

15)

Synthesis, Structure, and Reactivity of
Borabenzene and Boratabenzene Complexes

by
Diego Andrés Hoic

A.B., Chemistry (May 1993)
Columbia University

Submitted to the Department of Chemistry in Partial
Fulfillment of the Requirements for the Degree of

DOCTOR OF PHILOSOPHY

at the

Massachusetts Institute of Technology

September, 1998

© 1998 Massachusetts Institute of Technology.
All rights reserved.

Signature of Author

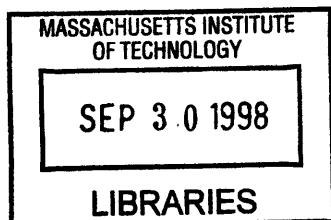
Department of Chemistry
July 30, 1998

Certified by

Professor Gregory C. Fu
Department of Chemistry
Thesis Supervisor

Accepted by

Dietmar Seyferth
Chairman, Departmental Committee on Graduate Students



science

v.1

This doctoral thesis has been examined by a committee of the Department of Chemistry as follows:

Professor Timothy M. Swager..... Chairman

Professor Gregory C. Fu Thesis Supervisor

Professor Frederick D. Greene.... ..

Synthesis, Structure, and Reactivity of Borabenzenes and Boratabenzenes
by
Diego A. Hoic

Submitted to the Department of Chemistry on July 30, 1998, in partial fulfillment of the requirements for the Degree of Doctor of Philosophy in Organic Chemistry

Abstract:

Although complexes derived from anionic borabenzenes (boratabenzenes) had been used for a long time, little was known about their neutral counterparts, mostly because an easy synthetic entry to them was not available. A facile three-step synthesis that allows the preparation of large quantities of neutral borabenzenes in three days, from commercially available starting materials is described in Chapter 2.

In Chapter 3 it is shown that neutral borabenzenes can be converted into anionic boratabenzenes, thereby providing a versatile new synthesis of this family of compounds. The solid state structures of these complexes are described. The developments in Chapters 2 and 3 allowed us to continue on to studies of both borabenzene and boratabenzene complexes.

Chapter 4 deals with the complexation of borabenzenes and boratabenzenes to some common transition metal fragments, mostly $\text{Cr}(\text{CO})_3$ and $[\text{Rh}(\text{olefin})_2]^+$, as well as structural studies thereof. We also discuss the interconversion between borabenzene- and boratabenzene-metal complexes.

Chapter 5 deals with the chemistry of the parent 1-*H*-boratabenzene. We discuss its synthesis, structure (in the solid state and in solution), and reactivity. In this chapter it is shown that the B-H is hydridic, and that the ring can form π -complexes with transition metals. The electron-donating ability of 1-*H*-boratabenzene is shown to lie somewhere between that of benzene and of Cp.

Chapter 6 is concerned with the chemistry of diphenylphosphidoboratabenzene. This molecule is unique among boratabenzenes in that it prefers to bind main group electrophiles and transition metals through its boron substituent. Solid state structural studies establish that it has the same steric bulk as triphenylphosphine. Comparative studies of its transition metal complexes show that it is considerably more electron-donating than triphenylphosphine.

Thesis Supervisor: Gregory C. Fu
Title: Associate Professor of Chemistry

**Esta tesis esta dedicada a
má, pá y Magui.**

ACKNOWLEDGEMENTS

To earn a Ph.D. we are required to work alone, so that our individual contributions may be properly identified. Notwithstanding, I owe many thanks to those people without whom I would never have obtained this degree.

The most influential person in my decision to attend graduate school was Tom Katz. He introduced me to an organic chemistry that did not consist of a purposeless stack of reactions, but of an intricate mixture of logic and randomness dictated by experiment. I am also very thankful of the unwavering support he provided throughout my graduate studies. From Columbia, I also want to thank the late Brian Bent, Clark Still, Ged Parkin, and Dave Horne for their teachings.

At MIT, I was fortunate that Greg allowed me to work on borabenzene chemistry. He always held me to the highest standards and for that I am grateful, as it has made me a better man. I also thank him for allowing me to have as much intellectual freedom as he is willing to allow anyone; this thesis stands as a testimony of how fruitful our relationship has been as a result. I must say that any person who may reads this thesis should be thankful of the two thorough (and I do mean *thorough*) readings he gave this entire manuscript. I thank Kit Cummins and Fred Greene for being interested in my research since my first year and Steve Buchwald for generously sharing his thoughts on my project. I thank Kit, Fred Greene and Tim for being so accommodating when the time came to set a thesis defense; I still wish Kit were in town today.

I am pleased that during my stay at MIT the following people entered my life, I hope never to leave: Dr. Bill Davis taught me all the crystallography I know, thus becoming somewhat responsible for the existence of Appendix II. I am fortunate that he shares his friendship, comments, and insults with me, as well as an occasional Budweiser. Mike Amendola, who started on borabenzene with me, is a wonderful human being and was a great researcher. I was sad to see him go, as we constantly exchanged ideas and thoughts. I believe that my life, this thesis, and the world of borabenzenes, would be orders of magnitude better if he had been around for a few more years. Dr. Dave Hays is simply the best and hardest-working chemist I ever met. He taught me, by example, to pay attention to detail, and to distinguish quality from crap. 3M is really lucky to have hired him. Dr. Ken Stockman taught me a considerable amount about coordination chemistry and general randomness. We also shared some good laughs. Dra. Rosa y Dr. Jordi (i.e., pelat), os habéis ganado un lugar especial en mi corazón por tantas cosas que no se pueden describir, pero que, de alguna manera, ya os he dicho. Thank you, Ike, for your teachings. Finally, I thank the remaining members of the Fu group for all their contributions to my life over the past five years.

Several graduate students and postdocs have helped make this thesis a reality; some are referenced in the text, but the following are not. Thank you, Aaron Odom, and the members of the Schrock and Cummins groups, for everything you've

taught me. I gratefully acknowledge the Buchwald group's generosity with chemicals, guidance and equipment, especially in the early years. I thank Jimmy and Jed for proofreading my entire thesis at different stages. Finally, I also feel that I must acknowledge the Stubbe group, with whom I shared a floor and an outlook.

My life outside of the lab made my stay at MIT fun, or at least bearable. I thank my "cousin" Marina U., Clau D., Pato M., Adam R., Elvira M., Ana Lisa P., Tuncay G., a en Sergi D., na Dolors S. i en Carles C., Adriano A., the rest of the Green Street Grill vampires, Chris M., Jed G., Marc J., Alex E.. I miss all of you already. Kevin and Aaron, my two roommates over the last 4 years, thank you for your patience. Merci, Becky, for the present.

Finally, a few people deserve a very special mention. Notably, it has just dawned upon me that I met most of them during a two-week span: Mr. Turkey Club, my soon-to-be neighbor Sal, and Cornish are my three pillars-of-strength and kept me sane throughout it all. I first met them nine years ago while settling into 9 Carman some time during the first week of September 1989. Lois and Arthur Katz (no relation to Tom - I'm surrounded by Katz!), and their rapidly growing family, generously opened their hearts to me. They have been my surrogate family since Lois and Brian picked me up at JFK on August 28, 1989; thank you, you know how much you mean to me.

Finalmente, al dedicarles esta tesis, agradezco a mi familia. Su amor y su apoyo incondicional me permitieron sobreponerme a todas las barreras que he encontrado hasta ahora.

Thus, everything has an end and what doesn't kill you makes you stronger. I'm outta here!!!!

De vez en cuando la vida
nos besa en la boca
y a colores se despliega
como un atlas.
nos pasea por las calles
en volandas
y nos sentimos en buenas manos;
se hace de nuestra medida,
coge nuestro paso
y saca un conejo de la vieja chistera
y uno es feliz como el niño
cuando sale de la escuela.

De vez en cuando la vida
toma conmigo café
y está tan bonita que
da gusto verla.
Se suelta el pelo y me invita
a salir con ella a escena.

De vez en cuando la vida
se nos brinda en cueros
y nos regala un sueño
tan escurridizo
que hay que andarlo de puntillas
por no romper el hechizo.

De vez en cuando la vida
afina con el pincel:
se nos eriza la piel
y faltan palabras
para nombrar lo que ofrece
a los que saben usarla.

De vez en cuando la vida
nos gasta una broma
y nos despertamos
sin saber qué pasa,
chupando un palo sentados
sobre una calabaza.

Joan Manuel Serrat

TABLE OF CONTENTS:

Title Page	1
Signature Page	2
Abstract	3
Dedication	4
Acknowledgements	5
Quotation	7
Table of Contents	8
Abbreviations	9
Chapter 1: Introduction	10
Chapter 2: Chemistry of Neutral Borabenzenes	18
Chapter 3: Synthesis and Structure of Alkali Metal Boratabenzenes	37
Chapter 4: Synthesis, Structure, and Reactivity of π -Bound Borabenzenes and Boratabenzenes	51
Chapter 5: Chemistry of 1- <i>H</i> -boratabenzene, BBH	83
Chapter 6: Chemistry of Diphenylphosphidoboratabenzene, DPB	100
Appendix I: ^1H NMR Spectra of Selected Compounds	119
Appendix II: Crystal Structure Determinations	155
Biographical Note and Publication List	391

ABBREVIATIONS

BB:	C ₅ H ₅ B
BBH:	C ₅ H ₅ BH
DPB:	C ₅ H ₅ BPh ₂
DAB:	C ₅ H ₅ BNPh ₂
Cy:	cyclohexyl
Nu:	nucleophile
E ⁺ :	electrophile
L:	ligand
L _n :	ligand system
py:	pyridine
lut:	2,6-lutidine
cod:	1,5-cyclooctadiene
nbd:	norbornadiene
diCp:	dicyclopentadiene
Tf:	trifluoromethanesulfonyl
Ts:	<i>p</i> -toluenesulfonyl
Fp:	Fe(CO) ₂ Cp
TMS:	trimethylsilyl
THF:	tetrahydrofuran
LDA:	lithium diisopropylamide
Cp:	cyclopentadienide
Cp*:	pentamethylcyclopentadienide

Chapter 1: Introduction.

Biologically active molecules are most often optically pure, and the recognition that only one enantiomer is usually responsible for the biological activity has spurred intense activity in the field of asymmetric synthesis. One of the most common carbon-carbon bond-forming reactions employed to prepare biologically active molecules is the addition of a reagent to one prochiral face of an aldehyde. Depending on the nature of the reagent, the reaction has been given well-recognized names such as aldol, Sakurai, Baylis-Hillman, and Alder ene, to name a few. Because these reactions can often be Lewis acid catalyzed,¹ a considerable amount of effort has been directed to the development of versatile chiral Lewis acid catalysts. Our goal is the development of a versatile chiral Lewis acid, based on a novel design feature that will be described below.

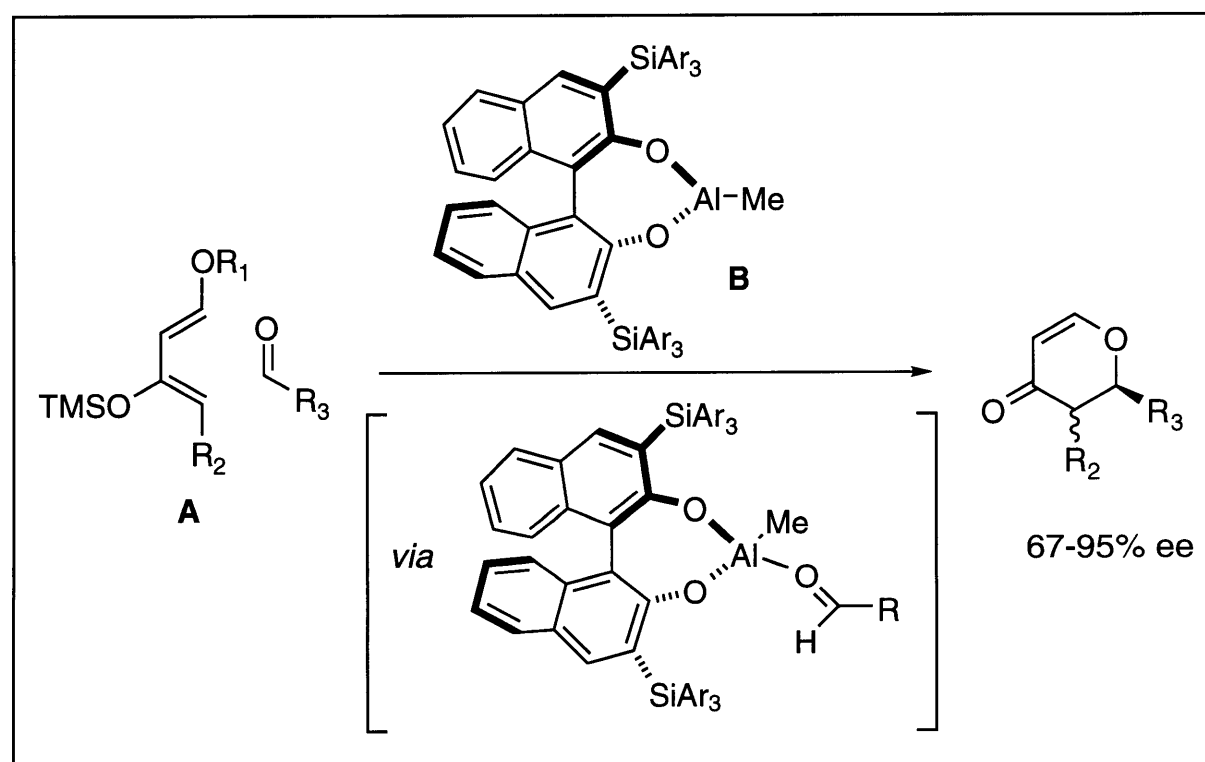


Figure 1.1. Yamamoto's Chiral Lewis Acid Catalyst.

¹ a) *Selectivities in Lewis Acid Promoted Reactions*; Schinzer, D., Ed.; Kluwer: Boston, 1989. b) Yamaguchi, M. In *Comprehensive Organic Synthesis*; Trost, B. M., Ed.; Pergamon: New York, 1991; Vol. 1, Chapter 1.11.

Several complexes that can catalyze enantioselective reactions of aldehydes have been reported over the past two decades. For example, in a landmark report Yamamoto and co-workers showed that the aluminum complex **B** (Figure 1.1) can catalyze enantioselective hetero Diels-Alder reactions, although the system appears to be highly specific for hetero Diels-Alder chemistry.² A possible explanation for this high selectivity (that highlights the need to employ elements other than sterics to effect organization of the transition state) is that the silyl substituents probably create such a tight pocket that that only particular diene/aldehyde combinations fit well in the reaction pocket. When the fit is good, the highly organized transition state results in high optical yields. However, for diene/aldehyde combinations for which the fit is worse, the pocket may be too large or too small, so that either the transition state is poorly-organized and the optical yields are low, or one reaction partner cannot get close to the other and catalysis is ineffective.

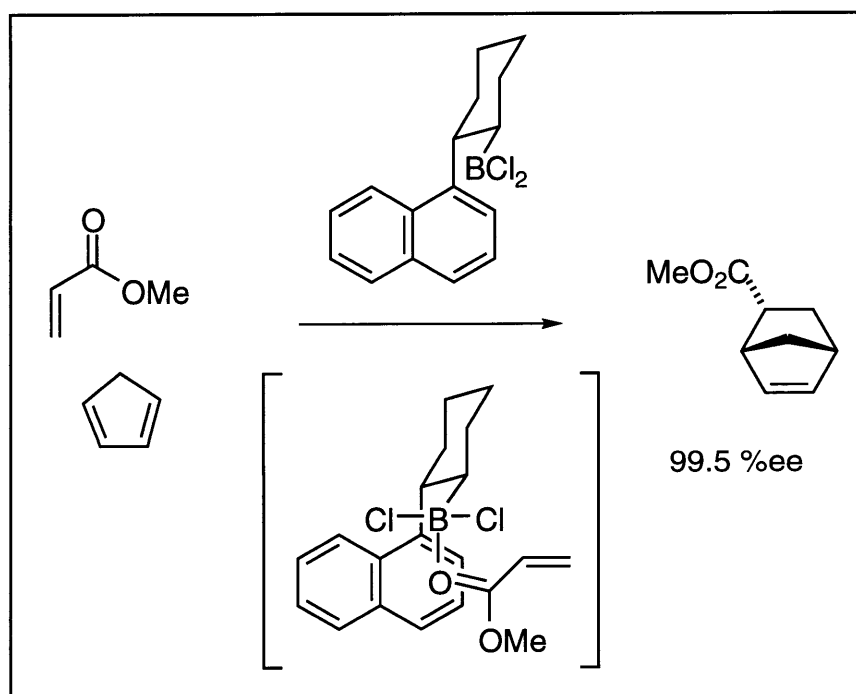


Figure 1.2. Hawkins' Chiral Lewis Acid Catalyst.

² Maruoka, K.; Itoh, T.; Shirasaka, T.; Yamamoto, H. *J. Am. Chem. Soc.* **1988**, *110*, 310-312.

In the early 1990's several research groups recognized that a new approach to a general Lewis acid catalyst was possible, not relying entirely on sterics to effect the stereodifferentiation. As a result, for example, the groups of Hawkins³ and Corey⁴ developed chiral Lewis acid catalysts that based the organization of the transition state on a π -stacking interaction between an aromatic ring in the catalyst and the aldehyde carbonyl group. Hawkins' system is illustrated in Figure 1.2. These approaches were quite successful, although the catalysts still were not general.

Our approach to the problem relies on the use of a partial multiple bond between the Lewis acid and the aldehyde. If a Lewis acid were to have orbitals that were of proper symmetry and energy to interact with the carbonyl π -system, rotation around the acid-oxygen bond would be hindered in the same manner that rotation around a carbon-carbon double bond is restricted. As a result, the degrees of freedom for the resulting Lewis acid-aldehyde complex would be reduced, possibly yielding a tightly organized transition state, the first requirement for a successful asymmetric reaction. A further advantage of this design is that the aldehyde behaves as a π -electron donor in the complex with the catalyst, so the carbonyl carbon should be the most electrophilic (i.e., reactive) in the conformation having π orbital overlap (Figure 1.3). Although nucleophiles add to the π^* -orbital of a carbonyl group, the direct activation of the carbonyl π -system has not been added as a design feature to any chiral Lewis acid explored to date. We call this design feature " π activation."

For π activation to be possible, the Lewis-acidic center must bear a π symmetry orbital. Furthermore, it is preferable that the Lewis-acidic atom belong to the first row, so that its p orbital overlaps better with the π system of the carbonyl group. Therefore, we have chosen boron as the Lewis-acidic element, and borabenzene (C, Figure 1.4) as the Lewis acid framework.

³ a) Hawkins, J. M.; Loren, S.; Nambu, M. *J. Am. Chem. Soc.* **1994**, *116*, 1657-1660.

b) Hawkins, J. M.; Loren, S. *J. Am. Chem. Soc.* **1991**, *113*, 7794-7795.

⁴ Corey, E. J.; Loh, T.-P. *J. Am. Chem. Soc.* **1991**, *113*, 8966-8967.

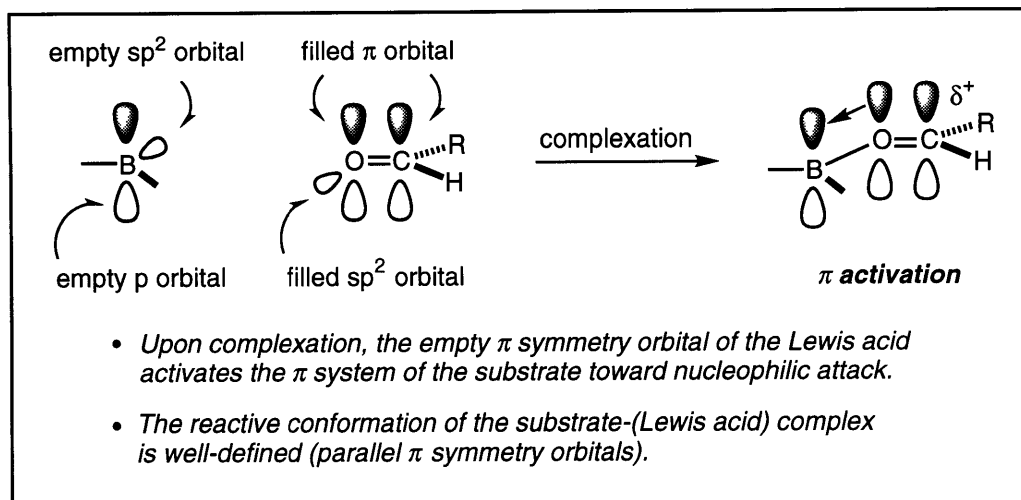


Figure 1.3. π Activation of a Prochiral Aldehyde.

Borabenzene is an achiral molecule by virtue of two mirror planes, one in the plane of the ring and a second one, perpendicular to the first, passing through the boron and the para carbon. It should be possible to destroy these mirror planes by π -complexing an ortho-substituted borabenzene ring to a transition metal (Figure 1.4), and we chose such a complex as our target chiral Lewis acid catalyst.

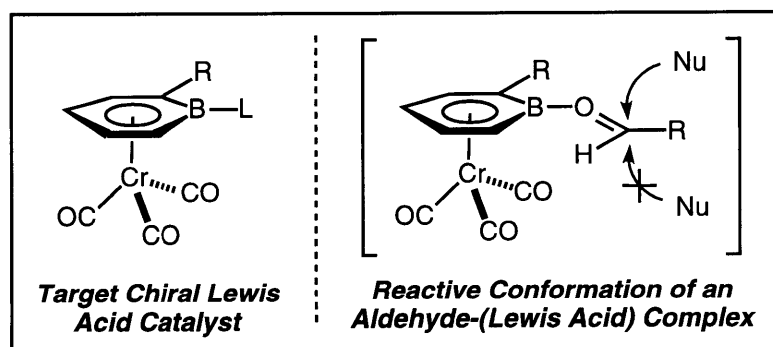


Figure 1.4. Target Chiral Lewis Acid Catalyst.

There are two different families of borabenzenes, and it is the nature of the base coordinated to boron that determines the family to which a specific borabenzene belongs. There are *neutral* borabenzenes, such as the PMe_3 adduct (D, Figure 1.5), and *anionic* ones, such as the hydride (E, Figure 1.5). It is a common practice in the literature to call both classes of complexes "borabenzenes" regardless of the nature of the boron substituent. For the purposes of the design of a chiral Lewis acid, we are mostly concerned with the chemistry of neutral borabenzenes.

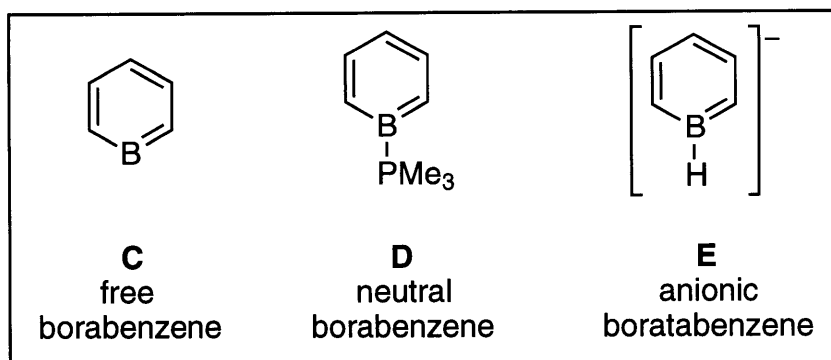


Figure 1.5. Different Classes of Borabenzenes.

Prior to our work, many complexes bearing the *boratabenzene* ring (Figure 1.6) were known,⁵ but only two well-characterized *borabenzene* complexes⁶ had been reported: the pyridine adduct⁷ and its $\text{Cr}(\text{CO})_3$ derivative, π -complexed via the borabenzene ring.⁸ Chapter 2 of this thesis presents a straightforward and versatile synthesis of borabenzenes stabilized by relatively strong Lewis bases, such as phosphines, amines, and an isocyanide. Our procedure allows the preparation of multigram quantities of the desired borabenzene compound. Studies of the properties of these compounds are also reported. The neutral borabenzenes can be purified either by crystallization or sublimation, the latter being the method of choice to reach analytical purity. As crystalline solids they are air stable. Also covered in Chapter 2 are our studies of the exchange of the Lewis base bound to boron. We had hoped that the intermediate in this reaction might be the hitherto unobserved free borabenzene (C, Figure 1.5), but experimentation showed otherwise. The ready availability of borabenzene complexes allowed their use as starting materials for the developments detailed in the following chapters.

⁵ Herberich, G. E.; Ohst, H. *Adv. Organomet. Chem.* **1986**, *25*, 199-236.

⁶ It should be noted that a considerable amount of unsuccessful experimental work has been directed to the observation of free borabenzene, C. This work is reviewed in Maier, G. *Pure Appl. Chem.* **1986**, *58*, 95-104.

⁷ Boese, R.; Finke, N.; Henkelmann, J.; Maier, G.; Paetzold, P.; Reisenauer, H. P.; Schmid, G. *Chem. Ber.* **1985**, *118*, 1644-1654.

⁸ Boese, R.; Finke, N.; Keil, T.; Paetzold, P.; Schmid, G. *Z. Naturforsch., B* **1985**, *40*, 1327-1332.

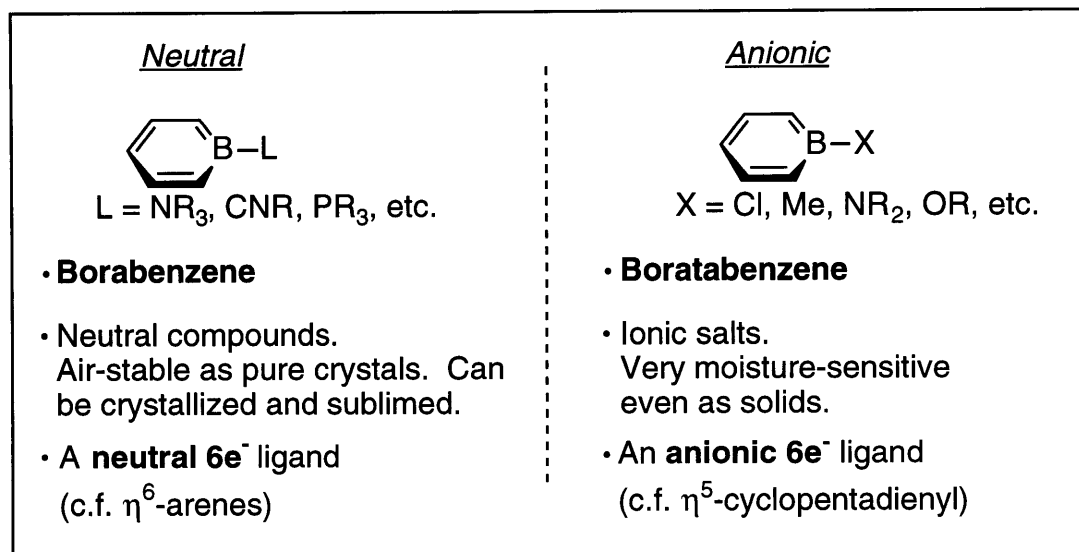


Figure 1.6. Borabenzenes vs. Boratabenzenes.

Chapter 3 discusses a versatile method for the synthesis of boratabenzenes, using neutral borabenzene- PMe_3 as starting material. The mechanism of this reaction is believed to be an associative bimolecular nucleophilic aromatic substitution. From borabenzene- PMe_3 , one can make boratabenzenes substituted with hydride, phosphides, alkoxides, amides, cyanide, and sulfides. Structural studies show that alkali metal boratabenzenes have similar structural motifs as alkali metal cyclopentadienides, although in some cases the boron substituent is not innocuous. Alkali metal boratabenzenes tend to be very moisture-sensitive powdery aggregates, rather than single crystals. When they do form a single crystal, there are often several solvent molecules incorporated into the crystal lattice, which are quite hard to remove. Crystallization, which is not always possible, is the only convenient method for their purification.

The chemistry of transition metal-bound borabenzenes and boratabenzenes forms the subject of Chapter 4. Borabenzenes resemble arenes when complexed to transition metals, and the borabenzene ligand is more electron-donating than benzene. Boratabenzenes resemble cyclopentadienides in their complexation to transition metals, as well as in their chemistry. Boratabenzene-containing transition metal complexes serve as effective surrogates for Cp ,⁹ especially when

⁹ a) Catalysis of the cyclotrimerization of olefins: Bonnemann, H. *Angew. Chem., Int. Ed. Engl.* **1985**, *24*, 248-262. Bonnemann, H.; Brijoux, W.; Brinkmann, R.; Meurers, W. *Helv. Chim. Acta* **1984**, *67*, 1616-1624. b) Mediation of zirconium

electron-deficient cyclopentadienides are needed.¹⁰ Chapter 4 also describes our unsuccessful attempts to correlate the electronic nature of the substituent on boron with the reactivity of a transition metal center π -complexed to the boratabenzene. As with unbound borabenzene, transition metal-bound borabenzene can sometimes be converted, via nucleophilic displacement, to the corresponding boratabenzene complex. Interestingly, we have found that in some instances alkoxy- or dialkylamido-boratabenzene metal complexes can be converted to the corresponding borabenzene metal complexes by reaction with a strong electrophile. These results are discussed from the perspective of the chemistry of our proposed chiral Lewis acid catalyst, as well as from the perspective of Ziegler-Natta polymerization chemistry.

Two boratabenzene complexes prepared in Chapter 3 were deemed worthy of detailed investigation. 1-*H*-Boratabenzene (BBH), the parent boratabenzene, occupies a special niche, as it is isostructural with benzene, but is uninegatively charged like Cp⁻. Its chemistry, as well as that of its transition metal complexes, is described in Chapter 5. The B-H bond is hydridic, a feature reflected by the fact that BBH reduces aldehydes and epoxides to alcohols and reacts with water to release H₂. BBH does not participate in olefin hydroboration reactions, probably because the p orbital on boron belongs to an aromatic ring and is thus less Lewis acidic than the p orbital in, for example, BH₃. Studies of the solid state and solution structures of BBH are also reported in Chapter 5. Finally, we have explored the use of BBH as a ligand for transition metals, and we have established that BBH has a donating ability that places it in between benzene and Cp.

Diphenylphosphidoboratabenzene (DPB) is the other special boratabenzene, and

(II) chemistry: Ashe, A. J., III; Al-Ahmad, S.; Kampf, J. W.; Young, V. G., Jr. *Angew. Chem., Int. Ed. Engl.* **1997**, *36*, 2014-2016.

- ¹⁰ Catalysis in Ziegler-Natta polymerization: a) Devore, D. D.; Timmers, F. J.; Neithamer, D. R. World Patent WO 97/36937. b) Herberich, G. E.; Schmidt, B.; Schmitz, A.; Fischer, A.; Riedel, M.; Herrmann, H.-F.; Ozdemir, D. World Patent WO 97/23512. c) Krishamurti, R.; Nagy, S.; Etherton, B. P. World Patent WO 96/23004. d) Herberich, G. E. German Patent DE 19549352 A1. e) Barnhart, R. W.; Bazan, G. C.; Mourey, T. J. *Am. Chem. Soc.* **1998**, *120*, 1082-1083. f) Sparry, C. K.; Rodriguez, G.; Bazan, G. C. *J. Organomet. Chem.* **1997**, *548*, 1-8. g) Rogers, J. S.; Bazan, G. C.; Sparry, C. K. *J. Am. Chem. Soc.* **1997**, *119*, 9305-9306. h) Bazan, G. C.; Rodriguez, G.; Ashe, A. J., III; Al-Ahmad, S.; Kampf, J. W. *Organometallics* **1997**, *16*, 2492-2494. i) Bazan, G. C.; Rodriguez, G.; Ashe, A. J., III; Al-Ahmad, S.; Muller, C. *J. Am. Chem. Soc.* **1996**, *118*, 2291-2292.

its chemistry is discussed in Chapter 6. DPB can be complexed with early (Zr), middle (Fe), and late (Rh) transition metal centers through phosphorus, rather than by the η^6 -complexation that is characteristic of other boratabenzenes. DPB is isostructural with triphenylphosphine, but negatively charged. We anticipate that DPB may become a useful tool for the separation of electronic and steric effects in mechanistic studies of organometallic reactions which employ PPh_3 complexes. Also discussed in Chapter 6 is how the degree of π -bonding between the borabenzene and the boron substituent can affect the reactivity of the boratabenzene complex.

We have not yet succeeded in making a chiral Lewis acid catalyst. This is hardly surprising, considering that no known working chiral catalyst was ever pre-designed to the extent that we had pre-designed our Lewis acid catalyst, with the possible exception of the Hawkins and Corey systems, and considering that the system presented a considerable number of unknowns when we started.¹¹ The work described herein, together with that described in two master's theses from our laboratory,^{12,13} should place us a considerable number of steps closer to the preparation of a chiral Lewis acid catalyst based on π -activation.

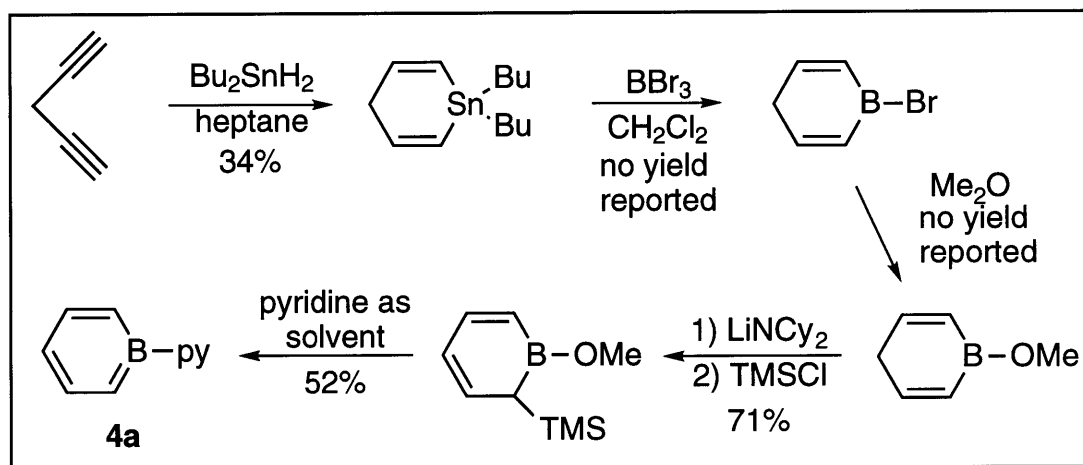
¹¹ For a colorful account of the discovery of the asymmetric epoxidation, which describes the most common catalyst discovery process, see Sharpless, K. B. *Chemistry in Britain* **1986**, 22(1), 38-44.

¹² Amendola, M. C. M.S. Thesis, MIT, 1995.

¹³ Tweddell, J. M.S. Thesis, MIT, 1997.

Chapter 2: Chemistry of Neutral Borabenzenes.

When we started working on borabenzene chemistry the only neutral borabenzene compound known was borabenzene-pyridine (BB-py).¹ The route to prepare it, outlined in Scheme 2.1,² was laborious and low-yielding, although it was sufficient for proper characterization of BB-py and for its complexation to $\text{Cr}(\text{CO})_3$.³



Scheme 2.1.

We have developed a new route,⁴ similar to the first one, but with a few crucial changes (Scheme 2.2).⁵ Indeed, Dr. Jennifer Robbins Wolf discovered that borabenzene-pyridine, -lutidine, and -trimethylphosphine could be efficiently prepared by incorporating the TMS group in the starting diyne (instead of adding it

¹ All other reports in which a neutral borabenzene complex has been mentioned deal with poorly characterized molecules: a) BB-N₂ and BB-CO: Maier, G.; Reisenauer, H. P.; Henkelmann, J.; Kliche, C. *Angew. Chem., Int. Ed. Engl.* **1988**, *27*, 295-296. b) 9-Boraanthracene-dimethylsulfide: Jutzi, P. *Angew. Chem., Int. Ed. Engl.* **1972**, *11*, 53-54. c) Boranaphthalene adducts were characterized in references 2 and 3.

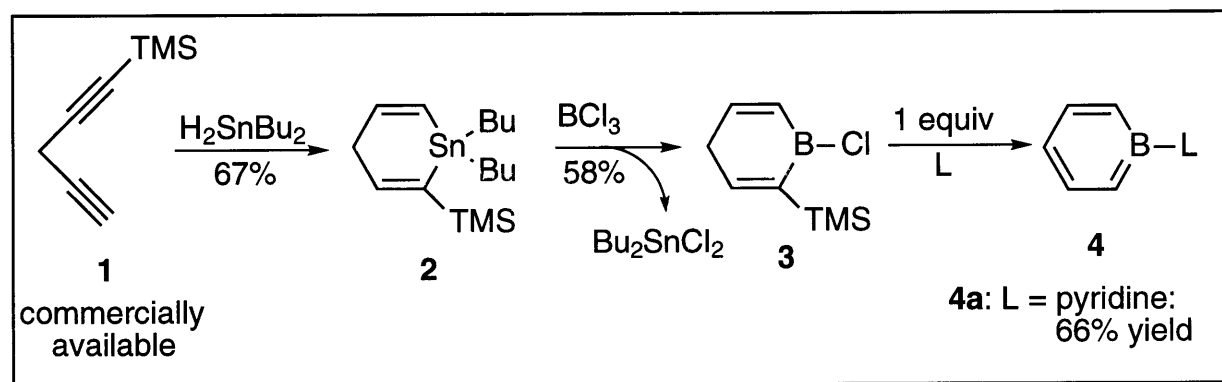
² Boese, R.; Finke, N.; Henkelmann, J.; Maier, G.; Paetzold, P.; Reisenauer, H. P.; Schmid, G. *Chem. Ber.* **1985**, *118*, 1644-1654.

³ Boese, R.; Finke, N.; Keil, T.; Paetzold, P.; Schmid, G. *Z. Naturforsch., B* **1985**, *40*, 1327-1332.

⁴ This work has appeared in print: Hoic, D. A.; Wolf, J. R.; Davis, W. M.; Fu, G. C. *Organometallics* **1996**, *15*, 1315-1317.

⁵ The initial experiments in this project were performed by Dr. Jennifer Robbins Wolf, who isolated small amounts of borabenzene-pyridine (**4a**), -2,6-lutidine (**4b**), and -PMe₃ (**4e**), and showed exchange of the PMe₃ in **4e** by pyridine.

later in the synthesis) and forming the borabenzene adduct **4** from chloroboracycle **3** (instead of from its methoxy analog). It was our task to scale up this procedure and to conclude the study of its scope. By the time our studies were completed, the net effect of these changes were an increase in the overall yield of borabenzene-pyridine by a factor of five.⁶ These changes have allowed the preparation of a family of complexes exhibiting varied substitution at boron, which has not been shown to be possible by the original route. Trialkylamine, tertiary phosphine, and isocyanide complexes can be prepared this way. An important advantage of our method is that the starting diyne is commercially available, whereas the synthesis of 1,4-pentadiyne, which is not commercially available, is laborious and low-yielding.⁷ Finally, the amount of time required for the preparation of borabenzene complexes has been reduced; now it is possible to obtain multi-gram quantities of the borabenzene in three days.



Scheme 2.2.

The first step is the free-radical cyclization of commercially available diyne **1** to stannacycle **2**. In their previous study of this reaction, Ashe and co-workers were able to obtain a 34% yield, refluxing the reagents in heptane (bp: 98 °C) for 16 hours.⁸ By halving the reflux time and running the reaction in toluene (bp: 111 °C), we were able to reproducibly obtain between 55 and 65% yield. The resulting

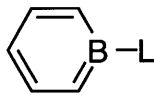
⁶ This number arises by assuming a combined 60% yield for the two reactions for which yields were not reported, the boron-for-tin transmetallation and the ether cleavage.

⁷ For its preparation, see: a) Ben-Efraim, D. A.; Sondheimer, F.; *Tetrahedron* **1969**, *25*, 2823-2835. b) Verkruisje, H. D.; Hasselaar, M. *Synthesis* **1979**, 292-293.

⁸ Ashe, A. J., III; Chan, W.-T.; Smith, T. W.; Taba, K. M. *J. Org. Chem.* **1981**, *46*, 881-885. Also see Chan, W.-T. Ph.D. Thesis, University of Michigan, 1977.

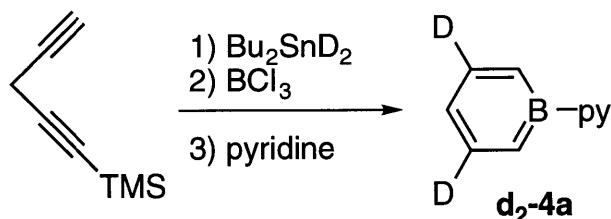
stannacycle **2** can be converted to boracycle **3** by its reaction with boron trichloride, a reaction analogous to that used in the original synthesis of borabenzene-pyridine (Scheme 2.1).

Boracycle **3** reacts with a variety of Lewis bases to form the neutral borabenzene complexes **4a-f**.⁹ The Lewis bases that were selected for the formation of the borabenzene complex are all relatively low boiling, in order to facilitate isolation.¹⁰ The Lewis base must also be relatively strong to effect the reaction; despite numerous attempts, we have been unable to isolate compounds with L = dialkyl ether or aldehyde.

 4	L = a pyridine	66%
	b lutidine	80%
	c NEt ₃	92%
	d NMe ₃	77%
	e PMe ₃	88%
	f CN- <i>t</i> -Bu	85%

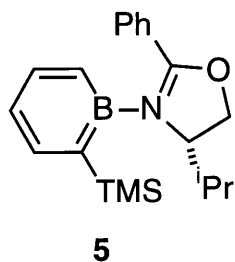
This protocol was extended by Michael Amendola to the synthesis of ortho-substituted borabenzene complexes.¹¹ This work was subsequently adapted by Jennifer Tweddell to the synthesis of the first optically pure borabenzene complex

⁹ We have also performed the aforementioned reactions starting with Bu₂SnD₂ (prepared from Bu₂SnCl₂ and LiAlH₄). Under the described conditions the resulting 3,5-dideuterio stannacycle forms cleanly but in lower yield than the unlabelled material, perhaps reflecting an isotope effect, although the reaction conditions were not optimized. The corresponding dideuterio boracycle forms in approximately the same yield as the unlabelled material, while treatment with a base cleanly affords the 3,5-dideuterio borabenzene complex.

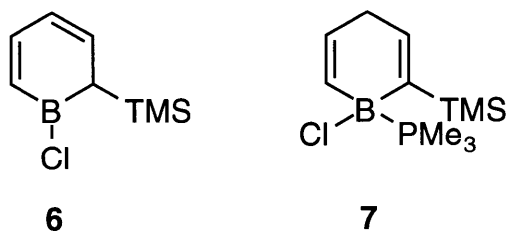


¹⁰ Notwithstanding, by mixing **3** with 4-phenylpyridine under the conditions prescribed for the synthesis of **4a**, the very crystalline borabenzene-(4-phenylpyridine) could be prepared by Shuang Qiao. Qiao, S.; Hoic, D. A.; Fu, G. C. *Organometallics* **1997**, *16*, 1501-1502.

¹¹ Amendola, M. C. M.S. Thesis, MIT, 1995.

(5).¹²

The reaction of boracycle **3** with Lewis bases to form **4a-f** is mechanistically interesting. It must involve the isomerization of a double bond (as in, for example, the conversion from **3** to **6**), formation of a boron-L bond, and loss of TMSCl. The question is the order in which these reactions occur. In principle, two reactions are most likely to take place when a base (such as PMe₃) is mixed with **3**: nucleophilic addition to boron to give adduct **7** or deprotonation at C₄ followed by reprotonation of the boratabenzene anion at C₂, resulting in isomerization from **3** to **6**.¹³ HCl elimination from **3** is unlikely: because of the sp² boron center, the molecule cannot meet the preferred conformation for an E2 elimination.¹⁴ An E1 elimination would require the intermediacy of a divalent boron cation, and these species are extremely high in energy.¹⁵ We cannot rule out HCl elimination from **7** based on our current information.



If the reaction **3** → **4e** is run in hexane for just four hours, one can isolate the

¹² a) Tweddell, J. M.S. Thesis, MIT, 1997. b) Tweddell, J.; Hoic, D. A.; Fu, G. C. *J. Org. Chem.* **1997**, *62*, 8286-8287.

¹³ A deuterium labelling experiment ruled out the possibility that this reaction occurs via successive hydrogen shifts. We thank Prof. Frederick Greene for suggesting this experiment.

¹⁴ March, J. *Advanced Organic Chemistry*, 4th ed.; Wiley: N.Y., 1992; Chapter 17.

¹⁵ Berndt, A. *Angew. Chem., Int. Ed. Engl.* **1993**, *32*, 985-1009.

acid-base complex **7** in 85% yield,¹⁶ contaminated with some borabenzene-trimethylphosphine, but no starting material. Stirring the isolated **7** in CH₂Cl₂ overnight results in complete conversion to borabenzene-trimethylphosphine.¹⁷

We have shown that the isomerized boracycle **6**¹⁸ is a chemically and kinetically competent intermediate for the formation of borabenzene-PMe₃ (**4e**). In the presence of 2 equivalents of PMe₃, the isomerized boracycle **6** rapidly reacts to form **4e** exclusively. We suspect that, upon mixing, **6** and PMe₃ transiently form a Lewis acid-base adduct from which TMSCl elimination to yield the borabenzene is fast.

It seems reasonable to propose that under basic conditions isomerization is more facile from the trivalent boron halide **3** than from the tetravalent boron halide **7**, because the intermediate resulting from deprotonation of the former is a 6π aromatic system (**A**, Figure 2.2).¹⁹ Deprotonation of **7** leads to a less-stable, albeit still resonance-stabilized, anion (**B**, Figure 2.2).

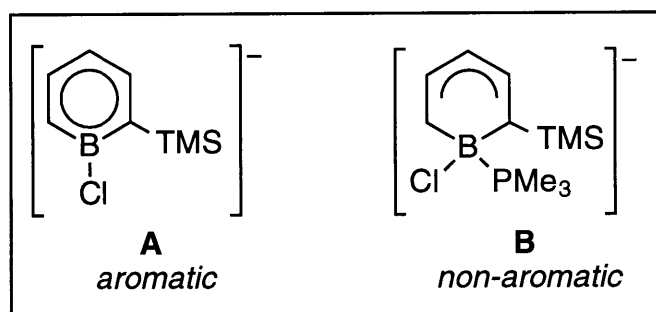


Figure 2.2. Products of the Deprotonation of 5 and 7.

When three NMR-tube reactions (in relative concentrations 1:4:10, with 1:1 boracycle **3**:PMe₃) were set up side-by-side and monitored, the more dilute sample resulted in qualitatively faster formation of BB-PMe₃ (**4e**). This suggests that an inhibitory pathway may be operating at increased concentration of either boracycle,

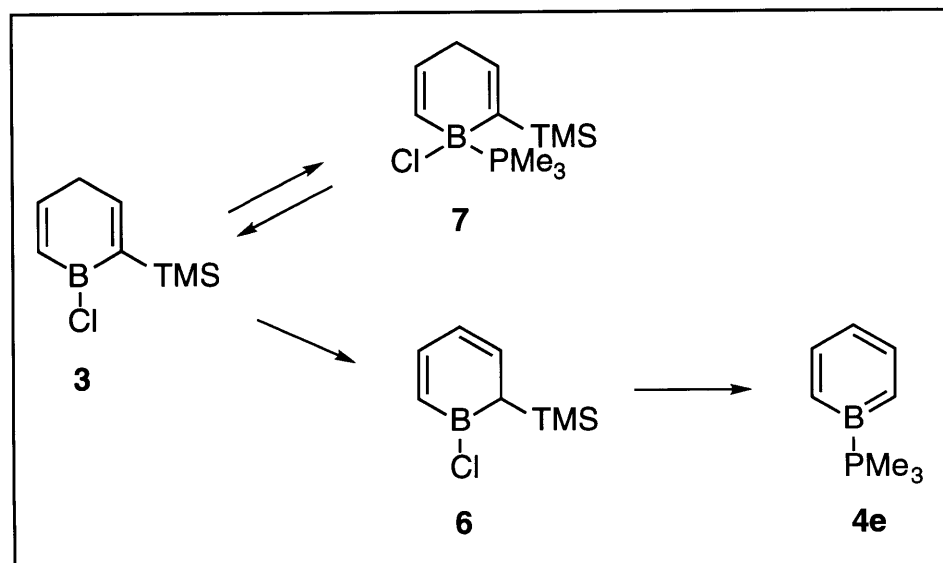
¹⁶ Characterized by ¹H, ¹¹B, and ³¹P NMR spectroscopy.

¹⁷ Notwithstanding the way this particular experiment was done, the published procedure for the synthesis of BB-PMe₃ (**4e**) calls for running the reaction in hexane overnight, resulting in the clean formation of borabenzene-trimethylphosphine in high yield.

¹⁸ Generously provided by Michael Amendola.

¹⁹ The acidity of an analogous system has been measured in the gas phase employing ion cyclotron resonance techniques. It has been found to be close to that of cyclopentadiene (pK_a ~ 15). Sullivan, S. A.; Sandford, H.; Beauchamp, J. L.; Ashe, A. J., III *J. Am. Chem. Soc.* **1978**, *100*, 3737-3742

phosphine, or both, perhaps as illustrated in Scheme 2.3.²⁰



Scheme 2.3.

We obtained crystal structures²¹ of the trimethylamine, trimethylphosphine, and *t*-butylisocyanide adducts (**4d**, **4e**, and **4f**) and compared them to that of the pyridine adduct (**4a**) which had been described in the literature.²² The interatomic distances within the borabenzene ring are the same, at the 3σ level, for all four crystal structures. The B-P distances in **4e** are 1.900(8) Å, 1.906(8) Å, 1.911(8) Å, and 1.918(8) Å (there are four independent molecules per asymmetric unit), similar to those of other acyclic boron-phosphorus single bonds.²³ The boron-isocyanide distances in **4f** are 1.560(3) Å and 1.559(3) Å (two molecules per unit), considerably shorter than in the only other known structure of a borane-isocyanide complex.²⁴ The B-N

²⁰ The resonances corresponding to **3**, **4e**, **6**, and **7** are observed in the ^{11}B NMR spectra of the reaction mixtures. It may be possible to, in the future, measure the parameters that affect the mechanism.

²¹ For details of these crystal structures, see the appendix.

²² Reference 2.

²³ Based on a search of the Cambridge Crystallographic Database, bonds between PMe_3 and any boron center range between 1.961 Å (Black, D. L.; Taylor, R. C. *Acta Crystallogr., Sect. B* **1975**, *31*, 1116-1120) and 1.883 Å (Mangion, M.; Hertz, R. K.; Denniston, M. L.; Long, J. R.; Clayton, W. R.; Shore, S. G. *J. Am. Chem. Soc.* **1976**, *98*, 449-453). There are no obvious trends in the eight different reports

²⁴ Tamm, M.; Lügger, T.; Hahn, F. E. *Organometallics* **1996**, *15*, 1251-1256. This compound is the only one of a borane-isocyanide complex, except for adducts

distances in BB-NMe₃ (**4d**) are 1.596(4) Å and 1.595(4) Å (two molecules per unit), significantly longer than the 1.558(3) Å observed in the crystal structure of **4a**.

Part of the turnover step in our proposed catalytic cycle is the exchange of the Lewis base on boron by another Lewis base. Because this step was unprecedented in borabenzene chemistry, we decided to explore its viability. Initially, Dr. Wolf found that treatment of borabenzene-trimethylphosphine with pyridine resulted in slow conversion of the colorless PMe₃ adduct to the red (in solution; yellow as a solid) pyridine adduct (Figure 2.3).

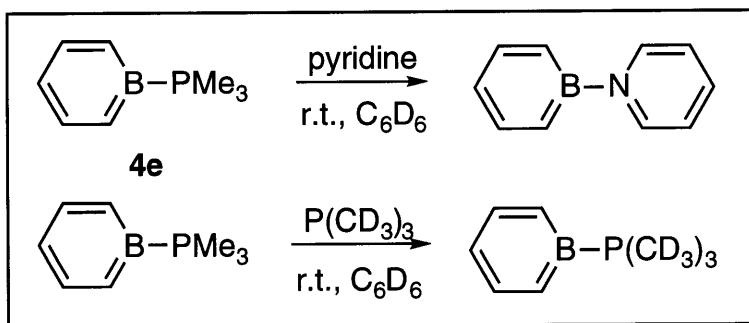
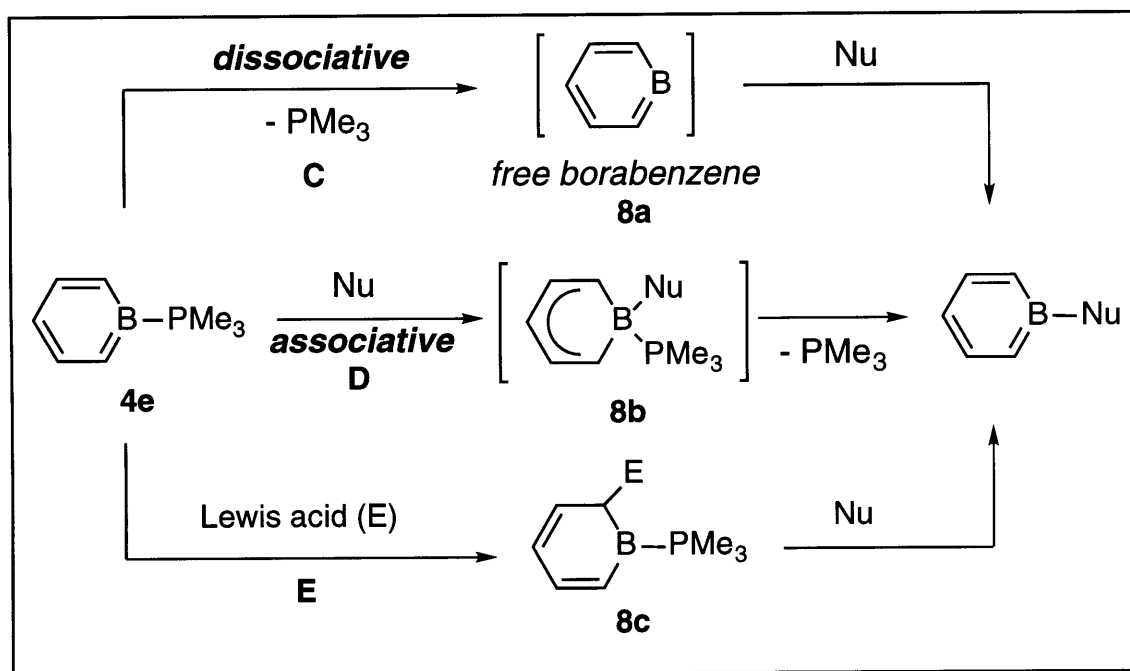


Figure 2.3. Initial Observations of Ligand Exchange.

We anticipated that there were two mechanisms by which this reaction was most likely to proceed, a dissociative pathway (C) involving free borabenzene (**8a**, Scheme 2.4) and an associative one (D) involving the tetrahedral intermediate **8b**. Initially, we did not think that a third pathway (E), in which the rate-limiting step was attack of the borabenzene by an electrophile to form **8c**, was likely, as we believed that we had removed the two most likely Lewis acidic impurities in the starting material: BCl₃ and Bu₂SnCl₂. We felt that BCl₃ is too volatile to survive the manipulations

with B-H bonds, where the B-C bond is shorter. This distinction appears justified as follows. In the Cambridge Crystallographic database there are 67 reports of B-C bonds between any boron center and an sp carbon connected to a nitrogen or an oxygen. The B-C bond distances in these compounds fall in a roughly Gaussian distribution with a median around 1.57 Å. However, once we remove all the molecules in which boron is bonded to at least one hydrogen, or forms part of a polyhedral borane, we are left with only nine structures. Of these, only one has a bond distance shorter than 1.618 Å (1.586 Å; ZIDJIF; Ansorge, A.; Brauer, D. J.; Buchheim-Spiegel, S.; Burger, G.; Hagen, T.; Pawelke, G. J. *Organomet. Chem.* **1995**, *501*, 347-358). The bond shortening of those structures containing boron hydrides or polyhedral boranes could be due to hyperconjugation effects.

involved in the conversion of **2** to **4e** (Scheme 2.2). Furthermore, it should react completely with excess PMe_3 . Bu_2SnCl_2 has six methyl protons and should easily be observed by high field ^1H NMR down to less than 0.5%, and it was not observed. Furthermore, to be present as an impurity, Bu_2SnCl_2 would have had to survive two distillations and at least one crystallization.



Scheme 2.4.

Free borabenzene (**8a**) has been of considerable interest to theoreticians²⁵ and experimentalists²⁶ alike, but it has thus far eluded observation. We therefore decided to try to distinguish the dissociative and associative mechanisms (**C** and **D**) by kinetics. Our initial experiments were encouraging, because the overall rate appeared to remain essentially constant as the concentration of Lewis base was

²⁵ a) Cioslowski, J.; Hay, P. J. *J. Am. Chem. Soc.* **1990**, *112*, 1707-1710. b) Schulman, J. M.; Disch, R. L. *Organometallics* **1989**, *8*, 733-737. c) Raabe, G.; Schleker, W.; Heyne, E.; Fleischhauer, J. *Z. Naturforsch., A* **1987**, *42*, 352-360. d) Schulman, J. M.; Disch, R. L.; Sabio, M. L. *J. Am. Chem. Soc.* **1982**, *104*, 3785-3788.

²⁶ a) Maier, G.; Wolf, H.-J.; Boese, R. *Chem. Ber.* **1990**, *123*, 505-511. b) Maier, G.; Reisenauer, H. P.; Henkelmann, J.; Kliche, C. *Angew. Chem., Int. Ed. Engl.* **1988**, *27*, 295-296. c) Maier, G. *Pure Appl. Chem.* **1986**, *58*, 95-104. d) Maier, G.; Henkelmann, J.; Reisenauer, H. P. *Angew. Chem., Int. Ed. Engl.* **1985**, *24*, 1065-1066.

increased ten-fold (Table 2.1). Indeed, the reaction appeared to *slow down* as the concentration of base increased, as might be expected for a dissociative pathway (vide infra). These experiments effectively rule out a direct $S_{\text{NAr}}2$ pathway.

[BB-PMe ₃] (M)	[d ₉ -PMe ₃] (M)	Rate constant (sec ⁻¹)
0.128	0.13	5.3 x 10 ⁻⁶
0.127	0.25	4.8 x 10 ⁻⁶
0.121	0.71	2.8 x 10 ⁻⁶

Table 2.1. Initial Experimental Rate Constant Determination.²⁷

Two possible explanations for this "slowing-down" phenomenon are a solvent effect and acid catalysis. The solvent effect argument goes as follows. A medium with a low dielectric constant should stabilize the neutral intermediates (free PMe₃ and free borabenzene, **8a**) better than it stabilizes the zwitterionic starting material and products. As a result, the rate-limiting dissociation of the ligand is more facile when the dielectric constant of the solvent is smaller (i.e., when less free phosphine is present). The alternative explanation involves catalysis by a Lewis acid that has been only partly neutralized by the excess base. At higher Lewis base concentration, there is less available Lewis acid catalyst, and the reaction slows down. It should be possible to distinguish these two mechanisms by reproducing the rate constant employing independently prepared reagents. If the rates are reproducible, then it is unlikely that a small amount of a Lewis acidic impurity is catalyzing the reaction, because it is nearly impossible to reproduce the purification of a reagent, while at the same time leaving the exact same amount of a very minor impurity.

Whereas within each batch of borabenzene-PMe₃, the trend shown in Table 2.1 was observed, we were unable to reproduce the observed rate from one batch to another. Therefore, we took a batch of borabenzene-trimethylphosphine and studied the kinetics of the reaction as we further recrystallized the starting material (Table 2.2). With dismay, we noted that the rate constant dropped upon further crystallization.

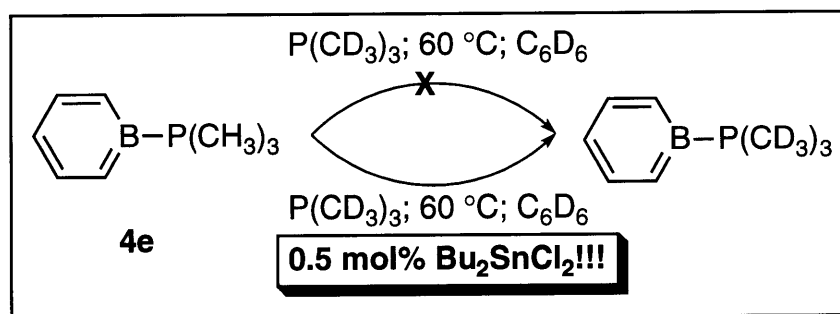
This trend could reflect the existence of a third mechanism that we had not considered up to that point, involving Lewis acid catalysis (E in Scheme 2.4).

²⁷ Solvent: C₆D₆; temperature: 48.0 - 48.2 °C.

Evidently, ^1H NMR was not a good enough assay for the purity of borabenzene-trimethylphosphine. Eventually, Dr. Kenneth Stockman showed that there was no exchange of the ligand when BB-PMe₃ was purified first by crystallization, then by sublimation, and finally by picking select single crystals from the sublimation.²⁸ He also showed that trace amounts of Bu₂SnCl₂ (the byproduct of the synthesis of boracycle **3**) is an excellent catalyst for the transformation (Scheme 2.5). His experiments show that the exchange of PMe₃ by another Lewis base does not proceed in the absence of a catalytic amount of an electrophile.

Recrystallizations	Rate constant
2	5.2×10^{-5}
3	2.0×10^{-5}
4	3.8×10^{-6}
5	3.2×10^{-6}
6	2.2×10^{-6}

Table 2.2. The Rate Constant Drops as Borabenzene-PMe₃ (**4e**) is Recrystallized.



Scheme 2.5.

Organotin compounds are known to be very resilient impurities.²⁹ Therefore, we suspect that Bu₂SnCl₂ remains throughout the purification of the borabenzene, even after two distillations and six crystallizations. The exchange of trimethylphosphine by pyridine occurs even when the starting BB-PMe₃ is pure by 500 MHz ^1H NMR, ^{13}C NMR, passes elemental analysis, and has a sharp, melting point. In other words, *none of the commonly used standards of purity for academic synthetic work was a good enough indicator of purity for BB-PMe₃ for the purposes*

²⁸ Stockman, K. E., unpublished results.

²⁹ For a discussion, see Crich, D.; Sun, S. J. *Org. Chem.* **1996**, *61*, 7200-7201.

of our study.

Conclusions:

We describe in this chapter a synthesis of neutral borabenzene that is superior to the one in the literature for several reasons. The compounds can be prepared in good overall yields, in three steps from commercially available starting materials, and in about three days. This route is also superior to the previous route because it allows the synthesis of borabenzene complexes bearing varied substitution at the boron atom. The exchange of Lewis bases bound to boron by other Lewis bases is a Lewis acid-catalyzed process.

Experimental Section.

General.

All reactions were carried out under an atmosphere of nitrogen in a glove box, or under argon using standard Schlenk techniques. Tetrahydrofuran, diethyl ether, benzene, hexane, pentane, pyridine, 2,6-lutidine, triethylamine, trimethylphosphine, and $P(CD_3)_3$ were distilled from sodium/benzophenone. Toluene was distilled from sodium. *t*-Butylisocyanide was distilled and stored at -35 °C. Methylene chloride was distilled from CaH_2 . $CDCl_3$, and C_6D_6 were purchased from Cambridge Isotope Laboratories and dried over basic alumina. $LiAlD_4$ was purchased from Cambridge Isotope Laboratories. All reagents were stored in the glove box after purification. BCl_3 (1.0 M in CH_2Cl_2) and trimethylamine (gas) were purchased from Aldrich Chemical Co. and used without further purification. 1-trimethylsilyl-1,4-pentadiyne was purchased from Farchan and distilled (stored at -35 °C).

1H nuclear magnetic resonance spectra were recorded on Varian XL-300, Unity 300, or VXR 500 NMR spectrometers at ambient temperature unless otherwise specified. 1H data are reported as follows: chemical shift (δ scale) (multiplicity (br = broad, s = singlet, d = doublet, t = triplet, q = quartet, and m = multiplet); coupling constant (Hz); integration). The spectra are referenced to residual solvent downfield from tetramethylsilane ($CDCl_3$: 7.25 ppm; C_6D_6 : 7.15 ppm; CD_2Cl_2 : 5.35 ppm; THF-d₈: 3.58 ppm). All ^{13}C spectra were determined with complete proton decoupling on Varian XL-300, Unity 300, or VXR 500 spectrometers and referenced to the solvent peak ($CDCl_3$: 77.0 ppm; C_6D_6 : 128.0 ppm; CD_2Cl_2 : 54.0 ppm; THF-d₈: 67.6 ppm). ^{11}B and ^{31}P NMR spectra (96 and 121 MHz, respectively) were obtained on XL-300 or Unity 300 spectrometers and were referenced to external $BF_3 \cdot OEt_2$ (0 ppm, ^{11}B), and 85% H_3PO_4 (0 ppm, ^{31}P), unless otherwise stated.

Infrared spectra were obtained as indicated on a Perkin-Elmer Series 1600 FT-IR spectrophotometer and are reported in cm^{-1} . Mass spectra were recorded on a Finnegan MAT System 8200 spectrometer.

Synthesis of Bu_2SnH_2 .

Prepared according to the literature procedure,³⁰ which consists of mixing dibutyltin oxide (42.8 grams, 0.172 mol) with polymethylhydrosiloxane (PMHS; 66

³⁰ Hayashi, K.; Iyoda, J.; Shiihara, I. *J. Organomet. Chem.* **1967**, *10*, 81-94.

mL; excess) and heating the mixture under vacuum (heating mantle) until the product distills out. Under these conditions the product vaporizes rather abruptly, so that very efficient cooling must be employed. In this particular case, 31.3 grams (78%) of product were isolated. However, Dr. Stockman found that the yield of the reaction could drop by ~20% depending on the source of PMHS and another ~20% depending on the source of Bu₂SnO. As of this writing, PMHS is purchased from Fluka and Bu₂SnO from Gelest, leading to reproducible yields of 65-70% of Bu₂SnH₂. Under identical conditions, reagents purchased from Aldrich resulted in reproducible yields of around 25%.

Synthesis of Stannacycle 2.³¹

A solution containing 1-trimethylsilyl-1,4-pentadiyne (5.00 g, 36.8 mmol) and dibutyltin dihydride³² (8.64 g, 36.8 mmol) in 18 mL of toluene was refluxed for 8 h. The toluene was then removed in vacuo, and stannacycle 6 was distilled under reduced pressure, providing a clear oil (bp 95-110 °C, 400 mtorr). Redistillation yielded 9.0 g (66%) of stannacycle 6 as a slightly air-sensitive colorless oil. ¹H NMR (300 MHz; C₆D₆): δ 6.84 (t; J = 3, J_{H-¹¹⁹Sn} = 35.4, J_{H-¹¹⁷Sn} = 34.5; 1H), 6.56 (dtd; J = 1.2, 4.0, 14.0; 1H), 6.29 (dtd; J = 0.9, 1.9, 13.9, J_{H-¹¹⁹Sn} = 66.6, J_{H-¹¹⁷Sn} = 63.5; 1H), 2.95 (m; 2H), 1.58 (m; 4H), 1.36 (m; 4H), 1.02 (m; 4H), 0.90 (t; J = 7.2; 6H), 0.15 (s; 9H). Coupling to tin was resolved at 500 MHz. ¹³C NMR (75 MHz; C₆D₆): δ 151.7, 145.0, 140.4, 126.4, 38.6, 29.7, 27.7, 13.9, 11.5, 0.4. IR (neat): 2956, 2929, 2871, 2852, 2175, 1824, 1602, 1566, 1463, 1399, 1245, 928, 836, 747, 687. HRMS: Calcd for C₁₆H₃₂SiSn: 372.1295. Found: 372.1293.

Synthesis of 3,5-Dideuteriostannacycle d₂-2.

Dibutyltin deuteride³³ (9.5 g, 40.1 mmol) was mixed with 1-trimethylsilyl-1,4-pentadiyne (5.46 g, 40.1 mmol) in 20 mL of toluene. The reaction was stirred for 8 hours, after which time the toluene was removed in vacuo, and the product distilled at 80 °C (~ 150 mTorr), yielding 3.17 g (21%) of a clear colorless oil. ¹H NMR

³¹ Ashe, A. J., III; Chan, W.-T.; Smith, T. W.; Taba, K. M. *J. Org. Chem.* **1981**, *46*, 881-885. These workers effect the same cyclization under somewhat different conditions (refluxing heptane, 16 h) and observe a 34% yield of stannacycle 6.

³² **CAUTION:** Dialkyltin dihydrides can evolve H₂ in the presence of metallic tin or other adventitious impurities (Kuivila, H. G. *Adv. Organomet. Chem.* **1964**, *1*, 47-87). We recommend that dibutyltin dihydride be prepared immediately prior to use.

³³ Davis, A. G. *Organotin Chemistry*; VCH: Weinheim, 1997; p 194.

(300 MHz; C₆D₆): δ 6.32 (s; 1H), 2.95 (s; 2H), 1.58 (m; 4H), 1.36 (m; 4H), 1.02 (m; 4H), 0.90 (t; 6H), 0.15 (s; 9H). ²H NMR (46 MHz; C₆H₆): δ 6.90 (s), 6.61(s).

Synthesis of Boracycle 3.

BCl₃ (15.0 mL, 15.0 mmol; 1.0 M in CH₂Cl₂) was added dropwise to a -78 °C solution of stannacycle 2 (5.57 g, 15.0 mmol) in ~1.5 mL of CH₂Cl₂. The reaction mixture immediately turned cloudy, canary yellow. Upon completion of the addition, the reaction was warmed to r.t., at which point it became homogeneous, and it was then stirred overnight. CH₂Cl₂ was distilled from the resulting clear gold solution at ambient pressure. Distillation of the residue³⁴ (bp 40-75 °C, 200 mtorr; oil bath temperature: 105 °C) afforded 1.9 g (70%) of product (>85% pure by NMR) as a clear, pale yellow oil. Redistillation (bath temperature: 50 °C; 180 mtorr) afforded 1.53 g (56%) of clear, colorless boracycle 3. ¹H NMR (300 MHz; C₆D₆): δ 7.22 (br s; 1H), 6.77 (br d; J = 11.7; 1H), 6.58 (dt; J = 11.7, 1.3; 1H), 2.47 (m; 2H), 0.31 (s; 9H). ¹³C NMR (75 MHz; C₆D₆): δ 164.2, 155.5, 144.5 (br), 134.5 (br), 38.0, -0.6. ¹¹B NMR (96 MHz; C₆D₆): δ +53.6. IR (neat): 3009, 2959, 2900, 1599, 1397, 1354, 1329, 1246, 1196, 1014, 999, 965, 838. EIMS: 169, 112, 93, 73. HRMS (M⁺-CH₃): Calcd for C₇H₁₁BClSi: 169.0412. Found: 169.0410.

This reaction is quite reliable, as long as care is exercised to start it at -78 °C. The yield appears to be unaffected by the rate of addition of BCl₃, at least up to a rate of 10 mL/min. It is likely that the transmetallation occurs below room temperature, as a color change from white to yellow is observed at -40 to -20 °C. One can wait from 1 to 12 hours after warming the reaction mixture to room temperature before isolation of the boracycle. Once the CH₂Cl₂ has been removed, however, the distillation of the product must be carried out as quickly as possible to avoid product decomposition. In order to isolate the product in good yield, one must also apply a good vacuum and cool the distillate efficiently.

Synthesis of 3,5-Dideuterioboracycle d₂-3.

3,5-Dideuteriostannacycle d₂-2 (3.17 g, 8.51 mmol) was dissolved in approx. 1 mL of CH₂Cl₂, taken out of the glovebox and cooled to -78 °C. BCl₃ (1.0 M in CH₂Cl₂, 8.51 mL, 8.51 mmol) was added dropwise with efficient stirring. The solution was brought to room temperature when the addition was over, and stirred for 2.5 h.

³⁴ If the product is not distilled quickly, some isomerization to boracycle 5 is observed.

After this time, the methylene chloride was removed in vacuo, leaving behind a clear brown solution, which was transferred via cannula into a 10 mL two-neck round-bottom flask and distilled, yielding 1.12 g (71%) of a clear oil. $^1\text{H NMR}$ (300 MHz; C_6D_6): δ 6.60 (s; 1 H), 2.45 (s; 2H), 0.43 (s; 3H). $^2\text{H NMR}$ (46 MHz; C_6H_6): δ 7.32 (s), 6.87 (br s);

Synthesis of Borabenzene-Pyridine (4a).

Pyridine (99 μL , 1.2 mmol) was added in a slow stream to a solution of boracycle **3** (225 mg, 1.22 mmol) in 1.5 mL of Et_2O . After 5 min,³⁵ the Et_2O was removed in vacuo, and the resulting orange solid was recrystallized from $\text{CH}_2\text{Cl}_2/\text{Et}_2\text{O}/\text{hexane}$, yielding 128 mg (67%) of borabenzene-pyridine as a crystalline yellow solid. The ^1H and ^{13}C NMR spectra (CD_3CN) of this compound were identical with those previously reported for borabenzene-pyridine.³⁶ $^1\text{H NMR}$ (300 MHz; CDCl_3): δ 9.04 (m; 2H), 8.07 (m; 1H), 7.74 (m; 2H), 7.57 (m; 2H), 6.72 (m; 3H). $^{13}\text{C NMR}$ (75 MHz; CDCl_3): δ 144.3, 140.1, 135.4, 126.3, 119 (br), 116.6. **Anal.** Calcd for $\text{C}_{10}\text{H}_{10}\text{BN}$: C, 77.49; H, 6.50. Found: C, 77.26; H, 6.66.

Synthesis of 3,5-Dideuterioborabenzene-Pyridine (d_2 -4a).

A drop of 3,5-dideuterioboracycle d_2 -**3** was dissolved in CD_2Cl_2 , and a drop of pyridine was added to it. The $^1\text{H NMR}$ of the product shows no ^1H at the meta position of the borabenzene ring. $^1\text{H NMR}$ (300 MHz): δ 9.05 (d; $J = 5.3$; 1H), 8.09 (tt; $J = 7.7, 1.5$; 1H), 7.76 (t; $J = 7.2$; 2H), 6.67 (s; 2H), 6.57 (s; 1H). $^2\text{H NMR}$ (46 MHz; CH_2Cl_2): δ 7.28 (s); $^{11}\text{B NMR}$: δ +33.0.

Synthesis of Borabenzene-Lutidine (4b).

Lutidine (140 μL , 1.2 mmol) was added dropwise to a solution of boracycle **3** (204 mg, 1.09 mmol) in 2.4 mL of hexane, resulting in the immediate precipitation of a yellow solid. The crystalline solid was collected, washed several times with hexane, and then dried, affording 160 mg (80%) of borabenzene-lutidine. $^1\text{H NMR}$ (300 MHz; CDCl_3): δ 7.89 (t; $J = 7.8$; 1H), 7.53 (t; $J = 8.5$; 2H), 7.43 (d; $J = 8.0$; 2H), 6.60 (td; $J = 6.8, 1.0$; 1H), 6.18 (dd; $J = 9.5, 1.0$; 2H), 2.65 (s; 6H). $^{13}\text{C NMR}$ (75 MHz; CDCl_3): δ 156.7, 140.4, 134.7, 124.3, 118.5 (br), 113.9, 25.9. $^{11}\text{B NMR}$ (96 MHz; CDCl_3): δ +33.4. **IR** (KBr

³⁵ Subsequent experiments showed that the pure product precipitates after stirring the reaction mixture overnight.

³⁶ Boese, R.; Finke, N.; Henkelmann, J.; Maier, G.; Paetzold, P.; Reisenauer, H. P.; Schmid, G. *Chem. Ber.* **1985**, *118*, 1644-1654.

pellet): 3058, 3004, 2979, 2918, 1618, 1533, 1480, 1412, 1376, 1286, 1147, 1054, 959, 792, 714. **HRMS** Calcd for $C_{12}H_{14}BN$: 183.1219. Found: 183.1218. mp: 162-164 °C. **Anal.** Calcd for $C_{12}H_{14}BN$: C, 78.73; H, 7.71. Found: C, 78.57; H, 7.93.

Synthesis of Borabenzene-Triethylamine (4c).

Triethylamine (174 μ L, 1.25 mmol) was added in a stream to a solution of boracycle **3** (208 mg, 1.13 mmol) in 2.4 mL of heptane, resulting in the precipitation of a white solid. After stirring for 5 min, the supernatant was decanted, and the solids were washed with heptane. Additional white solid precipitated from the heptane. The solids were combined and dried, affording 183 mg (92%) of borabenzene-triethylamine. **1H NMR** (300 MHz; C_6D_6): δ 8.03 (br t; J = 8.7; 2H), 7.13 (t; J = 7.3; 1H), 6.45 (d; J = 10.2; 2H), 2.55 (q; J = 7.2; 6H), 0.51 (t; J = 6.9; 9H). **^{13}C NMR** (75 MHz; C_6D_6): δ 135.3, 116.5 (br), 114.7, 50.2, 8.0. **^{11}B NMR** (96 MHz; C_6D_6): δ +34.0. **IR** ($CDCl_3$): 3013, 2989, 2943, 1537, 1421, 1008, 938. **EIMS**: 177, 162, 148, 134, 86, 77. **mp**: 86-88 °C. **Anal.** Calcd for $C_{11}H_{20}BN$: C, 74.60; H, 11.38. Found: C, 74.71; H, 11.53. **HRMS**: Calcd for $C_{11}H_{20}BN$: 177.1689. Found: 177.1688.

Synthesis of Borabenzene-Trimethylamine (4d).

Trimethylamine was bubbled through a solution of boracycle **3** (612 mg, 3.33 mmol) in 5 mL of CH_2Cl_2 until the resulting exotherm subsided. Hexanes (~5 mL) were added, and the solvent was evaporated to yield a white/colorless crystalline solid, a sample of which was used for the X-ray diffraction experiment. This solid was washed with hexanes three times and dried (348 mg; 77%). **1H NMR** (300 MHz; C_6D_6): δ 7.95 (br m; 2H), 7.11 (t; J = 7.0; 1H), 6.43 (d; J = 9.9; 2H), 1.97 (s; 9H). **^{13}C NMR** (125 MHz; C_6D_6): δ 135.3, 115.4, 114.0 (br), 52.9. **^{11}B NMR** (96 MHz; C_6D_6): δ +35.8. **IR** (KBr pellet): 3012, 2943, 2696, 1536, 1482, 1461, 1420, 1291, 1154, 1111, 1017, 973, 844, 713, 507. **HRMS** calcd for $C_8H_{13}BN$: 135.1219; found: 135.1219. The X-ray structure of this complex is in Appendix II.

Synthesis of Borabenzene-Trimethylphosphine (4e).

PMe_3 (773 μ L, 15.0 mmol) was added dropwise by pipette to a solution of boracycle **3** (1.37 g, 7.47 mmol) in hexane (15 mL), resulting in an exotherm and the precipitation of a white solid (this initial precipitate is betaine **7**). The reaction was stirred for 11 h, during which time additional white solid precipitated from the reaction mixture. The solution was decanted, and the remaining solids were washed twice with hexane, then dried, providing 1.04 g (92%) of borabenzene-

trimethylphosphine. ^1H NMR (300 MHz; C_6D_6): δ 8.05 (br s; 2H), 7.42 (br t; $J = 8.0$; 1H), 7.23 (br t; $J = 8.0$; 2H), 0.64 (d; $J_{\text{P-H}} = 9.0$; 9H). ^{13}C NMR (75 MHz; C_6D_6): δ 133.6 (d; $J_{\text{C-P}} = 17.5$), 128 (br), 120.7, 10.6 (d; $J_{\text{C-P}} = 42.0$). ^{11}B NMR (96 MHz; C_6D_6): δ +20.8 (d; $J_{\text{B-P}} = 110.0$). ^{31}P NMR (121 MHz; C_6D_6 ; referenced to PPh_3 in C_6D_6 at δ -5.95): δ -16.4 (q; $J_{\text{P-B}} = 102.6$). IR (KBr pellet): 3059, 3006, 2982, 2908, 1528, 1420, 1411, 1289, 1152, 1022, 951, 860, 762, 703; EIMS: 152, 109, 91, 76, 61. mp. 135-139 °C. Anal. Calcd for $\text{C}_8\text{H}_{14}\text{BP}$: C, 63.22; H, 9.28. Found: C, 63.05; H, 9.26. HRMS calcd for $\text{C}_8\text{H}_{14}\text{BP}$: 152.0927; found: 152.0926. The X-ray structure of this complex is in Appendix II.

Large-Scale Preparation of Borabenzene-Trimethylphosphine³⁷ (4e).

Inside the glovebox, boracycle **3** (7.23 grams, 39.4 mmol) was covered with 70 mL of toluene inside a 250 mL three-neck round-bottom flask equipped with a magnetic stirrer. Simultaneously, trimethylphosphine (3.00 grams, 4.08 mL, 39.4 mmol) was covered with 10 mL of toluene in a separate Schlenk flask. After attaching both flasks to the double manifold, the boracycle was cooled with a dry-ice/acetonitrile bath (-42 °C) before adding the trimethylphosphine in a slow stream. After a brief initial smoke evolution, a clear and colorless solution was obtained. After removal of the bath, the solution appeared to freeze as solids precipitated, although the stirbar still spun effortlessly. The solids dissolved between 0 °C and room temperature, and the reaction mixture was stirred overnight. The next morning a yellowish solution with suspended white solids was found. After removal of between 1/4 and 1/2 of the solvent, the flask was taken into the glove box, and the solution was filtered, yielding 3.2 grams (53%) of borabenzene trimethylphosphine, mp. 136-138 °C. Anal. Found, C: 63.31; H: 9.52. A second crop of pure (^1H NMR) material was also obtained, 1.1 grams (18%), for a total yield of 4.3 grams (72%).

Synthesis of Borabenzene-(*t*-Butylisocyanide) (4f).

t-Butylisocyanide³⁸ (61 mg, 0.73 mmol) was added dropwise to a solution of boracycle **3**³⁹ (134 mg, 0.730 mmol) in 3.5 mL of benzene. The solution was stirred for 3 h, after which time the volatiles were removed in vacuo, leaving a brown solid. The solid was washed three times with pentane and dried, affording 101 mg

³⁷ This experiment was performed in collaboration with Adam Littke.

³⁸ For the product of this reaction to precipitate out, the freshly purchased isocyanide must be distilled and stored at -35 °C.

³⁹ For the preparation of this compound to be successful, the boracycle **3** must be extremely pure, or the product will oil out of solution.

(87%) of **4f**, a light brown solid. $^1\text{H NMR}$ (300 MHz; C_6D_6): δ 8.01 (app d; $J = 3.6$; 4H), 7.48 (app quintet; $J = 4.3$; 1H), 0.58 (s; 9H). $^{13}\text{C NMR}$ (75 MHz; C_6D_6): δ 138.0 (br q; $J_{\text{C-B}} = 71.2$), 133.8, 123.3, 59.0 (t; $J_{\text{C-N}} = 4.6$), 28.6. $^{11}\text{B NMR}$ (96 MHz; C_6D_6): δ +11.9. IR (CD_2Cl_2): 3340, 3122, 3011, 2992, 2302, 2233, 2197, 1750, 1388. EIMS 159, 103, 76, 57. mp. 80-82 °C. Anal. Calcd for $\text{C}_{10}\text{H}_{14}\text{BN}$: C, 75.52; H, 8.87. Found: C, 75.25; H, 8.61. HRMS calcd for $\text{C}_{10}\text{H}_{14}\text{BN}$: 159.1219; found: 159.1222. The X-ray structure of this complex is in Appendix II.

Synthesis of Conjugated Boracycle 6.

A solution of 918 mg of boracycle **3** in ~3.5 mL of heptane was refluxed for ~30 hours, after which ^1H and ^{11}B NMR showed that the reaction was complete. Distillation of the product afforded 308 mg (33.5%) of product, slightly contaminated with heptane. $^1\text{H NMR}$ (300 MHz; C_6D_6): δ 7.19 (br; 1H), 6.63 (br; 1H), 6.47 (br; 1H), 6.20 (t; $J = 7.4$; 1H), 3.36 (br; 1H), -0.06 (s; 9H). $^{11}\text{B NMR}$ (96 MHz; C_6D_6): δ +56.4.

Synthesis of 3,5-Dideuterioisomerized Boracycle d_2 -6.

3,5-Dideuterioboracycle d_2 -**3** (20 μL) was dissolved in 480 μL of toluene- d_8 , and heated to 100 °C. The reaction was monitored by ^1H NMR. $^1\text{H NMR}$ (300 MHz; C_6D_6): δ 6.65 (br s; 1H), 6.20 (s; 1H), 3.35 (br s; 1H), -0.10 (s; 1H); $^2\text{H NMR}$ (46 MHz; C_6H_6): δ 8.5 (m), 4 (br).

Synthesis of Betaine 7.

Trimethylphosphine (362 μL , 3.50 mmol) was added quickly to a solution of chloroboracycle **3** (642 mg, 3.50 mmol) in 7 mL of hexane. A white powder formed immediately. After 4 hours, the reaction mixture was filtered, and the collected solids weighed (454 mg). They consisted of a mixture of BB- PMe_3 (**4e**, 20%) and betaine **7**, 80%. $^1\text{H NMR}$ (300 MHz; C_6D_6): δ 6.80 (br; 1H), 6.28 (br d.; $J = 11.2$ Hz; 1H), 6.13 (dt; $J_1 = 12.0$, 1.6 Hz; 1H), 2.70 (v br; 2H), 0.56 (d; $J = 10.2$ Hz; 9H), 0.41 (s; 9H). $^{11}\text{B NMR}$ (96 MHz; C_6D_6): δ -7.4 (br s). $^{31}\text{P NMR}$ (122 MHz; C_6D_6): δ -7.5 (br).

Study of the Kinetics of Ligand Exchange.⁴⁰

A stock solution of BB- PMe_3 (**4e**) in C_6D_6 (distilled from sodium/benzophenone prior to use) was prepared. The probe of the NMR spectrometer was warmed to the required temperature, to then be tuned and shimmed with a measured amount of

⁴⁰ NOTE: This is a standard procedure.

the stock solution. A ^1H NMR spectrum of this stock solution was then obtained to serve as an initial data point, as well as an indication of the purity of the starting borabenzene- PMe_3 . In the glove box, $\text{P}(\text{CD}_3)_3$ was added via a microliter syringe to the NMR tube, which was inserted into the probe of the spectrometer as quickly as possible. The data points were collected at regular intervals using an array. The relative concentrations were determined by computing the ratios

$$\frac{\{\text{BB} - \text{PMe}_3\}}{\{\text{BB} - \text{PMe}_3\} + \{\text{PMe}_3\}}$$

$$\frac{\{\text{PMe}_3\}}{\{\text{BB} - \text{PMe}_3\} + \{\text{PMe}_3\}}$$

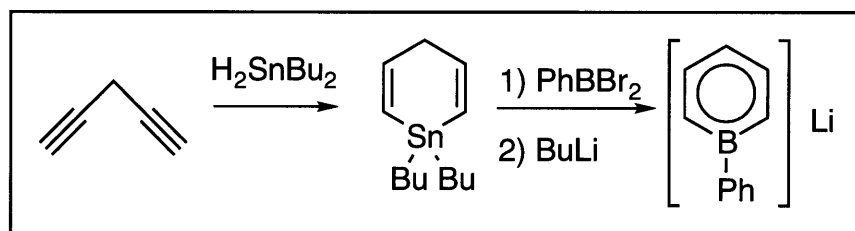
where $\{\text{BB} - \text{PMe}_3\}$ is the ^1H NMR integration of the PMe_3 that is bound to borabenzene and $\{\text{PMe}_3\}$ is the integration of free PMe_3 . The rate constants were determined by entering the data into the program Cricket Graph and plotting the appropriate equations⁴¹ for each mechanism under consideration. Error analysis was performed in the usual fashion.⁴²

⁴¹ Derived following: Castellan, G. W. *Physical Chemistry*, 3rd ed.; Benjamin/Cummings: Menlo Park, 1983; Chapters 32 and 33.

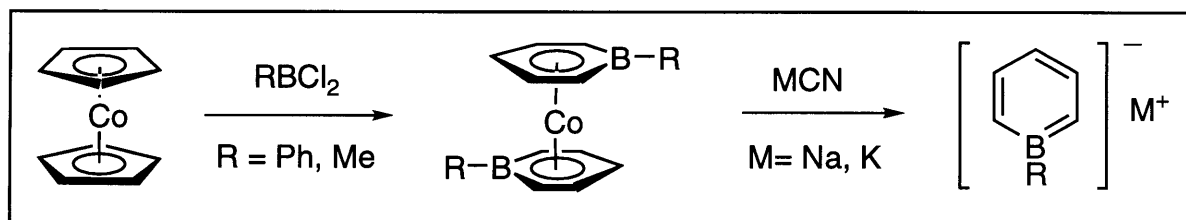
⁴² Shoemaker, D. P.; Garland, C. W.; Nibler, J. W. *Experiments in Physical Chemistry*, 5th ed.; McGraw-Hill: New York, 1989; Chapter 2.

Chapter 3: Synthesis and Structure of Alkali Metal Boratabenzenes.

Unlike borabenzenes, for which only one synthetic route was available prior to our work, several syntheses of boratabenzenes had been reported, but they all have drawbacks. The first two syntheses (Schemes 3.1¹ and 3.2²), while short, were limited in scope to methyl- and phenyl-substituted boratabenzenes.³ The approach outlined in Scheme 3.1 is also limited by the fact that the starting diyne is not commercially available and is synthesized in low yield.⁴



Scheme 3.1.



Scheme 3.2.

The third approach (Scheme 3.3) in which the boron-for-tin transmetallation is effected with BBr_3 , is limited by virtue of beginning with the same diyne as in Scheme 3.1.

Recently, a new synthesis of boratabenzenes (Scheme 3.4) has been reported by the Herberich group. It can be carried out on a large scale (about 40 grams), but

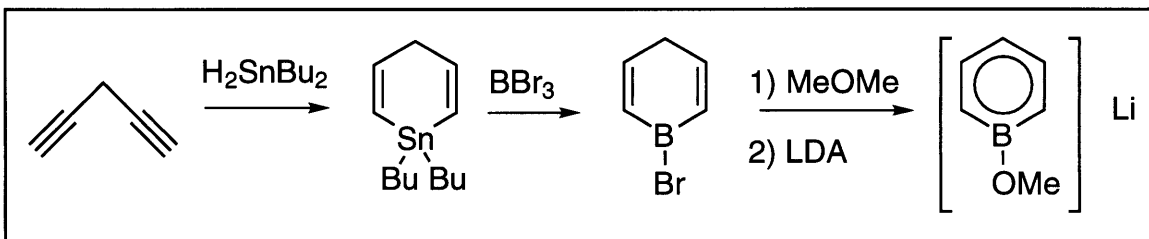
¹ Ashe, A. J., III; Shu, P. *J. Am. Chem. Soc.* **1971**, *93*, 1804-1805.

² Herberich, G. E.; Becker, H. J.; Carsten, K.; Engelke, C.; Koch, W. *Chem. Ber.* **1976**, *109*, 2382-2388.

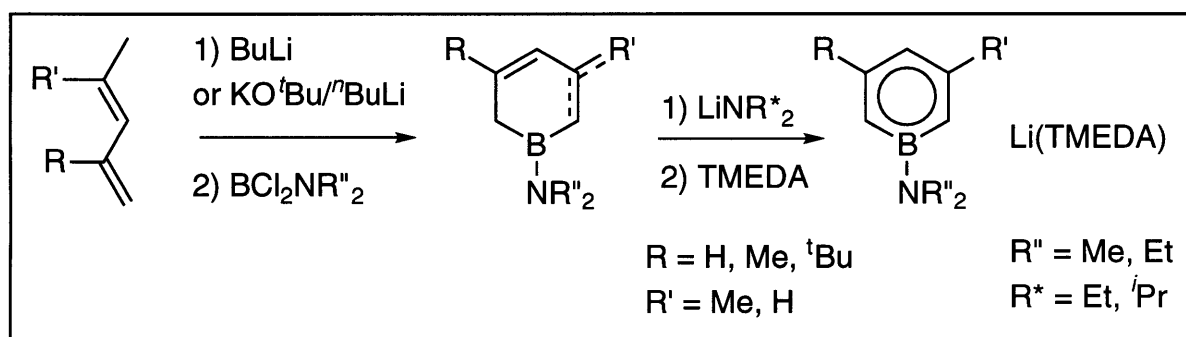
³ There is only one report in which this route has been used to prepare other boratabenzenes, by the reaction between cobaltocene and BCl_3 to afford bis(1-chloroboratabenzene)cobalt: Herberich, G. E.; Greiss, G.; Heil, H. F.; Muller, J. *J. Chem. Soc., Chem. Commun.* **1971**, 1328-1329.

⁴ For its preparation, see: a) Ben-Efraim, D. A.; Sondheimer, F.; *Tetrahedron* **1969**, *25*, 2823-2835. b) Verkrujisse, H. D.; Hasselaar, M. *Synthesis* **1979**, 292-293.

remains limited to methyl-, alkoxide-, and amide- substituted boratabenzenes.⁵ This route is the only one that can be adapted to the preparation of meta-substituted boratabenzenes.⁶



Scheme 3.3.



Scheme 3.4.

Because boratabenzenes have found wider application than borabenzenes,⁷ we decided to invest time exploring the reaction of neutral borabenzenes with alkali-metal salts of anionic nucleophiles. As shown in the previous chapter, neutral ligands that are bound to borabenzene can undergo nucleophilic substitution with other Lewis bases. We were interested in exploring the possibility that an anionic nucleophile might displace the neutral Lewis base from boron, leading to the formation of an alkali metal boratabenzene. In this chapter we describe how this strategy results in formation of the desired boratabenzenes (Scheme 3.5).⁸ We also discuss some structural studies we performed on the alkali metal boratabenzene

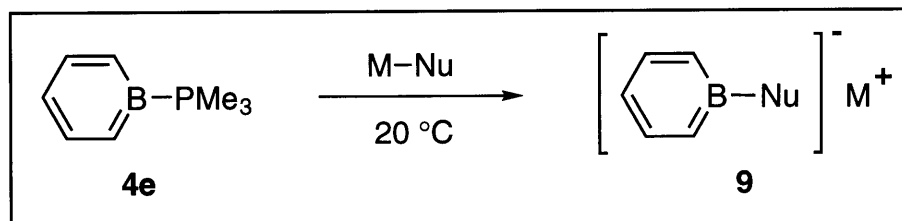
⁵ Herberich, G. E.; Schmidt, B.; Englert, U. *Organometallics* **1995**, *14*, 471-480.

⁶ Herberich, G. E.; Schmidt, M. U.; Standt, R. *Organometallics* **1996**, *15*, 2707-2712.

⁷ For a review of boratabenzene chemistry, see: Herberich, G. E.; Ohst, H. *Adv. Organomet. Chem.* **1986**, *25*, 199-236.

⁸ This work has appeared in print: Qiao, S.; Hoic, D. A.; Fu, G. C. *J. Am. Chem. Soc.* **1996**, *118*, 6329-6330.

complexes thus prepared.



Scheme 3.5.

The main advantage of our synthesis (Scheme 3.5) over the other existing syntheses of boratabenzenes is that it allows the preparation of compounds with varied substitution at boron in high yield and from a single precursor, as illustrated in Table 3.1.⁹ In fact, boratabenzenes bearing hydride, acetylide, dialkylamide, diarylamide, alkoxide, diarylphosphide, and cyanide substituents can be prepared.¹⁰ Tweddell has adapted this procedure to the synthesis of ortho-substituted boratabenzenes.¹¹

The use of good nucleophiles is required for the success of this reaction, indicating that the bimolecular nucleophilic aromatic substitution (S_NAr₂)¹² shown in Scheme 3.2 is the most likely mechanism for this transformation. For example, while treatment of BB-PMe₃ (**4e**) with LiNMe₂ cleanly and instantaneously afforded Li(BB-NMe₂), the reaction with LiN(*i*-Pr)₂ (LDA) in THF-d₈ is not clean (Scheme 3.6). Further support for an associative pathway, as well as the exclusion of other plausible mechanisms, came in the form of a combination of kinetics and labelling studies, employing BB-PMe₃ and lithium (2-trimethylsilylacetylide) performed by

⁹ These compounds need not be isolated prior to use. After preparation of the boratabenzene, one only needs to evaporate the volatiles to remove the PMe₃ that is released. The resulting boratabenzene can be redissolved in THF for further use. In this way, we have also prepared Li(BB-CN), Li(BB-SMe), and Li(BB-SPh), which are difficult to isolate; all these reactions must be heated to reflux in THF in order to proceed at an appreciable rate.

¹⁰ We have been informed that the Bazan group has succeeded in adding phenyllithium to the list of alkali metal nucleophiles. Bazan, G. C., personal communication to G. C. Fu.

¹¹ a) Tweddell, J. M.S. Thesis, MIT, 1997. b) Tweddell, J.; Hoic, D. A.; Fu, G. C. *J. Org. Chem.* **1997**, *62*, 8286-8287.

¹² March, J. *Advanced Organic Chemistry*, 4th ed.; Wiley: New York, 1992; Chapter 13.

Shuang Qiao.¹³

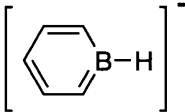
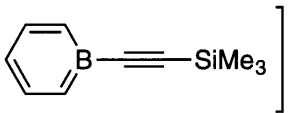
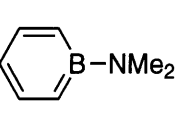
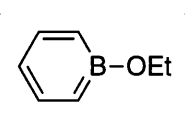
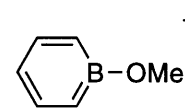
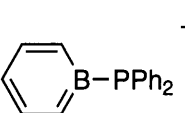
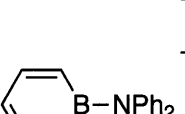

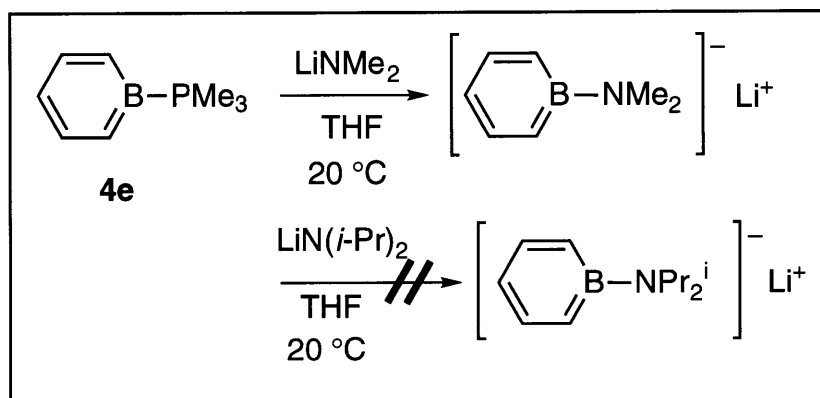
Nucleophile	Product	Yield (%)	Cpd. Nbr.
LiAlH ₄	Li ⁺ 	71	9a
Li—C≡SiMe ₃	Li ⁺ 	68	9b
Li—NMe ₂	Li ⁺ 	78	9c
Na—OEt	Na ⁺ 	78	9d
Na—OMe	Na ⁺ 	77	9e
K—PPh ₂	K ⁺ 	91	9f
K—NPh ₂	K ⁺ 	46	9g
Bu ₄ N ⁺ CN ⁻	Bu ₄ N ⁺ 	100 (NMR yield)	9h

Table 3.1. Synthesis of Boratabenzenes from Borabenzene-PMe₃ (4e).

The choice of starting borabenzene complex was based on the fact that we had a

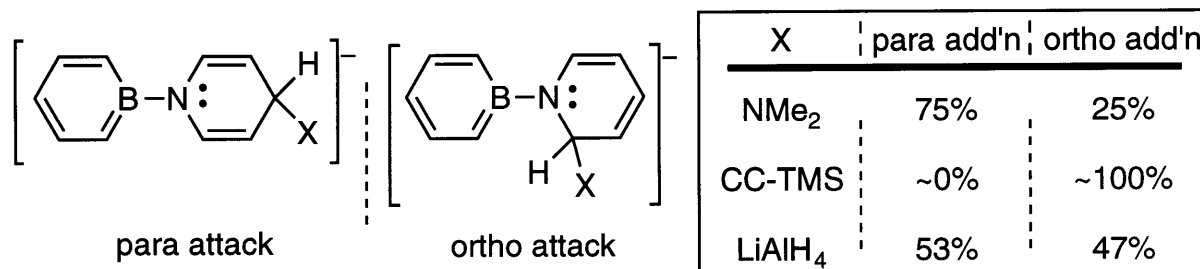
¹³ The author is responsible for all the synthetic work described in this chapter, as well as for the initial experiments comparing the reactivity of LDA and LiNMe₂. The detailed studies on the mechanism of this reaction were performed by Shuang Qiao.

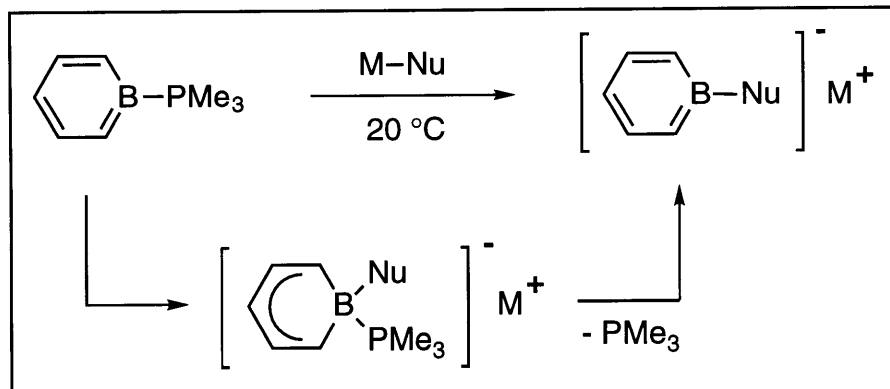
large quantity of BB-PMe₃ (**4e**) on hand, but very little of any other borabenzenes. Afterwards, we came to realize that this choice had been extremely fortuitous. BB-NEt₃ (**4c**) reacts cleanly with LiAlH₄ to form Li(BBH) (**4a**), but, unfortunately, the similarity between its reactivity and that of BB-PMe₃ (**4e**) stops there: reaction of BB-NEt₃ (**4c**) with LiNMe₂ results in formation of Li(BB-NEt₂), instead of the desired Li(BB-NMe₂) (**9c**, of which only a trace is present). Reaction of BB-py (**4a**) with LiNMe₂, Li-CC-TMS, or LiAlH₄ resulted in the formation of multiple products, presumably because of the existence of three electrophilic sites on the starting material.¹⁴ Therefore, from this point on, the alkali metal boratabenzene complexes were prepared from BB-PMe₃ (**4e**).



Scheme 3.6.

¹⁴ Besides boron, there are two electrophilic sites on the pyridine ring, the ortho and para positions. If steric and electronic effects combine to give sites of equal effective electrophilicity (i.e., a statistical mixture) one would expect a 2:1 ratio of addition for ortho:para. Hard nucleophiles add to the pyridine ring, in the ratios shown in the table below. The products of the reaction between BB-py and LiAlH₄ were assigned by a ¹H NMR decoupling experiment (The help of Dr. Rosa López Alvarez in this experiment is gratefully acknowledged). The remaining products were assigned by analogy.





Scheme 3.7.

Alkali metal cyclopentadienides have long been used as precursors to transition metal complexes of η^5 -cyclopentadienide.¹⁵ Nevertheless, an understanding of their structure and its relationship to their reactivity had been prevented by their tendency to precipitate as powders, rather than to form single crystals. Only over the last 15-20 years did researchers start using coordinating bases such as THF and TMEDA, instead of aromatic hydrocarbons, to obtain single crystals, allowing the routine crystallization of MCp derivatives and sparking intense research in the area. Structures of lithium salts of the parent $(\text{C}_5\text{H}_5)^-$, reported in the past few years, show that cyclopentadienide can crystallize to form rodlike polymers,¹⁶ piano-stool complexes,¹⁷ and triple-decker complexes.¹⁸ Finally, in 1994 Harder and Prosenc published the first structural study of the sandwiched lithocene anion, $[\text{Cp}_2\text{Li}]^-$, the simplest metallocene.¹⁹

Boratabenzenes are often touted as surrogates for Cp, with different electronic properties and the advantage of easier tunability.²⁰ Therefore, a structural comparison of boratabenzene-transfer agents to cyclopentadienide-transfer agents is of interest. Although the crystal structure of the boratanaphthalene complex **10** was

¹⁵ For example, see Elschenbroich, C.; Salzer, A. *Organometallics* 2nd ed.; VCH: Weinheim, 1992; Chapter 15.4.

¹⁶ Evans, W. J.; Boyle, T. J.; Ziller, J. W. *Organometallics* **1992**, *11*, 3903-3907.

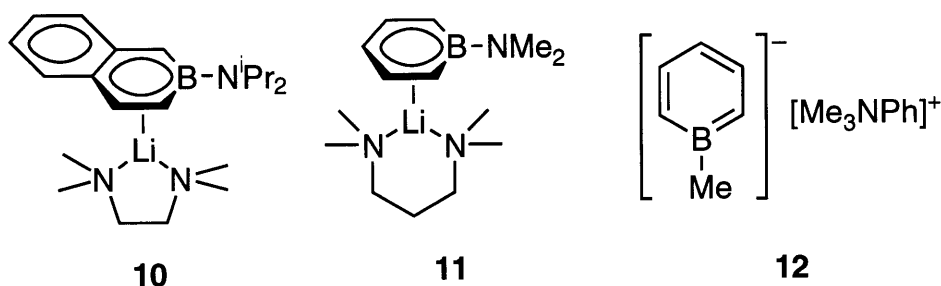
¹⁷ Chen, H.; Jutzi, P.; Leffers, W.; Olmstead, M. M.; Power, P. P. *Organometallics* **1991**, *10*, 1282-1286.

¹⁸ Stults, S. D.; Andersen, R. A.; Zalkin, A. *J. Am. Chem. Soc.* **1989**, *111*, 4507-4508.

¹⁹ Harder, S.; Prosenc, M. H., *Angew. Chem., Int. Ed. Eng.* **1994**, *33*, 1744-1746.

²⁰ See, for example, Barnhart, R. W.; Bazan, G. C.; Mourey, T. J. *Am. Chem. Soc.* **1998**, *120*, 1082-1083.

published as early as 1986,²¹ it was not until 1993 that the first crystal structure of an alkali metal boratabenzene complex was published,²² in the form of the piano-stool **11**, structurally related to **10**. Prior to our work, the only other known crystal structure of a boratabenzene salt not coordinated to a transition metal was that of the naked boratabenzene **12**, reported by Herberich.²³



We determined the crystal structure of several alkali-metal boratabenzenes, and through these studies we showed that alkali metal boratabenzenes can exhibit the same varied structural motifs as cyclopentadienides. For example, lithium (1-*H*-boratabenzene) crystallizes out of cold THF/toluene/hexane to form a metallocene anion (Figure 3.1). This structure will be discussed in more detail in Chapter 5.

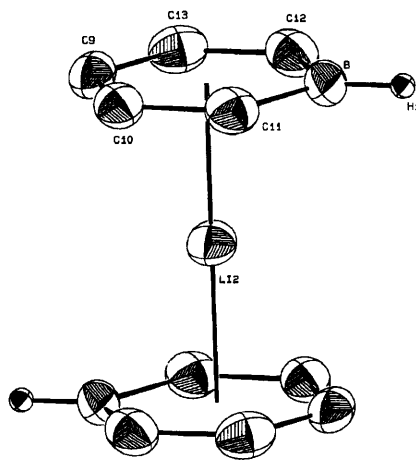


Figure 3.1. The Metallocene Anion [(BBH)₂Li]⁻. [Li(THF)₄]⁺ was omitted for clarity.

²¹ Paetzold, P.; Finke, N.; Wennek, P.; Schmid, G.; Boese, R. *Z. Naturforsch., B* **1986**, *41*, 167-174.

²² Herberich G. E.; Schmidt, B.; Englert, U.; Wagner, T. *Organometallics* **1993**, *12*, 2891-2893.

²³ Herberich, G. E.; Schmidt, B.; Englert, U. *Organometallics* **1995**, *14*, 471-480.

Potassium diphenylphosphidoboratabenzene (K-DPB), the subject of Chapter 6, crystallizes out of cold THF/Et₂O as a rod-like polymer (Figure 3.2). As will be discussed in Chapter 6, the aggregation of the polymer can be broken up by addition of a crown ether or a cryptand to form a piano-stool complex or a separated ion pair (i.e., a naked DPB anion), respectively. The structures depicted in Figures 3.1 and 3.2 will be discussed further in Chapter 6.

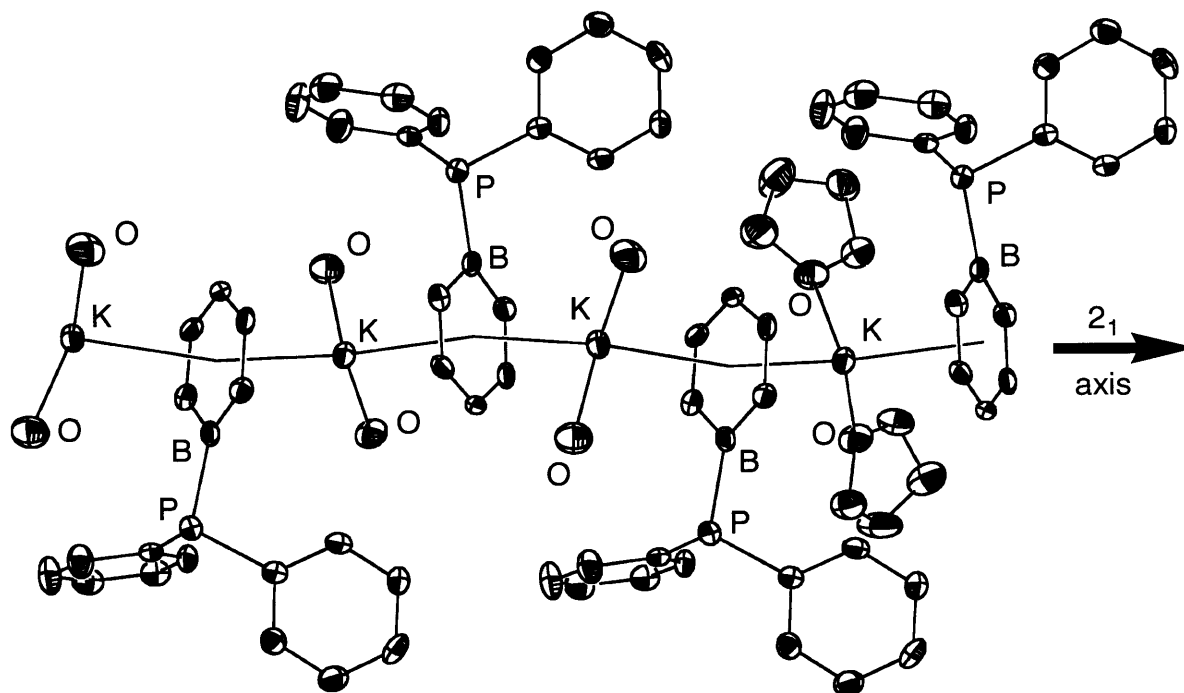


Figure 3.2. The Crystal Structure of $[(\text{DPB})\text{K}(\text{THF})_2]_n$, Four Monomers (Asymmetric Units) Shown. 24 THF carbons were omitted for clarity.

Our studies show that alkali metal boratabenzenes do exhibit the same structural motifs as alkali metal cyclopentadienides. However, the boron substituent on a boratabenzene can by itself add variety to the array of possible solid state structures. For example, the exo diphenylphosphido is essential in the weaving of the polymeric structure in the sheet-polymer $[\text{K}(\text{DPB}) \cdot \text{BH}_3]_n$ (13, Figure 3.3).

Also, in the case of $[\text{Li}(\text{BB-CN}) \cdot (12\text{-crown-4})]$, the boratabenzene ring is not π bound to the lithium, but rather the lithium(crown) fragment is coordinated via a σ bond from the lone pair on the nitrile (Figure 3.4). Until we performed the work described in this thesis, there had been no reports in the borabenzene literature of a

boron substituent serving as a Lewis-base. We have since encountered other examples where the boron substituent interacts with electrophiles, which are described in Chapters 4 and 6.

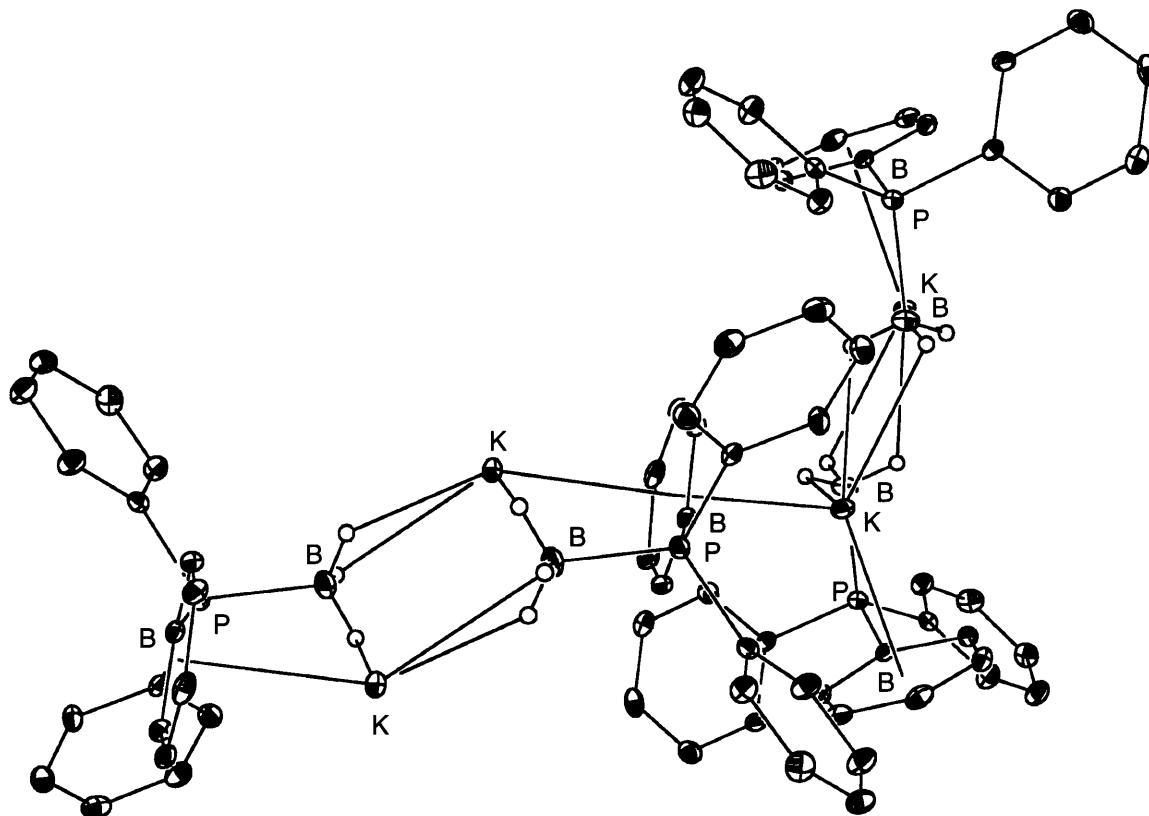


Figure 3.3. The Sheet-Polymer $[K(DPB) \cdot BH_3]$, 13.

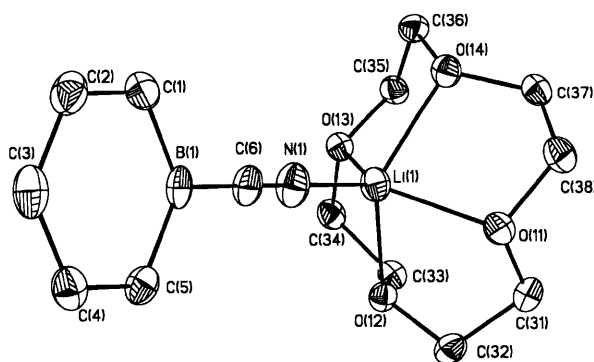


Figure 3.4. $(BB-CN)Li(12\text{-crown-}4)$, with a Bond Between the Lithium and the Boron Substituent.

Using nucleophilic additions we tried, unsuccessfully, to synthesize a compound

bearing a transition metal bound to boron.²⁴ A number of common transition-metal anions were employed, with BB-PMe₃ or BB-py as the borabenzene source. The metal anions included [MnL₂(CO)₃]⁻ (L = CO, PPh₃, or PMe₃), [Fe₂(CO)₄]²⁻, and [Fe(CO)₂Cp]⁻ (Fp⁻).²⁵

Conclusions:

Borabenzene-trimethylphosphine serves as a good precursor for the synthesis of alkali metal boratabenzenes with varied substitution at boron, via a nucleophilic displacement of PMe₃ by a hard nucleophile. These complexes exhibit similar structural motifs to those exhibited by cyclopentadienides. Their reactivity, as well as a more in-depth study of BBH and DPB, will be presented in the following chapters.

²⁴ Nöth, H. Schmidt, M. *Angew. Chem., Int. Ed. Engl.* **1996**, *35*, 292-293.

²⁵ Reaction of NaFp with BB-py in THF-d₈ at room temperature led to the formation of Fp₂, as well as multiple borabenzene-containing products (¹H NMR), while heating NaFp with BB-PMe₃ in THF-d₈ to 90 °C (sealed tube) resulted in no reaction. These observations suggest that the reduction potential of the bicyclic BB-py is lower, while the reduction potential of BB-PMe₃ is higher, than the oxidation potential of NaFp (known to be -1.2 eV in THF: Miholová, D.; Vlcek, A. A. *Inorg. Chim. Acta* **1980**, *41*, 119-122).

Experimental Section.

General.

The general experimental section from Chapter 2 applies. LiNMe₂ was purchased from Strem, while NaOEt, NaOMe, KPh₂ (0.5 M in THF), and Bu₄NCN were purchased from Aldrich and used as received. LiAlH₄ was purchased from Aldrich and purified by dissolving in ether, filtering through an Acrodisc, and drying. Li-CC-TMS could be used from commercial sources (0.5 M in THF; Aldrich), but the purification of the boratabenzene is greatly simplified if freshly prepared (H-CC-TMS + lithium hydride in hexane) Li-CC-TMS is used instead.

Synthesis of Li(BBH) (9a).²⁶

A solution of borabenzene-PMe₃ (370 mg, 2.43 mmol) in 10 mL of THF was added to a solution of LiAlH₄ (92.4 mg, 2.43 mmol) in 2 mL of THF. After stirring for 5 hours at room temperature, ~5 mL of THF were removed in vacuo. Toluene (~5 mL) was added, resulting in the formation of an amorphous white precipitate, which was removed by filtration. Further evaporation of ~3 mL of solvent resulted in the precipitation of additional amorphous white solids, which were also removed by filtration. Hexane was then added to the resulting yellow solution. Cooling to -35 °C overnight yielded colorless crystals, which were washed with cold toluene/hexane (1 : 2) three times and dried for 24 hours, yielding 146 mg (71%) of lithium boratabenzene as a white powder. Recrystallization of the mother liquor yielded two additional crops of crystals, each of which was somewhat impure. ¹H NMR (300 MHz; THF-d₈): δ 7.19 (dd; J = 8.8, 7.4; 2H), 6.57 (ddt; J = 10.2, 4.8, 1.4; 2H), 6.21 (td; J = 7.1, 1.4; 1H), 5.5-4.0 (br; 1H). ¹³C NMR (75 MHz; THF-d₈): δ 133.3, 128.2 (br), 111.8. ¹¹B NMR (96 MHz; THF-d₈): δ +32. IR (KBr pellet): 3009, 2992, 2497, 1404, 916, 827, 722, 630. The X-ray structure of this complex is in Appendix II.

NMR yield of Li(BBH) (9a).

Borabenzene-PMe₃ (23 mg, 0.15 mmol) was dissolved in ~0.5 mL of THF-d₈. Toluene (16 μL, 0.15 mmol) was added to the solution, and a ¹H NMR spectrum obtained. The NMR tube was taken into the glove box and its contents emptied into a vial containing LiAlH₄ (5.6 mg, 0.15 mmol), and the solution thus formed was stirred for 4.5 hours. The ensuing solution was pipetted into an NMR tube and a ¹H

²⁶ Hoic, D. A.; Davis, W. M.; Fu, G. C. *J. Am. Chem. Soc.* **1995**, *117*, 8480-8481.

NMR spectrum obtained. Integration of two different resonances versus the toluene standard and comparison with the initial spectrum indicated that the reaction had proceeded in 95 and 97% yields.

Synthesis of Li(BB-CCSiMe₃) (9b).

A solution of lithium trimethylsilylacetylide (42.6 mg, 0.409 mmol) in 1 mL of Et₂O was added to borabenzene-PMe₃ (62.1 mg, 0.409 mmol). The reaction mixture was stirred for 16 h at room temperature, then concentrated to a yellow oil, which was taken up in benzene and dried to a white solid. Crystallization from Et₂O/toluene provided 50.3 mg (68%) of Li(BB-CCSiMe₃) as white crystals. ¹H NMR (500 MHz; THF-d₈): δ 7.06 (dd; J = 10.0, 7.0; 2H), 6.52 (dd; J = 10.0, 1.2; 2H), 6.13 (tt; J = 7.0, 1.5; 1H), 0.09 (s; 9H). ¹³C NMR (300 MHz; THF-d₈): δ 132.5, 130.4 (br), 112.6, 103.6, 1.4 (J_{C-Si} = 27.2). ¹¹B NMR (96 MHz; THF-d₈): δ +23.3. IR (KBr pellet): 3013, 2959, 2919, 2081, 1420, 1248, 1090, 952, 843, 751. HRMS (EI, *m/e*) calcd for C₁₀H₁₄BLiSi (M⁺): 180.1118; found: 180.1119.

Synthesis of Li(BB-NMe₂) (9c).

A solution of borabenzene-PMe₃ (43.2 mg, 0.284 mmol) in 1.0 mL of THF was added to a solution of LiNMe₂ (14.5 mg, 0.284 mmol) in 2 mL of THF. After stirring for 10 minutes at room temperature, the mixture was filtered and then dried to provide a brown solid, which was washed with benzene, affording 28.0 mg (78%) of a creamy white solid. ¹H NMR (300 MHz; THF-d₈): δ 7.02 (dd; J = 10.8, 7.2; 2H), 5.63 (d; J = 10.8; 2H), 5.48 (t; J = 6.8; 1H), 2.68 (s; 6H). ¹³C NMR (75 MHz; THF-d₈): δ 134.5, 110 (br), 100.1, 39.9. ¹¹B NMR (96 MHz; THF-d₈): δ 31.7. IR (KBr pellet): 3025, 2990, 1425, 1390, 1343, 1243, 679, 588, 550. HRMS (EI, *m/e*) calcd for C₇H₁₁BN (M-Li⁺): 120.0985; found: 120.0982.

Synthesis of Na(BB-OEt) (9d).

A solution of borabenzene-PMe₃ (32.7 mg, 0.215 mmol) in 1 mL of THF was added to sodium ethoxide (13.9 mg, 0.204 mmol). The reaction was stirred vigorously. After four days, ¹¹B NMR showed the reaction to be complete,²⁷ and the resulting product was dried and then washed with benzene, affording 22.9 mg (78%) of the creamy white solid Li(BB-OEt). ¹H NMR (500 MHz; THF-d₈): δ 7.14 (dd; J =

²⁷ Since the reaction mixture is heterogeneous, the time required for the reaction to reach completion can vary significantly.

10.5, 7.0; 2H), 5.67 (m; 3H), 3.77 (q; $J = 6.8$; 2H), 1.18 (t; $J = 7.0$; 3H). ^{13}C NMR (75 MHz; THF- d_8): δ 135.7, 115.5 (br), 104.2, 60.2, 18.6. ^{11}B NMR (96 MHz; THF- d_8): δ +35.2. IR (KBr pellet): 2969, 2888, 1527, 1421, 1197, 1152, 742, 728. HRMS (EI, m/e) calcd for $\text{C}_6\text{H}_9\text{BO}$ (M^+-Na^+): 108.0746; found: 108.0746.

Synthesis of Na(BB-OMe) (9e).

BB-PMe₃ (76.5 mg, 0.503 mmol) was mixed with NaOMe (27.2 mg, 0.503 mmol) in 2 mL of THF. The resulting solution was stirred at reflux in a sealed tube for 12 hours (although 4 hours is usually enough). Solvents were removed in vacuo, and the resulting white solids were thoroughly washed with benzene (3 mL). After filtration, the white solid was dried. (50.3 mg, 77%). ^1H NMR (300 MHz; THF- d_8): δ 7.16 (dd; $J = 9.3, 7.2$; 2H), 5.72 (t, $J = 6.9$; 1H), 5.65 (d; $J = 10.8$; 2H), 3.46 (s; 3H). ^{13}C NMR (125 MHz; THF- d_8): δ 135.6, 110.6 (br), 104.9, 52.7. ^{11}B NMR (96 MHz; THF- d_8): δ +35.7. IR (KBr pellet): 3062, 3018, 2990, 2930, 2897, 2825, 1525, 1498, 1462, 1229, 1143, 1035, 745, 726, 714. HRMS (EI, m/e) calcd for $\text{C}_6\text{H}_9\text{BO}$ ($\text{M}+\text{H}-\text{Na}^+$): 122.0903; found: 122.0902.

Synthesis of K(DPB) (9f).

A solution of potassium diphenylphosphide (0.5 M in THF; 9.8 mL, 4.9 mmol) was added to a solution of BB-PMe₃ (739 mg, 4.87 mmol) in 4 mL of THF. To this solution was added 6 mL of THF, and the solution was cooled to -35 °C. Two batches of white crystals were collected (1.33 g, 91% yield). ^1H NMR (500 MHz; THF- d_8): δ 7.45 (t; $J = 6.8$; 4H), 7.14 (m; 2H), 7.07 (t; $J = 7.3$; 4H), 7.00 (t; $J = 7.3$; 2H), 6.50 (dd; $J = 9.5, 4.0$; 2H), 6.20 (t; $J = 7.0$; 1H). ^{13}C NMR (75 MHz; THF- d_8): δ 146.2 (d, $J_{\text{C-P}} = 16.2$), 135.5 (d, $J_{\text{C-P}} = 15.9$), 133.3 (d, $J_{\text{C-P}} = 8.9$), 130.5 (br), 128.0 ($J_{\text{C-P}} = 6.0$), 125.94, 113.04. ^{11}B NMR (96 MHz; THF- d_8): δ +32.5. ^{31}P NMR (121 MHz; THF- d_8): δ -31.9. IR (KBr pellet): 3062, 3004, 2978, 2860, 1523, 1408, 1053, 738, 722, 696, 488. HRMS (EI, m/e) calcd for $\text{C}_{17}\text{H}_{16}\text{BP}$ ($\text{M}+\text{H}-\text{K}^+$): 262.1083; found: 262.1081. The X-ray structure of this complex is in Appendix II.

Synthesis of K(DAB) (9g).

The preparation was identical to the synthesis of K(DPB) (KNPh₂ was prepared from KH and HNPh₂). K(DAB) was isolated in 46% unoptimized yield. ^1H NMR (300 MHz; THF- d_8): δ 7.14 (dd; $J = 8.4, 1.8$; 4H), 7.02 (m; 6H), 6.70 (t; $J = 6.9$; 2H), 5.99 (d; $J = 9.6$; 2H), 5.72 (t; $J = 7.2$; 1H). ^{13}C NMR (75 MHz; THF- d_8): δ 154.7, 134.7, 128.8, 126.6, 120.2, 118.9 (br), 106.1. ^{11}B NMR (96 MHz; THF- d_8): δ +33.2. IR (KBr pellet): 3012,

1584, 1526, 1488, 1417, 1310, 1242, 1132, 756, 739, 701. **HRMS** (EI) calcd for $C_{17}H_{15}BKN$: 283.0935; found: 283.0933. The X-ray structure of this complex is in Appendix II.

In situ synthesis of $Bu_4N(BB-CN)$ (9h).

$BB-PMe_3$ (42.0 mg, 0.276 mmol) and hexamethylbenzene (11.6 mg, 0.0691 mmol) were dissolved in 0.5 mL of THF- d_8 . This solution was mixed with Bu_4NCN (74.2 mg, 0.276 mmol), and the resulting clear, homogeneous solution was refluxed overnight in a J. Young tube. Comparison of the 1H NMR spectra obtained at the end of the reaction with those taken before the addition of Bu_4NCN showed 102% conversion. **1H NMR** (300 MHz; THF- d_8): δ 7.06 (dd; $J = 10.2, 7.2$; 2H), 6.62 (dd; $J = 10.2, 1.2$; 2H), 6.28 (td; $J = 7.2, 1.2$; 1H), 2.95 (m; 8H), 1.45-2.5 (m; 16 H), 0.95 (m; 12H). **^{13}C NMR** (75 MHz; THF- d_8): δ 133.2, 131.4 (br), 115.9, 59.3, 24.9, 20.7, 14.3. **^{11}B NMR** (96 MHz; THF- d_8): δ +19.3. **IR** (KBr pellet): ν_{CN} : 2168.

Chapter 4: Synthesis, Structure, and Reactivity of π -bound Borabenzenes and Boratabenzenes.

From the time that boratabenzenes were discovered,¹ their potential utility as ligands for transition metals has been recognized.^{2,3,4} Borabenzenes are very interesting ligands because one can vary their donating profile merely by changing the substituent on boron. If a neutral two-electron donor, such as pyridine or trimethylphosphine, is bound to boron, then the borabenzene acts as a *neutral* 6-electron donor (e.g., benzene in (benzene)Cr(CO)₃). If, on the other hand, the ligand on boron is an anionic two-electron donor, such as methyl, hydride, or alkoxide, then the borabenzene (now formally called a boratabenzene) acts as an *anionic* 6-electron donor (e.g., cyclopentadienide in Cp₂Fe). We have complexed a number of borabenzenes and boratabenzenes to chromium and rhodium. In this chapter we discuss their synthesis and the interconversion between (η^6 -boratabenzene)M complexes and (η^6 -borabenzene)M complexes, where M is a transition metal. We also mention unsuccessful attempts to correlate the reactivity of the transition metal with the nature of the substituent on boron.

Reaction of BB-py with (MeCN)₃Cr(CO)₃ had been reported to yield a π -complex in which the Cr is bonded to the borabenzene ring.⁵ We have found that this reaction is not limited to BB-py. Indeed, we have prepared chromium complexes in

¹ Herberich, G. E.; Greiss, G.; Heil, H. F. *Angew. Chem., Int. Ed. Engl.* **1970**, *9*, 805-806.

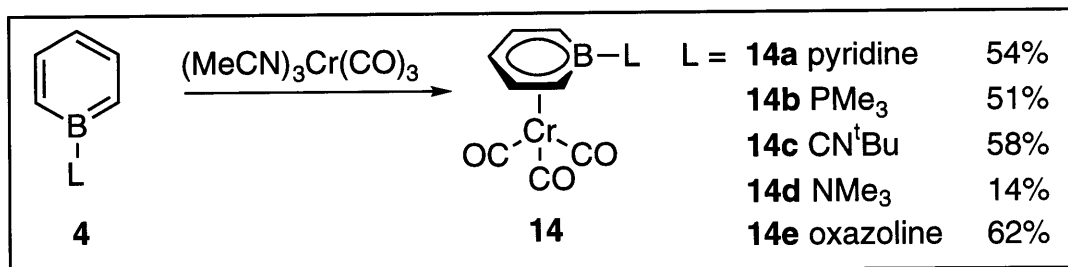
² Catalysis in Ziegler-Natta polymerization: a) Devore, D. D.; Timmers, F. J.; Neithamer, D. R. World Patent WO 97/36937. b) Herberich, G. E.; Schmidt, B.; Schmitz, A.; Fischer, A.; Riedel, M.; Herrmann, H.-F.; Ozdemir, D. World Patent WO 97/23512. c) Krishamurti, R.; Nagy, S.; Etherton, B. P. World Patent WO 96/23004. d) Herberich, G. E. German Patent DE 19549352 A1. e) Barnhart, R. W.; Bazan, G. C.; Mourey, T. J. *Am. Chem. Soc.* **1998**, *120*, 1082-1083. f) Sparry, C. K.; Rodriguez, G.; Bazan, G. C. *J. Organomet. Chem.* **1997**, *548*, 1-8. g) Rogers, J. S.; Bazan, G. C.; Sparry, C. K. *J. Am. Chem. Soc.* **1997**, *119*, 9305-9306. h) Bazan, G. C.; Rodriguez, G.; Ashe, A. J., III; Al-Ahmad, S.; Kampf, J. W. *Organometallics* **1997**, *16*, 2492-2494. i) Bazan, G. C.; Rodriguez, G.; Ashe, A. J., III; Al-Ahmad, S.; Muller, C. *J. Am. Chem. Soc.* **1996**, *118*, 2291-2292.

³ Mediation of zirconium (II) chemistry: Ashe, A. J., III; Al-Ahmad, S.; Kampf, J. W.; Young, V. G., Jr. *Angew. Chem., Int. Ed. Engl.* **1997**, *36*, 2014-2016.

⁴ Catalysis of the cyclotrimerization of alkynes: a) Bonnemann, H. *Angew. Chem., Int. Ed. Engl.* **1985**, *24*, 248-262. b) Bonnemann, H.; Brijoux, W.; Brinkmann, R.; Meurers, W. *Helv. Chim. Acta* **1984**, *67*, 1616-1624.

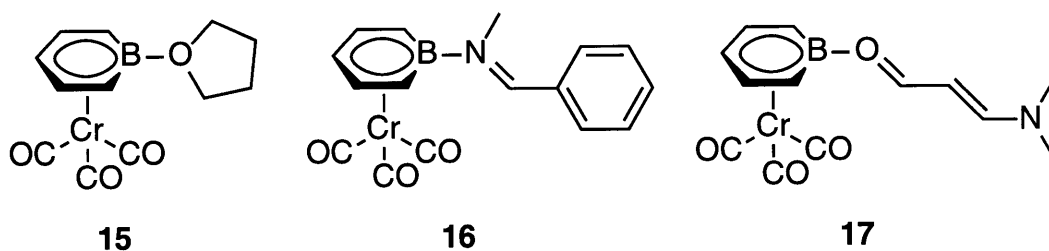
⁵ Boese, R.; Finke, N.; Keil, T.; Paetzold, P.; Schmid, G. *Z. Naturforsch., B* **1985**, *40*, 1327-1332.

which the boron is substituted with phosphine, isocyanide, trialkylamine, and oxazoline⁶ bases.



Scheme 4.1.

These results were further extended in work carried out by Michael Amendola and Dr. Kenneth Stockman, who succeeded in running the borabenzene formation and subsequent complexation in situ, with excellent results: The complexes **15**, **16**, and **17**, in which the borabenzene is stabilized by relatively weak Lewis bases, is clear evidence of the strong Lewis acidity of borabenzene.^{7,8}



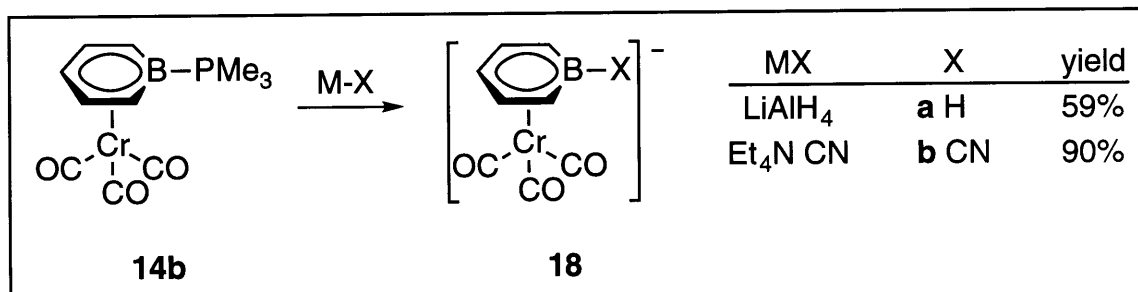
As is the case with uncoordinated BB-PMe₃ (**4e**), the trimethylphosphine in **14b** can be displaced from the coordination sphere of boron by hard nucleophiles, such as hydride or diphenylphosphide. By this method, we have prepared the anionic complexes [(BB-X)Cr(CO)₃]⁻, where X is H or CN (Scheme 4.2). The direct synthesis of these boratabenzene complexes, by reacting the corresponding alkali-metal

⁶ The oxazoline employed was (*S*)-4-isopropyl-2-phenyloxazoline: Tweddell, J.; Hoic, D. A.; Fu, G. C. *J. Org. Chem.* **1997**, *62*, 8286-8287.

⁷ Amendola, M. C.; Stockman, K. E.; Hoic, D. A.; Davis, W. M.; Fu, G. C. *Angew. Chem., Int. Ed. Eng.* **1997**, *36*, 267-269.

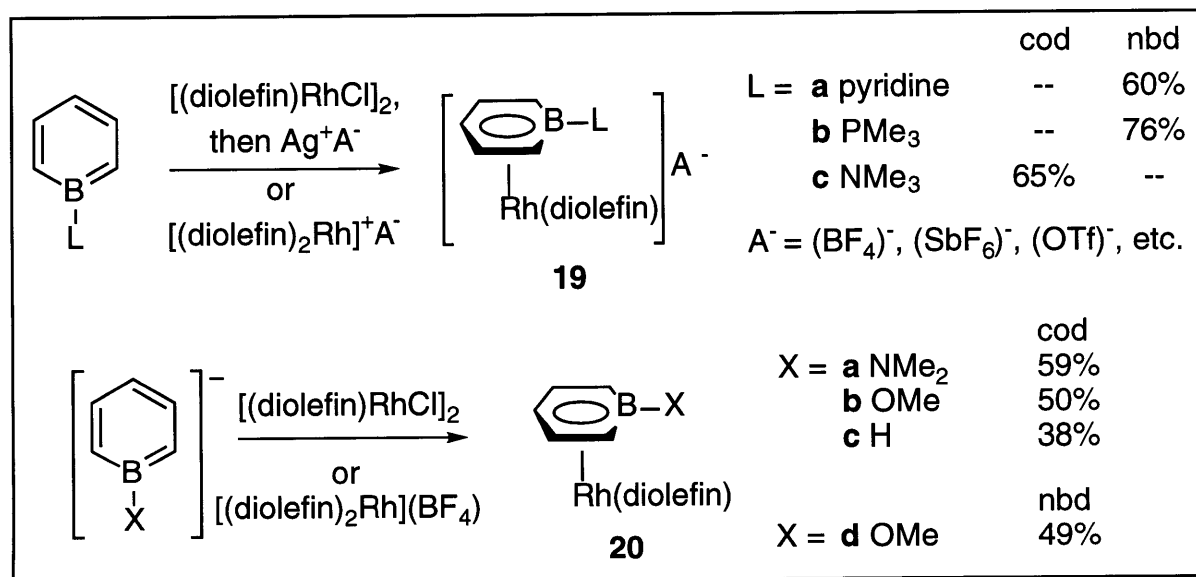
⁸ a) Cioslowski, J.; Hay, P. J. *J. Am. Chem. Soc.* **1990**, *112*, 1707-1710. b) Schulman, J. M.; Disch, R. L. *Organometallics* **1989**, *8*, 733-737. c) Raabe, G.; Schleker, W.; Heyne, E.; Fleischhauer, J. *Z. Naturforsch., A* **1987**, *42*, 352-360. d) Schulman, J. M.; Disch, R. L.; Sabio, M. L. *J. Am. Chem. Soc.* **1982**, *104*, 3785-3788.

boratabenzene with $(\text{MeCN})_3\text{Cr}(\text{CO})_3$, either yielded multiple products ($\text{X} = \text{CN}$), or the products could not be isolated easily from an apparently clean (^1H NMR) reaction mixture ($\text{X} = \text{H}$).⁹



Scheme 4.2.

Simultaneously, we learned how to prepare a series of rhodium diolefin complexes bearing borabenzenes and boratabenzenes as ligands (Scheme 4.3).



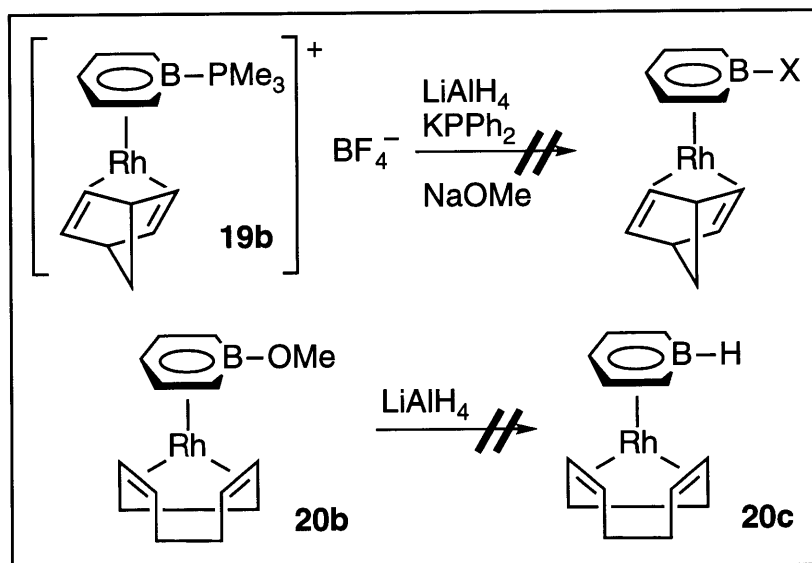
Scheme 4.3.

Borabenzenes react cleanly with [(diolefin)Rh]^+ sources,¹⁰ such as

⁹ Herberich has prepared the anion $\text{[(BB-X)Cr}(\text{CO})_3]^-$ where X is methyl (i.e., X has no lone electrons pairs), by reaction of $\text{Na}(\text{BB-Me})$ with $(\text{H}_3\text{N})_3\text{Cr}(\text{CO})_3$: Herberich, G. E.; Söhnen, D. J. *Organomet. Chem.* **1983**, 254, 143-147.

¹⁰ Schrock, R. R.; Osborn, J. A. J. *Am. Chem. Soc.* **1971**, 93, 3089-3090.

$[(\text{diolefin})\text{RhCl}]_2/\text{AgA}$ or $[(\text{diolefin})_2\text{Rh}](\text{A})$, where A is a non-coordinating anion, to form the cationic complexes **19a, b, c** in good yield (Scheme 4.3). Also, the family of $(\text{BB-X})\text{Rh}(\text{cod})$ can be isolated easily from the reaction of an alkali-metal boratabenzene with the desired $[(\text{diolefin})\text{Rh}]^+$ source.¹¹ In contrast with the $\text{Cr}(\text{CO})_3$ complexes, however, reaction of nucleophiles with the rhodium-bound borabenzene complexes results in the formation of multiple products, presumably due to attack of nucleophile on the rhodium-bound diolefins (Scheme 4.4).



Scheme 4.4.

The accessibility of borabenzene with varying substitution at boron should allow the fine tuning of the reactivity of their transition metal complexes by proper choice of the substituent, provided that different substituents have different donating properties to the borabenzene ring. We have data that suggests that this is the case. When one thinks of a tricoordinate boron center, one normally thinks of a strong Lewis acid that forms acid-base complexes through an empty p orbital on boron. The three substituents coordinate the boron in a trigonal planar fashion, and the empty, boron-centered, p orbital behaves as an electron-pair acceptor¹² (i.e., acts as a Lewis acid) either intermolecularly (e.g., $\text{F}_3\text{B}\cdot\text{OEt}_2$, forming a dative σ bond) or

¹¹ Herberich, G. E.; Becker, H. J.; Carsten, K.; Engelke, C.; Koch, W. *Chem. Ber.* **1976**, *109*, 2382-2388.

¹² For reviews, see: a) Paine, R. T.; Nöth, H. *Chem. Rev.* **1995**, *95*, 343-379. b) Power, P. P. *Angew. Chem., Int. Ed. Engl.* **1990**, *29*, 449-460.

intramolecularly (e.g., Ph_2BNPh_2 , forming a π bond) (Figure 4.1).

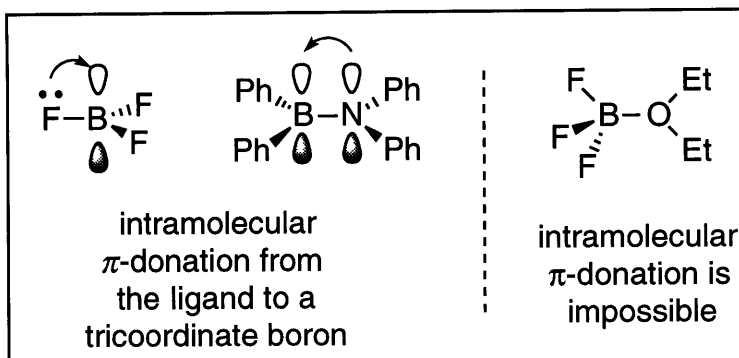


Figure 4.1. Boron-based Lewis Acid/Base Complexation.

Theoretical studies have proposed that, in a special case, a tricoordinate boron can behave as a π -donor as well (Figure 4.2).¹³ Cioslowski and Hay concluded that a charge transfer would occur from the π -symmetry orbitals on borabenzene to their counterparts at the ligand, when the boron-bound ligand was either CO ¹⁴ or N_2 .¹⁵

We set out to determine whether there might be experimental support for the prediction of Cioslowski and Hay that the boron center in borabenzene can act as both a π -acid and as a π -base to the boron substituent. To do this, we prepared a

¹³ Cioslowski, J.; Hay, P. J. *J. Am. Chem. Soc.* **1990**, *112*, 1707-1710. This conclusion is consistent with, but at the time was not linked to, the observation of a charge-transfer band in borabenzene-pyridine that is responsible for its characteristic yellow color (Boese, R.; Finke, N.; Henkelmann, J.; Maier, G.; Paetzold, P.; Reisenauer, H. P.; Schmid, G. *Chem. Ber.* **1985**, *118*, 1644-1654.). The direction of polarization of the π bond is inferred from the fact that the $\text{Cr}(\text{CO})_3$ fragment chooses to attach itself to the boron (rather than the nitrogen) heterocycle, suggesting that the borabenzene π -system is more electron-rich than that of pyridine: Boese, R.; Finke, N.; Keil, T.; Paetzold, P.; Schmid, G. *Z. Naturforsch., B* **1985**, *40*, 1327-1332.

¹⁴ A recent paper suggests that bonding between a trihaloborane and a weak base such as CO may be mostly due to van der Waals interactions (Jonas, V.; Frenking, G.; Reetz, M. T. *J. Am. Chem. Soc.* **1994**, *116*, 8741-8753). An isocyanide is much more basic than CO (For example, see Elschenbroich, C.; Salzer, A. *Organometallics*, 2nd ed.; VCH: Weinheim, 1992; pp 240-241), so that their conclusions are not pertinent to our discussion.

¹⁵ There is some evidence for the existence of borabenzene- CO and borabenzene- N_2 in an argon matrix: Maier, G.; Reisenauer, H. P.; Henkelmann, J.; Kliche, C. *Angew. Chem., Int. Ed. Engl.* **1988**, *27*, 295-296.

variety of neutral borabenzene adducts. These adducts were characterized by ^1H and ^{13}C NMR spectroscopy, as well as X-ray crystallography and IR spectroscopy. By comparing their properties, we hoped to determine if π -donation from a tricoordinate boron center to a ligand could occur when the ligand is a strong π -acid.

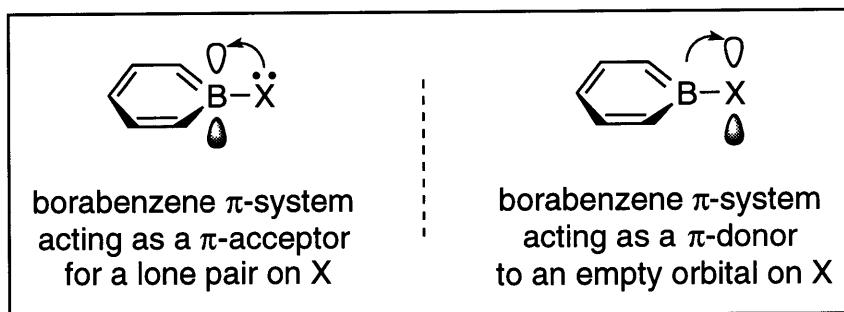


Figure 4.2. Oversimplified Drawing of Borabenzene as a π -Amphoteric Molecule.

The notion that the ^1H and ^{13}C NMR chemical shifts can be used to study π -bonding in boratabenzenes is not new. Herberich initially suggested¹⁶ that the NMR chemical shifts of the ortho and para protons and carbons can be used to assess the π -donor capacity of the boratabenzene substituent (**A** in Figure 4.3).¹⁷ We, in a different study, used the ^1H and ^{13}C NMR chemical shifts to confirm the presence of a B-N double bond, as well as absence of a B-P double bond (Chapter 6).

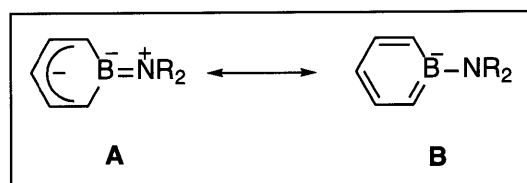


Figure 4.3. Resonance Structures for a Dialkylamidoboratabenzene

We decided to attempt to explore the π -basicity of borabenzene based on the following reasoning. Given that the chemical shifts of the ortho and para protons

¹⁶ Herberich, G. E.; Schmidt, B.; Englert, U. *Organometallics* **1995**, *14*, 471-480.

¹⁷ Ashe measured the barrier of rotation about the B-N π -bond to be 10.1 ± 0.5 kcal/mol for BB-N(Me)(Bn). This barrier increases to 16.6 ± 0.5 kcal/mol upon complexation of the boratabenzene to the powerfully electron-withdrawing $\text{Mn}(\text{CO})_3$ fragment: Ashe, A. J., III; Kampf, J. W.; Muller, C.; Schneider, M. *Organometallics* **1996**, *15*, 387-393.

and carbons of borabenzene can indicate the presence of π donation from the ligand to the boron, then it follows that they may also provide evidence for *reverse* π donation. Therefore, we tabulated the chemical shifts we had obtained for chromium tricarbonyl complexes of neutral borabenzene (Table 4.1). The trends observed for these chemical shifts are consistent with the existence of π donation from the borabenzene to the ligand in the case of the isocyanide, as well as π -acceptance by the borabenzene in the case of THF and 3-dimethylaminoacrolein.

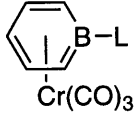
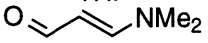
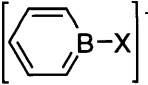
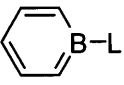
entry	ortho ^1H	ortho ^{13}C	para ^1H	para ^{13}C	
	L= CN- ^tBu	4.65	98.2	5.29	90.3
	pyridine	4.40	84.0	5.20	85.2
	PMe ₃	4.40	93.0	5.25	88.5
	THF	3.91	76.5	4.94	83.5
		3.89	81.3	4.86	82.5

Table 4.1. Chemical Shifts (in ppm) for Chromium-Bound Borabenzene Complexes. (^1H in CD_2Cl_2 , ^{13}C in THF-d_8)¹⁸

¹⁸ A similar trend is observed for uncomplexed borabenzene and boratabenzene complexes. The interpretation of this trend for boratabenzenes is not entirely straightforward, as the coordination environment around the alkali metal counterions (omitted for clarity) is fluxional. Unfortunately, we have yet to make a borabenzene with electron-donating substituents that is not bound to a transition metal. The chemical shifts for the meta positions do not change.

entry	ortho ^1H	ortho ^{13}C	para ^1H	para ^{13}C	
	X= CN	6.71		6.32	
	H	6.57	128	6.21	112
	PPh ₂	6.50	128	6.20	113
	Me	6.47	127	6.18	108
	NPh ₂	5.99	119	5.72	106
	OEt	5.67	115	5.67	104
	NMe ₂	5.65	110	5.50	100
	L= CN- ^tBu	8.01	138.0	7.48	123.3
	PMe ₃	7.23	128.0	7.42	120.7
	pyridine	6.75	119.2	6.75	116.6
	NEt ₃	6.45	116.5	7.20	114.7

The work presented in this chapter extends Herberich's NMR analysis of π -donating boron substituents to π -acidic ligands. We have shown that a π -electron-rich tricoordinate boron may act as a π -base to a suitable boron-bound ligand¹⁹ and that borabenzene is, therefore, a π -amphoteric molecule for which the extent and direction of the π interaction between borabenzene and the ligand depends on the nature of the ligand.

We became interested in the possibility that these effects could translate into differing reactivity at the metal center for different members of a family of borabenzene- or boratabenzene-metal complexes. Our interest ties in with that of several groups that are interested in the effect on the metal of replacing Cp with boratabenzenes. Most of their efforts have centered on early-metal metallocene chemistry, with excellent results. The rhodium(diolefin) complexes we prepared (**19** and **20**) were to be used as catalysts for a number of well-known reactions. We were particularly interested in catalyzing the hydrogenation and hydroformylation of α -olefins,²⁰ as well as the tail-to-tail dimerization of acrylates.²¹ Unfortunately, none of these efforts were successful.

In order to get meaningful comparisons, we decided to examine a simple one-step bimolecular process. One such reaction is the nucleophilic displacement of iodide from iodomethane by a nucleophilic transition metal complex, to form a metal alkyl. Angelici has reported a considerable amount of work on the methylation of iridium cyclopentadienide complexes **A** (Scheme 4.5) to form **B**.²²

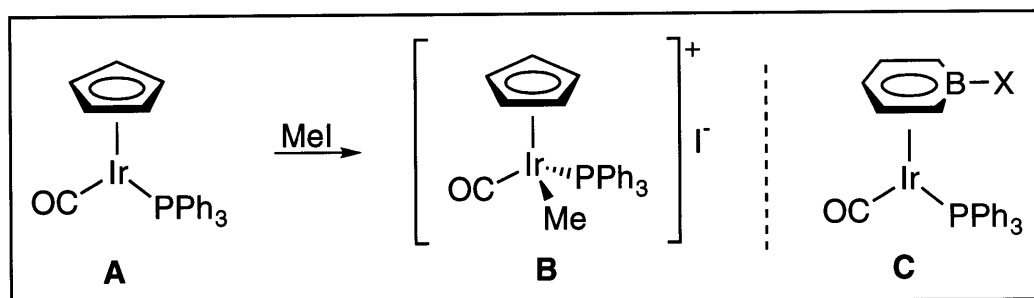
¹⁹ Since electrons are not localized in a specific atomic orbital, but rather they are delocalized over a molecular orbital, it would be surprising if borabenzene were the only boron fragment that could exhibit this π -backbonding phenomenon; we believe that our system is not unique in exhibiting such behavior. For example, a crystal structure of the hitherto unknown $(\text{Me}_2\text{N})_2\text{B-CN}$ should exhibit significant B-C double bond character, whereas the also unknown Me_2BCN adduct should not. Borabenzene is unique because it has allowed the study of the direction of the polarization of this double bond.

²⁰ Zhou, A.; James, B. R.; Alper, H. *Organometallics* **1995**, *14*, 4209-4212, and references therein.

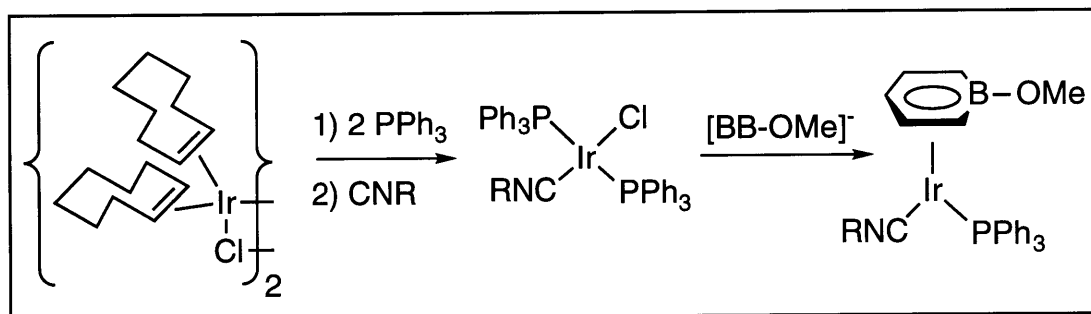
²¹ This process has been shown to require a Cp fragment that is electron-rich and sterically hindered (i.e., Cp*): Hauptman, E.; Sabo-Etienne, S.; White, P. S.; Brookhart, M.; Garner, J. M.; Fagan, P. J.; Calabrese, J. C. *J. Am. Chem. Soc.* **1994**, *116*, 8038-8060.

²² a) Wang, D.; Angelici, R. J. *J. Am. Chem. Soc.* **1996**, *35*, 1321-1331. b) Hart-Davis, A. J.; Graham, W. A. G. *Inorg. Chem.* **1971**, *10*, 1653-1657.

These reactions exhibit clean first-order kinetics in MeI and the iridium complex, although in certain instances the methyl group in **B** migrates to the carbonyl to form a metal-acyl complex.²³ We initially decided to focus on the family of complexes **C** (Scheme 4.5), but, unfortunately, we were unable to purify them. Their yellow Cp analogues are purified by flash chromatography on silica under nitrogen, but the boratabenzene complexes decomposed on silica. Furthermore, we were unable to purify these compounds by crystallization or sublimation.



Scheme 4.5.



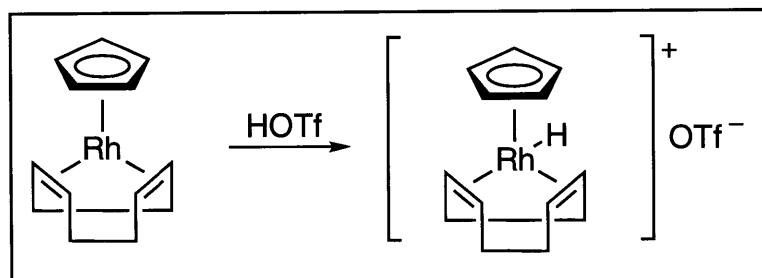
Scheme 4.6.

In order to impart increased crystallinity to the desired complexes, we decided to modify the ligand system around Ir. The simple solution of switching from PPh₃ to PMe₃ did not lead to crystalline complexes, so we replaced the CO with a series of isonitriles²⁴ (Scheme 4.6, R = *t*-butyl, 2,6-dimethylphenyl, and benzyl), in the hope that a bulkier substituent would dominate the packing of the solid. Unfortunately,

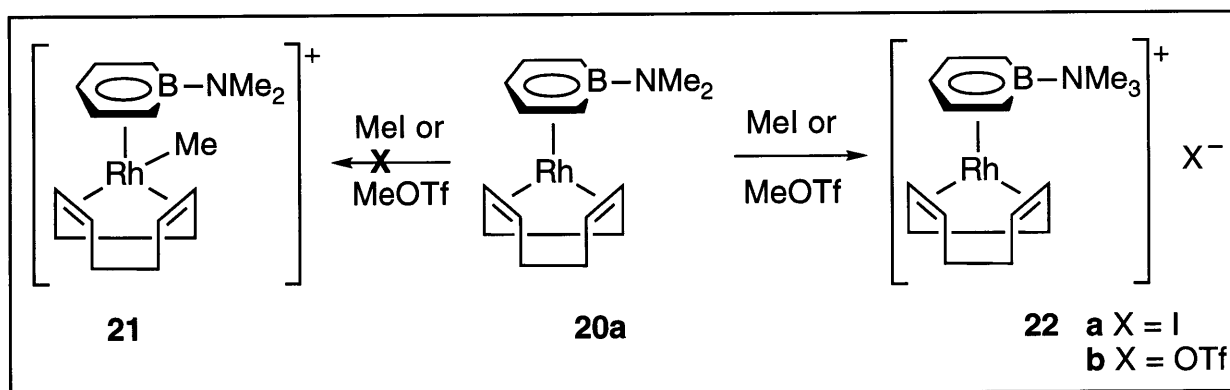
²³ a) Hart-Davis, A. J.; Graham, W. A. G. *Inorg. Chem.* **1970**, *9*, 2658-2663. b) Oliver, A. J.; Graham, W. A. G. *Inorg. Chem.* **1970**, *9*, 2653-2657.

²⁴ We prepared the isonitrile analogues of Vaska's complex by loosely following a literature procedure: Ent, A. v.d.; Onderdelinden A. L. *Inorg. Chim. Acta* **1973**, *7*, 203-208.

this approach was also unsuccessful. At this point, we decided to focus on rhodium(diolefin) complexes, based on a report that CpRh(cod), the boratabenzene analogues of which we had isolated, could be protonated by triflic acid (Scheme 4.7).²⁵



Scheme 4.7.



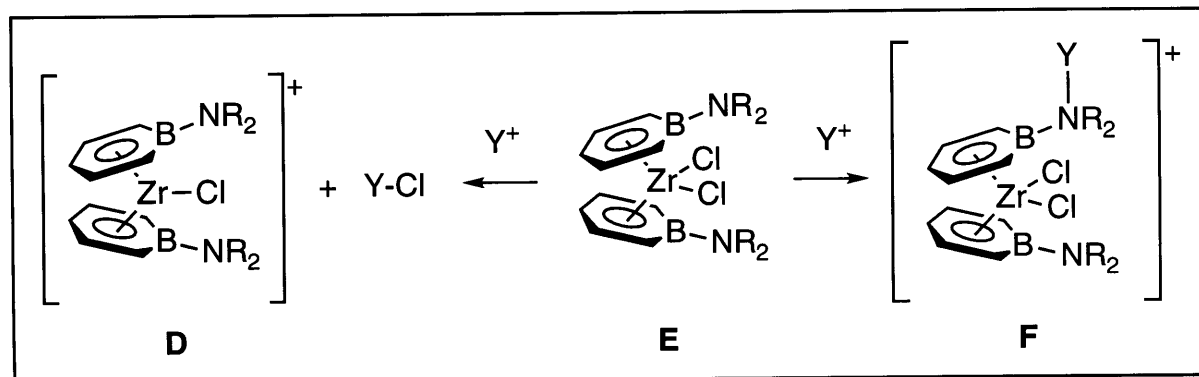
Scheme 4.8.

Since we had (BB-OMe)Rh(cod), (BBH)Rh(cod), and (BB-NMe₂)Rh(cod) in hand,²⁶ we decided to explore the possibility that they could be methylated at rhodium. Reaction of (BB-NMe₂)Rh(cod) with ¹³C labelled iodomethane resulted in a compound for which the ¹H NMR spectrum, as well as the crystal structure, establish unambiguously that *methylation occurs at nitrogen, instead of at rhodium*

²⁵ Sowa, J. R.; Angelici, R. J. *J. Am. Chem. Soc.* **1991**, *113*, 2537-2544.

²⁶ Recently, we have found that methylation at rhodium is extremely clean for the very crystalline and easy-to-purify complexes (BB-OMe)RhL₂ (where L₂ is a chelating bis(phosphine) such as dppe and dppm). The rates are somewhat fast, but it may be possible to study the kinetics of conversion to [(BB-OMe)RhL₂Me]⁺.

(Scheme 4.8). While unexpected, this was an extremely interesting development for several reasons, including boratabenzene-based Ziegler-Natta polymerization chemistry and our borabenzene-based chiral Lewis acid catalyst.



Scheme 4.9.

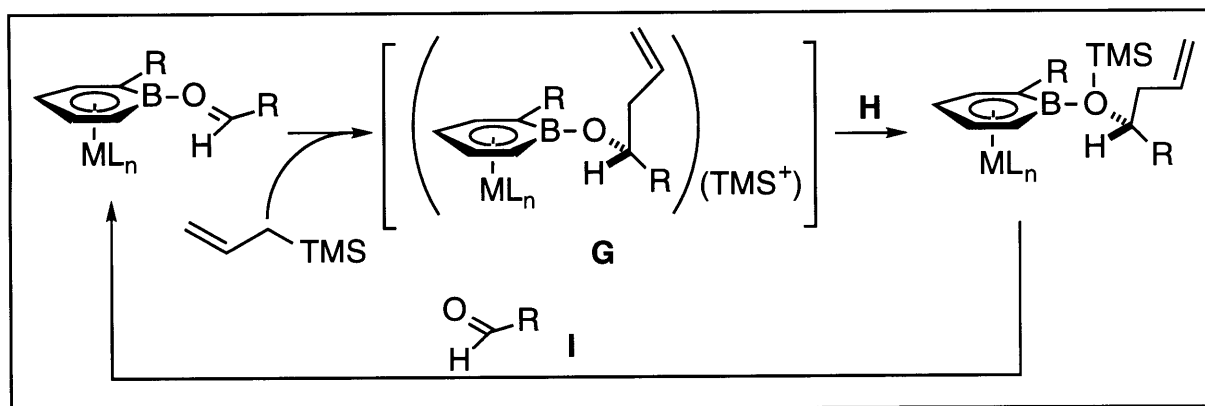
So far, it has been assumed that the substituent on boron is inert under the extremely Lewis-acidic conditions of the Ziegler-Natta polymerization of α -olefins.²⁷ B-X π -bonding has always been believed to be the overriding feature of the bonding between boron and the lone pair on the boron substituent (for rotation around the B-N double bond in (BB-NMeBn)Mn(CO)₃, a ΔG^\ddagger of 16.6 kcal/mol has been measured by Ashe²⁸), because no evidence had been found for interactions between the boron substituent and any electrophilic reagents (outside of DPB chemistry, Chapter 6). Yet, when formulating a mechanistic hypothesis, the validity of this assumption is a crucial point. For example, a recent report calls for the use of 100 to 20000 equivalents of the extremely Lewis acidic coactivator methylalumoxane (MAO) for every equivalent of bis(boratabenzene) zirconium catalyst.²⁹ The electrophile (Y⁺, MAO in this case) may react with the zirconocene E (Scheme 4.9) by either reacting at nitrogen or abstracting a halide. In both cases the resulting zirconocene is cationic, but in **D** the complex has an open coordination site and should be catalytically active, while the absence of an easily accessible open

²⁷ a) For a discussion based on crystal structures, see reference 2i. b) Also, see Ashe, A. J.; III; Kampf, J. W.; Waas, J. R. *Organometallics* **1997**, *16*, 163-167.

²⁸ Ashe, A. J., III; Kampf, J. W.; Müller, C.; Schneider, M. *Organometallics* **1996**, *15*, 387-393.

²⁹ In this example, the catalyst of interest is (BB-OEt)₂ZrCl₂: reference 2e. The analysis presented in Scheme 4.7 concerns the seminal system, (BB-NR₂)ZrCl₂: reference 2i. As is seen later, the analysis holds for BB-OR as well as BB-NR₂.

coordination site should render **F** catalytically less active.³⁰ That boratabenzene-based catalysts are quite active in Ziegler-Natta polymerizations suggests that complexes analogous to **D** do, indeed, form efficiently. The clean methylation of **20a**, however, serves notice that there is a chance that a pathway leading to analogues of **F** may also exist and should be considered as possible reaction pathways. The relative rates of the formation of **D** and **F**, as well as their relative stability, may have an effect on any postulated mechanism.



Scheme 4.10.

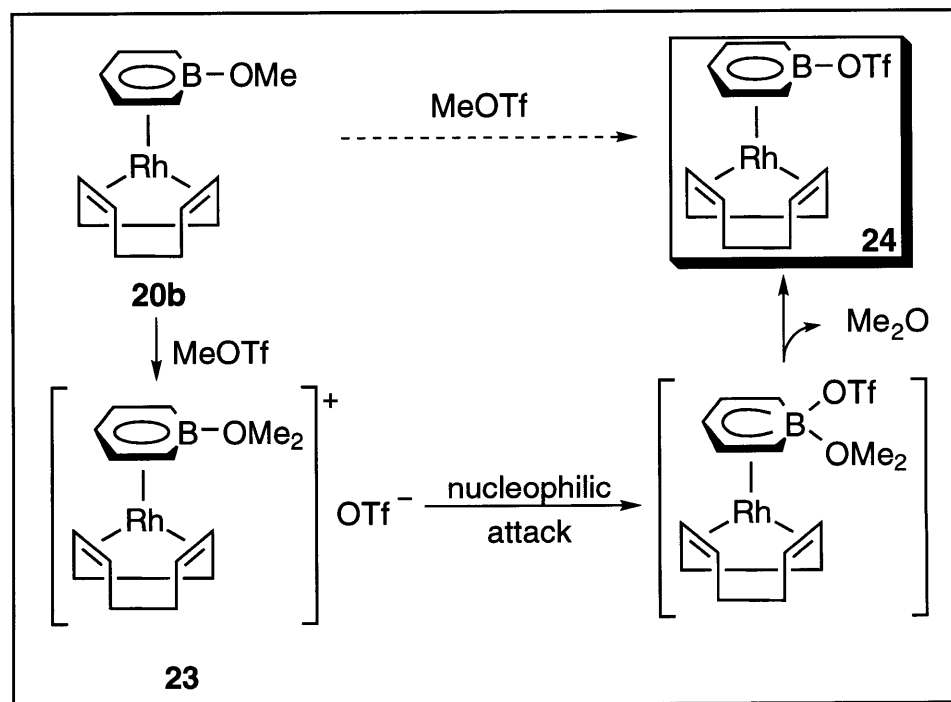
From the perspective of the synthesis of a chiral Lewis acid based on borabenzene (see Chapter 1), we were interested in the possibility that a rhodium-bound alkoxy(boratabenzene) could be methylated as well, even though an alkoxy substituent should be considerably less nucleophilic than the NMe₂ in (BB-NMe₂)Rh(cod) (**20a**). The turnover step for the desired catalytic cycle, depicted in Scheme 4.10 for a Sakurai reaction, includes two discrete steps: the reaction of a metal-bound alkoxyboratabenzene with an electrophile (Reaction **H**) and the exchange of the resulting boron-bound ether (or silyl ether) by an aldehyde (Reaction **I**). Proof-of-principle for step **I** had been furnished by Michael Amendola,³¹ who prepared the imine complex **16** and the vinylogous amide complex **17** by displacing THF from the coordination sphere of boron in (BB-THF)Cr(CO)₃ (**15**) with the appropriate Lewis base. In the first discrete step of the catalyst turnover process, an alkoxyboratabenzene-metal complex (**G**) must react with an electrophile (TMS⁺) at the alkoxy substituent (Reaction **H**), rather than at

³⁰ Bent metallocene dihalides have an empty orbital: Lauher, J. W.; Hoffmann, R. J. *Am. Chem. Soc.* **1976**, *98*, 1729-1742.

³¹ Amendola, M. C. M. S. Thesis, MIT, 1995. Also see: Reference 7.

the potentially nucleophilic metal center. Seeking proof-of-principle for reaction **H**, we reacted (BB-OMe)Rh(cod) (**20b**) with a range of methylating agents.

Although iodomethane does not react with (BB-OMe)Rh(cod), methyl triflate does. The structure of the resulting complex was originally assigned as the cationic dimethylether complex **23** (Scheme 4.11), by analogy with the amine complex **22**. Two observations, however, raised questions about this structural assignment. The unusually high solubility of this compound in a mixture of CH₂Cl₂/Et₂O was much more characteristic of the neutral (BB-X)Rh(cod) complexes than of all other [(BB-L)Rh(cod)]⁺ salts that we had prepared up to that point. Also, while ¹³C labelling established the presence of a H₃CO¹³CH₃ fragment, we had no proof that the ether was boron-bound. Indeed, when the solvent was evaporated and the compound was redissolved, the dimethyl ether resonances disappeared. The remainder of the spectrum remained the same, clearly indicating that our initial assignment was incorrect.



Scheme 4.11.

It was clear that we had not made **23**, so we hypothesized that the product of the reaction was either (BB-OTf)Rh(cod), or (BB-Cl)Rh(cod), arising from a nucleophilic displacement, because we saw triflate or chloride (from chloroform-*d*) as the most

likely nucleophiles. Both of these neutral molecules would likely form (Scheme 4.11; shown for the triflate, but the chloride is analogous) by rate-limiting methylation of the methoxyboratabenzene to yield the unobserved **23**, from which the dimethyl ether can be displaced by triflate. However, we cannot currently discard other substitution pathways, including a dissociative one involving rhodium-complexed free borabenzene.

A chemical ionization mass spectrum³² showed that **24** is the boron-bound triflate. This assignment is in agreement with its solubility properties, as well as with the IR spectrum (ν_{CO} : 1383 cm^{-1}); the S-O stretch for an unbound triflate should be at $\sim 1270 \text{ cm}^{-1}$, while the same stretch for a bound one should be at $\sim 1380 \text{ cm}^{-1}$.³³ When the reaction was performed with one equivalent of 1,3,5-trifluorobenzene as an internal standard, the integration of the ^1H and ^{19}F NMR spectra of these reactions showed that for every two meta protons of a borabenzene there were three fluorines, indicating the presence of one triflate per borabenzene. Finally, Table 4.2 shows that the ^{19}F NMR chemical shift is consistent with a boron-bound triflate.

sample	$\delta \text{ } ^{19}\text{F}$ NMR ³⁴	ν_{SO} (cm^{-1})
MeOTf	-75.5	
Cy ₂ B-OTf ³⁵	-76.7	
(BB-OTf)Rh(cod), 24	-77.4	1383
(BB-OTf)Rh(nbd), 26a	-77.5	1391
[(BB-NMe ₃)Rh(cod)](OTf), 19c	-79.4	1271
[(BB-PMe ₃)Rh(nbd)](OTf), 28	-80.1	1264
[(BB-py)Rh(nbd)](OTf), 27	-80.3	1260

Table 4.2. ^{19}F NMR Chemical Shifts and S-O Stretching Frequencies.

We were unable to crystallize **24**, either for purification or for a single-crystal X-ray diffraction experiment. Therefore, we prepared the analogous compounds where cod is replaced by nbd (**26a**; Scheme 4.12) or dicyclopentadiene (**26b**). We were also

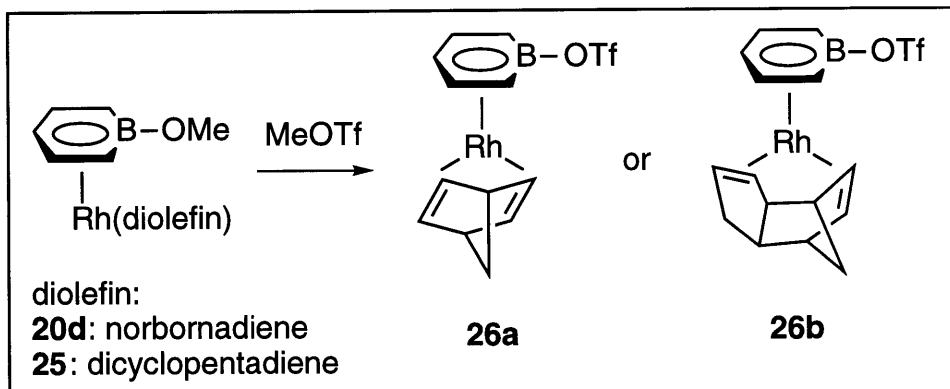
³² We thank Prof. Thomas Katz, and Ms. Vinka Parmakovich from Columbia University for this data.

³³ Lawrance, G. A. *Chem. Rev.* **1986**, *86*, 17-33.

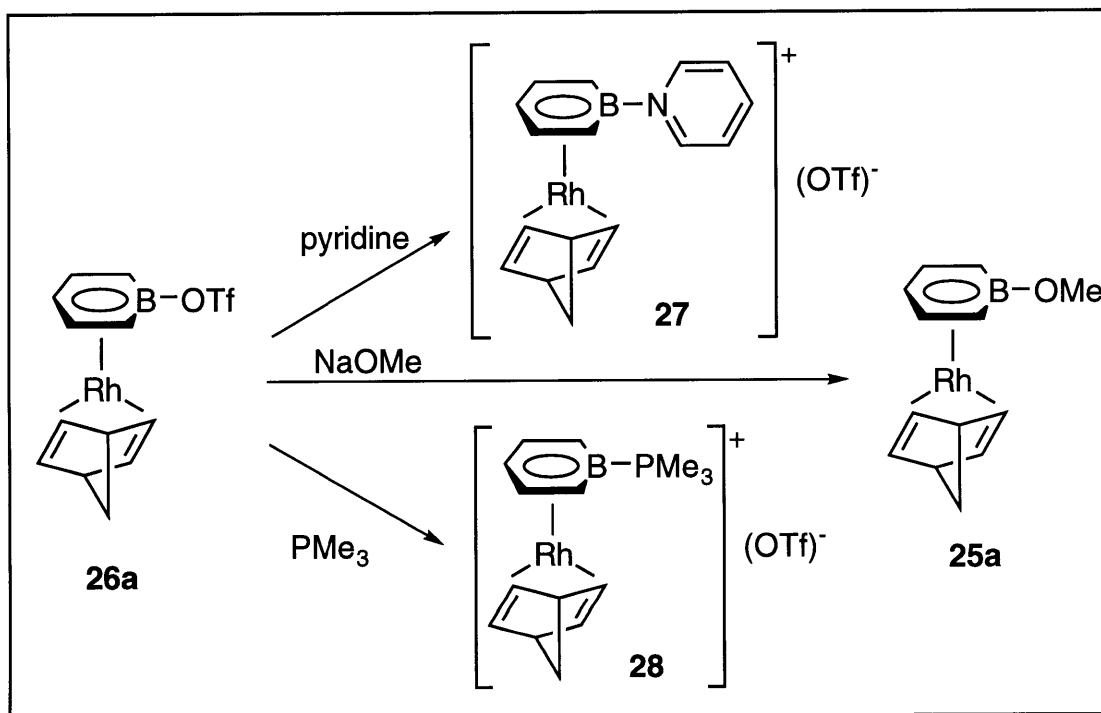
³⁴ Referenced to CF₃COOH, -76.54 ppm.

³⁵ We thank Ms. Dana Buske (Masamune group) for a gift of Cy₂B-OTf.

unable to crystallize these compounds.



Scheme 4.12.



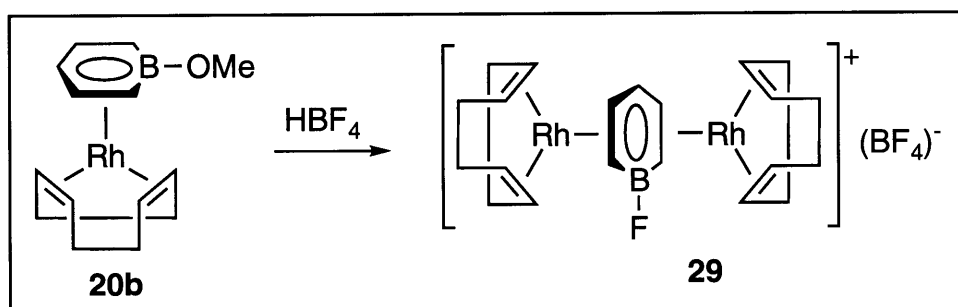
Scheme 4.13.

We were able to convert the boratabenzene compound **26a** to the borabenzene compounds **27** and **28** by reaction with pyridine and trimethylphosphine (Scheme 4.13).³⁶ Compound **26a** also reacts with sodium methoxide to return to (BB-

³⁶ THF and DMF are not sufficiently nucleophilic to react with complex **24** to form borabenzene complexes.

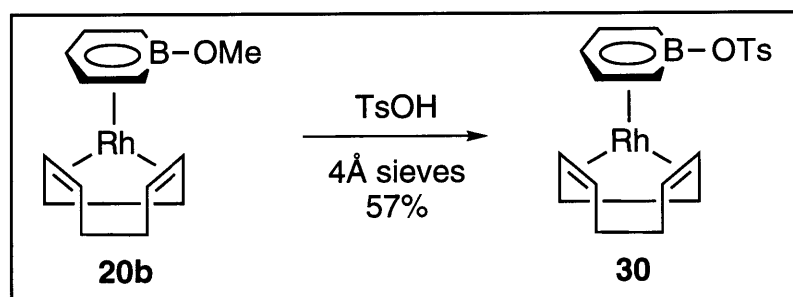
OMe)Rh(nbd) (**20b**) the compound from which it was originally prepared.

In order to further study the reaction of the boron substituent on borabenzene, we decided to attempt protonation of the oxygen in **20b**, with the hope of isolating a crystalline adduct. Initial experiments with HBF₄ at room temperature yielded a mixture of solids (¹H NMR) from which we were able to unambiguously characterize, by means of an X-ray structure, the crystalline triple-decker [(cod)Rh(C₅H₅BF)Rh(cod)](BF₄) (**29**; Scheme 4.14). We suspect that the fluoride in this product probably arises from the inevitable presence of HF or BF₃ in commercial HBF₄, and not from the relatively inert (BF₄)⁻.



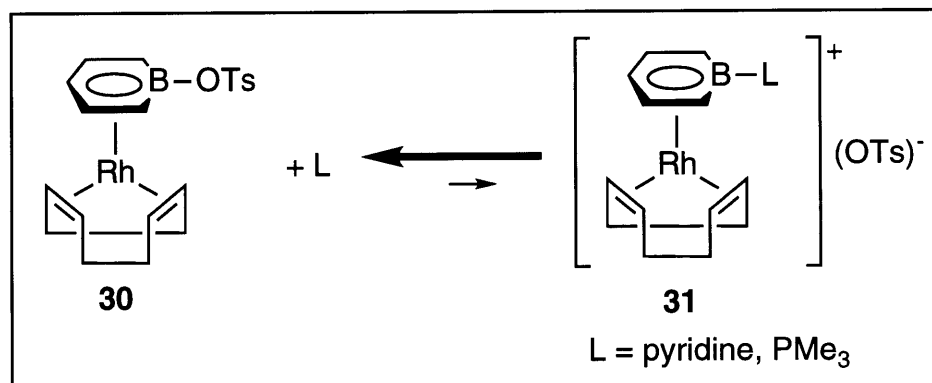
Scheme 4.14.

Hoping that a different acid might lead to the desired crystalline compound, we attempted the protonation of **20b** with triflic acid, (+)-camphorsulfonic acid (CSA) and *p*-toluenesulfonic acid (TsOH). Triflic acid appears to be too reactive, as the reaction results in a mixture of unidentifiable products. Reaction with CSA is somewhat cleaner, whereas reaction with TsOH (Scheme 4.15) led to the formation of a mixture of starting material, product (**30**) and methanol. The reaction stopped while there was still acid and starting material present, but addition of 4 Å molecular sieves drove the reaction to completion.



Scheme 4.15.

Compound **30** could be isolated and fully characterized. However, studies of its reactivity towards five different Lewis bases — pyridine, trimethylphosphine, 2,6-dimethylphenylisocyanide, 4-dimethylaminopyridine, and $\text{P}(\text{NMe}_2)_3$ — led to mixtures of products. We speculated that perhaps the equilibrium in these exchange reactions could lie towards **30** (Scheme 4.16), and that after a while an unidentified decomposition pathway led to the many products. Therefore, we attempted to prepare two of the products (**31**) independently. If the equilibrium truly lies towards compound **30**, then its formation should be observed upon preparing " $[(\text{BB-PMe}_3)\text{Rh}(\text{cod})](\text{OTs})$ " or " $[(\text{BB-py})\text{Rh}(\text{cod})](\text{OTs})$ ", employing the same solvent and similar concentration as the initial displacement reactions that failed. When we reacted BB-PMe₃ and BB-py with $[(\text{cod})\text{RhCl}]_2$,³⁷ followed by addition of Ag(OTs), we saw **30** appear quickly in the ^1H NMR spectrum of the reaction mixture. We therefore conclude that the equilibrium between **30** and **31** favors **30** when L is pyridine or PMe₃.



Scheme 4.16.

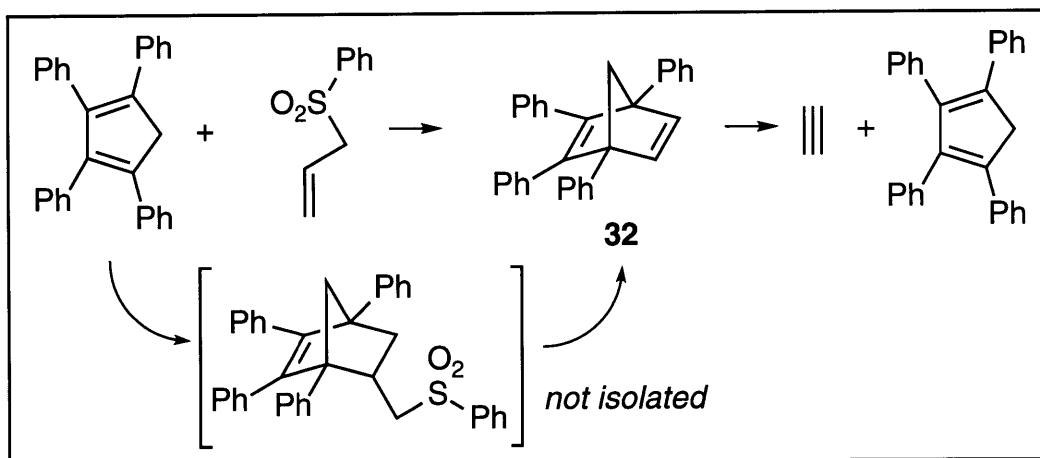
A second approach we took to overcoming the lack of crystallinity of triflates **24**, **26a**, and **26b** was to try to affect their packing by employing a bulkier diolefin. This approach came to mind because of our experience with the $(\text{C}_5\text{Ph}_5)\text{Fe}(\text{pyridine})$ -based nucleophilic catalysts,³⁸ in which the packing forces are dominated by the $(\text{C}_5\text{Ph}_5)\text{Fe}$ moiety.³⁹ The $(\text{C}_5\text{Ph}_5)\text{Fe}$ fragment tends to pack in a symmetry higher

³⁷ Addition of AgBF_4 to this mixture results in formation of $[(\text{BB-L})\text{Rh}(\text{cod})](\text{BF}_4)$.

³⁸ Ruble, J. C.; Latham, H. A.; Fu, G. C. *J. Am. Chem. Soc.* **1997**, *119*, 1492-1493.

³⁹ In contrast, the packing of the $\text{Cp}^*\text{Fe}(\text{pyridine})$ -based complexes is determined by the entire molecule.

than the true symmetry of the molecule.⁴⁰ We reasoned that a compound with a bulkier diolefin may make the BB-OTf complex more crystalline than **24**, **26a**, or **26b**, in which the diolefin clearly does not dominate the packing. In order to obtain simpler NMR spectra we decided to modify either nbd or cod.



Scheme 4.17.

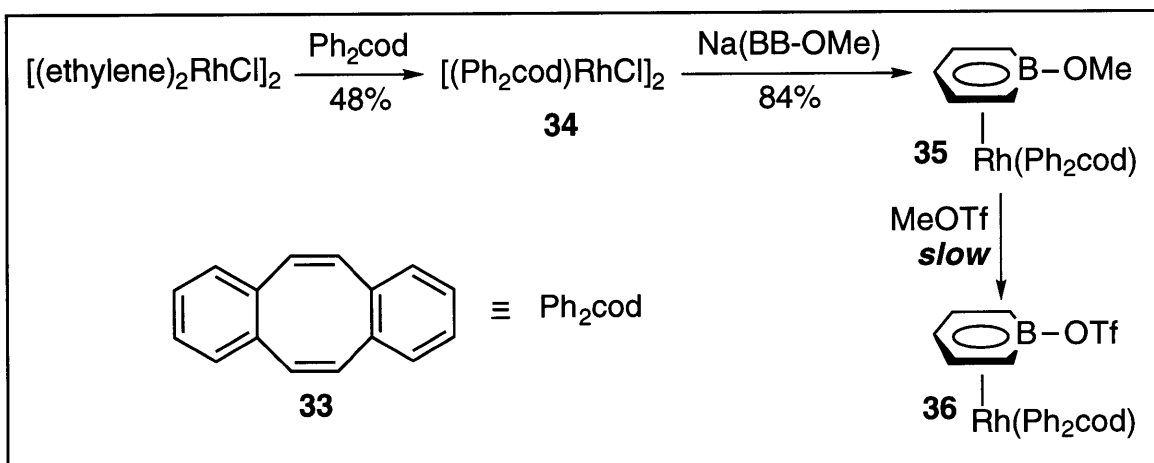
The norbornadiene skeleton is more easily modified than cod because it is accessible via the Diels-Alder reaction between a cyclopentadiene and an acetylene equivalent. Two known norbornadienes with substitution at the 1-, 2-, 3-, and 4-positions and which do not contain any carbonyl groups are 1,2,3,4-tetraphenylnorbornadiene (**32**) and 1,2,3,4,5-pentaphenylnorbornadiene. They can be made by reaction of tetraphenylcyclopentadiene with an allylphenylsulfone, which acts as an acetylene equivalent (Scheme 4.17).⁴¹ After considerable experimentation it was found that following the initial formation of some **32**, the ratio of **32**:tetraphenylcyclopentadiene remained constant for a short period of time, after which **32** disappeared. Apparently, a retro Diels Alder of **32** is occurring, and

⁴⁰ For example, the specimen employed in the first crystal structure determination of enantiopure (4-dimethylaminopyrindine)Fe(Ph₅C₅) crystallized in the space group P1, with four independent molecules in the asymmetric unit (Hoic, D. A., unpublished results). The Fe(C₅Ph₅) fragments were related by an inversion center, so that their packing (excluding the pyrindine fragment) was P-1, containing in the asymmetric unit two independent molecules that are "enantiomers" because of the propeller-shaped Fe(C₅Ph₅). The drawback of this approach is that a relatively low number of independent reflections can be observed, lowering the quality of the structural model.

⁴¹ Kumar, P. R. *J. Chem. Soc., Chem. Commun.* **1989**, 509-510.

the loss of acetylene gas is driving the reaction. Since most norbornadienes we would be interested in were liable to suffer from the same limitation, we decided to focus on derivatives of 1,5-cyclooctadiene with fused benzene rings, which are synthetically more challenging but likely to be more stable.

The preparation of dibenzo-(α,ϵ)-cyclooctatetraene (**33**; Ph₂cod) can be carried out in three steps.⁴² It is a stable, crystalline white solid that we hoped, as actually happens, would displace ethylene from the coordination sphere of rhodium in [(ethylene)₂RhCl]₂ to form [(Ph₂cod)RhCl]₂ (**34**, Scheme 4.18). Compound **34** reacts with Na(BB-OMe) to afford (BB-OMe)Rh(Ph₂cod) (**35**), a yellow solid the crystallinity of which is evident from the observation that X-ray quality crystals grew in less than 10 minutes. Unlike (BB-OMe)Rh(cod) (**20b**), however, **35** reacts slowly with methyl triflate to yield the desired triflate (**36**), accompanied by a small amount of unidentified decomposition products.



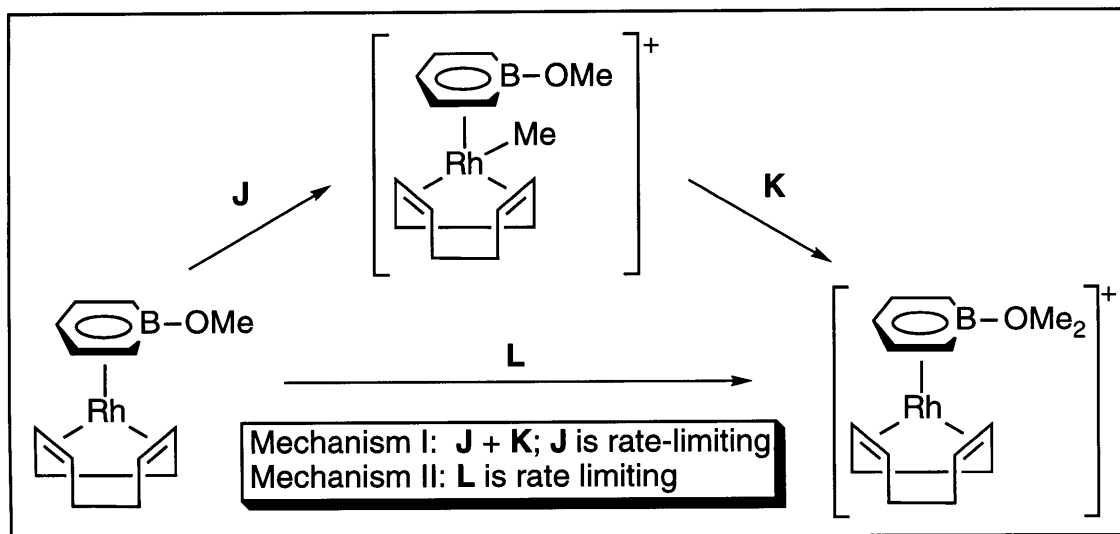
Scheme 4.18.

Although we were disappointed that **36** could not be cleanly prepared in this way, the slow conversion from **35** to **36** suggests some interesting mechanistic implications. Initially, we believed that the methylation occurs directly at the boron substituent (Scheme 4.19; L), but now we are not sure. The alternative mechanism (Scheme 4.13; J + K) involves the initial formation of a rhodium-methyl bond,⁴³

⁴² a) Rabideau, P. W.; Hamilton, J. B.; Friedman, L. J. *Am. Chem. Soc.* **1968**, *90*, 4465-4466, and references therein. b) Chan, T. L.; Mak, T. C. W.; Poon, C.-W.; Wong, H. N. C.; Jia, J. H.; Wang, L. L. *Tetrahedron* **1986**, *42*, 655-661. c) Mak, T. C. W.; Wong, H. N. C.; Sze, K. H.; Book, L. J. *Organomet. Chem.* **1983**, *255*, 123-134.

⁴³ Similar to the protonation of CpRh(cod) shown in equation 4.2.

followed by rapid migration of the methyl to the methoxy group.⁴⁴

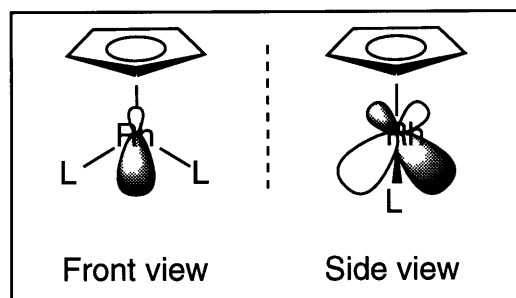


Scheme 4.19.

For the direct methylation mechanism to be operating, one of two things must be happening. Either the HOMO for (BB-OMe)Rh(diolefin) resides on the exo alkoxide (or amido for the case of **20a**), or the HOMO still resides on rhodium,⁴⁵ but it is blocked by the two-carbon bridge of the diolefin. In this case, the reaction occurs at methoxide because it is the only nucleophilic site available. When Ph₂cod is complexed to a metal, the π -systems of its benzene rings are orthogonal to the π -

⁴⁴ The reaction of CpCo(PMe₃)₂ with an electrophile (E⁺) to yield (C₅H₄E)Co(PMe₃)₂ (+ H⁺) has been shown to proceed via initial formation of a Co-E bond followed by migration of E to the Cp ring: Werner, H.; Hofmann, W. *Angew. Chem., Int. Ed. Eng.* **1977**, *16*, 794-795.

⁴⁵ The spatial orientation of the HOMO of an 18 ϵ complex with general formula CpML₂, known to reside on the metal M, is believed to be downwards and perpendicular to the L-M-L plane, (Hoffman, P. *Angew. Chem., Int. Ed. Eng.* **1977**, *16*, 536-537), as required by this second mechanism.



system of its olefins. As a result, the effect on the metal of replacing cod with Ph₂cod is probably relatively small.⁴⁶ If the electronics at the metal remain unchanged upon changing the olefin, then there should not be a great change in the nucleophilicity of the boron-bound oxygen or, for that matter, the rate of the methylation reaction, *unless the rhodium is intimately involved in the process*. The change between cod and Ph₂cod appears to have a dramatic effect⁴⁷ on the rate of the methylation at rhodium, suggesting that the reaction proceeds via the J + K mechanism, with J as the rate-limiting step.⁴⁸

Conclusions:

It was known from the literature that neutral borabenzene complexes bound to transition metals behave like π -bound arenes. We have extended this from the (arene)Cr(CO)₃ family to the cationic (arene)Rh(diolefin) family. We have also shown that, in some cases, metal-bound borabenzene complexes undergo ligand exchange at boron with hard nucleophiles, thereby providing a route to metal-bound boratabenzenes. The availability of boratabenzenes bearing an electron-rich transition metal fragment as well as a Lewis basic boron substituent led to the discovery of several reactions in which a metal-bound boratabenzene is converted into a metal-bound borabenzene by reaction of the boron substituent with an electrophile. This discovery is significant because it supports the feasibility of a catalytic cycle employing borabenzene complexes as catalysts for additions of nucleophiles to aldehydes. It is also significant because of its potential implications for catalysis of Ziegler-Natta

⁴⁶ We are alluding specifically to an inductive effect. This assertion can be checked by either X-ray photoelectron spectroscopy or ¹⁰³Rh NMR, none of which is readily available to us. As a first approximation, the ¹³C chemical shifts of the olefins in CD₂Cl₂ are close (cod: 70.2; Ph₂cod: 69.0), but this comparison falls quite short of ideal because the carbons in Ph₂cod are benzylic, and should still be affected by the aromatic ring current in Ph₂cod.

⁴⁷ It takes 30 minutes for the reaction to reach completion when the diolefin is cod, while it takes over 24 hours when the diolefin is Ph₂cod.

⁴⁸ (BB-OMe)Rh(dppe), in which the chelating bis(L) ligand has only one two-carbon bridge, is methylated at rhodium. Therefore, it would appear that having a second two-carbon bridge, or other similar shielding of the HOMO, is crucial for the methylation of the substituent on boron. Whereas the bridge in cod contains two methylene groups (with a C-C bond length of 1.533(4) Å), the bridge in Ph₂cod contains two aromatic carbons (C-C bond length: 1.41(2) Å). The shorter C-C bonds in Ph₂cod effectively close the cavity through which the HOMO on rhodium can attack the electrophile.

polymerizations which employ boratabenzene metal complexes as catalysts.

Experimental Section.

General.

The general considerations in the previous chapters apply. $\text{Cr}(\text{CO})_3(\text{MeCN})_3$ was prepared by the literature procedure.⁴⁹ Et_4NCN , MeI , MeOTf , and 1,3,5-trifluorobenzene were purchased from Aldrich and used as received. 1,2-bis(diphenylphosphino)ethane (dppe), $[(\text{cod})\text{RhCl}]_2$, $[(\text{nbd})\text{RhCl}]_2$, and $[(\text{ethylene})_2\text{RhCl}]_2$ were purchased from Strem Chemical Co. and used as received. $[(\text{nbd})_2\text{Rh}](\text{BF}_4)$ was purchased from Pressure Chemical Co. and recrystallized from $\text{CH}_2\text{Cl}_2/\text{Et}_2\text{O}$. $[(\text{cod})_2\text{Rh}](\text{OTf})$ was prepared by the literature procedure.⁵⁰ ^{13}C -labelled MeI was purchased from Cambridge Isotope Laboratories, while ^{13}C -labelled methyl triflate was purchased from Aldrich. *p*-Toluenesulfonic acid was purchased from Aldrich as the hydrate and dried by heating to 140 °C under vacuum (150 mTorr.) for four hours.⁵¹ Compound **33** was prepared by the literature procedure.⁵² ^{19}F NMR spectra were obtained at 288 MHz on a Varian Unity 300 spectrometer and referenced to external CF_3COOH (-76.54 ppm⁵³).

Synthesis of $(\text{BB-PMe}_3)\text{Cr}(\text{CO})_3$ (**14b**).

BB-PMe_3 (117 mg, 0.77 mmol) was placed in a vial and dissolved in CH_2Cl_2 (~10 mL). To this solution was added, in a slow stream, $\text{Cr}(\text{MeCN})_3(\text{CO})_3$ (200 mg, 0.77 mmol) in ~2 mL of CH_2Cl_2 , and the resulting homogeneous solution was immediately filtered through a Kimwipe. A ^{11}B NMR spectrum taken within 20 minutes of addition showed that the reaction was complete. The solvent was reduced to ~2 mL, and the solution was cooled to -35 °C. Large yellow crystals were collected (112 mg, 51% after one crystallization, and more product grew from mother liquors; the reaction is quantitative by NMR). X-ray quality crystals were grown

⁴⁹ Watkins, W. C.; Jaeger, T.; Kidd, C. E.; Fortier, S.; Baird, M. C.; Kiss, G.; Roper, G.; Hoff, C. D. *J. Am. Chem. Soc.* **1992**, *114*, 907-914.

⁵⁰ Schrock, R. R.; Osborn, J. A. *J. Am. Chem. Soc.* **1971**, *93*, 2397-2407.

⁵¹ Perrin, D. D.; Armarego, W. L. F. *Purification of Laboratory Chemicals*, 3rd ed.; Pergamon: Oxford, 1988; p 291.

⁵² a) Rabideau, P. W.; Hamilton, J. B.; Friedman, L. *J. Am. Chem. Soc.* **1968**, *90*, 4465-4466, and references therein. b) Chan, T. L.; Mak, T. C. W.; Poon, C.-W.; Wong, H. N. C.; Jia, J. H.; Wang, L. L. *Tetrahedron* **1986**, *42*, 655-661. c) Mak, T. C. W.; Wong, H. N. C.; Sze, K. H.; Book, L. *J. Organomet. Chem.* **1983**, *255*, 123-134.

⁵³ Bovey, F. A. *Nuclear Magnetic Resonance Spectroscopy*; 2nd ed.; Academic: San Diego, CA, 1988; p 438.

from cold (-35 °C) methylene chloride. Compound **14b** is air stable. $^1\text{H NMR}$ (300 MHz; CD_2Cl_2): δ 5.53 (m; 2H), 5.30 (t; $J = 5.8$; 1H), 4.42 (app t; 2H). $^{13}\text{C NMR}$ (125 MHz; CD_2Cl_2): δ 238.2, 103.3 (d; $J_{\text{Rh-C}} = 13.8$), 93.0 (br), 88.9, 10.4 (d; $J_{\text{C-P}} = 44.9$). $^{11}\text{B NMR}$ (96 MHz; CD_2Cl_2): δ +8.6 (d; $J_{\text{B-P}} = 140.3$). **IR** (KBr pellet): ν_{CO} : 1937, 1809. **mp.** it turns from yellow to brown at 171-180 °C before melting at 192-196 °C (dec). **HRMS** calcd for $\text{C}_{11}\text{H}_{14}\text{BCrO}_3\text{P}$: 288.0179; found: 288.0180. This compound was also characterized by X-ray crystallography; details are in Appendix II.

Synthesis of $(\text{BB-CN}^t\text{Bu})\text{Cr}(\text{CO})_3$ (**14c**).

$\text{Cr}(\text{CO})_3(\text{MeCN})_3$ (53.0 mg, 0.204 mmol) in 1.5 mL of CH_2Cl_2 was added dropwise to $\text{BB-CN}^t\text{Bu}$ (32.5 mg, 0.204 mmol) in 1.5 mL of CH_2Cl_2 . To this solution were added 3 mL of ether, and the solution was reduced to a total volume of 0.5 mL. A crystalline yellow product (35 mg, 58%) was isolated upon cooling to -35 °C overnight. $^1\text{H NMR}$ (300 MHz; THF-d_8): δ 5.39 (app t; 2H), 5.18 (t; $J = 6.2$; 1H), 4.50 (d; $J = 8.7$; 2H), 1.75 (s; 9H; overlaps with residual solvent). $^{13}\text{C NMR}$ (125 MHz; THF-d_8): δ 239.7, 104.6, 98.2 (br), 90.3, 64.8, 31.3. $^{11}\text{B NMR}$ (96 MHz; THF-d_8): δ +0.3. **IR** (KBr pellet): 2988, 2295 (CN), 1940 (CO), 1830 (CO), 1476, 1458, 1402, 1374, 1238, 1183, 930, 861, 808, 682, 635. **Anal.** calcd C: 52.92, H: 4.78; found C: 52.57, H: 4.62. This compound was also characterized by X-ray crystallography; details are in Appendix II.

Synthesis of $(\text{BB-NMe}_3)\text{Cr}(\text{CO})_3$ (**14d**).

The yield of this reaction was not optimized. BB-NMe_3 (23.7 mg, 0.176 mmol) was dissolved in 0.5 mL of CH_2Cl_2 . To this solution was added $(\text{MeCN})_3\text{Cr}(\text{CO})_3$ in 0.5 mL of CH_2Cl_2 . After filtration through an Acrodisc, ether (1 mL) and hexane were added (until cloudy) to the solution. Of the crystals that formed, a few were used to obtain the X-ray structure. The remaining crystals (6.5 mg, 14%) were characterized. $^1\text{H NMR}$ (300 MHz; THF-d_8): δ 5.42 (app t; 2H), 4.96 (t; $J = 6.0$; 1H), 4.04 (d; $J = 9$; 2H), 3.12 (s; 9H). $^{13}\text{C NMR}$ (125 MHz; THF-d_8): δ 238.4, 104.8, 85.5, 81.0 (br), 53.5. $^{11}\text{B NMR}$ (96 MHz; THF-d_8): δ +28.2. **IR** (KBr pellet): 3016, 1936 (CO), 1925 (CO), 1843 (CO), 1810, 1484, 1461, 1405, 1042, 958, 832, 684, 644. **mp.** >200 °C. **Anal.** calc'd for $\text{C}_{11}\text{H}_{14}\text{BCrNO}_3$ C: 48.75, H: 5.21; found C: 48.56, H: 4.98. This compound was also characterized by X-ray crystallography; details are in Appendix II.

Synthesis of $\text{Li}[(\text{C}_5\text{H}_5\text{BH})\text{Cr}(\text{CO})_3] \cdot \text{Et}_2\text{O}$ (**18a**).

A solution of $(C_5H_5B-PMe_3)Cr(CO)_3$ (117 mg, 0.406 mmol) in 5 mL of toluene was added to $LiAlH_4$ (15.4 mg, 0.406 mmol) in 0.5 mL toluene. Et_2O (~1 mL) was added to the mixture to help solubility. The solution was stirred for 40 minutes, at which time it was homogeneous. Stirring was stopped, and the solution was allowed to stand at room temperature for two days. From the reaction mixture yellow crystals grew, which were washed with hexane (70 mg, 59%). 1H NMR (300 MHz; THF- d_8): δ 5.28 (dd; J = 8.4, 6.4; 2H), 4.76 (t; J = 6.1; 1H), 3.97 (dd; J = 8.5, 4.4; 2H), 3.7 (v br; 1H), 3.38 (q; J = 7.0; 4H), 1.11 (t; J = 7.0; 6H). ^{13}C NMR (125 MHz; THF- d_8): δ 241.5, 106.7, 94.3 (br), 83.7, 66.5, 15.8. ^{11}B NMR (THF- d_8): δ +16.7. IR (KBr pellet): 2486 (B-H), 1911, 1807, 1750 (CO). mp. >195 °C dec. (at 127-129 °C there is a color change and at 180 °C it goes from lustrous to powdery). This compound was also characterized by its reaction with [2.2.1]-cryptand (see Chapter 5) and by X-ray crystallography; details are in Appendix II.

Synthesis of $(Et_4N)[(BB-CN)Cr(CO)_3]$ (18b).

$(BB-PMe_3)Cr(CO)_3$ (33.3 mg, 0.115 mmol) was dissolved in ~2 mL of THF. To this was added Et_4NCN (18.1 mmol, 0.115 mmol) dissolved in minimal THF. The resulting suspension was stirred at reflux in a sealed tube for 6 hours. The resulting clear yellow solution was dried and dissolved in THF (~700 μ L), ether (~500 μ L), and benzene (~200 μ L), and the ensuing homogeneous solution was cooled to -35 °C. Yellow crystals formed (37.9 mg, 90%). 1H NMR (300 MHz; $CDCl_3$): δ 5.27 (dd; J = 9.3, 6.0; 2H), 4.88 (tt; J = 6.0, 1.0; 1H), 4.12 (dd; J = 9.3, 1.2; 2H), 3.35 (q; J = 7.2; 8H), 1.32 (t; J = 5.6; 12H). ^{13}C NMR (125 MHz; $CDCl_3$): δ 239.6, 132.0 (v br; CN), 104.3, 94.0 (br), 85.5, 53.2 (t; J_{C-N} = 3.1 Hz), 7.8. ^{11}B NMR (96 MHz; $CDCl_3$): δ +7.8. IR (KBr pellet): 2985, 2203 (CN), 1934 (CO), 1916 (CO), 1805 (CO), 2486, 1174, 997, 788, 683, 640. mp. 78-79 °C. Anal. Calcd C: 55.40; H: 6.84. Found C: 55.19; H: 6.84. This compound was also characterized by X-ray crystallography; details are in Appendix II.

Synthesis of $[(BB-py)Rh(nbd)](BF_4)$ (19a).

$[(nbd)_2Rh](BF_4)$ (134 mg, 0.358 mmol) in ~1 mL of CH_2Cl_2 was added dropwise to BB-py (55.5 mg, 0.358 mmol) in ~2 mL of CH_2Cl_2 . Crystals were obtained by adding ~2 mL of ether and cooling to -35 °C (120 mg, 77%). The first crop was recrystallized from $CDCl_3$ /ether to yield 93.9 mg (60%) of pure product. 1H NMR (500 MHz; $CDCl_3$): δ 9.03 (d; J = 4.0; 2H), 8.43 (t; J = 8.0; 1H), 8.14 (d; J = 6.0; 2H), 6.44 (dd; J = 10.0, 6.0; 2H), 5.92 (d; J = 9.0; 2H), 5.72 (td; J = 6.0, 1.0; 1H), 3.62 (q; J = 2.0; 4H), 3.32 (m; 2H), 1.01 (t; J = 2; 2H). ^{13}C NMR (75 MHz; $CDCl_3$): δ 145.5, 145.0, 128.3, 107.6 (d; J = 3.3), 94.5

(br), 91.1 (d; $J = 4$), 58.1 (d; $J = 6$), 46.5, 38.6 (d; $J = 8.7$). **^{11}B NMR** (96 MHz; CDCl_3): δ +20.5. **IR** (KBr pellet): 3072, 3013, 2954, 2923, 1630, 1494, 1476, 1464, 1404, 1308, 1188, 1064.

Synthesis of [(BB-PMe₃)Rh(nbd)](BF₄) (19b).

[(nbd)₂Rh](BF₄) (360 mg, 0.963 mmol) in ~12 mL of CH_2Cl_2 was added dropwise over ~20 minutes to BB-PMe₃ (146 mg, 0.963 mmol) dissolved in ~1 mL of CH_2Cl_2 . The resulting yellow solution was stirred for 2 h and filtered through an Acrodisc. Et₂O (~3 mL) was added, resulting in the formation of yellow crystals, which were collected and dried (316 mg, 76% yield). **^1H NMR** (300 MHz; CDCl_3): δ 6.30 (m; 2H), 6.02 (t; $J = 5.7$; 1H), 5.78 (d; $J = 7.7$; 2H), 3.71 (m; 4H), 3.33 (m; 2H), 1.84 (d; $J = 12.5$; 9H), 1.06 (s, 4H). **^{13}C NMR** (75 MHz; CDCl_3): δ 106.5 (dd; $J = 12.0, 3.0$), 102.0 (br), 93.9, 58.4 (d; $J = 6.0$), 46.3 (d; $J = 2.0$), 36.9 (d; $J = 10.0$), 9.3 (d; $J = 46.0$). **^{11}B NMR** (96 MHz; CDCl_3): δ +11.3. **^{31}P NMR** (122 MHz; CDCl_3): δ -18 (br d). **IR** (KBr pellet): 2992, 2931, 1428, 1311, 1299, 1172, 1051, 956, 868. **mp.** 140-142 °C. **Anal.** calcd C: 41.53, H: 5.11; found C: 41.43, H: 5.06. This compound was also characterized by X-ray crystallography; the details are in Appendix II.

Synthesis of [(BB-NMe₃)Rh(cod)](OTf) (19c).

[(cod)₂Rh]OTf (66.6 mg; 0.142 mmol) was dissolved in ~1 mL of CH_2Cl_2 and added dropwise to BB-NMe₃ (19.2 mg; 0.142 mmol) in ~1 mL of CH_2Cl_2 with stirring. To the resulting yellow solution was added ether (~0.5 mL), and the total volume of the solvent was reduced to ~0.5 mL. At this point, ether was added until the solution became cloudy, and to this suspension was added 2-3 drops of CH_2Cl_2 . The resulting clear and colorless solution was cooled to -35 °C. The resulting slightly impure yellow crystals were washed with ether and dried (59.8 mg, 85%). Recrystallization from CH_2Cl_2 /ether yielded 45.7 mg of the desired product (65%). **^1H NMR** (300 MHz; CDCl_3): δ 6.15 (dd; $J = 8.9, 5.9$; 2H), 5.98 (t; $J = 6.0$; 1H), 5.32 (d; $J = 8.9$; 2H), 4.23 (br s; 4H), 3.26 (s; 9H), 2.25 (m; 4H), 2.03 (m; 4H). **^{13}C NMR** (125 MHz; CDCl_3): δ 108.0 (d; $J = 2.8$), 94.5, 90.8 (br), 72.0 (d; $J = 12.8$), 53.8, 31.8. **^{11}B NMR** (96 MHz; CDCl_3): δ +26.6. **^{19}F NMR** (282 MHz; CDCl_3): δ -79.4. **IR** (KBr pellet): 2984, 2943, 2872, 2840, 1481, 1466, 1412, 1271 (OTf), 1224, 1140, 1031, 960, 881, 834, 812, 752. **Anal.** Calcd, C: 41.24; H: 5.29. Found, C: 41.00; H: 5.14. The ^1H NMR spectrum of this compound is the same as the one resulting from treatment of the iodide (**22**) with AgOTf in CDCl_3 .

Synthesis of (BB-NMe₂)Rh(cod) (20a).

Li(BB-NMe₂) (21.6 mg, 0.170 mmol) was dissolved in 1 mL of THF and added to [(cod)RhCl]₂ (42 mg, 0.085 mmol) in 1 mL of THF. After stirring for 2 h, the solvent was evaporated and the resulting yellow solid was sublimed, affording 33.2 mg of yellow product (59%). ¹H NMR (300 MHz; CDCl₃): δ 6.08 (dd; J = 9.3, 6.0; 2H), 4.90 (d; J = 9.3; 2H), 4.67 (m; 1H); 4.05 (br s; 4H), 2.70 (s; 6H), 2.12 (m; 4H), 1.95 (m; 4H). ¹³C NMR (75 MHz; CDCl₃): δ 108.7 (d; J = 3.2), 90.3 (br s), 80.6, 67.1 (d; J = 12.7), 38.6, 32.1. ¹¹B NMR (96 MHz; CDCl₃): δ +21.6. IR (KBr pellet): 2988, 2904, 2832, 2814, 1514, 1415, 1349, 1120, 787, 634. mp. 99-101 °C. HRMS calc: 331.0979; found: 331.0978. This compound was also characterized by X-ray crystallography; the details are in Appendix II.

Synthesis of (BB-OMe)Rh(cod) (20b).

Na(BB-OMe) (16.6 mg, 0.128 mmol) was dissolved in 0.5 mL of THF and added to [(cod)RhCl]₂ (31.5 mg, 0.0639 mmol). A cloudy orange solution resulted, which was allowed to stir for 3 hours before being filtered through an Acrodisc. The solvent was removed, providing a brown oil, which was loaded onto a column and eluted with hexane and then ether. Two yellow bands formed, of which only the fast-moving one was collected and rechromatographed, providing 28.4 mg (67%) of a slightly impure yellow solid. This was sublimed at 90 °C (0.1 Torr) to yield 19.8 mg (46%) of a crystalline yellow solid which passed analysis after standing in air for 3 months. A second experiment yielded 57% of clean product. ¹H NMR (300 MHz; C₆D₆): δ 5.89 (dd; J = 9.3, 5.7; 2H), 5.16 (d; J = 8.7; 2H), 4.34 (t; J = 9.2; 1H), 4.05 (s; 4H), 3.58 (s; 3H), 2.06 (m; 4H), 1.85 (m; 4H). ¹³C NMR (125 MHz; C₆D₆): δ 110.0, 93.5 (br), 83.0, 68.3 (d; J = 12.5), 52.9, 32.4. ¹¹B NMR (96 MHz; C₆D₆): δ +19.4. IR (KBr pellet): 2986, 2938, 2880, 2833, 1502, 1454, 1398, 1322, 1242, 1136, 1026, 872, 796, 640, 484. mp. 91-93 °C. Anal. Calcd for C₁₄H₂₀BORh: C, 52.87; H, 6.34. Found: C, 53.15; H, 6.44. This compound was also characterized by X-ray crystallography; the details are in Appendix II.

Synthesis of (BBH)Rh(cod) (20c).

See Chapter 5.

Synthesis of (BB-OMe)Rh(nbd) (20d).

BB-PMe₃ (258 mg, 1.70 mmol) was dissolved in 3 mL of THF and added to NaOMe (91.6 mg, 1.70 mmol). The suspension was refluxed overnight in a sealed tube, after which time the volatiles were removed in vacuo (to remove PMe₃), and

the resulting white solid was redissolved in 3 mL of THF. To this solution was added [(nbd)RhCl]₂ (391 mg, 0.848 mmol) dissolved in 5 mL of THF. The resulting orange solution was refluxed for 1 h, and the solvent was removed. The residue was chromatographed (5% Et₂O/pentane; silica gel), providing 253 mg (49%) of a yellow oil (**20d**). ¹H NMR (300 MHz; CDCl₃): δ 6.13 (m; 2H), 4.97 (m; 3H), 3.52 (s; 3H), 3.48 (br s; 4H), 3.27 (s; 2H), 0.97 (s; 2H). ¹³C NMR (75 MHz; CDCl₃): δ 107.4 (d; J = 3.9), 88.3 (br s), 82.5 (d; J = 4.0), 57.7 (d; J = 6.2), 53.0, 46.7, 34.9. ¹¹B NMR (96 MHz; CDCl₃): δ +24.5. IR (CDCl₃ solution): 2998, 2902, 2831, 1467, 1406, 1383, 1242, 1096. HRMS calc (C₁₃H₁₆BORh): 302.0349; found: 302.0350.

Synthesis of [(BB-N(¹²CH₃)₂(¹³CH₃))Rh(cod)] I (**22a**).

(BB-NMe₂)Rh(cod) (**20a**; 7.1 mg, 0.021 mmol) was dissolved in 0.5 mL of Cl₂CDCDCl₂. To this solution was added ¹³CH₃I (13.4 μL, 0.214 mmol). After 4 h, ¹H and ¹³C NMR spectroscopy showed that the reaction was complete. The spectra are almost identical with those of **19c**, except that the peak at δ 2.72 ppm had become a dd (J = 142.8, 3.7), while for the unlabelled material this peak was a singlet. A single crystal grew from diffusing ether into the reaction mixture. Its X-ray structure is in Appendix II.

NMR Yield of (BB-OTf)Rh(cod) (**25**).

(BB-OMe)Rh(cod) (10.6 mg, 0.033 mmol) was dissolved in CDCl₃ (~0.8 mL). To this solution was added 1,3,5-trifluorobenzene (3.4 μL, 4.4 mg, 0.033 mmol) and MeOTf (18.9 mL, 27.3 mg, 0.167 mmol; 5 equiv.). ¹H and ¹⁹F NMR spectra were taken immediately with the ratios below:

resonances	ratio
meta BB/C ₆ H ₃ F ₃	1.04
cod/C ₆ H ₃ F ₃	6.63

Initial ratios, ¹H NMR.

resonances	ratio	yield
meta BB/C ₆ H ₃ F ₃	0.89	86%
cod/C ₆ H ₃ F ₃	4.64	70%

Final ratios, ¹H NMR.

The reaction mixture was heated to 70 °C, and the following spectra were

obtained, suggesting a level of conversion as high as 80-90%.

resonances	ratio
OTf/C ₆ H ₃ F ₃	0.16

Initial ratios ¹⁹F NMR.

resonance	ratio	yield
OTf/C ₆ H ₃ F ₃	0.14	88%

Final ratios ¹⁹F NMR.

A similar experiment was performed employing 29.5 mg (0.928 mmol) of (BB-OMe)Rh(cod) and 52.5 μ L (76.1 mg, 0.463 mmol) of MeOTf. Removal of the solvent resulted in 40.0 mg (99%) of crude compound, the ¹H NMR spectrum of which (300 MHz, CDCl₃) is included below. IR (KBr pellet) ν_{OTf} : 1383 cm⁻¹. There is debate in the literature as to whether ¹⁹F NMR chemical shifts can be used to determine the presence of a bound triflate, but there is agreement that IR stretching frequencies for the triflates are diagnostic.⁵⁴ Nevertheless, in this case NMR and IR are both consistent with the presence of a bound triflate. A clean chemical ionization mass spectrum revealed the presence of a M⁺ peak at e/z = 436 amu. HRMS (EI) calcd: 435.9999; found: 435.9998. All attempts at crystallizing this compound for purification or an X-ray structure have been unsuccessful.

Synthesis of (BB-OTf)Rh(nbd) (26a).

(BB-OMe)Rh(nbd) (**20d**; 247 mg, 0.818 mmol) dissolved in 1.3 mL of CDCl₃ was added MeOTf (92.5 μ L, 0.818 mmol). The orange solution was refluxed for 35 minutes, after which time a ¹H NMR spectrum showed that the reaction was complete. The solvent was removed in vacuo to quantitatively afford a green solid (a similar experiment with toluene as internal standard shows that the reaction proceeds with an 84% NMR yield). ¹H NMR (300 MHz; CDCl₃): δ 6.31 (dd; J = 9.0, 6.0; 2H), 5.54 (d; J = 8.4; 2H), 5.19 (t; J = 5.8; 1H), 3.70 (d; J = 2.1; 4H), 3.32 (s; 2H), 1.06 (t; J = 1.4; 2H). ¹³C NMR (125 MHz; CDCl₃): δ 107.6, 92.8 (br), 86.4, 58.1 (d; J = 6.9), 46.6, 37.2. ¹¹B NMR (96; CDCl₃): δ +23.2. ¹⁹F NMR (288 MHz; CDCl₃): δ -77.5. IR (KBr pellet): 3004, 2952, 2844, 1498, 1475, 1391 (OTf), 1304, 1249, 1203, 1150, 1060, 949, 803, 620. HRMS calc (C₁₃H₁₃BF₃O₃RhS): 419.9686; found: 419.9687.

⁵⁴ Lawrance, G. A. *Chem. Rev.* **1986**, *86*, 17-33.

Synthesis of [(BB-py)Rh(nbd)](OTf) (27).

Pyridine (14.0 μ L, 0.173 mmol) was added slowly to a burgundy solution of (BB-OTf)Rh(nbd) (**26a**; 65.1 mg, 0.149 mmol) in 0.5 mL of CD_2Cl_2 . There was an immediate color change to a greenish orange. ^1H , ^{13}C , ^{19}F , and ^{11}B NMR spectra taken after 1 h showed complete conversion to **27**. A few drops of benzene were added to this solution, as well as hexane until cloudy. After cooling to $-35\text{ }^\circ\text{C}$ overnight, large yellow crystals of **27** (43.0 mg, 58 %) resulted. NMR shows that the conversion in this reaction is quantitative (102%, toluene as internal standard). ^1H NMR (300 MHz; CD_2Cl_2): δ 9.02 (m; 2H), 8.51 (tt; $J = 7.5, 1.4$; 1H), 8.14 (m; 2H), 6.53 (dd; $J = 8.7, 6.3$; 2H), 5.93 (d; $J = 8.4$; 2H), 5.81 (t; $J = 6.0$; 1H), 3.68 (m; 4H), 3.38 (m; 2H), 1.09 (s; 2H). ^{13}C NMR (125 MHz; CD_2Cl_2): δ 146.0, 145.7, 128.7, 108.2 (d; $J = 3.0$), 95.2 (br s), 91.9 (d; $J = 3.0$), 58.7 (d; $J = 6.5$), 47.2 (d; $J = 1.9$), 39.2 (d; $J = 9.0$). ^{11}B NMR (96 MHz; CD_2Cl_2): δ +21.6. ^{19}F NMR (288 MHz; CD_2Cl_2): δ -80.3. IR (KBr pellet): 3115, 3047, 3021, 2944, 2915, 2815, 1626, 1495, 1474, 1462, 1413, 1260 (OTf), 1224, 1179, 1150, 1028, 823, 781, 693, 635. Anal. Calcd, C: 43.32 H: 3.64. Found, C: 43.38; H: 3.53. The X-ray structure of this compound is in Appendix II.

Synthesis of [(BB-PMe₃)Rh(nbd)](OTf) (28).

Trimethylphosphine (12.1 μ L, 0.117 mmol) was added dropwise as a solution in 1 mL of CH_2Cl_2 to (BB-OTf)Rh(nbd) (**26a**; 46.3 mg, 0.106 mmol) in 2 mL of CH_2Cl_2 . There was an immediate color change to yellow. Benzene (\sim 0.1 mL) was added, followed with hexane until cloudy. Because no crystals had formed overnight, but rather an oil, benzene (\sim 1 mL) was added, followed by enough CH_2Cl_2 to make the solution homogeneous, and enough ether to make the solution cloudy again. Cooling to $-35\text{ }^\circ\text{C}$ overnight resulted in the formation of crystalline yellow **28** (35.0 mg, 64%). NMR shows that the yield in this reaction is 90% (toluene as internal standard). ^1H NMR (300 MHz; CD_2Cl_2): δ 6.37 (br s; 2H), 6.13 (triplet of multiplets; $J = 6.2$; 1H), 5.77 (m; 2H), 3.75 (m; 4H), 3.37 (m; 2H), 1.85 (d; $J = 12.3$; 9H), 1.13 (t; $J = 1.6$; 2H). ^{13}C NMR (125 MHz; CD_2Cl_2): δ 107.2 (dd; $J = 11.9, 3.0$), 107.7 (br s), 94.8, 58.8 (d; $J = 6.0$), 46.9 (d; $J = 1.9$), 37.6 (d; $J = 9.6$), 10.1 (d; $J = 45.9$). ^{11}B NMR (96 MHz; CD_2Cl_2): δ +10.5 (d; $J = 136.4$). ^{31}P NMR (121 MHz; CD_2Cl_2): δ -16.8 (br d; $J = \sim 145$). ^{19}F NMR (288 MHz; CD_2Cl_2): δ -80.1. IR (KBr pellet): 3004, 2962, 2923, 1493, 1470, 1428, 1404, 1388, 1304, 1264 (OTf), 1225, 1140, 1031, 958, 867, 812, 790, 764, 752, 636, 570, 516. The X-ray structure of this compound is in Appendix II.

Reaction of (BB-OTf)Rh(nbd) (26a) with NaOMe to yield (BB-OTf)Rh(nbd), 20d.

(BB-OTf)Rh(nbd) (**26a**; 25.9 mg, 0.0594 mmol) was dissolved in \sim 1 mL of THF and

immediately added to NaOMe (3.2 mg, 0.0594 mmol). The burgundy suspension was stirred very efficiently for 2 h. The resulting yellow solution was extracted (5% Et₂O/water) and dried. The resulting orange oil was subjected to column chromatography on silica (1% Et₂O in pentane → 4% Et₂O in pentane), yielding 11 mg of the oily yellow (BB-OMe)Rh(nbd) (**20d**).

Synthesis of (BB-OTs)Rh(cod) (**30**).

p-Toluenesulfonic acid (45.0 mg, 0.261 mmol) was stirred for 10 minutes in 3 mL of CH₂Cl₂ with 4Å molecular sieves. To this was added (BB-OMe)Rh(cod) (**20b**; 55.4 mg, 0.174 mmol) in 2 mL CH₂Cl₂, and the resulting suspension was stirred overnight. The solubles were filtered, dried, washed with ether, and dried again, resulting in 45.5 mg (57 %) of **30**. ¹H NMR (500 MHz; CD₂Cl₂): δ 7.84 (d; J = 9.0; 2H), 7.35 (d; J = 8.5; 2H), 6.30 (dd; J = 9.5, 6.0; 2H), 5.47 (d; J = 8.5; 2H), 4.98 (t; J = 5.8; 1H), 4.23 (br s; 4H), 2.45 (s; 3H), 2.15 (m; 4H), 2.00 (m; 4H). ¹³C NMR (125 MHz; CD₂Cl₂): δ 144.4, 137.1, 130.1, 127.6, 110.2 (d; J = 3.0), 96.3 (br s), 86.5, 71.0 (d; J = 12.0), 32.4, 21.8. ¹¹B NMR (96 MHz; CD₂Cl₂): δ +22.3. IR (KBr pellet) 2934, 2870, 2830, 1500, 1402, 1344, 1177, 1085, 895, 802, 714, 660, 548. HRMS calcd (C₂₀H₂₄BO₃RhS): 458.0594; found: 458.0592. The X-ray structure of this compound is in Appendix II.

Synthesis of [(Ph₂cod)RhCl]₂ (**34**).

Ph₂cod (**33**; 88.3 mg; 0.432 mmol) and [(ethylene)₂RhCl]₂ (84.1 mg, 0.216 mmol) were both dissolved in minimal CH₂Cl₂, mixed, filtered, shaken, and allowed to stand. After 15 minutes the solution started to become cloudy. After the solution had been standing overnight, solid **34** was collected and dried (72.4 mg, 48%). ¹H NMR (300 MHz; DMSO-d₆): δ 7.00 (m; 8H), 5.02 (br s; 4H). This compound was not soluble enough in DMSO-d₆ to measure its ¹³C NMR spectrum in 15 hours. IR (KBr pellet): 2990, 1490, 1399, 1376, 1251, 1105, 982, 940, 828, 747, 663, 562, 490. HRMS calcd (C₃₂H₂₄Rh₂Cl₂): 683.9365; found: 683.9363.

Synthesis of (BB-OMe)Rh(Ph₂cod) (**35**).

BB-PMe₃ (41.4 mg, 0.272 mmol) was mixed with NaOMe (15.7 mg, 0.292 mmol) in 1.5 mL of THF and heated to 80 °C for 4 hours. The volatiles were evaporated, and the resulting white solids were dissolved in 4 mL of THF and added to [(Ph₂cod)RhCl]₂ (**34**; 66.6 mg, 0.0972 mmol) in ~1 mL of THF. The solution was stirred overnight and then extracted (water/CH₂Cl₂). The solvent was removed from the dried (MgSO₄) organic layer in vacuo, to afford **35** as a yellow solid (67 mg, 84%). ¹H NMR (500 MHz; CDCl₃): δ 6.84 (m; 8H), 6.46 (dd; J = 9.5, 5.5; 2H), 5.38 (d; J =

9.0; 2H), 4.95 (d; J = 2.5; 4H), 4.88 (t; J = 5.8; 1H), 3.66 (s; 3H). ^{13}C NMR (125 MHz; CDCl_3): δ 145.9, 127.2, 126.4, 112.1 (d; J = 3.4), 96.2 (br s), 83.7 (d; J = 3.8), 70.2 (d; J = 12.4), 53.6. ^{11}B NMR (96 MHz; CDCl_3): δ +24.4. IR (KBr pellet): 3006, 2830, 1578, 1508, 1489, 1458, 1402, 1254, 1136, 1028, 854, 826, 802, 754, 641, 561. HRMS calcd ($\text{C}_{22}\text{H}_{20}\text{BORh}$): 414.0662; found: 414.0662. The X-ray structure of this compound is in Appendix II.

Synthesis of (BB-OMe)Rh(dppe).

BB-PMe₃ (81.3 mg, 0.535 mmol) was mixed with NaOMe (28.9 mg, 0.535 mmol) in 3 mL of THF, stirred at reflux for 4 hours, stripped of volatiles, and redissolved in 3 mL THF to give a solution of Na(BB-OMe). Dppe (213 mg, 0.535 mmol) and [(ethylene)₂RhCl]₂ (104 mg, 0.268 mmol) were mixed in 3 mL of THF and stirred for 10 minutes, resulting in gas evolution. The resulting solution was slowly added to the Na(BB-OMe) solution and stirred for 18 hours. The resulting solution was filtered (Acrodisc) and dried, resulting in a yellow solid that was extracted with benzene. The extracts were filtered, and hexane was added. The solution was reduced to ~2 mL, at which point crystals started forming. Hexane (~2 mL) was added, resulting in the formation of additional crystals. The mother liquors were decanted and the solids were dried to afford **37** (78.4 mg, 37%). ^1H NMR (300 MHz; CDCl_3): δ 7.64 (m; 8H), 7.36 (m; 12H), 5.99 (dd; J = 9.2, 5.8; 2H), 4.97 (d; J = 8.9; 2H), 4.68 (t; J = 5.4; 1H), 3.10 (s; 3H), 2.02 (d; J = 19.8; 4H). ^{11}B NMR (96 MHz; CDCl_3): δ +25.0. ^{31}P NMR (121 MHz; CDCl_3): δ +75.4 (d; J = 124.6). IR (KBr pellet): 3000, 2827, 1500, 1432, 1399, 1239, 1132, 1095, 811, 744, 695, 526, 488. HRMS calcd ($\text{C}_{32}\text{H}_{32}\text{BOP}_2\text{Rh}$): 608.1076; found: 608.1079. The X-ray structure of this compound is in Appendix II.

Methylation of **37**.

(BB-OMe)Rh(dppe) (**37**; 16.5 mg, 0.027 mmol) was dissolved in ~0.5 mL of CDCl_3 . To this solution was added $^{13}\text{CH}_3\text{I}$ (1.7 μL , 0.027 mmol). A ^{13}C NMR spectrum, as well as a ^1H NMR spectrum, obtained within ~25 minutes clearly showed the formation of a Rh- $^{13}\text{CH}_3$ bond. In the same amount of time, the reaction of (BB-OMe)Rh(dppe) (**37**; 13.0 mg, 0.214 mmol) with 1 equivalent of ^{13}C -labelled MeOTf (2.4 μL , 3.5 mg) showed complete conversion to the same product. ^1H NMR (300 MHz; CDCl_3): δ -0.10 (doublet of broad triplets; J = 139.5, 4.4). ^{13}C NMR (75 MHz; CDCl_3): δ -1.65 ppm; dt; J = 20.0, 7.0.

Chapter 5: The Chemistry of 1-*H*-boratabenzene, BBH.

In Chapter 3 we described the synthesis and briefly discussed structural studies of the parent boratabenzene, 1-*H*-boratabenzene. This molecule is of interest in the context of the study of basic questions regarding heteroaromaticity because, together with the pyridinium cation and with benzene, it completes an isoelectronic series (Figure 5.1). It is also interesting in the context of the development of new Cp-like ligands for transition metals. Clearly, 1-*H*-boratabenzene fits a very special niche, as it is isostructural with benzene, but a uninegatively charged six-electron donor like cyclopentadienide.

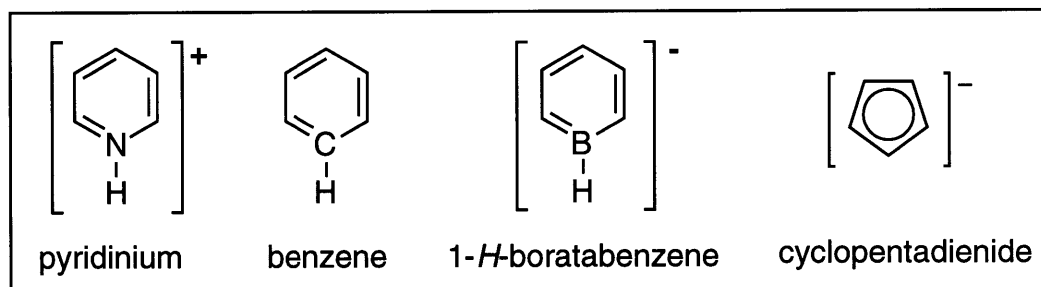
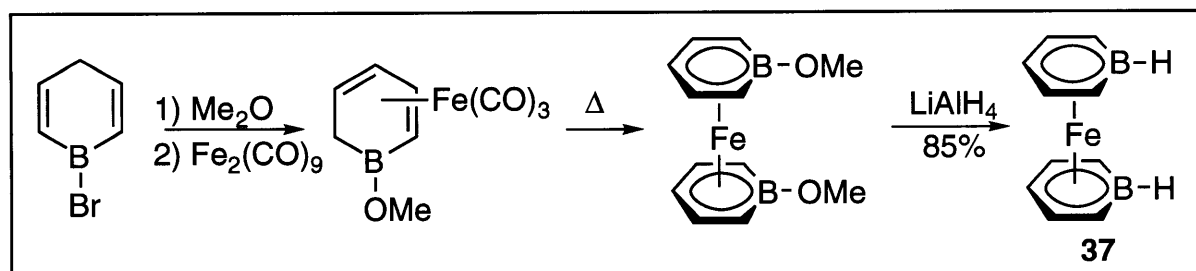


Figure 5.1. An Isoelectronic Series.



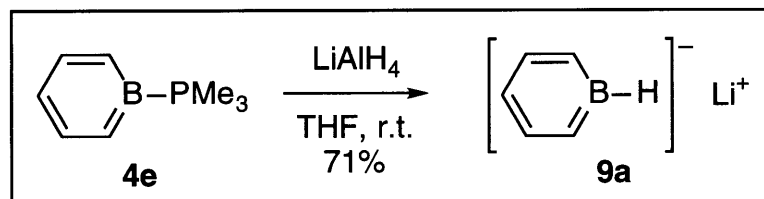
Scheme 5.1.

Prior to our work, the only experimental report involving 1-*H*-boratabenzene was a report by Ashe and co-workers that $(\text{BBH})_2\text{Fe}$ (**37**) could be prepared (Scheme 5.1) from LiAlH_4 reduction of $(\text{BB-OMe})_2\text{Fe}$.¹ Reactivity studies showed that $(\text{BBH})_2\text{Fe}$ reacts with a protic acid, CF_3COOH , to exchange deuterium into the ortho and para positions. The strong nucleophile BuLi displaced the hydride to afford a boron-bound butyl group. In spite of the considerable attention paid to the study of

¹ Ashe, A. J., III; Butler, W.; Sandford, H. F. *J. Am. Chem. Soc.* **1979**, *101*, 7066-7067.

other 1-substituted boratabenzenes,² 1-*H*-boratabenzene has received very little attention since Ashe's report, except by theoreticians.³

Reaction of readily available BB-PMe₃ (**4a**)⁴ with LiAlH₄ results in clean (>95% by NMR) conversion to Li(BBH) (**9a**, Scheme 5.2).^{5,6} Its isolation is relatively straightforward because this compound can be crystallized from a THF/toluene/hexane mixture to afford very large crystals of the desired product.⁷



Scheme 5.2.

The lithium salt of 1-*H*-boratabenzene crystallizes in the monoclinic space group

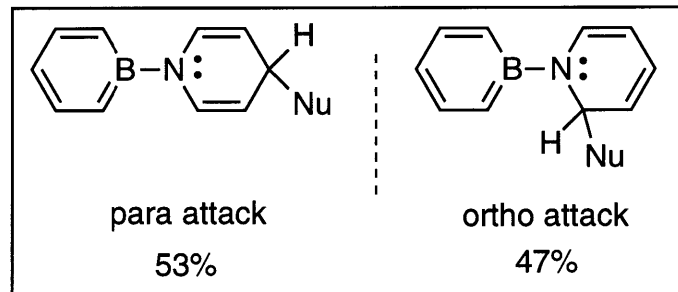
² Herberich, G. E.; Ohst, H. *Adv. Organomet. Chem.* **1986**, *25*, 199-236.

³ a) Kostic, N. M.; Fenske, R. F. *Organometallics* **1983**, *2*, 1319-1325. b) Clack, D. W.; Warren, K. D. *J. Organomet. Chem.* **1981**, *208*, 183-188, and earlier papers in this series.

⁴ Hoic, D. A.; Wolf, J. R.; Davis, W. M.; Fu, G. C. *Organometallics* **1996**, *15*, 1315-1518.

⁵ We have unsuccessfully attempted to reduce BB-PMe₃ using LiH, NaH, KH, LiBEt₃H, LiAl(OEt)₃H, L-, and LS-Selectride (Aldrich trademarks), Bu₄NBH₄, Bu₄NBH₃(CN), NaBH₃(CN), NaBH₄, and LiAl(*t*-Bu)₃H.

⁶ This reaction also works when NaAlH₄ is employed in place of LiAlH₄ and when BB-NEt₃ replaces BB-PMe₃. As was discussed in Chapter 3, the reaction cannot be effected using BB-py as a starting material because the hydride adds to the electrophilic 2 and 4 positions of the pyridine ring, instead of the boron center.



⁷ The aqueous workup usually employed in LiAlH₄ reductions (Fieser, L. F.; Fieser, M. *Reagents for Organic Synthesis*; Wiley: New York, 1967; p 583) cannot be used to isolate this compound, since it is air- and moisture-sensitive.

C₂/c, containing in the asymmetric unit one half of a metallocene anion⁸ balanced in charge by one half of a lithium cation tetrahedrally coordinated by 4 THF molecules (Figure 5.2). There are four asymmetric units per unit cell, as the molecule contains a crystallographically imposed center of symmetry. The position of the boron was established with the use of comparative thermal parameters.

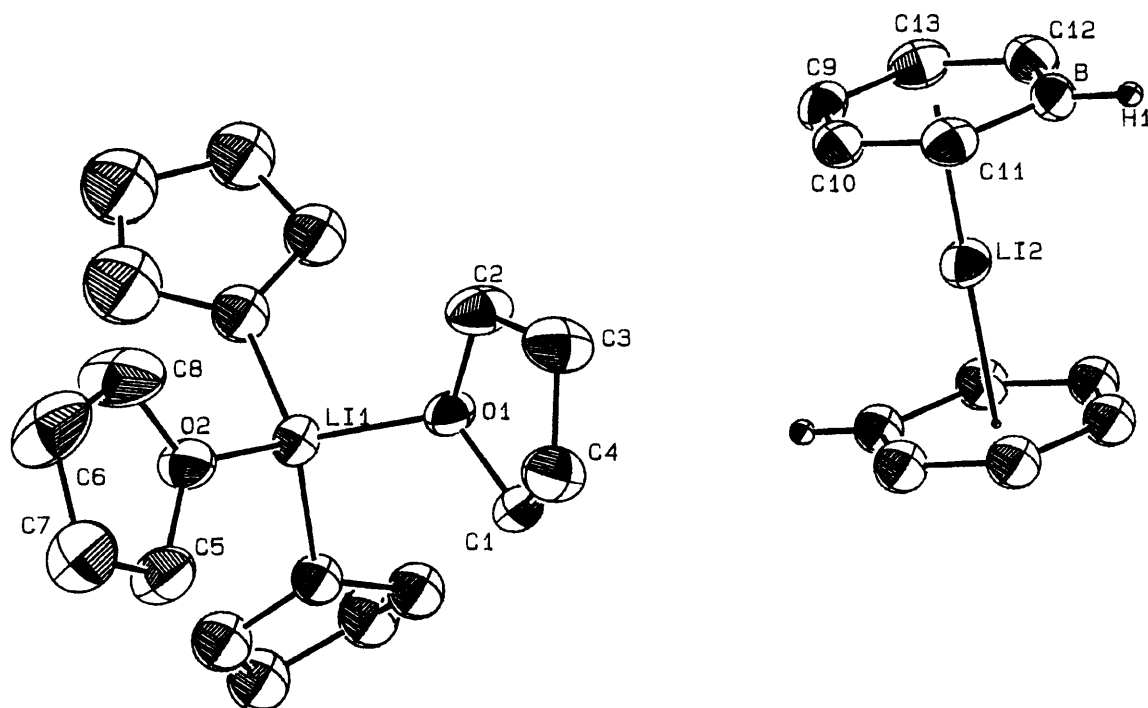


Figure 5.2. The Crystal Structure of $\text{Li}(\text{BBH})_2 \cdot \text{Li}(\text{THF})_4$.

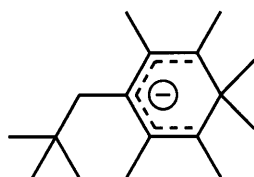
The boratabenzene fragment is planar, suggesting that it is aromatic. Consistent with aromaticity, the interatomic distances show negligible bond alternation at the 3σ level (C-C: 1.380(5) Å to 1.410(5) Å; C-B: 1.453(5) Å and 1.481(5) Å); the longer C-B bonds relative to C-C are probably due to the covalent radius of boron (0.82 Å) being larger than that of carbon (0.77 Å).⁹

If the metallocene structure were conserved in solution, two peaks around 0 (tetrahedral Li cation) and around -8 to -12 (metallocene) of approximately equal intensities should be observable in the ^7Li NMR spectrum. Such behavior has been

⁸ Stalke, D. *Angew. Chem., Int. Ed. Engl.* **1994**, *33*, 2168-2171.

⁹ Gordon, A. J.; Ford, R. A. *The Chemist's Companion*; Wiley: New York, 1972; pp 82-83.

documented by Fraenkel and coworkers, who studied the peralkylcyclohexadienyl lithium **38**.¹⁰ Compound **38** is a piano-stool at room temperature but a mixture of the piano-stool with the metallocene at $-65\text{ }^{\circ}\text{C}$. Their system was quite amenable to study, and they were able to determine kinetic and equilibrium constants for the dimer-monomer equilibrium by line-shape analysis.

**38**

The ^7Li NMR chemical shift for the half-sandwich **38**, -3.8 ppm , appears at lower-field than what is observed for Li-Cp, which is reasonable in light of the lower donicity of **38** vis-à-vis Cp.^{11,12,13} Other data has shown (vide infra) that (BBH)⁻ is generally less donating than Cp⁻, so we conclude that, with a temperature-dependent chemical shift between -2 and -4 ppm (Table 5.1), Li(BBH) is a monomeric contact ion pair (piano-stool) in THF-d₈.

The ^1H NMR resonance corresponding to the boron-bound hydride gets sharper as the solution becomes colder (Figure 5.3). If the variation of the line shape were due to the averaging of different states, one would expect the peak to sharpen at higher temperature. Instead, this behavior suggests that at low temperature the coupling between the proton and the quadrupole on boron becomes a less important mode of relaxation for the proton.

¹⁰ Fraenkel, G.; Hallden-Abberton, M. P. *J. Am. Chem. Soc.* **1981**, *103*, 5657-5664.

¹¹ A piano-stool Li-Cp has been encountered between -8.2 and -12.5 ppm : a) Jutzi, P.; Leffers, W.; Pohl, S.; Saak, W. *Chem. Ber.* **1989**, *122*, 1449-1456. b) Paquette, L. A.; Bauer, W.; Sivik, M. R.; Bühl, M.; Feigel, M.; Schleyer, P. v. R. *J. Am. Chem. Soc.* **1990**, *112*, 8776-8789.

¹² A piano stool with electron-withdrawing substituent has been observed at -5.6 ppm , and it undergoes an equilibrium to the metallocene-ate/lithium cation form: Eiermann, M.; Hafner, K. *J. Am. Chem. Soc.* **1992**, *114*, 135-140.

¹³ In the Li-Cp literature a separated ion pair, resonating in the neighborhood of -1 to -3 ppm , has also been observed: a) Cox, R. H.; Terry, H. W., Jr.; Harrison, L. W. *J. Am. Chem. Soc.* **1971**, *93*, 3297-3298. b) Cox, R. H.; Terry, H. W., Jr. *J. Magn. Res.* **1974**, *14*, 317-322.

temperature (°C)	chemical shift (ppm)
-93.3	-2.0
-60.5	-2.6
-32.6	-3.1
-15.5	-3.6
+20.6	-4.1

Table 5.1: Variable Temperature (VT) ^7Li NMR Study of Li(BBH).

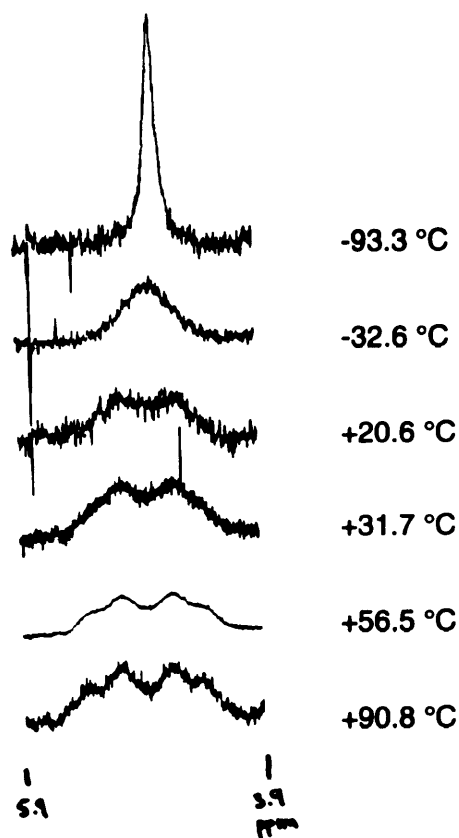


Figure 5.3. VT ^1H NMR Spectroscopy of the Boron-Bound Hydride.

Similar behavior had been previously observed for a number of cases in which there are hydrogen atoms that couple to quadrupoles, including molecules with more than one quadrupole, such as borazine.¹⁴ The physics behind this phenomenon received theoretical attention by Kubo's group, who showed that they

¹⁴ a) Mellon, E. K.; Coker, B. M.; Dillon, P. B. *Inorg. Chem.* **1972**, *11*, 852-857. b) Ito, K.; Watanabe, H.; Kubo, M. *J. Chem. Phys.* **1960**, *32*, 947-948.

could predict the shapes of the peaks employing a stochastic approach.¹⁵ The lineshape depends on a parameter called α , and this parameter is directly proportional to the quadrupole relaxation rate (p) divided by the coupling constant (J). It is quite remarkable that in the 180 degree difference of our experimental VT-NMR study we were able to clearly observe, for one molecule, all the different line shapes predicted by Kubo's theoretical work.

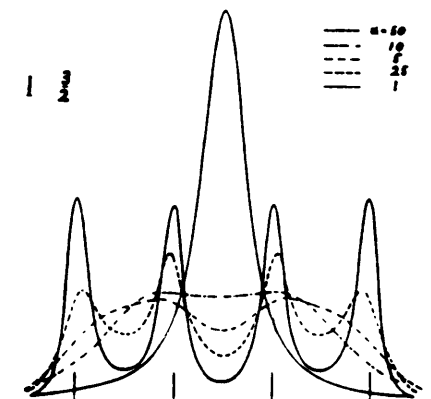


Figure 5.4. Theoretically Predicted VT ^1H NMR Spectra for Coupling Between a Nucleus with $I = 3/2$ and One with $I = 1/2$.¹⁶

Satisfied with our understanding of the structure of Li(BBH), we turned to a study of its reactivity. Because of the well-known tendency of B-H bonds to serve as hydride donors, we expected that it might serve as a reductant for organic functionalities.¹⁷ Indeed, Li(BBH) reduces aldehydes and epoxides to the corresponding alcohols, and it reacts with the isotopomers of water (H_2O , D_2O) to produce the corresponding isotopomers of dihydrogen (H_2 , D_2 , HD) (Scheme 5.3).

Unlike many other trivalent boron hydrides, Li(BBH) does not appear to add to an olefin, such as 1-dodecene, to afford the corresponding alkylborane.¹⁸ Furthermore, addition of the known hydroboration catalyst $\text{ClRh}(\text{PPh}_3)_3$

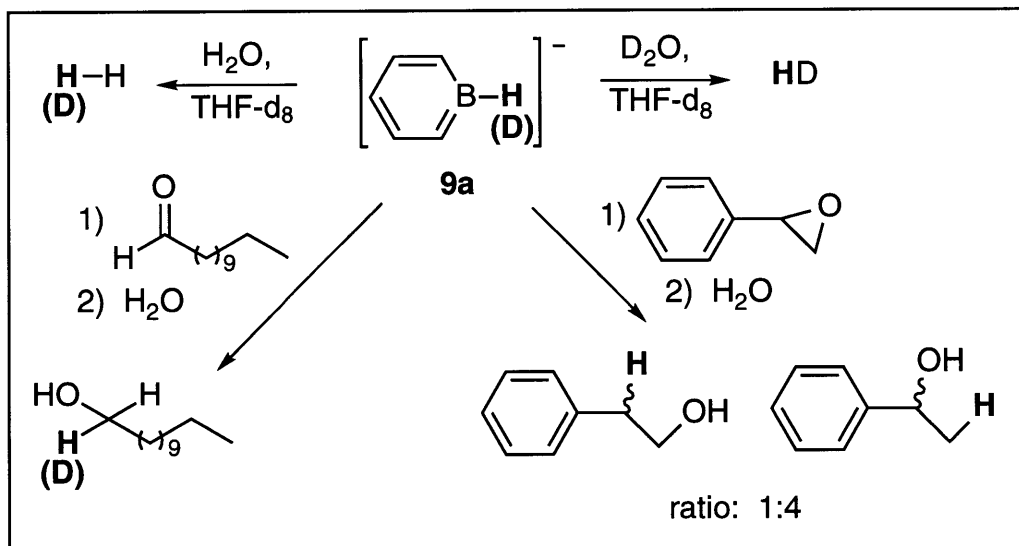
¹⁵ Suzuki, M.; Kubo, R. *Mol. Phys.* **1964**, *7*, 201-209.

¹⁶ Reproduced from reference 15 with permission from the publisher.

¹⁷ It should be pointed out that Ashe, in his original report, showed that $(\text{BBH})_2\text{Fe}$ reacts with CF_3COOD to incorporate up to 4 deuterium atoms in the bound heterocycle, but found no evidence for reaction at the boron-bound hydrogen.

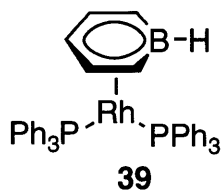
¹⁸ Smith, K.; Pelter, A. In *Comprehensive Organic Synthesis*; Trost, B. M., Ed.; Pergamon: New York, 1991; Vol. 8, Chapter 3.10.

(Wilkinson's catalyst)¹⁹ resulted in π -complexation of 1-*H*-boratabenzene to rhodium, rather than hydroboration.



Scheme 5.3.

The product is believed to be compound **39**, based on the ¹H NMR spectrum and precedent with cyclopentadienides.²⁰ Compound **39** could not be isolated, as it was unstable to the conditions employed for the isolation of its Cp analogue (chromatography on alumina), and it could not be crystallized from the reaction mixture.

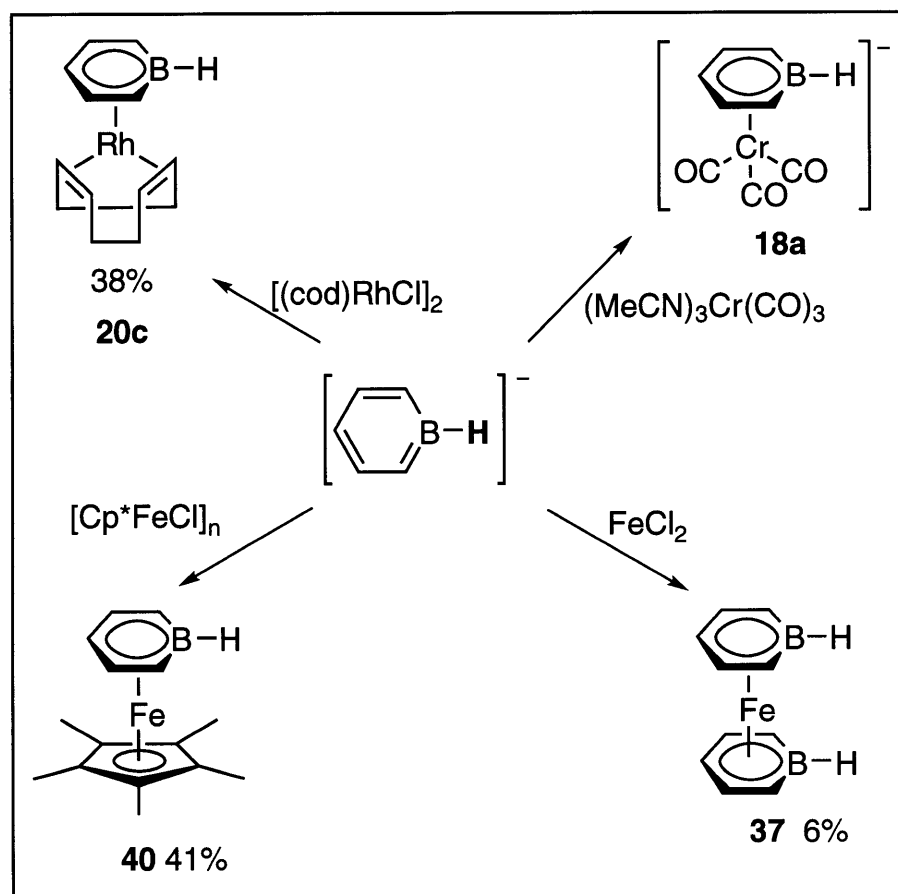


The reaction of Li(BBH) with Wilkinson's catalyst highlights the fact that BBH can react with a metal halide to form the corresponding (η^6 -BBH)M complex. This reaction is quite general, and it proceeds with several other transition metal electrophiles, such as [Cp*FeCl]_n, [(cod)RhCl]₂, and (MeCN)₃Cr(CO)₃ (Scheme 5.4),

¹⁹ a) Evans, D.A.; Fu, G. C.; Hoveyda, A. H. *J. Am. Chem. Soc.* **1992**, *114*, 6671-6679. b) Mannig, D.; Noth, H. *Angew. Chem., Int. Ed. Engl.* **1985**, *24*, 878-879.

²⁰ Wakatsuki, Y.; Yamazaki, H. *J. Organomet. Chem.* **1974**, *64*, 393-402.

although these reactions are not clean. We suspect that competitive reduction by Li(BBH) may be responsible for the side-reactions (the same metal halides cleanly form π -complexes when reacted with boratabenzenes where H is replaced by NMe₂ or OMe). More experimentation is needed in order to firmly establish this hypothesis.

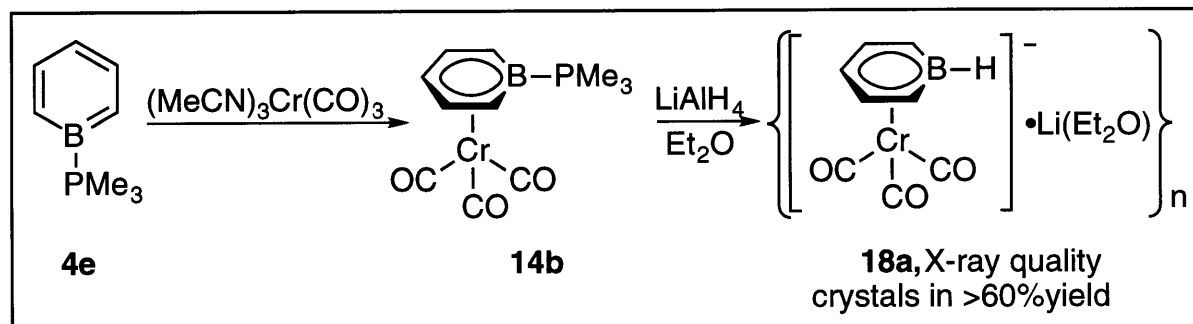


Scheme 5.4.

An alternative synthetic route (i.e., reduction of an *anionic* (boratabenzene)transition metal complex) had been employed in the Ashe synthesis of bis(borabenzene)iron (Scheme 5.1). We have found that the LiAlH_4 reduction of transition metal complexes of *neutral* borabenzenes, such as $(\text{BB-PMe}_3)\text{Cr}(\text{CO})_3$, is also viable (Scheme 5.5).

However, for the reduction on the metal to proceed, the ligand on the metal must be less reactive than the B-substituent bond. For example, $(\text{BBH})\text{Rh}(\text{diolenin})$ could not be prepared from either reduction of $(\text{BB-OEt})\text{Rh}(\text{cod})$ or $[(\text{BB-PMe}_3)\text{Rh}(\text{nbd})]\text{BF}_4$. Although less-versatile than the direct synthesis from the

reaction of transition metal electrophiles plus Li(BBH), the reduction route appears to be higher-yielding in certain instances.



Scheme 5.5.

The preparation of various transition metal complexes bearing π -complexed BBH as a ligand has allowed us to compare their properties to those of the corresponding complexes of benzene and Cp. Comparison of the high quality crystal structure of the unbound Li(BBH) with two high-quality crystal structures bearing $(\eta^6\text{-BBH})\text{M}$ (Table 5.4) shows that the intramolecular distances in the uncomplexed boratabenzene ring are not significantly different from those in the complexed ring. From the data, it follows that 1-*H*-boratabenzene does not become significantly distorted upon complexation to a transition metal.

	Li(BBH) ²¹	[(BBH)Cr(CO) ₃ Li • THF	[(BBH)Cr(CO) ₃ Li • [2,2,1] cryptand, 41	(BBH)Rh(cod) • 1/2 [(cod)RhCl] ₂
B-C1	1.453(5)	1.426(12)	1.503(6)	1.53(2)
C1-C2	1.389(5)	1.446(11)	1.395(4)	1.38(2)
C2-C3	1.388(5)	1.452(11)	1.370(4)	1.35(2)
C3-C4	1.380(5)	1.412(10)	1.379(5)	1.41(2)
C4-C5	1.410(5)	1.379(11)	1.376(5)	1.36(2)
C5-B	1.481(5)	1.446(12)	1.529(6)	1.48(2)

Table 5.4. Intramolecular Distances for 1-*H*-Boratabenzene.²²

²¹ The numbering scheme for the table is different than for the structure report: C1 should be C12; C2, C13; C3, C9; C4, C10; C5, C11. B remains B.

²² The position of the boron in these structures was located through the use of comparative thermal parameters.

From the the chemistry of 1-substituted boratabenzenes,²³ 1-*H*-boratabenzene is expected to be electron deficient vis-à-vis cyclopentadienide. To illustrate this point, Table 5.5 shows the results of an electrochemical study²⁴ of the family (BBH)FeL,²⁵ where L is Cp, Cp*, or BBH. It is clear from the data that complexes bearing BBH as a ligand are harder to oxidize than those bearing Cp.²⁶ Therefore, BBH is, as expected, less electron-rich than Cp.

iron complex		oxidation potential (V)
	40	+0.316
	42	+0.487
	37	+0.805

Table 5.5. Cyclic Voltammetry of Various Fe(BBH) Compounds.

²³ Reference 2.

²⁴ We gratefully acknowledge Rich Kingsborough, from the Swager group, who determined these values for us.

²⁵ A similar study of *substituted* boratabenzenes has been carried out for methyl- and phenyl- substituted bis(boratabenzene)iron complexes: Koelle, U. J. *Organomet. Chem.* **1978**, *157*, 327-334. In their case, the oxidations were reversible.

²⁶ Ferrocene was used as an internal and external reference (+ 0.138 V under our conditions): Gagne, R. R.; Koval, C. A.; Lisensky, G. C. *Inorg. Chem.* **1980**, *19*, 2854-2855.

Table 5.6 shows the IR stretching frequency for two chromium carbonyl complexes, as well as selected data from their crystal structures. They can be interpreted based on considerations of bond lengthening due to π -back-bonding from chromium to the π -acidic carbonyl (a more electron-rich metal center is capable of better π -backbonding to the carbonyl, resulting in a shorter M-C bond and a longer C-O bond; the latter is reflected in the IR spectrum as a shift towards lower cm^{-1}).²⁷ Such an analysis provides further support for the notion that the electron-donating ability of BBH lies between that of benzene and Cp^- .

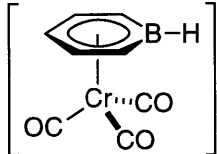
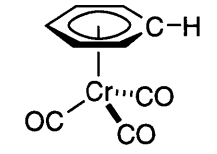
	av bond length (Å)		ν_{CO} (cm^{-1})
	Cr-C	C-O	
	1.818(3)	1.172(3)	1785 1802 1908
	1.844(2)	1.160(2)	1858 (s) 1968

Table 5.6. Structural and Spectroscopic Comparison of η^6 -1-*H*-Boratabenzene and η^6 -benzene Complexes of $\text{Cr}(\text{CO})_3$.

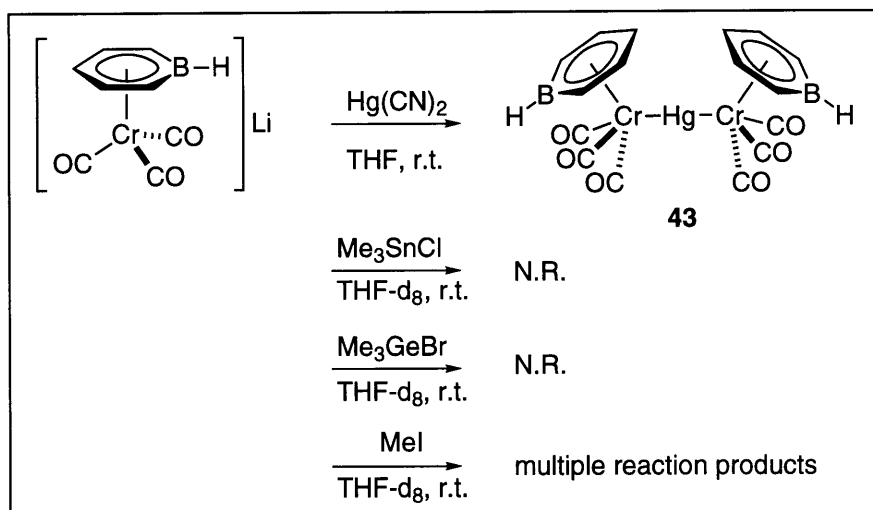
The reactivity that BBH imparts on a transition metal should provide some further indication of its electronic nature as a ligand, vis-à-vis benzene and Cp (Scheme 5.6). $[(\text{BBH})\text{Cr}(\text{CO})_3]^-$ reacts with $\text{Hg}(\text{CN})_2$ to form **43**, a molecule containing two Cr-Hg bonds. This is further evidence that 1-*H*-boratabenzene is more electron-rich than benzene,²⁸ since $(\eta^6\text{-benzene})\text{Cr}(\text{CO})_3$ does not react under otherwise identical conditions.²⁹ Unlike its cyclopentadienide analogue,

²⁷ Elschembroich, C.; Salzer, A. *Organometallics* 2nd ed.; VCH: Weinheim, 1992; Chapter 14.5.

²⁸ For a similar reaction involving 1-substituted boratabenzenes, see Herberich, G. E.; Söhnen, D. J. *Organomet. Chem.* **1983**, 254, 143-147.

²⁹ Except to slowly liberate minute amounts (less than 3% of the total benzene after 18 hours) of free benzene, a mode of reactivity inconsistent with Cr-Hg bond formation, but likely due to cyanide-mediated decomposition of the starting material.

$[(\text{BBH})\text{Cr}(\text{CO})_3]^-$ does not react at all with Me_3GeBr or Me_3SnBr ,³⁰ while reaction with MeI (rapid and clean³¹ at $-20\text{ }^\circ\text{C}$ for $[\text{CpCr}(\text{CO})_3]^-$) is slow and messy.



Scheme 5.6.

Conclusions

We have prepared the simplest boratabenzene, 1-*H*-boratabenzene, in good yield from LiAlH_4 reduction of the easily accessible borabenzene-trimethylphosphine. In the solid state, it adopts the structure of an anionic metallocene that does not interact with the tetrahedral $\text{Li}(\text{THF})_4$ that completes the asymmetric unit. In solution, on the other hand, variable-temperature ^7Li NMR studies suggest that it prefers a piano-stool structure. The boron-bound hydrogen is hydridic in nature, as evidenced by its reactions with epoxides, aldehydes, and water. However, the B-H fragment does not add to an olefin, as is observed for many other trivalent boron hydrides.

Various transition metal complexes incorporating BBH as a ligand are accessible by reaction of $\text{Li}(\text{BBH})$ with a suitable transition metal halide or pseudohalide. Comparative studies involving cyclic voltammetry, infrared spectroscopy, X-ray crystallography, and reactivity show that the 1-*H*-boratabenzene ligand is more electron donating than benzene, but less so than cyclopentadienyl.

³⁰ Baird, M. C. In *Progress in Inorganic Chemistry*; Cotton, F. A., Ed.; Interscience: New York, 1968; Vol. 9; p 1.

³¹ Alt, H. G. *J. Organomet. Chem.* **1977**, 124, 167-174.

Experimental Section.

General.

The general considerations in the previous chapters apply. Dodecanal and styrene oxide were purchased from Aldrich and distilled prior to use. 5,6-Benzo[2.2.2]cryptand was purchased from Aldrich and used as received. D₂O was of the highest purity available from Isotec, and used as received.³²

NMR yield for the Formation of Li(BBH) (9a).³³

Borabenzene-PMe₃ (23 mg, 0.15 mmol) was dissolved in ~0.5 mL of THF-d₈. Toluene (16 μL, 0.15 mmol) was added to the solution, and a ¹H NMR spectrum was obtained. The NMR tube was taken into the glove box, and its contents were emptied into a vial containing LiAlH₄ (5.6 mg, 0.15 mmol). The solution thus formed was stirred for 4.5 hours. The resulting solution was pipetted into an NMR tube, and a ¹H NMR spectrum was obtained. Integration of two different resonances versus the toluene standard and comparison with the initial spectrum indicated that the reaction had proceeded in 95 and 97% yields, for an average of 96%.

Reaction of Li(BBH) with Dodecanal.

In a vial, dodecanal (29.1 μL, 0.132 mmol) was mixed with a solution of Li(BBH) (12.3 mg, 0.147 mmol) in 0.7 mL of THF-d₈. The solution was pipetted into an NMR tube. After 10 minutes no aldehyde was observed (¹H NMR), but little or no loss of Li(BBH) was evident. After an additional 1.5 hours, 30.0 μL (0.136 mmol) of the aldehyde were added. ¹H NMR showed progress, with incomplete disappearance of boratabenzene. More aldehyde (50.0 μL, 0.226 mmol) was added, and the NMR showed complete disappearance of both starting materials. The following manipulations were performed in air: The contents of the NMR tube were poured into a flask, and the THF was evaporated. The resulting oil was purified by flash chromatography (silica gel; hexane:ethyl acetate gradient (from 0 to 25% ethyl acetate), which yielded 31 mg (113%) of dodecanol (by TLC and ¹H NMR), contaminated with a small amount of ethyl acetate and acetone. Further evaporation resulted in a clean NMR spectrum.

³² We thank Dr. Wei Wu (Stubbe group) for donating an ampule of D₂O.

³³ For the isolation of Li(BBH), see Chapter 3.

Reaction of Li(BBH) with Styrene Oxide.

To a solution of Li(BBH) (17.5 mg, 0.208 mmol) in 2 mL of THF was added 100 μ L (0.877 mmol) of styrene oxide. The vial was left sitting in the glove box without stirring for about 48 hours, after which time it was taken out and opened to air. The solvent was removed, and the resulting oil was flashed through a pipette containing silica gel. The fractions which contained α - and β - phenethyl alcohols were collected and combined, yielding 13 mg (51%) of a mixture consisting of 82% α -phenethyl alcohol and 18% β -phenethyl alcohol (^1H NMR).

Reaction of Li(BBH) with H₂O and D₂O.

In the glove box, two NMR tubes were charged with 5.1 mg (0.061 mmol) and 5.5 mg (0.066 mmol) of Li(BBH) in THF-*d*₈. To these tubes were added 1.1 μ L (0.061 mmol) and 1.3 μ L (0.066 mmol) of H₂O and D₂O, respectively. Gas evolution was noted immediately. ^1H NMR spectra taken within 30 minutes of beginning the experiment showed the presence of H₂ in the first tube and HD in the second one.

Synthesis of (BBH)Rh(cod) (20c).

To a solution of [(cod)RhCl]₂ (77.7 mg, 0.158 mmol) in ~1 mL of THF was added Li(BBH) (102 mg, 0.315 mmol). The solution turned black and was brought out of the glove box, where it was passed through a pad of silica gel using THF as eluent. The solvent was removed from the ochre-colored solution, and the resulting solid was chromatographed (hexane), yielding 36.9 mg (41%) of (BBH)Rh(cod), which was subsequently sublimed at 50 °C (250 mTorr) to yield 24.6 mg (27%) of pure (BBH)Rh(cod). In another experiment, after chromatography the product was crystallized from heptane at -35 °C for a 30% yield. ^1H NMR (300 MHz; C₆D₆): δ 5.95 (m; 4H), 4.52 (t; J = 5.4; 1H), 4.35 (v br; 1H), 4.15 (s; 4H), 1.97 (m; 4H), 1.76 (m; 4H). ^{13}C NMR (75 MHz; C₆D₆): δ 109.1, 109.0 (v br), 87.8, 67.7 (d; J = 13.0), 32.1. ^{11}B NMR (96 MHz; C₆D₆): δ +17.2 (J_{B-H} = 107). IR (KBr pellet): 2996, 2934, 2878, 2828, 2484 (v_{B-H}), 2429, 1461, 1390, 1325. mp. 128-129°C. Anal. calc: C: 54.22; H: 6.30; found: C: 54.31; found H: 6.20.

This compound was also characterized by X-ray diffraction; details are in Appendix II. The location of the boron was disordered between the positions assigned as B and C(5). Since the exact location of B was found by comparative thermal parameters in the next structure, no effort was made to model the disorder in this particular one.

(BBH)Rh(cod)•1/2 [(cod)RhCl]₂.

A crystal of this compound grew from an attempt at purifying (BBH)Rh(cod) by recrystallization. This compound was characterized by X-ray diffraction; details are in the Appendix II. The position of the boron was located through the use of comparative thermal parameters.

Synthesis of (BBH)₂Fe (37).

FeCl₂ (66.0 mg, 0.521 mmol) was added to a solution of Li(BBH) (87.4 mg, 1.04 mmol) in ~5 mL of THF. A black solution resulted from which the THF was removed, leaving a black solid. Extraction with ~5 mL of hexanes and flash chromatography yielded 5 mg (5% yield) of (BBH)₂Fe, which can be sublimed at 50 °C (250 mTorr.). ¹H NMR (300 MHz; CD₂Cl₂): δ 5.66 (tt; J = 5.8, 2.1; 2H), 5.51 (app t; 4H), 4.74 (ddd; J=8.7, 4.2, 2.1; 4H), 4.03 (v br; 2H). ¹³C NMR (125 MHz; CD₂Cl₂): δ 93.2, 86.2 (br), 79.7. ¹¹B NMR (96 MHz; CD₂Cl₂): δ +12.5 (J_{B-H} = 135). IR ν_{B-H}: 2505. mp. >195 °C. HRMS calcd for C₁₀H₁₂B₂Fe: 210.0474; found: 210.0475.

Synthesis of (BBH)FeCp* (40).

A suspension of LiCp* (37.1 mg, 0.261 mmol) in ~7 mL of THF was added slowly to a stirred suspension of FeCl₂ (33.1 mg, 0.261 mmol) in ~1 mL of THF. To the resulting green solution was added a solution of Li(BBH) (84.5 mg, 1.01 mmol) in ~3 mL of THF, resulting in a dark orange solution. The reaction mixture was taken out of the glove box, hexanes (~10 mL) was added, and the THF was evaporated. The solids were extracted with hexane and acetone, and the extracts were combined. Filtration of the resulting cloudy solution through an Acrodisc, followed by flash chromatography on silica (gradient: 1% Et₂O/hexanes to 1.5% Et₂O/hexanes) yielded 26.7 mg (38%) of desired product. On a small scale (< 60 mg product) the isolation of the product could more easily be achieved by filtration through a pad of silica gel to remove the first yellow band (decamethylferrocene), followed by preparative HPLC chromatography of the second orange band (Column: Econosphere Silica 10U from Alltech, 250 mm x 20 mm; 5% i-PrOH/hexane; flow rate approximately 20 mL/min). The desired compound sublimes at 55-75 °C (300-450 mTorr). ¹H NMR (300MHz; C₆D₆): δ 4.71 (dd; J = 8.4, 6.0; 2H), 4.49 (t; J = 5.8; 1H), 4.41 (dd; J = 8.1, 4.5; 2H), 4.20 (v br; 1H), 1.56 (s; 15H). ¹³C NMR (125 MHz; C₆D₆): δ 93.3, 87.7 (br), 83.3, 81.0, 10.5. ¹¹B NMR (96 MHz; C₆D₆): δ +13.3 (J_{B-H} = 106). IR (KBr pellet) ν_{B-H}: 2463. mp. 115-117 °C. HRMS calcd: 268.1086; found: 268.1085. Anal. calc: C: 67.23, H: 7.90; found: C: 67.44, H: 8.12.

This compound was also characterized by X-ray diffraction; details are in Appendix II. The position of the boron atom could not be located, as it seems to be disordered in all 6 ring positions. Charge considerations indicate that the boron must be present, so that further refinement seemed unwarranted at this point.

Synthesis of [(BBH)Cr(CO)₃]•[Li•(5,6-benzo[2.2.2.]cryptand)] (41).³⁴

[(BBH)Cr(CO)₃]Li•(Et₂O) (18a)³⁵ (30.2 mg, 0.102 mmol) was dissolved in ~6 mL of THF and added to 87.1 mg of 5,6-benzo[2.2.2.]cryptand solution (43.6 mg cryptand, 0.102 mmol) and shaken. When the solution was homogeneous, ~3 mL of Et₂O were added. At this point, pentane was added until cloudiness persisted for ~20 seconds. The solution was cooled to -35°C for two days, after which yellow needles had formed (65.1 mg, 99%). ¹H NMR (300 MHz; THF-d₈): δ 7.12 (m; 2H), 6.99 (m; 2H), 5.25 (app t; 2H), 4.72 (t; J = 6.0; 1H), 4.37 (m; 4H), 3.96 (dd; J = 9.0, 4.5; 2H), 3.74 (m; 8H), 3.58 (m; 8H), 2.75 (m; 12H). ¹³C NMR (125 MHz; THF-d₈): δ 241.2, 148.8, 123.4, 116.6, 106.1, 94.0 (br), 83.3, 69.8, 69.3, 69.1, 54.7, 54.1. ¹¹B NMR (96 MHz; THF-d₈): δ +17.1. IR (KBr pellet): 2464 (B-H), 1908, 1802, 1785 (CO). mp. 156-158 °C Anal. calc C: 55.92; H: 6.57; found C: 55.80; H: 6.76. This compound was also characterized by X-ray diffraction; details are in Appendix II. The position of the boron was located through the use of comparative thermal parameters.

Synthesis of CpFe(BBH) (42).

Anhydrous FeCl₂ (110 mg, 0.869 mmol) was added portionwise as a powder to a solution of NaCp (76.5 mg, 0.869 mmol) and Li(BBH) (72.9 mg, 0.869 mmol) in ~8 mL of THF. The solution turned green, and bubbling ensued. After 5 minutes, the THF was evaporated, and the black solid was extracted with 1% Et₂O/hexane to yield an orange solution with undissolved black solids. The extracts and the solids were loaded onto a silica gel column, and two orange bands were isolated. The first one was ferrocene (47.6 mg, 29%) and the second one (47.7 mg, 27% desired product) consisted of CpFe(C₅H₅BH) (92%) and (BBH)₂Fe (6%). These two products were separated by preparative HPLC, followed by sublimation (50 °C, 250 mTorr), to yield pure CpFe(BBH) 9.5 mg (5.5%). ¹H NMR (500 MHz; CD₂Cl₂): δ 5.52 (t; J = 5.8; 1H), 5.45 (app t; 2H), 4.60 (dd; J = 9.0, 4.5; 2H), 4.36 (s; 5H). ¹³C NMR (125 MHz; CD₂Cl₂): δ 91.2, 84.9 (br), 79.4, 70.6. ¹¹B NMR (96 MHz; CD₂Cl₂): δ +11.7 (J_{B-H} = 128). IR (KBr

³⁴ The actual name of 5,6-benzo[2.2.2.]cryptand is 5,6-benzo-4,7,13,16,21,24-hexaoxa-1,10-diazabicyclo[8.8.8]hexacosane.

³⁵ For its preparation, see Chapter 4.

pellet) $\nu_{\text{B-H}}$: 2482. **mp.** >195 °C. **HRMS** calcd for $\text{C}_{10}\text{H}_{11}\text{BFe}$: 198.0303; found: 198.0302.

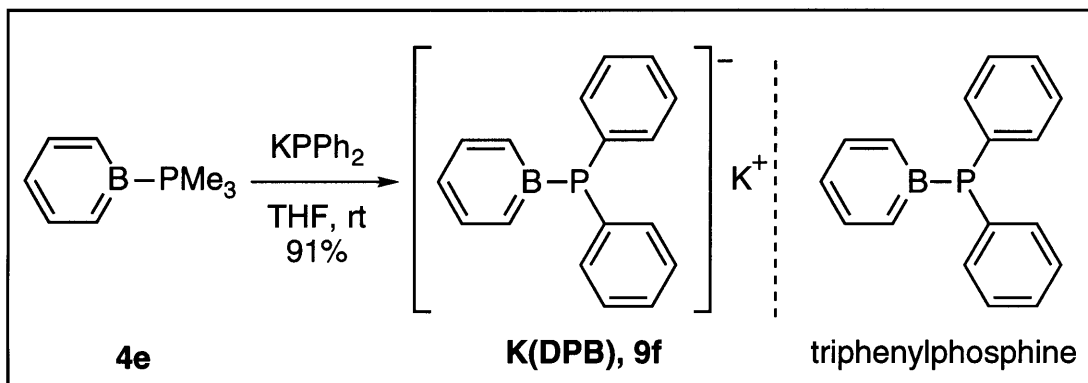
$[(\text{C}_6\text{H}_6)\text{Rh}(\text{cod})](\text{OTf})$.

Prepared following the literature procedure.³⁶ A crystal with dimensions of 0.08 x 0.08 x 0.05 mm³ was used for this crystal structure determination, following the procedure in 5.8. More details of this study are included in Appendix II.

³⁶ See: Hancock, K. S. B.; Steed, J. W. *J. Chem. Soc., Chem. Commun.* **1998**, 1409-1410.

Chapter 6: The Chemistry of Diphenylphosphidoboratabenzene (DPB).

In this chapter we introduce a potential new tool for the isolation of electronic effects from steric effects in the study of the reactivity of transition metal complexes. This separation is of great interest to any mechanism-oriented chemist. For example, during the course of their studies on the tail-to-tail dimerization of acrylates, Brookhart and co-workers¹ found a seventy-fold increase in the turnover frequency when the Cp ligand of the catalyst was replaced by the more electron-rich, as well as more sterically-demanding, Cp*. By employing CpRh(ethylene)₂, Cp*Rh(ethylene)₂, and (C₅Me₄CF₃)Rh(ethylene)₂, they were able to break down this phenomenon into its steric and electronic components (C₅Me₄CF₃ is as sterically demanding as Cp*, but relatively electron-poor like Cp). They showed that the turnover increases 10-fold because of the increased steric demand and 7-fold because of the more electron-rich metal.



Scheme 6.1.

In this context, should diphenylphosphidoboratabenzene (DPB, **9f**) bind transition metals through its phosphorus center, it could potentially behave as an anionic surrogate for the ubiquitous ligand triphenylphosphine. However, in the relatively extensive literature on borabenzenes,² there are no examples in which a

¹ Hauptman, E.; Sabo-Etienne, S.; White, P. S.; Brookhart, M.; Garner, J. M.; Fagan, P. J.; Calabrese, J. C. *J. Am. Chem. Soc.* **1994**, *116*, 8038-8060.

² For leading references to π -bound boratabenzene complexes, see: a) Herberich, G. E.; Ohst, H. *Adv. Organomet. Chem.* **1986**, *25*, 199-236. b) Herberich, G. E. In *Comprehensive Organometallic Chemistry II, Vol. 1*, Abel, E. W.; Stone, F. G. A.; Wilkinson, G., Eds.; Pergamon: New York, 1995, Chapter 5.

boratabenzene is bound to an electrophile through its boron substituent. Therefore, we had to establish a priori that DPB is capable of binding a transition metal through the phosphorus atom. These studies, as well as the synthesis, structure, and reactivity of DPB, form the body of this chapter.

Reaction of BB-PMe₃ with KPh₂ results in quantitative formation of K(DPB) (Scheme 6.1), an air-sensitive colorless solid that often exhibits a yellow coloration; this coloration appears not to affect the chemistry detailed in this chapter. K(DPB) is insoluble in hexane and very sparingly soluble in benzene, toluene, and ether. In tetrahydrofuran it has a sharp solubility profile, being quite soluble at room temperature, but not very soluble at -35 °C, which makes its isolation straightforward.

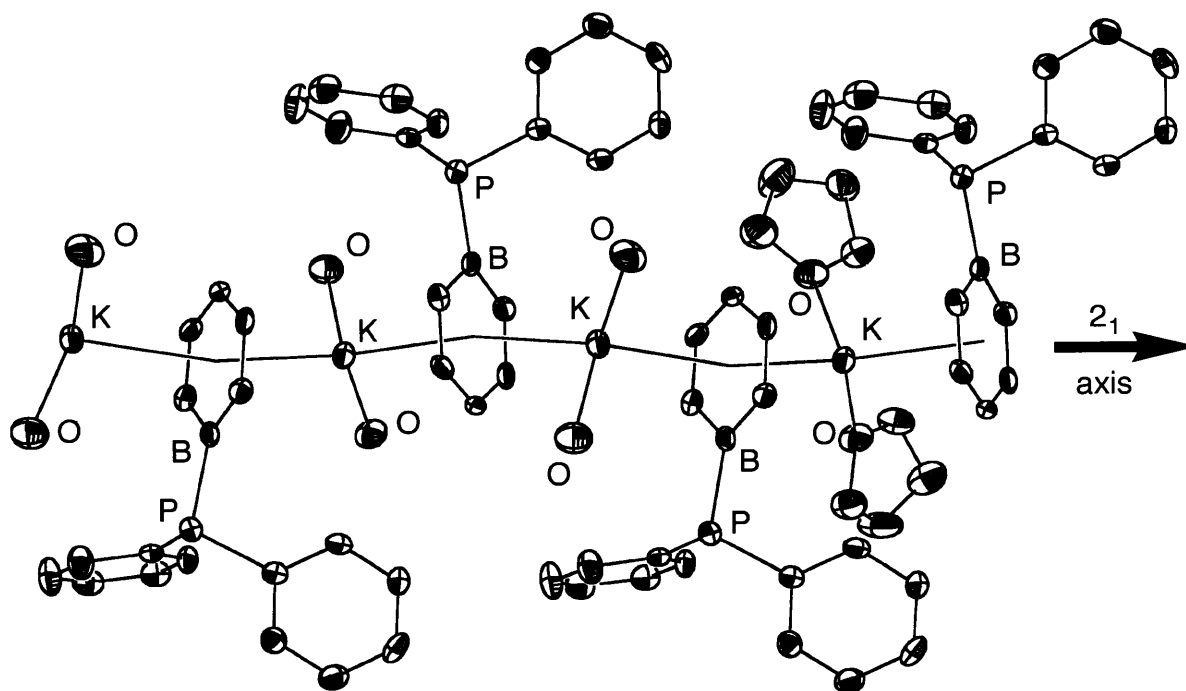


Figure 6.1. The Crystal Structure of the Polymeric [(DPB)K(THF)₂]_n.

DPB crystallizes from THF as needles that can be extremely long (in some cases, up to 25 mm), but slim (out of close to 50 crystallizations, in only three or four cases were we able to obtain needles greater than 0.03 mm in width). These macroscopic features are a direct consequence of the packing of K(DPB)(THF)₂ in the solid state. A single-crystal X-ray diffraction study shows that the molecule crystallizes as a rod-

like polymer³ in which boratabenzene rings and potassium atoms alternate. The polymer grows along the 2_1 axis characteristic of the monoclinic space group $P2_1/c$. Figure 6.1 shows an ORTEP drawing of the polymer as a four-monomer oligomer in which, for the sake of clarity, six THF molecules are shown as oxygen atoms.

The polymer can be broken up by addition of a chelating ether, such as 18-crown-6, to the crystallization mixture (Figure 6.2). The resulting material is slightly more soluble in solvents such as toluene and forms extremely beautiful, gem-like crystals that are evenly sized in all dimensions. The crystal structure of this molecule revealed a monomeric piano-stool structure in which the potassium and the borabenzene were still attached to one another.⁴

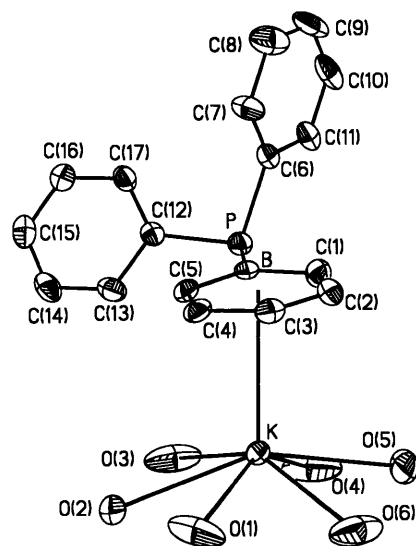


Figure 6.2. The Crystal Structure of (DPB)K(18-crown-6) with the Solvent Toluene and the Crown Carbons Omitted for Clarity.

Ultimately, we were able to obtain a structure of a separated ion pair by using a cryptand (Figure 6.3).⁵ The structure of the DPB fragment of the cryptand complex is quite similar to the crown ether complex. However, a meaningful detailed comparison could not be carried out because the structure of the cryptand complex is

³ $[\text{Cp}^*\text{K}(\text{pyridine})_2]_n$ shows a similar structure: Rabe, G.; Roesky, H. W.; Stalke, D.; Pauer, F.; Sheldrick, G. M. *J. Organomet. Chem.* **1991**, *403*, 11-19.

⁴ There is a one-half toluene molecule in the lattice, disordered about the center of symmetry of the aromatic ring. It was modeled as a xylene with half-occupancies for the methyl groups.

⁵ We used 4,7,13,16,21,24-hexaoxa-1,10-diazabicyclo[8.8.8]hexacosane. For simplicity, we call this molecule "[2.2.2] cryptand" throughout this thesis.

of marginal quality, as a result of a combination of the small size of the crystal, the large number of atoms, and the absence of a heavy scatterer. The ^1H NMR spectra of the different crystal forms of DPB are different. The two containing a coordinated borabenzene ring in the solid state have very similar chemical shifts, which are shifted downfield from those of the cryptate, presumed to be a solvent-separated ion pair because of its solid-state structure.

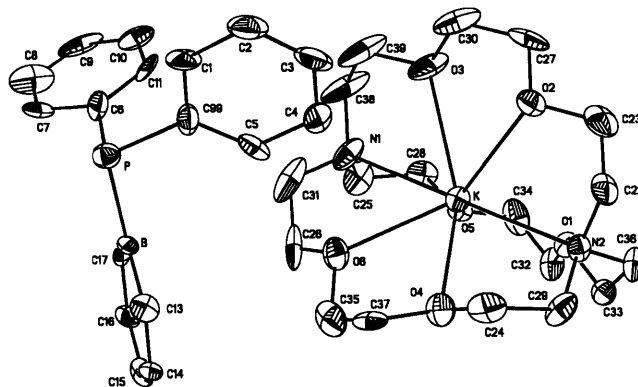


Figure 6.3. Crystal Structure of $(\text{DPB}) \cdot [\text{K}([2.2.2]\text{cryptand})]$.

PPh_3	DPB
<ul style="list-style-type: none"> • Σ°_{P}: $308.3(3)^\circ$ • Cone angle: 145° • Overall charge: 0 • Neutral 2ϵ ligand 	<ul style="list-style-type: none"> • Σ°_{P}: $310.1(8)^\circ$ • Cone angle: $\sim 145^\circ$ (estimated) • Overall charge: -1 • Anionic 2ϵ ligand

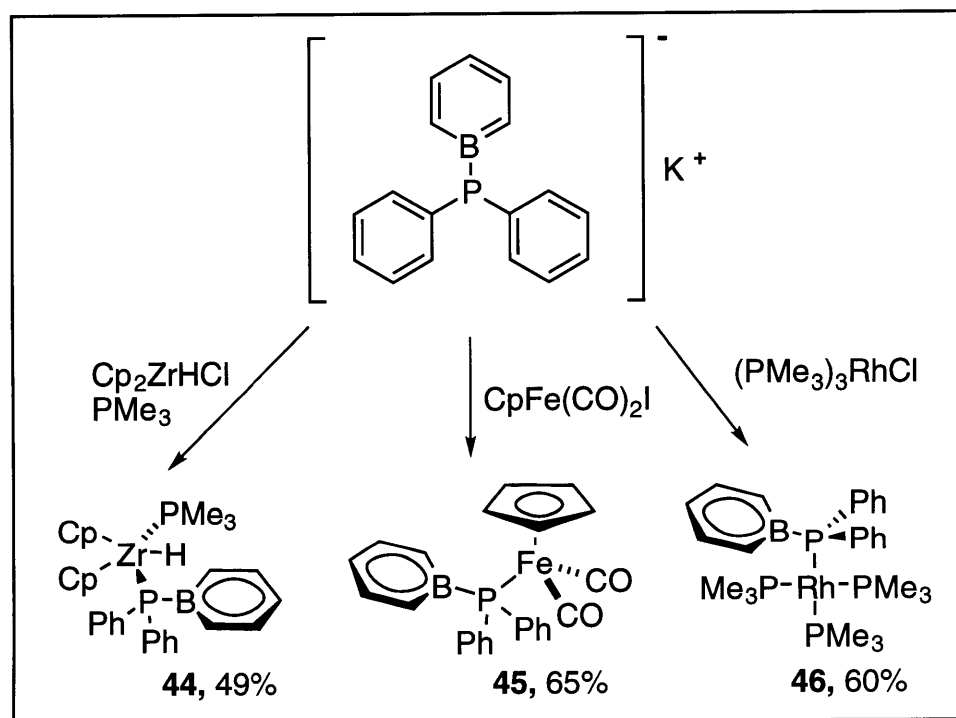
Table 6.1. A Head-to-head Comparison of Triphenylphosphine and DPB.

A comparison of the salient features of the three crystal structures shows that

DPB is indeed quite similar to triphenylphosphine (Table 6.1). Therefore, should it bind to transition metals through phosphorus, DPB is a molecule that could allow the isolation of steric and electronic effects on the reactivity of transition metal complexes containing triphenylphosphine.

As shown in Scheme 6.2, DPB reacts at phosphorus with early, middle, and late transition-metal halides, such as $\text{Cp}_2\text{ZrHCl}/\text{PMe}_3$, $\text{CpFe}(\text{CO})_2\text{I}$, and $(\text{Me}_3\text{P})_3\text{RhCl}$, to replace the halide with a P-bound DPB. As mentioned earlier, this was the first observation of a boratabenzene binding an electrophile of any sort through the substituent on boron, rather than through one or more of the ring carbons.

Structurally, and as a result of charge considerations, the resulting complexes are very closely related to the corresponding compounds in which DPB is replaced by triphenylsilicate. To illustrate this point, Table 6.2 shows that the cell constants for $(\text{Me}_3\text{P})_3\text{Rh}(\text{DPB})^6$ are essentially the same as they are for $(\text{Me}_3\text{P})_3\text{RhSiPh}_3$.⁷



Scheme 6.2.

⁶ $(\text{Me}_3\text{P})_3\text{Rh}(\text{DPB})$ reacts with hydrogen gas. When the reaction is performed in a J. Young NMR tube, the orange solution of **31** turns completely colorless within a few seconds. The ^1H NMR spectra show two different rhodium hydrides of unequal abundance (3:1).

⁷ Thorn, D. L.; Harlow, R. L. *Inorg. Chem.* **1990**, 29, 2017-2019.

	(Me ₃ P) ₃ Rh(DPB), 46	(Me ₃ P) ₃ RhSiPh ₃
space group	P2 ₁ /n	P2 ₁ /n
a (Å)	9.4031(8)	9.433(3)
b (Å)	17.692(2)	17.692(2)
c (Å)	17.672(2)	17.673(5)
β (°)	95.635(1)	96.03(1)

Table 6.2. A Comparison of the Cell Constants for (Me₃P)₃Rh(DPB) (46**) and (Ph₃Si)Rh(PMe₃)₃.**

This similarity between DPB and triphenylsilicate is further illustrated by comparison of our zirconium compound **44** with the isostructural Cp₂Zr(H)(PMe₃)(SiPh₃) (**47**), reported by Buchwald and co-workers (Table 6.3).⁸ The intramolecular bond distances and angles are essentially the same for both compounds, although their cell constants are different.

		bond		
Zr-H	2.657(2)	Zr-PMe ₃	2.677(2)	
Zr-P	2.7382(14)	Zr-X	2.721(2)	
Zr-B	1.81(5)	Zr-H	1.94(5)	
P-B	115.09(5)	Me ₃ P-Zr-X	112.68(5)	
	57(2)	Me ₃ P-Zr-H	59(1)	

Table 6.3. A Comparison of Zirconium Complexes of DPB and Ph₃Si (Bond Lengths in Å, Angles in °).

We wanted to establish the effect on the metal of replacing PPh₃ with DPB. Therefore, we compared the CO stretching frequencies in a series of compounds bearing the common fragment [CpFe(CO)₂]⁺. The results are shown in Table 6.4. Within experimental error, the donicity of DPB is comparable to that of [PPh₂]⁻⁹ and considerably greater than PPh₃,¹⁰ but considerably less so than [Ph₃Si]⁻¹¹

⁸ Kreutzer, K. A.; Fisher, R. A.; Davis, W. M.; Spaltenstein, E.; Buchwald, S. L. *Organometallics* **1991**, *10*, 4031-4035.

⁹ Burckett-St. Laurent, J. C. T. R.; Haines, R. J.; Nolte, C. R.; Steen, N. D. C. T. *Inorg. Chem.* **1980**, *19*, 577-587.

¹⁰ Riley, P. E.; Davis, R. E. *Organometallics* **1983**, *2*, 286-292.

¹¹ Gansow, O. A.; Schexnayder, D. A.; Kimura, B. Y. *J. Am. Chem. Soc.* **1972**, *94*, 3406-3408.

Phosphides are believed to be much less prone to form multiple bonds to transition metals than are amides. While the crystal structure of **50** has not been reported,¹² the crystal structure of Cp*Fe(CO)₂PPh₂ is known to bear a pyramidal phosphorus (Σ°_P : 319.8 °).¹³ Since DPB has no phosphorus-based "lone pairs" available for bonding to iron, our infrared data support the conclusion that there is little, if any P-Fe multiple bonding in **50**. This complements the observation that the average CO stretching frequency of [CpFe(CO)₂(H₃B•PPh₂)] is 2007 cm⁻¹,¹⁴ also consistent with PPh₂ being a poor π -donor in the case that the lone pair is not tied up (i.e., **49**).

	48	45	49	50
Avg ν_{CO} (cm ⁻¹):	2048	2003	1991	1968
Avg Fe-CO length (Å):	1.771(4)	1.742(10)	N/A	N/A
Avg C-O length (Å):	1.139(5)	1.168(9)	N/A	N/A

Table 6.4. A Comparison of Donating Abilities Through IR Spectroscopy and X-ray Crystallography.

Besides reacting with transition metal based electrophiles, DPB also reacts with main-group electrophiles. For example, reaction with borane also occurs at phosphorus. The solid state structure of this compound is that of a polymeric sheet, woven by three different types of interaction (Figure 6.4): a 3-center, 2-electron bond between the BH₃ and potassium, an electrostatic interaction between the boratabenzene and the potassium, and a dative phosphorus-boron bond. While in the unbound DPB the phosphorus atom lies in the plane of the boratabenzene, in the BH₃ adduct the phosphorus is displaced from the plane by a normal measuring

¹² Ashby, M. T.; Enemark, J. H. *Organometallics* **1987**, *6*, 1323-1327.

¹³ Weber, L.; Reizig, K.; Boese, R. *Chem. Ber.* **1985**, *118*, 1193-1203.

¹⁴ Nakazawa, H.; Veda, Y.; Nakamura, K.; Miyoshi, K. *Organometallics* **1997**, *16*, 1562-1566.

0.453(7) Å. This distortion is apparently caused by the interaction between the potassium and the boron-bound hydride.¹⁵

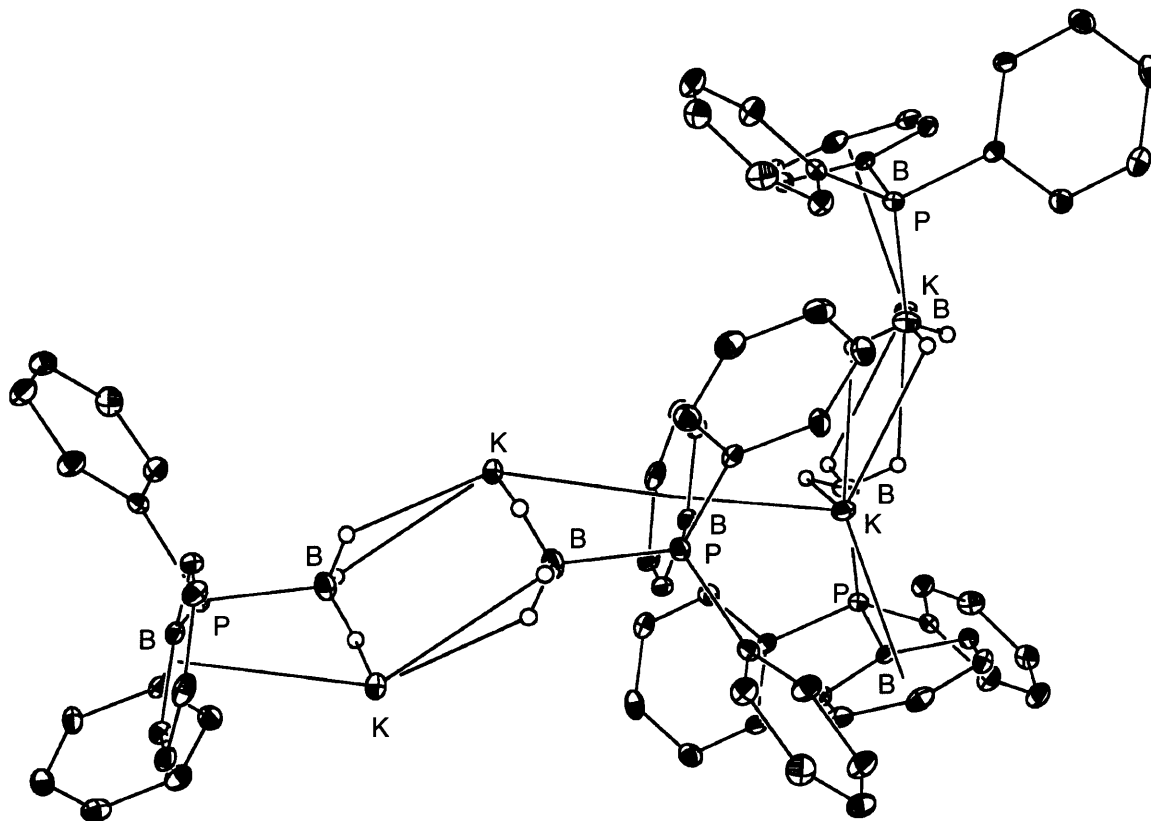
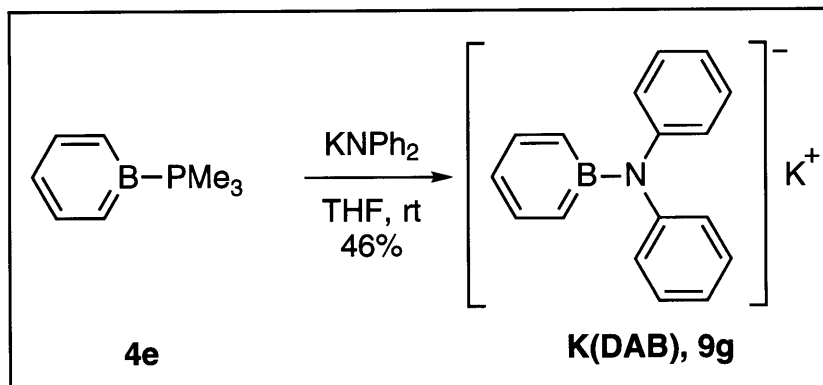


Figure 6.4. Crystal Structure of $[(\text{DPB})\text{K}(\text{BH}_3)]_n$.

We were determined to find out why DPB binds transition metal fragments at phosphorus, instead of π -complexing them, because this feature is what makes it unique among boratabenzenes. In principle, this uniqueness could merely be due to the two phenyl substituents. However, we suspected that the uniqueness was more likely to arise from the fact that the pnictogen is phosphorus, because phosphorus is known to be less prone than nitrogen to form multiple bonds to boron. In this case, the "lone pair" on DPB would be free to interact with electrophiles, while the "lone pair" on a corresponding amidoboratabenzene would be involved in multiple bonding with boron. To delve into the matter, we prepared (Scheme 6.3) potassium diphenylamidoboratabenzene $\text{K}(\text{DAB})$ (**9g**; identical to DPB, but for the group 15

¹⁵ We have tried to use BH_3 as a protecting group to prepare transition-metal π -complexes of DPB (Oshiki, T.; Hikosaka, T.; Imamoto, T. *Tetrahedron Lett.* **1991**, 32, 3371-3374), but these experiments have been unsuccessful.

element) and explored its structure and reactivity.



Scheme 6.3.

		X:	ortho H	para H	ortho C	para C
<i>σ-donors (A predominant)</i>	H		6.57	6.21	128	112
	PPh ₂		6.50	6.20	128	113
	Me		6.47	6.18	127	108

<i>σ- and π-donors (B contributes as well)</i>	NPh ₂		5.99	5.72	119	106
	OEt		5.67	5.67	115	104
	NMe ₂		5.65	5.50	110	100

↓ Increased contribution of the B resonance form

Table 6.5. Correlation Between ¹H NMR Chemical Shifts and π -Donor Ability.

First, we compared the ¹H and ¹³C NMR spectra of DPB and DAB in THF-d₈. Herberich has proposed that the chemical shifts of the ortho and para protons in boratabenzene rings can be indicative of the extent of delocalization of the lone pair

of a boron substituent with the π -system of the boratabenzene ring.¹⁶ A good donor such as a dialkylamide or an alkoxide group will lead to chemical shifts that are upfield from the corresponding resonances in the spectrum of a molecule for which the B-X π -overlap is negligible. Examination of the chemical shifts of DAB and DPB confirms that there is considerably more π overlap in DAB than in DPB (Table 6.5).¹⁷

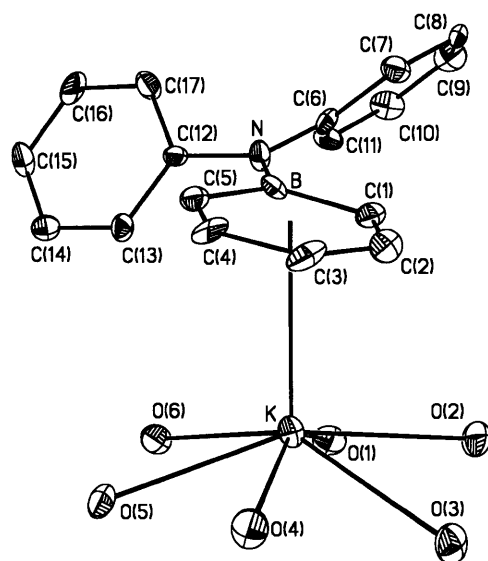


Figure 6.5. A Crystal Structure of (DAB)K(18-crown-6).

Second, we obtained a crystal structure of $K(\text{DAB}) \cdot (18\text{-crown-6})$ (Figure 6.5). A comparison of the crystal structures of $K(\text{DPB}) \cdot (18\text{-crown-6})$ and $K(\text{DAB}) \cdot (18\text{-crown-6})$, grown under identical conditions, is instructive.¹⁸ The phosphorus of $K(\text{DPB})$ is pyramidal (sp^3 , $\Sigma^\circ_P = 310^\circ$), while the nitrogen of $K(\text{DAB})$ is planar¹⁹ (sp^2 , $\Sigma^\circ_N = 360^\circ$).

¹⁶ Herberich, G. E.; Schmidt, B.; Englert, U.; Wagner, T. *Organometallics* **1993**, *12*, 2891-2893.

¹⁷ Preliminary data suggests that counterion and concentration effects on the ^1H or ^{13}C NMR chemical shifts are negligible, as long as the counterion is π -bound to the boratabenzene.

¹⁸ It should be pointed out, however, that the crystal structure of NPh_3 shows a planar pnictogen, whereas that of PPh_3 does not: a) NPh_3 : Sobolev, A. N.; Belsky, V. K.; Romm, I. P.; Chernikova, N. Y.; Guryanova, E. N. *Acta Crystallogr., Sect. C* **1985**, *41*, 967-971. b) PPh_3 : Bruckman, J.; Kruger, C.; Lutz, F. *Z. Naturforsch., B* **1995**, *50*, 351-360.

¹⁹ Based on a search of the Cambridge Structural Database, the B-N bond length in the structure of $K\text{-DAB}$ is the longest known between divalent boron and divalent nitrogen.

°). It is well-established in the literature on boron-pnictogen multiple bonding²⁰ that B-N π -bonds are much stronger than B-P π -bonds.

The conformations observed in the crystal structures are in good agreement with the lowest energy conformations found in *ab initio* calculations performed on this system by Prof. Marcello DiMare (University of California, Santa Barbara) (Figure 6.6).

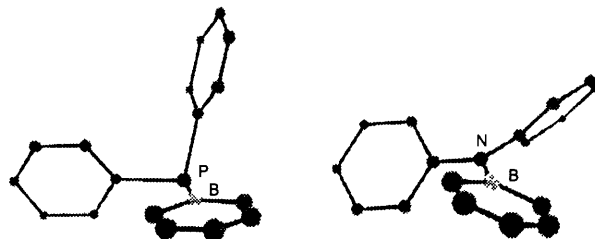
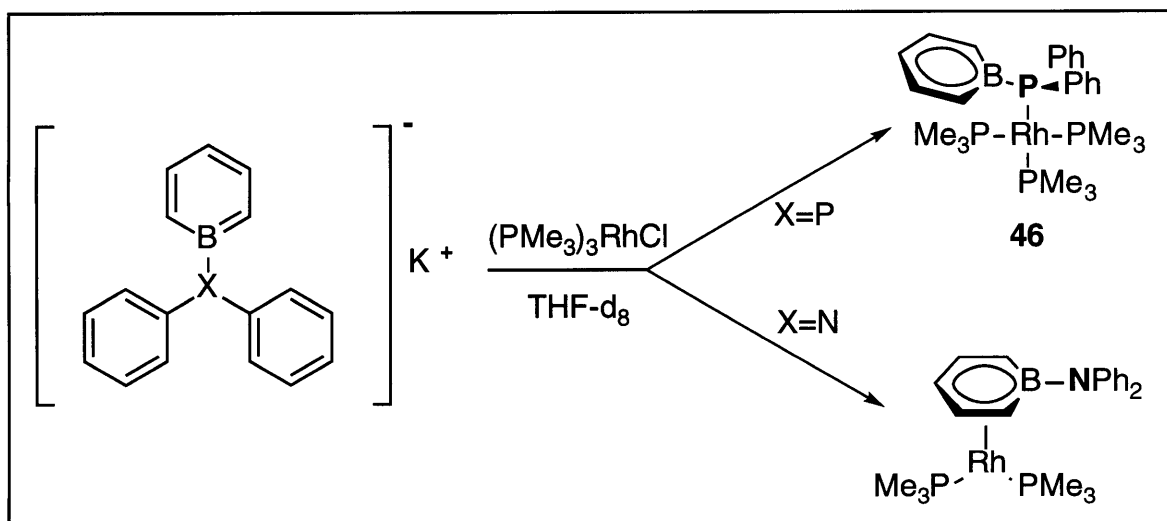


Figure 6.6. HF/6-31G*-minimized Conformations of DPB and DAB. (See Figures 6.2 and 6.5).



Scheme 6.2.

Finally, the reaction of K(DAB) with $(\text{Me}_3\text{P})_3\text{RhCl}$ resulted in formation of a π -complex, with no evidence for any intermediates (Scheme 6.4).²¹ This reactivity is

²⁰ a) Paine, R. T.; Nöth, H. *Chem. Rev.* **1995**, *95*, 343-379. b) Power, P. P. *Angew. Chem., Int. Ed. Engl.* **1990**, *29*, 449-460.

²¹ Reactions of DPB and DAB with methylating agents (carried out by Shuang Qiao) show that DPB reacts to form borabenzene-diphenylmethylphosphine, while DAB appears to methylate on the ring.

in contrast with that of K(DPB), which resulted in the formation of the σ complex **46**.

Conclusions:

We have begun to study the chemistry of DPB, a phosphine which is isostructural with triphenylphosphine, but bears a negative charge. Unlike all other well-characterized boratabenzenes, DPB binds a transition metal through the boron-bound heteroatom. Our structural, reactivity, and computational data suggest that this may be because the lone pair on phosphorus, unlike the lone pair on the nitrogen center of DAB, does not participate in multiple bonding with boron, and it is therefore more available to react as a nucleophile.

Experimental Section.

General.

The general considerations of the previous chapters apply. Cp_2ZrHCl and Fp-I were purchased from Strem and used as received. 18-crown-6 was purchased from Aldrich and used as received. $(\text{PMe}_3)_3\text{RhCl}$ was prepared according to the literature.²²

Synthesis of $\text{Cp}_2\text{Zr(H)(PMe}_3\text{)(DPB)}$ (44).

PMe_3 (40.2 μL , 29.5 mg, 0.389 mmol) was added to Cp_2ZrHCl (33.4 mg, 0.129 mmol) in ~0.2 mL of THF. K-DPB (38.9 mg, 0.129 mmol) in ~1.8 mL of THF (minimal amount) was added, resulting in a cloudy suspension. After shaking for approximately 5 minutes, during which time the solution became orange and just a little cloudy, the reaction mixture was filtered through an Acrodisc. The resulting clear orange solution was added ~0.4 mL of hexanes, and the vial was then cooled to $-35\text{ }^\circ\text{C}$ overnight. The solids that had formed by the next morning were removed with an Acrodisc, and the resulting solution was cooled to $-35\text{ }^\circ\text{C}$ in a 2-dram vial with a 4-dram vial on the outside which contained pentane. Wheat-colored crystals (40.6 mg, 56% yield) were obtained. This complex is unstable as a solid at room temperature, or in solution in the absence of excess PMe_3 . For spectroscopic characterization, a solution was prepared with one equivalent of this compound and approximately three equivalents of trimethylphosphine. $^1\text{H NMR}$ (300 MHz; THF- d_8): δ 7.77 (t; J = 7.3; 4H), 7.27 (m; 6H), 7.12 (m; 2H), 6.52 (dd; J = 9.8, 5.6; 2H), 6.24 (t; J = 7.0; 1H), 5.52 (s; 10H), 2.95 (dd; J = 116.9, 87.2; 1H; Zr-H), 1.52 (d; J = 7.4; 9H; bound $\text{P}(\text{CH}_3)_3$), 0.95 (d; J = 2.3; free $\text{P}(\text{CH}_3)_3$). $^{13}\text{C NMR}$ (75 MHz; THF- d_8): δ 136.0 (br s), 132.6 (d; J = 13.0), 128.1 (br s), 128.1 (d; J = 7.4), 115.3, 104.7, 19.9 (d; J = 26.0; bound $\text{P}(\text{CH}_3)_3$), 16.8 (d; J = 13.3; free $\text{P}(\text{CH}_3)_3$). $^{11}\text{B NMR}$ (96 MHz; THF- d_8): δ +29.3 (br s). $^{31}\text{P}\{^1\text{H}\}$ NMR (121 MHz; THF- d_8): δ +11.9 (br s), +5.9 (d; J = 45.6), -61.4 (s; free PMe_3). $^{31}\text{P NMR}$ (121 MHz; THF- d_8): +11.9 (v br s), +6.0 (dd; J = 141.1, 43.3), -61.4 (s; free PMe_3). IR (KBr pellet): 3072, 3005, 2906, 1528, 1430, 1408, 1287, 1019, 954, 812, 744. mp. 135-152 (slow dec). Anal. calcd C: 64.50%, H: 6.32%. Found C: 63.71%, H: 6.02%. The X-ray structure of this compound is in Appendix II.

Synthesis of $\text{CpFe(CO)}_2\text{(DPB)}$ (45).

²²Jones, R. A.; Real, F. M.; Wilkinson, G.; Galas, A. M. R.; Hursthouse, M. B.; Malik, K. M. A. *J. Chem. Soc., Dalton*, **1980**, 511-518.

To a black, -78 °C solution of Fp-I (49.0 mg, 0.202 mmol) in 1.5 mL of THF was slowly added a colorless THF (5 mL) solution of K-DPB (60.5 mg, 0.202 mmol). The reaction mixture, which turned cloudy and red, was allowed to warm to room temperature and left to stir overnight. To the solution was then taken into the dark drybox, filtered through an Acrodisc, and vacuum dried. Diffusion in the dark of hexanes into a THF solution of CpFe(CO)₂(DPB) yielded 57.1 mg (65%) of the desired product, a light-sensitive orange solid. ¹H NMR (300 MHz; THF-d₈): δ 7.70 (m; 4H), 7.35 (m; 6H), 7.21 (m; 2H), 6.50 (t; J = 8.6; 2H), 6.40 (t; J = 7.1; 1H), 5.12 (s; 5H). ¹³C NMR (75 MHz; THF-d₈): δ 214.0 (d; J = 19.8), 138.1 (d; J = 35.6), 135.1 (d; J = 9.6), 133.3 (d; J = 16.2), 130.1 (d; J = 4.3), 129.5 (v br s), 128.9 (d; J = 10.9), 117.6 (br s), 89.5. ¹¹B NMR (96 MHz; THF-d₈): δ 32.0. ³¹P NMR (121 MHz; THF-d₈): δ +19.5 (br s). IR (KBr pellet): 3407, 3084, 3003, 2024, 1982, 694, 581, 494. mp. 185 °C (dec). Anal. calcd C: 65.81%, H: 4.60%. Found C: 65.99%, H: 4.67%. The X-ray structure of this compound is in Appendix II.

Synthesis of (PMe₃)₃Rh(DPB) (46).

To a 5-dram vial charged with 52.5 mg (0.143 mmol) of the red (PMe₃)₃RhCl was added K-DPB (42.9 mg, 0.143 mmol) in THF (2 mL). After 5 minutes of vigorous shaking, the solution, which had turned deep-red immediately, was filtered through an Acrodisc. Diffusion of pentane into the THF solution provided the desired product (56.3 mg, 66%) as red prisms. ¹H NMR (500 MHz; THF-d₈): δ 8.05 (td; J = 8.3, 1.8; 4H), 7.18 (m; 8H), 6.85 (dd; J = 8.5, 6.5; 2H), 6.34 (t; J = 6.5; 1H), 1.17 (s; 27H). ¹³C NMR (75 MHz; THF-d₈): δ 143.2 (d; J = 26.2), 136.2 (d; J = 8.9), 134 (br s), 132.6 (d; J = 13.7), 128.1 (d; J = 33.3), 128.0, 116.5, 21.3 (br s). ¹¹B NMR (96 MHz; THF-d₈): δ +26.1 (br s). ³¹P NMR (121 MHz; THF-d₈): δ +7.0 (br), -15.0 (br). IR (KBr pellet): 2990, 2966, 2908, 1434, 1419, 1408, 1279, 938, 703. mp. 158-175 °C (turns darker red, then black (168 °C); dec.) Anal. calcd C: 52.73%, H: 7.15%. Found, C: 52.69%, H: 7.11%. The X-ray structure of this compound is in Appendix II.

Synthesis of K(DPB)•(18-crown-6)•(toluene)_{1/2}.

A solution of 18-crown-6 (15.2 mg, 0.0575 mmol) in ~1 mL of THF was added to K(DPB) (15.7 mg, 0.0523 mmol) in a 2-dram vial, producing a homogeneous, colorless solution. This 2-dram vial was placed inside a 4-dram vial that contained hexane, and the 4-dram vial was then capped (a diffusion chamber) and allowed to sit at room temperature overnight, resulting in the formation of clear, colorless crystals. The solvent was decanted, and the crystals were dried. ¹H NMR (300 MHz;

THF- d_8): δ 7.48 (td; $J = 7.2, 1.2$; 4H; ortho H of C_6H_5), 7.12 (ddd; $J = 9.9, 7.2, 2.7$; 2H; meta H of BC_5H_5), 7.02 (m; 6H; meta and para H of C_6H_5), 6.45 (ddd; $J = 10.2, 4.2, 1.5$; 2H; ortho H of BC_5H_5), 6.16 (t; $J = 7.0$; 1H; para H of BC_5H_5), 3.55 (s; 24H; H of 18-crown-6). ^{13}C NMR (125 MHz; THF- d_8): δ 147.1 (d; $J = 17.2$; ipso C of C_6H_5), 135.9 (d; $J = 15.9$; ortho C of C_6H_5), 133.0 (d; $J = 9.1$; meta C of BC_5H_5), 130.3 (br s; ortho C of BC_5H_5), 127.6 (d; $J = 6.0$; meta C of C_6H_5), 125.5 (s; para C of C_6H_5), 112.7 (s; para C of BC_5H_5), 71.2 (s; C of 18-crown-6). ^{11}B NMR (96 MHz; THF- d_8): δ 31.6. ^{31}P NMR (121 MHz; THF- d_8): δ -30.1. IR (KBr pellet): 3049, 2993, 2898, 1579, 1525, 1474, 1406, 1350, 1282, 1247, 1109, 963, 835, 742, 702. The X-ray structure of this compound is in Appendix II.

Synthesis of $K(DAB) \cdot (18\text{-crown-6})$.

A solution of 18-crown-6 (31.7 mg, 0.120 mmol) in ~1 mL of THF was added to $K(DAB)$ (30.9 mg, 0.109 mmol) in a 2-dram vial, producing a homogeneous, yellow solution. This 2-dram vial was placed inside a 4-dram vial that contained hexane, and the 4-dram vial was then capped (a diffusion chamber) and allowed to sit at room temperature overnight, resulting in the formation of clear, yellow crystals. The solvent was decanted, and the crystals were dried. 1H NMR (300 MHz; THF- d_8) δ 7.26 (d; $J = 6.5$; 4H; ortho H of C_6H_5), 7.00 (app t; $J = 7.9$; 4H; meta H of C_6H_5), 6.96 (dd; $J = 10.8, 6.9$; 2H; meta H of BC_5H_5), 6.66 (t; $J = 7.2$; 2H; para H of C_6H_5), 5.97 (d; $J = 9.7$; 2H; ortho H of BC_5H_5), 5.69 (t; $J = 6.8$; 1H; para H of BC_5H_5). ^{13}C NMR (75 MHz; THF- d_8) δ 155.0 (ipso C of C_6H_5), 134.3 (meta C of BC_5H_5), 128.6, 126.8, 119.7 (para C of C_6H_5), 119.0 (br; ortho C of BC_5H_5), 106.1 (para C of BC_5H_5), 71.2 (C of 18-crown-6). ^{11}B NMR (96 MHz; THF- d_8): δ 33.0. IR (KBr pellet): 3042, 2989, 2885, 1581, 1489, 1411, 1351, 1307, 1283, 1266, 1233, 1106, 962, 838, 755, 700. The X-ray structure of this compound is in Appendix II.

Calculations

B-P-C(12)	106.2(3)	[105.6]
B-P-C(6)	102.5(3)	[106.5]
C(12)-P-C(6)	101.4(2)	[99.9]
C(1)-B-P	117.9(4)	[119.2]
C(1)-B-C(5)	115.4(5)	[116.5]
C(5)-B-P	126.7(4)	[124.3]
C(6)-P-B-C(1)	-66.2(5)	[-72.6]
C(6)-P-C(12)-C(17)	16.0(5)	[-43.9]
C(12)-P-C(6)-C(11)	-112.7(4)	[-65.0]
C(12)-P-B-C(1)	-172.2(4)	[-178.2]
B-P-C(12)-C(13)	-62.3(5)	[-112.7]
B-P-C(6)-C(11)	137.7(4)	[-174.7]
P-B	1.968(7)	[1.988]
P-C(6)	1.840(6)	[1.865]
P-C(12)	1.835(5)	[1.861]

Table 1. Selected Crystallographic [and Calculated] Bond Angles ($^{\circ}$), Torsion Angles ($^{\circ}$), and Bond Distances (\AA) for $\text{K-DPB}\cdot(18\text{-crown-6})\cdot(\text{toluene})_{1/2}$ (3).

B-N-C(12)	120.2(6)	[121.0]
B-N-C(6)	122.7(6)	[121.0]
C(12)-N-C(6)	117.0(5)	[118.0]
C(1)-B-N	122.9(7)	[122.0]
C(1)-B-C(5)	113.2(7)	[116.0]
C(5)-B-N	123.8(7)	[122.0]
C(6)-N-C(12)-C(17)	-42.3(9)	[-41.4]
C(6)-N-B-C(1)	-21.9(10)	[-34.0]
C(12)-N-C(6)-C(11)	-39.6(9)	[-41.4]
C(12)-N-B-C(1)	162.7(6)	[145.9]
B-N-C(12)-C(13)	-47.9(9)	[-40.7]
B-N-C(6)-C(11)	144.9(7)	[138.6]
N-B	1.510(10)	[1.535]
N-C(12)	1.431(8)	[1.400]
N-C(6)	1.399(8)	[1.400]

Table 2. Selected Crystallographic [and Calculated] Bond Angles ($^{\circ}$), Torsion Angles ($^{\circ}$), and Bond Distances (\AA) for $\text{K-DAB}\cdot(18\text{-crown-6})$ (4).

Calculated (HF/6-31G*) Coordinates for DPB in Chem3D Cartesian Coordinates 2 Format

```
34 1.0 1.0 1.0 90 90 90
P 1 0.5768389279 -0.9863947119 -0.3523704075 159
B 2 0.4355180186 -0.8377593093 1.625417978 53
C 3 1.6894800165 -0.9092164494 2.4586736745 63
C 4 -0.8629928763 -0.7275413411 2.3753906301 63
C 5 1.5824929222 -0.8428274575 3.8394799398 63
C 6 -0.8306160193 -0.6829427899 3.7615783044 63
C 7 0.3555413761 -0.7322887824 4.4918913977 63
C 8 1.3164342847 0.6165263366 -0.9533268011 63
C 9 1.8299149683 1.5928027313 -0.1029117118 63
C 10 1.4275701912 0.8374809039 -2.3295977674 63
C 11 2.4251438295 2.7427722322 -0.6068845134 63
C 12 2.0067134802 1.9872787296 -2.8346594376 63
C 13 2.5131574041 2.9491651416 -1.9715785738 63
C 14 -1.1602183741 -0.7961149606 -0.9925138513 63
C 15 -1.7781366944 -1.8907875685 -1.5904508891 63
C 16 -1.8974072251 0.3863047455 -0.8943186514 63
C 17 -3.0792977047 -1.8176161001 -2.0704548417 63
C 18 -3.1900708012 0.4694973743 -1.3807442169 63
C 19 -3.7889205642 -0.6348488383 -1.9713261008 63
H 20 2.6891708119 -1.0102013057 2.052585821 11
H 21 2.4757977901 -0.8857957662 4.4514303011 11
H 22 0.3235429773 -0.6907081214 5.5701322221 11
H 23 -1.7578672092 -0.6037061853 4.3169514872 11
H 24 -1.8385434595 -0.6834690293 1.9113751827 11
H 25 1.7644534639 1.4502148425 0.9593643609 11
H 26 2.813664134 3.4800292655 0.075624298 11
H 27 2.9710485222 3.843050428 -2.3606241886 11
H 28 2.0705562211 2.1310181938 -3.9004986313 11
H 29 1.0512997981 0.0950002493 -3.0119722145 11
H 30 -1.2306244499 -2.8121857882 -1.6840016566 11
H 31 -3.5314479716 -2.6828795596 -2.5256973849 11
H 32 -4.7962148539 -0.5705865237 -2.3470241903 11
```

H 33 -3.7353617454 1.3941259494 -1.2924605336 11

H 34 -1.4523773219 1.2449471321 -0.4261981923 11

Calculated (HF/6-31G*) Coordinates for DAB in Chem3D Cartesian Coordinates 2 format

34 1.00 1.00 1.00 90 90 90

N 1 -0.0001808223 0.0012508033 -0.0354546454 73

B 2 0.0090145145 -0.0484569729 1.498582592 53

C 3 1.2623071888 -0.3599064162 2.2813400097 63

C 4 -1.2348022268 0.2107113762 2.3147928235 63

C 5 1.1994206095 -0.3870993808 3.6640653917 63

C 6 -1.1554531283 0.1479328533 3.6955139845 63

C 7 0.0261538775 -0.1423189477 4.3789371518 63

C 8 1.1143727275 0.458102912 -0.748688375 63

C 9 1.8416520806 1.5667014169 -0.3029576415 63

C 10 1.5562836801 -0.172651 -1.9166243678 63

C 11 2.9522275286 2.0160479189 -0.9927359773 63

C 12 2.6607602855 0.2915570505 -2.6094208112 63

C 13 3.3730330833 1.3897566817 -2.1566581107 63

C 14 -1.1233579397 -0.4089047908 -0.7633657483 63

C 15 -1.8458670985 -1.5441250916 -0.3814452097 63

C 16 -1.5788399602 0.2957967564 -1.8828092949 63

C 17 -2.9648207101 -1.9482986381 -1.0854829416 63

C 18 -2.691736139 -0.1230171626 -2.590889198 63

C 19 -3.3991371688 -1.2483222427 -2.2014727683 63

H 20 2.2251780075 -0.5719227101 1.8331971741 11

H 21 2.0937149537 -0.6146699572 4.2333577196 11

H 22 0.0325793412 -0.1774503885 5.4577776917 11

H 23 -2.0428360259 0.3375828481 4.2890030289 11

H 24 -2.2028845229 0.450936515 1.8928765764 11

H 25 1.5296092652 2.0567664219 0.5990461264 11

H 26 3.4888962945 2.872330026 -0.6194546134 11

H 27 4.2355346583 1.7462712728 -2.6932012616 11

H 28 2.9725069473 -0.2211846054 -3.5044401149 11

H 29 1.026767089 -1.0352845493 -2.2770530653 11

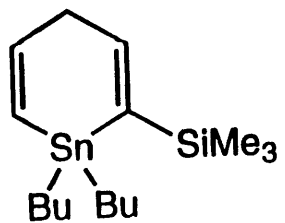
H 30 -1.5233621133 -2.091291106 0.4832788248 11
H 31 -3.4974523735 -2.8270116667 -0.7618488577 11
H 32 -4.2681579142 -1.5696864082 -2.7495764192 11
H 33 -3.0138611081 0.4463348522 -3.4471739983 11
H 34 -1.053219455 1.1800289252 -2.1931127548 11

Appendix I: Selected ^1H NMR Spectra

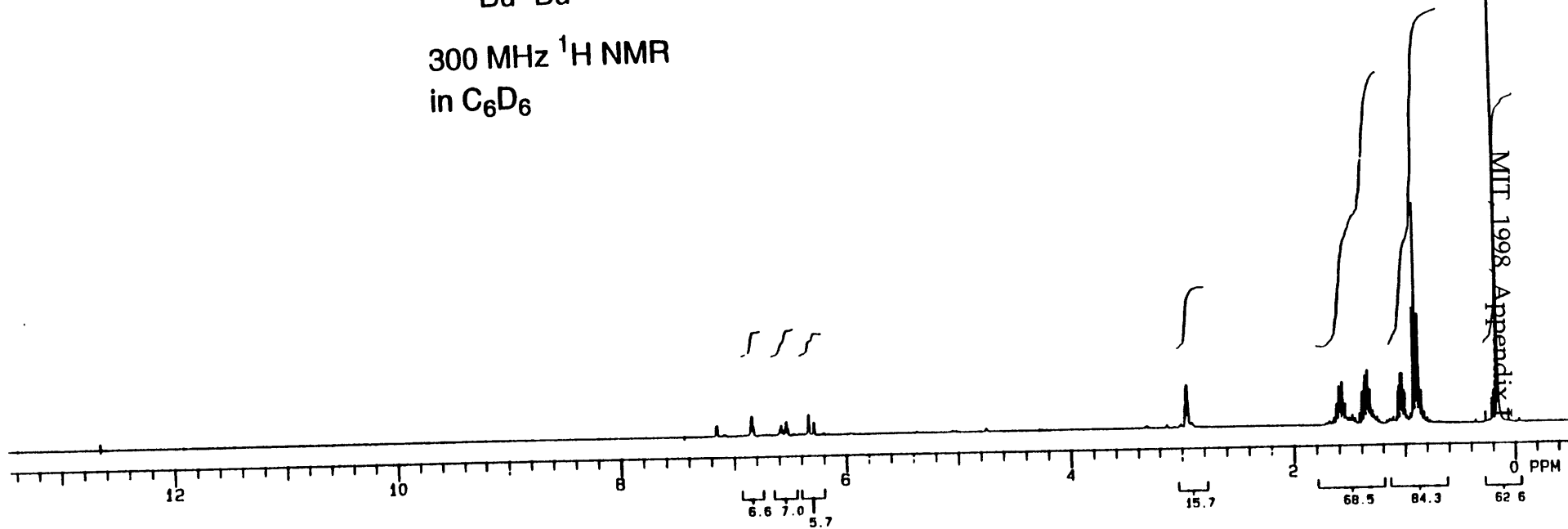
Chapter:	Compound Name (Number):
2	• Stannacycle 2
2	• Boracycle 3
2	• BB-py (4a)
2	• BB-lut (4b)
2	• BB-NEt ₃ (4c)
2	• BB-NMe ₃ (4d)
2	• BB-PMe ₃ (4e)
2	• BB-CN ^t Bu (4f)
2	• Isomerized Boracycle 5
2	• Betaine 7 + BB-PMe ₃ (4e)
3	• Li(BBH) (9a)
3	• Li(BB-CCSiMe ₃) (9b)
3	• Li(BB-NMe ₂) (9c)
3	• Na(BB-OEt) (9d)
3	• Na(BB-OMe) (9e)
3	• K(DPB) (9f)
3	• K(DAB) (9g)
3	• Bu ₄ N(BB-CN) (9h)
4	• (BB-PMe ₃)Cr(CO) ₃ (14b)
4	• Li(BBH)Cr(CO) ₃ •(Et ₂ O) (18a)
4	• [(BB-py)Rh(nbd)](BF ₄) (19a)
4	• (BB-NMe ₂)Rh(cod) (20a)
4	• (BB-OMe)Rh(nbd) (20d)
4	• (BB-N(¹³ CH ₃)(Me) ₂)Rh(cod)I (22a)
4	• (BB-OTf)Rh(nbd) (26a)
4	• [(BB-PMe ₃)Rh(nbd)](OTf) (28)
4	• (BB-OTs)Rh(cod) (30)
4	• [(Ph ₂ cod)RhCl] ₂ (34)
4	• (BB-OMe)Rh(Ph ₂ cod) (35)
4	• (BB-OMe)Rh(dppe)
5	• (BBH) ₂ Fe (37)
5	• CpFe(BBH) (40)

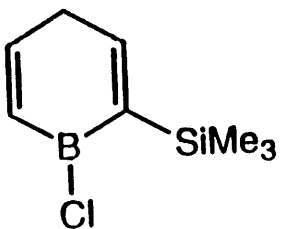
- 5 • [(BBH)Cr(CO)₃]₂Hg (43)
- 6 • Cp₂Zr(H)(PMe₃)(DPB) (44)

¹H NMR Spectrum of Stannacycle 2.

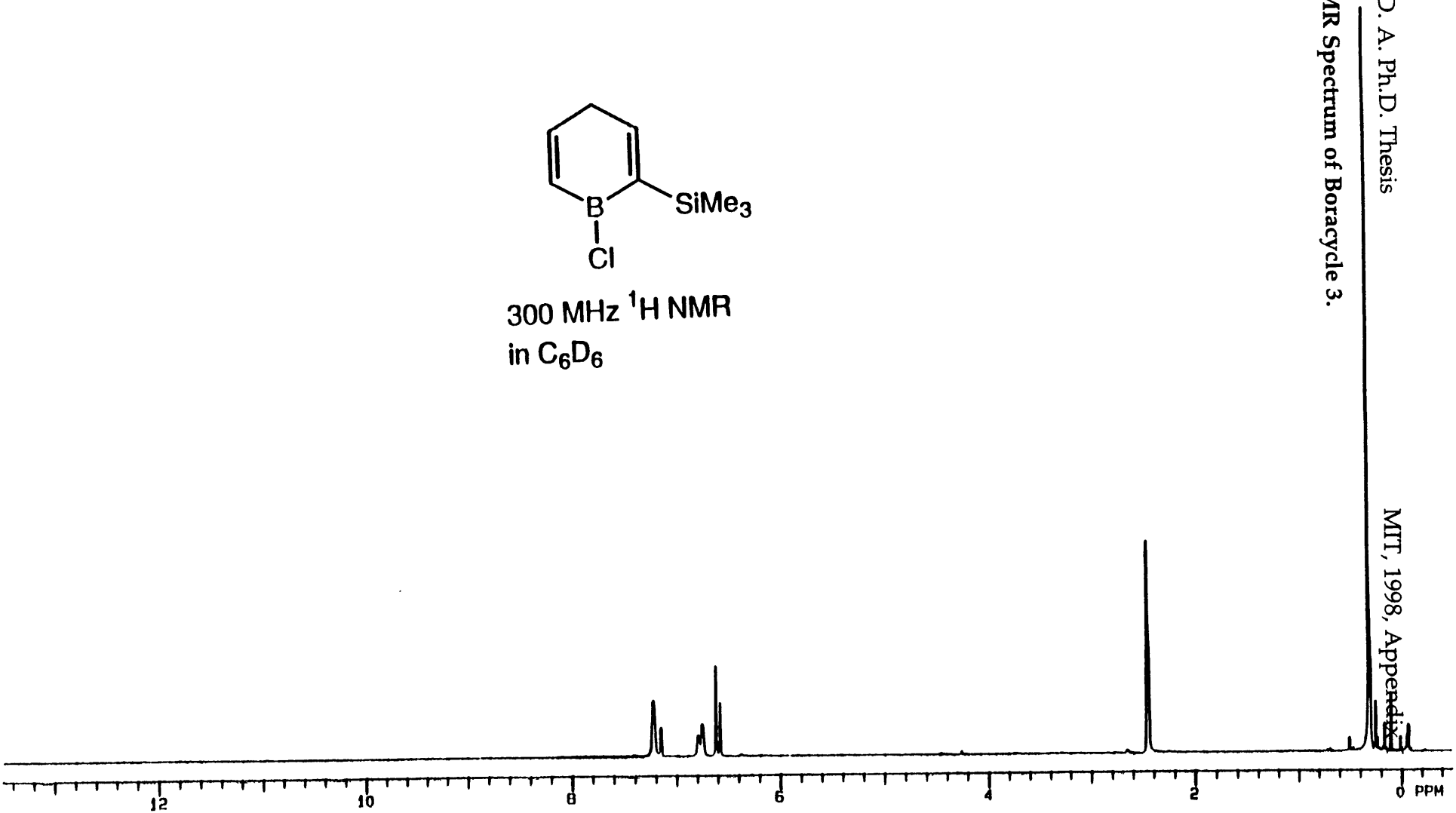


300 MHz ¹H NMR
in C₆D₆

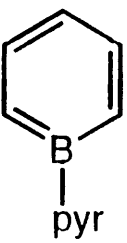




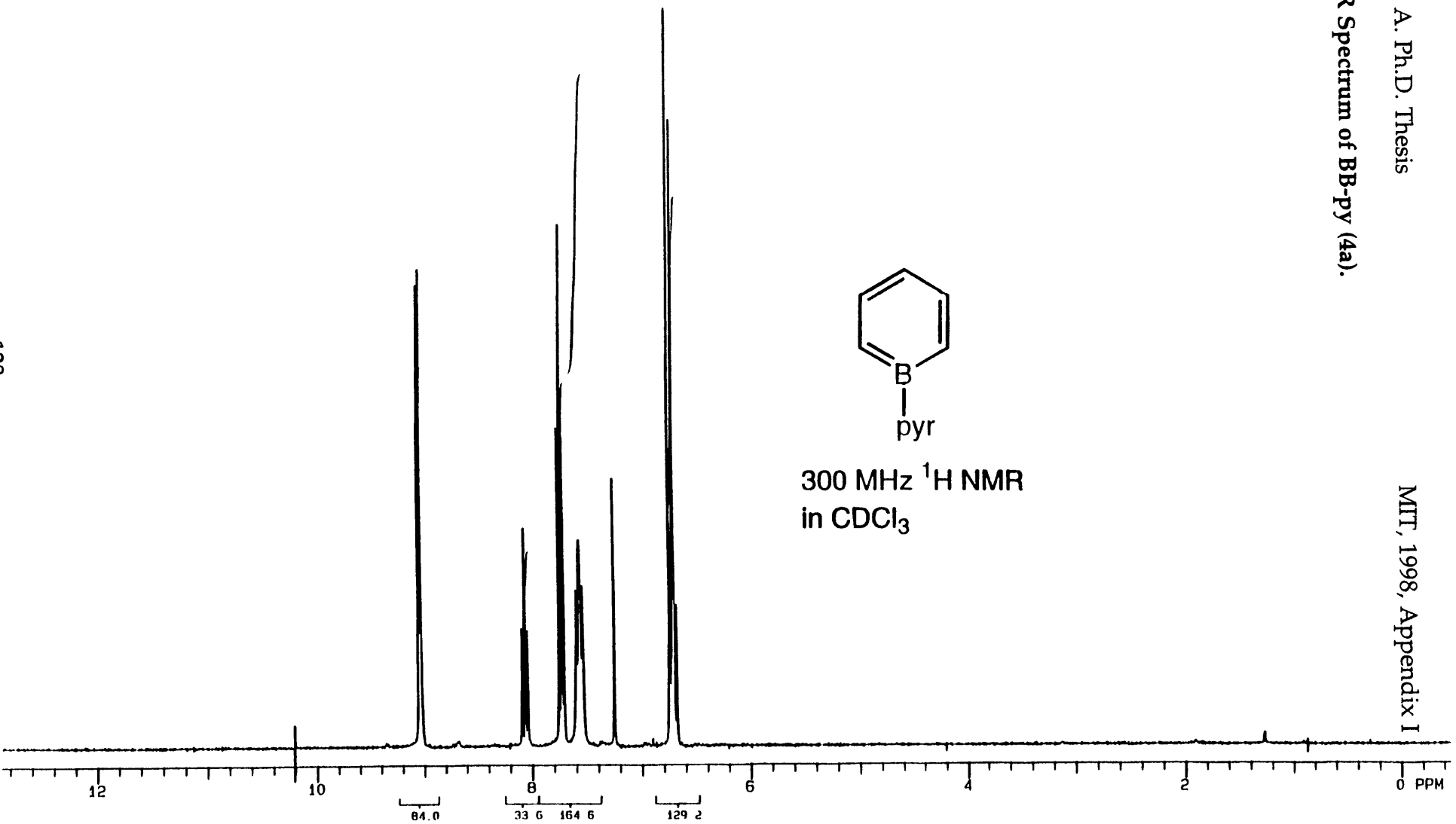
300 MHz ¹H NMR
in C₆D₆



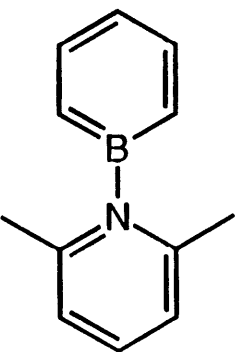
^1H NMR Spectrum of BB-py (4a).



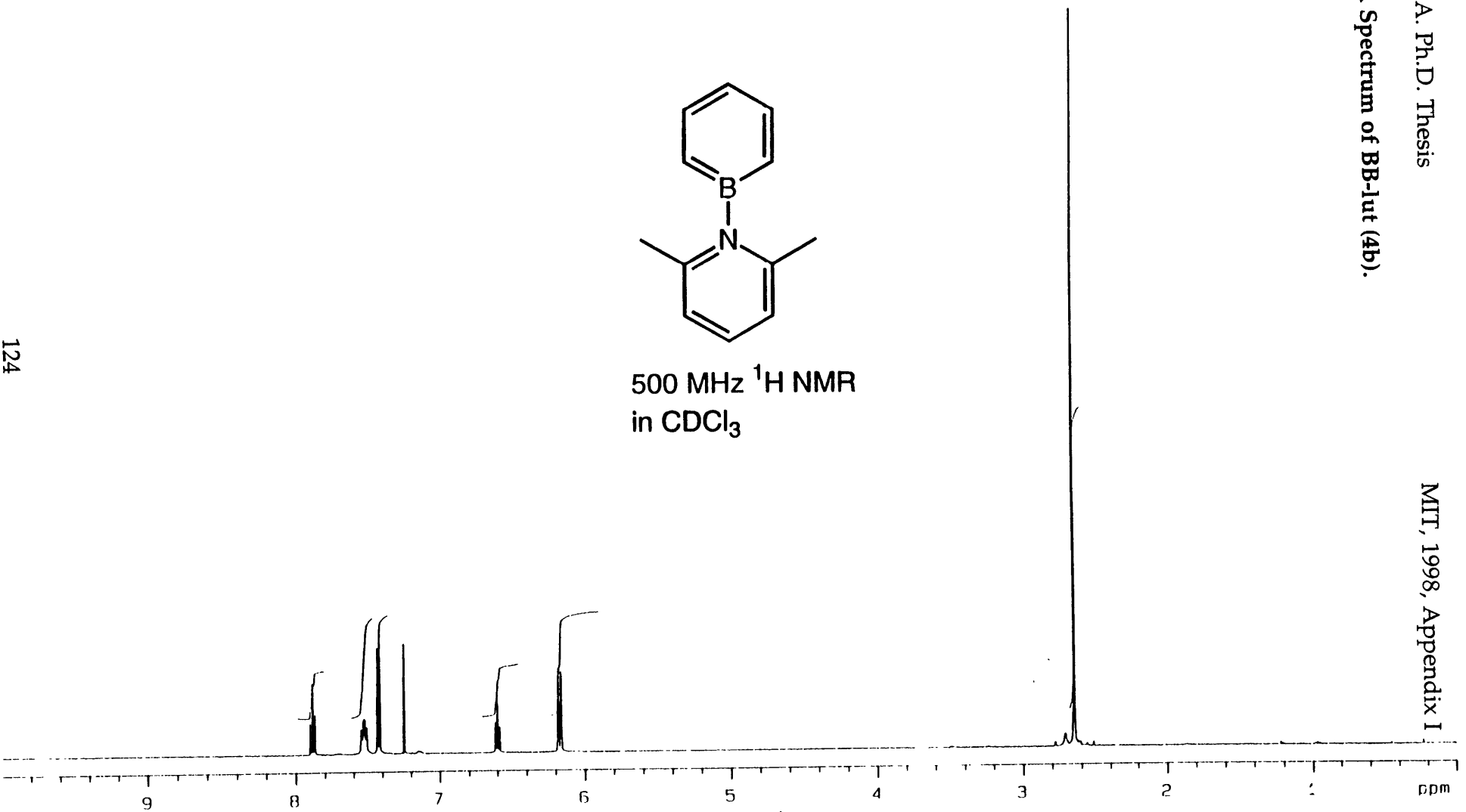
300 MHz ^1H NMR
in CDCl_3



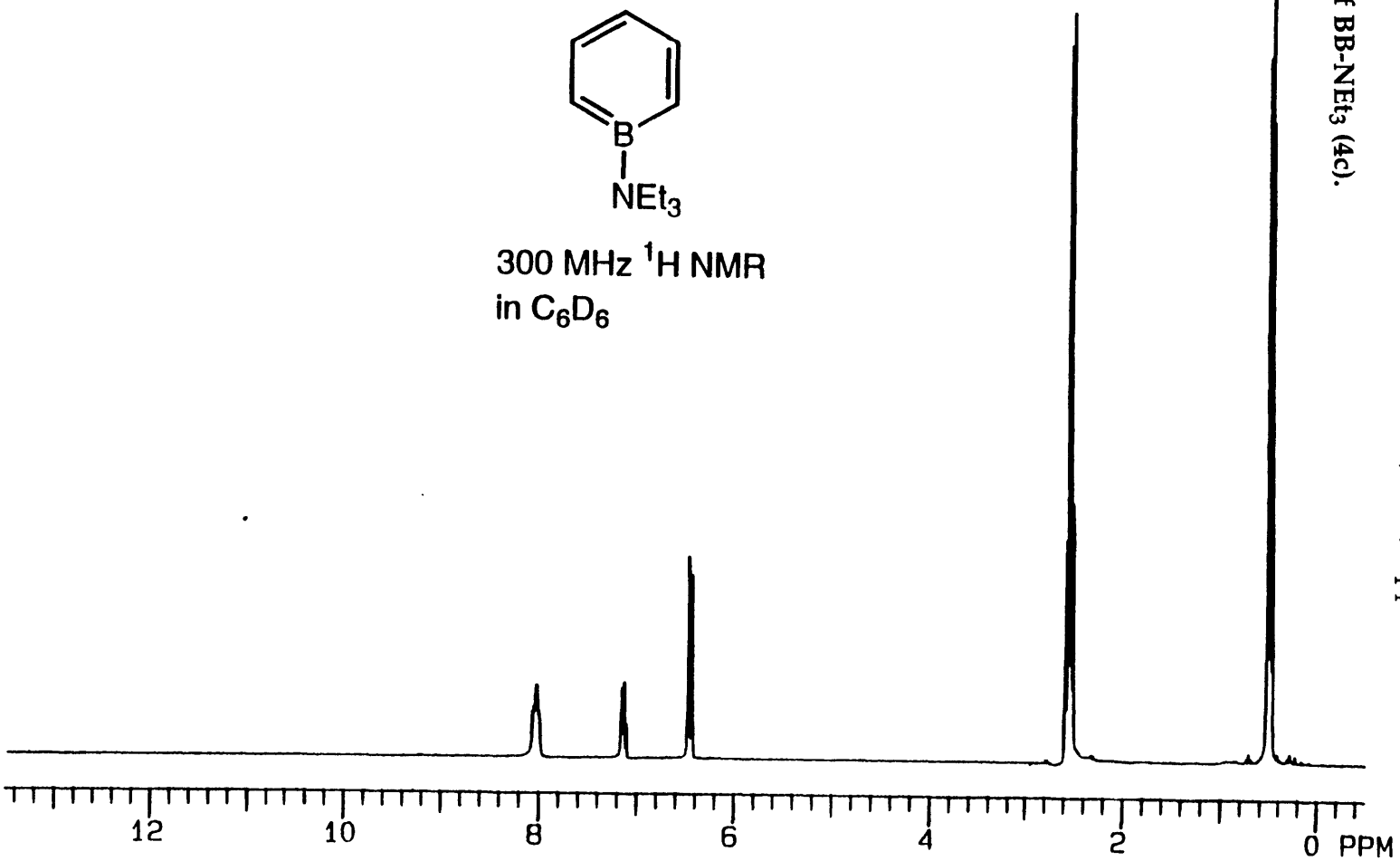
^1H NMR Spectrum of BB-Iut (4b).



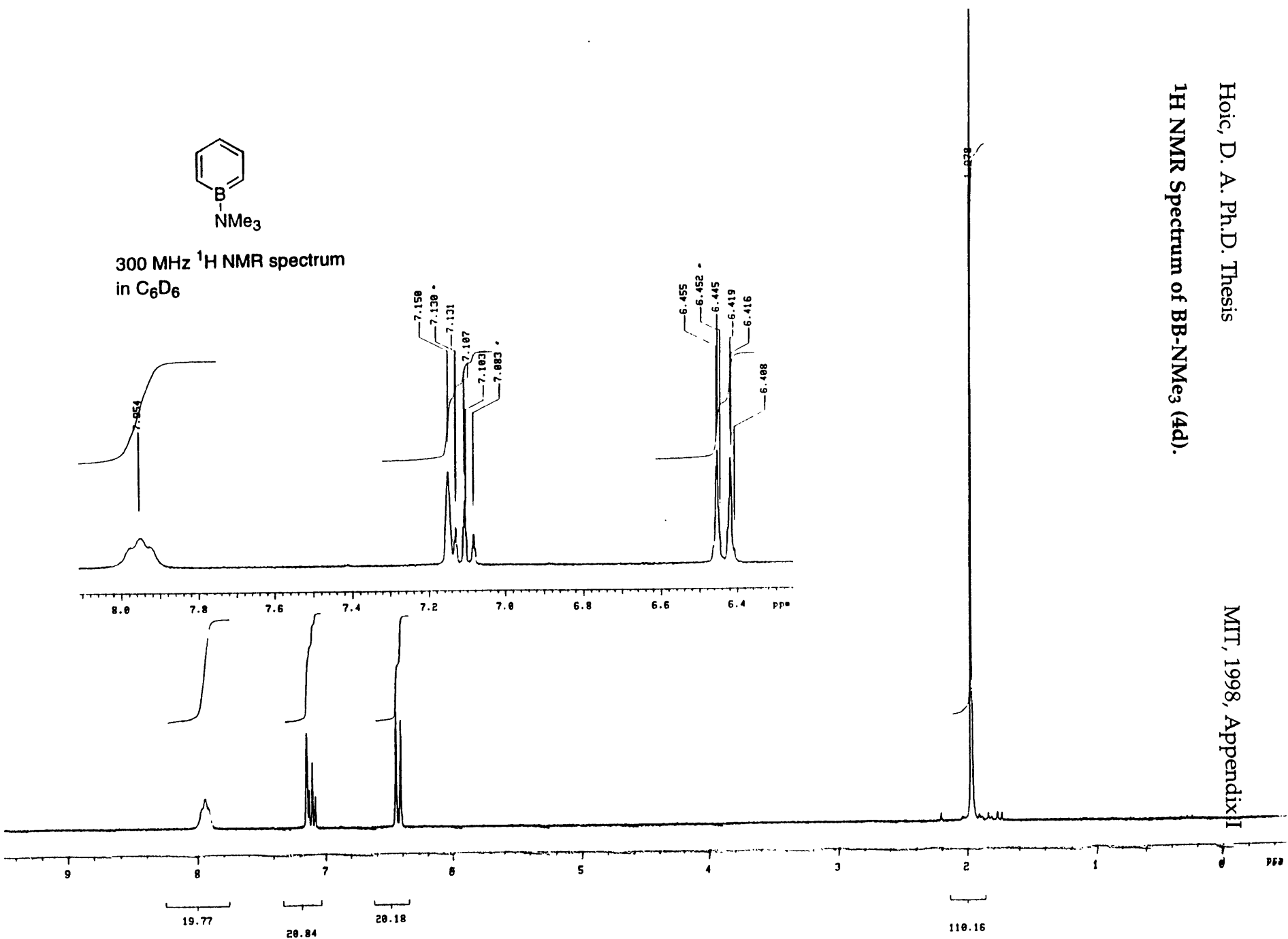
500 MHz ^1H NMR
in CDCl_3



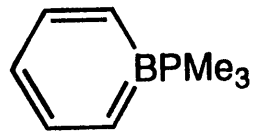
^1H NMR Spectrum of BB-NEt₃ (4c).



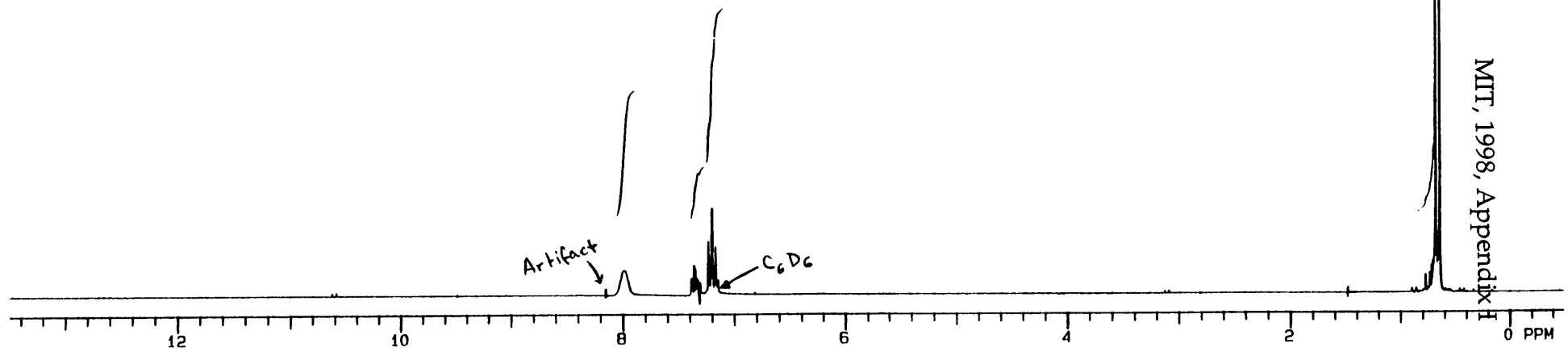
^1H NMR Spectrum of BB-NMe₃ (4d).



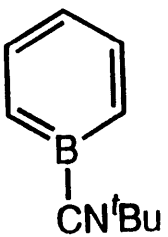
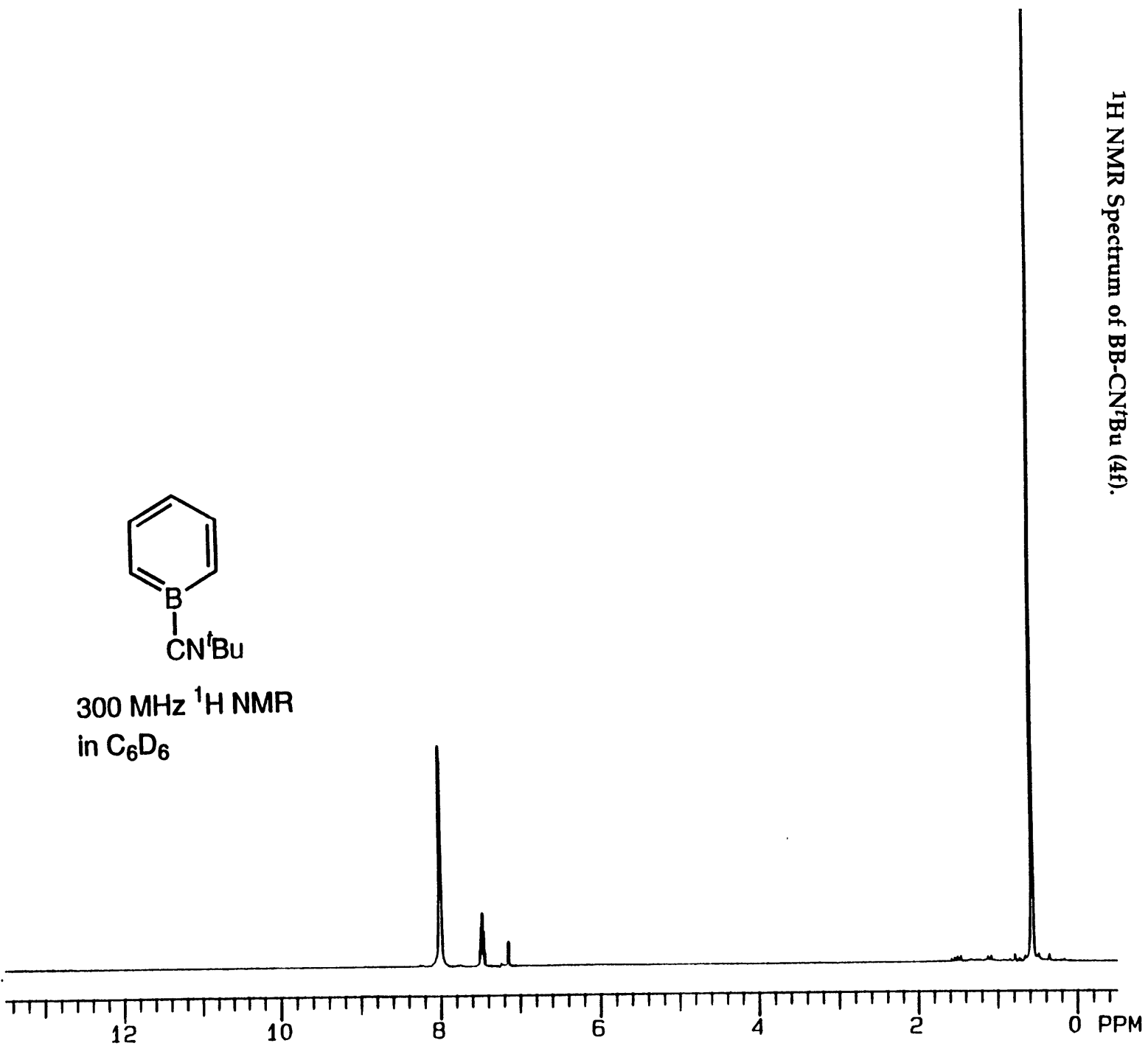
^1H NMR Spectrum of BB-PMe₃ (4e).



300 MHz ^1H NMR spectrum in C₆D₆

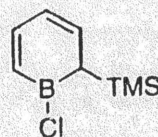


^1H NMR Spectrum of BB-CN^tBu (4f).



300 MHz ^1H NMR
in C_6D_6

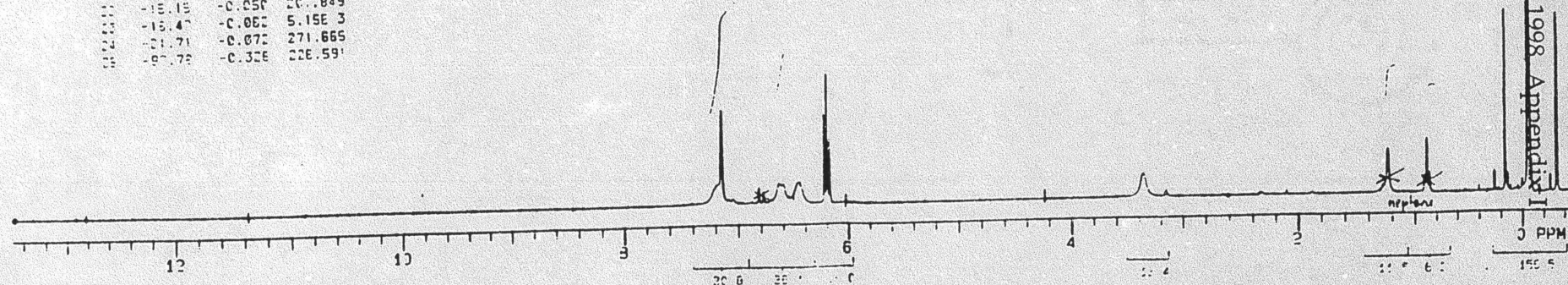
¹H NMR Spectrum of Isomerized Boracycle 5.



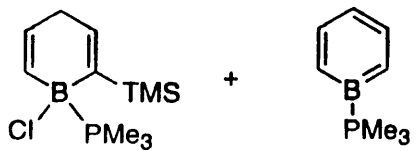
300 MHz ¹H NMR spectrum
in C₆D₆

300 MHz 1H NMR SPECTRUM
SPECTRAL LINES FOR THE
300 MHz 1H NMR SPECTRUM

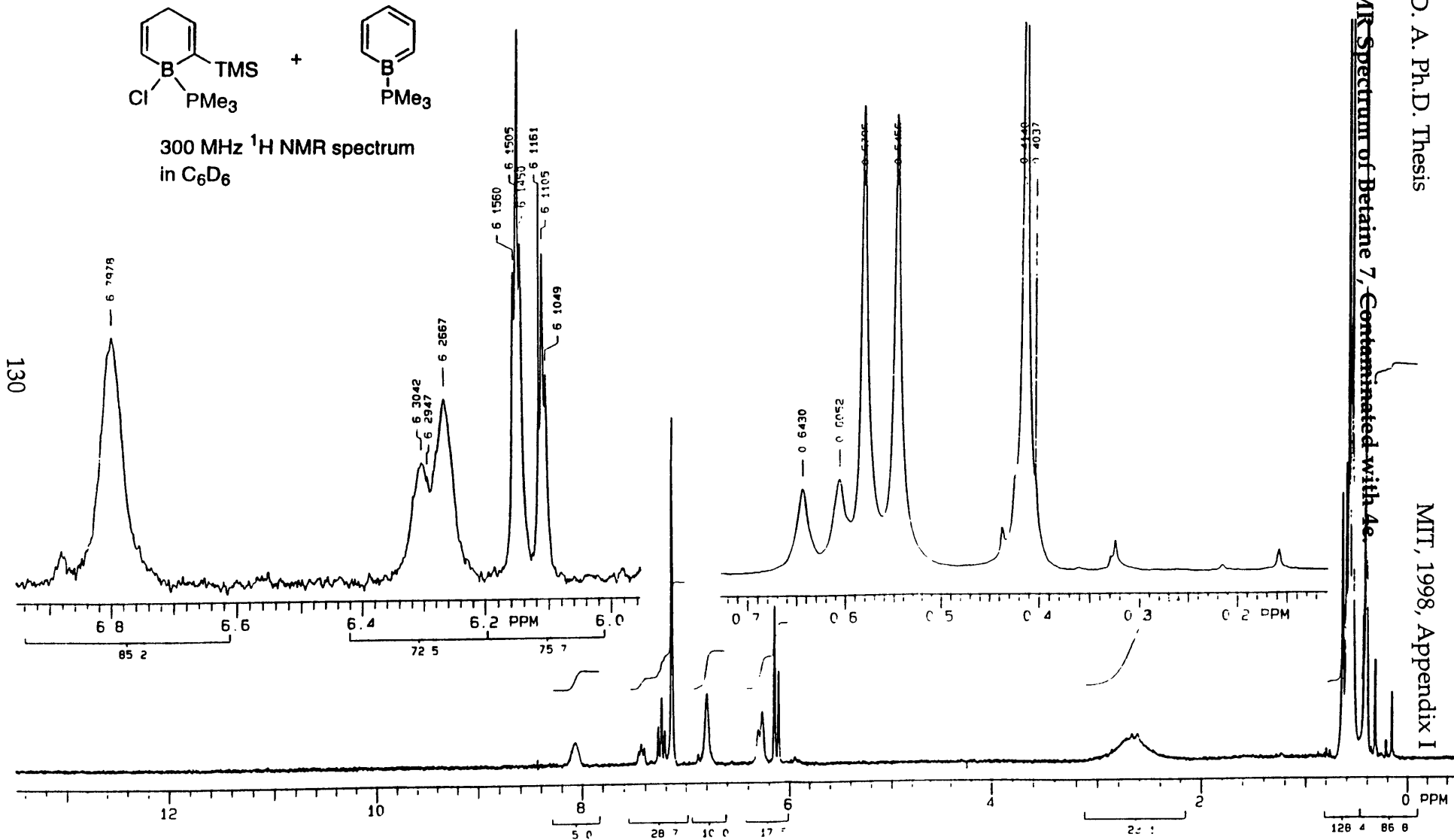
INDEX	FREQ	PPM	INTENSITY
1	145.45	7.196	24.604
2	142.72	7.150	121.792
3	132.74	6.644	27.156
4	129.27	6.622	25.159
5	126.56	6.627	25.677
6	121.01	6.607	25.517
7	122.94	6.601	25.296
8	122.49	6.596	24.121
9	133.76	6.467	27.845
10	133.99	6.456	27.677
11	122.72	6.456	27.071
12	122.00	6.226	114.316
13	132.60	6.202	164.328
14	122.29	6.179	62.714
15	122.41	6.365	25.376
16	122.95	6.362	29.001
17	122.46	6.235	55.632
18	122.32	6.668	70.726
19	122.32	6.655	25.681
20	122.15	6.261	24.925
21	122.57	6.150	242.871
22	122.15	-0.250	207.849
23	122.47	-0.062	5.1563
24	122.71	-0.072	271.665
25	122.72	-0.326	226.591

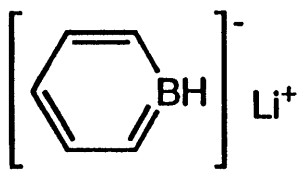


¹H NMR Spectrum of Betaine 7, Contaminated with 4e

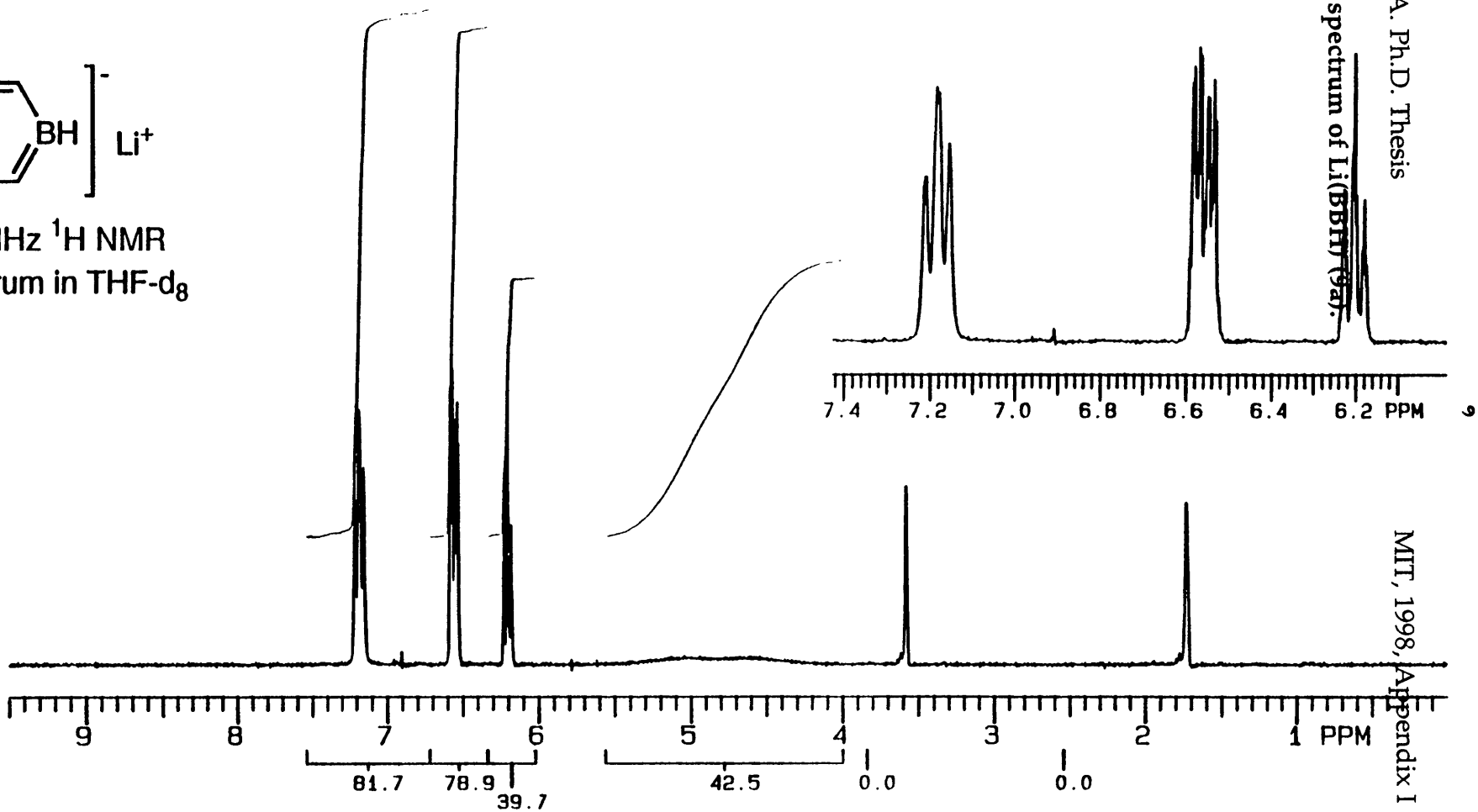


300 MHz ¹H NMR spectrum
in C₆D₆

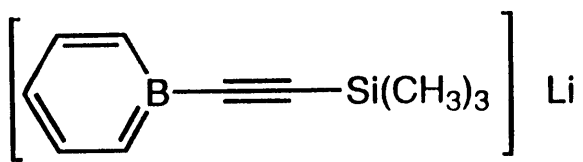




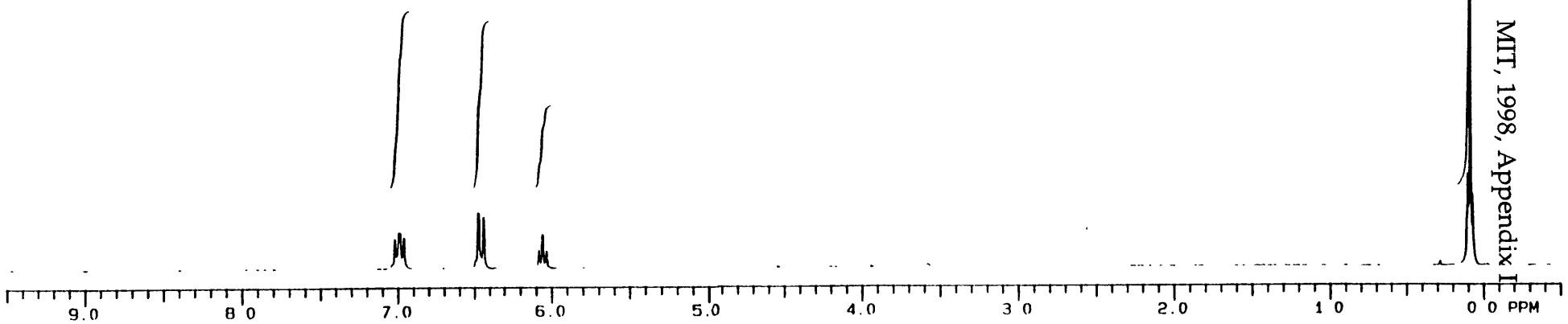
300 MHz ^1H NMR spectrum in THF-d_8



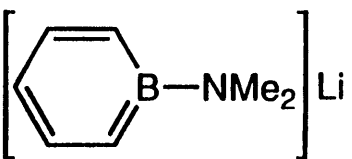
^1H NMR spectrum of $\text{Li}(\text{B}(\text{C}_6\text{H}_5)\text{CCSiMe}_3)$ (9b).



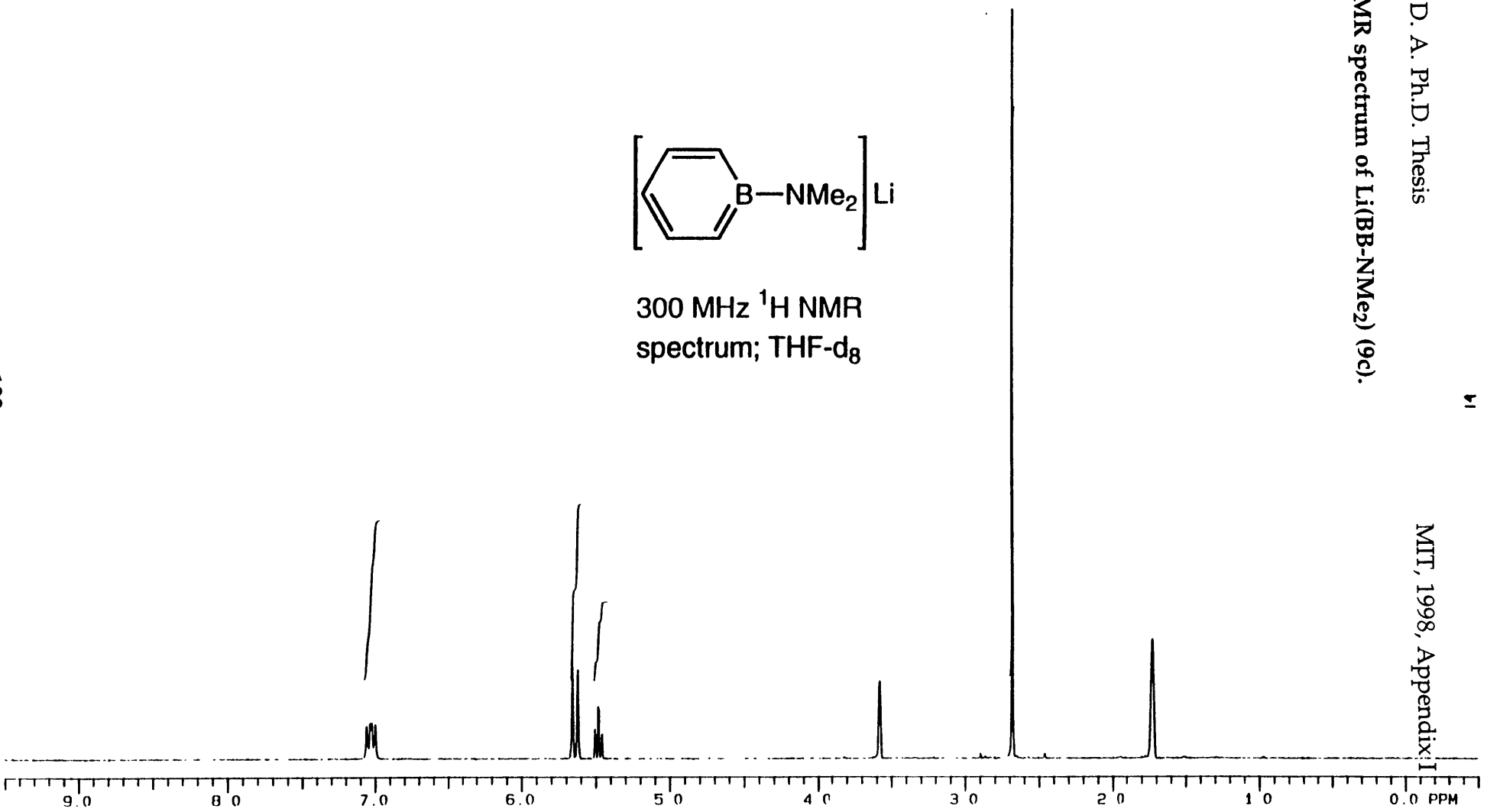
300 MHz ^1H NMR spectrum; THF- d_8



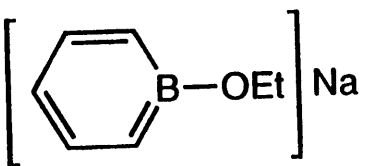
^1H NMR spectrum of $\text{Li}(\text{B}(\text{C}_6\text{H}_5)\text{NMe}_2)$ (9c).



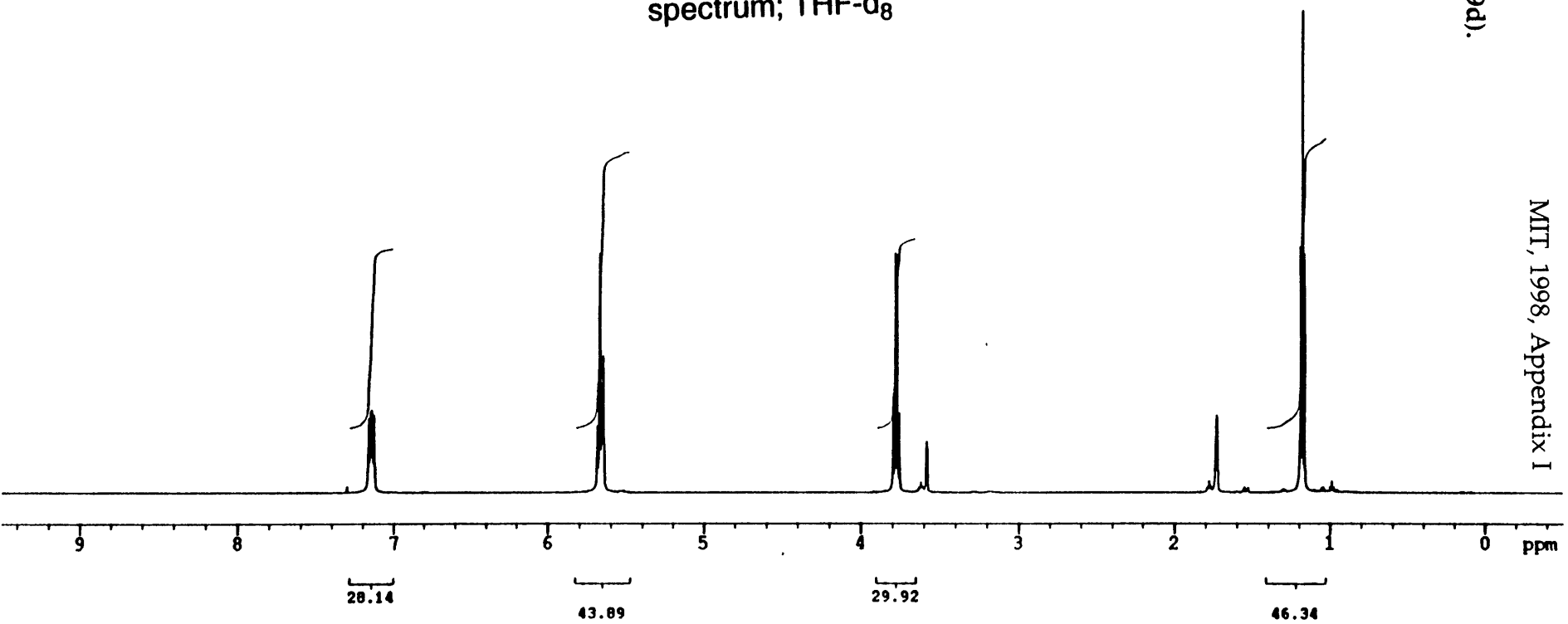
300 MHz ^1H NMR
spectrum; THF- d_8



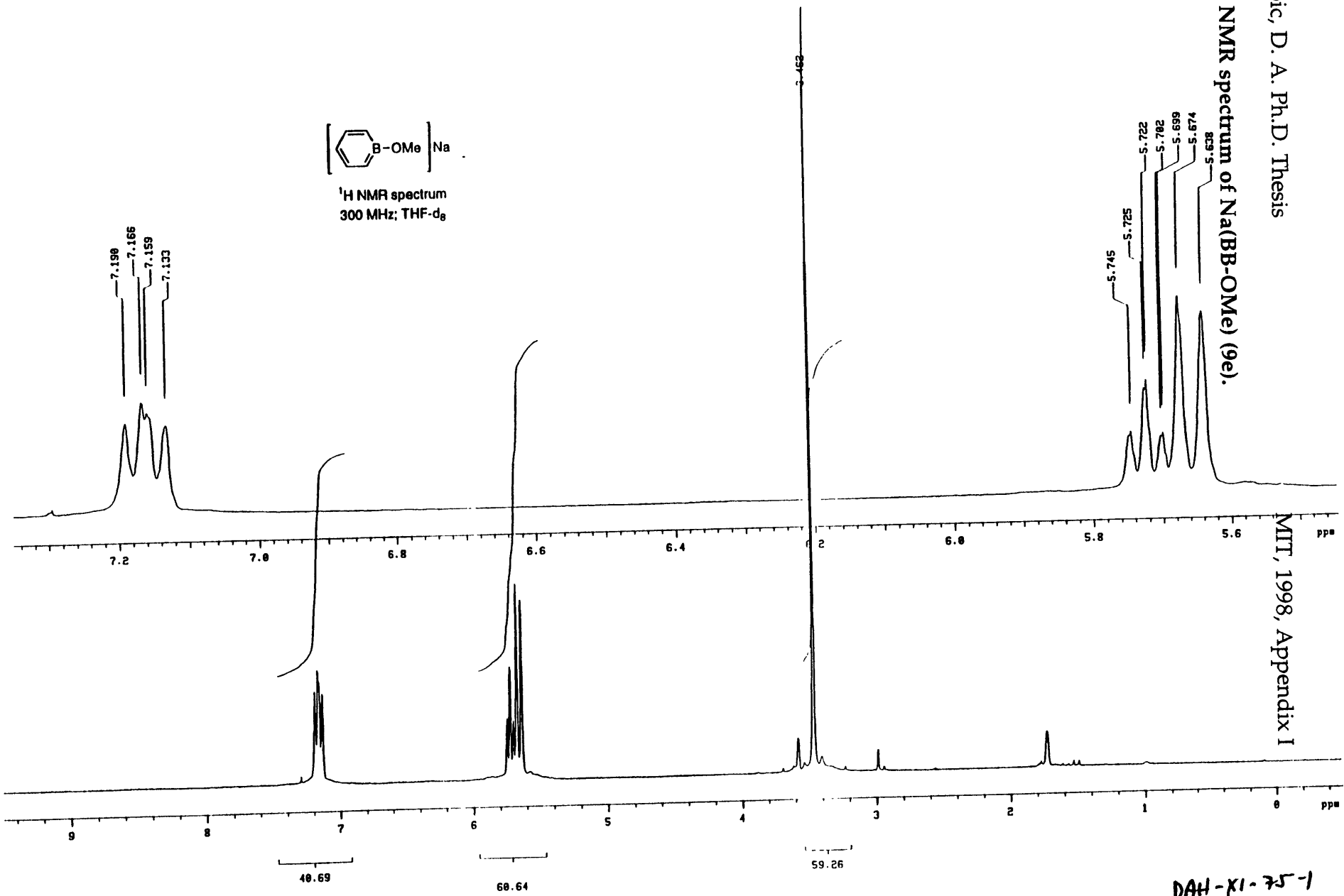
^1H NMR spectrum of $\text{Na}(\text{BB-OEt})$ (9d).



500 MHz ^1H NMR
spectrum; THF-d_8



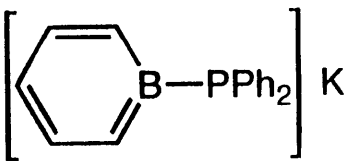
¹H NMR spectrum of Na(BB-OMe) (9e).



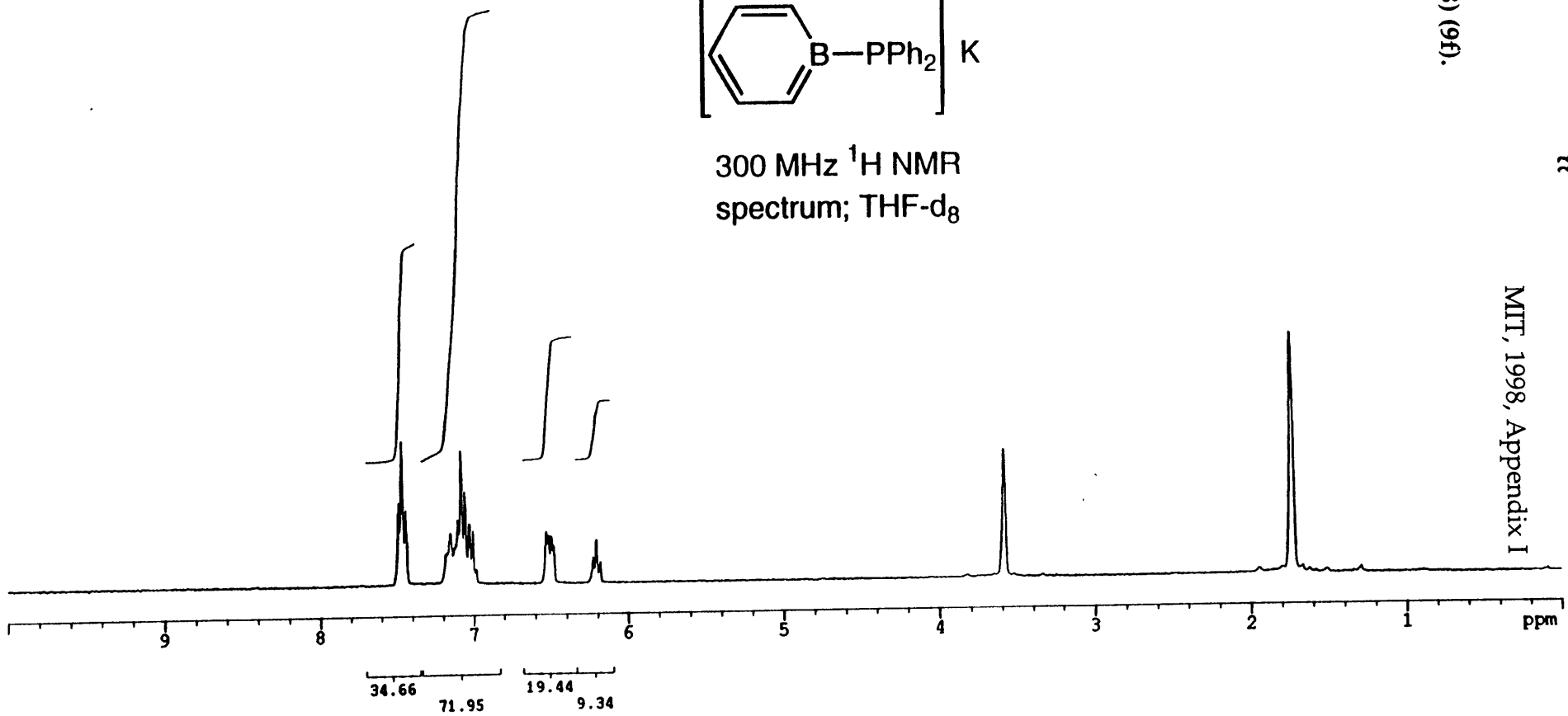
MIT, 1998, Appendix I

DAH-XI-75-1
THF₈

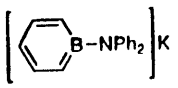
^1H NMR spectrum of K(DPB) (9f).



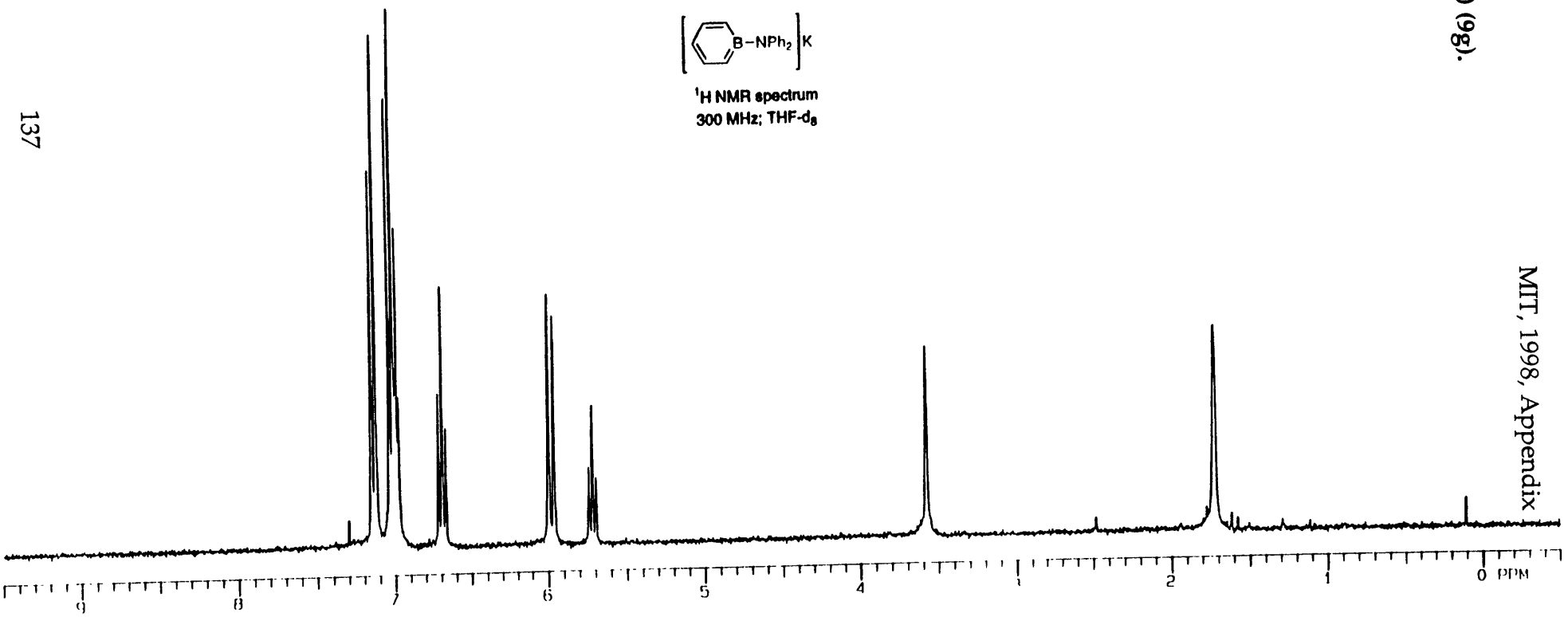
300 MHz ^1H NMR spectrum; THF- d_8



^1H NMR spectrum of K(DAB) (9g).

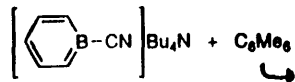


^1H NMR spectrum
300 MHz; THF-d₆

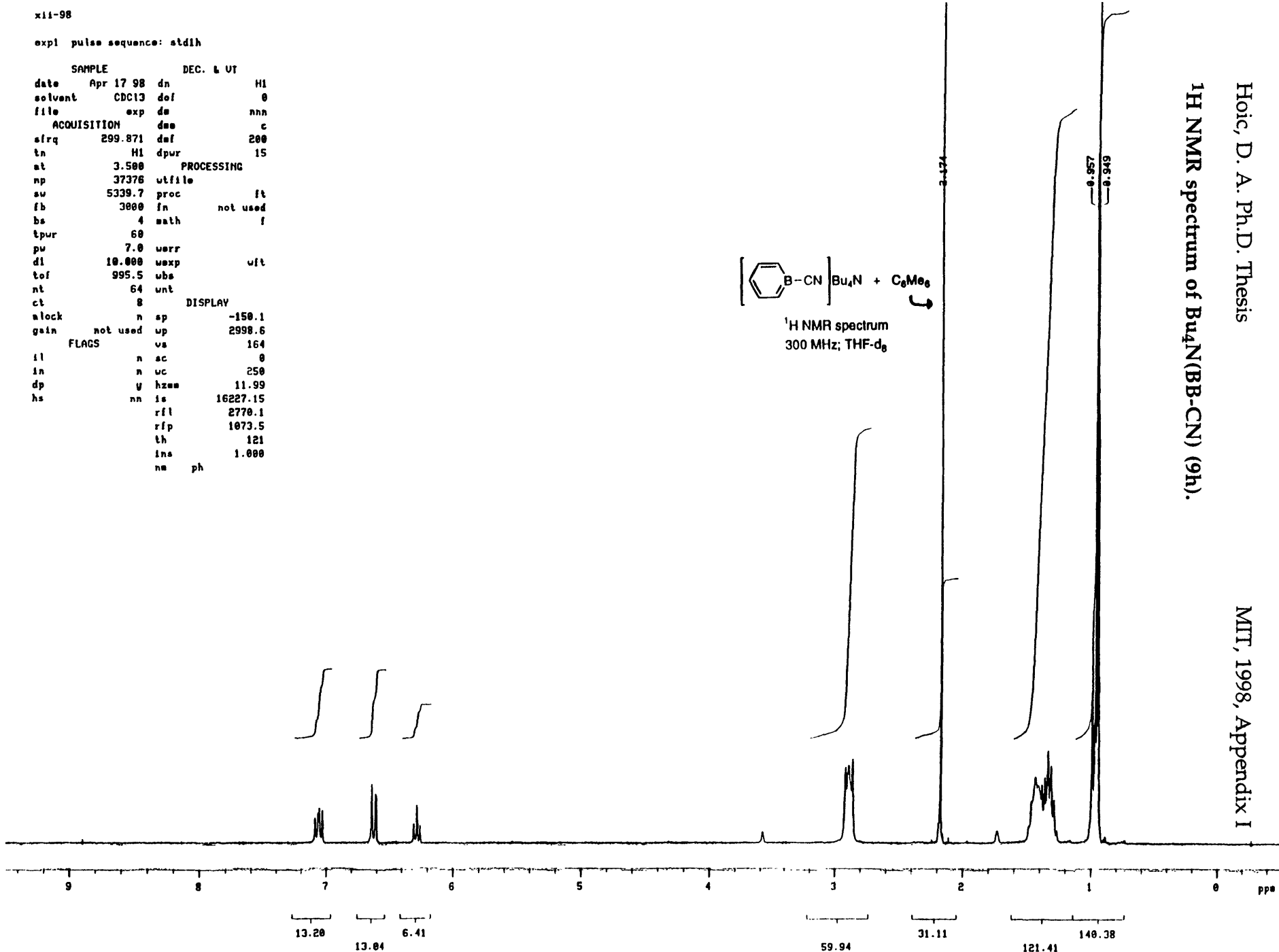


expl pulse sequence: std1h

SAMPLE		DEC. & UT	
date	Apr 17 98	dn	H1
solvent	CDC13	dof	0
file	exp	ds	nnn
ACQUISITION		das	c
sfrq	299.871	daf	200
tn	H1	dpur	15
at	3.500	PROCESSING	
np	37376	utfile	
su	5339.7	proc	ft
fb	3800	fn	not used
bs	4	math	f
tpur	60		
pu	7.0	uarr	
dl	10.000	uexp	uit
tof	995.5	ubs	
nt	64	unt	
ct	8	DISPLAY	
alock	n	sp	-150.1
gain	not used	up	2998.6
FLAGS		va	164
il	n	ac	0
in	n	uc	250
dp	y	hzam	11.99
hs	nn	is	16227.15
		rfl	2770.1
		rfp	1073.5
		th	121
		ina	1.000
		na	ph



¹H NMR spectrum
300 MHz; THF-d₆

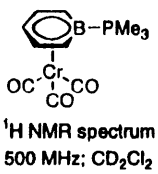
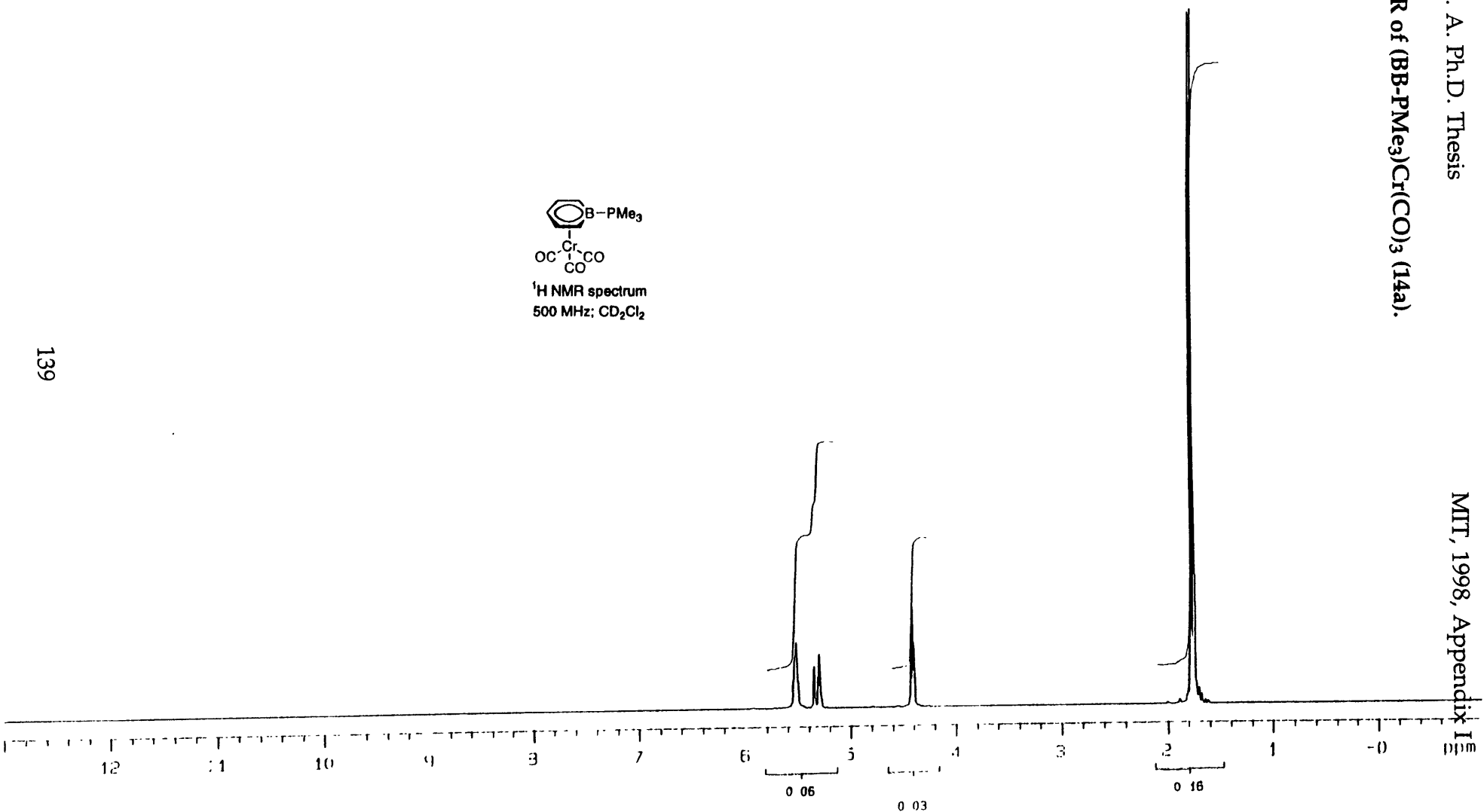


Hoic, D. A. Ph.D. Thesis
¹H NMR spectrum of Bu₄N(BB-CN) (9h).

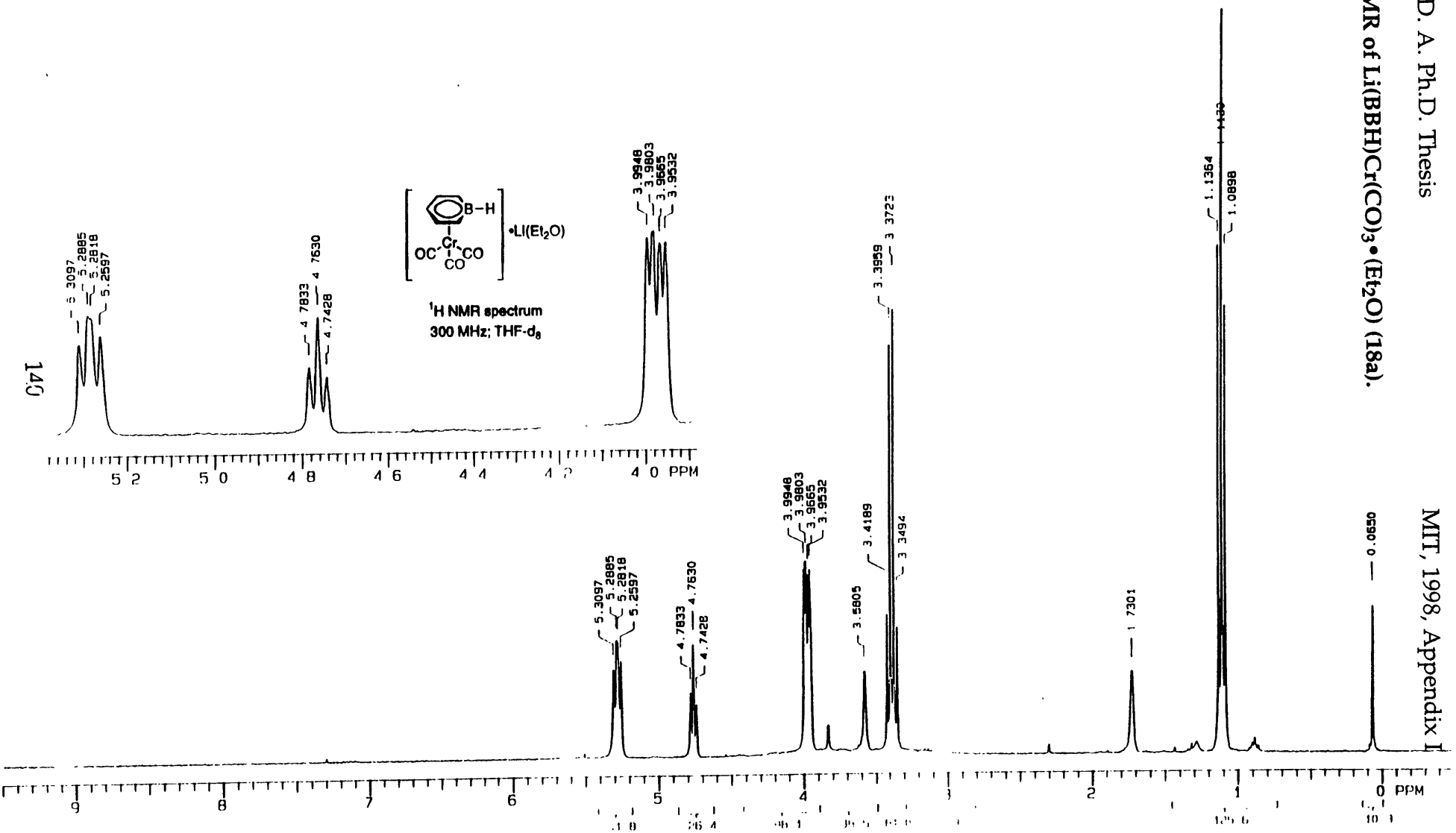
MIT, 1998, Appendix I

DAH-x-221-2
THF-d₆ U_n 300

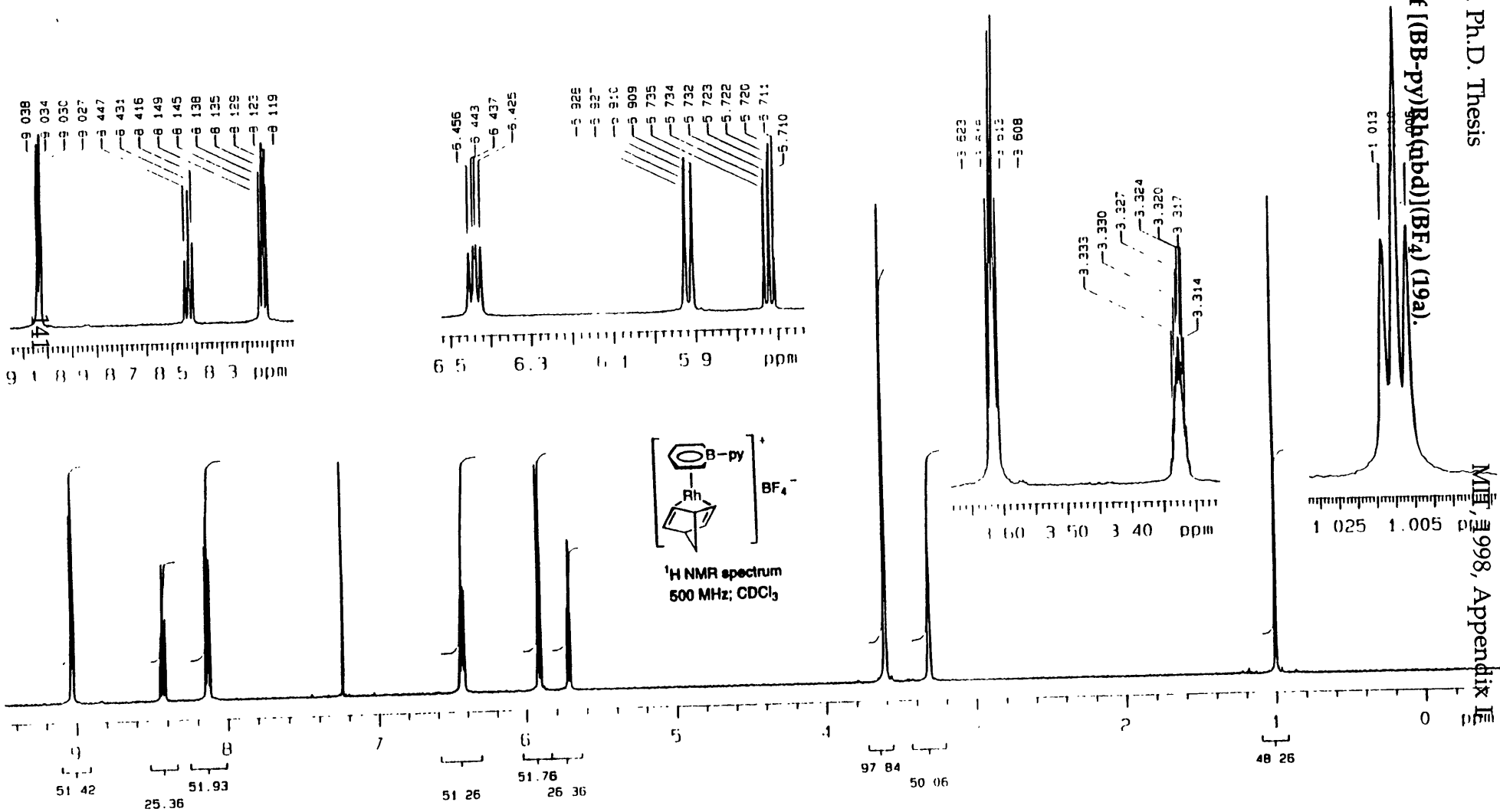
^1H NMR of $(\text{BB-PMe}_3)\text{Cr}(\text{CO})_3$ (14a).



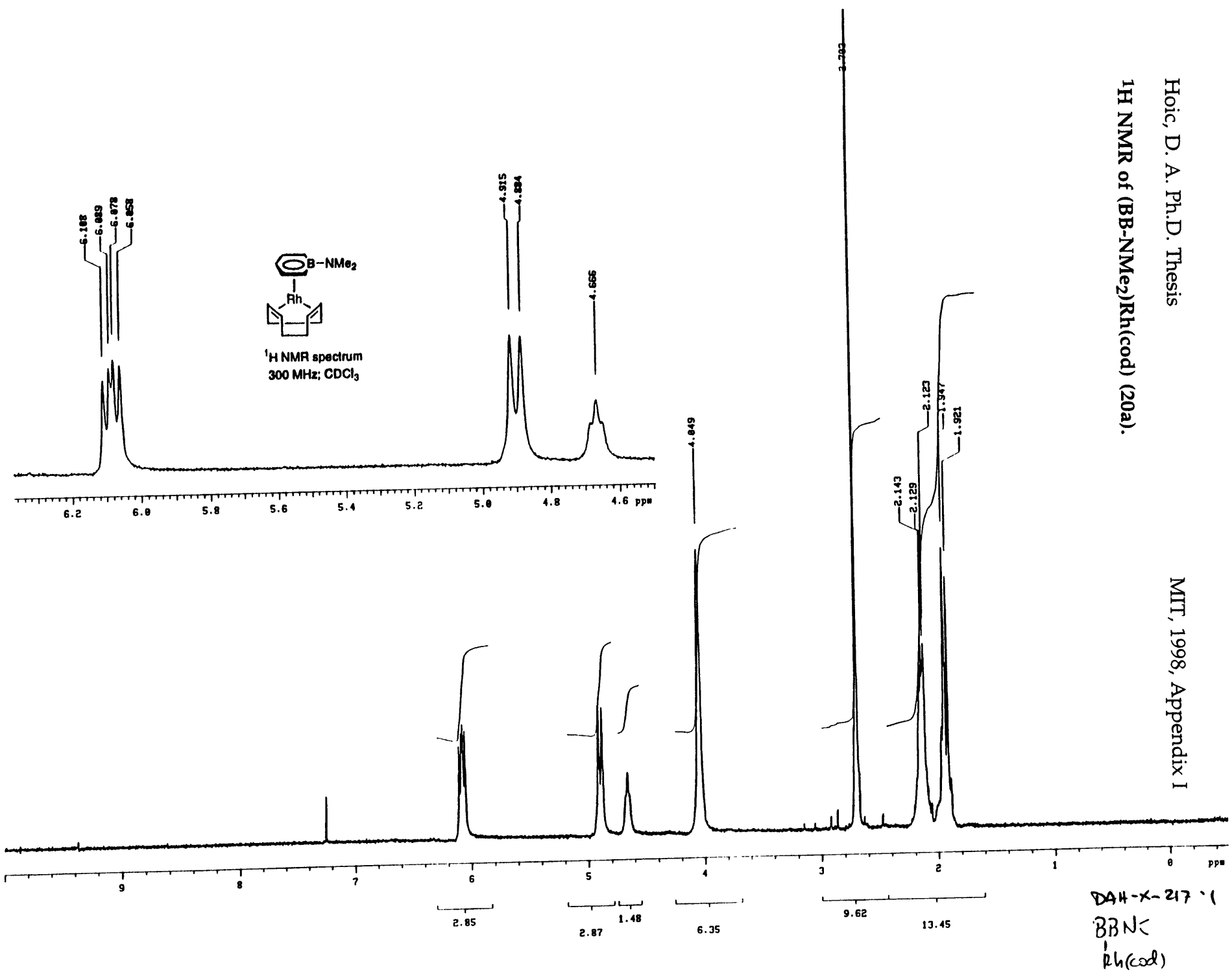
^1H NMR of $\text{Li}(\text{B}(\text{H})\text{C}(\text{CO})_3) \cdot (\text{Et}_2\text{O})$ (18a).



¹H NMR of [(BB-py)Rh(η⁵-bd)](BF₄) (19a).

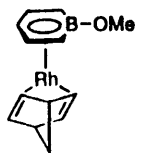
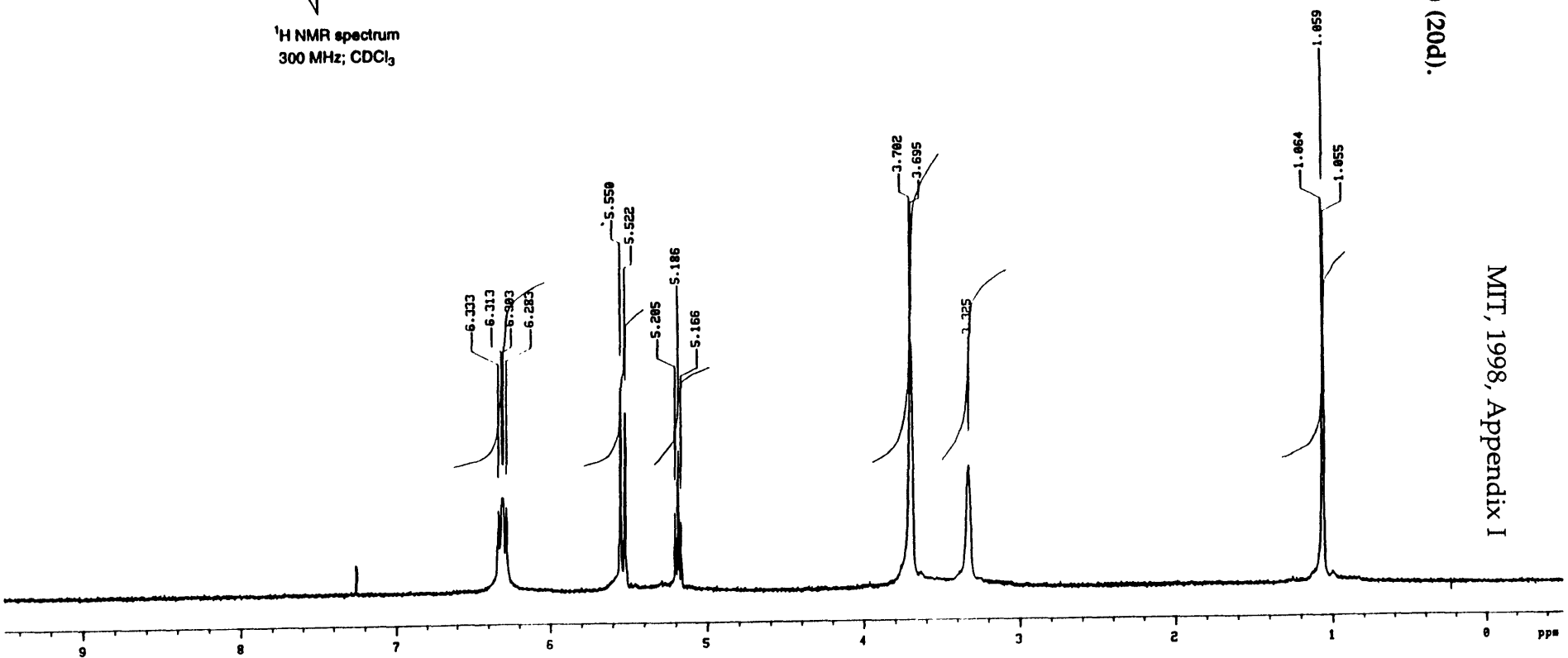


¹H NMR of (BB-NMe₂)Rh(cod) (20a).



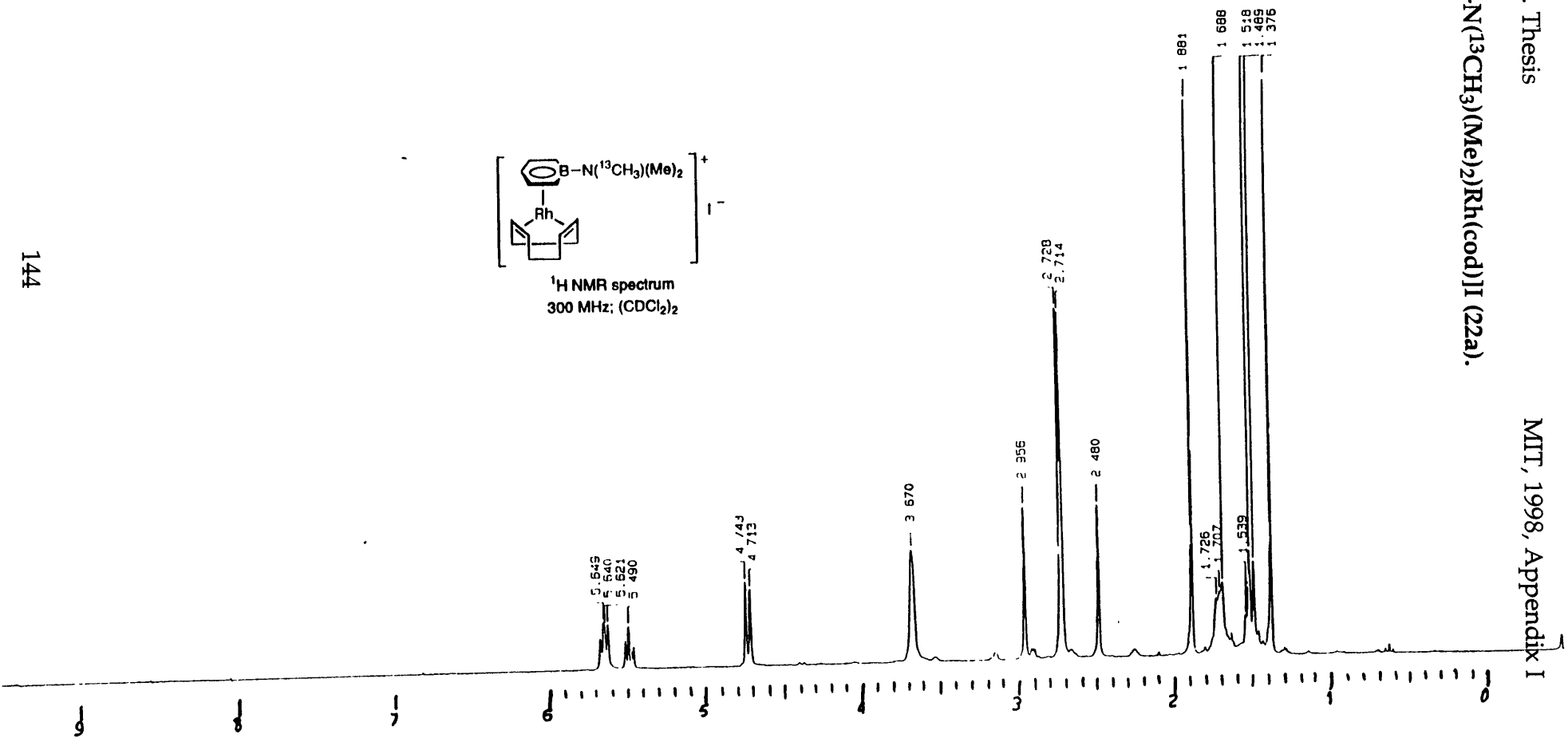
DAH-X-217-1
BBNc
Rh(cod)

^1H NMR of (BB-OMe)Rh(nbd) (20d).

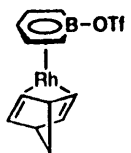


^1H NMR spectrum
300 MHz; CDCl_3

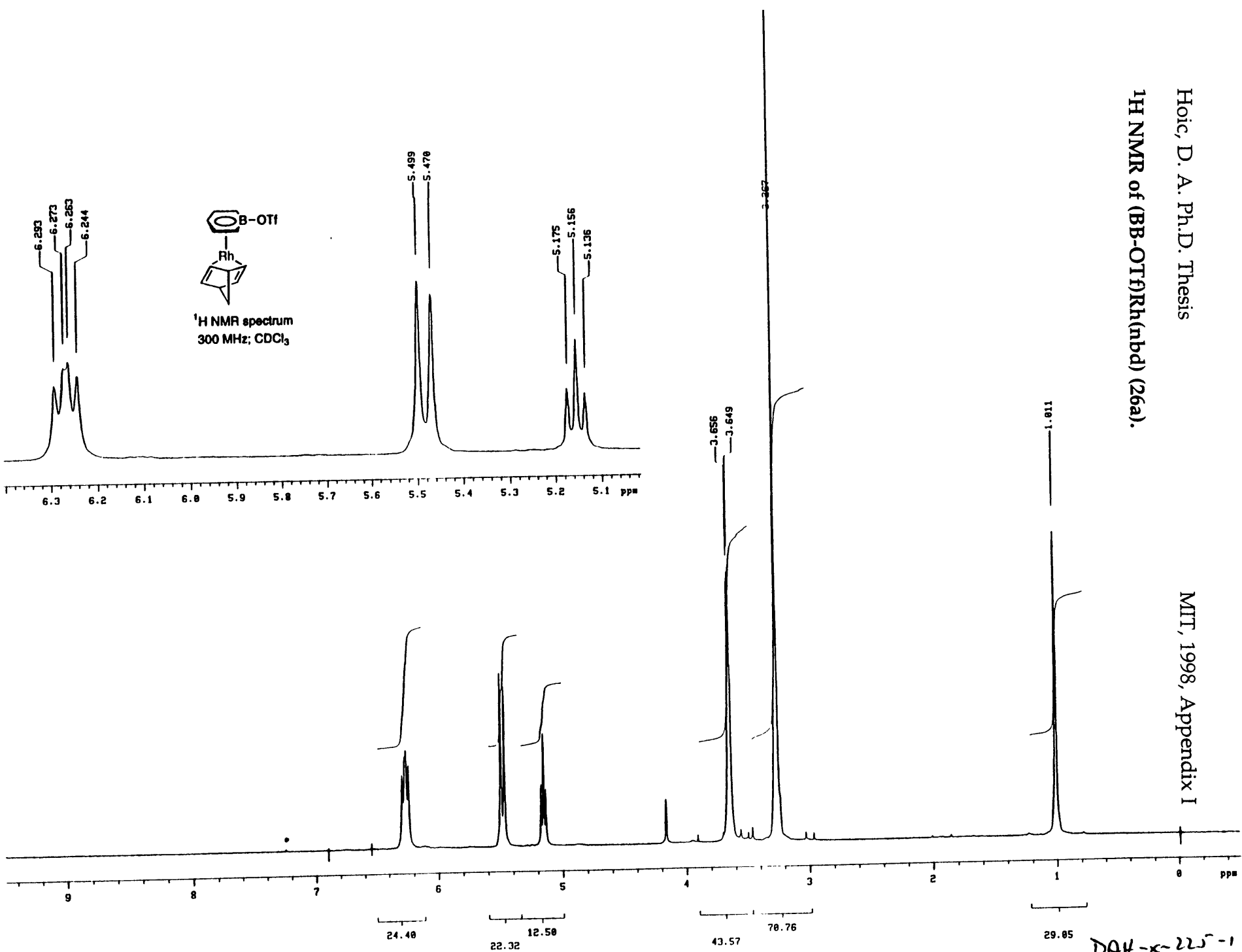
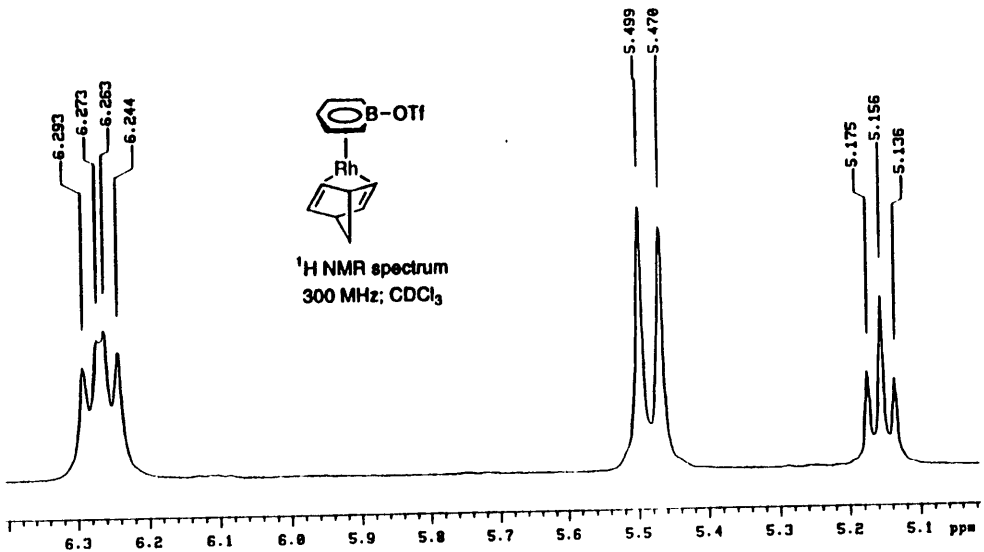
D9H-X-219-2
 CDCl_3
Un30

^1H NMR of $[(\text{BB}-\text{N}(\text{}^{13}\text{CH}_3)(\text{Me})_2)\text{Rh}(\text{cod})_2]\text{I}$ (22a).

¹H NMR of (BB-OTf)Rh(nbd) (26a).



¹H NMR spectrum
300 MHz; CDCl₃

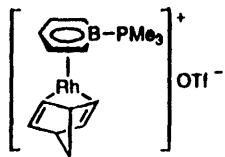


145

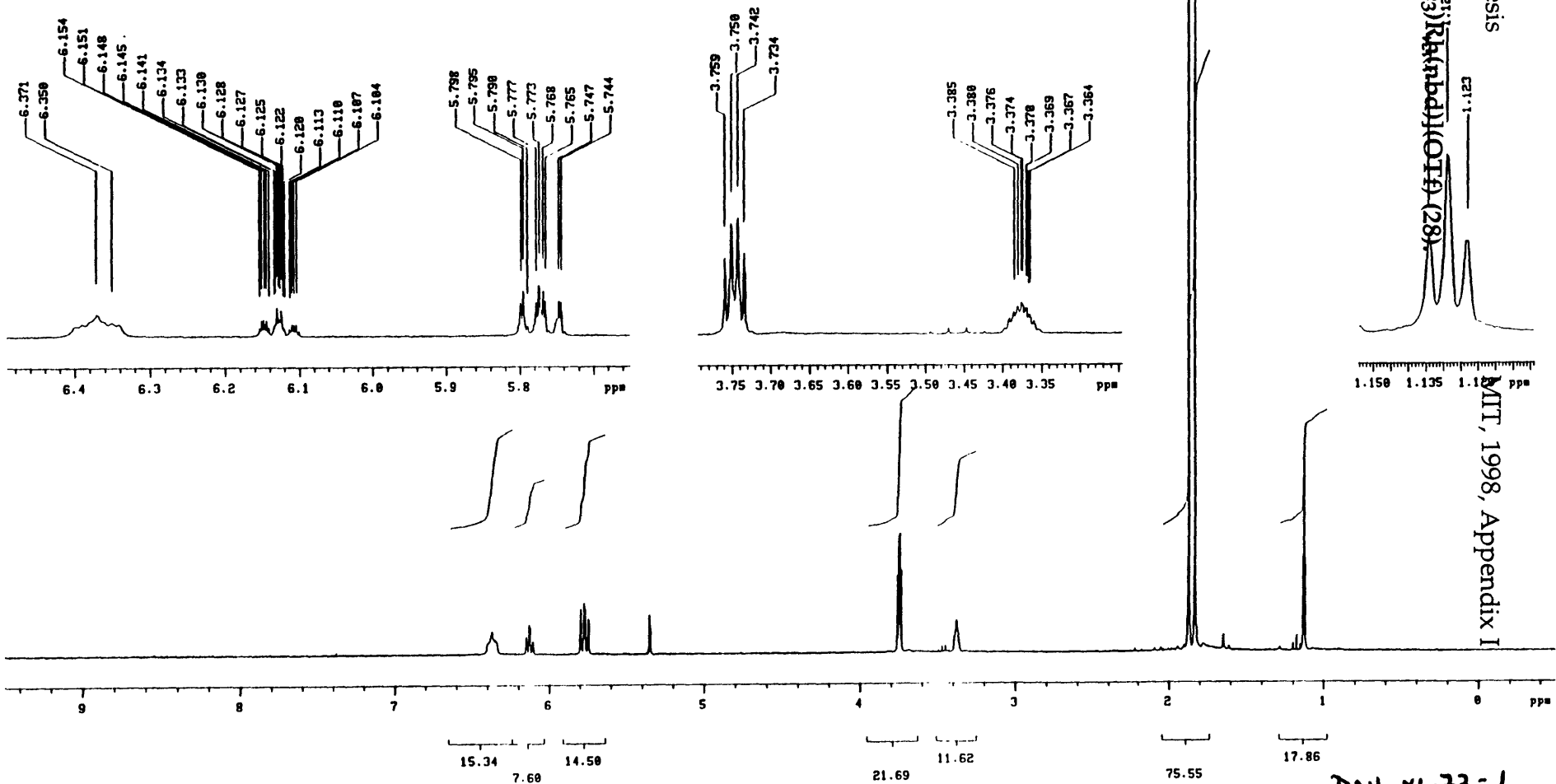
DAH-x-225-1
U₄ 380

^1H NMR of $[(\text{BB-PMe}_3^{\text{Et}})\text{Rh}(\text{hbd})](\text{OTf})_2$ (28)

MIT, 1998, Appendix I

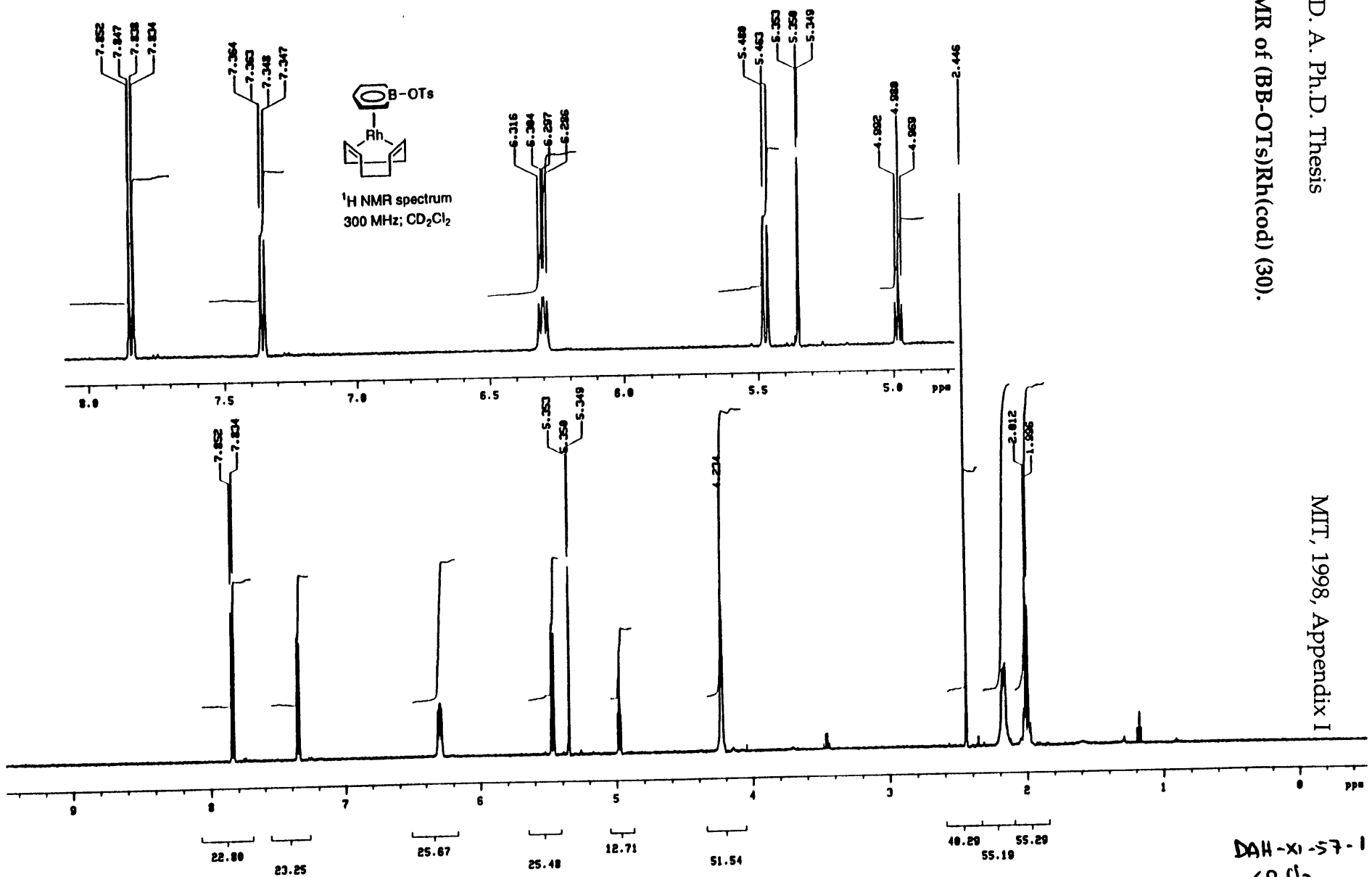


^1H NMR spectrum
300 MHz; CD_2Cl_2



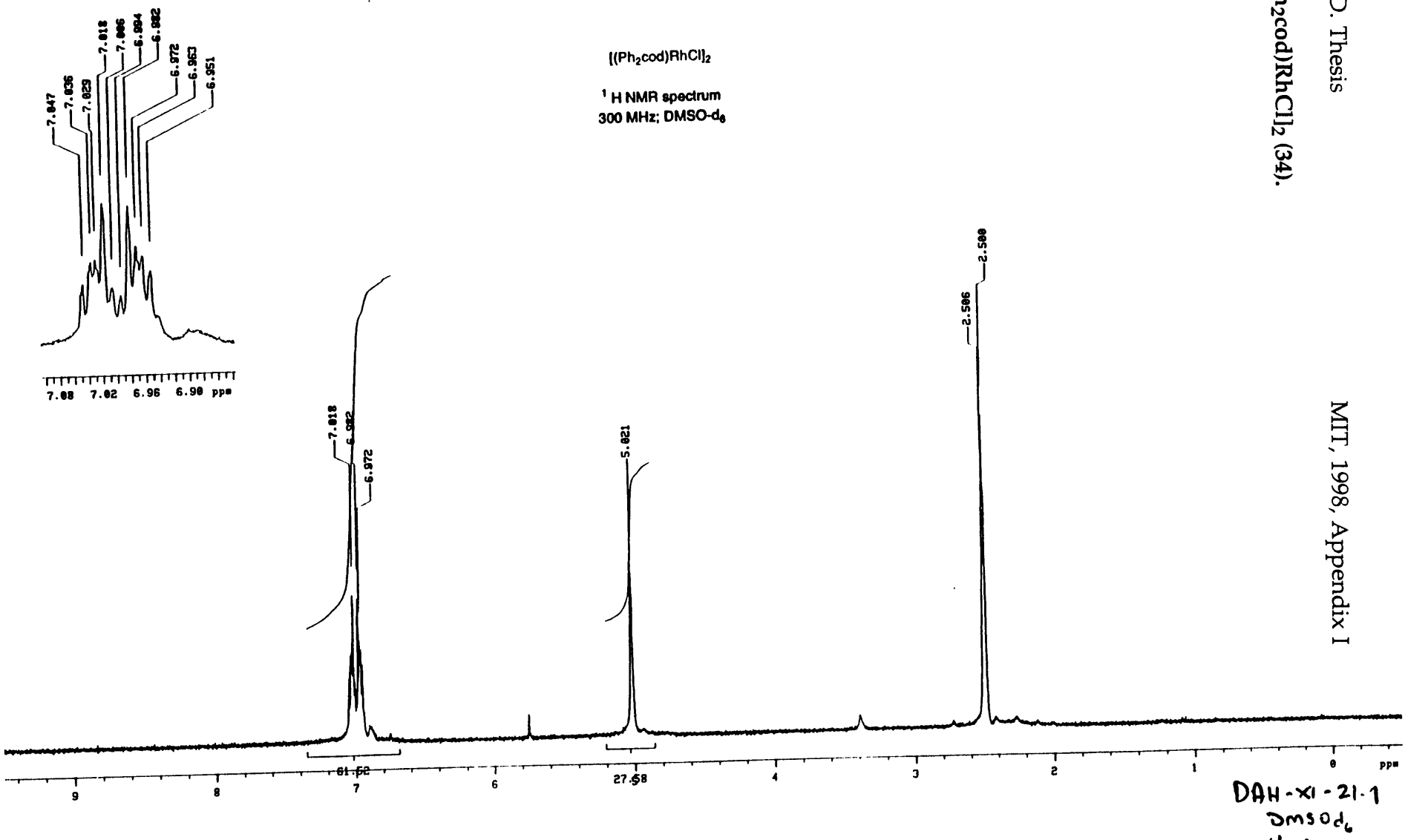
DAH-XI-77-1
 CD_2Cl_2
11 2 1

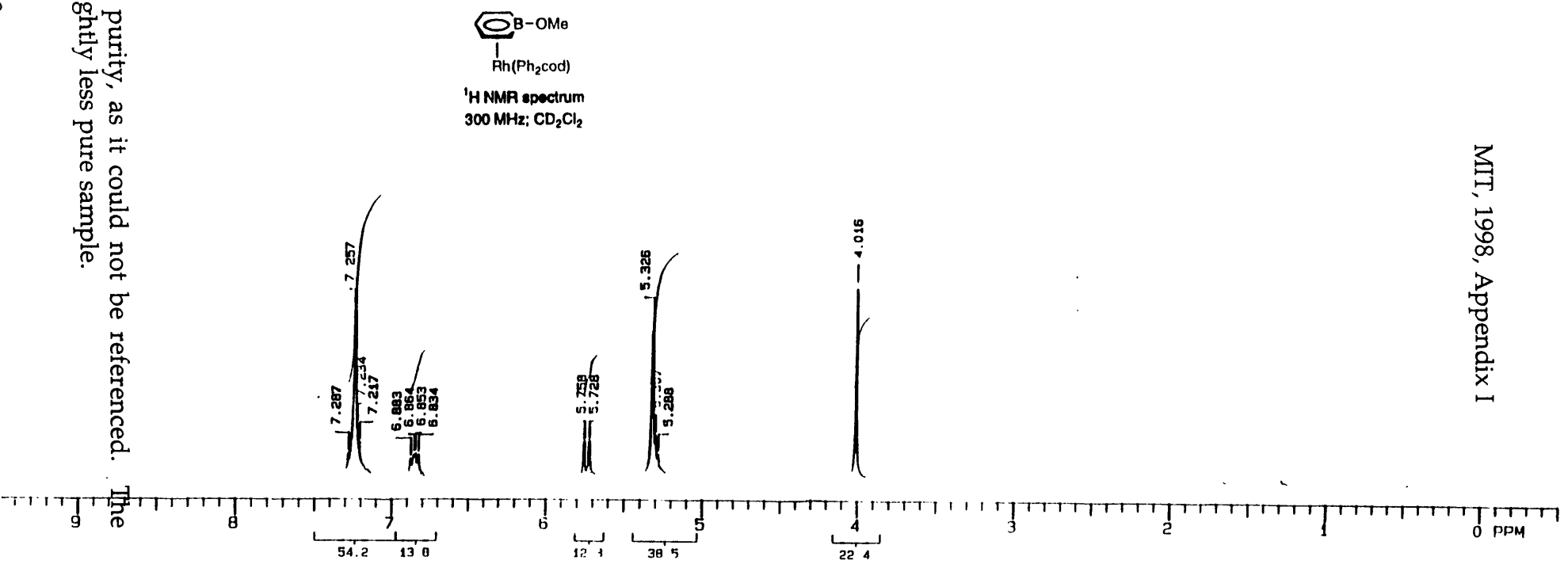
¹H NMR of (BB-OTs)Rh(cod) (30).



DAH-xi-57-1
CD₂Cl₂
VXR500

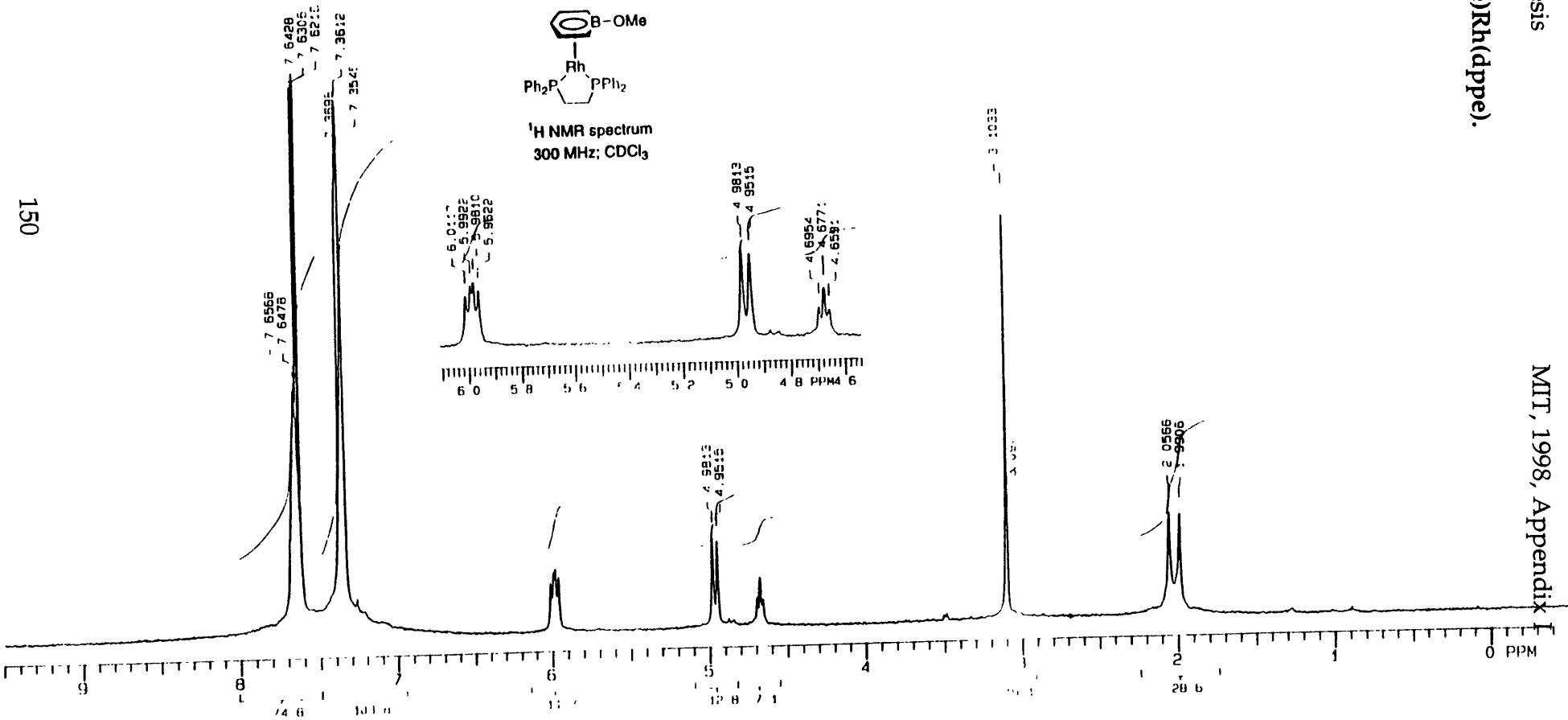
^1H NMR of $[(\text{Ph}_2\text{cod})\text{RhCl}]_2$ (34).



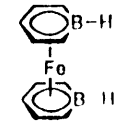
^1H NMR of (BB-OMe)Rh(Ph₂cod) (35).

Note: This spectrum is only to show purity, as it could not be referenced. The chemical shifts were obtained from a slightly less pure sample.

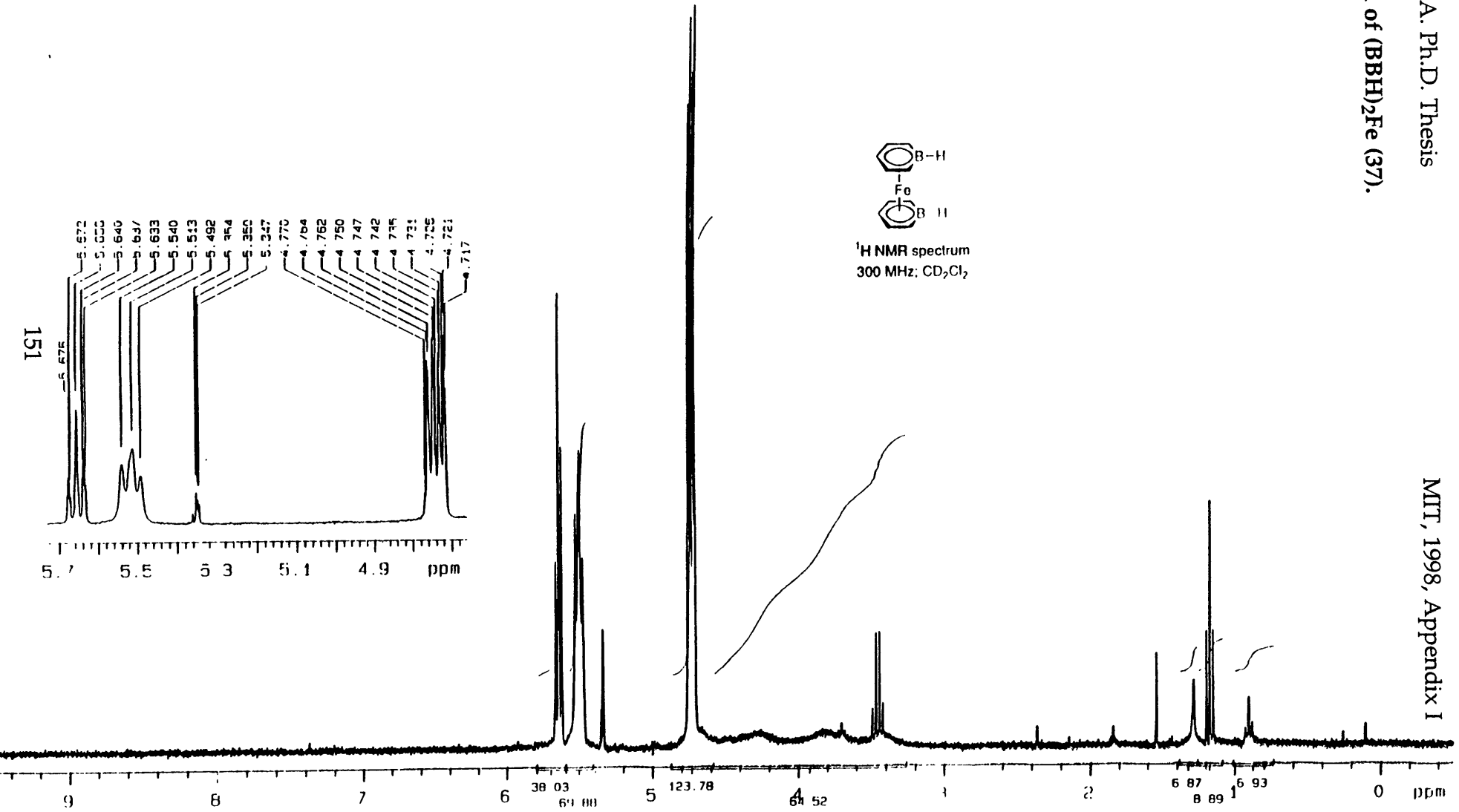
¹H NMR of (BB-OMe)Rh(dppe).



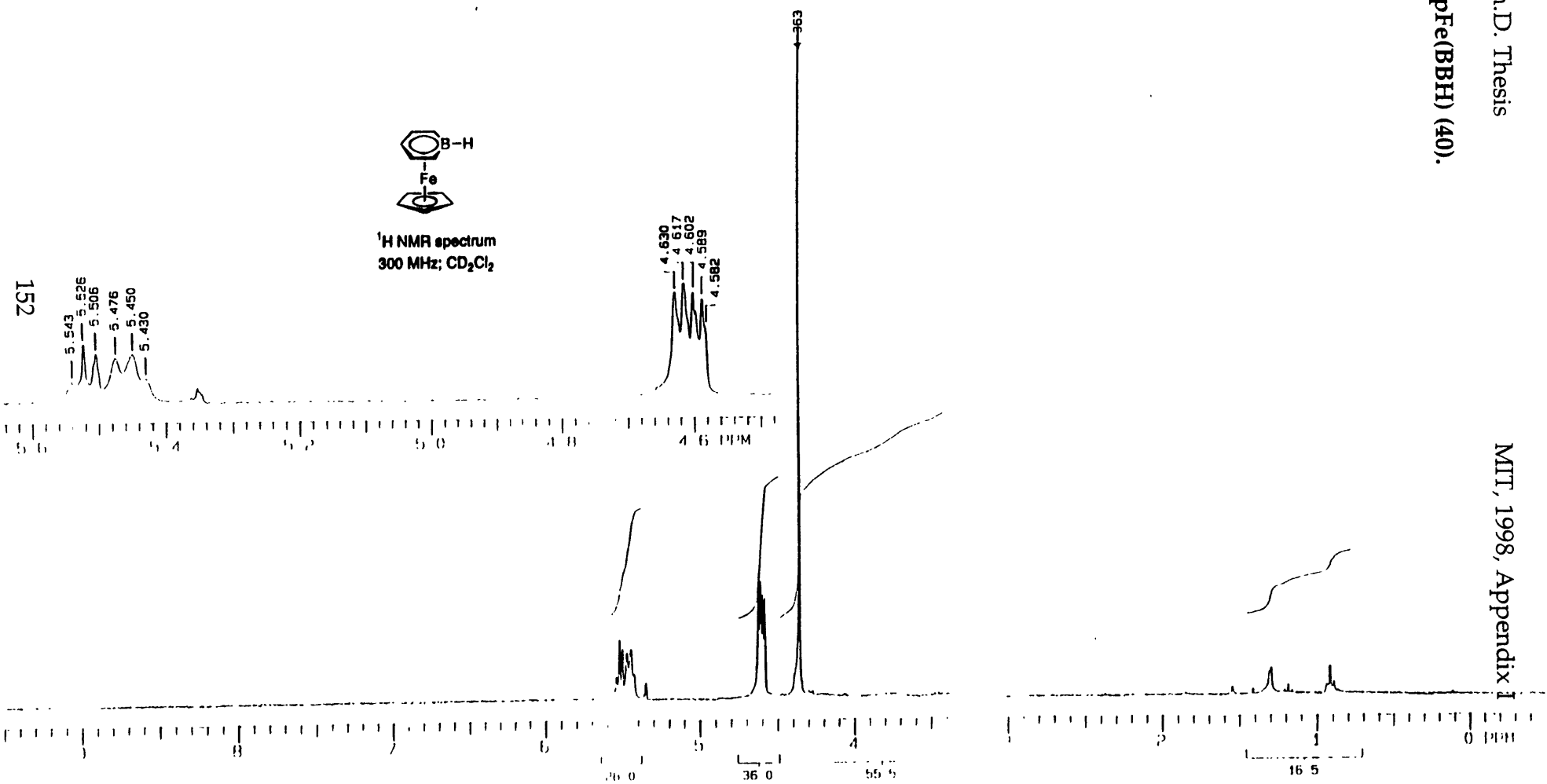
^1H NMR of $(\text{BBH})_2\text{Fe}$ (37).



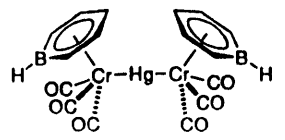
^1H NMR spectrum
300 MHz, CD_2Cl_2



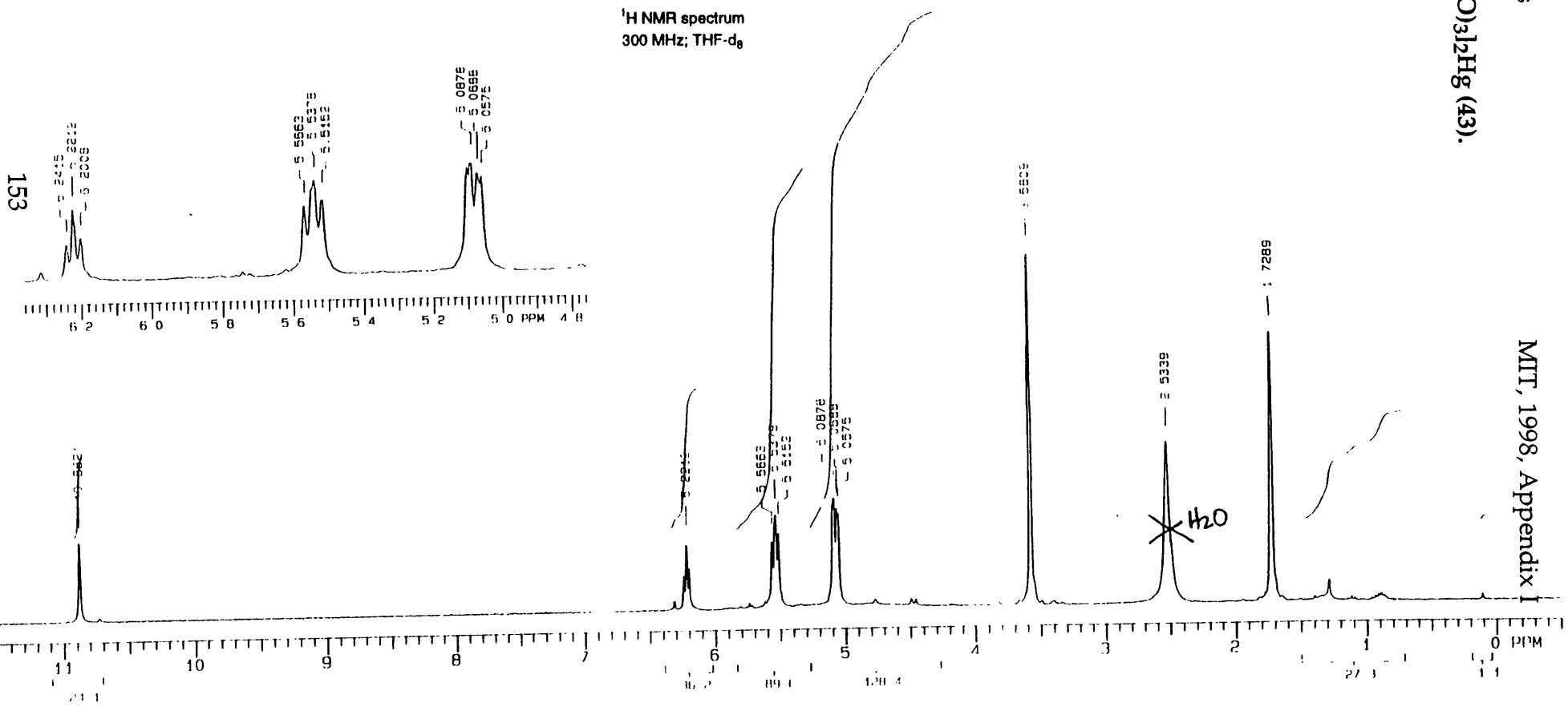
^1H NMR of $\text{CpFe}(\text{BBH})$ (40).



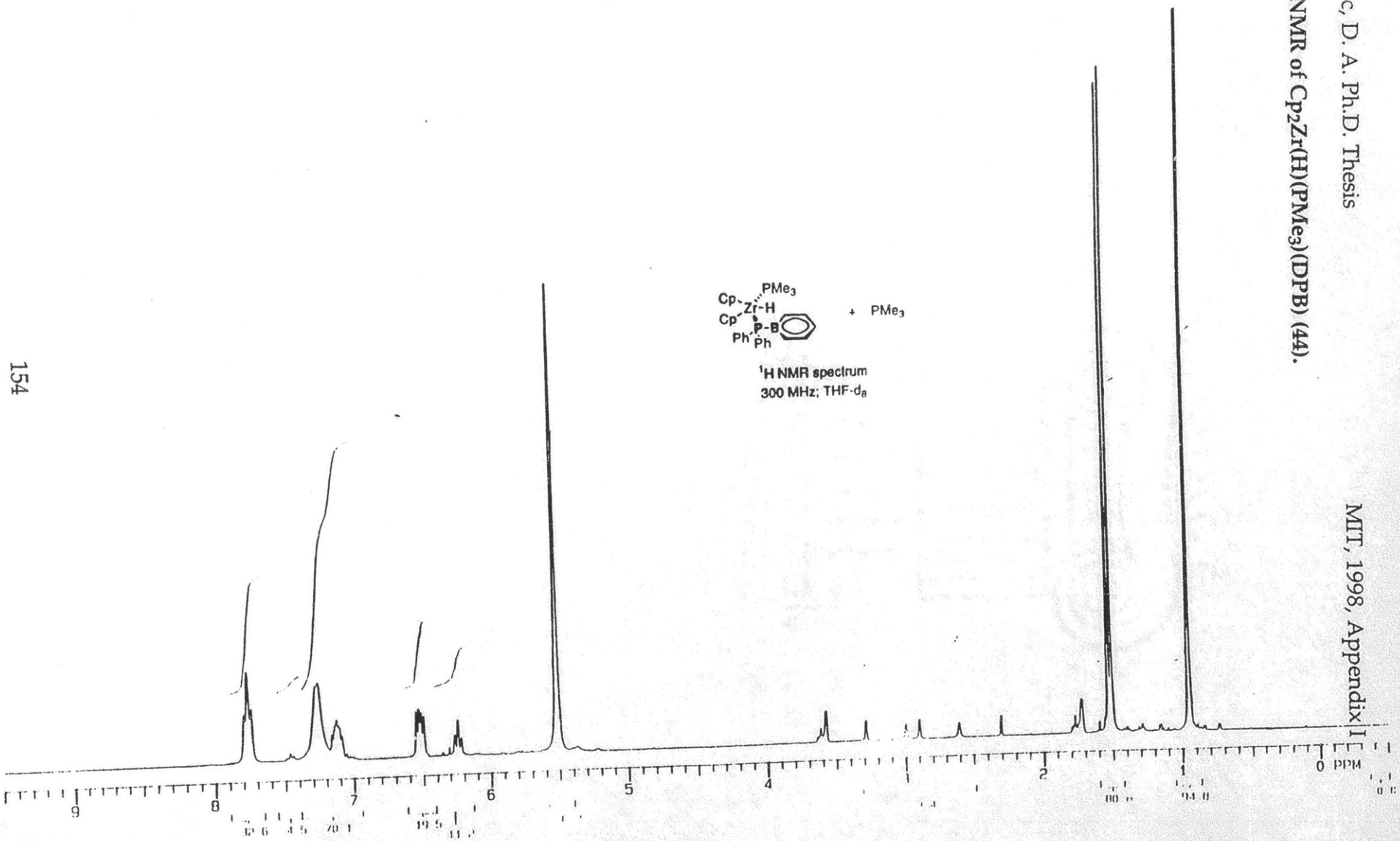
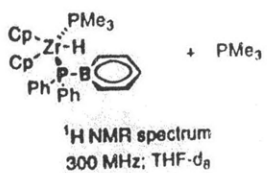
$^1\text{H NMR}$ of $[(\text{BBH})\text{Cr}(\text{CO})_3]_2\text{Hg}$ (43).



$^1\text{H NMR}$ spectrum
300 MHz; THF- d_6



^1H NMR of $\text{Cp}_2\text{Zr}(\text{H})(\text{PMe}_3)(\text{DPPB})$ (44).



Appendix: Crystal Structure Determinations.

Structures Determined on Enraf-Nonius CAD-4 or Rigaku AFC6R Serial Collection Diffractometers.

Structure # ¹	Compound	Thesis # ²	Page
95007	(BB-PMe ₃)Cr(CO) ₃	14b	159
95021	[(BBH) ₂ Li]•Li(THF) ₄	9a	165
95057	BB-PMe ₃	4e	170

Structures Determined on the Siemens-CCD Area Detector Diffractometer.

Structure #	Compound	Thesis #	Page
95097	CpFe(CO) ₂ (DPB)	45	176
95109	[(DPB•BH ₃)K] _n	--	181
95120	[(OC) ₃ Cr(DPB)]Rh(PMe ₃) ₃	--	187
95123	(DPB)Rh(PMe ₃) ₃	46	193
96001	Cp ₂ Zr(PMe ₃)(H)(DPB)	44	197
96020	[(DPB)K(THF) ₂] _n	9f	205
96040	[CpFe(CO) ₂] ₂	--	212
96054	(BB-NMe ₂)Rh(cod)	20a	217
96083	(BB-CN ^t Bu)Cr(CO) ₃	14c	223
96093	BB-CN ^t Bu	4f	228
96099	(DPB)K(18-c-6)(C ₇ H ₈) _{1/2}	9f	233
96103	Na[(BB-OMe)Cr(CO) ₃	--	239
96113	[(BBH)Cr(CO) ₃]Li(THF)	18a	246
96129	(DAB)K(18-crown-6)	9g	252
96159	(BBH)FeCp*	40	258
96161	(DPB)•[K(cryptand)]	9f	264
96172	(BBH)Rh(cod)•(cod)RhCl	20c	270
96186	[(benzene)Rh(cod)](OTf)	--	276

¹ This number corresponds to the number given to the structure in the x-ray diffraction facility.

² Compound number in this thesis.

96199	(BBH)Rh(cod)	20c	282
97006	[(BBH)Cr(CO) ₃]Li(Et ₂ O)	18a	287
97009	(BBH)Cr(CO) ₃ •Li(cryptand)	18a	293
97077	[(BB-NMe ₃)Rh(cod)] I	22a	299
97108	(BB-OEt)Rh(cod)	--	305
97112	(BB-CN)Li(12-crown-4)	--	311
97113	(BB-OMe)Rh(cod)	20b	317
97136	[(BB-PMe ₃)Rh(nbd)](BF ₄)	19a	323
98004	[(BBH)Cr(CO) ₃] ₂ Hg	43	329
98005	BB-NMe ₃	4d	335
98007	(BB-NMe ₃)Cr(CO) ₃	14d	340
98045	(Et ₄ N) [(BB-CN)Cr(CO) ₃]	18b	345
98130	[(cod)Rh(BB-F)Rh(cod)](BF ₄)	29	350
98147	(BB-OMe)Rh(Ph ₂ cod)	35	356
98148	(BB-OMe)Rh(dppe)	--	362
98157	[(BB-py)Rh(nbd)](OTf)	27	373
98158	(BB-OTs)Rh(cod)	30	379
98161	[(BB-PMe ₃)Rh(nbd)](OTf)	28	385

ADDENDA: Comparative thermal parameters show that we have located the boron in the following structures:

Li(BBH)Cr(CO)₃•THF (96113):

atom replaced	U for B	R ₁ (%)	wR ₂ (%)
none	0.052	6.43	11.79
C1	0.033	6.74	13.03
C2	0.034	6.51	12.60
C3	0.027	6.60	12.95
C4	0.026	6.66	12.98
C5	0.032	6.73	13.04

Li(BBH)Cr(CO)₃•cryptand (97009):

atom replaced	U for B	R ₁ (%)	wR ₂ (%)
none ³	0.071	4.33	10.82
C1	0.037	4.65	11.62
C2	0.035	4.59	11.62
C3	0.037	4.59	11.58
C4	0.041	4.57	11.53
C5	0.046	4.58	11.53

³ An absorption correction was added to this refinement only after comparing the thermal parameters, so the final residuals for the correct solution are lower.

(BBH)Rh(cod)•1/2 [(cod)RhCl]₂ (96172):

atom replaced	U for B	R ₁ (%)	wR ₂ (%)
none	0.062	4.57	8.93
C1	0.043	4.68	9.32
C2	0.045	4.70	9.35
C3	0.052	4.68	9.34
C4	0.052	4.70	9.37
C5	0.045	4.70	9.34

95007 Crystal Data table

Empirical Formula	C ₁₁ H ₁₄ BO ₃ PCr
Formula Weight	288.01
Crystal Color; Habit	yellow; prismatic
Crystal Dimensions (mm)	0.300 × 0.300 × 0.200
Crystal System	Monoclinic
Space Group	P2 ₁ (#4)
a (Å)	6.424(5)
b (Å)	11.352(3)
c (Å)	9.260(1)
β (deg)	98.60(2)
V (Å ³)	667.7(6)
Z; ρ _{calc}	2; 1.432
Radiation	Mo Kα (λ = 0.71069 Å)
Temperature (°C); μ(MoKα)	-96; 9.45 cm ⁻¹
Diffractometer	Rigaku AFC6R
Scan Type; Rate (min ⁻¹ in ω)	ω-2θ; 32.0 (8 rescans)
Scan Width	(1.57 + 0.30 tanθ) °
2θ _{max}	55.0°
Total Reflections	1744
Unique Reflections	1612 (R _{int} = 0.025)
Corrections	Lorentz-polarization; Absorption (trans. factors: 0.81 - 1.38)
Structure solution, refinement	Direct methods, Full-matrix least-squares
No. Observations (I > 3.00σ(I))	1449
No. Variables	163
Reflection/Parameter Ratio	8.89
R; R _w ; Goodness of Fit	0.036; 0.037; 2.07
Max./Min. electron density (e/Å ⁻³)	0.25/-0.30

Positional parameters and B(eq) for 95007 Hoic/Fu

atom	x	y	z	B(eq)
Cr	0.1590 (1)	0.8946	0.18580 (8)	1.65 (3)
P	0.3173 (2)	0.9202 (1)	0.6038 (1)	2.53 (6)
O(1)	0.3600 (7)	0.7159 (4)	0.0131 (5)	4.3 (2)
O(2)	0.008 (1)	0.6974 (5)	0.3544 (6)	6.2 (3)
O(3)	-0.2198 (6)	0.8647 (4)	-0.0400 (5)	4.0 (2)
C(1)	0.286 (1)	0.7855 (5)	0.0822 (7)	2.4 (2)
C(2)	0.065 (1)	0.7752 (6)	0.2881 (7)	3.2 (3)
C(3)	-0.0742 (8)	0.8772 (5)	0.0482 (6)	2.4 (2)
C(4)	0.070 (1)	0.892 (1)	0.6629 (8)	5.1 (4)
C(5)	0.453 (1)	1.0275 (7)	0.7283 (7)	4.9 (3)
C(6)	0.468 (1)	0.7854 (6)	0.6321 (8)	4.5 (3)
C(11)	0.4598 (8)	0.9652 (5)	0.3147 (6)	2.3 (2)
C(12)	0.433 (1)	1.0135 (5)	0.1755 (6)	2.9 (3)
C(13)	0.254 (1)	1.0725 (5)	0.1168 (6)	3.2 (3)
C(14)	0.084 (1)	1.0865 (5)	0.1951 (6)	2.9 (2)
C(15)	0.091 (1)	1.0427 (5)	0.3388 (6)	2.0 (2)
B	0.286 (1)	0.9787 (5)	0.4074 (6)	1.9 (2)
H(1)	-0.0182	0.9576	0.6531	7 (4)
H(2)	-0.0003	0.8267	0.6086	(2)
H(3)	0.0925	0.8674	0.7649	5.1
H(4)	0.4668	1.0022	0.8249	4.4
H(5)	0.5941	1.0407	0.7032	4.4
H(6)	0.3822	1.1019	0.7174	4.4
H(7)	0.4939	0.7625	0.7301	4.9
H(8)	0.3997	0.7219	0.5740	4.9
H(9)	0.6055	0.7955	0.5983	4.9
H(10)	0.5871	0.9205	0.3542	2.5
H(11)	0.5536	1.0082	0.1213	3.4
H(12)	0.2412	1.1037	0.0199	3.6
H(13)	-0.0489	1.1249	0.1553	2.9
H(14)	-0.0184	1.0571	0.3977	2.8

Intramolecular Distances Involving the Nonhydrogen Atoms

atom	atom	distance	atom	atom	distance
Cr	C(1)	1.830(6)	P	C(6)	1.809(7)
Cr	C(2)	1.807(6)	P	B	1.918(6)
Cr	C(3)	1.826(5)	O(1)	C(1)	1.164(7)
Cr	C(11)	2.261(5)	O(2)	C(2)	1.166(7)
Cr	C(12)	2.233(6)	O(3)	C(3)	1.155(6)
Cr	C(13)	2.230(6)	C(11)	C(12)	1.388(7)
Cr	C(14)	2.236(6)	C(11)	B	1.514(8)
Cr	C(15)	2.283(6)	C(12)	C(13)	1.375(8)
Cr	B	2.299(6)	C(13)	C(14)	1.407(8)
P	C(4)	1.788(7)	C(14)	C(15)	1.415(8)
P	C(5)	1.809(7)	C(15)	B	1.504(8)

Distances are in angstroms. Estimated standard deviations in the least significant figure are given in parentheses.

Intramolecular Bond Angles Involving the Nonhydrogen Atoms

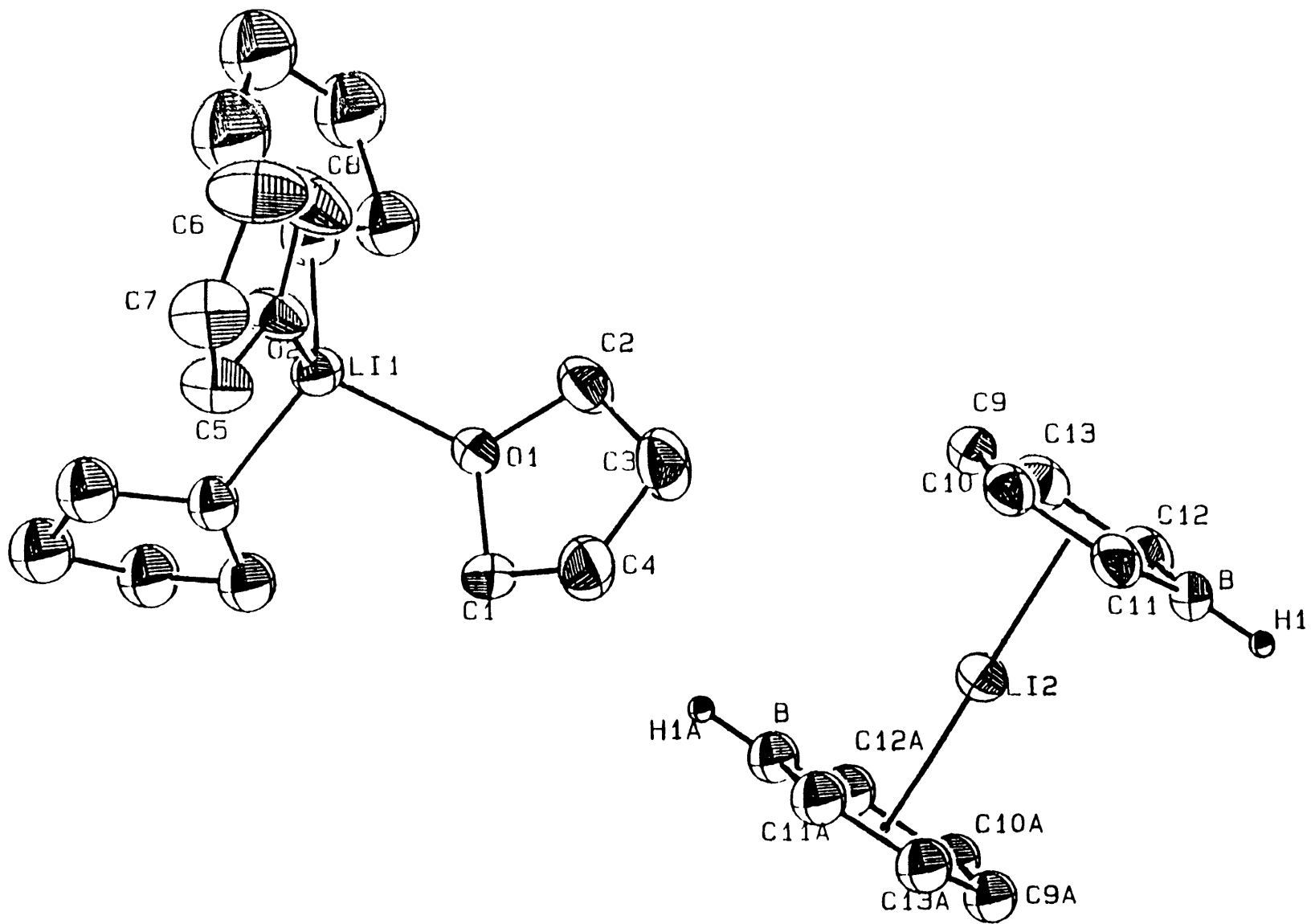
atom	atom	atom	angle	atom	atom	atom	angle
C(1)	Cr	C(2)	88.7(3)	C(12)	Cr	C(13)	35.9(2)
C(1)	Cr	C(3)	86.8(2)	C(12)	Cr	C(14)	65.8(2)
C(1)	Cr	C(11)	96.0(2)	C(12)	Cr	C(15)	78.9(2)
C(1)	Cr	C(12)	88.3(2)	C(12)	Cr	B	67.1(2)
C(1)	Cr	C(13)	107.5(3)	C(13)	Cr	C(14)	36.7(2)
C(1)	Cr	C(14)	142.7(3)	C(13)	Cr	C(15)	66.2(2)
C(1)	Cr	C(15)	164.8(2)	C(13)	Cr	B	78.7(2)
C(1)	Cr	B	128.5(2)	C(14)	Cr	C(15)	36.5(2)
C(2)	Cr	C(3)	89.0(3)	C(14)	Cr	B	67.1(2)
C(2)	Cr	C(11)	108.3(3)	C(15)	Cr	B	38.3(2)
C(2)	Cr	C(12)	143.3(3)	C(4)	P	C(5)	107.0(4)
C(2)	Cr	C(13)	162.9(3)	C(4)	P	C(6)	106.5(4)
C(2)	Cr	C(14)	128.3(3)	C(4)	P	B	112.4(3)
C(2)	Cr	C(15)	96.7(2)	C(5)	P	C(6)	106.3(3)
C(2)	Cr	B	86.8(2)	C(5)	P	B	110.1(3)
C(3)	Cr	C(11)	162.5(2)	C(6)	P	B	114.1(3)
C(3)	Cr	C(12)	127.3(2)	Cr	C(1)	O(1)	177.7(5)
C(3)	Cr	C(13)	97.4(2)	Cr	C(2)	O(2)	178.8(7)
C(3)	Cr	C(14)	88.4(2)	Cr	C(3)	O(3)	178.8(5)
C(3)	Cr	C(15)	107.4(2)	Cr	C(11)	C(12)	70.9(3)
C(3)	Cr	B	144.3(2)	Cr	C(11)	B	72.0(3)
C(11)	Cr	C(12)	36.0(2)	C(12)	C(11)	B	119.2(5)
C(11)	Cr	C(13)	65.3(2)	Cr	C(12)	C(11)	73.1(3)
C(11)	Cr	C(14)	78.9(2)	Cr	C(12)	C(13)	71.9(3)
C(11)	Cr	C(15)	68.8(2)	C(11)	C(12)	C(13)	122.6(5)
C(11)	Cr	B	38.8(2)	Cr	C(13)	C(12)	72.2(3)

Angles are in degrees. Estimated standard deviations in the least significant figure are given in parentheses.

Intramolecular Bond Angles Involving the Nonhydrogen Atoms (cont)

atom	atom	atom	angle	atom	atom	atom	angle
Cr	C(13)	C(14)	71.9(3)				
C(12)	C(13)	C(14)	121.5(5)				
Cr	C(14)	C(13)	71.4(3)				
Cr	C(14)	C(15)	73.5(3)				
C(13)	C(14)	C(15)	121.7(5)				
Cr	C(15)	C(14)	70.0(3)				
Cr	C(15)	B	71.4(3)				
C(14)	C(15)	B	118.4(5)				
Cr	B	P	132.5(3)				
Cr	B	C(11)	69.3(3)				
Cr	B	C(15)	70.3(3)				
P	B	C(11)	121.3(4)				
P	B	C(15)	122.0(4)				
C(11)	B	C(15)	116.6(5)				

Angles are in degrees. Estimated standard deviations in the least significant figure are given in parentheses.



95021 Crystal Data table

Empirical Formula	C ₂₆ H ₄₄ B ₂ Li ₂ O ₄
Formula Weight	456.13
Crystal Color, Habit	colorless, plate
Crystal Dimensions (mm)	0.380 x 0.280 x 0.120
Crystal System	Monoclinic
Space Group	C2/c (#15)
a (Å)	16.213(2)
b (Å)	8.403(2)
c (Å)	20.775(4)
β (deg)	95.15(1)
V (Å ³)	2819(2)
Z; ρ _{calc}	4; 1.075
Radiation	Cu Kα (λ = 1.54178 Å)
Temperature (°C); μ(CuKα)	-86; 4.93 cm ⁻¹
Diffractometer	Enraf-Nonius CAD-4
Scan Type; Rate (min ⁻¹ in ω)	ω; 1.9 ° to 16.5 °
Scan Width	(1.00 + 0.15 tanθ) °
2θ _{max}	109.9 °
Total Reflections	3989
Unique Reflections	3810 (R _{int} = 0.030)
Corrections	Lorentz-polarization; Secondary Extinction (coeff: 0.14573E-4)
Structure solution, refinement	Direct methods, Full-matrix least-squares
No. Observations (I>3.00σ(I))	1320
No. Variables	161
Reflection/Parameter Ratio	8.20
R; R _w ; Goodness of Fit	0.062; 0.055; 3.32
Max./Min. electron density (e/Å ³)	0.21/-0.20

Positional parameters and B(eq) for 95021 Hoic/GF

atom	x	y	z	B(eq)
O(1)	0.4593 (1)	0.2100 (3)	0.6816 (1)	4.2 (1)
O(2)	0.5841 (2)	0.4865 (3)	0.7211 (1)	5.3 (1)
C(1)	0.5060 (2)	0.0730 (4)	0.6661 (2)	5.1 (2)
C(2)	0.4135 (2)	0.2633 (5)	0.6239 (2)	5.7 (2)
C(3)	0.4393 (3)	0.1691 (5)	0.5702 (2)	6.2 (2)
C(4)	0.5144 (2)	0.0832 (5)	0.5954 (2)	5.9 (2)
C(5)	0.6689 (3)	0.4452 (5)	0.7258 (2)	6.1 (2)
C(6)	0.6498 (4)	0.6944 (6)	0.6773 (3)	9.2 (3)
C(7)	0.7131 (3)	0.5710 (6)	0.6943 (2)	7.4 (3)
C(8)	0.5746 (3)	0.6347 (6)	0.6886 (3)	9.8 (4)
Li(1)	1/2	0.353 (1)	3/4	4.0 (4)
H(7)	0.5589	0.0744	0.6899	5.2
H(8)	0.4774	-0.0213	0.6760	5.2
H(9)	0.3550	0.2534	0.6272	5.3
H(10)	0.4246	0.3750	0.6168	5.3
H(11)	0.3972	0.0931	0.5556	5.9
H(12)	0.4510	0.2329	0.5344	5.9
H(13)	0.5641	0.1379	0.5870	5.7
H(14)	0.5177	-0.0230	0.5773	5.7
H(15)	0.6890	0.4392	0.7713	6.4
H(16)	0.6770	0.3453	0.7068	6.4
H(17)	0.6635	0.7893	0.7028	9.5
H(18)	0.6528	0.7251	0.6325	9.5
H(19)	0.7582	0.6123	0.7231	7.9
H(20)	0.7360	0.5302	0.6569	7.9
H(21)	0.5427	0.6234	0.6474	10.1
H(22)	0.5473	0.7107	0.7135	10.1
C(9)	0.2060 (3)	0.0244 (4)	0.4950 (2)	4.2 (2)
C(10)	0.2589 (2)	0.0033 (4)	0.4473 (2)	4.0 (2)
C(11)	0.2424 (2)	-0.1084 (5)	0.3971 (2)	4.3 (2)
C(12)	0.1141 (2)	-0.1800 (4)	0.4482 (2)	4.6 (2)
C(13)	0.1346 (2)	-0.0667 (5)	0.4956 (2)	4.6 (2)
B	0.1664 (3)	-0.2064 (5)	0.3959 (2)	3.8 (2)
Li(2)	1/4	-1/4	1/2	4.2 (4)
H(1)	0.152 (2)	-0.284 (3)	0.364 (1)	3.9 (8)
H(23)	0.2183	0.1003	0.5283	4.0
H(24)	0.3084	0.0681	0.4475	3.8
H(25)	0.2808	-0.1228	0.3645	4.0
H(26)	0.0635	-0.2423	0.4501	4.2
H(27)	0.0983	-0.0488	0.5294	4.3

Intramolecular Distances Involving the Nonhydrogen Atoms

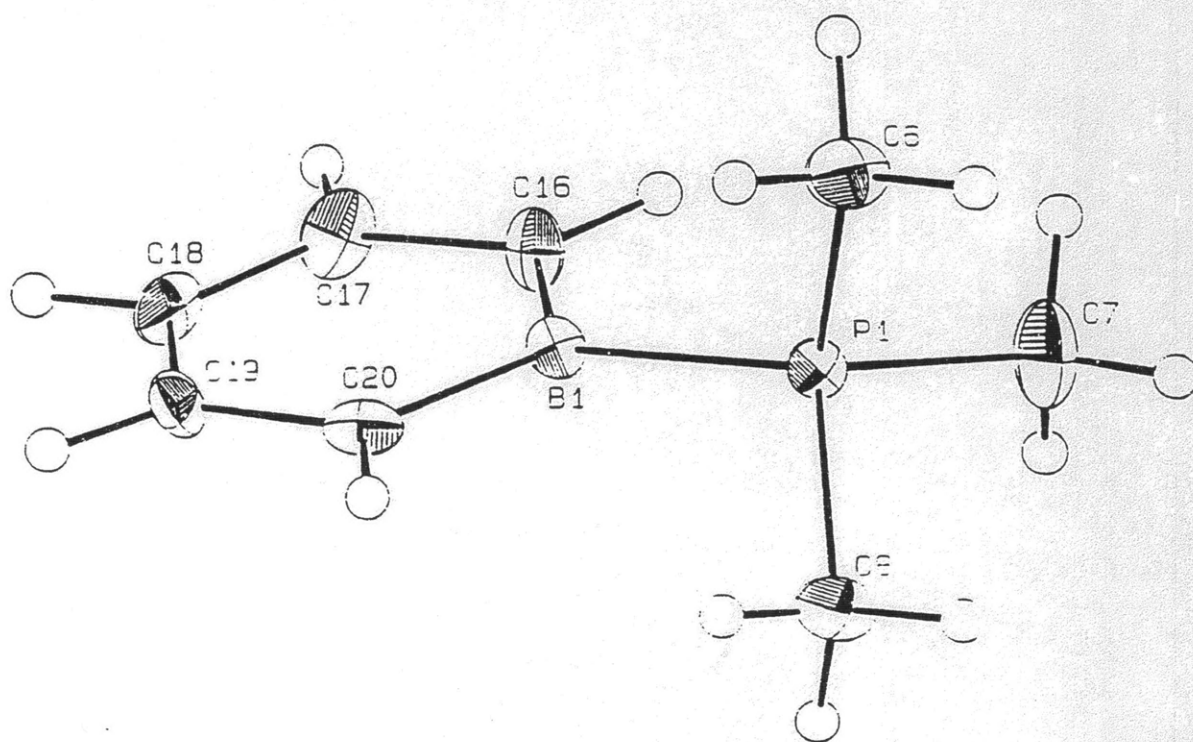
atom	atom	distance	atom	atom	distance
O(1)	C(1)	1.430(4)	C(9)	C(10)	1.380(5)
O(1)	C(2)	1.425(4)	C(9)	C(13)	1.388(5)
O(1)	Li(1)	1.929(5)	C(9)	Li(2)	2.413(3)
O(2)	C(5)	1.413(4)	C(10)	C(11)	1.410(5)
O(2)	C(8)	1.417(5)	C(10)	Li(2)	2.404(3)
O(2)	Li(1)	1.907(5)	C(11)	B	1.481(5)
C(1)	C(4)	1.491(5)	C(11)	Li(2)	2.439(3)
C(2)	C(3)	1.459(5)	C(12)	C(13)	1.389(5)
C(3)	C(4)	1.471(5)	C(12)	B	1.453(5)
C(5)	C(7)	1.463(5)	C(12)	Li(2)	2.436(3)
C(6)	C(7)	1.480(6)	C(13)	Li(2)	2.419(4)
C(6)	C(8)	1.358(6)	B	Li(2)	2.474(4)

Distances are in angstroms. Estimated standard deviations in the least significant figure are given in parentheses.

Intramolecular Bond Angles Involving the Nonhydrogen Atoms (cont)

atom	atom	atom	angle	atom	atom	atom	angle
C(9)	Li(2)	C(11)	60.3(1)	C(11)	Li(2)	C(12)	118.5(1)
C(9)	Li(2)	C(12)	120.1(1)	C(11)	Li(2)	C(13)	71.2(1)
C(9)	Li(2)	C(12)	59.9(1)	C(11)	Li(2)	C(13)	108.8(1)
C(9)	Li(2)	C(13)	146.6(1)	C(11)	Li(2)	B	35.1(1)
C(9)	Li(2)	C(13)	33.4(1)	C(11)	Li(2)	B	144.9(1)
C(9)	Li(2)	B	108.4(1)	C(11)	Li(2)	C(12)	118.5(1)
C(9)	Li(2)	B	71.6(1)	C(11)	Li(2)	C(12)	61.5(1)
C(10)	Li(2)	C(10)	180.00	C(11)	Li(2)	C(13)	108.8(1)
C(10)	Li(2)	C(11)	33.8(1)	C(11)	Li(2)	C(13)	71.2(1)
C(10)	Li(2)	C(11)	146.2(1)	C(11)	Li(2)	B	144.9(1)
C(10)	Li(2)	C(12)	70.9(1)	C(11)	Li(2)	B	35.1(1)
C(10)	Li(2)	C(12)	109.1(1)	C(12)	Li(2)	C(12)	180.00
C(10)	Li(2)	C(13)	59.8(1)	C(12)	Li(2)	C(13)	33.2(1)
C(10)	Li(2)	C(13)	120.2(1)	C(12)	Li(2)	C(13)	146.8(1)
C(10)	Li(2)	B	61.4(1)	C(12)	Li(2)	B	34.4(1)
C(10)	Li(2)	B	118.6(1)	C(12)	Li(2)	B	145.5(1)
C(10)	Li(2)	C(11)	146.2(1)	C(12)	Li(2)	C(13)	146.8(1)
C(10)	Li(2)	C(11)	33.8(1)	C(12)	Li(2)	C(13)	33.2(1)
C(10)	Li(2)	C(12)	109.1(1)	C(12)	Li(2)	B	145.5(1)
C(10)	Li(2)	C(12)	70.9(1)	C(12)	Li(2)	B	34.4(1)
C(10)	Li(2)	C(13)	120.2(1)	C(13)	Li(2)	C(13)	180.00
C(10)	Li(2)	C(13)	59.8(1)	C(13)	Li(2)	B	60.7(1)
C(10)	Li(2)	B	118.6(1)	C(13)	Li(2)	B	119.3(1)
C(10)	Li(2)	B	61.4(1)	C(13)	Li(2)	B	119.3(1)
C(11)	Li(2)	C(11)	180.00	C(13)	Li(2)	B	60.7(1)
C(11)	Li(2)	C(12)	61.5(1)	B	Li(2)	B	180.00

Angles are in degrees. Estimated standard deviations in the least significant figure are given in parentheses.



95057 Crystal Data table

Empirical Formula	C ₈ H ₁₄ BP
Formula Weight	151.98
Crystal Color, Habit	colorless, prismatic
Crystal Dimensions (mm)	0.340 x 0.380 x 0.420
Crystal System	Monoclinic
Space Group	P2/c (#13)
a (Å)	17.582(3)
b (Å)	6.286(1)
c (Å)	35.140(4)
β (deg)	102.93(2)
V (Å ³)	3785(1)
Z; ρ _{calc}	16; 1.067
Radiation	Mo Kα (λ = 0.71069 Å)
Temperature (°C); μ(MoKα)	-86; 2.13 cm ⁻¹
Diffractometer	Enraf-Nonius CAD-4
Scan Type; Rate (min ⁻¹ in ω)	ω-2θ; 1.9 ° to 16.5 °
Scan Width	(0.80 + 0.35 tanθ) °
2θ _{max}	45.0°
Total Reflections	5674
Unique Reflections	5467 (R _{int} = 0.177)
Corrections	Lorentz-polarization; Absorption (trans. factors: 0.33 - 1.69); Secondary Extinction (coeff: 0.39888E-6)
Structure solution, refinement	Direct methods, Full-matrix least-squares
No. Observations (I>3.00σ(I))	2735
No. Variables	362
Reflection/Parameter Ratio	7.56
R; R _w ; Goodness of Fit	0.065; 0.073; 2.14
Max./Min. electron density (e/Å ⁻³)	0.38/-0.37

Positional parameters and B(eq) for 95057 HOIC/GF

atom	x	y	z	B(eq)
P(1)	0.9123(1)	0.1241(3)	0.30548(5)	1.69(9)
P(2)	0.4114(1)	0.3818(4)	0.55638(5)	1.87(9)
P(3)	0.6080(1)	0.1291(4)	0.70488(5)	1.87(9)
P(4)	0.8954(1)	0.3847(3)	0.04346(5)	1.72(9)
C(1)	0.5453(4)	0.092(1)	0.5572(2)	2.3(4)
C(2)	0.5786(5)	0.462(1)	0.5846(2)	2.0(4)
C(3)	0.6250(6)	0.054(1)	0.5644(3)	3.4(4)
C(4)	0.6790(4)	0.208(2)	0.5798(2)	3.3(4)
C(5)	0.6571(4)	0.407(2)	0.5901(2)	2.7(4)
C(6)	0.8856(5)	-0.040(1)	0.2630(2)	3.2(4)
C(7)	0.8447(4)	0.341(1)	0.2986(2)	3.8(4)
C(8)	0.8912(5)	-0.034(1)	0.3441(2)	3.1(4)
C(9)	0.3823(5)	0.550(1)	0.5147(2)	2.8(4)
C(10)	0.3466(5)	0.161(2)	0.5484(3)	5.7(5)
C(11)	0.6707(4)	0.217(1)	0.7677(2)	2.3(3)
C(12)	0.6155(4)	-0.155(1)	0.7734(2)	2.4(4)
C(13)	0.6352(5)	-0.191(1)	0.8137(2)	3.4(4)
C(14)	0.6688(5)	-0.037(1)	0.8400(2)	2.6(4)
C(15)	0.3875(5)	0.523(2)	0.5957(2)	5.9(6)
C(16)	1.0455(4)	0.416(1)	0.3064(2)	2.2(4)
C(17)	1.1250(5)	0.459(1)	0.3141(3)	3.0(4)
C(18)	1.1789(4)	0.310(2)	0.3311(2)	3.0(4)
C(19)	1.1578(4)	0.110(2)	0.3419(2)	2.6(4)
C(20)	1.0791(5)	0.054(1)	0.3357(2)	2.4(4)
C(21)	0.5259(4)	0.304(1)	0.6922(2)	3.4(4)
C(22)	0.5866(6)	-0.090(2)	0.6723(2)	5.1(5)
C(23)	0.6865(4)	0.269(2)	0.6916(2)	5.2(5)
C(24)	0.8772(4)	0.346(1)	-0.0414(2)	2.0(3)
C(25)	0.8509(4)	0.420(1)	-0.0797(2)	2.5(4)
C(26)	0.8215(4)	0.622(1)	-0.0875(2)	2.2(4)
C(27)	0.8140(4)	0.761(1)	-0.0580(2)	2.5(4)
C(28)	0.8380(4)	0.702(1)	-0.0186(2)	2.9(3)
C(29)	0.8127(4)	0.256(2)	0.0553(2)	2.7(4)
C(30)	0.9249(5)	0.586(1)	0.0802(2)	3.2(4)
C(31)	0.9710(4)	0.137(1)	0.0513(2)	3.2(4)
C(32)	0.6860(4)	0.162(1)	0.8275(2)	2.5(4)
B(1)	1.0190(4)	0.206(1)	0.3158(2)	1.5(4)
B(2)	0.5186(4)	0.302(1)	0.5673(2)	1.5(4)
B(3)	0.6321(5)	0.054(2)	0.7539(2)	1.7(4)
B(4)	0.8700(5)	0.489(1)	-0.0092(2)	1.2(4)
H(1)	0.5083	-0.0163	0.5452	2.5
H(2)	0.5635	0.6034	0.5922	2.3
H(3)	0.6416	-0.0897	0.5590	4.0
H(4)	0.7364	0.1761	0.5337	3.5
H(5)	0.6968	0.5109	0.6010	3.1
H(6)	0.8332	-0.0774	0.2532	2.8
H(7)	0.8958	0.0367	0.2407	2.8
H(8)	0.9178	-0.1650	0.2662	2.8
H(9)	0.8537	0.4368	0.3198	4.3

Intramolecular Distances Involving the Nonhydrogen Atoms

atom	atom	distance	atom	atom	distance
P(1)	C(6)	1.791(8)	C(3)	C(4)	1.38(1)
P(1)	C(7)	1.788(8)	C(4)	C(5)	1.38(1)
P(1)	C(8)	1.785(8)	C(11)	C(32)	1.408(9)
P(1)	B(1)	1.900(8)	C(11)	B(3)	1.49(1)
P(2)	C(9)	1.785(7)	C(12)	C(13)	1.399(9)
P(2)	C(10)	1.776(9)	C(12)	B(3)	1.46(1)
P(2)	C(15)	1.770(9)	C(13)	C(14)	1.38(1)
P(2)	B(2)	1.906(8)	C(14)	C(32)	1.38(1)
P(3)	C(21)	1.789(7)	C(16)	C(17)	1.39(1)
P(3)	C(22)	1.778(9)	C(16)	B(1)	1.47(1)
P(3)	C(23)	1.783(8)	C(17)	C(18)	1.37(1)
P(3)	B(3)	1.911(8)	C(18)	C(19)	1.39(1)
P(4)	C(29)	1.796(7)	C(19)	C(20)	1.40(1)
P(4)	C(30)	1.800(8)	C(20)	B(1)	1.47(1)
P(4)	C(31)	1.797(8)	C(24)	C(25)	1.403(9)
P(4)	B(4)	1.918(8)	C(24)	B(4)	1.47(1)
C(1)	C(3)	1.39(1)	C(25)	C(26)	1.37(1)
C(1)	B(2)	1.47(1)	C(26)	C(27)	1.39(1)
C(2)	C(5)	1.40(1)	C(27)	C(28)	1.404(9)
C(2)	B(2)	1.49(1)	C(28)	B(4)	1.47(1)

Distances are in angstroms. Estimated standard deviations in the least significant figure are given in parentheses.

Intramolecular Bond Angles Involving the Nonhydrogen Atoms

atom	atom	atom	angle	atom	atom	atom	angle
C(6)	P(1)	C(7)	106.6(4)	C(1)	C(3)	C(4)	122.1(8)
C(6)	P(1)	C(8)	104.6(4)	C(3)	C(4)	C(5)	122.0(7)
C(6)	P(1)	B(1)	113.2(4)	C(2)	C(5)	C(4)	121.2(8)
C(7)	P(1)	C(8)	106.4(4)	C(32)	C(11)	B(3)	117.4(7)
C(7)	P(1)	B(1)	114.6(4)	C(13)	C(12)	B(3)	118.4(7)
C(8)	P(1)	B(1)	110.8(4)	C(12)	C(13)	C(14)	122.3(7)
C(9)	P(2)	C(10)	106.1(4)	C(13)	C(14)	C(32)	121.2(7)
C(9)	P(2)	C(15)	105.7(4)	C(17)	C(16)	B(1)	119.2(7)
C(9)	P(2)	B(2)	114.2(4)	C(16)	C(17)	C(18)	121.1(8)
C(10)	P(2)	C(15)	105.0(5)	C(17)	C(18)	C(19)	122.5(7)
C(10)	P(2)	B(2)	113.4(4)	C(18)	C(19)	C(20)	120.2(8)
C(15)	P(2)	B(2)	111.8(4)	C(19)	C(20)	B(1)	119.5(8)
C(21)	P(3)	C(22)	105.8(4)	C(25)	C(24)	B(4)	118.1(7)
C(21)	P(3)	C(23)	105.2(4)	C(24)	C(25)	C(26)	121.7(7)
C(21)	P(3)	B(3)	112.8(4)	C(25)	C(26)	C(27)	122.0(6)
C(22)	P(3)	C(23)	106.1(5)	C(26)	C(27)	C(28)	120.8(7)
C(22)	P(3)	B(3)	114.6(4)	C(27)	C(28)	B(4)	118.7(7)
C(23)	P(3)	B(3)	111.6(3)	C(27)	C(28)	C(29)	122.1(7)
C(29)	P(4)	C(30)	105.5(4)	P(1)	B(1)	C(16)	123.0(6)
C(29)	P(4)	C(31)	105.2(4)	P(1)	B(1)	C(20)	119.6(6)
C(29)	P(4)	B(4)	110.8(3)	C(16)	B(1)	C(20)	117.4(7)
C(30)	P(4)	C(31)	107.0(4)	P(2)	B(2)	C(1)	122.9(6)
C(30)	P(4)	B(4)	114.8(4)	P(2)	B(2)	C(2)	118.8(6)
C(31)	P(4)	B(4)	112.9(3)	C(1)	B(2)	C(2)	118.3(7)
C(3)	C(1)	B(2)	118.1(7)	P(3)	B(3)	C(11)	117.9(6)
C(5)	C(2)	B(2)	118.3(7)	P(3)	B(3)	C(12)	123.5(6)

Angles are in degrees. Estimated standard deviations in the least significant figure are given in parentheses.

Intramolecular Bond Angles Involving the Nonhydrogen Atoms (cont)

atom	atom	atom	angle	atom	atom	atom	angle
C(11)	B(3)	C(12)	118.6(7)				
P(4)	B(4)	C(24)	119.5(5)				
P(4)	B(4)	C(28)	121.7(6)				
C(24)	B(4)	C(28)	118.6(6)				

Angles are in degrees. Estimated standard deviations in the least significant figure are given in parentheses.

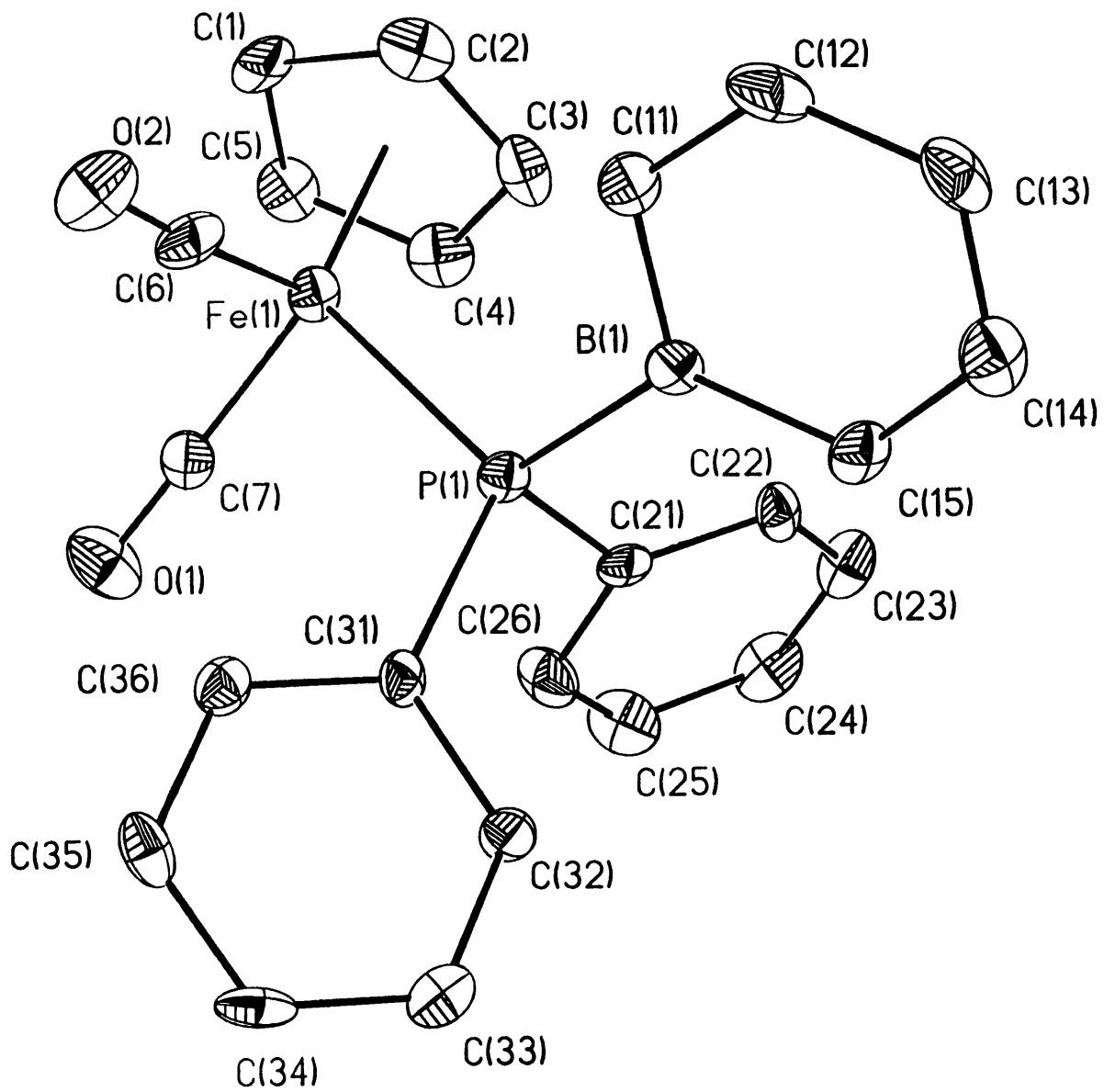


Table 6. Crystal data and structure refinement for 4.

Identification code	95097
Empirical formula	$C_{24}H_{20}BF_2O_2P$
Formula weight	438.03
Temperature	188(2) K
Wavelength	0.71073 Å
Crystal system	Monoclinic
Space group	C2/c
Unit cell dimensions	a = 17.1939(14) Å alpha = 90° b = 15.0376(13) Å beta = 92.5420(10)° c = 15.9249(13) Å gamma = 90°
Volume, Z	4113.4(6) Å ³ , 8
Density (calculated)	1.415 Mg/m ³
Absorption coefficient	0.829 mm ⁻¹
F(000)	1808
Crystal size	0.28 x 0.12 x 0.07 mm
θ range for data collection	1.80 to 20.00°
Limiting indices	-16 ≤ h ≤ 19, -16 ≤ k ≤ 16, -17 ≤ l ≤ 16
Reflections collected	5705
Independent reflections	1914 (R _{int} = 0.0713)
Absorption correction	None
Refinement method	Full-matrix least-squares on F ²
Data / restraints / parameters	1898 / 0 / 262
Goodness-of-fit on F ²	1.290
Final R indices [I > 2σ(I)]	R1 = 0.0649, wR2 = 0.1389
R indices (all data)	R1 = 0.0825, wR2 = 0.1982
Largest diff. peak and hole	0.460 and -0.363 eÅ ⁻³

Table 7. Atomic coordinates [$\times 10^4$] and equivalent isotropic displacement parameters [$\text{\AA}^2 \times 10^3$] for 4. $U(\text{eq})$ is defined as one third of the trace of the orthogonalized U_{ij} tensor.

	x	y	z	$U(\text{eq})$
Fe(1)	2545(1)	9749(1)	727(1)	25(1)
P(1)	2086(1)	9390(1)	2002(1)	22(1)
O(1)	1152(4)	10739(4)	211(4)	49(2)
O(2)	3454(4)	11288(4)	1284(4)	46(2)
C(1)	3313(5)	9500(6)	-246(5)	35(2)
C(2)	3552(5)	9011(6)	499(5)	41(2)
C(3)	2946(6)	8435(6)	687(5)	37(2)
C(4)	2327(5)	8560(6)	86(5)	38(2)
C(5)	2562(5)	9203(6)	-482(5)	37(2)
C(6)	3071(5)	10675(6)	1083(5)	33(2)
C(7)	1706(5)	10346(5)	440(5)	30(2)
C(11)	3706(5)	9275(5)	2781(5)	29(2)
C(12)	4250(5)	8961(6)	3380(5)	38(2)
C(13)	4052(5)	8421(6)	4043(5)	36(2)
C(14)	3283(6)	8182(6)	4132(5)	37(2)
C(15)	2683(5)	8450(5)	3585(5)	29(2)
C(21)	1387(4)	8477(5)	1815(4)	23(2)
C(22)	1573(5)	7614(5)	1994(5)	27(2)
C(23)	1072(6)	6927(6)	1775(5)	37(2)
C(24)	366(5)	7098(6)	1373(6)	42(2)
C(25)	169(5)	7968(6)	1203(6)	46(3)
C(26)	667(5)	8655(6)	1419(5)	37(2)
C(31)	1509(4)	10267(5)	2484(5)	22(2)
C(32)	1013(4)	10033(5)	3107(5)	26(2)
C(33)	616(5)	10671(6)	3546(5)	33(2)
C(34)	690(5)	11560(6)	3345(5)	33(2)
C(35)	1170(5)	11798(5)	2717(5)	31(2)
C(36)	1578(4)	11160(5)	2292(5)	26(2)
B(1)	2880(5)	9013(6)	2855(5)	24(2)

Table 8. Bond lengths [Å] and angles [°] for 4.

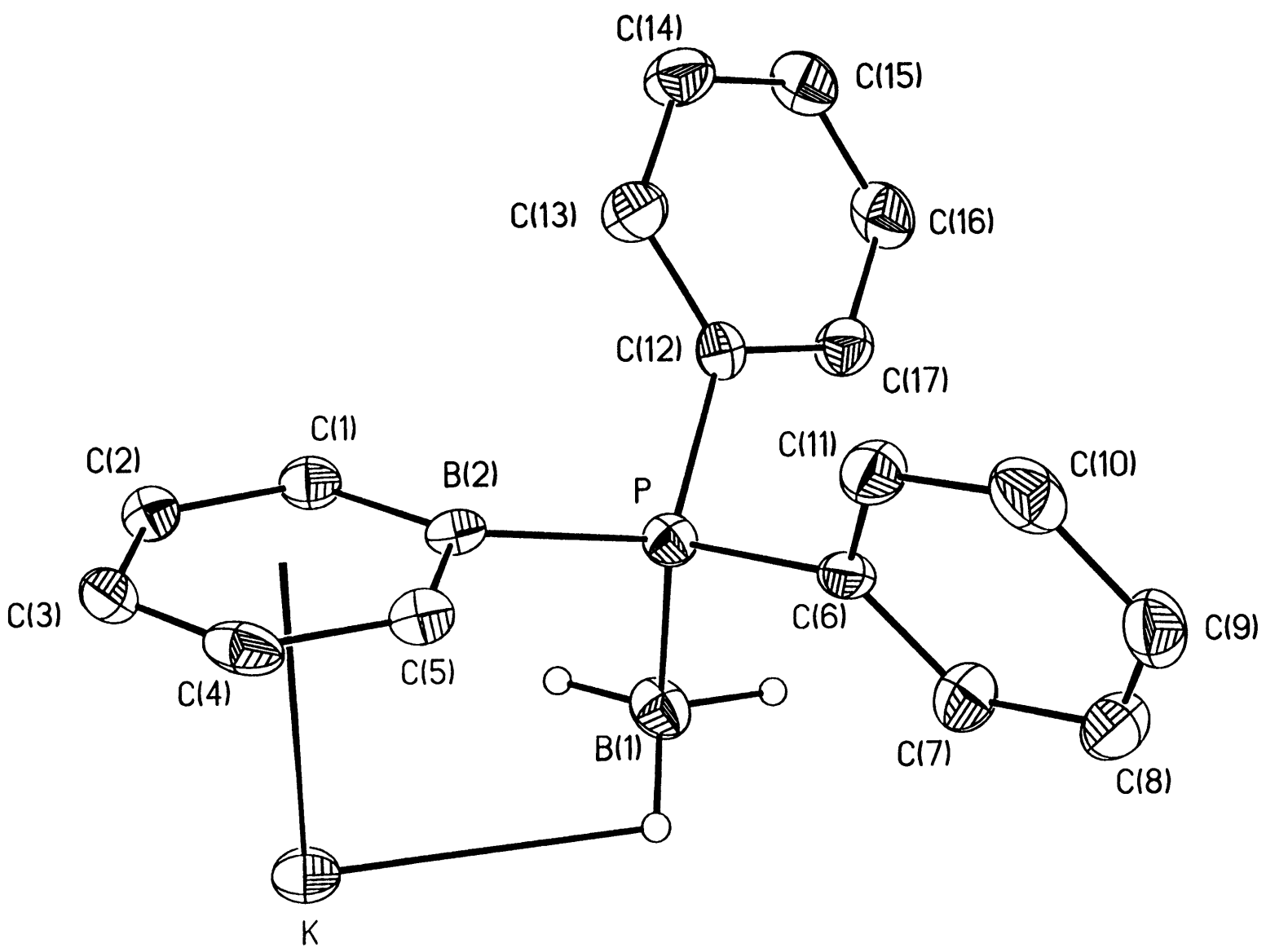
Fe(1)-C(6)	1.741(10)	Fe(1)-C(7)	1.743(10)
Fe(1)-C(4)	2.084(8)	Fe(1)-C(5)	2.094(8)
Fe(1)-C(3)	2.094(8)	Fe(1)-C(2)	2.102(9)
Fe(1)-C(1)	2.112(8)	Fe(1)-P(1)	2.276(2)
P(1)-C(31)	1.838(8)	P(1)-C(21)	1.840(8)
P(1)-B(1)	1.967(9)	O(1)-C(7)	1.167(9)
O(2)-C(6)	1.170(9)	C(1)-C(5)	1.402(12)
C(1)-C(2)	1.439(12)	C(2)-C(3)	1.398(12)
C(3)-C(4)	1.412(11)	C(4)-C(5)	1.396(12)
C(11)-C(12)	1.389(11)	C(11)-B(1)	1.483(12)
C(12)-C(13)	1.386(12)	C(13)-C(14)	1.385(12)
C(14)-C(15)	1.381(11)	C(15)-B(1)	1.489(12)
C(21)-C(22)	1.363(10)	C(21)-C(26)	1.390(11)
C(22)-C(23)	1.381(11)	C(23)-C(24)	1.370(12)
C(24)-C(25)	1.375(12)	C(25)-C(26)	1.375(11)
C(31)-C(36)	1.384(10)	C(31)-C(32)	1.383(10)
C(32)-C(33)	1.384(11)	C(33)-C(34)	1.383(11)
C(34)-C(35)	1.372(11)	C(35)-C(36)	1.384(11)
C(6)-Fe(1)-C(7)	94.8(4)	C(6)-Fe(1)-C(4)	157.7(4)
C(7)-Fe(1)-C(4)	100.7(4)	C(6)-Fe(1)-C(5)	125.8(4)
C(7)-Fe(1)-C(5)	90.4(4)	C(4)-Fe(1)-C(5)	39.0(3)
C(6)-Fe(1)-C(3)	126.7(4)	C(7)-Fe(1)-C(3)	138.4(4)
C(4)-Fe(1)-C(3)	39.5(3)	C(5)-Fe(1)-C(3)	65.4(3)
C(6)-Fe(1)-C(2)	93.4(4)	C(7)-Fe(1)-C(2)	154.9(3)
C(4)-Fe(1)-C(2)	66.1(3)	C(5)-Fe(1)-C(2)	65.7(3)
C(3)-Fe(1)-C(2)	38.9(3)	C(6)-Fe(1)-C(1)	92.8(4)
C(7)-Fe(1)-C(1)	115.8(4)	C(4)-Fe(1)-C(1)	66.0(3)
C(5)-Fe(1)-C(1)	38.9(3)	C(3)-Fe(1)-C(1)	66.0(3)
C(2)-Fe(1)-C(1)	39.9(3)	C(6)-Fe(1)-P(1)	95.4(3)
C(7)-Fe(1)-P(1)	92.3(3)	C(4)-Fe(1)-P(1)	99.9(3)
C(5)-Fe(1)-P(1)	138.3(3)	C(3)-Fe(1)-P(1)	86.0(2)
C(2)-Fe(1)-P(1)	110.5(3)	C(1)-Fe(1)-P(1)	149.9(3)
C(31)-P(1)-C(21)	104.0(3)	C(31)-P(1)-B(1)	106.8(3)
C(21)-P(1)-B(1)	109.0(4)	C(31)-P(1)-Fe(1)	114.7(3)
C(21)-P(1)-Fe(1)	106.4(2)	B(1)-P(1)-Fe(1)	115.3(3)
C(5)-C(1)-C(2)	106.5(8)	C(5)-C(1)-Fe(1)	69.8(5)
C(2)-C(1)-Fe(1)	69.6(5)	C(3)-C(2)-C(1)	107.7(8)
C(3)-C(2)-Fe(1)	70.3(5)	C(1)-C(2)-Fe(1)	70.4(5)
C(2)-C(3)-C(4)	108.6(8)	C(2)-C(3)-Fe(1)	70.8(5)
C(4)-C(3)-Fe(1)	69.9(5)	C(5)-C(4)-C(3)	107.5(8)
C(5)-C(4)-Fe(1)	70.9(5)	C(3)-C(4)-Fe(1)	70.6(5)
C(4)-C(5)-C(1)	109.7(8)	C(4)-C(5)-Fe(1)	70.1(5)
C(1)-C(5)-Fe(1)	71.2(5)	O(2)-C(6)-Fe(1)	175.9(7)
O(1)-C(7)-Fe(1)	177.0(7)	C(12)-C(11)-B(1)	118.2(8)
C(13)-C(12)-C(11)	122.8(8)	C(14)-C(13)-C(12)	119.9(8)
C(15)-C(14)-C(13)	123.4(8)	C(14)-C(15)-B(1)	117.9(8)
C(22)-C(21)-C(26)	118.3(7)	C(22)-C(21)-P(1)	122.1(6)
C(26)-C(21)-P(1)	119.5(6)	C(21)-C(22)-C(23)	121.4(8)
C(24)-C(23)-C(22)	120.5(8)	C(23)-C(24)-C(25)	118.4(8)
C(24)-C(25)-C(26)	121.3(9)	C(25)-C(26)-C(21)	120.1(8)
C(36)-C(31)-C(32)	117.8(7)	C(36)-C(31)-P(1)	123.4(6)
C(32)-C(31)-P(1)	118.6(6)	C(31)-C(32)-C(33)	121.4(7)
C(34)-C(33)-C(32)	120.1(8)	C(35)-C(34)-C(33)	119.0(8)
C(34)-C(35)-C(36)	120.7(8)	C(35)-C(36)-C(31)	121.0(7)

C(11)-B(1)-C(15)
C(15)-B(1)-P(1)

117.8(7)
121.8(6)

C(11)-B(1)-P(1)

120.4(6)



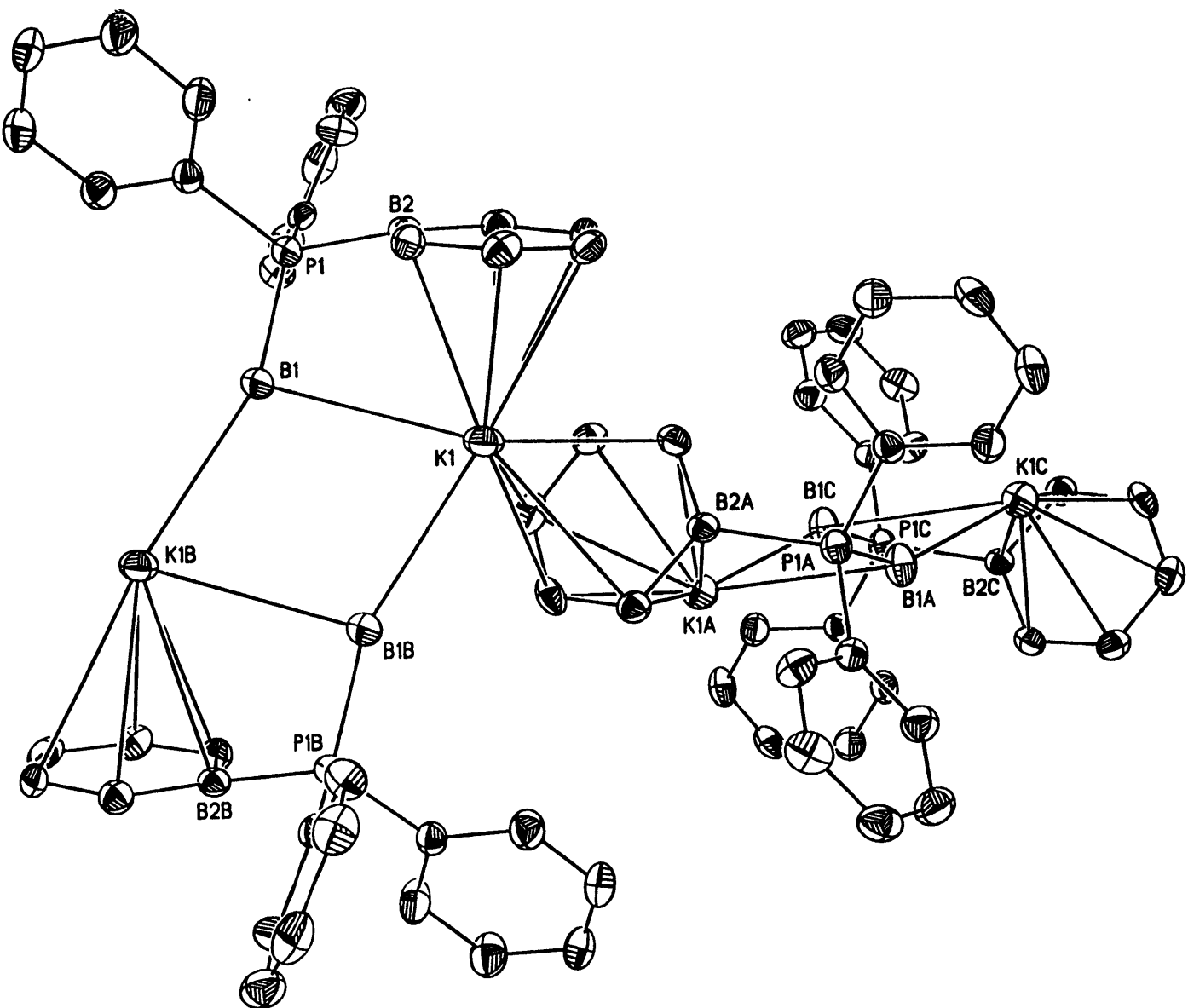


Table 1. Crystal data and structure refinement for 1.

A. Crystal data

Identification code	95109
Empirical formula	$C_{17}H_{18}B_2KP$
Formula weight	314.00
Temperature	188(2) K
Wavelength	0.71073 Å
Crystal system	Monoclinic
Space group	$P2_1/c$
Unit cell dimensions	$a = 11.044(2)$ Å $\alpha = 90^\circ$ $b = 9.952(2)$ Å $\beta = 91.871(2)^\circ$ $c = 15.546(3)$ Å $\gamma = 90^\circ$
Volume, Z	1707.7(6) Å ³ , 4
Density (calculated)	1.221 Mg/m ³
Absorption coefficient	0.394 mm ⁻¹
F(000)	656
Crystal morphology	colorless
Crystal size	? x ? x ? mm

B. Data Collection and Reduction

Diffractometer	Siemens SMART/CCD
Crystal-Detector distance	6.0 cm
Scan type	ω Scans
Scan angle	0.30 ^o
θ range for data collection	1.84 to 20.00 ^o
Limiting indices	$-11 \leq h \leq 12, -11 \leq k \leq 11, -14 \leq l \leq 17$
Reflections collected	4839
Independent reflections	1596 ($R_{int} = 0.0472$)
Absorption correction	None

C. Structure Solution and Refinement

Refinement method	Full-matrix least-squares on F^2
Data / restraints / parameters	1588 / 0 / 200
Goodness-of-fit on F^2	1.404
Final R indices [$I > 2\sigma(I)$]	$R_1 = 0.0549$, $wR_2 = 0.0987$
R indices (all data)	$R_1 = 0.0653$, $wR_2 = 0.1104$
Maximum shift/esd	0.000
Largest diff. peak and hole	0.143 and -0.190 \AA^{-3}

Notes: E

$$R_1 = \frac{\sum |F_o| - |F_c|}{\sum |F_o|}$$

$$wR_2 = \left[\frac{\sum [w(F_o^2 - F_c^2)^2]}{\sum (F_o^2)^2} \right]^{1/2}$$

Weighting scheme

calc $w = 1 / [\sigma^2(F_o^2) + (0.0000P)^2 + 2.6130P]$ where $P = (F_o^2 + 2F_c^2) / 3$

Refinement on F^2 for ALL reflections. Weighted R-factors wR and all goodnesses of fit S are based on F^2 , conventional R-factors R are based on F , with F set to zero for negative F^2 . The observed criterion of $F^2 > 2\sigma(F^2)$ is used only for calculating R_1 and is not relevant to the choice of reflections for refinement. R-factors based on F^2 are statistically about twice as large as those based on F , and R-factors based on ALL data will be even larger.

Table 2. Atomic coordinates [$\times 10^4$] and equivalent isotropic displacement parameters [$\text{\AA}^2 \times 10^3$] for 1. $U(\text{eq})$ is defined as one third of the trace of the orthogonalized U_{ij} tensor.

	x	y	z	$U(\text{eq})$
K(1)	4474(1)	98(1)	1570(1)	39(1)
P(1)	7340(1)	2312(1)	929(1)	29(1)
C(1)	4964(4)	3240(5)	1564(3)	32(1)
C(2)	4041(5)	3172(5)	2138(4)	36(1)
C(3)	4181(5)	2542(5)	2925(4)	40(1)
C(4)	5287(5)	1975(5)	3190(3)	38(1)
C(5)	6280(5)	1998(5)	2669(3)	32(1)
C(6)	8788(4)	1797(5)	1427(3)	29(1)
C(7)	9406(5)	699(5)	1122(3)	41(1)
C(8)	10517(5)	347(6)	1486(4)	47(2)
C(10)	11026(5)	1069(6)	2158(4)	46(2)
C(11)	10423(5)	2165(6)	2466(4)	47(2)
C(12)	9313(4)	2531(5)	2098(3)	38(1)
C(13)	7726(4)	3832(5)	348(3)	29(1)
C(14)	8445(5)	3759(6)	-359(3)	40(1)
C(15)	8796(5)	4901(7)	-783(3)	49(2)
C(16)	8428(5)	6141(6)	-508(3)	45(2)
C(17)	7687(5)	6238(6)	179(4)	49(2)
C(18)	7335(5)	5080(5)	607(3)	44(2)
B(1)	6719(6)	912(7)	162(4)	39(2)
B(2)	6159(5)	2628(5)	1805(3)	28(2)

Table 3. Bond lengths [Å] and angles [°] for 1.

K(1)-H(99A)	2.94(4)	P(1)-C(13)	1.820(5)
P(1)-C(6)	1.827(5)	P(1)-B(2)	1.941(6)
P(1)-B(1)	1.944(6)	C(1)-C(2)	1.378(7)
C(1)-B(2)	1.491(7)	C(1)-H(1A)	0.95
C(2)-C(3)	1.380(7)	C(2)-H(2A)	0.95
C(3)-C(4)	1.395(7)	C(3)-H(3A)	0.95
C(4)-C(5)	1.386(6)	C(4)-H(4A)	0.95
C(5)-B(2)	1.484(7)	C(5)-H(5A)	0.95
C(6)-C(7)	1.381(7)	C(6)-C(12)	1.385(7)
C(7)-C(8)	1.379(7)	C(7)-H(7A)	0.95
C(8)-C(10)	1.373(7)	C(8)-H(8A)	0.95
C(10)-C(11)	1.373(7)	C(10)-H(10A)	0.95
C(11)-C(12)	1.385(7)	C(11)-H(11A)	0.95
C(12)-H(12A)	0.95	C(13)-C(14)	1.378(6)
C(13)-C(18)	1.380(7)	C(14)-C(15)	1.376(7)
C(14)-H(14A)	0.95	C(15)-C(16)	1.372(7)
C(15)-H(15A)	0.95	C(16)-C(17)	1.369(7)
C(16)-H(16A)	0.95	C(17)-C(18)	1.393(7)
C(17)-H(17A)	0.95	C(18)-H(18A)	0.95
B(1)-H(99A)	1.13(5)	B(1)-H(99B)	1.15(4)
B(1)-H(99C)	1.13(4)		
C(13)-P(1)-C(6)	103.1(2)	C(13)-P(1)-B(2)	112.8(2)
C(6)-P(1)-B(2)	110.3(2)	C(13)-P(1)-B(1)	112.0(3)
C(6)-P(1)-B(1)	110.2(3)	B(2)-P(1)-B(1)	108.3(3)
C(2)-C(1)-B(2)	119.1(5)	C(2)-C(1)-H(1A)	120.5(3)
B(2)-C(1)-H(1A)	120.5(3)	C(1)-C(2)-C(3)	122.2(5)
C(1)-C(2)-H(2A)	118.9(3)	C(3)-C(2)-H(2A)	118.9(3)
C(2)-C(3)-C(4)	121.1(5)	C(2)-C(3)-H(3A)	119.4(3)
C(4)-C(3)-H(3A)	119.4(3)	C(5)-C(4)-C(3)	121.5(5)
C(5)-C(4)-H(4A)	119.2(3)	C(3)-C(4)-H(4A)	119.2(3)
C(4)-C(5)-B(2)	119.1(5)	C(4)-C(5)-H(5A)	120.4(3)
B(2)-C(5)-H(5A)	120.4(3)	C(7)-C(6)-C(12)	118.4(5)
C(7)-C(6)-P(1)	120.9(4)	C(12)-C(6)-P(1)	120.7(4)
C(8)-C(7)-C(6)	120.3(5)	C(8)-C(7)-H(7A)	119.9(3)
C(6)-C(7)-H(7A)	119.9(3)	C(10)-C(8)-C(7)	121.1(5)
C(10)-C(8)-H(8A)	119.5(3)	C(7)-C(8)-H(8A)	119.5(3)
C(11)-C(10)-C(8)	119.3(5)	C(11)-C(10)-H(10A)	120.3(3)
C(8)-C(10)-H(10A)	120.3(3)	C(10)-C(11)-C(12)	119.9(5)
C(10)-C(11)-H(11A)	120.1(3)	C(12)-C(11)-H(11A)	120.1(3)
C(11)-C(12)-C(6)	121.1(5)	C(11)-C(12)-H(12A)	119.5(3)
C(6)-C(12)-H(12A)	119.5(3)	C(14)-C(13)-C(18)	118.3(5)
C(14)-C(13)-P(1)	120.2(4)	C(18)-C(13)-P(1)	121.5(4)
C(15)-C(14)-C(13)	121.1(5)	C(15)-C(14)-H(14A)	119.4(3)
C(13)-C(14)-H(14A)	119.4(3)	C(16)-C(15)-C(14)	120.2(5)
C(16)-C(15)-H(15A)	119.9(3)	C(14)-C(15)-H(15A)	119.9(3)
C(17)-C(16)-C(15)	119.8(5)	C(17)-C(16)-H(16A)	120.1(3)
C(15)-C(16)-H(16A)	120.1(3)	C(16)-C(17)-C(18)	119.8(5)
C(16)-C(17)-H(17A)	120.1(3)	C(18)-C(17)-H(17A)	120.1(3)
C(13)-C(18)-C(17)	120.7(5)	C(13)-C(18)-H(18A)	119.7(3)
C(17)-C(18)-H(18A)	119.7(3)	P(1)-B(1)-H(99A)	106(2)
P(1)-B(1)-H(99B)	107(2)	H(99A)-B(1)-H(99B)	116(3)
P(1)-B(1)-H(99C)	103(2)	H(99A)-B(1)-H(99C)	112(3)
H(99B)-B(1)-H(99C)	112(3)	C(5)-B(2)-C(1)	116.9(5)
C(5)-B(2)-P(1)	121.6(4)	C(1)-B(2)-P(1)	120.0(4)

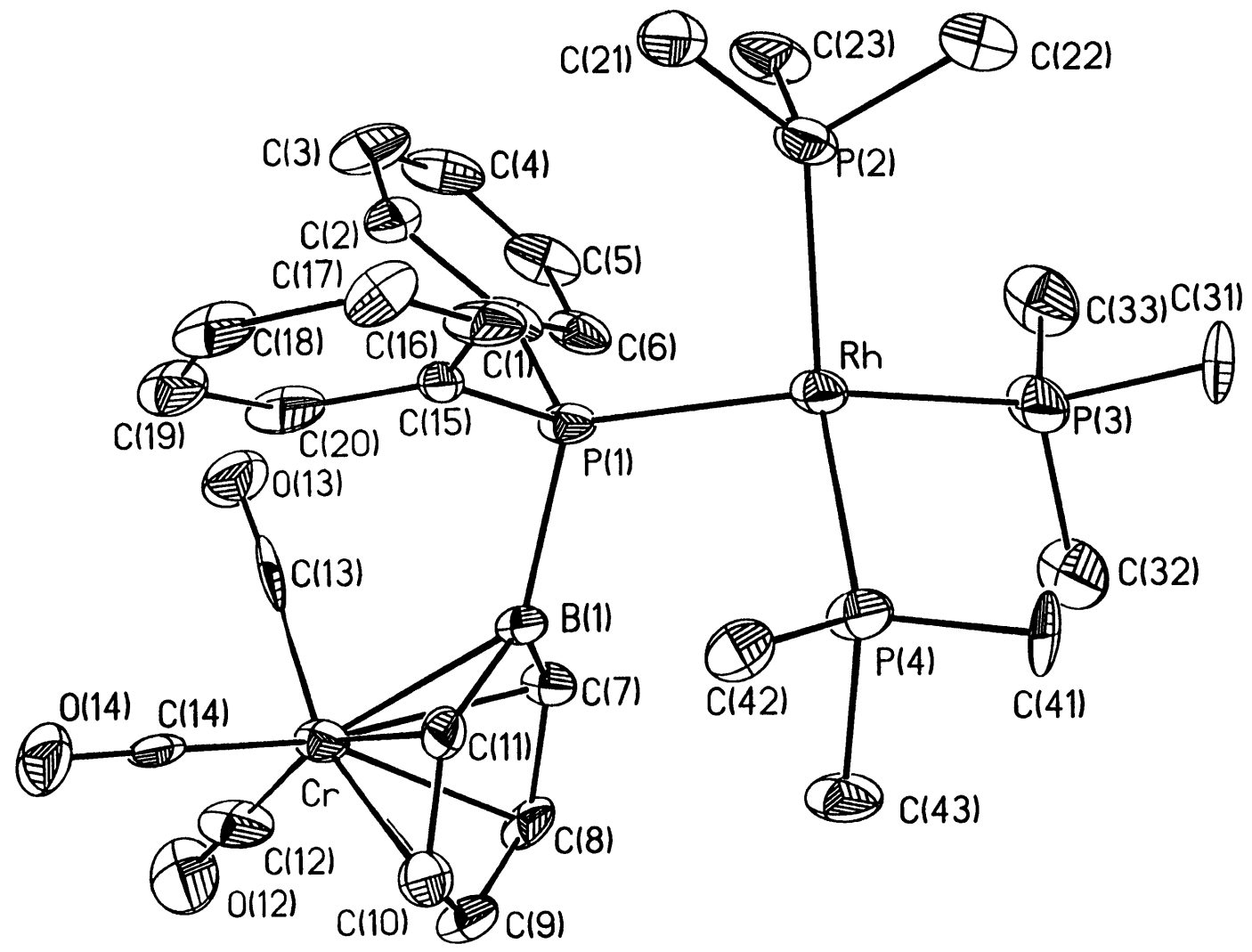


Table 1. Crystal data and structure refinement for 1.

A. Crystal Data

Identification code	95120
Empirical formula	$C_{29}H_{42}BCrO_3P_4Rh$
Formula weight	728.23
Temperature	-90(2) K
Wavelength	0.71073 Å
Crystal morphology	block
Crystal size	0.45 x 0.28 x 0.25 mm
Crystal system	Triclinic
Space group	$P\bar{1}$
Unit cell dimensions	$a = 10.6761(9) \text{ \AA}$ $\alpha = 87.7960(10)^\circ$ $b = 11.9753(10) \text{ \AA}$ $\beta = 83.6300(10)^\circ$ $c = 14.2747(12) \text{ \AA}$ $\gamma = 67.7310(10)^\circ$
Volume, Z	$1678.5(2) \text{ \AA}^3, 2$
Density (calculated)	1.441 Mg/m^3
Absorption coefficient	1.034 mm^{-1}
F(000)	748

B. Data Collection and Reduction

Diffractometer	Siemens SMART/CCD
Scan Type	ω Scans
Scan angle	0.30°
θ range for data collection	1.84 to 20.00°
Limiting indices	$-10 \leq h \leq 11, -11 \leq k \leq 13, -15 \leq l \leq 14$

Reflections collected	4244
Independent reflections	3012 ($R_{int} = 0.1266$)

C. Solution and Refinement

Refinement method	Full-matrix least-squares on F^2
Data / restraints / parameters	2978 / 0 / 353
Goodness-of-fit on F^2	1.199
Final R indices [$I > 2\sigma(I)$]	$R1 = 0.0947$, $wR2 = 0.2952$
R indices (all data)	$R1 = 0.1149$, $wR2 = 0.3358$
Extinction coefficient	0.024(5)
Largest diff. peak and hole	1.638 and $-3.521 \text{ e}\text{\AA}^{-3}$

Table 2. Atomic coordinates [$\times 10^4$] and equivalent isotropic displacement parameters [$\text{\AA}^2 \times 10^3$] for 1. $U(\text{eq})$ is defined as one third of the trace of the orthogonalized U_{ij} tensor.

	x	y	z	$U(\text{eq})$
Rh	7116(1)	3551(1)	2923(1)	36(1)
Cr	10371(2)	-1507(2)	1759(2)	37(1)
P(1)	7376(4)	1526(4)	2871(3)	35(1)
P(2)	4766(4)	4280(4)	2982(3)	47(1)
P(3)	7243(4)	5271(4)	2217(3)	52(1)
P(4)	9147(4)	3093(4)	3556(3)	40(1)
O(12)	11895(15)	-3379(13)	298(11)	82(4)
O(13)	7838(13)	-1483(12)	999(11)	76(4)
O(14)	10354(12)	-3507(11)	3067(9)	57(3)
C(1)	6319(14)	1429(13)	2022(9)	34(4)
C(2)	5334(15)	817(14)	2119(12)	43(4)
C(3)	4530(17)	852(19)	1460(14)	64(5)
C(4)	4663(18)	1356(19)	588(14)	68(6)
C(5)	5588(17)	1878(16)	414(11)	50(5)
C(6)	6400(15)	1927(14)	1104(12)	52(5)
C(7)	9892(14)	475(13)	1393(9)	33(4)
C(8)	11277(15)	-173(14)	1149(11)	41(4)
C(9)	12101(15)	-908(15)	1830(11)	44(4)
C(10)	11558(16)	-992(14)	2737(12)	48(4)
C(11)	10181(14)	-374(12)	3045(10)	33(4)
C(12)	11284(17)	-2644(22)	857(15)	68(6)
C(13)	8788(21)	-1456(12)	1301(12)	49(5)
C(14)	10351(13)	-2730(15)	2550(12)	42(4)
C(15)	7011(13)	746(12)	3923(10)	29(3)
C(16)	6551(14)	1274(16)	4766(11)	46(4)
C(17)	6345(15)	683(15)	5575(10)	41(4)
C(18)	6607(15)	-574(17)	5489(12)	50(5)
C(19)	7053(15)	-1151(16)	4658(12)	50(5)
C(20)	7231(14)	-490(16)	3877(10)	45(4)
C(21)	3937(17)	3530(16)	3831(15)	68(6)
C(22)	3964(18)	5815(17)	3516(15)	69(6)
C(23)	3793(17)	4402(17)	1994(14)	65(5)
C(31)	6900(20)	6676(14)	2849(14)	63(5)
C(32)	8901(18)	5052(17)	1578(14)	67(6)
C(33)	6171(20)	5825(17)	1255(13)	71(6)
C(41)	9300(18)	4314(13)	4099(11)	48(4)
C(42)	9370(15)	2093(14)	4592(10)	41(4)
C(43)	10826(15)	2448(16)	2882(13)	57(5)
B(1)	9264(15)	505(14)	2419(11)	28(4)

Table 3. Bond lengths [Å] and angles [°] for 1.

Rh-P(3)	2.302(4)	Rh-P(4)	2.306(4)
Rh-P(2)	2.315(4)	Rh-P(1)	2.337(4)
Cr-C(14)	1.82(2)	Cr-C(12)	1.82(3)
Cr-C(13)	1.86(2)	Cr-C(9)	2.233(14)
Cr-C(10)	2.23(2)	Cr-C(8)	2.263(13)
Cr-C(11)	2.27(2)	Cr-C(7)	2.283(14)
Cr-B(1)	2.42(2)	P(1)-C(1)	1.780(14)
P(1)-C(15)	1.822(13)	P(1)-B(1)	1.97(2)
P(2)-C(23)	1.81(2)	P(2)-C(21)	1.83(2)
P(2)-C(22)	1.86(2)	P(3)-C(33)	1.83(2)
P(3)-C(32)	1.83(2)	P(3)-C(31)	1.83(2)
P(4)-C(41)	1.750(13)	P(4)-C(43)	1.83(2)
P(4)-C(42)	1.844(14)	O(12)-C(12)	1.16(2)
O(13)-C(13)	1.16(2)	O(14)-C(14)	1.16(2)
C(1)-C(6)	1.43(2)	C(1)-C(2)	1.49(2)
C(2)-C(3)	1.33(2)	C(3)-C(4)	1.38(3)
C(4)-C(5)	1.35(3)	C(5)-C(6)	1.40(2)
C(7)-C(8)	1.40(2)	C(7)-B(1)	1.54(2)
C(8)-C(9)	1.42(2)	C(9)-C(10)	1.37(2)
C(10)-C(11)	1.40(2)	C(11)-B(1)	1.48(2)
C(15)-C(16)	1.33(2)	C(15)-C(20)	1.41(2)
C(16)-C(17)	1.37(2)	C(17)-C(18)	1.43(2)
C(18)-C(19)	1.34(2)	C(19)-C(20)	1.38(2)
P(3)-Rh-P(4)	92.4(2)	P(3)-Rh-P(2)	93.1(2)
P(4)-Rh-P(2)	154.2(2)	P(3)-Rh-P(1)	151.7(2)
P(4)-Rh-P(1)	92.73(14)	P(2)-Rh-P(1)	94.36(14)
C(14)-Cr-C(12)	87.8(8)	C(14)-Cr-C(13)	90.4(6)
C(12)-Cr-C(13)	86.5(8)	C(14)-Cr-C(9)	115.5(6)
C(12)-Cr-C(9)	94.1(7)	C(13)-Cr-C(9)	154.1(6)
C(14)-Cr-C(10)	89.4(6)	C(12)-Cr-C(10)	118.9(7)
C(13)-Cr-C(10)	154.6(6)	C(9)-Cr-C(10)	35.8(6)
C(14)-Cr-C(8)	152.4(6)	C(12)-Cr-C(8)	94.0(7)
C(13)-Cr-C(8)	117.1(6)	C(9)-Cr-C(8)	36.9(5)
C(10)-Cr-C(8)	65.7(6)	C(14)-Cr-C(11)	88.4(6)
C(12)-Cr-C(11)	154.9(7)	C(13)-Cr-C(11)	118.4(6)
C(9)-Cr-C(11)	65.4(6)	C(10)-Cr-C(11)	36.2(5)
C(8)-Cr-C(11)	78.4(5)	C(14)-Cr-C(7)	153.6(6)
C(12)-Cr-C(7)	118.6(6)	C(13)-Cr-C(7)	91.4(6)
C(9)-Cr-C(7)	65.6(5)	C(10)-Cr-C(7)	77.9(5)
C(8)-Cr-C(7)	35.7(5)	C(11)-Cr-C(7)	67.7(5)
C(14)-Cr-B(1)	115.6(7)	C(12)-Cr-B(1)	156.6(6)
C(13)-Cr-B(1)	92.4(6)	C(9)-Cr-B(1)	77.0(6)
C(10)-Cr-B(1)	65.0(5)	C(8)-Cr-B(1)	65.8(6)
C(11)-Cr-B(1)	36.7(5)	C(7)-Cr-B(1)	38.0(5)
C(1)-P(1)-C(15)	107.1(7)	C(1)-P(1)-B(1)	107.4(7)
C(15)-P(1)-B(1)	103.3(6)	C(1)-P(1)-Rh	106.3(5)
C(15)-P(1)-Rh	121.4(5)	B(1)-P(1)-Rh	110.6(5)
C(23)-P(2)-C(21)	99.7(10)	C(23)-P(2)-C(22)	102.6(9)
C(21)-P(2)-C(22)	97.2(9)	C(23)-P(2)-Rh	126.0(6)
C(21)-P(2)-Rh	115.1(6)	C(22)-P(2)-Rh	111.8(6)
C(33)-P(3)-C(32)	99.5(9)	C(33)-P(3)-C(31)	101.2(9)
C(32)-P(3)-C(31)	100.4(9)	C(33)-P(3)-Rh	114.0(7)
C(32)-P(3)-Rh	114.0(6)	C(31)-P(3)-Rh	124.1(6)
C(41)-P(4)-C(43)	100.4(9)	C(41)-P(4)-C(42)	97.3(8)

C(43)-P(4)-C(42)	101.7(7)	C(41)-P(4)-Rh	114.2(6)
C(43)-P(4)-Rh	124.2(6)	C(42)-P(4)-Rh	114.8(5)
C(6)-C(1)-C(2)	111.5(14)	C(6)-C(1)-P(1)	120.6(12)
C(2)-C(1)-P(1)	127.8(11)	C(3)-C(2)-C(1)	123(2)
C(2)-C(3)-C(4)	122(2)	C(5)-C(4)-C(3)	119(2)
C(4)-C(5)-C(6)	121(2)	C(5)-C(6)-C(1)	123(2)
C(8)-C(7)-B(1)	120.5(12)	C(8)-C(7)-Cr	71.4(8)
B(1)-C(7)-Cr	75.8(8)	C(7)-C(8)-C(9)	120.3(13)
C(7)-C(8)-Cr	72.9(8)	C(9)-C(8)-Cr	70.4(8)
C(10)-C(9)-C(8)	121.1(14)	C(10)-C(9)-Cr	72.1(9)
C(8)-C(9)-Cr	72.7(8)	C(9)-C(10)-C(11)	123(2)
C(9)-C(10)-Cr	72.1(9)	C(11)-C(10)-Cr	73.3(9)
C(10)-C(11)-B(1)	120.5(13)	C(10)-C(11)-Cr	70.5(9)
B(1)-C(11)-Cr	77.2(9)	O(12)-C(12)-Cr	178(2)
O(13)-C(13)-Cr	176.5(14)	O(14)-C(14)-Cr	178.7(13)
C(16)-C(15)-C(20)	116.3(13)	C(16)-C(15)-P(1)	123.7(12)
C(20)-C(15)-P(1)	120.1(11)	C(15)-C(16)-C(17)	124(2)
C(16)-C(17)-C(18)	117(2)	C(19)-C(18)-C(17)	121.5(14)
C(18)-C(19)-C(20)	118(2)	C(19)-C(20)-C(15)	123(2)
C(11)-B(1)-C(7)	114.0(12)	C(11)-B(1)-P(1)	121.8(11)
C(7)-B(1)-P(1)	124.1(11)	C(11)-B(1)-Cr	66.1(8)
C(7)-B(1)-Cr	66.1(8)	P(1)-B(1)-Cr	134.8(8)

Symmetry transformations used to generate equivalent atoms:

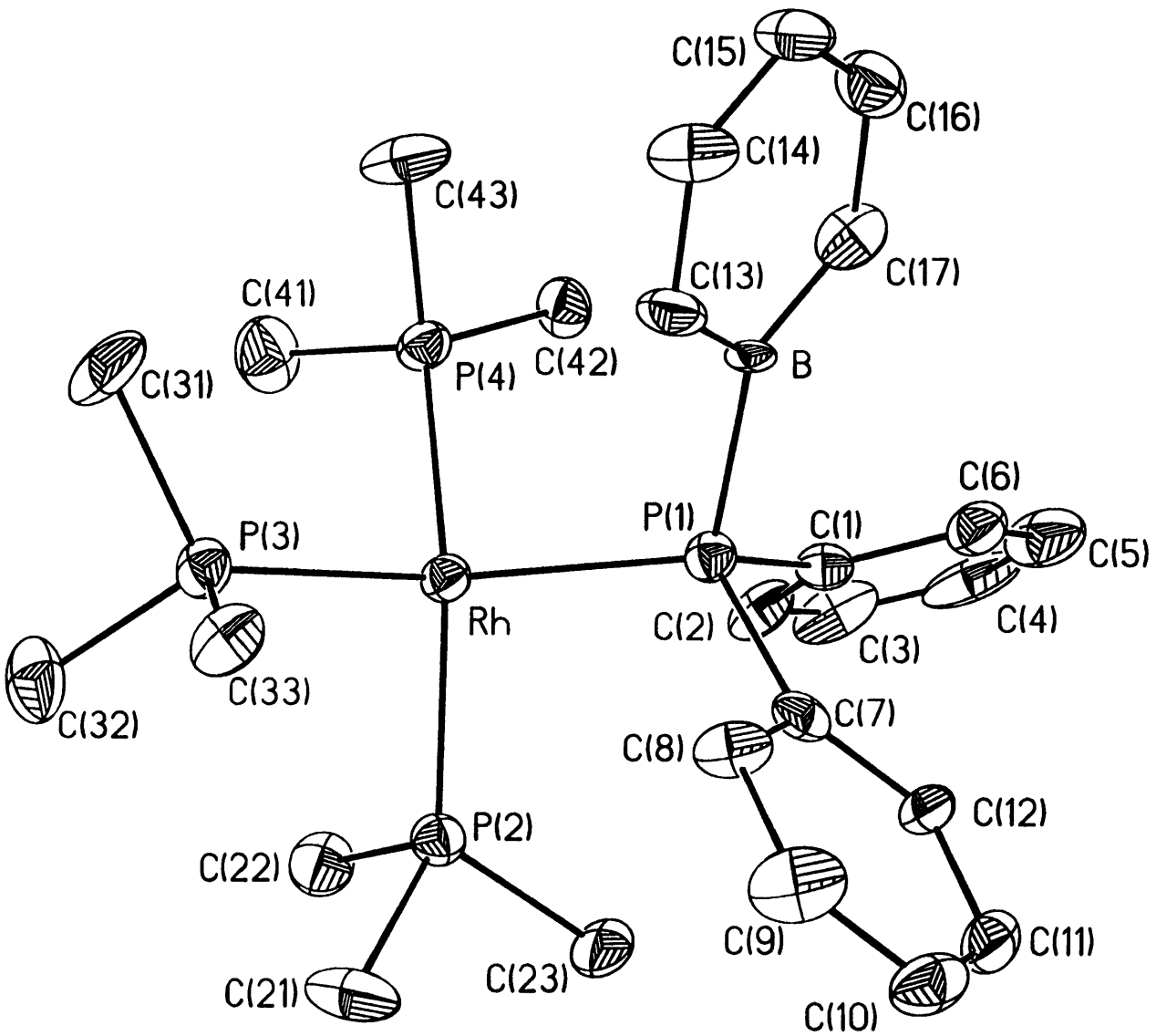


Table 11. Crystal data and structure refinement for 5.

Identification code	95123
Empirical formula	$C_{26}H_{42}BP_4Rh$
Formula weight	592.20
Temperature	188(2) K
Wavelength	0.71073 Å
Crystal system	Monoclinic
Space group	$P2_1/n$
Unit cell dimensions	$a = 9.4031(8)$ Å $\alpha = 90^\circ$ $b = 17.692(2)$ Å $\beta = 95.6350(10)^\circ$ $c = 17.672(2)$ Å $\gamma = 90^\circ$
Volume, Z	$2925.8(4)$ Å ³ , 4
Density (calculated)	1.344 Mg/m ³
Absorption coefficient	0.815 mm ⁻¹
F(000)	1232
Crystal size	0.22 x 0.22 x 0.13 mm
θ range for data collection	1.63 to 19.99°
Limiting indices	$-10 \leq h \leq 10$, $-19 \leq k \leq 17$, $-11 \leq l \leq 19$
Reflections collected	7705
Independent reflections	2710 ($R_{int} = 0.1446$)
Absorption correction	None
Refinement method	Full-matrix least-squares on F^2
Data / restraints / parameters	2640 / 0 / 290
Goodness-of-fit on F^2	1.166
Final R indices [$I > 2\sigma(I)$]	$R1 = 0.0572$, $wR2 = 0.1000$
R indices (all data)	$R1 = 0.0817$, $wR2 = 0.1497$
Extinction coefficient	$0.0019(4)$
Largest diff. peak and hole	0.707 and -1.317 eÅ ⁻³

Table 12. Atomic coordinates [$\times 10^4$] and equivalent isotropic displacement parameters [$\text{\AA}^2 \times 10^3$] for 5. $U(\text{eq})$ is defined as one third of the trace of the orthogonalized U_{ij} tensor.

	x	y	z	U(eq)
Rh	1389(1)	8553(1)	7602(1)	27(1)
P(1)	-1028(2)	8329(1)	7404(1)	29(1)
P(2)	1651(2)	8951(1)	6394(1)	33(1)
P(3)	3170(2)	9335(1)	8145(1)	34(1)
P(4)	1721(2)	7609(1)	8502(1)	34(1)
C(1)	-1810(9)	7473(4)	6920(4)	32(2)
C(2)	-973(10)	7002(4)	6547(4)	44(2)
C(3)	-1524(15)	6343(6)	6197(5)	69(3)
C(4)	-2935(18)	6188(5)	6198(6)	75(4)
C(5)	-3810(13)	6652(6)	6561(6)	74(3)
C(6)	-3278(9)	7294(5)	6925(4)	43(2)
C(7)	-1946(8)	9116(4)	6842(4)	31(2)
C(8)	-1571(9)	9854(4)	7058(4)	38(2)
C(9)	-2188(11)	10455(4)	6648(5)	55(3)
C(10)	-3157(9)	10345(5)	6034(5)	46(2)
C(11)	-3536(9)	9620(6)	5811(4)	44(2)
C(12)	-2944(8)	9015(4)	6218(4)	34(2)
C(13)	-1262(9)	9051(4)	8888(4)	40(2)
C(14)	-1653(10)	9090(5)	9623(5)	51(2)
C(15)	-2459(10)	8524(5)	9918(5)	54(3)
C(16)	-2907(10)	7911(5)	9482(5)	50(2)
C(17)	-2550(9)	7821(4)	8739(5)	46(2)
C(21)	2117(11)	9919(5)	6132(5)	64(3)
C(23)	334(9)	8754(5)	5591(4)	53(3)
C(22)	3170(9)	8413(4)	6096(4)	50(2)
C(31)	3753(10)	9269(5)	9174(4)	64(3)
C(32)	4885(9)	9473(5)	7784(5)	59(3)
C(33)	2420(9)	10288(4)	8140(4)	44(2)
C(41)	3526(9)	7226(5)	8494(5)	65(3)
C(42)	680(9)	6744(4)	8317(5)	44(2)
C(43)	1532(10)	7713(5)	9516(4)	63(3)
B	-1673(9)	8402(4)	8403(4)	21(2)

Table 13. Bond lengths [Å] and angles [°] for 5.

Rh-P(2)	2.285(2)	Rh-P(1)	2.299(2)
Rh-P(4)	2.306(2)	Rh-P(3)	2.307(2)
P(1)-C(1)	1.856(8)	P(1)-C(7)	1.871(7)
P(1)-B	1.927(8)	P(2)-C(23)	1.823(7)
P(2)-C(22)	1.836(8)	P(2)-C(21)	1.838(8)
P(3)-C(32)	1.808(9)	P(3)-C(33)	1.827(7)
P(3)-C(31)	1.851(7)	P(4)-C(43)	1.827(7)
P(4)-C(41)	1.828(9)	P(4)-C(42)	1.829(7)
C(1)-C(2)	1.360(10)	C(1)-C(6)	1.418(10)
C(2)-C(3)	1.397(12)	C(3)-C(4)	1.36(2)
C(4)-C(5)	1.37(2)	C(5)-C(6)	1.376(11)
C(7)-C(12)	1.387(10)	C(7)-C(8)	1.395(9)
C(8)-C(9)	1.382(10)	C(9)-C(10)	1.360(11)
C(10)-C(11)	1.378(10)	C(11)-C(12)	1.376(10)
C(13)-C(14)	1.385(11)	C(13)-B	1.462(10)
C(14)-C(15)	1.388(11)	C(15)-C(16)	1.373(11)
C(16)-C(17)	1.395(11)	C(17)-B	1.479(11)
P(2)-Rh-P(1)	96.13(7)	P(2)-Rh-P(4)	148.03(8)
P(1)-Rh-P(4)	92.59(7)	P(2)-Rh-P(3)	93.60(8)
P(1)-Rh-P(3)	146.36(8)	P(4)-Rh-P(3)	95.96(8)
C(1)-P(1)-C(7)	102.8(3)	C(1)-P(1)-B	109.3(3)
C(7)-P(1)-B	105.4(3)	C(1)-P(1)-Rh	123.5(3)
C(7)-P(1)-Rh	110.5(3)	B-P(1)-Rh	104.2(3)
C(23)-P(2)-C(22)	99.6(4)	C(23)-P(2)-C(21)	98.2(4)
C(22)-P(2)-C(21)	101.5(4)	C(23)-P(2)-Rh	122.8(3)
C(22)-P(2)-Rh	105.4(3)	C(21)-P(2)-Rh	125.0(3)
C(32)-P(3)-C(33)	103.3(4)	C(32)-P(3)-C(31)	99.6(4)
C(33)-P(3)-C(31)	98.0(4)	C(32)-P(3)-Rh	124.8(3)
C(33)-P(3)-Rh	106.7(3)	C(31)-P(3)-Rh	120.2(3)
C(43)-P(4)-C(41)	103.0(4)	C(43)-P(4)-C(42)	99.1(4)
C(41)-P(4)-C(42)	99.8(4)	C(43)-P(4)-Rh	125.7(3)
C(41)-P(4)-Rh	109.0(3)	C(42)-P(4)-Rh	116.6(3)
C(2)-C(1)-C(6)	118.5(7)	C(2)-C(1)-P(1)	120.1(7)
C(6)-C(1)-P(1)	121.4(6)	C(1)-C(2)-C(3)	121.3(9)
C(4)-C(3)-C(2)	119.3(10)	C(3)-C(4)-C(5)	121.0(10)
C(4)-C(3)-C(6)	120.5(11)	C(5)-C(6)-C(1)	119.4(9)
C(12)-C(7)-C(8)	118.0(7)	C(12)-C(7)-P(1)	124.5(6)
C(8)-C(7)-P(1)	117.4(6)	C(9)-C(8)-C(7)	119.7(7)
C(10)-C(9)-C(8)	121.5(7)	C(9)-C(10)-C(11)	119.7(7)
C(12)-C(11)-C(10)	119.6(7)	C(11)-C(12)-C(7)	121.5(7)
C(14)-C(13)-B	120.6(7)	C(13)-C(14)-C(15)	121.4(8)
C(16)-C(15)-C(14)	120.5(8)	C(15)-C(16)-C(17)	122.0(8)
C(16)-C(17)-B	119.6(8)	C(13)-B-C(17)	115.9(7)
C(13)-B-P(1)	120.0(6)	C(17)-B-P(1)	124.0(6)

Symmetry transformations used to generate equivalent atoms:

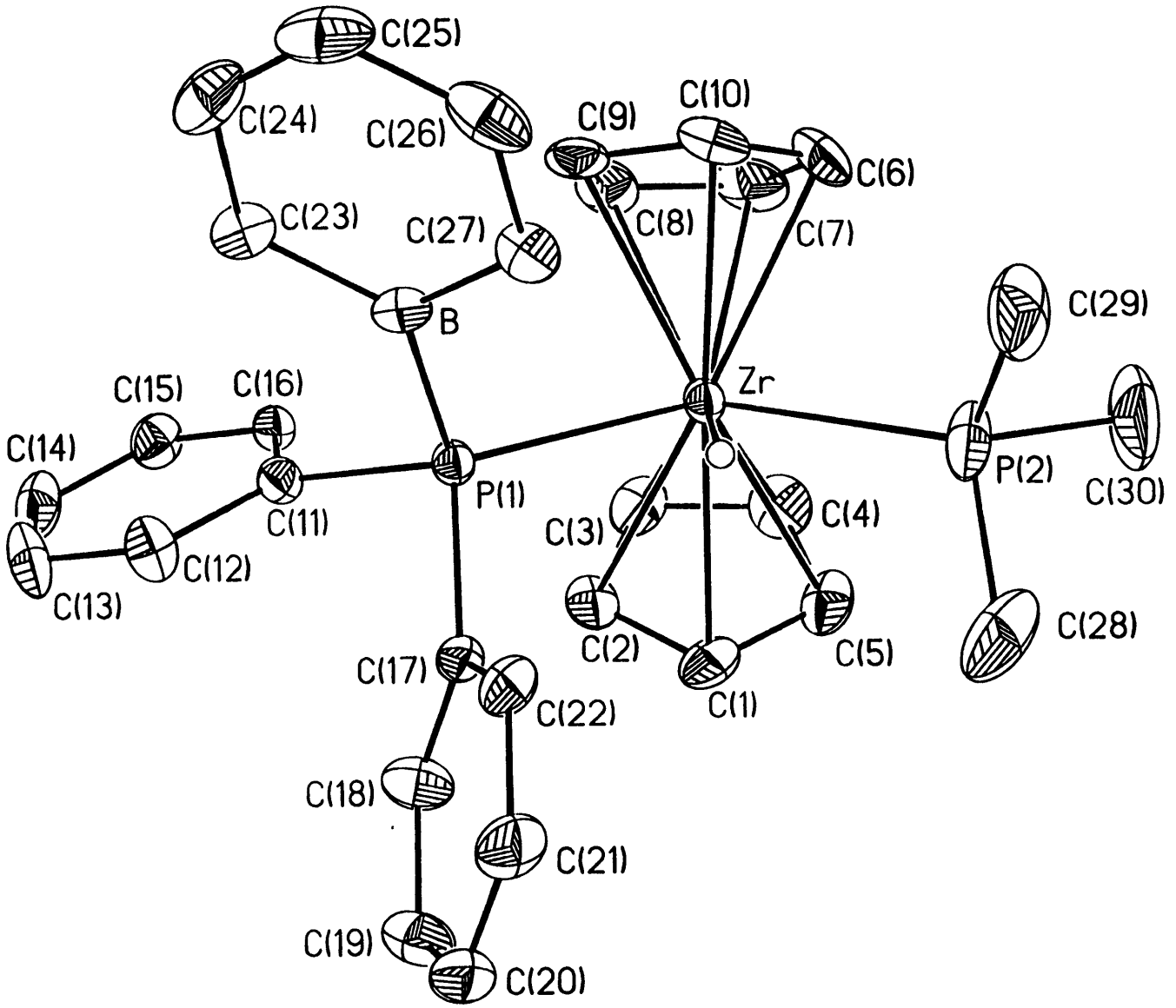


Table 6. Crystal data and structure refinement for 1.

A. Crystal Data

Identification code	96001
Empirical formula	$C_{30}H_{35}BP_2Zr$
Formula weight	559.55
Temperature	293(2) K
Wavelength	0.71073 Å
Crystal morphology	prismatic
Crystal size	0.39 x 0.09 x 0.08 mm
Crystal system	Monoclinic
Space group	$P2_1/c$
Unit cell dimensions	$a = 9.1017(6)$ Å $\alpha = 90^\circ$ $b = 17.6952(12)$ Å $\beta = 104.2750(10)^\circ$ $c = 17.8481(12)$ Å $\gamma = 90^\circ$
Volume, Z	2785.8(3) Å ³ , 4
Density (calculated)	1.334 Mg/m ³
Absorption coefficient	0.526 mm ⁻¹
F(000)	1160

B. Data Collection and Reduction

Diffractometer	Siemens SMART/CCD
Scan Type	ω Scans
Scan angle	0.30°
θ range for data collection	1.65 to 23.28°
Limiting indices	$-10 \leq h \leq 10, -10 \leq k \leq 19, -19 \leq l \leq 19$

Reflections collected	10886
Independent reflections	3977 ($R_{int} = 0.0550$)
Absorption correction	None

C. Solution and Refinement

Refinement method	Full-matrix least-squares on F^2
Data / restraints / parameters	3971 / 0 / 312
Goodness-of-fit on F^2	1.411
Final R indices [$I > 2\sigma(I)$]	R1 = 0.0641, wR2 = 0.1104
R indices (all data)	R1 = 0.0759, wR2 = 0.1215
Extinction coefficient	0.0007(3)
Largest diff. peak and hole	0.417 and -0.492 $e\text{\AA}^{-3}$

Table 7. Atomic coordinates [$\times 10^4$] and equivalent isotropic displacement parameters [$\text{\AA}^2 \times 10^3$] for 1. $U(\text{eq})$ is defined as one third of the trace of the orthogonalized U_{ij} tensor.

	x	y	z	$U(\text{eq})$
Zr	7881(1)	6441(1)	1717(1)	25(1)
P(1)	7830(2)	7559(1)	651(1)	23(1)
P(2)	9385(2)	5201(1)	1517(1)	52(1)
B	6573(7)	7322(4)	-386(3)	27(1)
C(1)	10373(7)	6973(4)	2435(3)	42(2)
C(2)	9268(7)	7499(3)	2503(3)	41(2)
C(3)	8340(7)	7184(4)	2939(3)	44(2)
C(4)	8902(8)	6460(4)	3164(3)	50(2)
C(5)	10163(7)	6335(4)	2864(3)	45(2)
C(6)	5944(8)	5408(4)	1515(4)	56(2)
C(7)	5660(7)	5875(4)	2098(4)	55(2)
C(8)	5176(7)	6575(4)	1767(4)	46(2)
C(9)	5134(6)	6541(4)	985(4)	42(2)
C(10)	5636(7)	5824(4)	830(4)	46(2)
C(11)	7218(6)	8517(3)	857(3)	29(1)
C(12)	7511(7)	9143(3)	438(3)	41(2)
C(13)	7048(8)	9863(3)	581(4)	53(2)
C(14)	6288(7)	9971(3)	1150(3)	46(2)
C(15)	5969(7)	9368(3)	1564(3)	39(2)
C(16)	6431(6)	8647(3)	1423(3)	30(1)
C(17)	9742(6)	7771(3)	535(3)	28(1)
C(18)	10677(7)	8285(4)	1011(3)	43(2)
C(19)	12111(7)	8454(4)	898(4)	47(2)
C(20)	12612(7)	8119(4)	322(4)	43(2)
C(21)	11710(7)	7604(4)	-148(4)	46(2)
C(22)	10280(6)	7433(3)	-42(3)	37(1)
C(23)	5382(6)	7843(3)	-803(3)	33(1)
C(24)	4440(7)	7621(4)	-1497(3)	48(2)
C(25)	4588(7)	6934(4)	-1830(3)	52(2)
C(26)	5713(7)	6418(4)	-1471(3)	48(2)
C(27)	6701(7)	6579(3)	-767(3)	36(1)
C(28)	11330(8)	5371(5)	1464(5)	79(3)
C(29)	8590(9)	4688(4)	620(4)	76(3)
C(30)	9637(11)	4428(4)	2215(5)	100(3)

Table 8. Bond lengths [Å] and angles [°] for 1.

Zr-C(2)	2.489(5)	Zr-C(3)	2.492(6)
Zr-C(7)	2.495(6)	Zr-C(8)	2.496(6)
Zr-C(1)	2.498(6)	Zr-C(6)	2.503(6)
Zr-C(10)	2.506(6)	Zr-C(4)	2.520(6)
Zr-C(9)	2.526(6)	Zr-C(5)	2.538(6)
Zr-P(2)	2.657(2)	Zr-P(1)	2.7382(14)
Zr-H	1.81(5)	P(1)-C(17)	1.841(5)
P(1)-C(11)	1.848(6)	P(1)-B	1.966(6)
P(2)-C(28)	1.821(8)	P(2)-C(29)	1.826(7)
P(2)-C(30)	1.827(7)	B-C(23)	1.476(8)
B-C(27)	1.498(8)	C(1)-C(2)	1.398(8)
C(1)-C(5)	1.402(9)	C(1)-H(1A)	0.98
C(2)-C(3)	1.398(8)	C(2)-H(2A)	0.98
C(3)-C(4)	1.402(9)	C(3)-H(3A)	0.98
C(4)-C(5)	1.398(9)	C(4)-H(4A)	0.98
C(5)-H(5A)	0.98	C(6)-C(10)	1.395(9)
C(6)-C(7)	1.402(9)	C(6)-H(6A)	0.98
C(7)-C(8)	1.396(9)	C(7)-H(7A)	0.98
C(8)-C(9)	1.388(8)	C(8)-H(8A)	0.98
C(9)-C(10)	1.399(8)	C(9)-H(9A)	0.98
C(10)-H(10A)	0.98	C(11)-C(16)	1.393(7)
C(11)-C(12)	1.399(7)	C(12)-C(13)	1.385(8)
C(12)-H(12A)	0.93	C(13)-C(14)	1.376(9)
C(13)-H(13A)	0.93	C(14)-C(15)	1.370(8)
C(14)-H(14A)	0.93	C(15)-C(16)	1.385(7)
C(15)-H(15A)	0.93	C(16)-H(16A)	0.93
C(17)-C(22)	1.381(7)	C(17)-C(18)	1.385(8)
C(18)-C(19)	1.401(8)	C(18)-H(18A)	0.93
C(19)-C(20)	1.361(8)	C(19)-H(19A)	0.93
C(20)-C(21)	1.366(8)	C(20)-H(20A)	0.93
C(21)-C(22)	1.394(8)	C(21)-H(21A)	0.93
C(22)-H(22A)	0.93	C(23)-C(24)	1.379(8)
C(23)-H(23A)	0.93	C(24)-C(25)	1.374(9)
C(24)-H(24A)	0.93	C(25)-C(26)	1.403(9)
C(25)-H(25A)	0.93	C(26)-C(27)	1.382(8)
C(26)-H(26A)	0.93	C(27)-H(27A)	0.93
C(28)-H(28A)	0.96	C(28)-H(28B)	0.96
C(28)-H(28C)	0.96	C(29)-H(29A)	0.96
C(29)-H(29B)	0.96	C(29)-H(29C)	0.96
C(30)-H(30A)	0.96	C(30)-H(30B)	0.96
C(30)-H(30C)	0.96		
C(2)-Zr-C(3)	32.6(2)	C(2)-Zr-C(7)	118.7(2)
C(3)-Zr-C(7)	86.9(2)	C(2)-Zr-C(8)	106.0(2)
C(3)-Zr-C(8)	82.7(2)	C(7)-Zr-C(8)	32.5(2)
C(2)-Zr-C(1)	32.6(2)	C(3)-Zr-C(1)	54.4(2)
C(7)-Zr-C(1)	134.9(2)	C(8)-Zr-C(1)	136.4(2)
C(2)-Zr-C(6)	150.7(2)	C(3)-Zr-C(6)	118.2(2)
C(7)-Zr-C(6)	32.6(2)	C(8)-Zr-C(6)	53.8(2)
C(1)-Zr-C(6)	150.1(2)	C(2)-Zr-C(10)	154.9(2)
C(3)-Zr-C(10)	135.8(2)	C(7)-Zr-C(10)	53.7(2)
C(8)-Zr-C(10)	53.6(2)	C(1)-Zr-C(10)	169.8(2)
C(6)-Zr-C(10)	32.3(2)	C(2)-Zr-C(4)	53.5(2)
C(3)-Zr-C(4)	32.5(2)	C(7)-Zr-C(4)	81.1(2)
C(8)-Zr-C(4)	94.6(2)	C(1)-Zr-C(4)	53.9(2)

C(6) -Zr-C(4)	103.1(2)	C(10) -Zr-C(4)	133.7(2)
C(2) -Zr-C(9)	122.6(2)	C(3) -Zr-C(9)	110.3(2)
C(7) -Zr-C(9)	53.4(2)	C(8) -Zr-C(9)	32.1(2)
C(1) -Zr-C(9)	153.8(2)	C(6) -Zr-C(9)	53.5(2)
C(10) -Zr-C(9)	32.3(2)	C(4) -Zr-C(9)	126.7(2)
C(2) -Zr-C(5)	53.2(2)	C(3) -Zr-C(5)	53.6(2)
C(7) -Zr-C(5)	107.9(2)	C(8) -Zr-C(5)	126.6(2)
C(1) -Zr-C(5)	32.3(2)	C(6) -Zr-C(5)	118.0(2)
C(10) -Zr-C(5)	148.8(2)	C(4) -Zr-C(5)	32.1(2)
C(9) -Zr-C(5)	158.7(2)	C(2) -Zr-P(2)	119.4(2)
C(3) -Zr-P(2)	125.0(2)	C(7) -Zr-P(2)	100.6(2)
C(8) -Zr-P(2)	129.0(2)	C(1) -Zr-P(2)	87.0(2)
C(6) -Zr-P(2)	75.3(2)	C(10) -Zr-P(2)	85.5(2)
C(4) -Zr-P(2)	94.4(2)	C(9) -Zr-P(2)	117.7(2)
C(5) -Zr-P(2)	72.6(2)	C(2) -Zr-P(1)	76.54(14)
C(3) -Zr-P(1)	101.4(2)	C(7) -Zr-P(1)	127.1(2)
C(8) -Zr-P(1)	96.2(2)	C(1) -Zr-P(1)	86.7(2)
C(6) -Zr-P(1)	122.5(2)	C(10) -Zr-P(1)	90.2(2)
C(4) -Zr-P(1)	129.9(2)	C(9) -Zr-P(1)	75.20(14)
C(5) -Zr-P(1)	118.9(2)	P(2) -Zr-P(1)	115.09(5)
C(2) -Zr-H	107(2)	C(3) -Zr-H	139(2)
C(7) -Zr-H	134(2)	C(8) -Zr-H	131(2)
C(1) -Zr-H	87(2)	C(6) -Zr-H	102(2)
C(10) -Zr-H	83(2)	C(4) -Zr-H	135(2)
C(9) -Zr-H	99(2)	C(5) -Zr-H	103(2)
P(2) -Zr-H	57(2)	P(1) -Zr-H	58(2)
C(17) -P(1) -C(11)	100.1(2)	C(17) -P(1) -B	106.6(2)
C(11) -P(1) -B	104.4(3)	C(17) -P(1) -Zr	111.8(2)
C(11) -P(1) -Zr	118.5(2)	B -P(1) -Zr	114.0(2)
C(28) -P(2) -C(29)	102.6(4)	C(28) -P(2) -C(30)	101.5(4)
C(29) -P(2) -C(30)	100.5(4)	C(28) -P(2) -Zr	114.2(3)
C(29) -P(2) -Zr	115.0(2)	C(30) -P(2) -Zr	120.5(3)
C(23) -B -C(27)	116.6(5)	C(23) -B -P(1)	121.8(4)
C(27) -B -P(1)	121.5(4)	C(2) -C(1) -C(5)	106.9(6)
C(2) -C(1) -Zr	73.4(3)	C(5) -C(1) -Zr	75.4(3)
C(2) -C(1) -H(1A)	126.0(4)	C(5) -C(1) -H(1A)	126.0(4)
Zr -C(1) -H(1A)	126.00(14)	C(1) -C(2) -C(3)	109.2(6)
C(1) -C(2) -Zr	74.1(3)	C(3) -C(2) -Zr	73.8(3)
C(1) -C(2) -H(2A)	125.1(4)	C(3) -C(2) -H(2A)	125.1(4)
Zr -C(2) -H(2A)	125.13(14)	C(2) -C(3) -C(4)	107.2(6)
C(2) -C(3) -Zr	73.6(3)	C(4) -C(3) -Zr	74.8(3)
C(2) -C(3) -H(3A)	125.9(4)	C(4) -C(3) -H(3A)	125.9(4)
Zr -C(3) -H(3A)	125.92(14)	C(5) -C(4) -C(3)	108.1(6)
C(5) -C(4) -Zr	74.7(3)	C(3) -C(4) -Zr	72.7(3)
C(5) -C(4) -H(4A)	125.6(4)	C(3) -C(4) -H(4A)	125.6(4)
Zr -C(4) -H(4A)	125.6(2)	C(4) -C(5) -C(1)	108.5(6)
C(4) -C(5) -Zr	73.2(3)	C(1) -C(5) -Zr	72.3(3)
C(4) -C(5) -H(5A)	125.6(4)	C(1) -C(5) -H(5A)	125.6(4)
Zr -C(5) -H(5A)	125.59(14)	C(10) -C(6) -C(7)	107.7(6)
C(10) -C(6) -Zr	73.9(3)	C(7) -C(6) -Zr	73.4(4)
C(10) -C(6) -H(6A)	125.8(4)	C(7) -C(6) -H(6A)	125.8(4)
Zr -C(6) -H(6A)	125.8(2)	C(8) -C(7) -C(6)	107.8(6)
C(8) -C(7) -Zr	73.8(3)	C(6) -C(7) -Zr	74.0(4)
C(8) -C(7) -H(7A)	125.7(4)	C(6) -C(7) -H(7A)	125.7(4)
Zr -C(7) -H(7A)	125.7(2)	C(9) -C(8) -C(7)	108.3(6)
C(9) -C(8) -Zr	75.1(3)	C(7) -C(8) -Zr	73.7(4)
C(9) -C(8) -H(8A)	125.4(4)	C(7) -C(8) -H(8A)	125.4(4)
Zr -C(8) -H(8A)	125.4(2)	C(8) -C(9) -C(10)	108.0(6)
C(8) -C(9) -Zr	72.8(3)	C(10) -C(9) -Zr	73.1(3)

C(8)-C(9)-H(9A)	125.8(4)	C(10)-C(9)-H(9A)	125.8(4)
Zr-C(9)-H(9A)	125.79(13)	C(6)-C(10)-C(9)	108.1(6)
C(6)-C(10)-Zr	73.7(4)	C(9)-C(10)-Zr	74.6(3)
C(6)-C(10)-H(10A)	125.5(4)	C(9)-C(10)-H(10A)	125.5(4)
Zr-C(10)-H(10A)	125.6(2)	C(16)-C(11)-C(12)	117.1(5)
C(16)-C(11)-P(1)	122.0(4)	C(12)-C(11)-P(1)	120.8(4)
C(13)-C(12)-C(11)	121.5(6)	C(13)-C(12)-H(12A)	119.2(4)
C(11)-C(12)-H(12A)	119.2(3)	C(14)-C(13)-C(12)	119.7(6)
C(14)-C(13)-H(13A)	120.2(4)	C(12)-C(13)-H(13A)	120.2(4)

C(15)-C(14)-C(13)	120.1(6)	C(15)-C(14)-H(14A)	119.9(4)
C(13)-C(14)-H(14A)	119.9(4)	C(14)-C(15)-C(16)	120.3(6)
C(14)-C(15)-H(15A)	119.8(4)	C(16)-C(15)-H(15A)	119.8(3)
C(15)-C(16)-C(11)	121.2(5)	C(15)-C(16)-H(16A)	119.4(3)
C(11)-C(16)-H(16A)	119.4(3)	C(22)-C(17)-C(18)	117.7(5)
C(22)-C(17)-P(1)	121.0(4)	C(18)-C(17)-P(1)	121.3(4)
C(17)-C(18)-C(19)	120.4(6)	C(17)-C(18)-H(18A)	119.8(3)
C(19)-C(18)-H(18A)	119.8(4)	C(20)-C(19)-C(18)	120.9(6)
C(20)-C(19)-H(19A)	119.6(4)	C(18)-C(19)-H(19A)	119.6(4)
C(19)-C(20)-C(21)	119.5(6)	C(19)-C(20)-H(20A)	120.3(4)
C(21)-C(20)-H(20A)	120.3(4)	C(20)-C(21)-C(22)	120.1(6)
C(20)-C(21)-H(21A)	120.0(4)	C(22)-C(21)-H(21A)	120.0(4)
C(17)-C(22)-C(21)	121.5(6)	C(17)-C(22)-H(22A)	119.3(3)
C(21)-C(22)-H(22A)	119.3(4)	C(24)-C(23)-B	119.4(6)
C(24)-C(23)-H(23A)	120.3(4)	B-C(23)-H(23A)	120.3(3)
C(25)-C(24)-C(23)	122.4(6)	C(25)-C(24)-H(24A)	118.8(4)
C(23)-C(24)-H(24A)	118.8(4)	C(24)-C(25)-C(26)	121.0(6)
C(24)-C(25)-H(25A)	119.5(4)	C(26)-C(25)-H(25A)	119.5(4)
C(27)-C(26)-C(25)	121.3(6)	C(27)-C(26)-H(26A)	119.4(4)
C(25)-C(26)-H(26A)	119.4(4)	C(26)-C(27)-B	119.2(6)
C(26)-C(27)-H(27A)	120.4(4)	B-C(27)-H(27A)	120.4(3)
P(2)-C(28)-H(28A)	109.5(2)	P(2)-C(28)-H(28B)	109.5(3)
H(28A)-C(28)-H(28B)	109.5	P(2)-C(28)-H(28C)	109.5(3)
H(28A)-C(28)-H(28C)	109.5	H(28B)-C(28)-H(28C)	109.5
P(2)-C(29)-H(29A)	109.5(3)	P(2)-C(29)-H(29B)	109.5(2)
H(29A)-C(29)-H(29B)	109.5	P(2)-C(29)-H(29C)	109.5(3)
H(29A)-C(29)-H(29C)	109.5	H(29B)-C(29)-H(29C)	109.5
P(2)-C(30)-H(30A)	109.5(3)	P(2)-C(30)-H(30B)	109.5(3)
H(30A)-C(30)-H(30B)	109.5	P(2)-C(30)-H(30C)	109.5(3)
H(30A)-C(30)-H(30C)	109.5	H(30B)-C(30)-H(30C)	109.5

Symmetry transformations used to generate equivalent atoms:

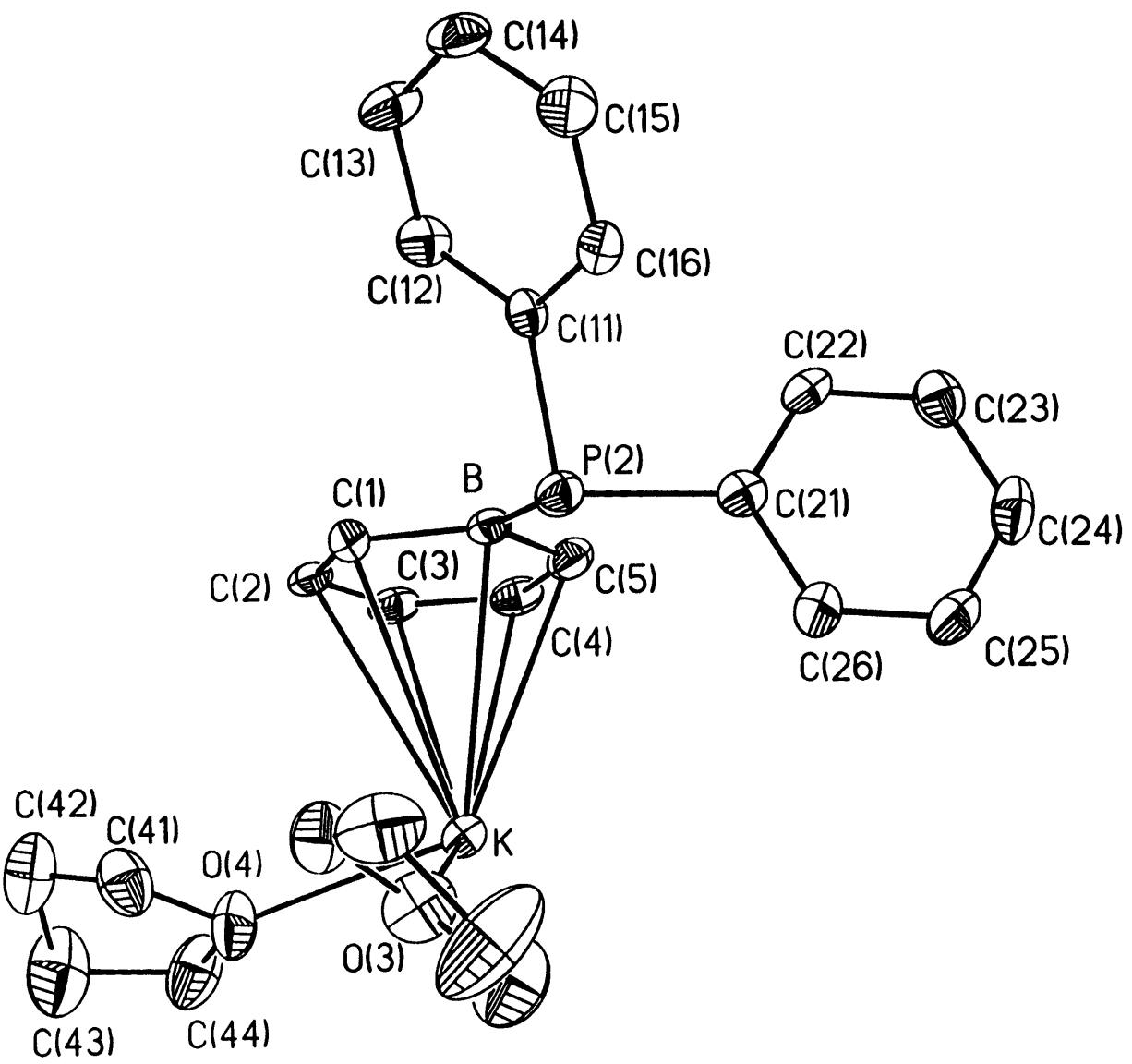


Table 1. Crystal data and structure refinement for 3.

A. Crystal Data

Identification code	96020
Empirical formula	$C_{25}H_{31}BKO_2P$
Formula weight	444.38
Temperature	187(2) K
Wavelength	0.71073 Å
Crystal morphology	needle
Crystal size	0.36 x 0.13 x 0.03 mm
Crystal system	Monoclinic
Space group	$P2_1/c$
Unit cell dimensions	$a = 13.3281(14)$ Å $\alpha = 90^\circ$ $b = 10.0091(11)$ Å $\beta = 104.063(2)^\circ$ $c = 18.835(2)$ Å $\gamma = 90^\circ$
Volume, Z	2437.3(5) Å ³ , 4
Density (calculated)	1.211 Mg/m ³
Absorption coefficient	0.302 mm ⁻¹
F(000)	944

B. Data Collection and Reduction

Diffractometer	Siemens SMART/CCD
Scan Type	ω Scans
Scan angle	0.30°
θ range for data collection	1.58 to 19.99°
Limiting indices	$-14 \leq h \leq 12, -9 \leq k \leq 11, -16 \leq l \leq 20$

Reflections collected	6707
Independent reflections	2259 ($R_{int} = 0.0796$)
Absorption correction	None

C. Solution and Refinement

Refinement method	Full-matrix least-squares on F^2
Data / restraints / parameters	2190 / 0 / 272
Goodness-of-fit on F^2	1.222
Final R indices [$I > 2\sigma(I)$]	$R1 = 0.0683$, $wR2 = 0.1155$
R indices (all data)	$R1 = 0.1000$, $wR2 = 0.1553$
Extinction coefficient	0.0044(8)
Largest diff. peak and hole	0.234 and $-0.217 \text{ e}\text{\AA}^{-3}$

Table 2. Atomic coordinates [$\times 10^4$] and equivalent isotropic displacement parameters [$\text{\AA}^2 \times 10^3$] for 3. $U(\text{eq})$ is defined as one third of the trace of the orthogonalized U_{ij} tensor.

	x	y	z	$U(\text{eq})$
K	351 (1)	2037 (1)	1823 (1)	37 (1)
P (2)	-2606 (1)	4261 (2)	1211 (1)	33 (1)
O (3)	-687 (4)	1553 (5)	418 (2)	64 (2)
O (4)	1958 (4)	2517 (5)	1256 (3)	61 (2)
C (1)	-400 (4)	5235 (6)	1598 (3)	32 (2)
C (2)	602 (5)	5284 (6)	2034 (4)	37 (2)
C (3)	864 (5)	4695 (6)	2727 (4)	34 (2)
C (4)	118 (5)	4054 (6)	3004 (3)	36 (2)
C (5)	-908 (5)	3969 (6)	2613 (3)	36 (2)
C (11)	-3300 (5)	5866 (6)	1079 (3)	28 (2)
C (12)	-2818 (5)	7095 (7)	1156 (3)	38 (2)
C (13)	-3367 (5)	8267 (7)	961 (3)	44 (2)
C (14)	-4419 (6)	8227 (7)	667 (3)	44 (2)
C (15)	-4915 (5)	7016 (8)	586 (3)	45 (2)
C (16)	-4364 (5)	5851 (7)	786 (3)	36 (2)
C (21)	-3300 (4)	3350 (6)	1787 (3)	30 (2)
C (22)	-3665 (5)	3938 (6)	2345 (4)	39 (2)
C (23)	-4144 (5)	3191 (8)	2784 (3)	44 (2)
C (24)	-4258 (5)	1845 (8)	2676 (4)	48 (2)
C (25)	-3904 (6)	1245 (7)	2133 (4)	57 (2)
C (26)	-3432 (5)	1990 (7)	1690 (4)	49 (2)
C (31)	-932 (5)	2586 (8)	-119 (4)	60 (2)
C (32)	-1982 (6)	2284 (8)	-584 (4)	71 (2)
C (33)	-2128 (8)	875 (10)	-466 (5)	124 (4)
C (34)	-1352 (6)	467 (9)	157 (4)	84 (3)
C (41)	1873 (5)	3456 (8)	669 (4)	62 (2)
C (42)	2870 (7)	4163 (9)	818 (4)	77 (3)
C (43)	3608 (6)	3172 (10)	1156 (5)	92 (3)
C (44)	3028 (6)	2385 (8)	1620 (4)	71 (2)
B	-1245 (5)	4570 (7)	1861 (4)	30 (2)

Table 3. Bond lengths [Å] and angles [°] for 3.

K-O(4)	2.659(4)	K-O(3)	2.716(5)
K-C(4)	3.074(6)	K-C(3)#1	3.082(6)
K-C(4)#1	3.084(6)	K-C(3)	3.143(6)
K-C(5)	3.159(6)	K-C(2)#1	3.264(6)
K-C(5)#1	3.275(6)	K-C(2)	3.281(6)
K-B	3.322(7)	K-C(1)	3.350(6)
P(2)-C(21)	1.831(6)	P(2)-C(11)	1.840(6)
P(2)-B	1.951(7)	O(3)-C(34)	1.414(8)
O(3)-C(31)	1.427(7)	O(4)-C(44)	1.431(8)
O(4)-C(41)	1.435(8)	C(1)-C(2)	1.388(7)
C(1)-B	1.493(8)	C(1)-K#2	3.464(6)
C(2)-C(3)	1.397(8)	C(2)-K#2	3.264(6)
C(3)-C(4)	1.387(8)	C(3)-K#2	3.082(6)
C(4)-C(5)	1.390(8)	C(4)-K#2	3.084(6)
C(5)-B	1.504(9)	C(5)-K#2	3.275(6)
C(11)-C(12)	1.379(8)	C(11)-C(16)	1.391(8)
C(12)-C(13)	1.385(8)	C(13)-C(14)	1.377(8)
C(14)-C(15)	1.372(8)	C(15)-C(16)	1.380(8)
C(21)-C(26)	1.379(8)	C(21)-C(22)	1.391(8)
C(22)-C(23)	1.381(8)	C(23)-C(24)	1.365(9)
C(24)-C(25)	1.364(9)	C(25)-C(26)	1.380(9)
C(31)-C(32)	1.491(9)	C(32)-C(33)	1.448(10)
C(33)-C(34)	1.423(10)	C(41)-C(42)	1.470(9)
C(42)-C(43)	1.433(10)	C(43)-C(44)	1.521(10)
B-K#2	3.496(7)		
O(4)-K-O(3)	84.8(2)	O(4)-K-C(4)	113.9(2)
O(3)-K-C(4)	134.8(2)	O(4)-K-C(3)#1	140.9(2)
O(3)-K-C(3)#1	87.4(2)	C(4)-K-C(3)#1	98.5(2)
O(4)-K-C(4)#1	114.9(2)	O(3)-K-C(4)#1	82.1(2)
C(4)-K-C(4)#1	120.05(8)	C(3)#1-K-C(4)#1	26.0(2)
O(4)-K-C(3)	88.5(2)	O(3)-K-C(3)	132.1(2)
C(4)-K-C(3)	25.8(2)	C(3)#1-K-C(3)	123.69(6)
C(4)#1-K-C(3)	141.8(2)	O(4)-K-C(5)	130.6(2)
O(3)-K-C(5)	111.4(2)	C(4)-K-C(5)	25.73(14)
C(3)#1-K-C(5)	87.8(2)	C(4)#1-K-C(5)	113.5(2)
C(3)-K-C(5)	45.4(2)	O(4)-K-C(2)#1	147.4(2)
O(3)-K-C(2)#1	111.1(2)	C(4)-K-C(2)#1	75.7(2)
C(3)#1-K-C(2)#1	25.23(14)	C(4)#1-K-C(2)#1	44.7(2)
C(3)-K-C(2)#1	99.6(2)	C(5)-K-C(2)#1	71.5(2)
O(4)-K-C(5)#1	99.1(2)	O(3)-K-C(5)#1	99.8(2)
C(4)-K-C(5)#1	115.8(2)	C(3)#1-K-C(5)#1	44.8(2)
C(4)#1-K-C(5)#1	25.03(14)	C(3)-K-C(5)#1	128.0(2)
C(5)-K-C(5)#1	121.73(8)	C(2)#1-K-C(5)#1	51.4(2)
O(4)-K-C(2)	78.5(2)	O(3)-K-C(2)	107.9(2)
C(4)-K-C(2)	44.6(2)	C(3)#1-K-C(2)	139.9(2)
C(4)#1-K-C(2)	164.5(2)	C(3)-K-C(2)	25.01(14)
C(5)-K-C(2)	52.2(2)	C(2)#1-K-C(2)	119.82(10)
C(5)#1-K-C(2)	151.8(2)	O(4)-K-B	116.9(2)
O(3)-K-B	88.8(2)	C(4)-K-B	46.0(2)
C(3)#1-K-B	101.1(2)	C(4)#1-K-B	126.1(2)
C(3)-K-B	53.0(2)	C(5)-K-B	26.7(2)
C(2)#1-K-B	92.4(2)	C(5)#1-K-B	143.6(2)
C(2)-K-B	44.6(2)	O(4)-K-C(1)	91.2(2)
O(3)-K-C(1)	88.9(2)	C(4)-K-C(1)	52.0(2)

C(3)#1-K-C(1)	126.9(2)	C(4)#1-K-C(1)	151.2(2)
C(3)-K-C(1)	43.8(2)	C(5)-K-C(1)	45.43(14)
C(2)#1-K-C(1)	116.4(2)	C(5)#1-K-C(1)	167.0(2)
C(2)-K-C(1)	24.14(13)	B-K-C(1)	25.9(2)
C(21)-P(2)-C(11)	101.8(3)	C(21)-P(2)-B	103.5(3)
C(11)-P(2)-B	107.8(3)	C(34)-O(3)-C(31)	107.2(5)
C(34)-O(3)-K	127.1(4)	C(31)-O(3)-K	122.4(4)
C(44)-O(4)-C(41)	108.2(5)	C(44)-O(4)-K	126.7(4)
C(41)-O(4)-K	120.5(4)	C(2)-C(1)-B	121.0(6)
C(2)-C(1)-K	75.1(3)	B-C(1)-K	76.0(3)
C(2)-C(1)-K#2	70.1(3)	B-C(1)-K#2	78.8(3)
K-C(1)-K#2	116.5(2)	C(1)-C(2)-C(3)	121.6(6)
C(1)-C(2)-K#2	86.3(3)	C(3)-C(2)-K#2	70.1(3)
C(1)-C(2)-K	80.7(3)	C(3)-C(2)-K	71.9(3)
K#2-C(2)-K	124.6(2)	C(4)-C(3)-C(2)	120.5(5)
C(4)-C(3)-K#2	77.1(3)	C(2)-C(3)-K#2	84.7(3)
C(4)-C(3)-K	74.4(3)	C(2)-C(3)-K	83.1(3)
K#2-C(3)-K	137.1(2)	C(3)-C(4)-C(5)	122.1(6)
C(3)-C(4)-K	79.9(4)	C(5)-C(4)-K	80.5(3)
C(3)-C(4)-K#2	76.9(4)	C(5)-C(4)-K#2	85.2(3)
K-C(4)-K#2	140.4(2)	C(4)-C(5)-B	120.3(6)
C(4)-C(5)-K	73.7(3)	B-C(5)-K	82.7(3)
C(4)-C(5)-K#2	69.8(3)	B-C(5)-K#2	85.6(4)
K-C(5)-K#2	128.5(2)	C(12)-C(11)-C(16)	117.1(6)
C(12)-C(11)-P(2)	123.9(5)	C(16)-C(11)-P(2)	118.3(5)
C(11)-C(12)-C(13)	121.6(5)	C(14)-C(13)-C(12)	120.2(6)
C(15)-C(14)-C(13)	119.1(6)	C(14)-C(15)-C(16)	120.4(6)
C(15)-C(16)-C(11)	121.5(6)	C(26)-C(21)-C(22)	117.5(6)
C(26)-C(21)-P(2)	118.6(5)	C(22)-C(21)-P(2)	123.8(5)
C(23)-C(22)-C(21)	121.3(6)	C(24)-C(23)-C(22)	119.7(6)
C(25)-C(24)-C(23)	120.0(6)	C(24)-C(25)-C(26)	120.4(7)
C(21)-C(26)-C(25)	121.0(6)	O(3)-C(31)-C(32)	106.8(6)
C(33)-C(32)-C(31)	104.4(6)	C(34)-C(33)-C(32)	107.9(7)
O(3)-C(34)-C(33)	109.6(7)	O(4)-C(41)-C(42)	105.6(5)
C(43)-C(42)-C(41)	104.1(7)	C(42)-C(43)-C(44)	102.9(6)
O(4)-C(44)-C(43)	105.2(6)	C(1)-B-C(5)	114.5(5)
C(1)-B-P(2)	121.6(5)	C(5)-B-P(2)	123.1(5)
C(1)-B-K	78.2(3)	C(5)-B-K	70.6(3)
P(2)-B-K	111.6(3)	C(1)-B-K#2	76.4(3)
C(5)-B-K#2	69.1(3)	P(2)-B-K#2	131.4(3)
K-B-K#2	116.4(2)		

Symmetry transformations used to generate equivalent atoms:

#1 -x,y-1/2,-z+1/2 #2 -x,y+1/2,-z+1/2

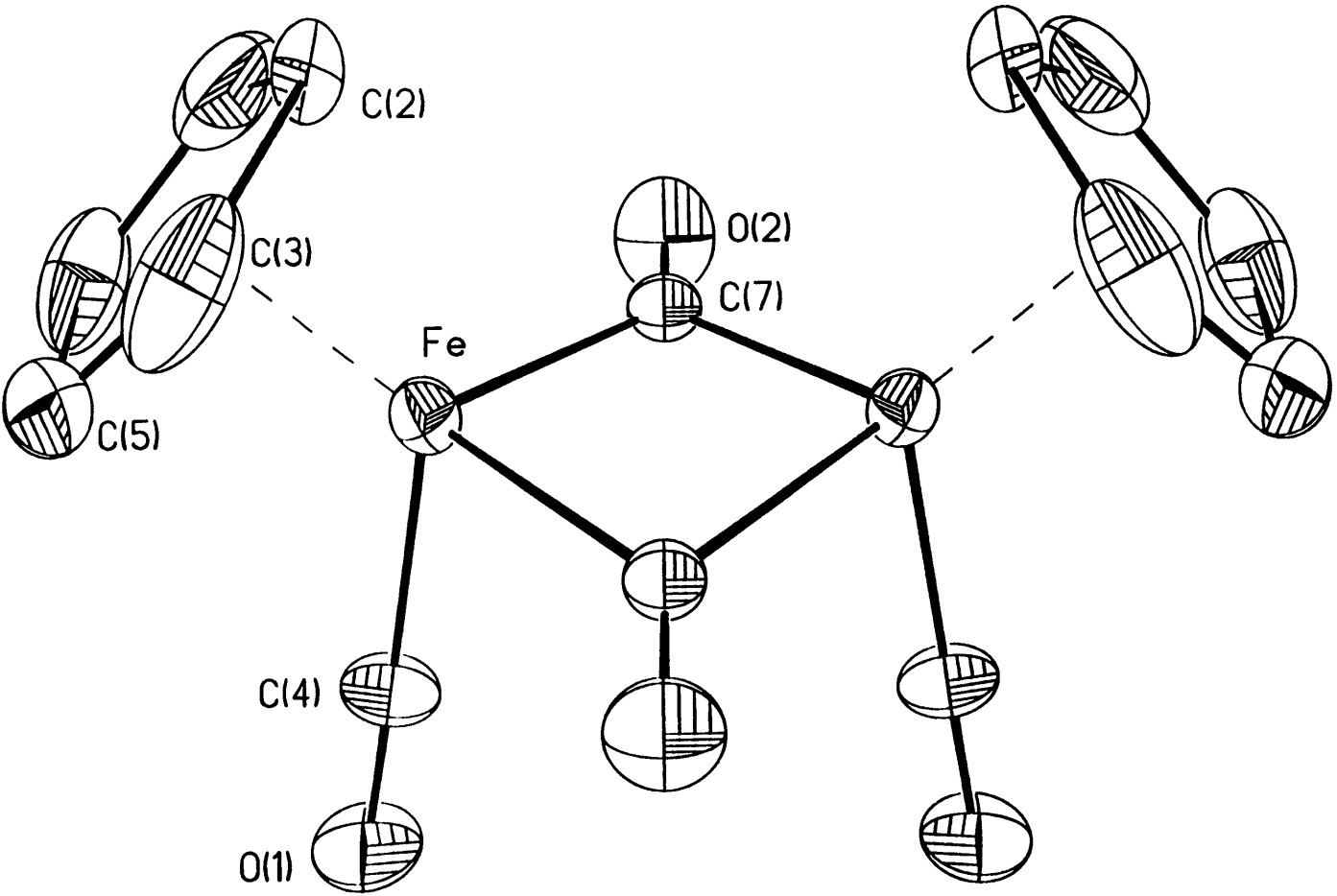


Table 1. Crystal data and structure refinement for 1.

A. Crystal Data

Identification code	1 96040
Empirical formula	$C_{14}H_{10}Fe_2O_4$
Formula weight	353.92
Temperature	293(2) K
Wavelength	0.71073 Å
Crystal morphology	plate
Crystal size	0.18 x 0.03 x 0.02 mm
Crystal system	Orthorhombic
Space group	Fmm2
Unit cell dimensions	$a = 10.037(6) \text{ \AA}$ $\alpha = 90^\circ$ $b = 16.075(10) \text{ \AA}$ $\beta = 90^\circ$ $c = 8.126(5) \text{ \AA}$ $\gamma = 90^\circ$
Volume, Z	1311.0(13) Å ³ , 4
Density (calculated)	1.793 Mg/m ³
Absorption coefficient	2.220 mm ⁻¹
F(000)	712

B. Data Collection and Reduction

Diffractometer	Siemens SMART/CCD
Scan Type	ω Scans
Scan angle	0.30°
θ range for data collection	2.53 to 19.90°
Limiting indices	$-11 \leq h \leq 6, -14 \leq k \leq 17, -7 \leq l \leq 6$

Reflections collected	453
Independent reflections	261 ($R_{int} = 0.0331$)
Absorption correction	None

C. Solution and Refinement

Refinement method	Full-matrix least-squares on F^2
Data / restraints / parameters	259 / 1 / 56
Goodness-of-fit on F^2	1.197
Final R indices [$I > 2\sigma(I)$]	$R1 = 0.0354$, $wR2 = 0.0881$
R indices (all data)	$R1 = 0.0371$, $wR2 = 0.0911$
Absolute structure parameter	0.59(11)
Extinction coefficient	0.0008(7)
Largest diff. peak and hole	0.384 and -0.480 $e\text{\AA}^{-3}$

Table 2. Atomic coordinates [$\times 10^4$] and equivalent isotropic displacement parameters [$\text{\AA}^2 \times 10^3$] for 1. $U(\text{eq})$ is defined as one third of the trace of the orthogonalized U_{ij} tensor.

	x	y	z	$U(\text{eq})$
Fe	0	5790(1)	908(4)	24(1)
C(2)	0	6095(16)	-1586(29)	83(12)
O(1)	0	6084(7)	4392(18)	53(3)
C(3)	1114(12)	6455(9)	-831(24)	71(5)
C(5)	693(12)	6970(7)	309(16)	59(5)
O(2)	-2584(9)	5000	1248(18)	50(5)
C(7)	-1423(12)	5000	1080(27)	27(3)
C(4)	0	5965(13)	3054(33)	37(7)

Table 3. Bond lengths [Å] and angles [°] for 1.

Fe-C(4)	1.77(3)	Fe-C(7)	1.916(9)
Fe-C(7)#1	1.917(9)	Fe-C(5)#2	2.079(11)
Fe-C(5)	2.079(11)	Fe-C(2)	2.08(2)
Fe-C(3)	2.095(12)	Fe-C(3)#2	2.095(12)
Fe-Fe#1	2.540(3)	C(2)-C(3)	1.40(2)
C(2)-C(3)#2	1.40(2)	O(1)-C(4)	1.10(2)
C(3)-C(5)	1.31(2)	C(5)-C(5)#2	1.39(2)
O(2)-C(7)	1.173(13)	C(7)-Fe#1	1.916(9)
C(4)-Fe-C(7)	91.9(8)	C(4)-Fe-C(7)#1	91.9(8)
C(7)-Fe-C(7)#1	96.4(5)	C(4)-Fe-C(5)#2	94.9(8)
C(7)-Fe-C(5)#2	111.9(5)	C(7)#1-Fe-C(5)#2	150.6(4)
C(4)-Fe-C(5)	94.9(8)	C(7)-Fe-C(5)	150.6(4)
C(7)#1-Fe-C(5)	111.9(5)	C(5)#2-Fe-C(5)	39.1(7)
C(4)-Fe-C(2)	157.2(6)	C(7)-Fe-C(2)	103.1(8)
C(7)#1-Fe-C(2)	103.1(8)	C(5)#2-Fe-C(2)	63.8(7)
C(5)-Fe-C(2)	63.8(7)	C(4)-Fe-C(3)	125.8(6)
C(7)-Fe-C(3)	141.7(8)	C(7)#1-Fe-C(3)	89.4(6)
C(5)#2-Fe-C(3)	63.6(4)	C(5)-Fe-C(3)	36.7(5)
C(2)-Fe-C(3)	39.2(5)	C(4)-Fe-C(3)#2	125.8(6)
C(7)-Fe-C(3)#2	89.4(6)	C(7)#1-Fe-C(3)#2	141.7(8)
C(5)#2-Fe-C(3)#2	36.7(5)	C(5)-Fe-C(3)#2	63.6(4)
C(2)-Fe-C(3)#2	39.2(5)	C(3)-Fe-C(3)#2	64.5(8)
C(4)-Fe-Fe#1	99.2(7)	C(7)-Fe-Fe#1	48.5(2)
C(7)#1-Fe-Fe#1	48.5(2)	C(5)#2-Fe-Fe#1	155.9(4)
C(5)-Fe-Fe#1	155.9(4)	C(2)-Fe-Fe#1	103.6(7)
C(3)-Fe-Fe#1	120.7(5)	C(3)#2-Fe-Fe#1	120.7(5)
C(3)-C(2)-C(3)#2	106(2)	C(3)-C(2)-Fe	70.8(11)
C(3)#2-C(2)-Fe	70.8(11)	C(5)-C(3)-C(2)	108.2(12)
C(5)-C(3)-Fe	71.0(8)	C(2)-C(3)-Fe	70.0(10)
C(3)-C(5)-C(5)#2	108.8(8)	C(3)-C(5)-Fe	72.4(6)
C(5)#2-C(5)-Fe	70.5(3)	O(2)-C(7)-Fe#1	138.5(3)
O(2)-C(7)-Fe	138.5(3)	Fe#1-C(7)-Fe	83.0(5)
O(1)-C(4)-Fe	179(2)		

Symmetry transformations used to generate equivalent atoms:

#1 -x, -y+1, z #2 -x, y, z

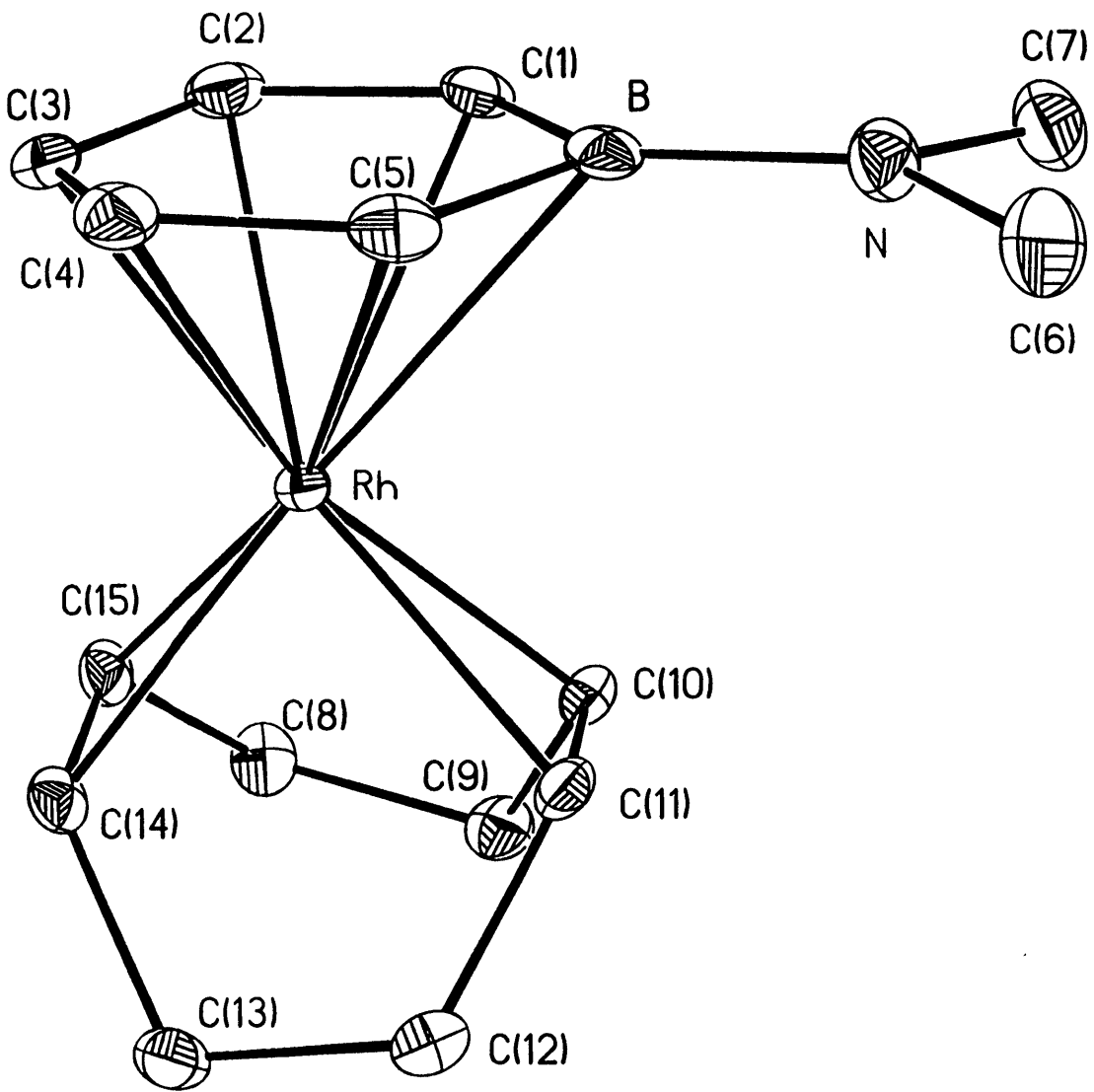


Table 1. Crystal data and structure refinement for 1.

A. Crystal data

Identification code	96053
Empirical formula	$C_{15}H_{23}BNRh$
Formula weight	331.06
Temperature	293(2) K
Wavelength	0.71073 Å
Crystal system	Triclinic
Space group	$P\bar{1}$
Unit cell dimensions	$a = 6.4131(2) \text{ \AA}$ $\alpha = 103.4290(10)^\circ$ $b = 8.327 \text{ \AA}$ $\beta = 92.1100(10)^\circ$ $c = 14.1959(4) \text{ \AA}$ $\gamma = 109.901(2)^\circ$
Volume, Z	$687.73(3) \text{ \AA}^3$, 2
Density (calculated)	1.599 Mg/m^3
Absorption coefficient	1.222 mm^{-1}
F(000)	340
Crystal morphology	yellow prism
Crystal size	0.32 x 0.12 x 0.12 mm

B. Data Collection and Reduction

Diffractometer	Siemens SMART/CCD
Crystal-Detector distance	6.0 cm
Scan type	ω Scans
Scan angle	0.30°
θ range for data collection	1.49 to 23.24°
Limiting indices	$-4 \leq h \leq 7$, $-9 \leq k \leq 9$, $-13 \leq l \leq 15$
Reflections collected	2808
Independent reflections	1919 ($R_{int} = 0.0303$)
Absorption correction	Semi-empirical from psi-scans

Max. and min. transmission 0.8926 and 0.6267

C. Structure Solution and Refinement

Refinement method	Full-matrix least-squares on F^2
Data / restraints / parameters	1917 / 0 / 164
Goodness-of-fit on F^2	1.075
Final R indices [$I > 2\sigma(I)$]	$R_1 = 0.0225$, $wR_2 = 0.0554$
R indices (all data)	$R_1 = 0.0242$, $wR_2 = 0.0667$
Maximum shift/esd	-0.001
Extinction coefficient	0.0162(13)
Largest diff. peak and hole	0.350 and -0.328 $e\text{\AA}^{-3}$

Notes: E

$$R_1 = \frac{\sum |F_o| - |F_c|}{\sum |F_o|}$$
$$wR_2 = \left[\frac{\sum [w(F_o^2 - F_c^2)^2]}{\sum (F_o^2)^2} \right]^{1/2}$$

Weighting scheme

calc $w = 1 / [\sigma^2(F_o^2) + (0.0182P)^2 + 1.3046P]$ where $P = (F_o^2 + 2F_c^2) / 3$

Refinement on F^2 for ALL reflections. Weighted R-factors wR and all goodnesses of fit S are based on F^2 , conventional R-factors R are based on F , with F set to zero for negative F^2 . The observed criterion of $F^2 > 2\sigma(F^2)$ is used only for calculating R_1 and is not relevant to the choice of reflections for refinement. R-factors based on F^2 are statistically about twice as large as those based on F , and R-factors based on ALL data will be even larger.

Table 2. Atomic coordinates [$\times 10^4$] and equivalent isotropic displacement parameters [$\text{\AA}^2 \times 10^3$] for 1. $U(\text{eq})$ is defined as one third of the trace of the orthogonalized U_{ij} tensor.

	x	y	z	$U(\text{eq})$
Rh	2380 (1)	4765 (1)	2033 (1)	13 (1)
N	4377 (5)	7747 (4)	4424 (2)	24 (1)
C (1)	4876 (6)	7751 (4)	2604 (2)	20 (1)
C (2)	3885 (6)	7418 (4)	1654 (2)	23 (1)
C (3)	1521 (6)	6659 (4)	1401 (2)	23 (1)
C (4)	73 (6)	6388 (4)	2130 (3)	24 (1)
C (5)	907 (6)	6654 (4)	3096 (2)	22 (1)
C (6)	3067 (7)	7355 (5)	5210 (3)	37 (1)
C (7)	6768 (6)	8279 (5)	4728 (3)	32 (1)
C (8)	4617 (6)	2401 (5)	878 (2)	24 (1)
C (9)	5111 (6)	2312 (4)	1925 (2)	23 (1)
C (10)	4388 (5)	3596 (4)	2674 (2)	19 (1)
C (11)	2282 (5)	3117 (4)	2998 (2)	19 (1)
C (12)	453 (6)	1315 (4)	2632 (2)	22 (1)
C (13)	-3 (6)	699 (4)	1513 (2)	23 (1)
C (14)	556 (5)	2252 (4)	1041 (2)	18 (1)
C (15)	2656 (5)	2993 (4)	739 (2)	18 (1)
B	3449 (6)	7442 (5)	3446 (3)	19 (1)

Table 3. Bond lengths [Å] and angles [°] for 1.

Rh-C(15)	2.128(3)	Rh-C(14)	2.139(3)
Rh-C(11)	2.140(3)	Rh-C(10)	2.147(3)
Rh-C(3)	2.194(3)	Rh-C(2)	2.290(3)
Rh-C(4)	2.307(3)	Rh-C(5)	2.378(3)
Rh-C(1)	2.379(3)	Rh-B	2.498(4)
N-B	1.421(5)	N-C(6)	1.452(5)
N-C(7)	1.460(5)	C(1)-C(2)	1.393(5)
C(1)-B	1.548(5)	C(2)-C(3)	1.425(5)
C(3)-C(4)	1.421(5)	C(4)-C(5)	1.393(5)
C(5)-B	1.548(5)	C(8)-C(15)	1.521(4)
C(8)-C(9)	1.531(5)	C(9)-C(10)	1.528(5)
C(10)-C(11)	1.400(5)	C(11)-C(12)	1.513(5)
C(12)-C(13)	1.535(5)	C(13)-C(14)	1.535(4)
C(14)-C(15)	1.406(5)		
C(15)-Rh-C(14)	38.48(12)	C(15)-Rh-C(11)	97.32(12)
C(14)-Rh-C(11)	81.26(12)	C(15)-Rh-C(10)	81.49(12)
C(14)-Rh-C(10)	89.91(12)	C(11)-Rh-C(10)	38.11(12)
C(15)-Rh-C(3)	100.04(12)	C(14)-Rh-C(3)	104.09(12)
C(11)-Rh-C(3)	157.73(13)	C(10)-Rh-C(3)	159.45(13)
C(15)-Rh-C(2)	100.90(12)	C(14)-Rh-C(2)	126.86(12)
C(11)-Rh-C(2)	150.26(12)	C(10)-Rh-C(2)	122.47(12)
C(3)-Rh-C(2)	36.98(13)	C(15)-Rh-C(4)	124.90(12)
C(14)-Rh-C(4)	106.09(12)	C(11)-Rh-C(4)	121.06(12)
C(10)-Rh-C(4)	152.39(13)	C(3)-Rh-C(4)	36.70(13)
C(2)-Rh-C(4)	65.18(12)	C(15)-Rh-C(5)	158.69(12)
C(14)-Rh-C(5)	127.48(12)	C(11)-Rh-C(5)	94.64(12)
C(10)-Rh-C(5)	118.17(12)	C(3)-Rh-C(5)	64.74(12)
C(2)-Rh-C(5)	76.22(12)	C(4)-Rh-C(5)	34.54(12)
C(15)-Rh-C(1)	123.26(12)	C(14)-Rh-C(1)	159.29(12)
C(11)-Rh-C(1)	115.79(12)	C(10)-Rh-C(1)	96.93(12)
C(3)-Rh-C(1)	64.91(12)	C(2)-Rh-C(1)	34.64(12)
C(4)-Rh-C(1)	76.06(12)	C(5)-Rh-C(1)	65.62(11)
C(15)-Rh-B	159.23(13)	C(14)-Rh-B	162.28(12)
C(11)-Rh-B	90.95(12)	C(10)-Rh-B	93.73(12)
C(3)-Rh-B	77.54(12)	C(2)-Rh-B	64.62(12)
C(4)-Rh-B	64.46(12)	C(5)-Rh-B	36.91(12)
C(1)-Rh-B	36.91(12)	B-N-C(6)	124.3(3)
B-N-C(7)	123.5(3)	C(6)-N-C(7)	111.8(3)
C(2)-C(1)-B	121.3(3)	C(2)-C(1)-Rh	69.2(2)
B-C(1)-Rh	75.7(2)	C(1)-C(2)-C(3)	121.6(3)
C(1)-C(2)-Rh	76.2(2)	C(3)-C(2)-Rh	67.8(2)
C(4)-C(3)-C(2)	120.9(3)	C(4)-C(3)-Rh	76.0(2)
C(2)-C(3)-Rh	75.2(2)	C(5)-C(4)-C(3)	121.3(3)
C(5)-C(4)-Rh	75.5(2)	C(3)-C(4)-Rh	67.3(2)
C(4)-C(5)-B	121.6(3)	C(4)-C(5)-Rh	69.9(2)
B-C(5)-Rh	75.8(2)	C(15)-C(8)-C(9)	113.2(3)
C(10)-C(9)-C(8)	112.3(3)	C(11)-C(10)-C(9)	122.9(3)
C(11)-C(10)-Rh	70.7(2)	C(9)-C(10)-Rh	113.6(2)
C(10)-C(11)-C(12)	124.5(3)	C(10)-C(11)-Rh	71.2(2)
C(12)-C(11)-Rh	111.9(2)	C(11)-C(12)-C(13)	112.7(3)
C(14)-C(13)-C(12)	112.4(3)	C(15)-C(14)-C(13)	122.6(3)
C(15)-C(14)-Rh	70.3(2)	C(13)-C(14)-Rh	113.8(2)
C(14)-C(15)-C(8)	124.1(3)	C(14)-C(15)-Rh	71.2(2)
C(8)-C(15)-Rh	111.6(2)	N-B-C(5)	123.6(3)

N-B-C(1)	123.5(3)	C(5)-B-C(1)	112.8(3)
N-B-Rh	131.1(2)	C(5)-B-Rh	67.3(2)
C(1)-B-Rh	67.4(2)		

Symmetry transformations used to generate equivalent atoms:

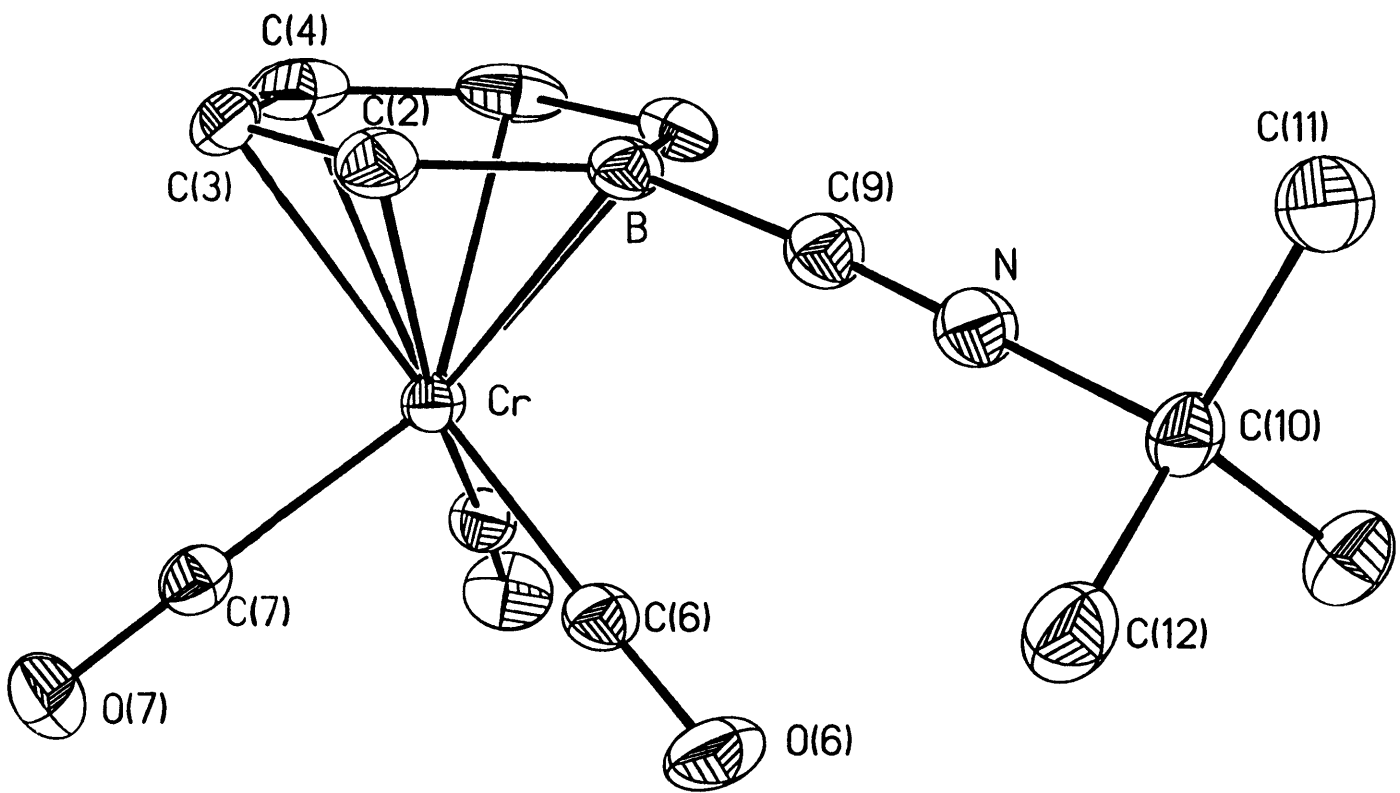


Table 1. Crystal data and structure refinement for 1.

A. Crystal Data

Identification code	96083
Empirical formula	$C_{13}H_{14}BCrNO_3$
Formula weight	295.06
Temperature	183(2) K
Wavelength	0.71073 Å
Crystal morphology	polygon
Crystal size	0.53 x 0.23 x 0.15 mm
Crystal system	Orthorhombic
Space group	Pnma
Unit cell dimensions	$a = 11.129(14)$ Å $\alpha = 90^\circ$ $b = 10.32(2)$ Å $\beta = 90^\circ$ $c = 11.92(2)$ Å $\gamma = 90^\circ$
Volume, Z	1370(4) Å ³ , 4
Density (calculated)	1.431 Mg/m ³
Absorption coefficient	0.836 mm ⁻¹
F(000)	608

B. Data Collection and Reduction

Diffractometer	Siemens SMART/CCD
Scan Type	ω Scans
Scan angle	0.30°
θ range for data collection	2.50 to 23.25°
Limiting indices	$-11 \leq h \leq 12, -11 \leq k \leq 10, -11 \leq l \leq 13$

Reflections collected	5246
Independent reflections	1046 ($R_{int} = 0.0581$)
Absorption correction	None

C. Solution and Refinement

Refinement method	Full-matrix least-squares on F^2
Data / restraints / parameters	1046 / 0 / 131
Goodness-of-fit on F^2	1.203
Final R indices [$I > 2\sigma(I)$]	$R1 = 0.0294$, $wR2 = 0.0702$
R indices (all data)	$R1 = 0.0309$, $wR2 = 0.0712$
Extinction coefficient	0.020(3)
Largest diff. peak and hole	0.296 and -0.278 $e\text{\AA}^{-3}$

Table 2. Atomic coordinates [$\times 10^4$] and equivalent isotropic displacement parameters [$\text{\AA}^2 \times 10^3$] for 1. $U(\text{eq})$ is defined as one third of the trace of the orthogonalized U_{ij} tensor.

	x	y	z	$U(\text{eq})$
Cr	8812 (1)	2500	5040 (1)	22 (1)
O(6)	10636 (2)	2500	3195 (2)	47 (1)
O(7)	7336 (1)	530 (2)	3805 (1)	44 (1)
N	12735 (2)	2500	5195 (2)	31 (1)
C(2)	9847 (2)	1251 (2)	6287 (2)	32 (1)
C(3)	8635 (2)	1310 (3)	6602 (2)	42 (1)
C(4)	8040 (3)	2500	6754 (2)	48 (1)
C(6)	9913 (2)	2500	3894 (2)	30 (1)
C(7)	7913 (2)	1280 (2)	4298 (2)	29 (1)
C(9)	11811 (2)	2500	5610 (2)	30 (1)
C(10)	13923 (2)	2500	4653 (2)	29 (1)
C(11)	14851 (3)	2500	5597 (3)	44 (1)
C(12)	13996 (2)	1277 (2)	3943 (2)	40 (1)
B	10505 (3)	2500	6114 (2)	27 (1)

Table 3. Bond lengths [Å] and angles [°] for 1.

Cr-C(6)	1.835(3)	Cr-C(7)#1	1.835(3)
Cr-C(7)	1.836(3)	Cr-C(4)	2.216(4)
Cr-C(3)#1	2.239(3)	Cr-C(3)	2.239(3)
Cr-B	2.278(4)	Cr-C(2)#1	2.280(3)
Cr-C(2)	2.280(3)	O(6)-C(6)	1.159(4)
O(7)-C(7)	1.165(3)	N-C(9)	1.141(4)
N-C(10)	1.472(4)	C(2)-C(3)	1.402(3)
C(2)-B	1.497(3)	C(3)-C(4)	1.407(4)
C(4)-C(3)#1	1.407(4)	C(9)-B	1.573(4)
C(10)-C(12)#1	1.522(3)	C(10)-C(12)	1.522(3)
C(10)-C(11)	1.527(4)	B-C(2)#1	1.497(3)
C(6)-Cr-C(7)#1	90.28(11)	C(6)-Cr-C(7)	90.28(11)
C(7)#1-Cr-C(7)	86.6(2)	C(6)-Cr-C(4)	160.89(12)
C(7)#1-Cr-C(4)	103.51(10)	C(7)-Cr-C(4)	103.51(10)
C(6)-Cr-C(3)#1	132.66(10)	C(7)#1-Cr-C(3)#1	88.69(13)
C(7)-Cr-C(3)#1	136.83(10)	C(4)-Cr-C(3)#1	36.80(9)
C(6)-Cr-C(3)	132.66(10)	C(7)#1-Cr-C(3)	136.83(10)
C(7)-Cr-C(3)	88.69(13)	C(4)-Cr-C(3)	36.80(9)
C(3)#1-Cr-C(3)	66.5(2)	C(6)-Cr-B	82.3(2)
C(7)#1-Cr-B	136.20(8)	C(7)-Cr-B	136.20(8)
C(4)-Cr-B	78.60(14)	C(3)#1-Cr-B	66.77(10)
C(3)-Cr-B	66.77(10)	C(6)-Cr-C(2)#1	98.50(12)
C(7)#1-Cr-C(2)#1	101.65(14)	C(7)-Cr-C(2)#1	167.86(8)
C(4)-Cr-C(2)#1	66.09(11)	C(3)#1-Cr-C(2)#1	36.12(9)
C(3)-Cr-C(2)#1	79.20(13)	B-Cr-C(2)#1	38.35(8)
C(6)-Cr-C(2)	98.50(12)	C(7)#1-Cr-C(2)	167.85(8)
C(7)-Cr-C(2)	101.65(14)	C(4)-Cr-C(2)	66.09(11)
C(3)#1-Cr-C(2)	79.20(13)	C(3)-Cr-C(2)	36.12(9)
B-Cr-C(2)	38.35(8)	C(2)#1-Cr-C(2)	68.9(2)
C(9)-N-C(10)	179.7(3)	C(3)-C(2)-B	118.0(2)
C(3)-C(2)-Cr	70.35(13)	B-C(2)-Cr	70.8(2)
C(2)-C(3)-C(4)	121.7(2)	C(2)-C(3)-Cr	73.52(12)
C(4)-C(3)-Cr	70.7(2)	C(3)#1-C(4)-C(3)	121.6(3)
C(3)#1-C(4)-Cr	72.5(2)	C(3)-C(4)-Cr	72.5(2)
O(6)-C(6)-Cr	177.9(2)	O(7)-C(7)-Cr	178.3(2)
N-C(9)-B	176.7(3)	N-C(10)-C(12)#1	106.9(2)
N-C(10)-C(12)	106.9(2)	C(12)#1-C(10)-C(12)	112.1(3)
N-C(10)-C(11)	106.5(3)	C(12)#1-C(10)-C(11)	112.0(2)
C(12)-C(10)-C(11)	112.0(2)	C(2)#1-B-C(2)	118.9(3)
C(2)#1-B-C(9)	120.32(14)	C(2)-B-C(9)	120.32(14)
C(2)#1-B-Cr	70.88(14)	C(2)-B-Cr	70.88(14)
C(9)-B-Cr	123.4(2)		

Symmetry transformations used to generate equivalent atoms:

#1 x, -y+1/2, z

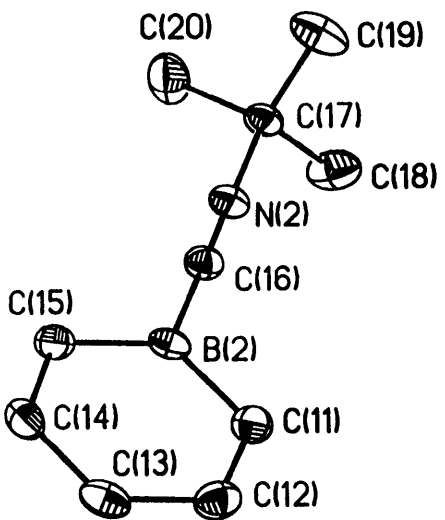
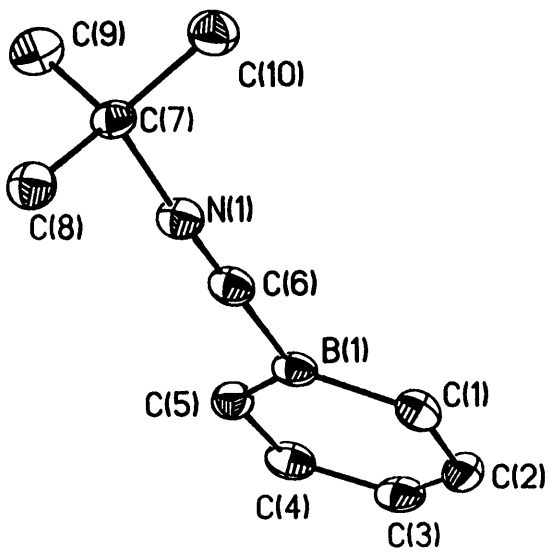


Table 1. Crystal data and structure refinement for 1.

A. Crystal Data

Identification code	96093
Empirical formula	$C_{10}H_{14}BN$
Formula weight	159.03
Temperature	293(2) K
Wavelength	0.71073 Å
Crystal morphology	orange prism
Crystal size	0.75 x 0.38 x 0.30 mm
Crystal system	Monoclinic
Space group	$P2_1/c$
Unit cell dimensions	$a = 15.6191(2) \text{ \AA}$ $\alpha = 90^\circ$ $b = 11.4952(2) \text{ \AA}$ $\beta = 101.5150(10)^\circ$ $c = 11.3923(2) \text{ \AA}$ $\gamma = 90^\circ$
Volume, Z	2004.26(6) Å ³ , 8
Density (calculated)	1.054 Mg/m ³
Absorption coefficient	0.060 mm ⁻¹
F(000)	688

B. Data Collection and Reduction

Diffractometer	Siemens SMART/CCD
Scan Type	ω Scans
Scan angle	0.30°
θ range for data collection	1.33 to 23.31°
Limiting indices	$-17 \leq h \leq 17, -12 \leq k \leq 12, -6 \leq l \leq 12$

Reflections collected	7978
Independent reflections	2875 ($R_{int} = 0.0458$)
Absorption correction	None

C. Solution and Refinement

Refinement method	Full-matrix least-squares on F^2
Data / restraints / parameters	2872 / 0 / 218
Goodness-of-fit on F^2	1.139
Final R indices [$I > 2\sigma(I)$]	$R1 = 0.0476$, $wR2 = 0.1061$
R indices (all data)	$R1 = 0.0604$, $wR2 = 0.1171$
Extinction coefficient	0.0060(14)
Largest diff. peak and hole	0.151 and -0.141 $e\text{\AA}^{-3}$

Table 2. Atomic coordinates [$\times 10^4$] and equivalent isotropic displacement parameters [$\text{\AA}^2 \times 10^3$] for 1. $U(\text{eq})$ is defined as one third of the trace of the orthogonalized U_{ij} tensor.

	x	y	z	U(eq)
N(1)	835(1)	6196(1)	1843(1)	33(1)
N(2)	5770(1)	854(1)	3138(1)	33(1)
C(1)	2164(1)	4853(2)	-194(2)	35(1)
C(2)	2608(1)	3955(2)	-624(2)	40(1)
C(3)	2746(1)	2890(2)	-38(2)	40(1)
C(4)	2458(1)	2677(2)	1018(2)	39(1)
C(5)	2011(1)	3508(2)	1543(2)	34(1)
C(6)	1273(1)	5565(2)	1445(2)	33(1)
C(7)	214(1)	6937(2)	2317(2)	29(1)
C(8)	737(1)	7747(2)	3250(2)	35(1)
C(9)	-359(1)	6120(2)	2876(2)	42(1)
C(10)	-303(1)	7607(2)	1257(2)	40(1)
C(11)	7397(1)	3230(2)	3455(2)	33(1)
C(12)	7859(1)	4188(2)	3982(2)	37(1)
C(13)	7788(1)	4587(2)	5113(2)	35(1)
C(14)	7243(1)	4045(2)	5771(2)	34(1)
C(15)	6740(1)	3087(2)	5335(2)	32(1)
C(16)	6226(1)	1591(2)	3572(2)	31(1)
C(17)	5130(1)	-3(2)	2534(2)	31(1)
C(18)	5598(2)	-805(2)	1810(2)	54(1)
C(19)	4414(2)	680(2)	1739(2)	56(1)
C(20)	4794(2)	-673(2)	3497(2)	60(1)
B(1)	1833(1)	4648(2)	926(2)	31(1)
B(2)	6806(1)	2632(2)	4136(2)	28(1)

Table 3. Bond lengths [Å] and angles [°] for 1.

N(1)-C(6)	1.150(2)	N(1)-C(7)	1.472(2)
N(2)-C(16)	1.153(2)	N(2)-C(17)	1.472(2)
C(1)-C(2)	1.386(3)	C(1)-B(1)	1.488(3)
C(2)-C(3)	1.390(3)	C(3)-C(4)	1.387(3)
C(4)-C(5)	1.388(3)	C(5)-B(1)	1.486(3)
C(6)-B(1)	1.560(3)	C(7)-C(10)	1.521(3)
C(7)-C(9)	1.521(3)	C(7)-C(8)	1.523(3)
C(11)-C(12)	1.387(3)	C(11)-B(2)	1.488(3)
C(12)-C(13)	1.393(3)	C(13)-C(14)	1.388(3)
C(14)-C(15)	1.385(3)	C(15)-B(2)	1.486(3)
C(16)-B(2)	1.559(3)	C(17)-C(19)	1.511(3)
C(17)-C(20)	1.517(3)	C(17)-C(18)	1.518(3)
<hr/>			
C(6)-N(1)-C(7)	175.2(2)	C(16)-N(2)-C(17)	174.7(2)
C(2)-C(1)-B(1)	118.0(2)	C(1)-C(2)-C(3)	121.8(2)
C(4)-C(3)-C(2)	121.7(2)	C(3)-C(4)-C(5)	122.0(2)
C(4)-C(5)-B(1)	117.8(2)	N(1)-C(6)-B(1)	176.5(2)
N(1)-C(7)-C(10)	106.6(2)	N(1)-C(7)-C(9)	106.4(2)
C(10)-C(7)-C(9)	112.4(2)	N(1)-C(7)-C(8)	108.01(14)
C(10)-C(7)-C(8)	111.7(2)	C(9)-C(7)-C(8)	111.3(2)
C(12)-C(11)-B(2)	117.7(2)	C(11)-C(12)-C(13)	122.1(2)
C(14)-C(13)-C(12)	121.5(2)	C(15)-C(14)-C(13)	121.9(2)
C(14)-C(15)-B(2)	118.1(2)	N(2)-C(16)-B(2)	177.1(2)
N(2)-C(17)-C(19)	106.5(2)	N(2)-C(17)-C(20)	107.6(2)
C(19)-C(17)-C(20)	112.1(2)	N(2)-C(17)-C(18)	107.8(2)
C(19)-C(17)-C(18)	111.6(2)	C(20)-C(17)-C(18)	110.9(2)
C(5)-B(1)-C(1)	118.7(2)	C(5)-B(1)-C(6)	118.9(2)
C(1)-B(1)-C(6)	122.3(2)	C(15)-B(2)-C(11)	118.7(2)
C(15)-B(2)-C(16)	120.6(2)	C(11)-B(2)-C(16)	120.6(2)

Symmetry transformations used to generate equivalent atoms:

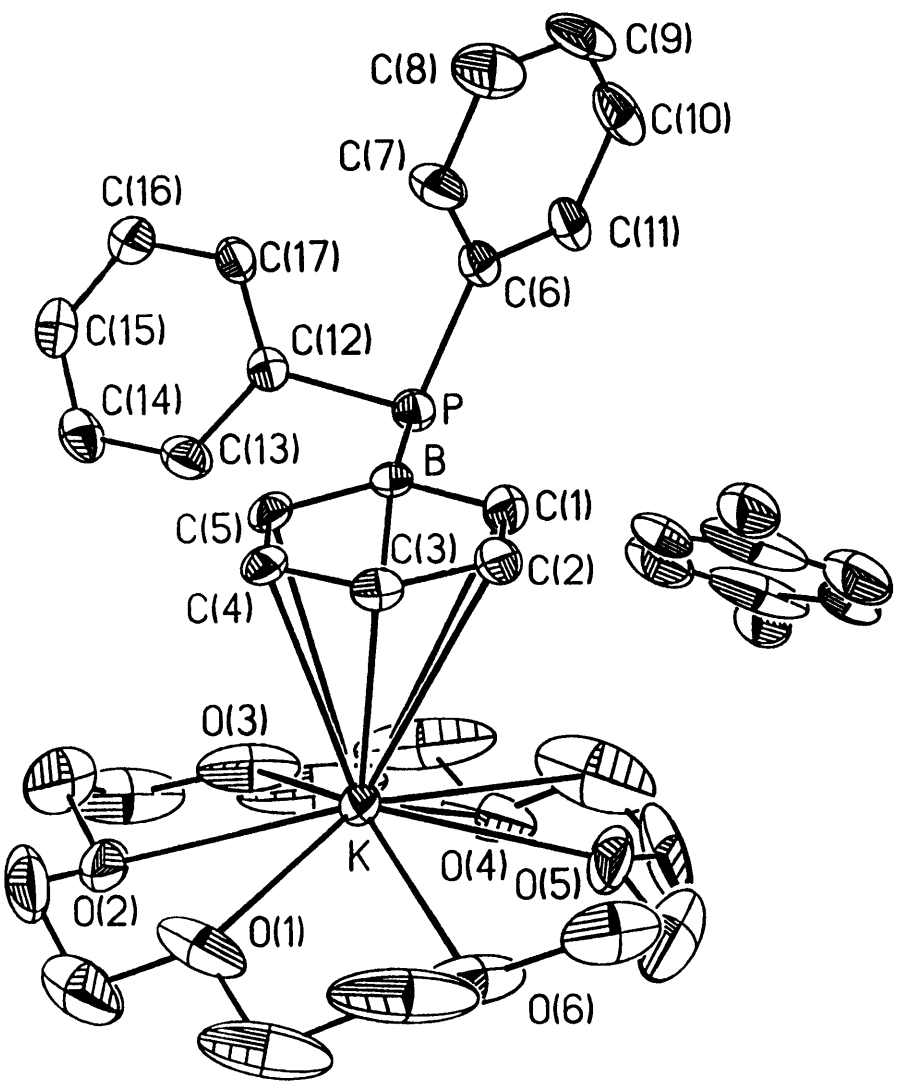


Table 1. Crystal data and structure refinement for 3.

A. Crystal Data

Identification code	96099
Empirical formula	$C_{32.50}H_{42.50}BKO_6P$
Formula weight	610.04
Temperature	187(2) K
Wavelength	0.71073 Å
Crystal morphology	parallelepiped
Crystal size	0.18 x 0.15 x 0.15 mm
Crystal system	Monoclinic
Space group	$P2_1/c$
Unit cell dimensions	$a = 13.3633(9) \text{ \AA}$ $\alpha = 90^\circ$ $b = 13.6716(9) \text{ \AA}$ $\beta = 108.9030(10)^\circ$ $c = 19.0550(12) \text{ \AA}$ $\gamma = 90^\circ$
Volume, Z	$3293.6(4) \text{ \AA}^3$, 4
Density (calculated)	1.230 Mg/m^3
Absorption coefficient	0.250 mm^{-1}
F(000)	1298

B. Data Collection and Reduction

Diffractometer	Siemens SMART/CCD
Scan Type	ω Scans
Scan angle	0.30°
θ range for data collection	1.61 to 20.50°

Reflections collected	9980
Independent reflections	3302 ($R_{int} = 0.0608$)
Absorption correction	None

C. Solution and Refinement

Refinement method	Full-matrix least-squares on F^2
Data / restraints / parameters	3085 / 0 / 380
Goodness-of-fit on F^2	1.058
Final R indices [$I > 2\sigma(I)$]	$R1 = 0.0643$, $wR2 = 0.1206$
R indices (all data)	$R1 = 0.0917$, $wR2 = 0.1555$
Extinction coefficient	0.0013(3)
Largest diff. peak and hole	0.264 and $-0.356 \text{ e}\text{\AA}^{-3}$

Table 2. Atomic coordinates [$\times 10^4$] and equivalent isotropic displacement parameters [$\text{\AA}^2 \times 10^3$] for 3. $U(\text{eq})$ is defined as one third of the trace of the orthogonalized U_{ij} tensor.

	x	y	z	$U(\text{eq})$
K	5781 (1)	3021 (1)	753 (1)	32 (1)
P	8266 (1)	610 (1)	2204 (1)	37 (1)
O (1)	4032 (4)	4258 (4)	811 (4)	84 (2)
O (2)	6117 (5)	4720 (3)	1691 (3)	76 (2)
O (3)	7814 (4)	3751 (5)	1540 (4)	97 (2)
O (4)	7506 (7)	2768 (5)	202 (5)	116 (3)
O (5)	5503 (8)	2093 (4)	-581 (3)	121 (3)
O (6)	3824 (5)	3166 (4)	-459 (3)	105 (2)
C (1)	6036 (5)	544 (4)	1219 (3)	40 (2)
C (2)	4966 (5)	770 (4)	982 (3)	40 (2)
C (3)	4549 (5)	1451 (4)	1358 (3)	38 (2)
C (4)	5204 (5)	1931 (4)	1980 (3)	36 (2)
C (5)	6284 (5)	1738 (4)	2260 (3)	35 (2)
C (6)	8211 (4)	-682 (4)	2460 (3)	35 (1)
C (7)	7571 (5)	-998 (4)	2860 (3)	51 (2)
C (8)	7565 (6)	-1970 (6)	3060 (4)	71 (2)
C (9)	8184 (6)	-2639 (5)	2849 (4)	70 (2)
C (10)	8811 (5)	-2348 (5)	2451 (4)	61 (2)
C (11)	8814 (4)	-1374 (4)	2254 (3)	43 (2)
C (12)	8895 (4)	1173 (4)	3115 (3)	32 (1)
C (13)	8903 (5)	2195 (4)	3155 (3)	48 (2)
C (14)	9433 (5)	2680 (5)	3810 (4)	50 (2)
C (15)	9977 (5)	2163 (5)	4433 (4)	48 (2)
C (16)	9973 (5)	1154 (5)	4406 (3)	47 (2)
C (17)	9431 (4)	677 (4)	3758 (3)	40 (2)
C (21)	2966 (8)	3388 (9)	-249 (7)	156 (6)
C (22)	3155 (7)	4370 (8)	133 (7)	129 (4)
C (23)	4305 (9)	5134 (7)	1184 (7)	111 (4)
C (24)	5165 (11)	4968 (6)	1877 (5)	116 (4)
C (25)	6995 (12)	4610 (7)	2289 (5)	138 (5)
C (26)	7912 (10)	4596 (9)	2028 (8)	161 (8)
C (27)	8571 (8)	3705 (12)	1212 (9)	180 (10)
C (28)	8522 (13)	2803 (14)	843 (10)	194 (12)
C (29)	7386 (18)	1929 (13)	-140 (11)	235 (14)
C (30)	6490 (17)	1939 (8)	-805 (8)	185 (10)
C (31)	4659 (17)	2121 (8)	-1148 (7)	195 (10)
C (32)	3705 (9)	2227 (7)	-877 (6)	146 (6)
C (50)	9148 (9)	-229 (9)	89 (12)	127 (5)
C (51)	9935 (15)	284 (9)	618 (9)	119 (6)
C (52)	9071 (24)	-578 (12)	-561 (10)	264 (18)
C (53)	8357 (15)	-484 (12)	229 (9)	86 (5)
B	6769 (5)	1001 (5)	1894 (3)	31 (2)

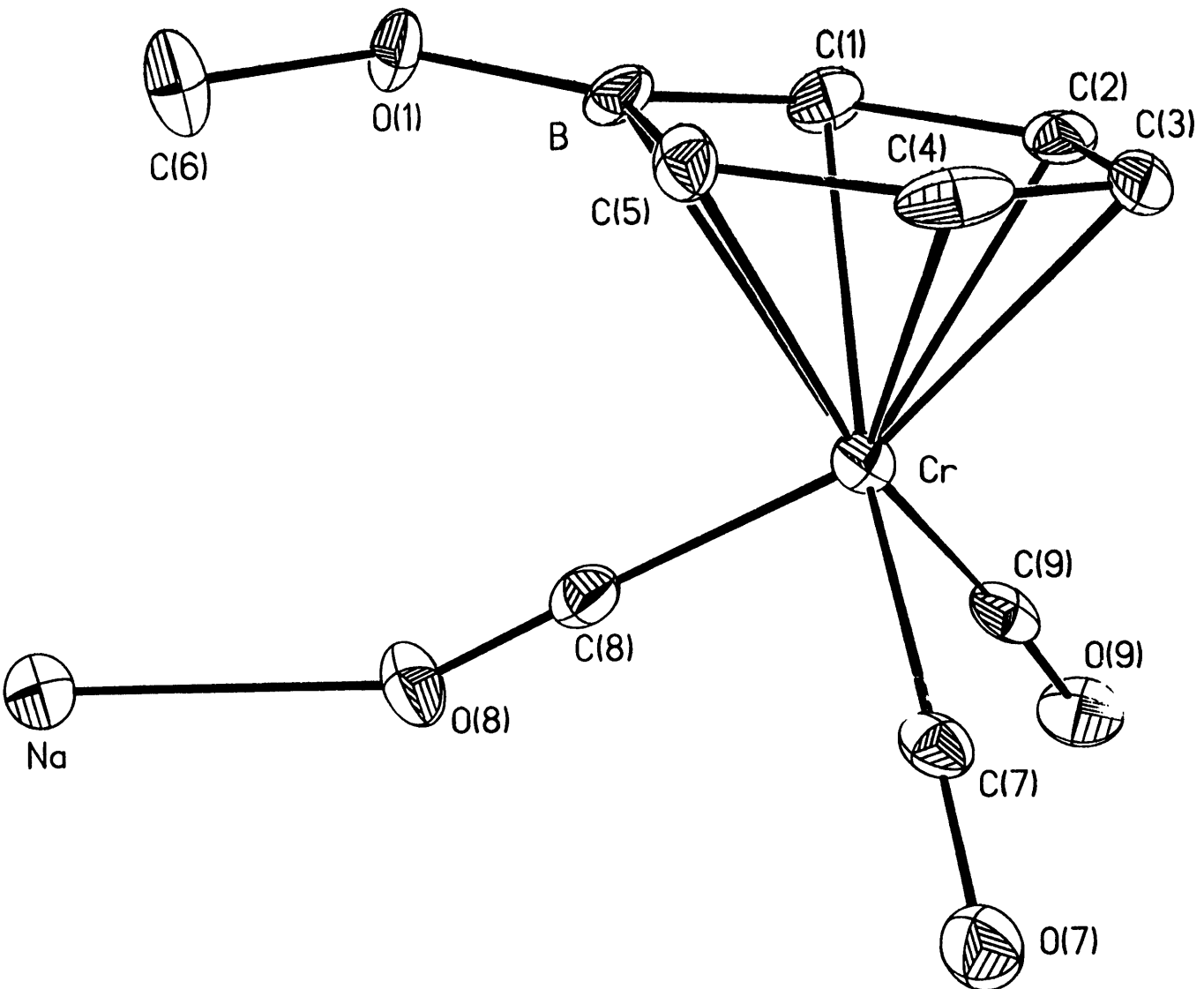
Table 3. Bond lengths [Å] and angles [°] for 3.

K-O(5)	2.756 (5)	K-O(3)	2.826 (5)
K-O(4)	2.847 (5)	K-O(2)	2.876 (5)
K-O(6)	2.880 (5)	K-O(1)	2.915 (5)
K-C(4)	3.075 (5)	K-C(3)	3.143 (5)
K-C(5)	3.245 (5)	K-C(2)	3.341 (5)
K-C(29)	3.477 (12)	K-C(1)	3.491 (6)
P-C(12)	1.835 (5)	P-C(6)	1.840 (6)
P-B	1.968 (7)	O(1)-C(23)	1.381 (11)
O(1)-C(22)	1.444 (10)	O(2)-C(25)	1.353 (11)
O(2)-C(24)	1.466 (11)	O(3)-C(27)	1.35 (2)
O(3)-C(26)	1.46 (2)	O(4)-C(29)	1.30 (2)
O(4)-C(28)	1.50 (2)	O(5)-C(31)	1.28 (2)
O(5)-C(30)	1.53 (2)	O(6)-C(21)	1.365 (14)
O(6)-C(32)	1.492 (12)	C(1)-C(2)	1.388 (7)
C(1)-B	1.480 (8)	C(2)-C(3)	1.396 (7)
C(3)-C(4)	1.389 (7)	C(4)-C(5)	1.393 (7)
C(5)-B	1.488 (8)	C(6)-C(11)	1.379 (7)
C(6)-C(7)	1.387 (8)	C(7)-C(8)	1.383 (9)
C(8)-C(9)	1.377 (10)	C(9)-C(10)	1.359 (9)
C(10)-C(11)	1.383 (8)	C(12)-C(17)	1.380 (7)
C(12)-C(13)	1.399 (8)	C(13)-C(14)	1.388 (8)
C(14)-C(15)	1.371 (8)	C(15)-C(16)	1.380 (8)
C(16)-C(17)	1.376 (8)	C(21)-C(22)	1.51 (2)
C(23)-C(24)	1.460 (13)	C(25)-C(26)	1.46 (2)
C(27)-C(28)	1.41 (2)	C(29)-C(30)	1.43 (2)
C(31)-C(32)	1.53 (2)	C(50)-C(53)	1.22 (2)
C(50)-C(52)	1.30 (2)	C(50)-C(51)	1.39 (2)
C(51)-C(52)#1	1.43 (3)	C(52)-C(51)#1	1.43 (3)
O(5)-K-O(3)	118.1 (3)	O(5)-K-O(4)	59.2 (3)
O(3)-K-O(4)	59.0 (3)	O(5)-K-O(2)	153.18 (14)
O(3)-K-O(2)	57.0 (2)	O(4)-K-O(2)	110.2 (2)
O(5)-K-O(6)	58.4 (3)	O(3)-K-O(6)	150.3 (2)
O(4)-K-O(6)	110.3 (3)	O(2)-K-O(6)	111.2 (2)
O(5)-K-O(1)	115.6 (2)	O(3)-K-O(1)	114.8 (2)
O(4)-K-O(1)	147.10 (14)	O(2)-K-O(1)	58.3 (2)
O(6)-K-O(1)	57.3 (2)	O(5)-K-C(4)	119.1 (2)
O(3)-K-C(4)	101.7 (2)	O(4)-K-C(4)	130.8 (2)
O(2)-K-C(4)	86.89 (14)	O(6)-K-C(4)	104.9 (2)
O(1)-K-C(4)	81.40 (14)	O(5)-K-C(3)	95.4 (2)
O(3)-K-C(3)	125.0 (2)	O(4)-K-C(3)	129.4 (2)
O(2)-K-C(3)	108.6 (2)	O(6)-K-C(3)	83.9 (2)
O(1)-K-C(3)	81.99 (14)	C(4)-K-C(3)	25.78 (14)
O(5)-K-C(5)	119.7 (2)	O(3)-K-C(5)	80.40 (14)
O(4)-K-C(5)	107.5 (2)	O(2)-K-C(5)	86.56 (13)
O(6)-K-C(5)	128.4 (2)	O(1)-K-C(5)	102.6 (2)
C(4)-K-C(5)	25.27 (13)	C(3)-K-C(5)	44.67 (14)
O(5)-K-C(2)	75.2 (2)	O(3)-K-C(2)	123.6 (2)
O(4)-K-C(2)	105.9 (2)	O(2)-K-C(2)	130.87 (14)
O(6)-K-C(2)	85.33 (14)	O(1)-K-C(2)	103.3 (2)
C(4)-K-C(2)	44.02 (14)	C(3)-K-C(2)	24.62 (13)
C(5)-K-C(2)	50.87 (14)	O(5)-K-C(29)	43.2 (5)
O(3)-K-C(29)	76.8 (5)	O(4)-K-C(29)	20.9 (4)
O(2)-K-C(29)	130.8 (4)	O(6)-K-C(29)	100.4 (4)
O(1)-K-C(29)	153.7 (3)	C(4)-K-C(29)	120.7 (3)

C(3) -K-C(29)	111.4(3)	C(5) -K-C(29)	102.6(3)
C(2) -K-C(29)	87.0(3)	O(5) -K-C(1)	76.2(2)
O(3) -K-C(1)	102.1(2)	O(4) -K-C(1)	87.2(2)
O(2) -K-C(1)	129.98(13)	O(6) -K-C(1)	105.0(2)
O(1) -K-C(1)	124.51(14)	C(4) -K-C(1)	50.50(14)
C(3) -K-C(1)	42.55(14)	C(5) -K-C(1)	43.53(13)
C(2) -K-C(1)	23.31(13)	C(29) -K-C(1)	71.5(3)
C(12) -P-C(6)	101.4(2)	C(12) -P-B	106.2(3)
C(6) -P-B	102.5(3)	C(23) -O(1) -C(22)	111.8(7)
C(23) -O(1) -K	116.2(5)	C(22) -O(1) -K	117.1(5)
C(25) -O(2) -C(24)	114.0(8)	C(25) -O(2) -K	110.6(5)
C(24) -O(2) -K	111.3(5)	C(27) -O(3) -C(26)	113.9(10)
C(27) -O(3) -K	118.3(8)	C(26) -O(3) -K	119.3(6)
C(29) -O(4) -C(28)	111.5(11)	C(29) -O(4) -K	108.0(9)
C(28) -O(4) -K	108.8(6)	C(31) -O(5) -C(30)	111.8(10)
C(31) -O(5) -K	125.5(10)	C(30) -O(5) -K	116.8(8)
C(21) -O(6) -C(32)	113.2(9)	C(21) -O(6) -K	114.2(6)
C(32) -O(6) -K	106.3(5)	C(2) -C(1) -B	120.6(5)
C(2) -C(1) -K	72.3(3)	B-C(1) -K	78.1(3)
C(1) -C(2) -C(3)	121.5(5)	C(1) -C(2) -K	84.4(3)
C(3) -C(2) -K	69.7(3)	C(4) -C(3) -C(2)	120.5(5)
C(4) -C(3) -K	74.4(3)	C(2) -C(3) -K	85.7(3)
C(3) -C(4) -C(5)	121.7(5)	C(3) -C(4) -K	79.8(3)
C(5) -C(4) -K	84.2(3)	C(4) -C(5) -B	120.2(5)
C(4) -C(5) -K	70.5(3)	B-C(5) -K	87.0(3)
C(11) -C(6) -C(7)	117.6(5)	C(11) -C(6) -P	120.4(4)
C(7) -C(6) -P	122.0(4)	C(8) -C(7) -C(6)	120.7(6)
C(9) -C(8) -C(7)	120.0(7)	C(10) -C(9) -C(8)	120.4(6)
C(9) -C(10) -C(11)	119.3(7)	C(6) -C(11) -C(10)	122.0(6)
C(17) -C(12) -C(13)	116.7(5)	C(17) -C(12) -P	125.5(4)
C(13) -C(12) -P	117.6(5)	C(14) -C(13) -C(12)	121.3(6)
C(15) -C(14) -C(13)	120.3(6)	C(14) -C(15) -C(16)	119.2(6)
C(17) -C(16) -C(15)	120.2(6)	C(16) -C(17) -C(12)	122.3(6)
O(6) -C(21) -C(22)	108.3(8)	O(1) -C(22) -C(21)	107.3(7)
O(1) -C(23) -C(24)	109.3(7)	C(23) -C(24) -O(2)	108.0(6)
O(2) -C(25) -C(26)	107.9(9)	C(25) -C(26) -O(3)	108.3(8)
O(3) -C(27) -C(28)	110.5(11)	C(27) -C(28) -O(4)	108.5(11)
O(4) -C(29) -C(30)	112(2)	O(4) -C(29) -K	51.1(6)
C(30) -C(29) -K	87.5(9)	C(29) -C(30) -O(5)	107.7(9)
O(5) -C(31) -C(32)	108.7(10)	O(6) -C(32) -C(31)	107.8(8)
C(53) -C(50) -C(52)	107(2)	C(53) -C(50) -C(51)	119(2)
C(52) -C(50) -C(51)	133(2)	C(50) -C(51) -C(52) #1	126(2)
C(50) -C(52) -C(51) #1	100(2)	C(1) -B-C(5)	115.4(5)
C(1) -B-P	117.9(4)	C(5) -B-P	126.7(4)
C(1) -B-K	77.4(3)	C(5) -B-K	67.8(3)
P-B-K	122.9(2)		

Symmetry transformations used to generate equivalent atoms:

#1 -x+2, -y, -z



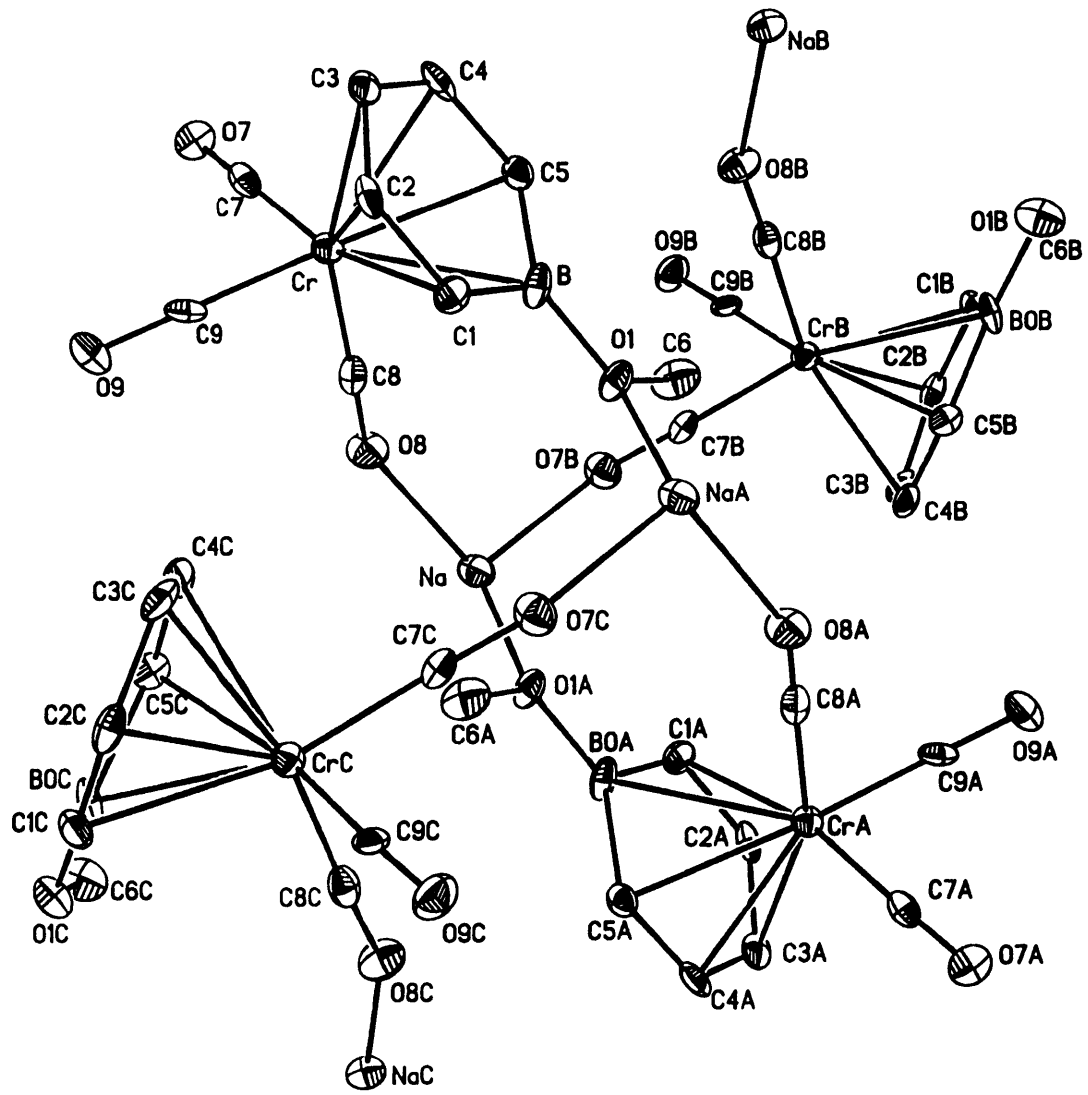


Table 1. Crystal data and structure refinement for 1.

A. Crystal Data

Identification code	96103a
Empirical formula	$C_9H_8BCrNaO_4$
Formula weight	265.95
Temperature	293(2) K
Wavelength	0.71073 Å
Crystal morphology	light yellow prism
Crystal size	0.18 x 0.05 x 0.03 mm
Crystal system	Monoclinic
Space group	$P2_1/c$
Unit cell dimensions	$a = 10.727(2)$ Å $\alpha = 90^\circ$ $b = 7.659(2)$ Å $\beta = 94.678(3)^\circ$ $c = 12.973(3)$ Å $\gamma = 90^\circ$
Volume, Z	$1062.2(4)$ Å ³ , 4
Density (calculated)	1.663 Mg/m ³
Absorption coefficient	1.108 mm ⁻¹
F(000)	536

B. Data Collection and Reduction

Diffractometer	Siemens SMART/CCD
Scan Type	ω Scans
Scan angle	0.30°
θ range for data collection	1.90 to 23.23°

Reflections collected	4195
Independent reflections	1518 ($R_{int} = 0.1243$)
Absorption correction	Semi-empirical from psi-scans
Max. and min. transmission	0.0590 and 0.0372

C. Solution and Refinement

Refinement method	Full-matrix least-squares on F^2
Data / restraints / parameters	1518 / 0 / 146
Goodness-of-fit on F^2	1.124
Final R indices [$I > 2\sigma(I)$]	$R1 = 0.0722$, $wR2 = 0.1072$
R indices (all data)	$R1 = 0.1499$, $wR2 = 0.1335$
Extinction coefficient	0.0020(10)
Largest diff. peak and hole	0.394 and $-0.408 \text{ e}\text{\AA}^{-3}$

Table 2. Atomic coordinates [$\times 10^4$] and equivalent isotropic displacement parameters [$\text{\AA}^2 \times 10^3$] for 1. $U(\text{eq})$ is defined as one third of the trace of the orthogonalized U_{ij} tensor.

	x	y	z	$U(\text{eq})$
Cr	7807(1)	-8076(2)	1679(1)	26(1)
Na	3158(3)	-7438(4)	466(2)	33(1)
O(1)	6380(5)	-4039(7)	954(4)	30(2)
O(7)	7412(5)	-10962(8)	3160(5)	36(2)
O(8)	5132(5)	-8451(7)	877(4)	37(2)
O(9)	8498(5)	-10940(8)	275(4)	38(2)
C(1)	8411(8)	-5621(10)	823(7)	30(2)
C(2)	9454(8)	-6509(10)	1285(7)	30(2)
C(3)	9562(7)	-6876(11)	2355(7)	32(2)
C(4)	8616(8)	-6391(10)	777(6)	36(2)
C(5)	7526(7)	-5527(10)	287(6)	27(2)
C(6)	5315(7)	-3661(11)	1406(6)	40(3)
C(7)	7579(8)	-9825(11)	2589(7)	28(2)
C(8)	6191(8)	-8285(11)	1171(6)	29(2)
C(9)	8264(8)	-9780(11)	818(6)	28(2)
B	7379(9)	-4970(12)	1453(8)	28(3)

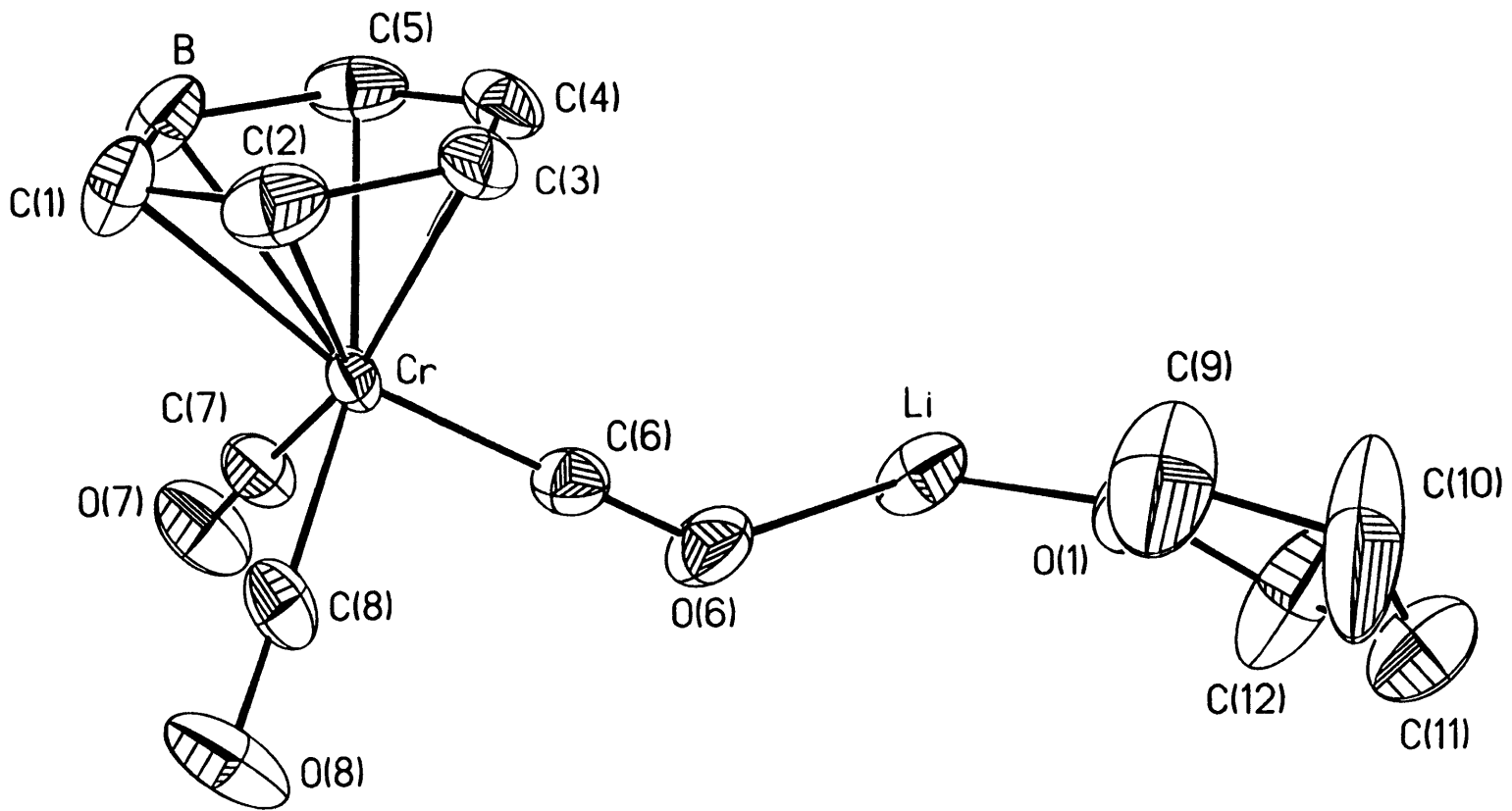
Table 3. Bond lengths [Å] and angles [°] for 1.

Cr-C(9)	1.811(10)	Cr-C(8)	1.810(9)
Cr-C(7)	1.815(9)	Cr-C(3)	2.212(8)
Cr-C(2)	2.229(8)	Cr-C(4)	2.236(8)
Cr-C(1)	2.303(8)	Cr-C(5)	2.312(8)
Cr-B	2.436(9)	Na-O(7)#1	2.237(7)
Na-O(1)#2	2.252(6)	Na-O(8)	2.277(6)
Na-O(9)#3	2.311(6)	Na-C(9)#3	3.037(9)
Na-B#2	3.114(10)	O(1)-B	1.400(10)
O(1)-C(6)	1.419(9)	O(1)-Na#2	2.252(6)
O(7)-C(7)	1.167(9)	O(7)-Na#4	2.237(7)
O(8)-C(8)	1.176(8)	O(9)-C(9)	1.173(9)
O(9)-Na#3	2.311(6)	C(1)-C(2)	1.402(10)
C(1)-B	1.514(12)	C(2)-C(3)	1.411(11)
C(3)-C(4)	1.394(11)	C(4)-C(5)	1.401(10)
C(5)-B	1.525(12)	C(9)-Na#3	3.037(9)
B-Na#2	3.114(10)		
C(9)-Cr-C(8)	90.7(4)	C(9)-Cr-C(7)	85.8(3)
C(8)-Cr-C(7)	89.8(4)	C(9)-Cr-C(3)	106.2(3)
C(8)-Cr-C(3)	160.1(3)	C(7)-Cr-C(3)	101.8(3)
C(9)-Cr-C(2)	89.3(3)	C(8)-Cr-C(2)	135.9(3)
C(7)-Cr-C(2)	134.2(3)	C(3)-Cr-C(2)	37.1(3)
C(9)-Cr-C(4)	140.4(4)	C(8)-Cr-C(4)	128.7(4)
C(7)-Cr-C(4)	90.1(3)	C(3)-Cr-C(4)	36.5(3)
C(2)-Cr-C(4)	66.1(3)	C(9)-Cr-C(1)	101.0(3)
C(8)-Cr-C(1)	101.3(3)	C(7)-Cr-C(1)	166.9(3)
C(3)-Cr-C(1)	65.7(3)	C(2)-Cr-C(1)	36.0(3)
C(4)-Cr-C(1)	77.5(3)	C(9)-Cr-C(5)	167.3(3)
C(8)-Cr-C(5)	95.7(3)	C(7)-Cr-C(5)	105.2(3)
C(3)-Cr-C(5)	65.7(3)	C(2)-Cr-C(5)	78.5(3)
C(4)-Cr-C(5)	35.8(3)	C(1)-Cr-C(5)	67.0(3)
C(9)-Cr-B	133.4(4)	C(8)-Cr-B	82.9(3)
C(7)-Cr-B	139.9(4)	C(3)-Cr-B	77.8(3)
C(2)-Cr-B	65.9(3)	C(4)-Cr-B	65.4(3)
C(1)-Cr-B	37.1(3)	C(5)-Cr-B	37.4(3)
O(7)#1-Na-O(1)#2	119.4(2)	O(7)#1-Na-O(8)	107.1(2)
O(1)#2-Na-O(8)	95.8(2)	O(7)#1-Na-O(9)#3	110.6(2)
O(1)#2-Na-O(9)#3	98.2(2)	O(8)-Na-O(9)#3	125.6(2)
O(7)#1-Na-C(9)#3	129.3(3)	O(1)#2-Na-C(9)#3	92.2(2)
O(8)-Na-C(9)#3	107.8(2)	O(9)#3-Na-C(9)#3	20.0(2)
O(7)#1-Na-B#2	107.0(3)	O(1)#2-Na-B#2	24.1(2)
O(8)-Na-B#2	119.8(3)	O(9)#3-Na-B#2	84.3(2)
C(9)#3-Na-B#2	85.7(2)	B-O(1)-C(6)	119.4(6)
B-O(1)-Na#2	115.0(5)	C(6)-O(1)-Na#2	122.9(5)
C(7)-O(7)-Na#4	161.7(6)	C(8)-O(8)-Na	153.5(6)
C(9)-O(9)-Na#3	117.5(6)	C(2)-C(1)-B	121.5(8)
C(2)-C(1)-Cr	69.1(4)	B-C(1)-Cr	76.2(5)
C(1)-C(2)-C(3)	121.1(8)	C(1)-C(2)-Cr	74.9(5)
C(3)-C(2)-Cr	70.8(5)	C(4)-C(3)-C(2)	120.4(8)
C(4)-C(3)-Cr	72.7(5)	C(2)-C(3)-Cr	72.2(4)
C(3)-C(4)-C(5)	123.1(8)	C(3)-C(4)-Cr	70.8(4)
C(5)-C(4)-Cr	75.0(5)	C(4)-C(5)-B	119.7(8)
C(4)-C(5)-Cr	69.1(4)	B-C(5)-Cr	75.8(5)
O(7)-C(7)-Cr	178.5(8)	O(8)-C(8)-Cr	177.4(7)
O(9)-C(9)-Cr	175.9(8)	O(9)-C(9)-Na#3	42.4(4)

Cr-C(9)-Na#3	134.0(4)	O(1)-B-C(1)	118.9(8)
O(1)-B-C(5)	127.1(8)	C(1)-B-C(5)	113.9(8)
O(1)-B-Cr	133.0(6)	C(1)-B-Cr	66.7(4)
C(5)-B-Cr	66.9(4)	O(1)-B-Na#2	40.9(3)
C(1)-B-Na#2	81.9(5)	C(5)-B-Na#2	159.0(6)
Cr-B-Na#2	134.0(4)		

Symmetry transformations used to generate equivalent atoms:

#1 $-x+1, y+1/2, -z+1/2$ #2 $-x+1, -y-1, -z$ #3 $-x+1, -y-2, -z$
#4 $-x+1, y-1/2, -z+1/2$



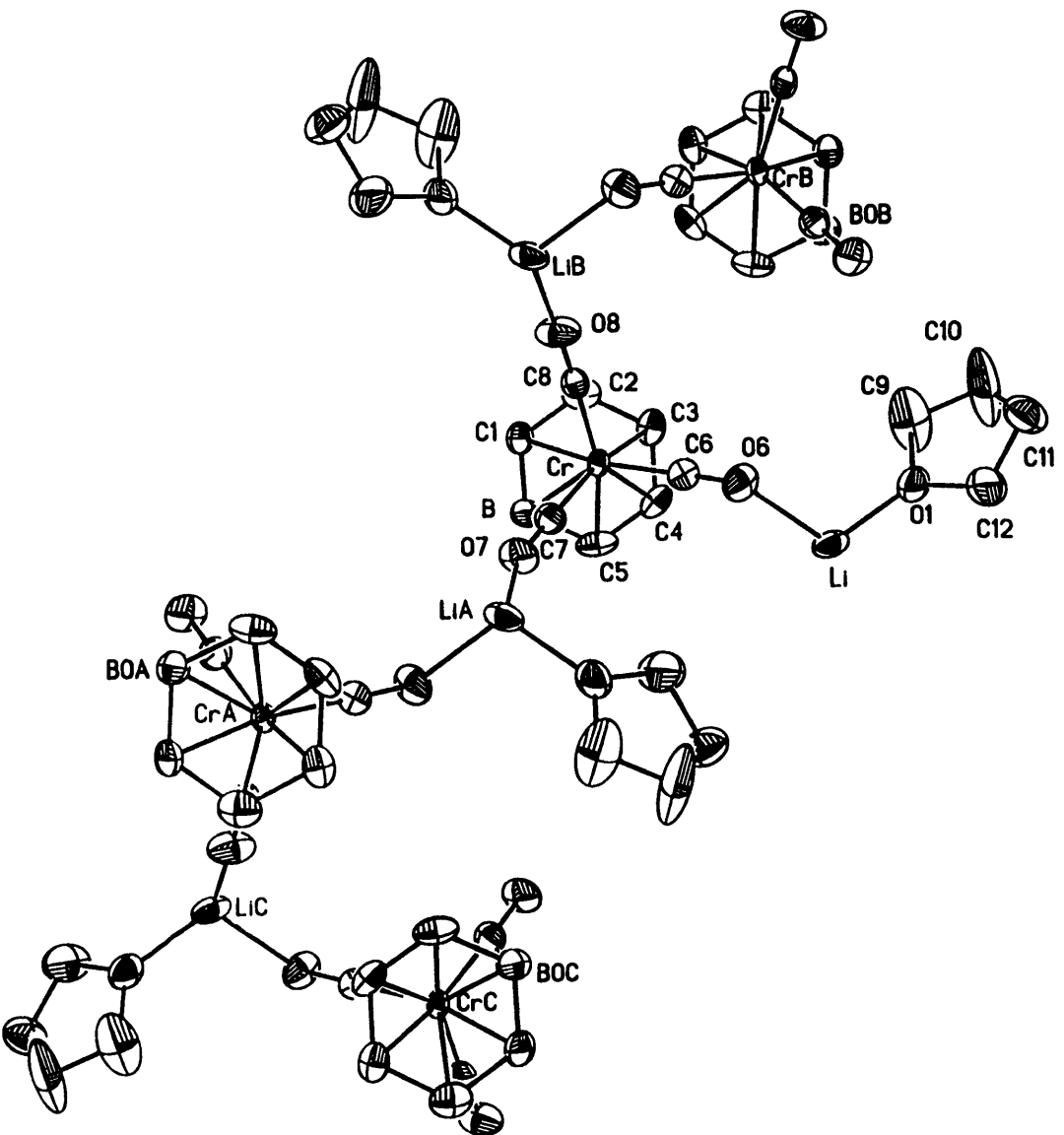


Table 1. Crystal data and structure refinement for 1.

A. Crystal Data

Identification code	thesis 96113
Empirical formula	$C_{12}H_{14}BCrLiO_4$
Formula weight	291.98
Temperature	161(2) K
Wavelength	0.71073 Å
Crystal morphology	brick
Crystal size	0.08 x 0.10 x 0.12 mm
Crystal system	Monoclinic
Space group	$P2_1/c$
Unit cell dimensions	$a = 11.2187(9) \text{ \AA}$ $\alpha = 90^\circ$ $b = 11.7209(9) \text{ \AA}$ $\beta = 99.332(2)^\circ$ $c = 10.7367(9) \text{ \AA}$ $\gamma = 90^\circ$
Volume, Z	$1393.1(2) \text{ \AA}^3$, 4
Density (calculated)	1.392 Mg/m^3
Absorption coefficient	0.823 mm^{-1}
F(000)	600

B. Data Collection and Reduction

Diffractometer	Siemens SMART/CCD
Scan Type	ω Scans
Scan angle	0.30°
θ range for data collection	1.84 to 21.00°
Limiting indices	$-10 \leq h \leq 12$, $-10 \leq k \leq 12$, $-9 \leq l \leq 11$

Reflections collected	4400
Independent reflections	1494 ($R_{int} = 0.0727$)
Absorption correction	None

C. Solution and Refinement

Refinement method	Full-matrix least-squares on F^2
Data / restraints / parameters	1443 / 0 / 173
Goodness-of-fit on F^2	1.135
Final R indices [$I > 2\sigma(I)$]	$R_1 = 0.0635$, $wR_2 = 0.1174$
R indices (all data)	$R_1 = 0.0822$, $wR_2 = 0.1317$
Extinction coefficient	0.0014(10)
Largest diff. peak and hole	0.317 and $-0.391 \text{ e}\text{\AA}^{-3}$

Table 2. Atomic coordinates [$\times 10^4$] and equivalent isotropic displacement parameters [$\text{\AA}^2 \times 10^3$] for 1. $U(\text{eq})$ is defined as one third of the trace of the orthogonalized U_{ij} tensor.

	x	y	z	$U(\text{eq})$
Cr	7764(1)	1270(1)	1786(1)	31(1)
O(1)	6496(5)	6075(4)	1633(5)	64(2)
O(6)	6304(5)	3397(5)	1478(5)	62(2)
O(7)	5624(5)	6(5)	2375(5)	70(2)
O(8)	6902(5)	658(5)	-909(5)	75(2)
C(1)	9359(7)	49(6)	2063(7)	55(2)
C(2)	9713(6)	1049(7)	1425(8)	56(2)
C(3)	9565(6)	2151(6)	1993(7)	46(2)
C(4)	9126(6)	2221(7)	3157(7)	47(2)
C(5)	8795(6)	1257(8)	3768(6)	54(2)
C(6)	6887(6)	2549(6)	1595(6)	40(2)
C(7)	6484(7)	494(6)	2152(7)	48(2)
C(8)	7266(6)	916(6)	147(8)	47(2)
B	8957(8)	129(8)	3261(8)	51(3)
Li	6023(12)	4773(12)	2443(11)	58(4)
C(11)	6332(9)	7730(9)	376(9)	84(3)
C(9)	7484(8)	6118(9)	969(13)	127(5)
C(12)	5782(12)	7096(9)	1357(10)	122(5)
C(10)	7462(11)	7245(9)	403(18)	179(8)

Table 3. Bond lengths [Å] and angles [°] for 1.

Cr-C(6)	1.787 (8)	Cr-C(7)	1.796 (8)
Cr-C(8)	1.806 (8)	Cr-C(4)	2.239 (7)
Cr-C(3)	2.247 (7)	Cr-C(5)	2.251 (7)
Cr-C(1)	2.273 (7)	Cr-C(2)	2.296 (7)
Cr-B	2.323 (8)	O(1)-C(9)	1.413 (10)
O(1)-C(12)	1.444 (10)	O(1)-Li	1.88 (2)
O(6)-C(6)	1.185 (8)	O(6)-Li	1.970 (14)
O(7)-C(7)	1.179 (8)	O(7)-Li#1	1.910 (13)
O(8)-C(8)	1.180 (8)	O(8)-Li#2	1.948 (13)
C(1)-B	1.434 (11)	C(1)-C(2)	1.445 (10)
C(2)-C(3)	1.451 (10)	C(3)-C(4)	1.417 (10)
C(4)-C(5)	1.387 (10)	C(5)-B	1.452 (11)
Li-O(7)#3	1.910 (13)	Li-O(8)#4	1.948 (13)
C(11)-C(10)	1.386 (13)	C(11)-C(12)	1.501 (12)
C(9)-C(10)	1.452 (13)		
C(6)-Cr-C(7)	90.3 (3)	C(6)-Cr-C(8)	90.2 (3)
C(7)-Cr-C(8)	88.0 (3)	C(6)-Cr-C(4)	87.8 (3)
C(7)-Cr-C(4)	126.3 (3)	C(8)-Cr-C(4)	145.6 (3)
C(6)-Cr-C(3)	95.4 (3)	C(7)-Cr-C(3)	161.5 (3)
C(8)-Cr-C(3)	109.5 (3)	C(4)-Cr-C(3)	36.8 (2)
C(6)-Cr-C(5)	107.6 (3)	C(7)-Cr-C(5)	95.5 (3)
C(8)-Cr-C(5)	161.8 (3)	C(4)-Cr-C(5)	36.0 (3)
C(3)-Cr-C(5)	66.0 (3)	C(6)-Cr-C(1)	161.9 (3)
C(7)-Cr-C(1)	107.0 (3)	C(8)-Cr-C(1)	95.5 (3)
C(4)-Cr-C(1)	77.8 (3)	C(3)-Cr-C(1)	66.5 (3)
C(5)-Cr-C(1)	66.4 (3)	C(6)-Cr-C(2)	126.7 (3)
C(7)-Cr-C(2)	142.8 (3)	C(8)-Cr-C(2)	87.8 (3)
C(4)-Cr-C(2)	66.5 (3)	C(3)-Cr-C(2)	37.2 (3)
C(5)-Cr-C(2)	78.6 (3)	C(1)-Cr-C(2)	36.9 (3)
C(6)-Cr-B	143.7 (3)	C(7)-Cr-B	87.2 (3)
C(8)-Cr-B	125.8 (3)	C(4)-Cr-B	65.3 (3)
C(3)-Cr-B	77.8 (3)	C(5)-Cr-B	37.0 (3)
C(1)-Cr-B	36.3 (3)	C(2)-Cr-B	65.9 (3)
C(9)-O(1)-C(12)	108.8 (7)	C(9)-O(1)-Li	124.5 (6)
C(12)-O(1)-Li	125.5 (7)	C(6)-O(6)-Li	139.8 (6)
C(7)-O(7)-Li#1	158.0 (8)	C(8)-O(8)-Li#2	169.8 (7)
B-C(1)-C(2)	121.5 (7)	B-C(1)-Cr	73.8 (4)
C(2)-C(1)-Cr	72.4 (4)	C(1)-C(2)-C(3)	117.6 (7)
C(1)-C(2)-Cr	70.7 (4)	C(3)-C(2)-Cr	69.6 (4)
C(4)-C(3)-C(2)	120.2 (7)	C(4)-C(3)-Cr	71.3 (4)
C(2)-C(3)-Cr	73.2 (4)	C(5)-C(4)-C(3)	121.9 (7)
C(5)-C(4)-Cr	72.5 (4)	C(3)-C(4)-Cr	71.9 (4)
C(4)-C(5)-B	120.3 (7)	C(4)-C(5)-Cr	71.5 (4)
B-C(5)-Cr	74.2 (4)	O(6)-C(6)-Cr	179.5 (6)
O(7)-C(7)-Cr	178.2 (7)	O(8)-C(8)-Cr	177.3 (6)
C(1)-B-C(5)	118.2 (8)	C(1)-B-Cr	69.9 (4)
C(5)-B-Cr	68.8 (4)	O(1)-Li-O(7)#3	106.4 (6)
O(1)-Li-O(8)#4	119.5 (8)	O(7)#3-Li-O(8)#4	107.5 (6)
O(1)-Li-O(6)	110.0 (6)	O(7)#3-Li-O(6)	114.3 (8)
O(8)#4-Li-O(6)	99.5 (6)	C(10)-C(11)-C(12)	105.1 (9)
O(1)-C(9)-C(10)	106.4 (9)	O(1)-C(12)-C(11)	106.1 (8)
C(11)-C(10)-C(9)	109.6 (10)		

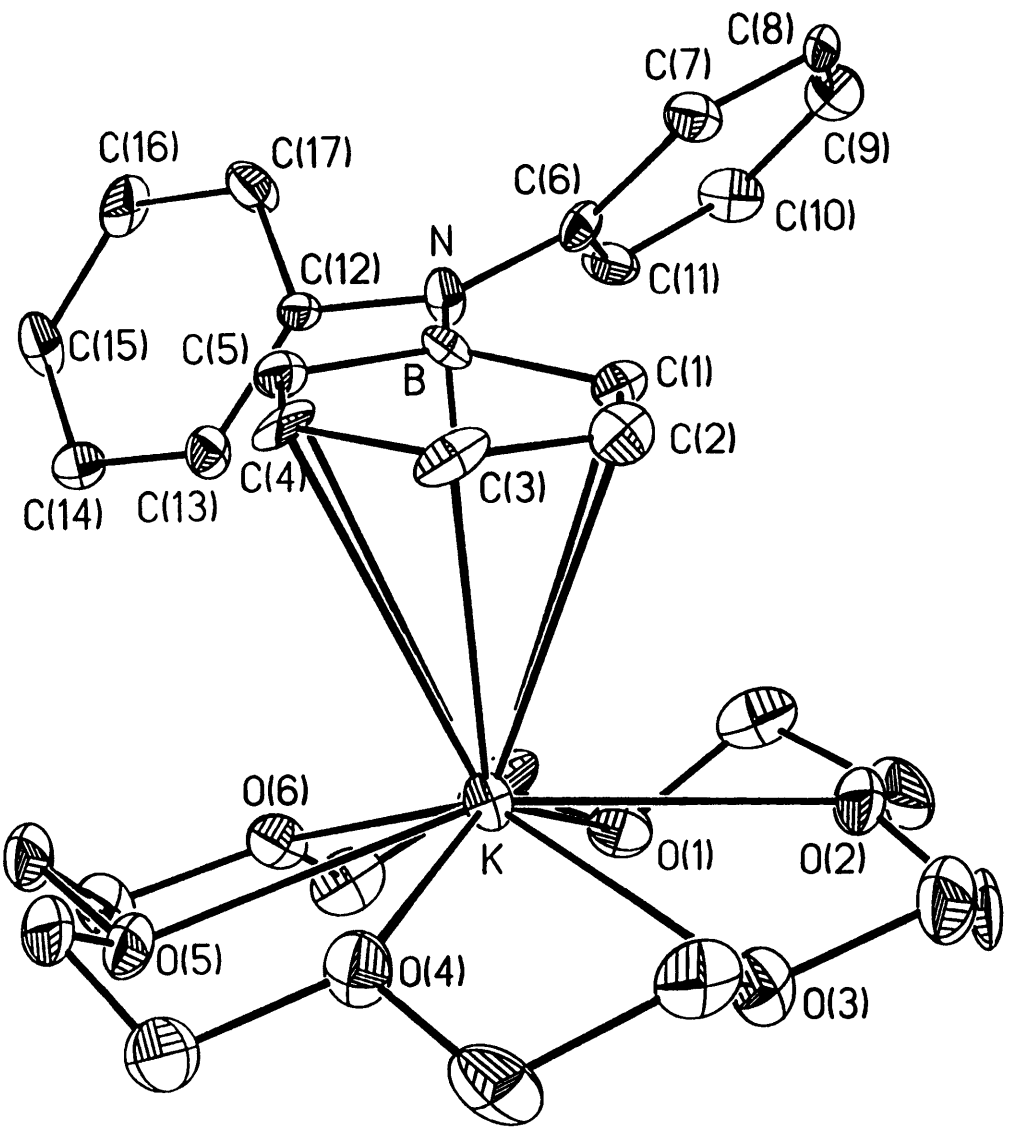


Table 6. Crystal data and structure refinement for 4.

A. Crystal Data

Identification code	96129
Empirical formula	$C_{29}H_{39}BKNO_6$
Formula weight	547.52
Temperature	138(2) K
Wavelength	0.71073 Å
Crystal morphology	irregular block
Crystal size	0.24 x 0.12 x 0.08 mm
Crystal system	Orthorhombic
Space group	$Pna2_1$
Unit cell dimensions	$a = 17.289(6)$ Å $\alpha = 90^\circ$ $b = 15.269(7)$ Å $\beta = 90^\circ$ $c = 10.929(4)$ Å $\gamma = 90^\circ$
Volume, Z	2885(2) Å ³ , 4
Density (calculated)	1.261 Mg/m ³
Absorption coefficient	0.226 mm ⁻¹
F(000)	1168

B. Data Collection and Reduction

Diffractometer	Siemens SMART/CCD
Scan Type	ω Scans
Scan angle	0.30°
θ range for data collection	1.78 to 21.50°

Reflections collected	9670
Independent reflections	3206 ($R_{int} = 0.0807$)
Absorption correction	None

C. Solution and Refinement

Refinement method	Full-matrix least-squares on F^2
Data / restraints / parameters	3145 / 1 / 343
Goodness-of-fit on F^2	1.247
Final R indices [$I > 2\sigma(I)$]	$R1 = 0.0690$, $wR2 = 0.1184$
R indices (all data)	$R1 = 0.0865$, $wR2 = 0.1283$
Absolute structure parameter	-0.05(9)
Largest diff. peak and hole	0.239 and -0.254 $e\text{\AA}^{-3}$

Table 7. Atomic coordinates [$\times 10^4$] and equivalent isotropic displacement parameters [$\text{\AA}^2 \times 10^3$] for 4. $U(\text{eq})$ is defined as one third of the trace of the orthogonalized U_{ij} tensor.

	x	y	z	$U(\text{eq})$
K	1759(1)	3444(1)	6966(1)	24(1)
O(1)	1241(3)	4215(3)	4653(5)	36(1)
O(2)	164(3)	3738(3)	6451(5)	35(1)
O(3)	672(3)	3982(3)	8873(4)	35(1)
O(4)	2246(3)	3579(3)	9424(4)	35(1)
O(5)	3312(3)	3850(3)	7599(4)	32(1)
O(6)	2806(3)	3973(3)	5200(4)	30(1)
N	1817(3)	1381(4)	3947(5)	24(2)
C(1)	1044(4)	1606(4)	6032(6)	27(2)
C(2)	1047(4)	1637(4)	7307(6)	27(2)
C(3)	1726(5)	1554(4)	8000(7)	31(2)
C(4)	2424(5)	1429(4)	7399(7)	26(2)
C(5)	2488(4)	1380(4)	6131(6)	23(2)
C(6)	1168(4)	1172(4)	3240(6)	22(2)
C(7)	597(4)	600(4)	3652(7)	28(2)
C(8)	-46(4)	381(4)	2935(7)	29(2)
C(9)	-125(4)	748(5)	1785(8)	37(2)
C(10)	421(4)	1316(4)	1371(7)	33(2)
C(11)	1052(4)	1544(4)	2081(7)	30(2)
C(12)	2537(4)	1471(4)	3315(6)	21(2)
C(13)	3030(3)	2146(4)	3577(6)	24(2)
C(14)	3717(4)	2257(5)	2924(6)	29(2)
C(15)	3913(4)	1692(5)	2017(8)	34(2)
C(16)	3428(4)	992(5)	1743(7)	34(2)
C(17)	2743(4)	883(5)	2403(7)	33(2)
C(31)	558(5)	3729(6)	4371(7)	43(2)
C(32)	-59(5)	4008(6)	5245(8)	49(3)
C(33)	-304(4)	4109(6)	7371(8)	47(3)
C(34)	-97(4)	3728(6)	8576(9)	50(3)
C(35)	924(4)	3611(5)	9989(6)	37(2)
C(36)	1723(5)	3924(6)	10283(8)	46(2)
C(37)	3026(4)	3818(5)	9701(8)	42(2)
C(38)	3522(4)	3447(5)	8728(7)	41(2)
C(39)	3802(4)	3598(5)	6596(7)	38(2)
C(40)	3596(4)	4153(6)	5546(7)	40(2)
C(41)	2561(5)	4483(5)	4180(7)	43(2)
C(42)	1819(5)	4120(6)	3723(8)	47(2)
B	1789(5)	1446(5)	5325(8)	24(2)

Table 8. Bond lengths [Å] and angles [°] for 4.

K-O(6)	2.767(5)	K-O(4)	2.823(5)
K-O(5)	2.842(5)	K-O(2)	2.849(5)
K-O(3)	2.923(5)	K-O(1)	2.928(5)
K-C(2)	3.043(7)	K-C(3)	3.099(7)
K-C(1)	3.231(7)	K-C(4)	3.318(7)
K-C(5)	3.514(7)	K-B	3.539(8)
O(1)-C(31)	1.428(9)	O(1)-C(42)	1.433(9)
O(2)-C(33)	1.409(9)	O(2)-C(32)	1.434(9)
O(3)-C(35)	1.414(8)	O(3)-C(34)	1.423(9)
O(4)-C(36)	1.405(9)	O(4)-C(37)	1.431(8)
O(5)-C(38)	1.426(9)	O(5)-C(39)	1.438(8)
O(6)-C(41)	1.425(8)	O(6)-C(40)	1.444(8)
N-C(6)	1.399(8)	N-C(12)	1.431(8)
N-B	1.510(10)	C(1)-C(2)	1.394(9)
C(1)-B	1.523(11)	C(2)-C(3)	1.404(10)
C(3)-C(4)	1.387(10)	C(4)-C(5)	1.392(9)
C(5)-B	1.499(11)	C(6)-C(7)	1.392(9)
C(6)-C(11)	1.404(10)	C(7)-C(8)	1.401(9)
C(8)-C(9)	1.382(10)	C(9)-C(10)	1.359(10)
C(10)-C(11)	1.383(10)	C(12)-C(13)	1.368(9)
C(12)-C(17)	1.388(9)	C(13)-C(14)	1.395(9)
C(14)-C(15)	1.357(10)	C(15)-C(16)	1.392(9)
C(16)-C(17)	1.396(10)	C(31)-C(32)	1.494(11)
C(33)-C(34)	1.483(12)	C(35)-C(36)	1.497(11)
C(37)-C(38)	1.479(10)	C(39)-C(40)	1.469(10)
C(41)-C(42)	1.485(11)		
O(6)-K-O(4)	116.6(2)	O(6)-K-O(5)	59.2(2)
O(4)-K-O(5)	58.04(14)	O(6)-K-O(2)	116.7(2)
O(4)-K-O(2)	117.7(2)	O(5)-K-O(2)	158.11(14)
O(6)-K-O(3)	146.69(14)	O(4)-K-O(3)	59.50(14)
O(5)-K-O(3)	111.8(2)	O(2)-K-O(3)	58.3(2)
O(6)-K-O(1)	58.72(14)	O(4)-K-O(1)	152.0(2)
O(5)-K-O(1)	114.3(2)	O(2)-K-O(1)	58.02(14)
O(3)-K-O(1)	107.8(2)	O(6)-K-C(2)	127.9(2)
O(4)-K-C(2)	94.0(2)	O(5)-K-C(2)	123.4(2)
O(2)-K-C(2)	77.0(2)	O(3)-K-C(2)	84.7(2)
O(1)-K-C(2)	110.3(2)	O(6)-K-C(3)	122.5(2)
O(4)-K-C(3)	74.1(2)	O(5)-K-C(3)	97.6(2)
O(2)-K-C(3)	101.6(2)	O(3)-K-C(3)	89.4(2)
O(1)-K-C(3)	133.1(2)	C(2)-K-C(3)	26.4(2)
O(6)-K-C(1)	106.5(2)	O(4)-K-C(1)	118.6(2)
O(5)-K-C(1)	128.9(2)	O(2)-K-C(1)	72.8(2)
O(3)-K-C(1)	102.9(2)	O(1)-K-C(1)	87.7(2)
C(2)-K-C(1)	25.4(2)	C(3)-K-C(1)	45.6(2)
O(6)-K-C(4)	98.2(2)	O(4)-K-C(4)	80.1(2)
O(5)-K-C(4)	80.8(2)	O(2)-K-C(4)	120.7(2)
O(3)-K-C(4)	112.4(2)	O(1)-K-C(4)	127.0(2)
C(2)-K-C(4)	44.2(2)	C(3)-K-C(4)	24.7(2)
C(1)-K-C(4)	51.1(2)	O(6)-K-C(5)	81.1(2)
O(4)-K-C(5)	101.9(2)	O(5)-K-C(5)	85.4(2)
O(2)-K-C(5)	115.9(2)	O(3)-K-C(5)	131.9(2)
O(1)-K-C(5)	104.2(2)	C(2)-K-C(5)	50.5(2)
C(3)-K-C(5)	42.8(2)	C(1)-K-C(5)	43.7(2)
O(4)-K-C(5)	23.2(2)	O(6)-K-C(5)	83.6(2)

O(4) -K-B	122.8(2)	O(5) -K-B	107.3(2)
O(2) -K-B	92.9(2)	O(3) -K-B	127.8(2)
O(1) -K-B	85.0(2)	C(2) -K-B	44.5(2)
C(3) -K-B	51.9(2)	C(1) -K-B	25.5(2)
C(4) -K-B	42.9(2)	C(5) -K-B	24.5(2)
C(31) -O(1) -C(42)	111.8(6)	C(31) -O(1) -K	103.3(4)
C(42) -O(1) -K	111.0(4)	C(33) -O(2) -C(32)	112.7(6)
C(33) -O(2) -K	118.6(4)	C(32) -O(2) -K	119.2(4)
C(35) -O(3) -C(34)	112.0(6)	C(35) -O(3) -K	107.7(4)
C(34) -O(3) -K	111.2(4)	C(36) -O(4) -C(37)	111.7(5)
C(36) -O(4) -K	118.1(4)	C(37) -O(4) -K	120.1(5)
C(38) -O(5) -C(39)	113.2(5)	C(38) -O(5) -K	110.9(4)
C(39) -O(5) -K	108.2(4)	C(41) -O(6) -C(40)	112.4(6)
C(41) -O(6) -K	120.7(4)	C(40) -O(6) -K	119.5(4)
C(6) -N-C(12)	117.0(5)	C(6) -N-B	122.7(6)
C(12) -N-B	120.2(6)	C(2) -C(1) -B	120.7(7)
C(2) -C(1) -K	69.7(4)	B-C(1) -K	88.7(4)
C(1) -C(2) -C(3)	122.6(7)	C(1) -C(2) -K	84.8(4)
C(3) -C(2) -K	79.0(4)	C(4) -C(3) -C(2)	119.0(7)
C(4) -C(3) -K	86.5(4)	C(2) -C(3) -K	74.6(4)
C(3) -C(4) -C(5)	123.2(8)	C(3) -C(4) -K	68.8(4)
C(5) -C(4) -K	86.3(4)	C(4) -C(5) -B	121.1(8)
C(4) -C(5) -K	70.4(4)	B-C(5) -K	78.7(4)
C(7) -C(6) -N	122.2(6)	C(7) -C(6) -C(11)	116.4(6)
N-C(6) -C(11)	121.4(6)	C(6) -C(7) -C(8)	122.1(7)
C(9) -C(8) -C(7)	119.4(7)	C(10) -C(9) -C(8)	119.5(7)
C(9) -C(10) -C(11)	121.5(7)	C(10) -C(11) -C(6)	121.1(7)
C(13) -C(12) -C(17)	118.6(6)	C(13) -C(12) -N	120.9(6)
C(17) -C(12) -N	120.4(6)	C(12) -C(13) -C(14)	120.9(7)
C(15) -C(14) -C(13)	120.6(7)	C(14) -C(15) -C(16)	119.7(7)
C(15) -C(16) -C(17)	119.4(7)	C(12) -C(17) -C(16)	120.7(7)
O(1) -C(31) -C(32)	107.7(6)	O(2) -C(32) -C(31)	108.3(6)
O(2) -C(33) -C(34)	109.7(6)	O(3) -C(34) -C(33)	108.7(7)
O(3) -C(35) -C(36)	109.9(6)	O(4) -C(36) -C(35)	109.3(6)
O(4) -C(37) -C(38)	107.3(6)	O(5) -C(38) -C(37)	108.0(6)
O(5) -C(39) -C(40)	107.4(6)	O(6) -C(40) -C(39)	108.8(6)
O(6) -C(41) -C(42)	108.4(6)	O(1) -C(42) -C(41)	109.1(7)
C(5) -B-N	123.8(7)	C(5) -B-C(1)	113.2(7)
N-B-C(1)	122.9(7)	C(5) -B-K	76.8(4)
N-B-K	124.2(5)	C(1) -B-K	65.9(4)

Symmetry transformations used to generate equivalent atoms:

Table 1. Crystal data and structure refinement for 1.

A. Crystal Data

Identification code	96159
Empirical formula	$C_{15}H_{21}BFe$
Formula weight	267.98
Temperature	183(2) K
Wavelength	0.71073 Å
Crystal morphology	?
Crystal size	? x ? x ? mm
Crystal system	?
Space group	?
Unit cell dimensions	$a = 10.214(9) \text{ \AA}$ $\alpha = 90^\circ$ $b = 12.372(5) \text{ \AA}$ $\beta = 90^\circ$ $c = 10.980(6) \text{ \AA}$ $\gamma = 90^\circ$
Volume, Z	$1388(2) \text{ \AA}^3$, 4
Density (calculated)	1.283 Mg/m^3
Absorption coefficient	1.062 mm^{-1}
F(000)	568

B. Data Collection and Reduction

Diffractometer	Siemens SMART/CCD
Scan Type	ω Scans
Scan angle	0.30°
θ range for data collection	2.48 to 20.50°

Reflections collected	3991
Independent reflections	734 ($R_{\text{int}} = 0.0818$)

C. Solution and Refinement

Refinement method	Full-matrix least-squares on F^2
Data / restraints / parameters	714 / 0 / 117
Goodness-of-fit on F^2	1.238
Final R indices [$I > 2\sigma(I)$]	$R_1 = 0.0640$, $wR_2 = 0.1108$
R indices (all data)	$R_1 = 0.0818$, $wR_2 = 0.1206$
Extinction coefficient	0.0012(5)
Largest diff. peak and hole	0.323 and $-0.262 \text{ e}\text{\AA}^{-3}$

Table 2. Atomic coordinates [$\times 10^4$] and equivalent isotropic displacement parameters [$\text{\AA}^2 \times 10^3$] for 1. $U(\text{eq})$ is defined as one third of the trace of the orthogonalized U_{ij} tensor.

	x	y	z	$U(\text{eq})$
Fe	1634 (1)	7500	5084 (1)	31 (1)
C(1)	1119 (20)	6582 (13)	6506 (16)	178 (16)
C(2)	138 (23)	6582 (16)	5747 (20)	224 (19)
C(3)	1640 (24)	7500	6906 (19)	178 (23)
C(4)	3603 (9)	7500	4660 (8)	26 (3)
C(5)	2971 (6)	6574 (5)	4160 (6)	23 (2)
C(6)	1979 (6)	6921 (5)	3346 (6)	26 (2)
C(7)	4741 (15)	7500	5512 (13)	55 (4)
C(8)	3314 (10)	5415 (7)	4397 (10)	43 (2)
C(9)	1101 (10)	6214 (8)	2590 (9)	49 (2)
B	-357 (24)	7500	5382 (35)	265 (40)

Table 3. Bond lengths [Å] and angles [°] for 1.

Fe-C(1)#1	2.00(2)	Fe-C(1)	2.00(2)
Fe-C(3)	2.00(2)	Fe-C(2)	2.04(2)
Fe-C(2)#1	2.04(2)	Fe-C(5)#1	2.052(7)
Fe-C(5)	2.052(7)	Fe-B	2.06(3)
Fe-C(4)	2.065(10)	Fe-C(6)#1	2.069(7)
Fe-C(6)	2.069(7)	C(1)-C(2)	1.30(3)
C(1)-C(3)	1.33(2)	C(2)-B	1.31(3)
C(3)-C(1)#1	1.33(2)	C(4)-C(5)	1.425(8)
C(4)-C(5)#1	1.425(8)	C(4)-C(7)	1.49(2)
C(5)-C(6)	1.418(9)	C(5)-C(8)	1.498(11)
C(6)-C(6)#1	1.433(13)	C(6)-C(9)	1.503(10)
B-C(2)#1	1.31(3)		
C(1)#1-Fe-C(1)	69.2(10)	C(1)#1-Fe-C(3)	38.8(7)
C(1)-Fe-C(3)	38.8(7)	C(1)#1-Fe-C(2)	80.8(6)
C(1)-Fe-C(2)	37.6(8)	C(3)-Fe-C(2)	69.2(8)
C(1)#1-Fe-C(2)#1	37.6(8)	C(1)-Fe-C(2)#1	80.8(6)
C(3)-Fe-C(2)#1	69.2(8)	C(2)-Fe-C(2)#1	67.8(13)
C(1)#1-Fe-C(5)#1	104.1(5)	C(1)-Fe-C(5)#1	151.4(7)
C(3)-Fe-C(5)#1	119.5(6)	C(2)-Fe-C(5)#1	170.7(7)
C(2)#1-Fe-C(5)#1	111.4(6)	C(1)#1-Fe-C(5)	151.4(7)
C(1)-Fe-C(5)	104.1(5)	C(3)-Fe-C(5)	119.5(6)
C(2)-Fe-C(5)	111.4(6)	C(2)#1-Fe-C(5)	170.7(7)
C(5)#1-Fe-C(5)	67.9(4)	C(1)#1-Fe-B	67.4(10)
C(1)-Fe-B	67.4(10)	C(3)-Fe-B	81.0(13)
C(2)-Fe-B	37.2(9)	C(2)#1-Fe-B	37.2(9)
C(5)#1-Fe-B	137.4(6)	C(5)-Fe-B	137.4(6)
C(1)#1-Fe-C(4)	115.6(6)	C(1)-Fe-C(4)	115.6(6)
C(3)-Fe-C(4)	102.9(7)	C(2)-Fe-C(4)	144.2(7)
C(2)#1-Fe-C(4)	144.2(8)	C(5)#1-Fe-C(4)	40.5(2)
C(5)-Fe-C(4)	40.5(2)	B-Fe-C(4)	176.1(11)
C(1)#1-Fe-C(6)#1	124.6(6)	C(1)-Fe-C(6)#1	164.0(7)
C(3)-Fe-C(6)#1	157.2(4)	C(2)-Fe-C(6)#1	130.6(7)
C(2)#1-Fe-C(6)#1	105.3(6)	C(5)#1-Fe-C(6)#1	40.2(3)
C(5)-Fe-C(6)#1	67.9(3)	B-Fe-C(6)#1	108.4(10)
C(4)-Fe-C(6)#1	68.0(3)	C(1)#1-Fe-C(6)	164.0(6)
C(1)-Fe-C(6)	124.6(6)	C(3)-Fe-C(6)	157.2(4)
C(2)-Fe-C(6)	105.3(6)	C(2)#1-Fe-C(6)	130.6(7)
C(5)#1-Fe-C(6)	67.9(3)	C(5)-Fe-C(6)	40.2(3)
B-Fe-C(6)	108.4(10)	C(4)-Fe-C(6)	68.0(3)
C(6)#1-Fe-C(6)	40.5(4)	C(2)-C(1)-C(3)	121(2)
C(2)-C(1)-Fe	72.8(11)	C(3)-C(1)-Fe	70.6(11)
C(1)-C(2)-B	120(2)	C(1)-C(2)-Fe	69.6(11)
B-C(2)-Fe	72.3(14)	C(1)-C(3)-C(1)#1	117(2)
C(1)-C(3)-Fe	70.6(12)	C(1)#1-C(3)-Fe	70.6(12)
C(5)-C(4)-C(5)#1	107.1(8)	C(5)-C(4)-C(7)	126.5(4)
C(5)#1-C(4)-C(7)	126.5(4)	C(5)-C(4)-Fe	69.3(4)
C(5)#1-C(4)-Fe	69.3(4)	C(7)-C(4)-Fe	128.1(8)
C(6)-C(5)-C(4)	108.8(6)	C(6)-C(5)-C(8)	124.5(7)
C(4)-C(5)-C(8)	126.6(7)	C(6)-C(5)-Fe	70.5(4)
C(4)-C(5)-Fe	70.2(5)	C(8)-C(5)-Fe	127.1(6)
C(5)-C(6)-C(6)#1	107.6(4)	C(5)-C(6)-C(9)	126.8(7)
C(6)#1-C(6)-C(9)	125.6(5)	C(5)-C(6)-Fe	69.2(4)
C(6)#1-C(6)-Fe	69.7(2)	C(9)-C(6)-Fe	127.6(6)
C(2)#1-C(6)-C(9)	121(3)	C(2)#1-C(6)-Fe	70.5(14)

C(2)-B-Fe

70.5(14)

Symmetry transformations used to generate equivalent atoms:

#1 $x, -y+3/2, z$

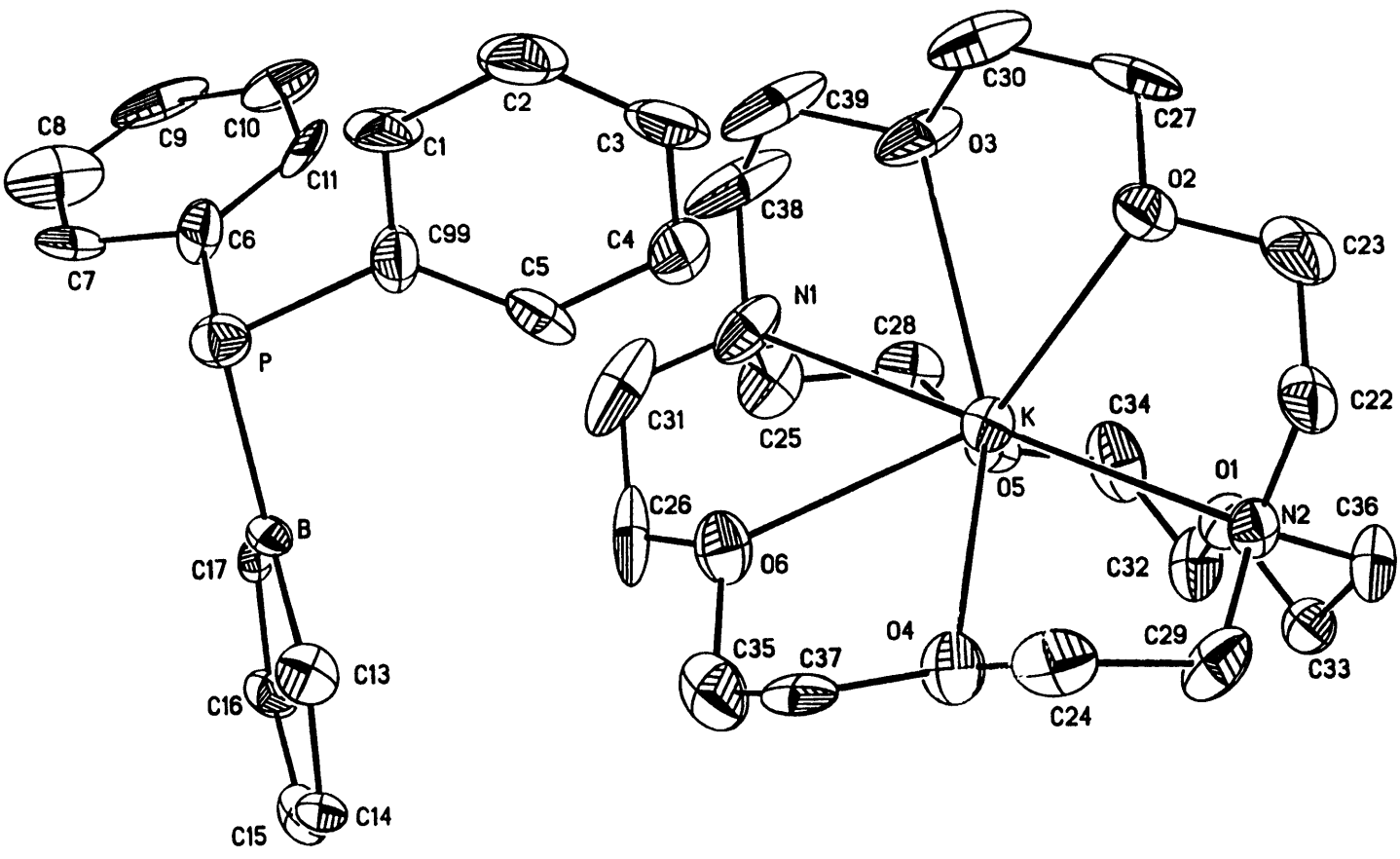


Table 1. Crystal data and structure refinement for 1.

A. Crystal Data

Identification code	96161
Empirical formula	$C_{35}H_{51}BKN_2O_6P$
Formula weight	676.66
Temperature	183(2) K
Wavelength	0.71073 Å
Crystal morphology	prism
Crystal size	0.09 x 0.08 x 0.03 mm
Crystal system	Triclinic
Space group	$P\bar{1}$
Unit cell dimensions	$a = 10.221(2) \text{ \AA}$ $\alpha = 91.082(3)^\circ$ $b = 11.352(2) \text{ \AA}$ $\beta = 97.167(3)^\circ$ $c = 16.784(2) \text{ \AA}$ $\gamma = 104.567(3)^\circ$
Volume, Z	$1867.4(5) \text{ \AA}^3$, 2
Density (calculated)	1.203 Mg/m^3
Absorption coefficient	0.229 mm^{-1}
F(000)	724

B. Data Collection and Reduction

Diffractionmeter	Siemens SMART/CCD
Scan Type	ω Scans
Scan angle	0.30°
θ range for data collection	1.86 to 19.50°
Limiting indices	$-9 \leq h \leq 11$, $-12 \leq k \leq 12$, $-18 \leq l \leq 17$

Reflections collected	4986
Independent reflections	3163 ($R_{int} = 0.0963$)
Absorption correction	None

C. Solution and Refinement

Refinement method	Full-matrix least-squares on F^2
Data / restraints / parameters	2810 / 0 / 416
Goodness-of-fit on F^2	1.310
Final R indices [$I > 2\sigma(I)$]	$R_1 = 0.1133$, $wR_2 = 0.1870$
R indices (all data)	$R_1 = 0.1839$, $wR_2 = 0.2373$
Extinction coefficient	0.0052(11)
Largest diff. peak and hole	0.294 and -0.295 $e\text{\AA}^{-3}$

Table 2. Atomic coordinates [$\times 10^4$] and equivalent isotropic displacement parameters [$\text{\AA}^2 \times 10^3$] for 1. $U(\text{eq})$ is defined as one third of the trace of the orthogonalized U_{ij} tensor.

	x	y	z	$U(\text{eq})$
K	2753 (3)	1627 (3)	2817 (2)	35 (1)
N(1)	2425 (15)	4140 (11)	2405 (8)	60 (4)
O(2)	2786 (9)	-32 (9)	1535 (6)	52 (3)
O(3)	2211 (11)	2235 (11)	1199 (6)	72 (4)
O(4)	5052 (9)	1375 (10)	3929 (6)	53 (3)
P	8666 (4)	6611 (3)	2114 (2)	39 (1)
C(17)	7375 (11)	7377 (10)	3504 (8)	29 (4)
O(1)	730 (8)	-33 (8)	3480 (5)	40 (2)
C(14)	8728 (13)	6150 (12)	4649 (3)	38 (4)
O(5)	531 (9)	2338 (8)	3200 (5)	39 (2)
C(1)	8452 (15)	4749 (14)	957 (8)	51 (4)
C(11)	6235 (15)	6878 (12)	1202 (8)	42 (4)
C(7)	7858 (16)	8693 (16)	1709 (8)	48 (4)
C(16)	7251 (13)	7481 (12)	4311 (9)	37 (4)
O(6)	4750 (10)	3648 (8)	3462 (6)	52 (3)
C(8)	6993 (25)	9371 (19)	1395 (11)	88 (6)
C(3)	7078 (19)	2725 (16)	940 (10)	65 (5)
C(15)	7904 (14)	6872 (13)	4863 (9)	42 (4)
C(99)	7983 (14)	5059 (12)	1659 (9)	45 (4)
B	8255 (16)	6627 (13)	3221 (9)	31 (4)
N(2)	3134 (11)	-896 (9)	3200 (5)	35 (3)
C(13)	8914 (13)	5998 (11)		38 (4)
C(23)	2452 (16)	-1270 (15)		65 (5)
C(6)	7502 (15)	7415 (15)		48 (4)
C(4)	6588 (16)	2965 (14)	529 (11)	61 (5)
C(24)	5466 (13)	300 (14)	3752 (9)	55 (4)
C(22)	3358 (15)	-1475 (12)	2449 (8)	53 (4)
C(5)	7066 (14)	4158 (14)	1995 (8)	43 (4)
C(2)	7972 (18)	3581 (17)	595 (9)	63 (5)
C(37)	6169 (13)	2430 (15)	4019 (8)	46 (4)
C(36)	1875 (14)	-1627 (11)	3484 (9)	48 (4)
C(35)	5628 (16)	3505 (15)	4169 (10)	67 (5)
C(34)	-617 (14)	1402 (14)	3342 (10)	66 (5)
C(33)	1214 (13)	-866 (12)	3981 (8)	40 (4)
C(32)	-140 (14)	529 (13)	3876 (9)	51 (4)
C(10)	5372 (15)	7566 (18)	885 (8)	55 (5)
C(9)	5722 (22)	8814 (19)	995 (10)	68 (6)
C(31)	3761 (21)	5003 (16)	2694 (13)	85 (7)
C(30)	2505 (18)	1455 (19)	623 (10)	84 (6)
C(29)	4286 (13)	-779 (13)	3818 (9)	51 (4)
C(28)	135 (14)	3296 (13)	2794 (9)	52 (4)
C(39)	2747 (21)	3477 (18)	1026 (10)	101 (7)
C(27)	1986 (16)	162 (17)	824 (9)	71 (5)
C(26)	4386 (16)	4773 (14)	3510 (12)	74 (6)
C(25)	1341 (16)	4394 (13)	2832 (10)	59 (5)
C(38)	2081 (20)	4217 (17)	1537 (10)	103 (7)

Table 4. Bond lengths [Å] and angles [°] for 1.

K-O(5)	2.740(9)	K-O(6)	2.757(10)
K-O(1)	2.785(9)	K-O(3)	2.837(10)
K-O(2)	2.842(9)	K-O(4)	2.890(10)
K-N(1)	3.038(11)	K-N(2)	3.046(10)
N(1)-C(38)	1.47(2)	N(1)-C(25)	1.47(2)
N(1)-C(31)	1.48(2)	O(2)-C(23)	1.41(2)
O(2)-C(27)	1.41(2)	O(3)-C(30)	1.41(2)
O(3)-C(39)	1.43(2)	O(4)-C(37)	1.42(2)
O(4)-C(24)	1.43(2)	P-C(6)	1.81(2)
P-C(99)	1.836(14)	P-B	1.96(2)
C(17)-C(16)	1.38(2)	C(17)-B	1.49(2)
C(17)-C(14)	1.416(14)	O(1)-C(32)	1.435(14)
C(14)-C(15)	1.39(2)	C(14)-C(13)	1.39(2)
O(5)-C(28)	1.415(14)	O(5)-C(34)	1.42(2)
C(1)-C(2)	1.39(2)	C(1)-C(99)	1.40(2)
C(11)-C(6)	1.38(2)	C(11)-C(10)	1.38(2)
C(7)-C(8)	1.38(2)	C(7)-C(6)	1.40(2)
C(16)-C(15)	1.37(2)	O(6)-C(26)	1.42(2)
O(6)-C(35)	1.43(2)	C(8)-C(9)	1.38(2)
C(3)-C(2)	1.35(2)	C(3)-C(4)	1.36(2)
C(99)-C(5)	1.38(2)	B-C(13)	1.48(2)
N(2)-C(29)	1.44(2)	N(2)-C(36)	1.48(2)
N(2)-C(22)	1.49(2)	C(23)-C(22)	1.50(2)
C(4)-C(5)	1.42(2)	C(24)-C(29)	1.50(2)
C(37)-C(35)	1.49(2)	C(36)-C(33)	1.52(2)
C(34)-C(32)	1.48(2)	C(10)-C(9)	1.37(2)
C(31)-C(26)	1.49(2)	C(30)-C(27)	1.49(2)
C(28)-C(25)	1.51(2)	C(39)-C(38)	1.52(2)
O(5)-K-O(6)	98.2(3)	O(5)-K-O(1)	60.7(3)
O(6)-K-O(1)	132.5(3)	O(5)-K-O(3)	91.1(3)
O(6)-K-O(3)	102.2(4)	O(1)-K-O(3)	118.9(3)
O(5)-K-O(2)	126.6(3)	O(6)-K-O(2)	129.3(3)
O(1)-K-O(2)	93.5(3)	O(3)-K-O(2)	59.8(3)
O(5)-K-O(4)	126.2(3)	O(6)-K-O(4)	59.2(3)
O(1)-K-O(4)	97.5(3)	O(3)-K-O(4)	138.4(3)
O(2)-K-O(4)	101.3(3)	O(5)-K-N(1)	60.3(3)
O(6)-K-N(1)	61.2(4)	O(1)-K-N(1)	120.9(3)
O(3)-K-N(1)	58.7(4)	O(2)-K-N(1)	118.2(3)
O(4)-K-N(1)	120.3(4)	O(5)-K-N(2)	121.0(3)
O(6)-K-N(2)	118.4(3)	O(1)-K-N(2)	60.4(3)
O(3)-K-N(2)	120.6(3)	O(2)-K-N(2)	61.0(3)
O(4)-K-N(2)	59.4(3)	N(1)-K-N(2)	178.7(3)
C(38)-N(1)-C(25)	110.1(13)	C(38)-N(1)-C(31)	110.2(14)
C(25)-N(1)-C(31)	110.9(13)	C(38)-N(1)-K	111.4(10)
C(25)-N(1)-K	108.4(8)	C(31)-N(1)-K	105.8(9)
C(23)-O(2)-C(27)	111.3(12)	C(23)-O(2)-K	114.6(8)
C(27)-O(2)-K	111.8(8)	C(30)-O(3)-C(39)	110.1(12)
C(30)-O(3)-K	114.8(9)	C(39)-O(3)-K	116.4(10)
C(37)-O(4)-K	111.9(11)	C(6)-P-C(99)	113.6(8)
C(24)-O(4)-K	112.4(8)	C(99)-P-B	108.8(7)
C(16)-C(17)-B	120.5(12)	C(33)-O(1)-C(32)	110.8(10)
C(33)-O(1)-K	114.5(7)	C(32)-O(1)-K	113.5(7)
C(15)-C(14)-C(13)	120.7(13)	C(28)-O(5)-C(34)	111.4(11)

C(28)-O(5)-K	119.1(8)	C(34)-O(5)-K	116.9(8)
C(2)-C(1)-C(99)	120.8(14)	C(6)-C(11)-C(10)	121.6(14)
C(8)-C(7)-C(6)	122(2)	C(15)-C(16)-C(17)	120.6(12)
C(26)-O(6)-C(35)	111.0(13)	C(26)-O(6)-K	117.7(9)
C(35)-O(6)-K	117.7(8)	C(9)-C(8)-C(7)	121(2)
C(2)-C(3)-C(4)	123(2)	C(16)-C(15)-C(14)	122.5(13)
C(5)-C(99)-C(1)	117.8(14)	C(5)-C(99)-P	123.3(12)
C(1)-C(99)-P	118.8(12)	C(13)-B-C(17)	115.4(12)
C(13)-B-P	121.7(11)	C(17)-B-P	122.6(11)
C(29)-N(2)-C(36)	110.1(10)	C(29)-N(2)-C(22)	110.5(11)
C(36)-N(2)-C(22)	109.1(10)	C(29)-N(2)-K	110.3(8)
C(36)-N(2)-K	109.1(7)	C(22)-N(2)-K	107.7(8)
C(14)-C(13)-B	120.2(12)	O(2)-C(23)-C(22)	110.8(13)
C(11)-C(6)-C(7)	116.2(14)	C(11)-C(6)-P	125.4(12)
C(7)-C(6)-P	118.2(13)	C(3)-C(4)-C(5)	118(2)
O(4)-C(24)-C(29)	107.9(11)	N(2)-C(22)-C(23)	113.5(12)
C(99)-C(5)-C(4)	121.3(14)	C(3)-C(2)-C(1)	120(2)
O(4)-C(37)-C(35)	107.9(11)	N(2)-C(36)-C(33)	112.1(11)
O(6)-C(35)-C(37)	108.2(12)	O(5)-C(34)-C(32)	108.4(11)
O(1)-C(33)-C(36)	109.0(11)	O(1)-C(32)-C(34)	109.5(12)
C(9)-C(10)-C(11)	122(2)	C(10)-C(9)-C(8)	118(2)
N(1)-C(31)-C(26)	114.5(13)	O(3)-C(30)-C(27)	109.8(14)
N(2)-C(29)-C(24)	114.3(11)	O(5)-C(28)-C(25)	109.8(11)
O(3)-C(39)-C(38)	105.7(14)	O(2)-C(27)-C(30)	107.8(13)
O(6)-C(26)-C(31)	108.3(14)	N(1)-C(25)-C(28)	111.7(12)
N(1)-C(38)-C(39)	114.1(13)		

Symmetry transformations used to generate equivalent atoms:

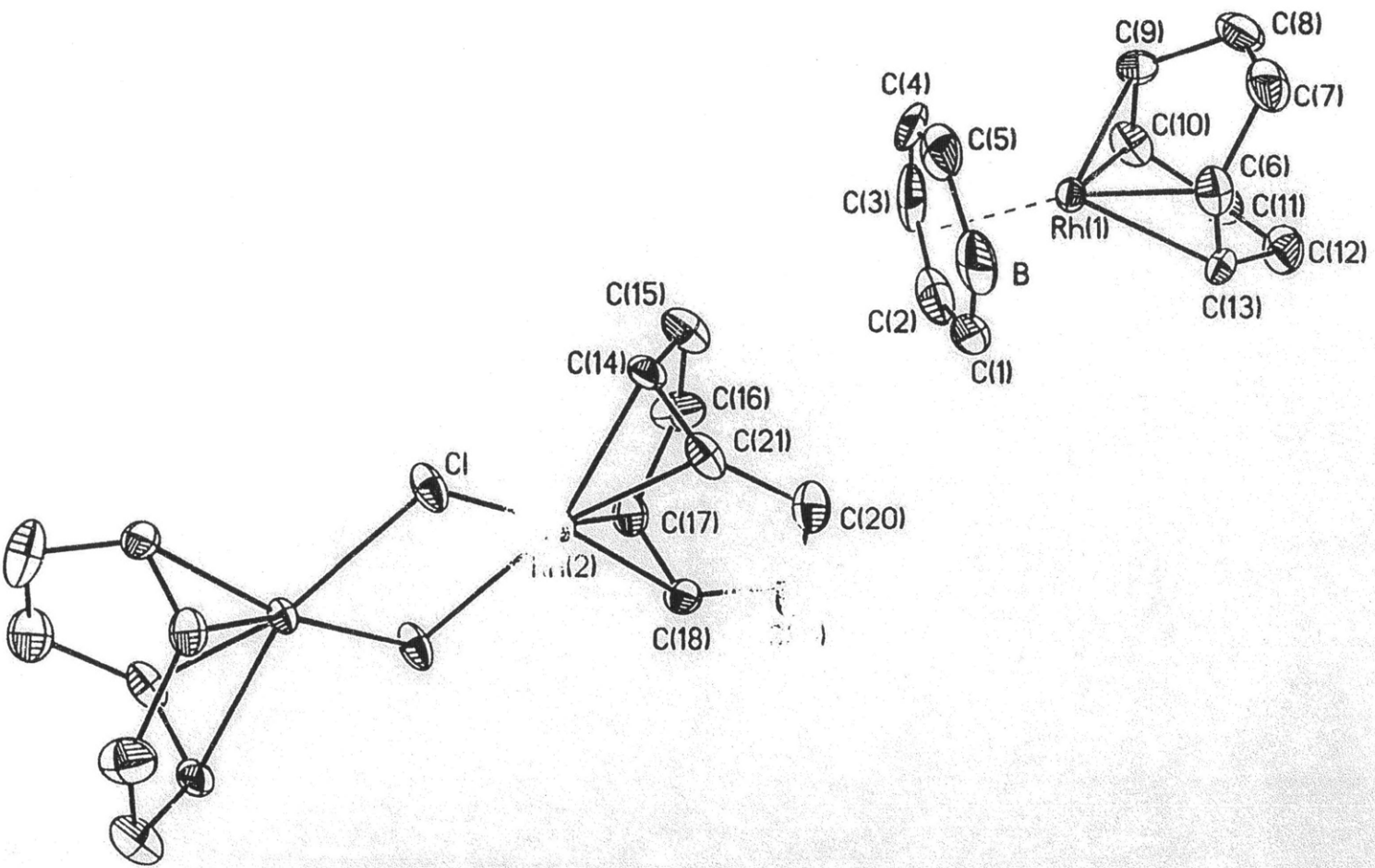


Table 1. Crystal data and structure refinement for 1.

A. Crystal Data

Identification code	96172
Empirical formula	$C_{21}H_{30}BClRh_2$
Formula weight	534.53
Temperature	183(2) K
Wavelength	0.71073 Å
Crystal morphology	Plate
Crystal size	.03 x .11 x .21 mm
Crystal system	Monoclinic
Space group	$P2_1/n$
Unit cell dimensions	$a = 6.6145(2) \text{ \AA}$ $\alpha = 90^\circ$ $b = 27.8629(7) \text{ \AA}$ $\beta = 95.4760(10)^\circ$ $c = 10.7880(2) \text{ \AA}$ $\gamma = 90^\circ$
Volume, Z	$1979.15(9) \text{ \AA}^3$, 4
Density (calculated)	1.794 Mg/m^3
Absorption coefficient	1.804 mm^{-1}
F(000)	1072

B. Data Collection and Reduction

Diffractometer	Siemens SMART/CCD
Scan Type	ω Scans
Scan angle	0.30°
θ range for data collection	1.46 to 23.24°
Limiting indices	$-7 \leq h \leq 6$, $-30 \leq k \leq 30$, $-7 \leq l \leq 11$

Reflections collected	7976
Independent reflections	2828 ($R_{int} = 0.0398$)
Absorption correction	Semi-empirical from psi-scans
Max. and min. transmission	0.3426 and 0.3195

C. Solution and Refinement

Refinement method	Full-matrix least-squares on F^2
Data / restraints / parameters	2827 / 0 / 226
Goodness-of-fit on F^2	1.254
Final R indices [$I > 2\sigma(I)$]	$R1 = 0.0457$, $wR2 = 0.0893$
R indices (all data)	$R1 = 0.0528$, $wR2 = 0.1059$
Largest diff. peak and hole	1.982 and $-0.516 \text{ e}\text{\AA}^{-3}$

Table 2. Atomic coordinates [$\times 10^4$] and equivalent isotropic displacement parameters [$\text{\AA}^2 \times 10^3$] for 1. $U(\text{eq})$ is defined as one third of the trace of the orthogonalized U_{ij} tensor.

	x	y	z	U(eq)
Rh(1)	1904(1)	1564(1)	2753(1)	27(1)
Rh(2)	-4145(1)	374(1)	-3693(1)	22(1)
Cl	-2891(3)	89(1)	-5589(2)	37(1)
C(1)	-806(15)	1396(4)	1328(10)	64(3)
C(2)	-859(17)	1077(4)	2301(10)	63(3)
C(3)	810(22)	817(3)	2683(10)	73(4)
C(4)	2571(19)	824(4)	2039(12)	72(4)
C(5)	2735(16)	1114(4)	1039(10)	64(3)
C(6)	3091(13)	2246(3)	2409(7)	41(2)
C(7)	5225(14)	2307(3)	2987(9)	56(3)
C(8)	5670(13)	2018(3)	4169(9)	53(2)
C(9)	4298(12)	1580(3)	4223(7)	41(2)
C(10)	2441(13)	1592(3)	4734(7)	44(2)
C(11)	1574(14)	2031(3)	5271(8)	52(2)
C(12)	1427(14)	2455(3)	4394(8)	53(2)
C(13)	1353(12)	2310(3)	3023(8)	38(2)
C(14)	-1212(10)	502(3)	-2829(7)	32(2)
C(15)	-1060(13)	428(3)	-1442(8)	48(2)
C(16)	-3053(13)	379(4)	-899(7)	53(2)
C(17)	-4876(11)	390(3)	-1842(7)	33(2)
C(18)	-5624(11)	802(3)	-2447(7)	32(2)
C(19)	-4680(16)	1286(3)	-2226(9)	56(3)
C(20)	-2671(14)	1347(3)	-2711(10)	60(3)
C(21)	-1955(11)	926(3)	-3415(7)	35(2)
B	1052(21)	1438(4)	584(10)	62(3)

Table 3. Bond lengths [Å] and angles [°] for 1.

Rh(1)-C(6)	2.104(8)	Rh(1)-C(9)	2.132(7)
Rh(1)-C(10)	2.134(8)	Rh(1)-C(13)	2.135(7)
Rh(1)-C(3)	2.203(9)	Rh(1)-C(4)	2.257(9)
Rh(1)-C(2)	2.290(9)	Rh(1)-C(1)	2.295(8)
Rh(1)-C(5)	2.341(9)	Rh(1)-B	2.380(10)
Rh(2)-C(17)	2.100(7)	Rh(2)-C(14)	2.102(7)
Rh(2)-C(18)	2.107(7)	Rh(2)-C(21)	2.115(7)
Rh(2)-Cl#1	2.412(2)	Rh(2)-Cl	2.413(2)
Cl-Rh(2)#1	2.412(2)	C(1)-C(2)	1.38(2)
C(1)-B	1.53(2)	C(2)-C(3)	1.35(2)
C(3)-C(4)	1.41(2)	C(4)-C(5)	1.36(2)
C(5)-B	1.48(2)	C(6)-C(13)	1.392(11)
C(6)-C(7)	1.497(12)	C(7)-C(8)	1.514(13)
C(8)-C(9)	1.526(12)	C(9)-C(10)	1.394(11)
C(10)-C(11)	1.491(12)	C(11)-C(12)	1.511(13)
C(12)-C(13)	1.530(11)	C(14)-C(21)	1.406(10)
C(14)-C(15)	1.504(11)	C(15)-C(16)	1.499(12)
C(16)-C(17)	1.502(11)	C(17)-C(18)	1.389(10)
C(18)-C(19)	1.495(11)	C(19)-C(20)	1.484(13)
C(20)-C(21)	1.499(12)		
C(6)-Rh(1)-C(9)	81.3(3)	C(6)-Rh(1)-C(10)	96.5(3)
C(9)-Rh(1)-C(10)	38.1(3)	C(6)-Rh(1)-C(13)	38.3(3)
C(9)-Rh(1)-C(13)	90.2(3)	C(10)-Rh(1)-C(13)	80.9(3)
C(6)-Rh(1)-C(3)	167.2(4)	C(9)-Rh(1)-C(3)	105.3(4)
C(10)-Rh(1)-C(3)	95.3(4)	C(13)-Rh(1)-C(3)	149.9(5)
C(6)-Rh(1)-C(4)	132.5(4)	C(9)-Rh(1)-C(4)	96.7(4)
C(10)-Rh(1)-C(4)	110.9(4)	C(13)-Rh(1)-C(4)	167.5(4)
C(3)-Rh(1)-C(4)	36.9(4)	C(6)-Rh(1)-C(2)	143.2(4)
C(9)-Rh(1)-C(2)	133.8(4)	C(10)-Rh(1)-C(2)	106.8(4)
C(13)-Rh(1)-C(2)	117.5(4)	C(3)-Rh(1)-C(2)	35.0(4)
C(4)-Rh(1)-C(2)	64.2(4)	C(6)-Rh(1)-C(1)	110.3(4)
C(9)-Rh(1)-C(1)	168.4(4)	C(10)-Rh(1)-C(1)	136.3(4)
C(13)-Rh(1)-C(1)	99.0(3)	C(3)-Rh(1)-C(1)	63.4(4)
C(4)-Rh(1)-C(1)	75.6(4)	C(2)-Rh(1)-C(1)	35.0(4)
C(6)-Rh(1)-C(5)	103.0(4)	C(9)-Rh(1)-C(5)	112.6(4)
C(10)-Rh(1)-C(5)	141.4(4)	C(13)-Rh(1)-C(5)	133.2(4)
C(3)-Rh(1)-C(5)	64.5(4)	C(4)-Rh(1)-C(5)	34.3(4)
C(2)-Rh(1)-C(5)	76.0(4)	C(1)-Rh(1)-C(5)	65.8(4)
C(6)-Rh(1)-B	91.0(4)	C(9)-Rh(1)-B	145.4(4)
C(10)-Rh(1)-B	172.4(4)	C(13)-Rh(1)-B	104.5(4)
C(3)-Rh(1)-B	77.3(4)	C(4)-Rh(1)-B	64.3(4)
C(2)-Rh(1)-B	66.1(4)	C(1)-Rh(1)-B	38.3(4)
C(5)-Rh(1)-B	36.5(4)	C(17)-Rh(2)-C(14)	82.0(3)
C(17)-Rh(2)-C(18)	38.5(3)	C(14)-Rh(2)-C(18)	94.9(3)
C(17)-Rh(2)-C(21)	93.8(3)	C(14)-Rh(2)-C(21)	38.9(3)
C(18)-Rh(2)-C(21)	81.4(3)	C(17)-Rh(2)-Cl#1	93.6(2)
C(14)-Rh(2)-Cl#1	157.1(2)	C(18)-Rh(2)-Cl#1	95.5(2)
C(21)-Rh(2)-Cl#1	163.6(2)	C(17)-Rh(2)-Cl	160.4(2)
C(14)-Rh(2)-Cl	93.1(2)	C(18)-Rh(2)-Cl	160.9(2)
C(21)-Rh(2)-Cl	94.2(2)	Cl#1-Rh(2)-Cl	83.49(6)
Rh(2)#1-Cl-Rh(2)	96.51(6)	C(2)-C(1)-B	121.8(9)
C(2)-C(1)-Rh(1)	72.3(5)	B-C(1)-Rh(1)	73.9(5)
C(3)-C(2)-C(1)	119.9(10)	C(3)-C(2)-Rh(1)	69.0(6)
C(1)-C(2)-Rh(1)	72.7(5)	C(2)-C(3)-C(4)	122.0(10)

C(2)-C(3)-Rh(1)	76.0(6)	C(4)-C(3)-Rh(1)	73.7(6)
C(5)-C(4)-C(3)	122.1(10)	C(5)-C(4)-Rh(1)	76.2(6)
C(3)-C(4)-Rh(1)	69.5(5)	C(4)-C(5)-B	120.7(10)
C(4)-C(5)-Rh(1)	69.4(5)	B-C(5)-Rh(1)	73.2(5)
C(13)-C(6)-C(7)	125.2(7)	C(13)-C(6)-Rh(1)	72.0(4)
C(7)-C(6)-Rh(1)	112.5(6)	C(6)-C(7)-C(8)	113.0(7)
C(7)-C(8)-C(9)	112.9(7)	C(10)-C(9)-C(8)	123.0(8)
C(10)-C(9)-Rh(1)	71.0(4)	C(8)-C(9)-Rh(1)	113.0(5)
C(9)-C(10)-C(11)	124.1(8)	C(9)-C(10)-Rh(1)	70.8(5)
C(11)-C(10)-Rh(1)	112.7(6)	C(10)-C(11)-C(12)	113.7(7)
C(11)-C(12)-C(13)	113.1(7)	C(6)-C(13)-C(12)	122.8(7)
C(6)-C(13)-Rh(1)	69.7(4)	C(12)-C(13)-Rh(1)	113.5(6)
C(21)-C(14)-C(15)	123.3(7)	C(21)-C(14)-Rh(2)	71.0(4)
C(15)-C(14)-Rh(2)	112.9(5)	C(16)-C(15)-C(14)	115.1(7)
C(15)-C(16)-C(17)	114.4(7)	C(18)-C(17)-C(16)	124.3(7)
C(18)-C(17)-Rh(2)	71.0(4)	C(16)-C(17)-Rh(2)	113.6(5)
C(17)-C(18)-C(19)	123.1(7)	C(17)-C(18)-Rh(2)	70.5(4)
C(19)-C(18)-Rh(2)	113.6(5)	C(20)-C(19)-C(18)	114.9(7)
C(19)-C(20)-C(21)	115.2(7)	C(14)-C(21)-C(20)	122.9(7)
C(14)-C(21)-Rh(2)	70.0(4)	C(20)-C(21)-Rh(2)	113.3(5)
C(5)-B-C(1)	113.3(9)	C(5)-B-Rh(1)	70.3(5)
C(1)-B-Rh(1)	67.9(5)		

Symmetry transformations used to generate equivalent atoms:

#1 -x-1, -y, -z-1

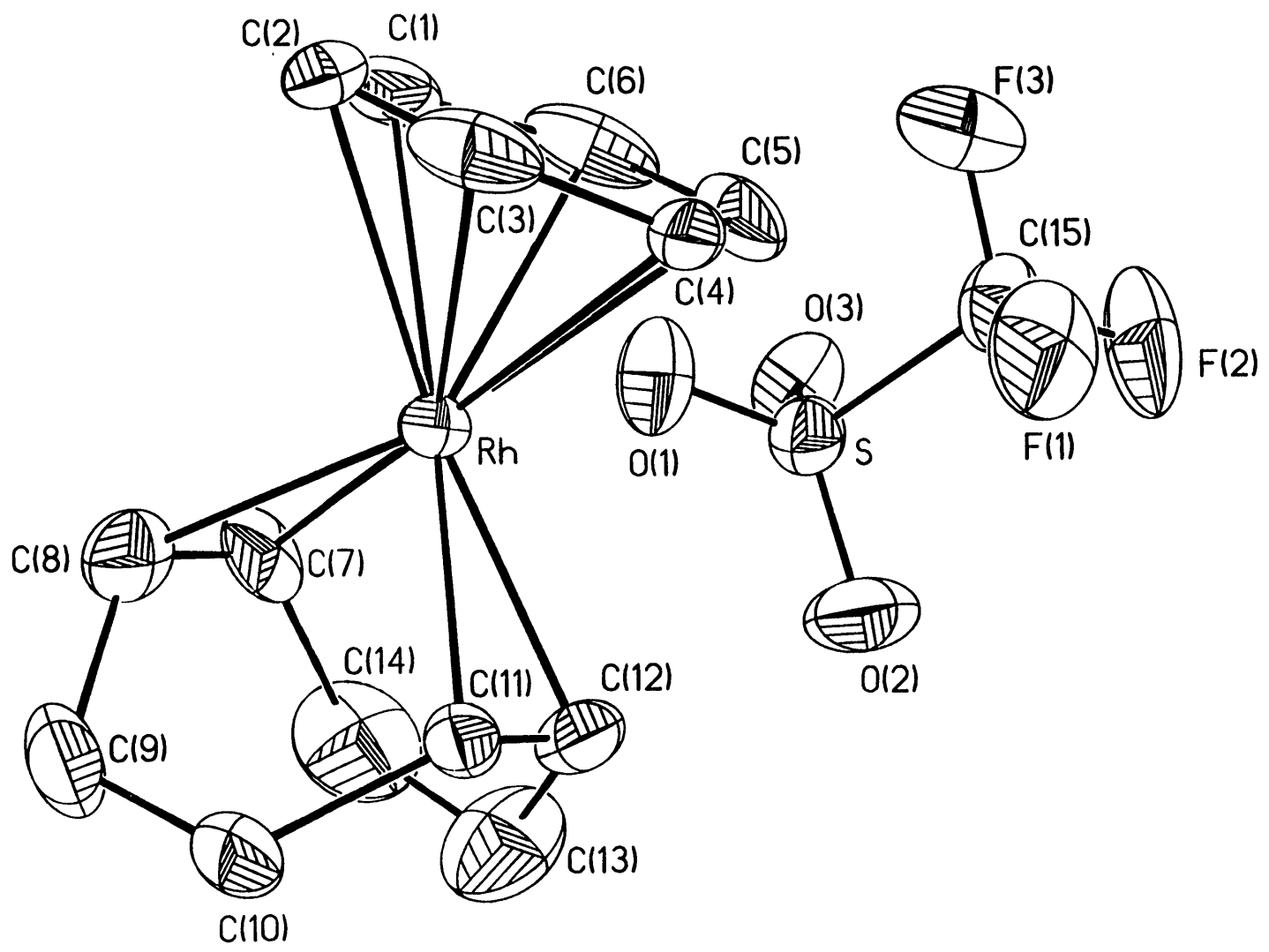


Table 1. Crystal data and structure refinement for 1.

A. Crystal Data

Identification code	96186 96186
Empirical formula	C ₁₅ H ₁₈ F ₃ O ₃ Rhs
Formula weight	438.26
Temperature	183(2) K
Wavelength	0.71073 Å
Crystal morphology	block
Crystal size	.05 x .08 x .08 mm
Crystal system	Orthorhombic
Space group	P2 ₁ ² ₁ ² ₁
Unit cell dimensions	a = 7.6554(6) Å alpha = 90° b = 14.4837(10) Å beta = 90° c = 15.1690(11) Å gamma = 90°
Volume, Z	1681.9(2) Å ³ , 4
Density (calculated)	1.731 Mg/m ³
Absorption coefficient	1.179 mm ⁻¹
F(000)	880

B. Data Collection and Reduction

Diffractometer	Siemens SMART/CCD
Scan Type	ω Scans
Scan angle	0.30°
θ range for data collection	1.94 to 23.29°
Limiting indices	-4 ≤ h ≤ 8, -15 ≤ k ≤ 16, -16 ≤ l ≤ 16

Reflections collected	6784
Independent reflections	2419 ($R_{int} = 0.0683$)
Absorption correction	Semi-empirical from ψ 1-scans
Max. and min. transmission	0.8339 and 0.6756

C. Solution and Refinement

Refinement method	Full-matrix least-squares on F^2
Data / restraints / parameters	2418 / 0 / 209
Goodness-of-fit on F^2	1.213
Final R indices [$I > 2\sigma(I)$]	$R1 = 0.0486$, $wR2 = 0.0903$
R indices (all data)	$R1 = 0.0601$, $wR2 = 0.0966$
Absolute structure parameter	-0.11(9)
Extinction coefficient	0.0019(3)
Largest diff. peak and hole	0.486 and -0.773 $e\text{\AA}^{-3}$

Table 2. Atomic coordinates [$\times 10^4$] and equivalent isotropic displacement parameters [$\text{\AA}^2 \times 10^3$] for 1. $U(\text{eq})$ is defined as one third of the trace of the orthogonalized U_{ij} tensor.

	x	y	z	U(eq)
Rh	-2316 (1)	-601 (1)	-6924 (1)	30 (1)
S	2963 (4)	334 (2)	-4722 (2)	56 (1)
F (1)	140 (12)	1322 (6)	-4500 (6)	111 (3)
F (2)	2243 (15)	1748 (6)	-3716 (5)	120 (3)
F (3)	2234 (17)	2050 (5)	-5109 (6)	133 (3)
O (1)	2459 (16)	131 (5)	-5605 (5)	77 (2)
O (2)	2386 (16)	-249 (5)	-4051 (6)	96 (3)
O (3)	4809 (8)	563 (7)	-4635 (5)	71 (2)
C (1)	-990 (19)	481 (10)	-7741 (9)	66 (4)
C (2)	-2601 (22)	344 (5)	-8142 (6)	65 (3)
C (3)	-4100 (15)	443 (9)	-7632 (9)	59 (4)
C (4)	-3964 (15)	680 (8)	-6747 (7)	52 (3)
C (5)	-2343 (25)	907 (5)	-6386 (7)	67 (4)
C (6)	-856 (15)	807 (8)	-6897 (13)	72 (4)
C (7)	-254 (12)	-1595 (6)	-6969 (9)	53 (3)
C (8)	-1536 (14)	-1851 (7)	-7591 (8)	53 (3)
C (9)	-2874 (17)	-2621 (7)	-7451 (7)	67 (3)
C (10)	-4294 (15)	-2426 (7)	-6835 (8)	64 (3)
C (11)	-4141 (14)	-1532 (6)	-6325 (6)	40 (3)
C (12)	-2843 (15)	-1323 (6)	-5727 (6)	50 (3)
C (13)	-1351 (19)	-1995 (11)	-5487 (10)	96 (5)
C (14)	19 (19)	-2083 (10)	-6098 (9)	91 (5)
C (15)	1881 (17)	1446 (9)	-4506 (7)	68 (4)

Table 3. Bond lengths [Å] and angles [°] for 1.

Rh-C(12)	2.134 (9)	Rh-C(7)	2.138 (8)
Rh-C(11)	2.144 (9)	Rh-C(8)	2.159 (10)
Rh-C(1)	2.241 (12)	Rh-C(4)	2.259 (11)
Rh-C(3)	2.302 (12)	Rh-C(2)	2.309 (8)
Rh-C(6)	2.326 (10)	Rh-C(5)	2.332 (8)
S-O(2)	1.395 (7)	S-O(1)	1.425 (8)
S-O(3)	1.458 (7)	S-C(15)	1.840 (12)
F(1)-C(15)	1.345 (14)	F(2)-C(15)	1.306 (11)
F(3)-C(15)	1.294 (13)	C(1)-C(6)	1.37 (2)
C(1)-C(2)	1.39 (2)	C(2)-C(3)	1.39 (2)
C(3)-C(4)	1.39 (2)	C(4)-C(5)	1.40 (2)
C(5)-C(6)	1.39 (2)	C(7)-C(8)	1.41 (2)
C(7)-C(14)	1.51 (2)	C(8)-C(9)	1.529 (14)
C(9)-C(10)	1.461 (14)	C(10)-C(11)	1.513 (13)
C(11)-C(12)	1.378 (14)	C(12)-C(13)	1.54 (2)
C(13)-C(14)	1.41 (2)		
C(12)-Rh-C(7)	80.6 (4)	C(12)-Rh-C(11)	37.6 (4)
C(7)-Rh-C(11)	94.1 (4)	C(12)-Rh-C(8)	92.3 (4)
C(7)-Rh-C(8)	38.3 (4)	C(11)-Rh-C(8)	81.5 (4)
C(12)-Rh-C(1)	154.0 (5)	C(7)-Rh-C(1)	96.8 (4)
C(11)-Rh-C(1)	165.8 (5)	C(8)-Rh-C(1)	101.7 (5)
C(12)-Rh-C(4)	101.3 (4)	C(7)-Rh-C(4)	165.7 (4)
C(11)-Rh-C(4)	95.9 (4)	C(8)-Rh-C(4)	154.0 (4)
C(1)-Rh-C(4)	75.2 (5)	C(12)-Rh-C(3)	127.3 (4)
C(7)-Rh-C(3)	149.9 (5)	C(11)-Rh-C(3)	102.9 (4)
C(8)-Rh-C(3)	119.7 (5)	C(1)-Rh-C(3)	63.4 (4)
C(4)-Rh-C(3)	35.5 (4)	C(12)-Rh-C(2)	162.4 (5)
C(7)-Rh-C(2)	116.3 (5)	C(11)-Rh-C(2)	130.6 (5)
C(8)-Rh-C(2)	98.5 (4)	C(1)-Rh-C(2)	35.5 (5)
C(4)-Rh-C(2)	63.6 (4)	C(3)-Rh-C(2)	35.1 (4)
C(12)-Rh-C(6)	120.4 (5)	C(7)-Rh-C(6)	103.7 (4)
C(11)-Rh-C(6)	149.0 (5)	C(8)-Rh-C(6)	127.6 (5)
C(1)-Rh-C(6)	34.8 (5)	C(4)-Rh-C(6)	63.0 (4)
C(3)-Rh-C(6)	73.6 (4)	C(2)-Rh-C(6)	62.6 (5)
C(12)-Rh-C(5)	99.2 (4)	C(7)-Rh-C(5)	130.5 (5)
C(11)-Rh-C(5)	115.8 (5)	C(8)-Rh-C(5)	162.2 (5)
C(1)-Rh-C(5)	62.8 (5)	C(4)-Rh-C(5)	35.3 (5)
C(3)-Rh-C(5)	62.8 (4)	C(2)-Rh-C(5)	74.0 (3)
C(6)-Rh-C(5)	34.6 (5)	O(2)-S-O(1)	118.4 (6)
O(2)-S-O(3)	112.3 (6)	O(1)-S-O(3)	113.2 (6)
O(2)-S-C(15)	104.9 (5)	O(1)-S-C(15)	103.0 (5)
O(3)-S-C(15)	102.8 (6)	C(6)-C(1)-C(2)	121.7 (11)
C(6)-C(1)-Rh	76.0 (7)	C(2)-C(1)-Rh	74.9 (7)
C(1)-C(2)-C(3)	118.3 (9)	C(1)-C(2)-Rh	69.6 (6)
C(3)-C(2)-Rh	72.2 (6)	C(4)-C(3)-C(2)	120.0 (10)
C(4)-C(3)-Rh	70.6 (7)	C(2)-C(3)-Rh	72.7 (6)
C(3)-C(4)-C(5)	120.3 (10)	C(3)-C(4)-Rh	74.0 (7)
C(5)-C(4)-Rh	75.2 (6)	C(6)-C(5)-C(4)	119.1 (9)
C(6)-C(5)-Rh	72.5 (6)	C(4)-C(5)-Rh	69.5 (6)
C(1)-C(6)-C(5)	119.9 (11)	C(1)-C(6)-Rh	69.2 (7)
C(5)-C(6)-Rh	72.9 (6)	C(8)-C(7)-C(14)	123.9 (10)
C(8)-C(7)-Rh	71.6 (6)	C(14)-C(7)-Rh	112.8 (8)
C(7)-C(8)-C(9)	124.3 (10)	C(7)-C(8)-Rh	70.1 (6)
C(9)-C(8)-Rh	111.2 (6)	C(10)-C(9)-C(8)	116.5 (8)

C(9)-C(10)-C(11)	115.8(8)	C(12)-C(11)-C(10)	125.4(10)
C(12)-C(11)-Rh	70.8(5)	C(10)-C(11)-Rh	111.8(6)
C(11)-C(12)-C(13)	123.4(10)	C(11)-C(12)-Rh	71.6(5)
C(13)-C(12)-Rh	111.7(8)	C(14)-C(13)-C(12)	116.9(11)
C(13)-C(14)-C(7)	115.6(11)	F(3)-C(15)-F(2)	112.2(12)
F(3)-C(15)-F(1)	107.6(11)	F(2)-C(15)-F(1)	104.4(11)
F(3)-C(15)-S	111.8(9)	F(2)-C(15)-S	111.2(8)
F(1)-C(15)-S	109.3(9)		

Symmetry transformations used to generate equivalent atoms:

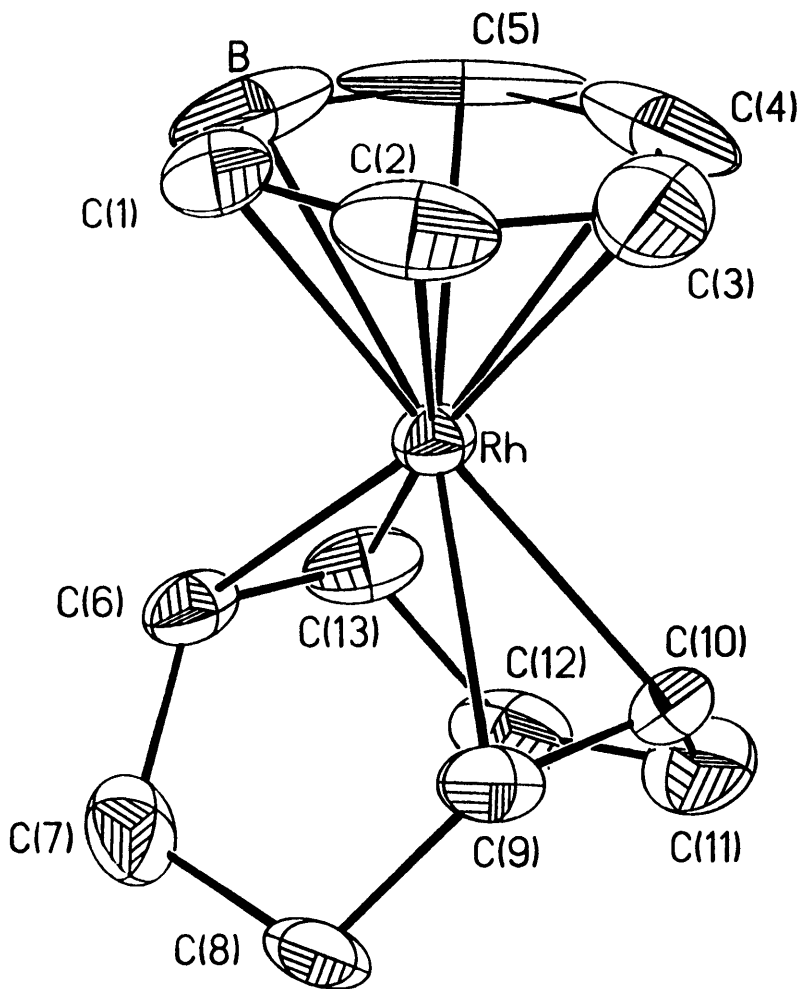


Table 1. Crystal data and structure refinement for 1.

A. Crystal Data

Identification code	96199
Empirical formula	$C_{13}H_{18}BRh$
Formula weight	287.99
Temperature	183(2) K
Wavelength	0.71073 Å
Crystal morphology	rhombus-shaped plate
Crystal size	.08 x .23 x .26 mm
Crystal system	Monoclinic
Space group	$P2_1/c$
Unit cell dimensions	$a = 8.247(3) \text{ \AA}$ $\alpha = 90^\circ$ $b = 13.393(7) \text{ \AA}$ $\beta = 107.01(2)^\circ$ $c = 11.002(3) \text{ \AA}$ $\gamma = 90^\circ$
Volume, Z	$1162.0(8) \text{ \AA}^3$, 4
Density (calculated)	1.646 Mg/m^3
Absorption coefficient	1.431 mm^{-1}
F(000)	584

B. Data Collection and Reduction

Diffractometer	Siemens SMART/CCD
Scan Type	ω Scans
Scan angle	0.30°
θ range for data collection	2.46 to 23.24°

Reflections collected	2123
Independent reflections	1265 ($R_{int} = 0.0340$)
Absorption correction	None

C. Solution and Refinement

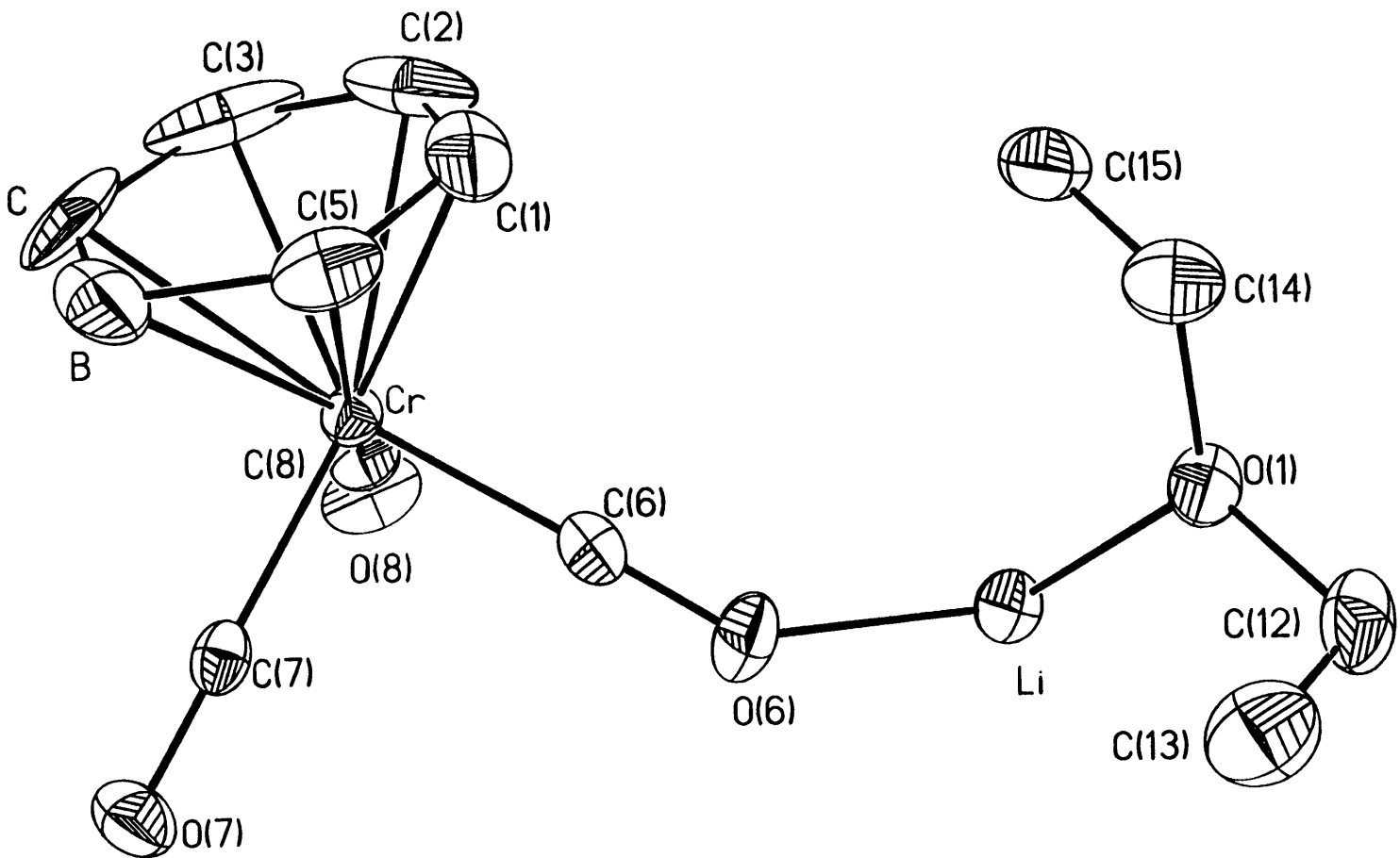
Refinement method	Full-matrix least-squares on F^2
Data / restraints / parameters	1261 / 0 / 136
Goodness-of-fit on F^2	1.151
Final R indices [$I > 2\sigma(I)$]	$R1 = 0.0288$, $wR2 = 0.0649$
R indices (all data)	$R1 = 0.0320$, $wR2 = 0.0702$
Largest diff. peak and hole	0.292 and $-0.271 \text{ e}\text{\AA}^{-3}$

Table 2. Atomic coordinates [$\times 10^4$] and equivalent isotropic displacement parameters [$\text{\AA}^2 \times 10^3$] for 1. $U(\text{eq})$ is defined as one third of the trace of the orthogonalized U_{ij} tensor.

	x	y	z	U(eq)
Rh	1104 (1)	3780 (1)	2533 (1)	34 (1)
C(1)	-1188 (7)	2875 (5)	2769 (10)	84 (3)
C(2)	-999 (8)	3708 (6)	3539 (7)	76 (2)
C(3)	-949 (8)	4696 (5)	2998 (9)	84 (3)
C(4)	-1191 (9)	4789 (7)	1703 (11)	94 (3)
C(5)	-1346 (10)	3926 (12)	927 (8)	135 (6)
C(6)	2734 (7)	2643 (4)	2224 (6)	46 (2)
C(7)	4112 (8)	2399 (4)	3399 (7)	62 (2)
C(8)	4632 (7)	3265 (4)	4337 (6)	52 (2)
C(9)	3213 (7)	4024 (4)	4168 (6)	45 (2)
C(10)	3031 (7)	4836 (4)	3330 (6)	56 (2)
C(11)	4108 (9)	5040 (5)	2486 (7)	82 (2)
C(12)	4260 (8)	4164 (5)	1663 (7)	68 (2)
C(13)	2772 (7)	3438 (5)	1421 (6)	55 (2)
B	-1293 (11)	2978 (9)	1521 (13)	89 (4)

Table 3. Bond lengths [Å] and angles [°] for 1.

Rh-C(10)	2.117(5)	Rh-C(6)	2.123(5)
Rh-C(9)	2.130(6)	Rh-C(13)	2.141(5)
Rh-B	2.239(9)	Rh-C(3)	2.267(6)
Rh-C(5)	2.270(9)	Rh-C(4)	2.287(7)
Rh-C(2)	2.316(6)	Rh-C(1)	2.322(5)
C(1)-B	1.358(14)	C(1)-C(2)	1.382(10)
C(2)-C(3)	1.456(10)	C(3)-C(4)	1.386(12)
C(4)-C(5)	1.420(14)	C(5)-B	1.42(2)
C(6)-C(13)	1.390(8)	C(6)-C(7)	1.487(9)
C(7)-C(8)	1.529(8)	C(8)-C(9)	1.519(7)
C(9)-C(10)	1.405(8)	C(10)-C(11)	1.486(8)
C(11)-C(12)	1.509(9)	C(12)-C(13)	1.527(8)
C(10)-Rh-C(6)	96.4(2)	C(10)-Rh-C(9)	38.6(2)
C(6)-Rh-C(9)	81.1(2)	C(10)-Rh-C(13)	81.3(2)
C(6)-Rh-C(13)	38.0(2)	C(9)-Rh-C(13)	90.7(2)
C(10)-Rh-B	166.7(4)	C(6)-Rh-B	94.8(3)
C(9)-Rh-B	151.4(4)	C(13)-Rh-B	103.6(3)
C(10)-Rh-C(3)	93.7(2)	C(6)-Rh-C(3)	166.8(2)
C(9)-Rh-C(3)	101.9(3)	C(13)-Rh-C(3)	153.1(3)
B-Rh-C(3)	76.3(3)	C(10)-Rh-C(5)	130.9(4)
C(6)-Rh-C(5)	113.5(4)	C(9)-Rh-C(5)	164.8(4)
C(13)-Rh-C(5)	98.5(3)	B-Rh-C(5)	36.8(4)
C(3)-Rh-C(5)	64.9(3)	C(10)-Rh-C(4)	101.8(3)
C(6)-Rh-C(4)	148.0(4)	C(9)-Rh-C(4)	128.5(3)
C(13)-Rh-C(4)	119.5(3)	B-Rh-C(4)	65.0(4)
C(3)-Rh-C(4)	35.4(3)	C(5)-Rh-C(4)	36.3(4)
C(10)-Rh-C(2)	113.9(3)	C(6)-Rh-C(2)	130.1(3)
C(9)-Rh-C(2)	98.2(2)	C(13)-Rh-C(2)	163.8(3)
B-Rh-C(2)	62.8(3)	C(3)-Rh-C(2)	37.0(3)
C(5)-Rh-C(2)	75.8(3)	C(4)-Rh-C(2)	64.4(3)
C(10)-Rh-C(1)	147.0(3)	C(6)-Rh-C(1)	102.6(2)
C(9)-Rh-C(1)	118.4(3)	C(13)-Rh-C(1)	129.2(3)
B-Rh-C(1)	34.6(3)	C(3)-Rh-C(1)	64.6(3)
C(5)-Rh-C(1)	64.2(3)	C(4)-Rh-C(1)	75.4(3)
C(2)-Rh-C(1)	34.7(3)	B-C(1)-C(2)	120.1(7)
B-C(1)-Rh	69.3(4)	C(2)-C(1)-Rh	72.4(3)
C(1)-C(2)-C(3)	119.6(7)	C(1)-C(2)-Rh	72.9(3)
C(3)-C(2)-Rh	69.7(3)	C(4)-C(3)-C(2)	119.3(7)
C(4)-C(3)-Rh	73.1(4)	C(2)-C(3)-Rh	73.3(3)
C(3)-C(4)-C(5)	120.3(8)	C(3)-C(4)-Rh	71.5(4)
C(5)-C(4)-Rh	71.2(5)	C(4)-C(5)-B	117.7(7)
C(4)-C(5)-Rh	72.5(5)	B-C(5)-Rh	70.4(6)
C(13)-C(6)-C(7)	124.6(5)	C(13)-C(6)-Rh	71.7(3)
C(7)-C(6)-Rh	112.2(3)	C(6)-C(7)-C(8)	114.3(5)
C(9)-C(8)-C(7)	111.8(5)	C(10)-C(9)-C(8)	122.0(5)
C(10)-C(9)-Rh	70.2(4)	C(8)-C(9)-Rh	114.3(4)
C(9)-C(10)-C(11)	125.7(5)	C(9)-C(10)-Rh	71.2(3)
C(11)-C(10)-Rh	112.2(4)	C(10)-C(11)-C(12)	113.7(5)
C(11)-C(12)-C(13)	113.3(5)	C(6)-C(13)-C(12)	122.9(6)
C(6)-C(13)-Rh	70.3(3)	C(12)-C(13)-Rh	112.5(4)
C(1)-B-C(5)	122.6(8)	C(1)-B-Rh	76.1(5)
C(5)-B-Rh	72.8(5)		



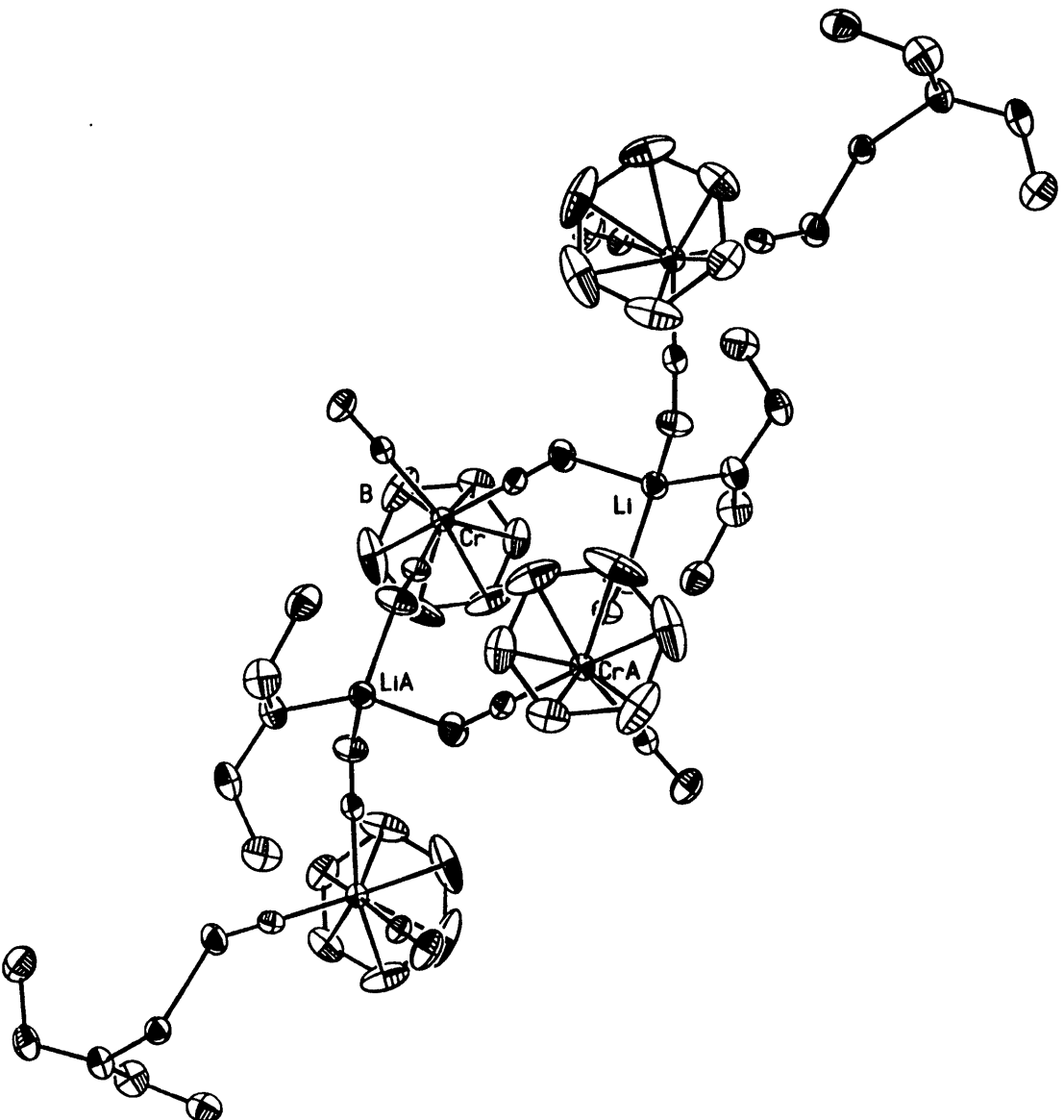


Table 1. Crystal data and structure refinement for 1.

A. Crystal Data

Identification code	97006
Empirical formula	$C_{12}H_{16}BCrLiO_4$
Formula weight	294.00
Temperature	293(2) K
Wavelength	0.71073 Å
Crystal morphology	yellow block
Crystal size	0.20 x 0.15 x 0.10 mm
Crystal system	Orthorhombic
Space group	Pbca
Unit cell dimensions	$a = 11.09(2) \text{ \AA}$ $\alpha = 90^\circ$ $b = 12.05(2) \text{ \AA}$ $\beta = 90^\circ$ $c = 21.54(4) \text{ \AA}$ $\gamma = 90^\circ$
Volume, Z	$2876(8) \text{ \AA}^3, 8$
Density (calculated)	1.358 Mg/m^3
Absorption coefficient	0.798 mm^{-1}
F(000)	1216

B. Data Collection and Reduction

Diffractometer	Siemens SMART/CCD
Scan Type	ω Scans
Scan angle	0.30°
θ range for data collection	2.64 to 23.32°

Reflections collected	3560
Independent reflections	1789 ($R_{int} = 0.0347$)
Absorption correction	None

C. Solution and Refinement

Refinement method	Full-matrix least-squares on F^2
Data / restraints / parameters	1789 / 0 / 172
Goodness-of-fit on F^2	1.299
Final R indices [$I > 2\sigma(I)$]	$R1 = 0.0470$, $wR2 = 0.0955$
R indices (all data)	$R1 = 0.0570$, $wR2 = 0.1005$
Largest diff. peak and hole	0.198 and $-0.227 \text{ e}\text{\AA}^{-3}$

Table 2. Atomic coordinates [$\times 10^4$] and equivalent isotropic displacement parameters [$\text{\AA}^2 \times 10^3$] for 1. $U(\text{eq})$ is defined as one third of the trace of the orthogonalized U_{ij} tensor.

	x	y	z	U(eq)
Cr	-747 (1)	1621 (1)	3762 (1)	25 (1)
C(5)	-88 (5)	2194 (4)	2812 (2)	47 (1)
C(1)	244 (4)	1107 (4)	2904 (2)	51 (1)
C	-2194 (5)	1623 (8)	3020 (3)	87 (2)
C(2)	-571 (7)	296 (4)	3057 (2)	67 (2)
B	-1368 (7)	2519 (6)	2845 (3)	68 (2)
C(6)	649 (4)	1685 (3)	4191 (2)	30 (1)
O(8)	-1779 (3)	462 (3)	4858 (2)	53 (1)
C(8)	-1371 (4)	895 (3)	4414 (2)	33 (1)
Li	2779 (6)	743 (5)	4831 (3)	34 (2)
C(3)	-1773 (7)	546 (7)	3117 (3)	86 (3)
O(7)	-1594 (3)	3670 (2)	4395 (2)	45 (1)
C(7)	-1245 (3)	2872 (3)	4127 (2)	28 (1)
O(6)	1543 (3)	1729 (2)	4481 (2)	44 (1)
O(1)	4087 (2)	602 (2)	4263 (1)	37 (1)
C(12)	5141 (4)	1296 (4)	4335 (3)	49 (1)
C(14)	3918 (4)	204 (4)	3643 (2)	53 (1)
C(13)	4940 (5)	2459 (4)	4095 (3)	62 (2)
C(15)	2911 (4)	-612 (4)	3634 (2)	53 (1)

Table 3. Bond lengths [Å] and angles [°] for 1.

Cr-C(7)	1.787(5)	Cr-C(8)	1.793(5)
Cr-C(6)	1.804(5)	Cr-C(2)	2.211(5)
Cr-C(3)	2.213(6)	Cr-C(1)	2.237(5)
Cr-C	2.264(6)	Cr-C(5)	2.279(6)
Cr-B	2.354(7)	C(5)-C(1)	1.374(7)
C(5)-B	1.474(9)	C(1)-C(2)	1.371(8)
C-C(3)	1.395(10)	C-B	1.465(10)
C(2)-C(3)	1.372(9)	C(6)-O(6)	1.173(5)
O(8)-C(8)	1.179(5)	O(8)-Li#1	1.946(7)
Li-O(1)	1.904(8)	Li-O(8)#1	1.946(7)
Li-O(7)#2	1.940(8)	Li-O(6)	1.964(7)
O(7)-C(7)	1.185(5)	O(7)-Li#3	1.940(8)
O(1)-C(14)	1.431(6)	O(1)-C(12)	1.445(5)
C(12)-C(13)	1.509(7)	C(14)-C(15)	1.488(7)
C(7)-Cr-C(8)	87.0(2)	C(7)-Cr-C(6)	90.2(2)
C(8)-Cr-C(6)	87.2(2)	C(7)-Cr-C(2)	159.7(2)
C(8)-Cr-C(2)	102.7(2)	C(6)-Cr-C(2)	107.9(2)
C(7)-Cr-C(3)	127.7(3)	C(8)-Cr-C(3)	90.4(2)
C(6)-Cr-C(3)	141.9(3)	C(2)-Cr-C(3)	36.1(3)
C(7)-Cr-C(1)	138.4(2)	C(8)-Cr-C(1)	134.5(2)
C(6)-Cr-C(1)	90.8(2)	C(2)-Cr-C(1)	35.9(2)
C(3)-Cr-C(1)	64.7(2)	C(7)-Cr-C	95.2(3)
C(8)-Cr-C	106.2(3)	C(6)-Cr-C	165.7(2)
C(2)-Cr-C	65.1(3)	C(3)-Cr-C	36.3(3)
C(1)-Cr-C	76.5(2)	C(7)-Cr-C(5)	103.8(2)
C(8)-Cr-C(5)	166.9(2)	C(6)-Cr-C(5)	99.9(2)
C(2)-Cr-C(5)	64.8(2)	C(3)-Cr-C(5)	77.2(2)
C(1)-Cr-C(5)	35.4(2)	C-Cr-C(5)	66.0(2)
C(7)-Cr-B	83.8(2)	C(8)-Cr-B	140.2(3)
C(6)-Cr-B	131.4(3)	C(2)-Cr-B	77.4(2)
C(3)-Cr-B	66.0(3)	C(1)-Cr-B	65.0(2)
C-Cr-B	36.9(3)	C(5)-Cr-B	37.0(2)
C(1)-C(5)-B	120.3(5)	C(1)-C(5)-Cr	70.6(3)
B-C(5)-Cr	74.2(3)	C(5)-C(1)-C(2)	122.5(5)
C(5)-C(1)-Cr	74.0(3)	C(2)-C(1)-Cr	71.0(3)
C(3)-C-B	121.0(5)	C(3)-C-Cr	69.9(3)
B-C-Cr	74.9(3)	C(3)-C(2)-C(1)	120.4(5)
C(3)-C(2)-Cr	72.0(3)	C(1)-C(2)-Cr	73.1(3)
C-B-C(5)	114.7(5)	C-B-Cr	68.2(3)
C(5)-B-Cr	68.7(3)	O(6)-C(6)-Cr	178.7(4)
C(8)-O(8)-Li#1	145.8(4)	O(8)-C(8)-Cr	176.9(4)
O(1)-Li-O(8)#1	126.1(4)	O(1)-Li-O(7)#2	108.1(4)
O(8)#1-Li-O(7)#2	100.4(4)	O(1)-Li-O(6)	109.8(4)
O(8)#1-Li-O(6)	100.7(3)	O(7)#2-Li-O(6)	111.0(4)
C(2)-C(3)-C	121.0(5)	C(2)-C(3)-Cr	71.9(3)
C-C(3)-Cr	73.9(3)	C(7)-O(7)-Li#3	146.2(4)
O(7)-C(7)-Cr	176.6(4)	C(6)-O(6)-Li	140.0(4)
C(14)-O(1)-C(12)	113.5(3)	C(14)-O(1)-Li	121.9(4)
C(12)-O(1)-Li	119.8(4)	O(1)-C(12)-C(13)	112.4(4)
O(1)-C(14)-C(15)	109.4(4)		

Symmetry transformations used to generate equivalent atoms:

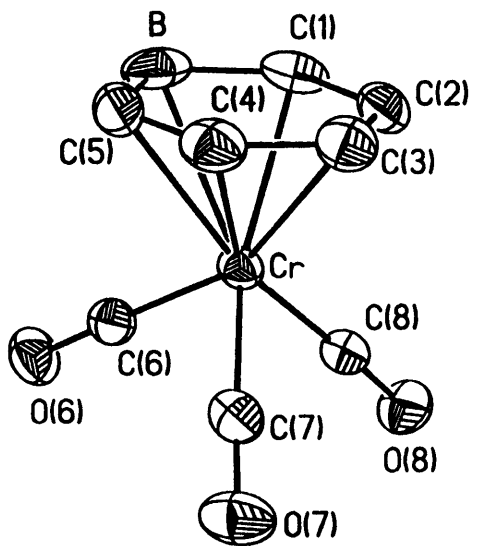
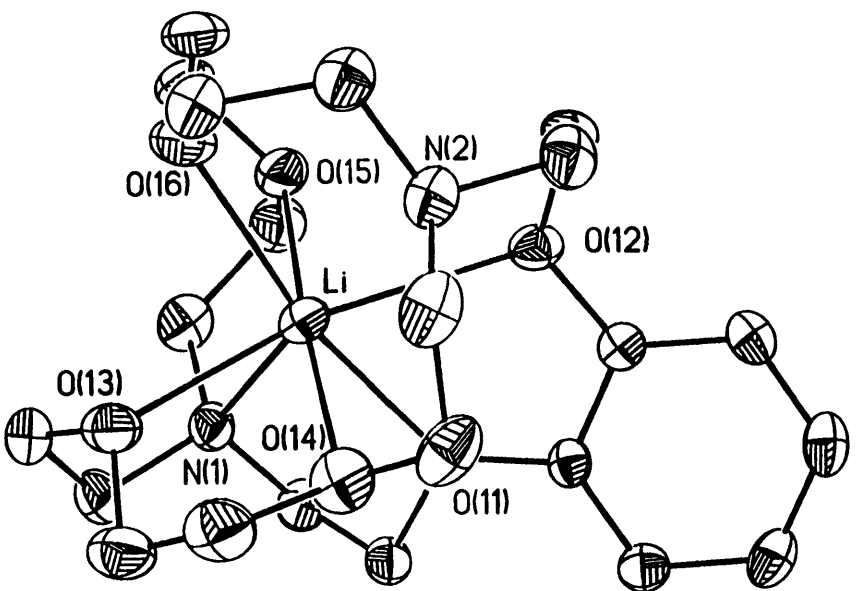


Table 6. Crystal data and structure refinement for 3.

A. Crystal Data

Identification code	→ 97009
Empirical formula	$C_{30}H_{42}BCrLiN_2O_9$
Formula weight	644.41
Temperature	183(2) K
Wavelength	0.71073 Å
Crystal morphology	parallelepi
Crystal size	.23 x .30 x .46 mm
Crystal system	Monoclinic
Space group	$P2_1/c$
Unit cell dimensions	$a = 10.9469(2) \text{ \AA}$ $\alpha = 90^\circ$ $b = 13.18610(10) \text{ \AA}$ $\beta = 94.6310(10)^\circ$ $c = 21.6955(4) \text{ \AA}$ $\gamma = 90^\circ$
Volume, Z	$3121.45(8) \text{ \AA}^3$, 4
Density (calculated)	1.371 Mg/m^3
Absorption coefficient	0.422 mm^{-1}
F(000)	1360

B. Data Collection and Reduction

Diffractometer	Siemens SMART/CCD
Scan Type	ω Scans
Scan angle	0.30°
θ range for data collection	1.81 to 23.25°
Limiting indices	$-12 \leq h \leq 8$, $-11 \leq k \leq 14$, $-24 \leq l \leq 21$

Reflections collected	12320
Independent reflections	4449 ($R_{int} = 0.0506$)
Absorption correction	None

C. Solution and Refinement

Refinement method	Full-matrix least-squares on F^2
Data / restraints / parameters	4447 / 0 / 397
Goodness-of-fit on F^2	1.130
Final R indices [$I > 2\sigma(I)$]	$R1 = 0.0433$, $wR2 = 0.1042$
R indices (all data)	$R1 = 0.0485$, $wR2 = 0.1098$
Largest diff. peak and hole	0.237 and $-0.509 \text{ e}\text{\AA}^{-3}$

Table 7. Atomic coordinates [$\times 10^4$] and equivalent isotropic displacement parameters [$\text{\AA}^2 \times 10^3$] for 3. $U(\text{eq})$ is defined as one third of the trace of the orthogonalized U_{ij} tensor.

	x	y	z	U(eq)
Cr	461(1)	7373(1)	4704(1)	35(1)
O(6)	3100(2)	7060(2)	4496(1)	56(1)
O(7)	817(2)	6446(2)	5964(1)	64(1)
O(8)	1236(2)	9303(2)	5344(1)	53(1)
O(11)	5066(2)	2280(1)	3616(1)	44(1)
O(12)	3051(2)	2589(2)	2986(1)	42(1)
O(13)	5112(2)	-623(2)	3381(1)	50(1)
O(14)	3697(2)	468(2)	4074(1)	55(1)
O(15)	4531(2)	1325(2)	2089(1)	60(1)
O(16)	3134(2)	-259(2)	2377(1)	65(1)
N(1)	6584(2)	1017(2)	2992(1)	40(1)
N(2)	1579(2)	828(2)	3179(1)	47(1)
C(1)	-490(3)	8097(3)	3842(1)	52(1)
C(2)	-1305(3)	8032(2)	4302(1)	49(1)
C(3)	-1553(3)	7134(2)	4584(2)	50(1)
C(4)	-1005(3)	6236(2)	4432(2)	56(1)
C(5)	-185(3)	6199(3)	3984(2)	63(1)
C(6)	2063(3)	7180(2)	4574(1)	41(1)
C(7)	679(3)	6784(2)	5463(2)	45(1)
C(8)	900(2)	8560(2)	5089(1)	38(1)
C(9)	7049(2)	1894(2)	3352(1)	46(1)
C(10)	6300(2)	2131(2)	3883(1)	42(1)
C(11)	4341(2)	3001(2)	3862(1)	33(1)
C(12)	4607(2)	3528(2)	4405(1)	41(1)
C(13)	3803(3)	4269(2)	4581(1)	49(1)
C(14)	2737(3)	4469(2)	4223(1)	48(1)
C(15)	2445(2)	3918(2)	3690(1)	42(1)
C(16)	3233(2)	3180(2)	3506(1)	34(1)
C(17)	1822(3)	2490(2)	2706(1)	48(1)
C(18)	1065(3)	1851(2)	3104(2)	52(1)
C(19)	7120(3)	61(2)	3232(2)	51(1)
C(20)	6239(3)	-804(2)	3109(2)	53(1)
C(21)	5181(3)	-810(3)	4028(1)	61(1)
C(22)	3949(3)	-560(3)	4236(2)	62(1)
C(23)	2525(3)	796(3)	4243(1)	59(1)
C(24)	1487(3)	421(3)	3800(1)	56(1)
C(25)	6721(3)	1150(3)	2331(1)	52(1)
C(26)	5699(3)	1790(3)	2034(2)	63(1)
C(27)	4251(3)	549(3)	1641(2)	65(1)
C(28)	3038(3)	121(3)	1761(1)	64(1)
C(29)	2011(3)	-675(3)	2557(2)	63(1)
C(30)	1095(3)	141(2)	2690(2)	55(1)
B	140(3)	7158(4)	3636(2)	71(1)
Li	4186(4)	872(3)	3063(2)	42(1)

Table 8. Bond lengths [Å] and angles [°] for 3.

Cr-C(6)	1.817(3)	Cr-C(8)	1.820(3)
Cr-C(7)	1.820(3)	Cr-C(3)	2.222(3)
Cr-C(2)	2.232(3)	Cr-C(4)	2.241(3)
Cr-C(5)	2.271(3)	Cr-C(1)	2.275(3)
Cr-B	2.332(4)	O(6)-C(6)	1.171(3)
O(7)-C(7)	1.173(3)	O(8)-C(8)	1.170(3)
O(11)-C(11)	1.375(3)	O(11)-C(10)	1.440(3)
O(11)-Li	2.371(5)	O(12)-C(16)	1.373(3)
O(12)-C(17)	1.437(3)	O(12)-Li	2.581(5)
O(13)-C(21)	1.421(4)	O(13)-C(20)	1.430(4)
O(13)-Li	2.297(5)	O(14)-C(22)	1.422(4)
O(14)-C(23)	1.429(4)	O(14)-Li	2.359(5)
O(15)-C(27)	1.426(4)	O(15)-C(26)	1.431(4)
O(15)-Li	2.258(5)	O(16)-C(28)	1.422(4)
O(16)-C(29)	1.429(4)	O(16)-Li	2.343(5)
N(1)-C(9)	1.463(4)	N(1)-C(25)	1.464(4)
N(1)-C(19)	1.467(4)	N(1)-Li	2.649(5)
N(2)-C(30)	1.460(4)	N(2)-C(24)	1.463(4)
N(2)-C(18)	1.464(4)	C(1)-C(2)	1.395(4)
C(1)-B	1.503(6)	C(2)-C(3)	1.370(4)
C(3)-C(4)	1.379(5)	C(4)-C(5)	1.376(5)
C(5)-B	1.529(6)	C(9)-C(10)	1.501(4)
C(11)-C(12)	1.378(4)	C(11)-C(16)	1.404(4)
C(12)-C(13)	1.389(4)	C(13)-C(14)	1.373(4)
C(14)-C(15)	1.382(4)	C(15)-C(16)	1.381(4)
C(17)-C(18)	1.503(4)	C(19)-C(20)	1.504(4)
C(21)-C(22)	1.494(5)	C(23)-C(24)	1.510(5)
C(25)-C(26)	1.506(5)	C(27)-C(28)	1.486(5)
C(29)-C(30)	1.515(4)		
C(6)-Cr-C(8)	88.24(12)	C(6)-Cr-C(7)	91.34(13)
C(8)-Cr-C(7)	86.65(12)	C(6)-Cr-C(3)	157.41(12)
C(8)-Cr-C(3)	113.50(12)	C(7)-Cr-C(3)	95.80(12)
C(6)-Cr-C(2)	144.17(12)	C(8)-Cr-C(2)	91.90(11)
C(7)-Cr-C(2)	124.45(12)	C(3)-Cr-C(2)	35.84(11)
C(6)-Cr-C(4)	123.04(12)	C(8)-Cr-C(4)	148.58(12)
C(7)-Cr-C(4)	89.51(12)	C(3)-Cr-C(4)	36.00(12)
C(2)-Cr-C(4)	65.02(12)	C(6)-Cr-C(5)	92.77(12)
C(8)-Cr-C(5)	163.28(13)	C(7)-Cr-C(5)	110.00(13)
C(3)-Cr-C(5)	64.65(12)	C(2)-Cr-C(5)	77.58(11)
C(4)-Cr-C(5)	35.50(12)	C(6)-Cr-C(1)	108.32(12)
C(8)-Cr-C(1)	95.89(12)	C(7)-Cr-C(1)	160.22(12)
C(3)-Cr-C(1)	65.16(11)	C(2)-Cr-C(1)	36.04(11)
C(4)-Cr-C(1)	78.09(12)	C(5)-Cr-C(1)	67.95(12)
C(6)-Cr-B	84.17(12)	C(8)-Cr-B	125.0(2)
C(7)-Cr-B	147.7(2)	C(3)-Cr-B	78.36(12)
C(2)-Cr-B	66.61(13)	C(4)-Cr-B	67.0(2)
C(5)-Cr-B	38.8(2)	C(1)-Cr-B	38.0(2)
C(11)-O(11)-C(10)	119.3(2)	C(11)-O(11)-Li	120.9(2)
C(10)-O(11)-Li	115.3(2)	C(16)-O(12)-C(17)	117.9(2)
C(16)-O(12)-Li	114.0(2)	C(17)-O(12)-Li	112.2(2)
C(21)-O(13)-C(20)	113.6(2)	C(21)-O(13)-Li	115.6(2)
C(20)-O(13)-Li	113.2(2)	C(22)-O(14)-C(23)	112.6(2)
C(22)-O(14)-Li	113.1(2)	C(23)-O(14)-Li	116.5(2)
C(27)-O(15)-C(26)	113.3(2)	C(27)-O(15)-Li	113.9(2)

C(26)-O(15)-Li	114.2(2)	C(28)-O(16)-C(29)	113.0(2)
C(28)-O(16)-Li	111.6(2)	C(29)-O(16)-Li	117.4(2)
C(9)-N(1)-C(25)	111.6(2)	C(9)-N(1)-C(19)	112.2(2)
C(25)-N(1)-C(19)	112.4(2)	C(9)-N(1)-Li	109.2(2)
C(25)-N(1)-Li	104.3(2)	C(19)-N(1)-Li	106.7(2)
C(30)-N(2)-C(24)	113.2(2)	C(30)-N(2)-C(18)	112.2(2)
C(24)-N(2)-C(18)	112.7(2)	C(2)-C(1)-B	119.8(3)
C(2)-C(1)-Cr	70.3(2)	B-C(1)-Cr	73.0(2)
C(3)-C(2)-C(1)	122.3(3)	C(3)-C(2)-Cr	71.7(2)
C(1)-C(2)-Cr	73.7(2)	C(2)-C(3)-C(4)	121.9(3)
C(2)-C(3)-Cr	72.5(2)	C(4)-C(3)-Cr	72.7(2)
C(5)-C(4)-C(3)	121.4(3)	C(5)-C(4)-Cr	73.4(2)
C(3)-C(4)-Cr	71.3(2)	C(4)-C(5)-B	120.7(3)
C(4)-C(5)-Cr	71.1(2)	B-C(5)-Cr	72.8(2)
O(6)-C(6)-Cr	179.2(2)	O(7)-C(7)-Cr	177.1(3)
O(8)-C(8)-Cr	176.9(2)	N(1)-C(9)-C(10)	112.7(2)
O(11)-C(10)-C(9)	105.7(2)	O(11)-C(11)-C(12)	126.3(2)
O(11)-C(11)-C(16)	113.7(2)	C(12)-C(11)-C(16)	120.0(2)
C(11)-C(12)-C(13)	119.6(3)	C(14)-C(13)-C(12)	120.5(3)
C(13)-C(14)-C(15)	120.0(3)	C(16)-C(15)-C(14)	120.3(3)
O(12)-C(16)-C(15)	125.8(2)	O(12)-C(16)-C(11)	114.8(2)
C(15)-C(16)-C(11)	119.4(2)	O(12)-C(17)-C(18)	110.4(2)
N(2)-C(18)-C(17)	110.8(2)	N(1)-C(19)-C(20)	110.9(2)
O(13)-C(20)-C(19)	111.2(2)	O(13)-C(21)-C(22)	106.4(3)
O(14)-C(22)-C(21)	107.3(3)	O(14)-C(23)-C(24)	112.5(2)
N(2)-C(24)-C(23)	111.2(2)	N(1)-C(25)-C(26)	110.9(2)
O(15)-C(26)-C(25)	111.2(3)	O(15)-C(27)-C(28)	107.4(2)
O(16)-C(28)-C(27)	107.4(3)	O(16)-C(29)-C(30)	112.1(3)
N(2)-C(30)-C(29)	111.9(3)	C(1)-B-C(5)	113.9(3)
C(1)-B-Cr	69.0(2)	C(5)-B-Cr	68.5(2)
O(15)-Li-O(13)	113.9(2)	O(15)-Li-O(16)	71.6(2)
O(13)-Li-O(16)	80.0(2)	O(15)-Li-O(14)	176.0(2)
O(13)-Li-O(14)	69.8(2)	O(16)-Li-O(14)	108.1(2)
O(15)-Li-O(11)	100.1(2)	O(13)-Li-O(11)	111.6(2)
O(16)-Li-O(11)	168.0(2)	O(14)-Li-O(11)	79.7(2)
O(15)-Li-O(12)	79.8(2)	O(13)-Li-O(12)	166.1(2)
O(16)-Li-O(12)	107.9(2)	O(14)-Li-O(12)	96.6(2)
O(11)-Li-O(12)	61.35(12)	O(15)-Li-N(1)	71.62(14)
O(13)-Li-N(1)	70.35(14)	O(16)-Li-N(1)	116.5(2)
O(14)-Li-N(1)	111.8(2)	O(11)-Li-N(1)	66.98(13)
O(12)-Li-N(1)	114.0(2)		

Symmetry transformations used to generate equivalent atoms:

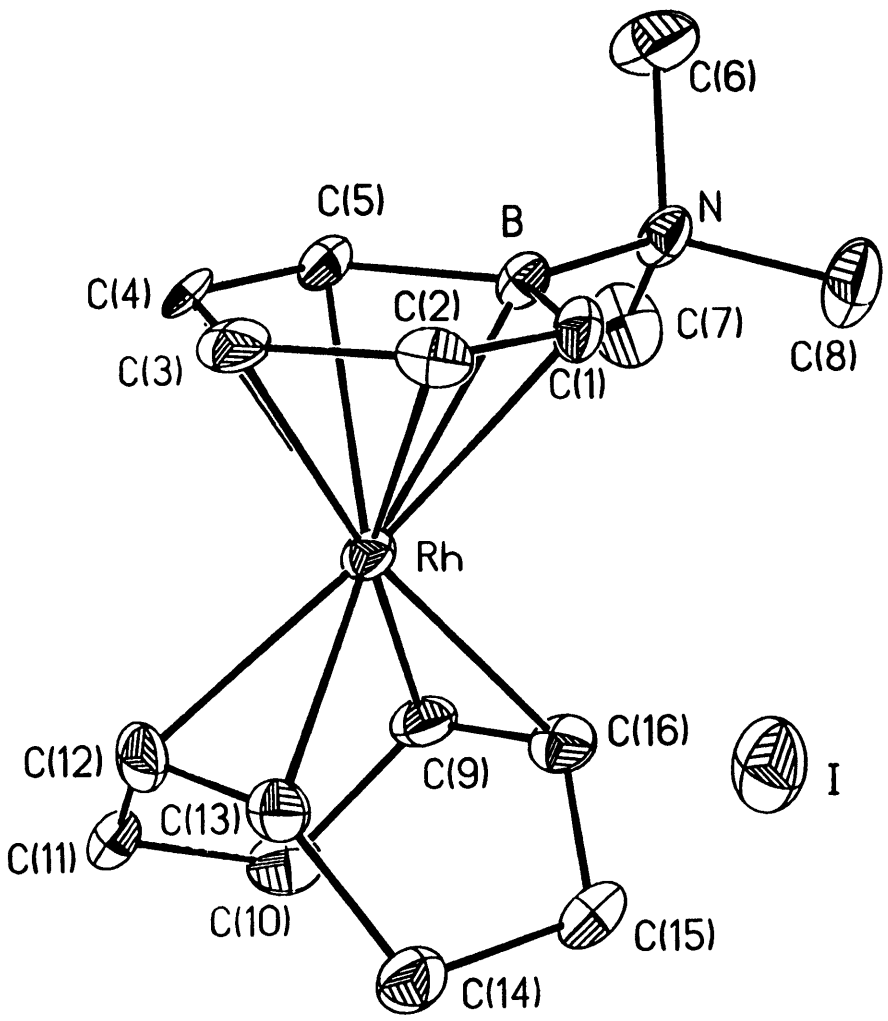


Table 1. Crystal data and structure refinement for 1.

A. Crystal Data

Identification code	97077
Empirical formula	$C_{16}H_{26}BINRh$
Formula weight	473.00
Temperature	183(2) K
Wavelength	0.71073 Å
Crystal morphology	needle
Crystal size	0.05 x 0.05 x 0.21 mm
Crystal system	Monoclinic
Space group	$P2_1/c$
Unit cell dimensions	$a = 10.0153(7) \text{ \AA}$ $\alpha = 90^\circ$ $b = 15.4985(10) \text{ \AA}$ $\beta = 110.7770(10)^\circ$ $c = 11.8622(8) \text{ \AA}$ $\gamma = 90^\circ$
Volume, Z	$1721.5(2) \text{ \AA}^3$, 4
Density (calculated)	1.825 Mg/m^3
Absorption coefficient	2.776 mm^{-1}
F(000)	928

B. Data Collection and Reduction

Diffractometer	Siemens SMART/CCD
Scan Type	ω Scans
Scan angle	0.30°
θ range for data collection	2.17 to 23.23°

Reflections collected	6874
Independent reflections	2459 ($R_{int} = 0.0780$)
Absorption correction	Semi-empirical from psi-scans
Max. and min. transmission	0.6967 and 0.3293

C. Solution and Refinement

Refinement method	Full-matrix least-squares on F^2
Data / restraints / parameters	2455 / 0 / 181
Goodness-of-fit on F^2	1.140
Final R indices [$I > 2\sigma(I)$]	$R_1 = 0.0457$, $wR_2 = 0.1011$
R indices (all data)	$R_1 = 0.0655$, $wR_2 = 0.1149$
Largest diff. peak and hole	0.898 and $-0.766 \text{ e}\text{\AA}^{-3}$

Table 2. Atomic coordinates [$\times 10^4$] and equivalent isotropic displacement parameters [$\text{\AA}^2 \times 10^3$] for 1. $U(\text{eq})$ is defined as one third of the trace of the orthogonalized U_{ij} tensor.

	x	y	z	$U(\text{eq})$
I	1244 (1)	3733 (1)	2268 (1)	41 (1)
Rh	3874 (1)	1136 (1)	1840 (1)	24 (1)
N	7484 (7)	1566 (5)	3999 (6)	29 (2)
C(1)	5206 (8)	2409 (5)	2460 (7)	29 (2)
C(2)	4219 (9)	2515 (5)	1295 (8)	34 (2)
C(3)	4168 (9)	1898 (6)	384 (7)	34 (2)
C(4)	5145 (8)	1215 (5)	566 (7)	29 (2)
C(5)	6194 (8)	1063 (5)	1705 (7)	29 (2)
C(6)	8834 (9)	1828 (9)	3830 (9)	64 (4)
C(7)	7630 (11)	659 (6)	4462 (9)	51 (3)
C(8)	7293 (10)	2128 (7)	4952 (8)	51 (3)
C(9)	3801 (9)	91 (6)	3027 (8)	34 (2)
C(10)	2672 (9)	-588 (6)	2408 (8)	38 (2)
C(11)	2102 (9)	-490 (6)	1038 (8)	38 (2)
C(12)	2078 (9)	421 (6)	648 (7)	34 (2)
C(13)	1583 (8)	1133 (5)	1100 (7)	28 (2)
C(14)	892 (9)	1058 (6)	2046 (8)	38 (2)
C(15)	1963 (9)	1174 (5)	3331 (8)	34 (2)
C(16)	3459 (9)	876 (6)	3458 (7)	32 (2)
B	6255 (9)	1674 (6)	2726 (8)	22 (2)

Table 3. Bond lengths [Å] and angles [°] for 1.

Rh-C(16)	2.142(8)	Rh-C(13)	2.146(8)
Rh-C(12)	2.158(8)	Rh-C(9)	2.165(8)
Rh-C(3)	2.196(8)	Rh-C(2)	2.294(8)
Rh-C(4)	2.298(7)	Rh-C(1)	2.349(8)
Rh-C(5)	2.388(8)	Rh-B	2.389(9)
N-C(6)	1.492(11)	N-C(8)	1.492(11)
N-C(7)	1.497(11)	N-B	1.583(10)
C(1)-C(2)	1.395(11)	C(1)-B	1.506(12)
C(2)-C(3)	1.431(12)	C(3)-C(4)	1.404(12)
C(4)-C(5)	1.407(11)	C(5)-B	1.521(12)
C(9)-C(16)	1.408(12)	C(9)-C(10)	1.529(12)
C(10)-C(11)	1.527(12)	C(11)-C(12)	1.484(12)
C(12)-C(13)	1.392(11)	C(13)-C(14)	1.517(12)
C(14)-C(15)	1.532(12)	C(15)-C(16)	1.523(11)
C(16)-Rh-C(13)	81.2(3)	C(16)-Rh-C(12)	96.2(3)
C(13)-Rh-C(12)	37.8(3)	C(16)-Rh-C(9)	38.2(3)
C(13)-Rh-C(9)	89.2(3)	C(12)-Rh-C(9)	80.2(3)
C(16)-Rh-C(3)	158.3(4)	C(13)-Rh-C(3)	95.9(3)
C(12)-Rh-C(3)	94.3(3)	C(9)-Rh-C(3)	163.5(3)
C(16)-Rh-C(2)	121.6(3)	C(13)-Rh-C(2)	97.7(3)
C(12)-Rh-C(2)	117.9(3)	C(9)-Rh-C(2)	157.4(3)
C(3)-Rh-C(2)	37.1(3)	C(16)-Rh-C(4)	158.1(3)
C(13)-Rh-C(4)	119.5(3)	C(12)-Rh-C(4)	97.1(3)
C(9)-Rh-C(4)	128.5(3)	C(3)-Rh-C(4)	36.3(3)
C(2)-Rh-C(4)	65.9(3)	C(16)-Rh-C(1)	98.4(3)
C(13)-Rh-C(1)	122.4(3)	C(12)-Rh-C(1)	152.3(3)
C(9)-Rh-C(1)	124.8(3)	C(3)-Rh-C(1)	64.9(3)
C(2)-Rh-C(1)	34.9(3)	C(4)-Rh-C(1)	77.1(3)
C(16)-Rh-C(5)	123.6(3)	C(13)-Rh-C(5)	153.8(3)
C(12)-Rh-C(5)	122.4(3)	C(9)-Rh-C(5)	105.4(3)
C(3)-Rh-C(5)	64.4(3)	C(2)-Rh-C(5)	77.2(3)
C(4)-Rh-C(5)	34.9(3)	C(1)-Rh-C(5)	66.6(3)
C(16)-Rh-B	98.7(3)	C(13)-Rh-B	159.4(3)
C(12)-Rh-B	159.6(3)	C(9)-Rh-B	103.5(3)
C(3)-Rh-B	76.5(3)	C(2)-Rh-B	64.7(3)
C(4)-Rh-B	64.6(3)	C(1)-Rh-B	37.1(3)
C(5)-Rh-B	37.1(3)	C(6)-N-C(8)	108.0(7)
C(6)-N-C(7)	109.2(8)	C(8)-N-C(7)	107.0(7)
C(6)-N-B	106.1(6)	C(8)-N-B	113.3(6)
C(7)-N-B	113.0(7)	C(2)-C(1)-B	119.6(7)
C(2)-C(1)-Rh	70.4(5)	B-C(1)-Rh	72.9(5)
C(1)-C(2)-C(3)	119.5(8)	C(1)-C(2)-Rh	74.7(5)
C(3)-C(2)-Rh	67.7(4)	C(4)-C(3)-C(2)	123.5(8)
C(4)-C(3)-Rh	75.8(5)	C(2)-C(3)-Rh	75.2(5)
C(3)-C(4)-C(5)	121.1(7)	C(3)-C(4)-Rh	67.9(4)
C(5)-C(4)-Rh	76.0(4)	C(4)-C(5)-B	117.7(7)
C(4)-C(5)-Rh	69.1(4)	B-C(5)-Rh	71.5(4)
C(16)-C(9)-C(10)	122.4(7)	C(16)-C(9)-Rh	70.1(5)
C(10)-C(9)-Rh	113.1(6)	C(11)-C(10)-C(9)	112.1(7)
C(12)-C(11)-C(10)	112.6(7)	C(13)-C(12)-C(11)	127.1(8)
C(13)-C(12)-Rh	70.7(5)	C(11)-C(12)-Rh	111.6(5)
C(12)-C(13)-C(14)	122.8(7)	C(12)-C(13)-Rh	71.6(5)
C(14)-C(13)-Rh	113.6(5)	C(13)-C(14)-C(15)	112.6(7)
C(16)-C(15)-C(14)	112.3(7)	C(9)-C(16)-C(15)	125.7(8)

C(9)-C(16)-Rh	71.8(5)	C(15)-C(16)-Rh	110.5(5)
C(1)-B-C(5)	118.5(7)	C(1)-B-N	121.9(7)
C(5)-B-N	119.5(7)	C(1)-B-Rh	70.0(4)
C(5)-B-Rh	71.4(4)	N-B-Rh	134.4(6)

Symmetry transformations used to generate equivalent atoms:

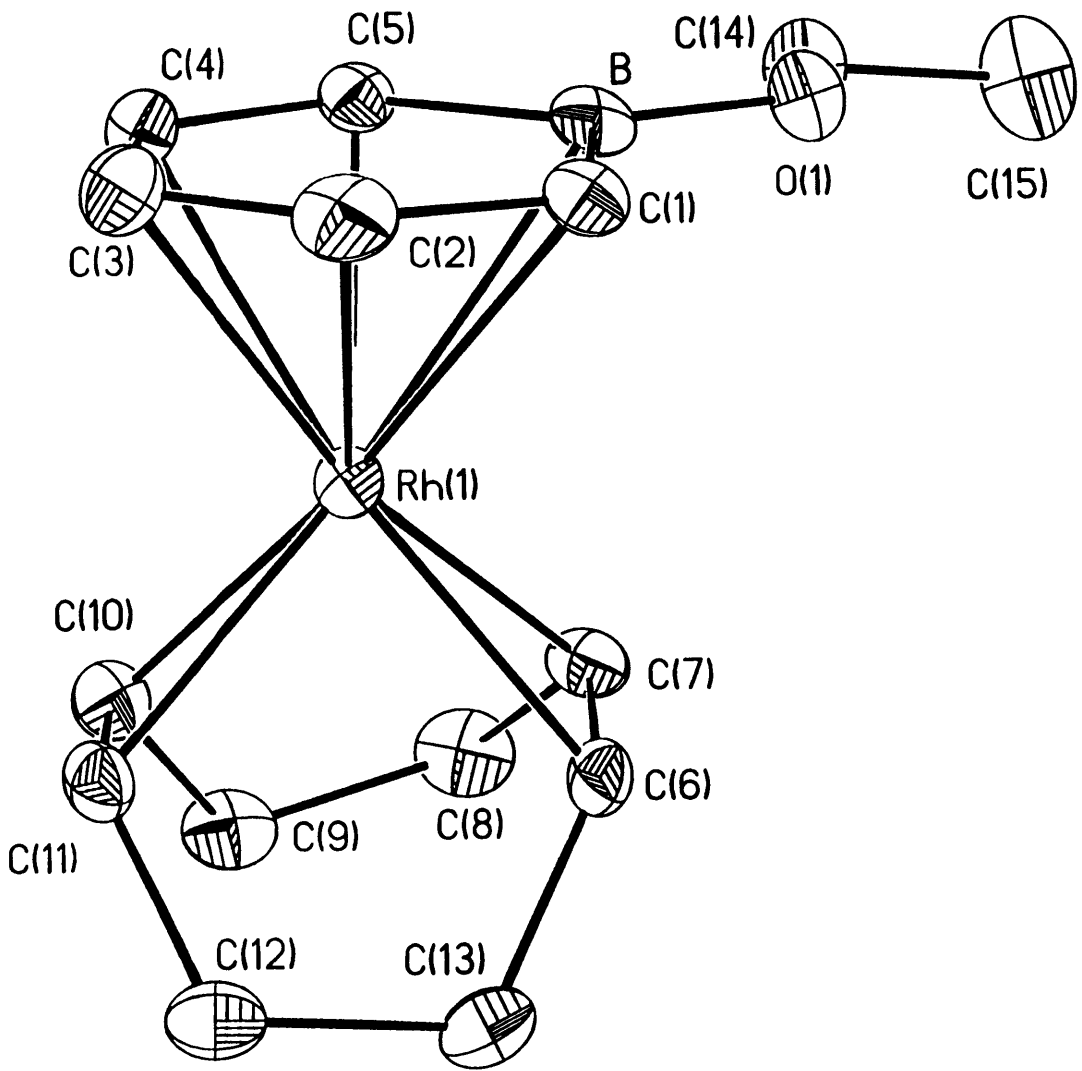


Table 1. Crystal data and structure refinement for 1.

A. Crystal Data

Identification code	9710 9 ₀
Empirical formula	C ₁₅ H ₂₂ BORh
Formula weight	332.05
Temperature	293(2) K
Wavelength	0.71073 Å
Crystal morphology	prism
Crystal size	.17 x .17 x .12 mm
Crystal system	Triclinic
Space group	P $\bar{1}$
Unit cell dimensions	a = 6.6593(3) Å alpha = 78.0780(10) ^o b = 8.2992(3) Å beta = 78.129(2) ^o c = 14.0348(6) Å gamma = 67.9650(10) ^o
Volume, Z	696.43(5) Å ³ , 2
Density (calculated)	1.583 Mg/m ³
Absorption coefficient	1.211 mm ⁻¹
F(000)	340

B. Data Collection and Reduction

Diffractometer	Siemens SMART/CCD
Scan Type	ω Scans
Scan angle	0.30 ^o
θ range for data collection	1.50 to 23.28 ^o
Limiting indices	-7 \leq h \leq 7, -8 \leq k \leq 9, -11 \leq l \leq 15

Reflections collected	2889
Independent reflections	1976 ($R_{int} = 0.0425$)
Absorption correction	Semi-empirical from psi-scans
Max. and min. transmission	0.4717 and 0.2505

C. Solution and Refinement

Refinement method	Full-matrix least-squares on F^2
Data / restraints / parameters	1974 / 0 / 163
Goodness-of-fit on F^2	1.175
Final R indices [$I > 2\sigma(I)$]	$R_1 = 0.0515$, $wR_2 = 0.1315$
R indices (all data)	$R_1 = 0.0547$, $wR_2 = 0.1419$
Largest diff. peak and hole	1.314 and $-1.504 \text{ e}\text{\AA}^{-3}$

Table 2. Atomic coordinates [$\times 10^4$] and equivalent isotropic displacement parameters [$\text{\AA}^2 \times 10^3$] for 1. $U(\text{eq})$ is defined as one third of the trace of the orthogonalized U_{ij} tensor.

	x	y	z	U(eq)
Rh(1)	-1227(1)	5423(1)	-1977(1)	20(1)
O(1)	2350(8)	7653(7)	-3216(3)	28(1)
B	417(14)	7693(11)	-2597(6)	27(2)
C(1)	501(12)	6999(9)	-1509(5)	26(2)
C(2)	-1413(13)	7095(10)	-841(6)	33(2)
C(3)	-3434(13)	7655(10)	-1198(6)	34(2)
C(4)	-3638(12)	8257(10)	-2200(6)	32(2)
C(5)	-1831(12)	8289(9)	-2911(6)	27(2)
C(6)	1451(11)	2995(9)	-1968(5)	27(2)
C(7)	1174(13)	3771(10)	-2951(5)	30(2)
C(8)	114(15)	3186(12)	-3600(6)	41(2)
C(9)	-2056(14)	2958(11)	-3099(6)	38(2)
C(10)	-3242(13)	4196(10)	-2331(6)	31(2)
C(11)	-2973(12)	3681(10)	-1341(5)	28(2)
C(12)	-1505(13)	1913(10)	-917(6)	32(2)
C(13)	835(13)	1417(10)	-1475(6)	34(2)
C(14)	2373(13)	8066(11)	-4262(5)	34(2)
C(15)	4659(16)	7688(15)	-4754(6)	54(3)

Table 3. Bond lengths [\AA] and angles [$^{\circ}$] for 1.

Rh(1)-C(11)	2.131(7)	Rh(1)-C(7)	2.130(7)
Rh(1)-C(6)	2.132(7)	Rh(1)-C(10)	2.142(7)
Rh(1)-C(3)	2.218(8)	Rh(1)-C(2)	2.277(7)
Rh(1)-C(1)	2.294(7)	Rh(1)-C(4)	2.297(7)
Rh(1)-C(5)	2.398(7)	Rh(1)-B	2.446(8)
O(1)-B	1.390(10)	O(1)-C(14)	1.434(9)
B-C(5)	1.519(11)	B-C(1)	1.521(11)
C(1)-C(2)	1.404(11)	C(2)-C(3)	1.410(11)
C(3)-C(4)	1.408(11)	C(4)-C(5)	1.401(11)
C(6)-C(7)	1.414(11)	C(6)-C(13)	1.508(11)
C(7)-C(8)	1.506(11)	C(8)-C(9)	1.534(12)
C(9)-C(10)	1.530(11)	C(10)-C(11)	1.394(11)
C(11)-C(12)	1.505(11)	C(12)-C(13)	1.537(11)
C(14)-C(15)	1.480(12)		
C(11)-Rh(1)-C(7)	97.5(3)	C(11)-Rh(1)-C(6)	81.0(3)
C(7)-Rh(1)-C(6)	38.8(3)	C(11)-Rh(1)-C(10)	38.1(3)
C(7)-Rh(1)-C(10)	81.8(3)	C(6)-Rh(1)-C(10)	89.9(3)
C(11)-Rh(1)-C(3)	96.3(3)	C(7)-Rh(1)-C(3)	165.7(3)
C(6)-Rh(1)-C(3)	148.8(3)	C(10)-Rh(1)-C(3)	107.1(3)
C(11)-Rh(1)-C(2)	109.3(3)	C(7)-Rh(1)-C(2)	139.1(3)
C(6)-Rh(1)-C(2)	115.0(3)	C(10)-Rh(1)-C(2)	137.5(3)
C(3)-Rh(1)-C(2)	36.5(3)	C(11)-Rh(1)-C(1)	139.9(3)
C(7)-Rh(1)-C(1)	105.7(3)	C(6)-Rh(1)-C(1)	97.0(3)
C(10)-Rh(1)-C(1)	172.3(3)	C(3)-Rh(1)-C(1)	65.2(3)
C(2)-Rh(1)-C(1)	35.8(3)	C(11)-Rh(1)-C(4)	109.8(3)
C(7)-Rh(1)-C(4)	133.3(3)	C(6)-Rh(1)-C(4)	168.7(3)
C(10)-Rh(1)-C(4)	96.8(3)	C(3)-Rh(1)-C(4)	36.3(3)
C(2)-Rh(1)-C(4)	65.3(3)	C(1)-Rh(1)-C(4)	76.9(3)
C(11)-Rh(1)-C(5)	139.6(3)	C(7)-Rh(1)-C(5)	102.4(3)
C(6)-Rh(1)-C(5)	134.2(3)	C(10)-Rh(1)-C(5)	111.0(3)
C(3)-Rh(1)-C(5)	64.2(3)	C(2)-Rh(1)-C(5)	76.8(3)
C(1)-Rh(1)-C(5)	66.2(2)	C(4)-Rh(1)-C(5)	34.7(3)
C(11)-Rh(1)-B	173.0(3)	C(7)-Rh(1)-B	89.5(3)
C(6)-Rh(1)-B	105.3(3)	C(10)-Rh(1)-B	143.3(3)
C(3)-Rh(1)-B	76.6(3)	C(2)-Rh(1)-B	65.3(3)
C(1)-Rh(1)-B	37.3(3)	C(4)-Rh(1)-B	64.2(3)
C(5)-Rh(1)-B	36.5(3)	B-O(1)-C(14)	120.3(6)
O(1)-B-C(5)	125.9(7)	O(1)-B-C(1)	119.1(7)
C(5)-B-C(1)	115.0(7)	O(1)-B-Rh(1)	131.2(5)
C(5)-B-Rh(1)	70.0(4)	C(1)-B-Rh(1)	66.0(4)
C(2)-C(1)-B	121.4(7)	C(2)-C(1)-Rh(1)	71.4(4)
B-C(1)-Rh(1)	76.8(4)	C(1)-C(2)-C(3)	119.5(7)
C(1)-C(2)-Rh(1)	72.8(4)	C(3)-C(2)-Rh(1)	69.4(4)
C(4)-C(3)-C(2)	122.2(7)	C(4)-C(3)-Rh(1)	74.9(4)
C(2)-C(3)-Rh(1)	74.0(4)	C(5)-C(4)-C(3)	122.0(7)
C(5)-C(4)-Rh(1)	76.6(4)	C(3)-C(4)-Rh(1)	68.8(4)
C(4)-C(5)-B	119.4(7)	C(4)-C(5)-Rh(1)	68.7(4)
B-C(5)-Rh(1)	73.5(4)	C(7)-C(6)-C(13)	123.5(7)
C(7)-C(6)-Rh(1)	70.5(4)	C(13)-C(6)-Rh(1)	114.1(5)
C(6)-C(7)-C(8)	123.9(7)	C(6)-C(7)-Rh(1)	70.7(4)
C(8)-C(7)-Rh(1)	111.0(5)	C(7)-C(8)-C(9)	113.4(6)
C(10)-C(9)-C(8)	111.9(6)	C(11)-C(10)-C(9)	121.9(7)
C(11)-C(10)-Rh(1)	70.5(4)	C(9)-C(10)-Rh(1)	113.1(5)
C(10)-C(11)-C(12)	124.9(7)	C(10)-C(11)-Rh(1)	71.4(4)

C(12)-C(11)-Rh(1)	112.2(5)	C(11)-C(12)-C(13)	112.2(6)
C(6)-C(13)-C(12)	112.9(6)	O(1)-C(14)-C(15)	109.5(6)

Symmetry transformations used to generate equivalent atoms:

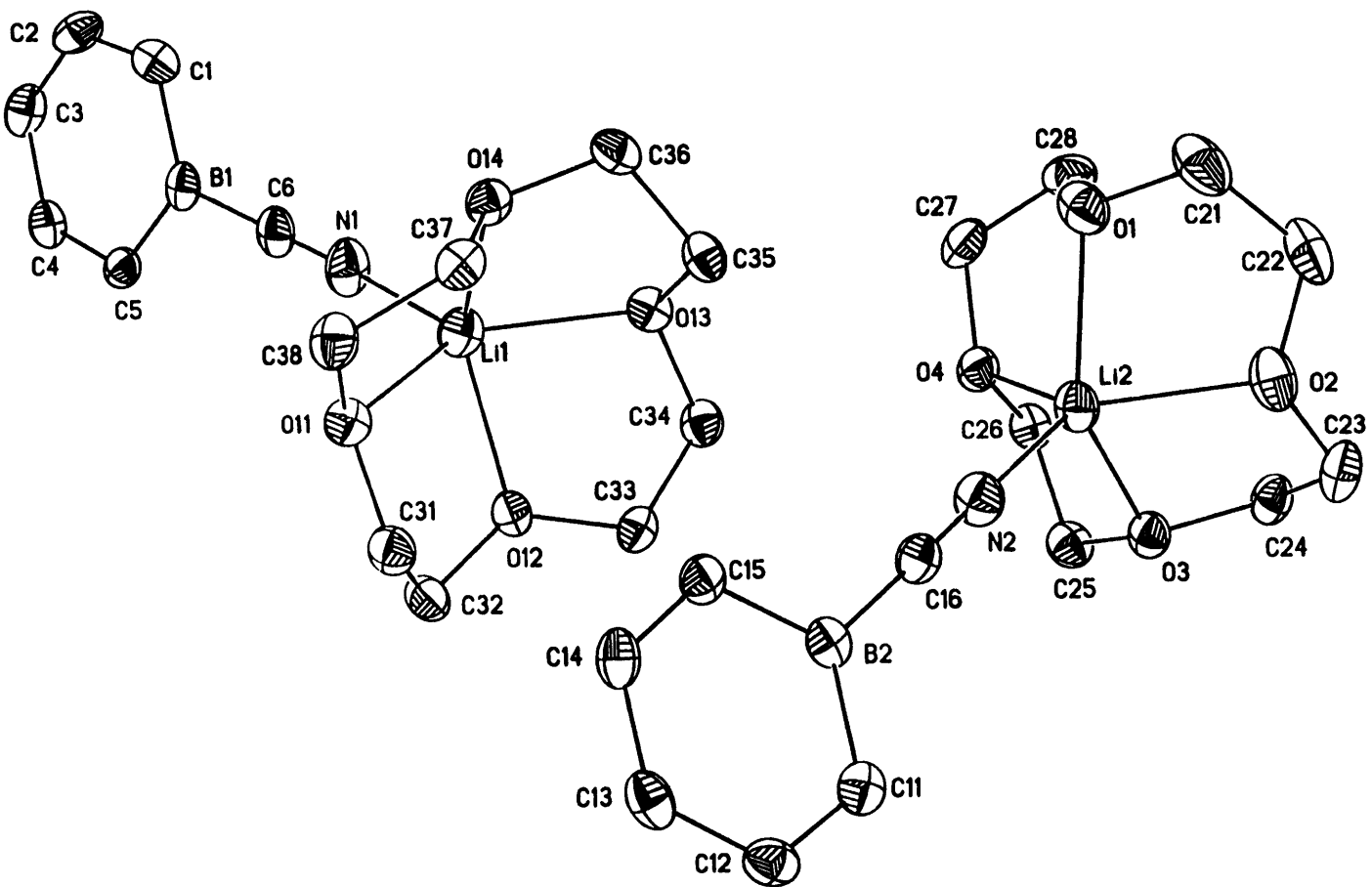


Table 1. Crystal data and structure refinement for 1.

CA. Crystal Data

Identification code	97112
Empirical formula	$C_{14}H_{21}BLiNO_4$
Formula weight	285.07
Temperature	183(2) K
Wavelength	0.71073 Å
Crystal size	0.23 x 0.23 x 0.30 mm
Crystal system	Monoclinic
Space group	$P2_1/c$
Unit cell dimensions	$a = 14.4640(2)$ Å $\alpha = 90^\circ$ $b = 13.7771(2)$ Å $\beta = 92.4490(10)^\circ$ $c = 15.75620(10)$ Å $\gamma = 90^\circ$
Volume, Z	$3136.90(7)$ Å ³ , 8
Density (calculated)	1.207 Mg/m ³
Absorption coefficient	0.085 mm ⁻¹
F(000)	1216

CB. Data Collection and Reduction

Diffractometer	Siemens SMART/CCD
Scan Type	ω Scans
Scan angle	0.30°
θ range for data collection	1.41 to 23.26°
Limiting indices	$-7 \leq h \leq 16$, $-15 \leq k \leq 15$, $-17 \leq l \leq 17$
Reflections collected	12469
Independent reflections	4491 ($R_{int} = 0.0362$)
Absorption correction	None

Refinement method Full-matrix least-squares on F^2

Data / restraints / parameters	4488 / 0 / 380
Goodness-of-fit on F^2	1.182
Final R indices [$I > 2\sigma(I)$]	R1 = 0.0442, wR2 = 0.0854
R indices (all data)	R1 = 0.0564, wR2 = 0.0911
Extinction coefficient	0.0058(4)
Largest diff. peak and hole	0.141 and -0.155 eÅ ⁻³

Table 2. Atomic coordinates [$\times 10^4$] and equivalent isotropic displacement parameters [$\text{\AA}^2 \times 10^3$] for 1. $U(\text{eq})$ is defined as one third of the trace of the orthogonalized U_{ij} tensor.

	x	y	z	$U(\text{eq})$
O(11)	7767(1)	1802(1)	646(1)	36(1)
O(12)	8509(1)	2975(1)	-522(1)	32(1)
O(14)	6226(1)	2918(1)	641(1)	33(1)
O(13)	6990(1)	4119(1)	-495(1)	34(1)
C(33)	8644(1)	3978(1)	-306(1)	33(1)
C(32)	9093(2)	2321(2)	-37(1)	38(1)
C(37)	6694(1)	2736(2)	1447(1)	35(1)
C(38)	7194(2)	1790(2)	1366(1)	40(1)
C(36)	5883(1)	3896(2)	536(1)	36(1)
C(35)	6639(2)	4551(2)	253(1)	35(1)
C(34)	7860(1)	4515(2)	-742(1)	36(1)
C(31)	8699(1)	2123(2)	815(1)	38(1)
O(4)	7500(1)	6794(1)	-1323(1)	36(1)
O(3)	8811(1)	8091(1)	-808(1)	35(1)
O(1)	6338(1)	7537(1)	-200(1)	45(1)
O(2)	7638(1)	8886(1)	288(1)	46(1)
C(25)	8906(2)	7559(2)	-1584(1)	39(1)
C(26)	7973(1)	7297(2)	-1970(1)	36(1)
C(24)	8569(2)	9096(2)	-926(1)	39(1)
C(27)	6519(2)	6721(2)	-1489(2)	44(1)
C(23)	8341(2)	9471(2)	-73(1)	48(1)
C(28)	6045(2)	7553(2)	-1083(1)	45(1)
C(22)	6712(2)	9214(2)	86(2)	54(1)
C(21)	6075(2)	8385(2)	258(2)	59(1)
N(2)	8452(1)	6568(1)	763(1)	42(1)
C(15)	8890(1)	4445(1)	2167(1)	32(1)
C(12)	10704(2)	4876(2)	2812(1)	37(1)
C(16)	8839(1)	6059(2)	1239(1)	33(1)
C(13)	10244(2)	4042(2)	3057(1)	35(1)
C(14)	9355(2)	3837(2)	2743(1)	35(1)
C(11)	10303(1)	5543(2)	2244(1)	34(1)
B(2)	9354(2)	5346(2)	1884(1)	29(1)
C(4)	6080(2)	-1160(2)	-3137(1)	36(1)
N(1)	6586(1)	1668(1)	-1158(1)	46(1)
C(6)	6280(2)	1045(2)	-1568(1)	37(1)
C(1)	4858(2)	-3(2)	-2199(1)	39(1)
C(3)	5132(2)	-1315(2)	-3183(1)	41(1)
C(5)	6477(1)	-431(1)	-2635(1)	32(1)
C(2)	4542(2)	-747(2)	-2728(1)	43(1)
B(1)	5868(2)	194(2)	-2133(1)	31(1)
Li(1)	7125(2)	2620(3)	-339(2)	37(1)
Li(2)	7803(3)	7438(2)	-113(2)	38(1)

Table 3. Bond lengths [Å] and angles [°] for 1.

O(11)-C(38)	1.433 (2)	O(11)-C(31)	1.434 (2)
O(11)-Li(1)	2.102 (4)	O(12)-C(32)	1.433 (2)
O(12)-C(33)	1.434 (2)	O(12)-Li(1)	2.093 (4)
O(14)-C(37)	1.435 (2)	O(14)-C(36)	1.443 (2)
O(14)-Li(1)	2.102 (4)	O(13)-C(35)	1.432 (2)
O(13)-C(34)	1.441 (2)	O(13)-Li(1)	2.089 (4)
C(33)-C(34)	1.498 (3)	C(32)-C(31)	1.505 (3)
C(37)-C(38)	1.500 (3)	C(36)-C(35)	1.501 (3)
O(4)-C(26)	1.431 (2)	O(4)-C(27)	1.435 (2)
O(4)-Li(2)	2.131 (4)	O(3)-C(25)	1.437 (2)
O(3)-C(24)	1.439 (2)	O(3)-Li(2)	2.066 (4)
O(1)-C(21)	1.433 (3)	O(1)-C(28)	1.437 (3)
O(1)-Li(2)	2.122 (4)	O(2)-C(23)	1.435 (3)
O(2)-C(22)	1.436 (3)	O(2)-Li(2)	2.110 (4)
C(25)-C(26)	1.500 (3)	C(24)-C(23)	1.491 (3)
C(27)-C(28)	1.494 (3)	C(22)-C(21)	1.499 (3)
N(2)-C(16)	1.154 (3)	N(2)-Li(2)	2.028 (4)
C(15)-C(14)	1.387 (3)	C(15)-B(2)	1.489 (3)
C(12)-C(13)	1.390 (3)	C(12)-C(11)	1.392 (3)
C(16)-B(2)	1.577 (3)	C(13)-C(14)	1.387 (3)
C(11)-B(2)	1.488 (3)	C(4)-C(3)	1.386 (3)
C(4)-C(5)	1.387 (3)	N(1)-C(6)	1.151 (3)
N(1)-Li(1)	1.976 (4)	C(6)-B(1)	1.575 (3)
C(1)-C(2)	1.386 (3)	C(1)-B(1)	1.485 (3)
C(3)-C(2)	1.382 (3)	C(5)-B(1)	1.484 (3)
C(38)-O(11)-C(31)	115.3 (2)	C(38)-O(11)-Li(1)	109.8 (2)
C(31)-O(11)-Li(1)	110.7 (2)	C(32)-O(12)-C(33)	114.1 (2)
C(32)-O(12)-Li(1)	108.9 (2)	C(33)-O(12)-Li(1)	108.29 (14)
C(37)-O(14)-C(36)	114.3 (2)	C(37)-O(14)-Li(1)	109.44 (14)
C(36)-O(14)-Li(1)	108.6 (2)	C(35)-O(13)-C(34)	114.2 (2)
C(35)-O(13)-Li(1)	110.4 (2)	C(34)-O(13)-Li(1)	109.2 (2)
O(12)-C(33)-C(34)	105.9 (2)	O(12)-C(32)-C(31)	110.7 (2)
O(14)-C(37)-C(38)	106.7 (2)	O(11)-C(38)-C(37)	110.7 (2)
O(14)-C(36)-C(35)	110.2 (2)	O(13)-C(35)-C(36)	106.4 (2)
O(13)-C(34)-C(33)	110.0 (2)	O(11)-C(31)-C(32)	106.2 (2)
C(26)-O(4)-C(27)	113.8 (2)	C(26)-O(4)-Li(2)	110.4 (2)
C(27)-O(4)-Li(2)	110.9 (2)	C(25)-O(3)-C(24)	114.3 (2)
C(25)-O(3)-Li(2)	108.9 (2)	C(24)-O(3)-Li(2)	108.4 (2)
C(21)-O(1)-C(28)	113.6 (2)	C(21)-O(1)-Li(2)	107.8 (2)
C(28)-O(1)-Li(2)	108.4 (2)	C(23)-O(2)-C(22)	113.9 (2)
C(23)-O(2)-Li(2)	108.7 (2)	C(22)-O(2)-Li(2)	110.4 (2)
O(3)-C(25)-C(26)	110.5 (2)	O(4)-C(26)-C(25)	106.1 (2)
O(3)-C(24)-C(23)	106.1 (2)	O(4)-C(27)-C(28)	109.7 (2)
O(2)-C(23)-C(24)	110.6 (2)	O(1)-C(28)-C(27)	106.3 (2)
O(2)-C(22)-C(21)	107.1 (2)	O(1)-C(21)-C(22)	110.7 (2)
C(16)-N(2)-Li(2)	177.6 (2)	C(14)-C(15)-B(2)	119.1 (2)
C(13)-C(12)-C(11)	122.2 (2)	N(2)-C(16)-B(2)	178.8 (2)
C(14)-C(13)-C(12)	121.1 (2)	C(13)-C(14)-C(15)	121.8 (2)
C(12)-C(11)-B(2)	118.5 (2)	C(11)-B(2)-C(15)	117.3 (2)
C(11)-B(2)-C(16)	122.4 (2)	C(15)-B(2)-C(16)	120.4 (2)
C(3)-C(4)-C(5)	121.8 (2)	C(6)-N(1)-Li(1)	172.9 (2)
N(1)-C(6)-B(1)	179.6 (2)	C(2)-C(1)-B(1)	118.4 (2)
C(2)-C(3)-C(4)	121.2 (2)	C(4)-C(5)-B(1)	118.8 (2)
C(3)-C(2)-C(1)	122.4 (2)	C(5)-B(1)-C(1)	117.5 (2)

C(5)-B(1)-C(6)	120.9(2)	C(1)-B(1)-C(6)	121.5(2)
N(1)-Li(1)-O(13)	123.2(2)	N(1)-Li(1)-O(12)	114.7(2)
O(13)-Li(1)-O(12)	80.66(13)	N(1)-Li(1)-O(14)	111.7(2)
O(13)-Li(1)-O(14)	80.53(13)	O(12)-Li(1)-O(14)	132.9(2)
N(1)-Li(1)-O(11)	106.0(2)	O(13)-Li(1)-O(11)	130.8(2)
O(12)-Li(1)-O(11)	80.34(13)	O(14)-Li(1)-O(11)	80.19(13)
N(2)-Li(2)-O(3)	107.6(2)	N(2)-Li(2)-O(2)	114.2(2)
O(3)-Li(2)-O(2)	80.74(13)	N(2)-Li(2)-O(1)	120.9(2)
O(3)-Li(2)-O(1)	131.5(2)	O(2)-Li(2)-O(1)	80.36(14)
N(2)-Li(2)-O(4)	115.8(2)	O(3)-Li(2)-O(4)	80.22(13)
O(2)-Li(2)-O(4)	129.8(2)	O(1)-Li(2)-O(4)	78.61(14)

Symmetry transformations used to generate equivalent atoms:

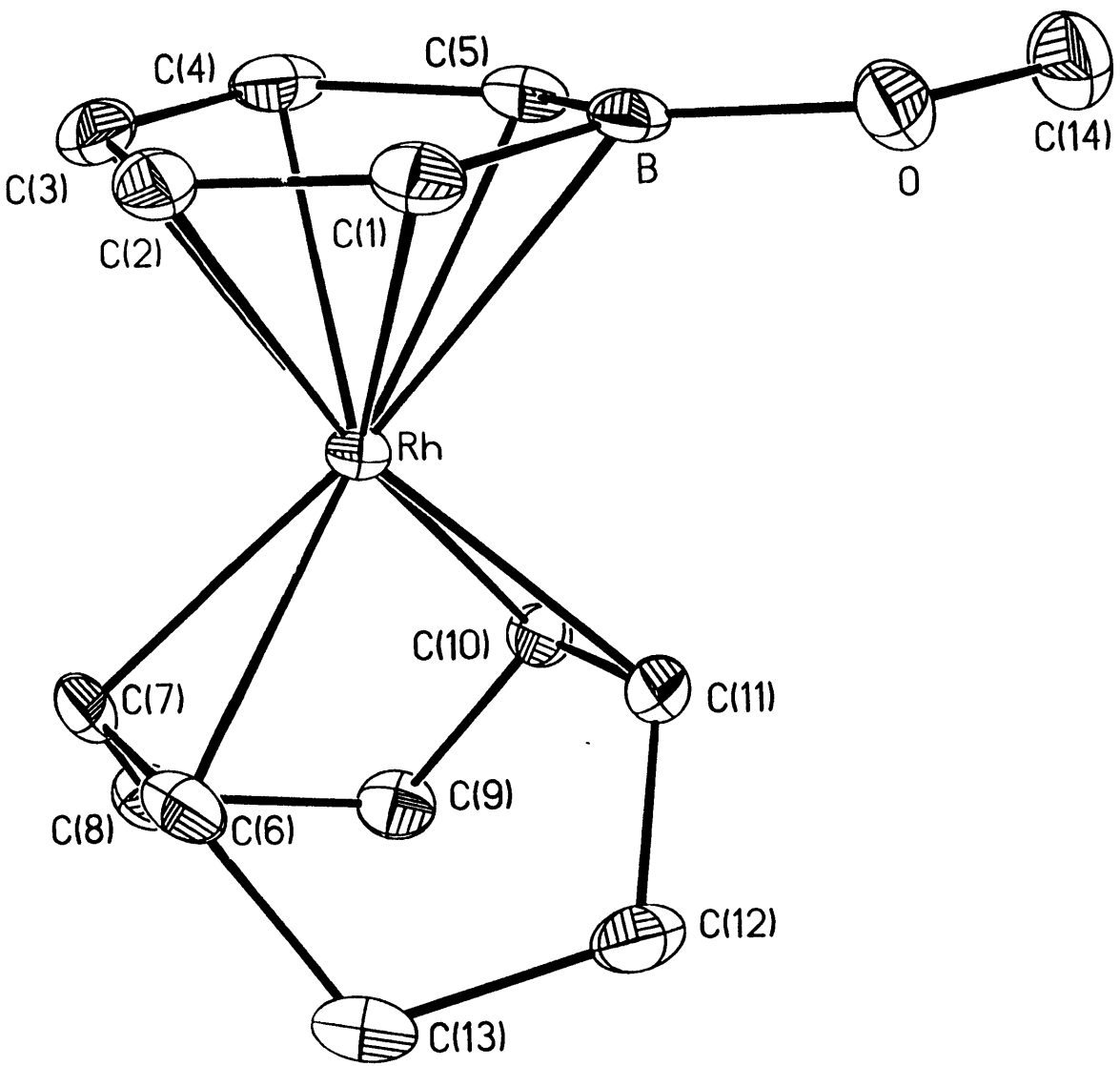


Table 1. Crystal data and structure refinement for 1.

A. Crystal Data

Identification code	97113
Empirical formula	$C_{14}H_{20}BORh$
Formula weight	318.02
Temperature	183(2) K
Wavelength	0.71073 Å
Crystal morphology	block
Crystal size	0.24 x 0.30 x 0.34 mm
Crystal system	Monoclinic
Space group	$P2_1/c$
Unit cell dimensions	$a = 8.3192(3)$ Å $\alpha = 90^\circ$ $b = 12.0618(4)$ Å $\beta = 103.7910(10)^\circ$ $c = 12.9856(5)$ Å $\gamma = 90^\circ$
Volume, Z	1265.47(8) Å ³ , 4
Density (calculated)	1.669 Mg/m ³
Absorption coefficient	1.328 mm ⁻¹
F(000)	648

B. Data Collection and Reduction

Diffractometer	Siemens SMART/CCD
Scan Type	ω Scans
Scan angle	0.30°
θ range for data collection	2.34 to 23.23°
Limiting indices	$-8 \leq h \leq 9$, $-11 \leq k \leq 13$, $-14 \leq l \leq 12$

Reflections collected	4996
Independent reflections	1798 ($R_{int} = 0.0237$)
Absorption correction	Semi-empirical from psi-scans
Max. and min. transmission	0.5478 and 0.4535

C. Solution and Refinement

Refinement method	Full-matrix least-squares on F^2
Data / restraints / parameters	1798 / 0 / 155
Goodness-of-fit on F^2	1.091
Final R indices [$I > 2\sigma(I)$]	$R1 = 0.0179$, $wR2 = 0.0466$
R indices (all data)	$R1 = 0.0184$, $wR2 = 0.0468$
Extinction coefficient	0.0341(12)
Largest diff. peak and hole	0.287 and $-0.247 \text{ e}\text{\AA}^{-3}$

Table 2. Atomic coordinates [$\times 10^4$] and equivalent isotropic displacement parameters [$\text{\AA}^2 \times 10^3$] for 1. $U(\text{eq})$ is defined as one third of the trace of the orthogonalized U_{ij} tensor.

	x	y	z	$U(\text{eq})$
Rh	6082 (1)	1707 (1)	6654 (1)	18 (1)
O	2796 (2)	3682 (1)	6226 (1)	30 (1)
B	3347 (3)	2602 (2)	6452 (2)	22 (1)
C(1)	4047 (3)	2262 (2)	7602 (2)	26 (1)
C(2)	4581 (3)	1178 (2)	7843 (2)	31 (1)
C(3)	4488 (3)	345 (2)	7056 (2)	33 (1)
C(4)	3891 (3)	590 (2)	5974 (2)	32 (1)
C(5)	3456 (3)	1695 (2)	5643 (2)	25 (1)
C(6)	8469 (3)	1761 (2)	7771 (2)	28 (1)
C(7)	8365 (3)	796 (2)	7154 (2)	27 (1)
C(8)	9214 (3)	670 (2)	6254 (2)	29 (1)
C(9)	8854 (3)	1630 (2)	5457 (2)	27 (1)
C(10)	7216 (3)	2205 (2)	5436 (2)	23 (1)
C(11)	7071 (3)	3135 (2)	6077 (2)	25 (1)
C(12)	8488 (3)	3631 (2)	6889 (2)	33 (1)
C(13)	9509 (3)	2757 (2)	7619 (2)	30 (1)
C(14)	2189 (3)	4041 (2)	5160 (2)	41 (1)

Table 3. Bond lengths [Å] and angles [°] for 1.

Rh-C(10)	2.113 (2)	Rh-C(11)	2.121 (2)
Rh-C(7)	2.156 (2)	Rh-C(6)	2.163 (3)
Rh-C(3)	2.249 (2)	Rh-C(5)	2.265 (2)
Rh-C(4)	2.269 (2)	Rh-C(2)	2.295 (2)
Rh-C(1)	2.412 (2)	Rh-B	2.475 (2)
O-B	1.390 (3)	O-C(14)	1.422 (3)
B-C(1)	1.524 (4)	B-C(5)	1.534 (4)
C(1)-C(2)	1.393 (4)	C(2)-C(3)	1.422 (4)
C(3)-C(4)	1.406 (4)	C(4)-C(5)	1.420 (4)
C(6)-C(7)	1.404 (4)	C(6)-C(13)	1.520 (4)
C(7)-C(8)	1.511 (3)	C(8)-C(9)	1.534 (3)
C(9)-C(10)	1.524 (3)	C(10)-C(11)	1.419 (3)
C(11)-C(12)	1.506 (4)	C(12)-C(13)	1.532 (4)
C(10)-Rh-C(11)	39.15 (9)	C(10)-Rh-C(7)	81.47 (9)
C(11)-Rh-C(7)	97.59 (9)	C(10)-Rh-C(6)	89.47 (9)
C(11)-Rh-C(6)	80.85 (9)	C(7)-Rh-C(6)	37.94 (9)
C(10)-Rh-C(3)	140.72 (10)	C(11)-Rh-C(3)	167.11 (9)
C(7)-Rh-C(3)	94.79 (9)	C(6)-Rh-C(3)	111.38 (9)
C(10)-Rh-C(5)	96.24 (9)	C(11)-Rh-C(5)	101.67 (9)
C(7)-Rh-C(5)	146.08 (9)	C(6)-Rh-C(5)	173.50 (9)
C(3)-Rh-C(5)	65.74 (9)	C(10)-Rh-C(4)	109.72 (9)
C(11)-Rh-C(4)	133.42 (10)	C(7)-Rh-C(4)	112.50 (10)
C(6)-Rh-C(4)	143.41 (9)	C(3)-Rh-C(4)	36.25 (10)
C(5)-Rh-C(4)	36.49 (9)	C(10)-Rh-C(2)	173.76 (9)
C(11)-Rh-C(2)	141.51 (10)	C(7)-Rh-C(2)	103.73 (9)
C(6)-Rh-C(2)	96.75 (9)	C(3)-Rh-C(2)	36.46 (10)
C(5)-Rh-C(2)	77.52 (9)	C(4)-Rh-C(2)	65.27 (10)
C(10)-Rh-C(1)	142.72 (9)	C(11)-Rh-C(1)	109.48 (9)
C(7)-Rh-C(1)	131.52 (9)	C(6)-Rh-C(1)	107.08 (9)
C(3)-Rh-C(1)	63.94 (9)	C(5)-Rh-C(1)	66.45 (9)
C(4)-Rh-C(1)	76.55 (9)	C(2)-Rh-C(1)	34.30 (9)
C(10)-Rh-B	111.08 (9)	C(11)-Rh-B	91.88 (9)
C(7)-Rh-B	167.37 (9)	C(6)-Rh-B	137.07 (9)
C(3)-Rh-B	76.43 (9)	C(5)-Rh-B	37.44 (9)
C(4)-Rh-B	65.46 (9)	C(2)-Rh-B	63.83 (9)
C(1)-Rh-B	36.31 (8)	B-O-C(14)	120.9 (2)
O-B-C(1)	119.3 (2)	O-B-C(5)	126.5 (2)
C(1)-B-C(5)	114.1 (2)	O-B-Rh	132.8 (2)
C(1)-B-Rh	69.61 (12)	C(5)-B-Rh	63.82 (13)
C(2)-C(1)-B	120.0 (2)	C(2)-C(1)-Rh	68.25 (13)
B-C(1)-Rh	74.09 (13)	C(1)-C(2)-C(3)	122.8 (2)
C(1)-C(2)-Rh	77.45 (13)	C(3)-C(2)-Rh	70.01 (13)
C(4)-C(3)-C(2)	121.0 (2)	C(4)-C(3)-Rh	72.66 (14)
C(2)-C(3)-Rh	73.53 (14)	C(3)-C(4)-C(5)	120.2 (2)
C(3)-C(4)-Rh	71.09 (14)	C(5)-C(4)-Rh	71.57 (14)
C(4)-C(5)-B	121.0 (2)	C(4)-C(5)-Rh	71.94 (14)
B-C(5)-Rh	78.73 (14)	C(7)-C(6)-C(13)	122.7 (2)
C(7)-C(6)-Rh	70.76 (14)	C(13)-C(6)-Rh	113.4 (2)
C(6)-C(7)-C(8)	123.2 (2)	C(6)-C(7)-Rh	71.30 (14)
C(8)-C(7)-Rh	111.1 (2)	C(7)-C(8)-C(9)	113.2 (2)
C(10)-C(9)-C(8)	112.7 (2)	C(11)-C(10)-C(9)	123.4 (2)
C(11)-C(10)-Rh	70.70 (13)	C(9)-C(10)-Rh	114.5 (2)
C(10)-C(11)-C(12)	124.3 (2)	C(10)-C(11)-Rh	70.15 (13)
C(12)-C(11)-Rh	112.3 (2)	C(11)-C(12)-C(13)	112.7 (2)

C(6)-C(13)-C(12)

112.0(2)

Symmetry transformations used to generate equivalent atoms:

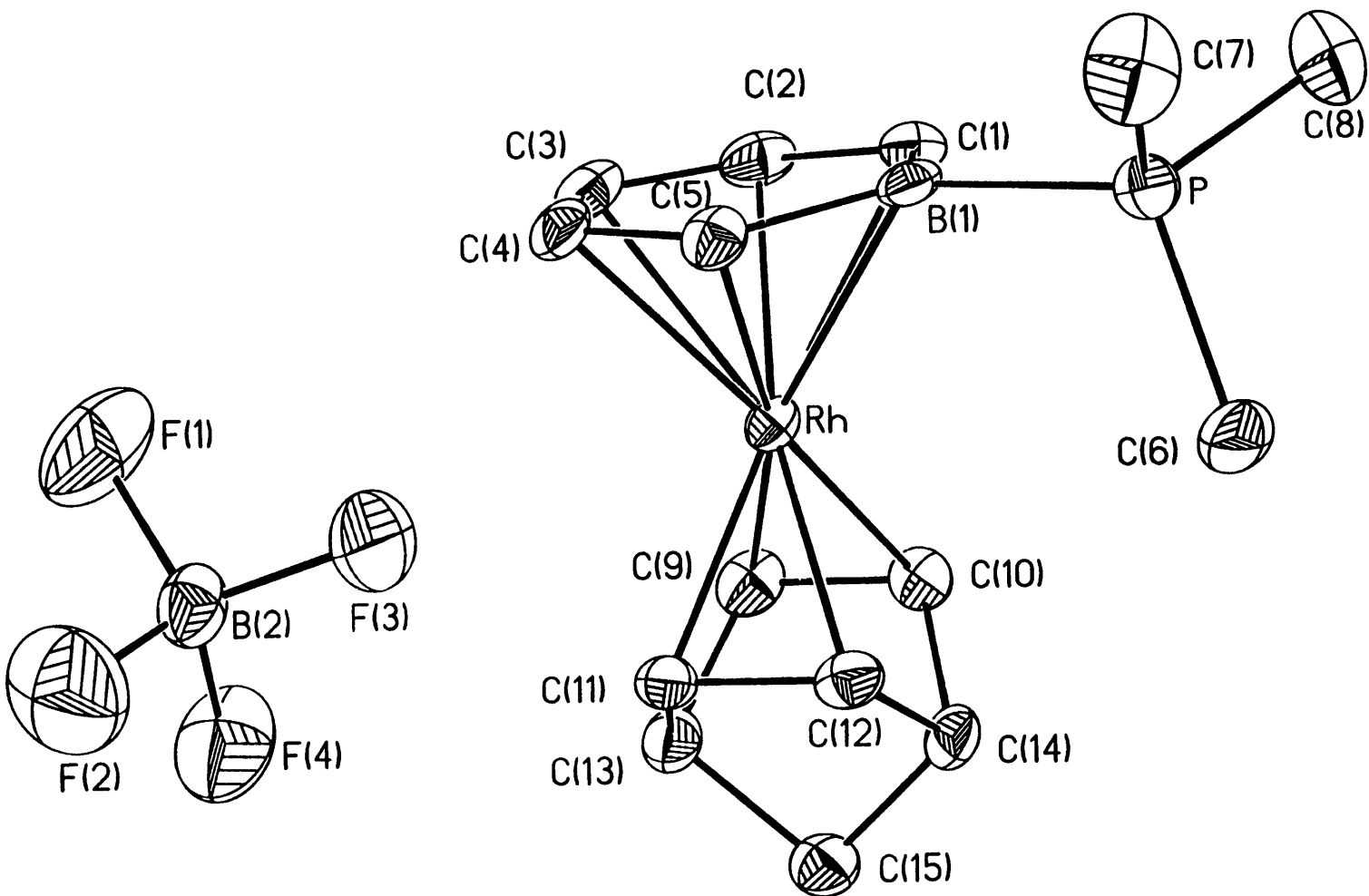


Table 7. Crystal data and structure refinement for 1.

A. Crystal Data

Identification code	97136
Empirical formula	$C_{15}H_{22}B_2F_4PRh$
Formula weight	433.83
Temperature	182(2) K
Wavelength	0.71073 Å
Crystal morphology	plate
Crystal size	0.06 x 0.12 x 0.18 mm
Crystal system	Monoclinic
Space group	$P2_1/c$
Unit cell dimensions	$a = 9.7280(2)$ Å $\alpha = 90^\circ$ $b = 15.4212(4)$ Å $\beta = 110.1830(10)^\circ$ $c = 12.5515(3)$ Å $\gamma = 90^\circ$
Volume, Z	$1767.32(7)$ Å ³ , 4
Density (calculated)	1.630 Mg/m ³
Absorption coefficient	1.088 mm ⁻¹
F(000)	872

B. Data Collection and Reduction

Diffractometer	Siemens SMART/CCD
Scan Type	ω Scans
Scan angle	0.30°
θ range for data collection	2.18 to 23.21°
Limiting indices	$-10 \leq h \leq 10, -16 \leq k \leq 17, -13 \leq l \leq 8$

Reflections collected	6933
Independent reflections	2510 ($R_{int} = 0.0452$)
Absorption correction	Semi-empirical from psi-scans
Max. and min. transmission	0.7251 and 0.5867

C. Solution and Refinement

Refinement method	Full-matrix least-squares on F^2
Data / restraints / parameters	2510 / 0 / 209
Goodness-of-fit on F^2	1.194
Final R indices [$I > 2\sigma(I)$]	$R1 = 0.0355$, $wR2 = 0.0700$
R indices (all data)	$R1 = 0.0408$, $wR2 = 0.0723$
Extinction coefficient	0.0012(2)
Largest diff. peak and hole	0.470 and $-0.362 \text{ e}\text{\AA}^{-3}$

Table 8. Atomic coordinates [$\times 10^4$] and equivalent isotropic displacement parameters [$\text{\AA}^2 \times 10^3$] for 1. $U(\text{eq})$ is defined as one third of the trace of the orthogonalized U_{ij} tensor.

	x	y	z	U(eq)
Rh	4647 (1)	1409 (1)	1917 (1)	25 (1)
P	8539 (1)	1958 (1)	3978 (1)	33 (1)
F(1)	1544 (4)	4312 (3)	1584 (3)	89 (1)
F(2)	1160 (5)	4542 (3)	3204 (4)	97 (1)
F(3)	3033 (3)	3719 (3)	3177 (3)	82 (1)
F(4)	740 (4)	3225 (2)	2419 (3)	84 (1)
C(1)	6840 (5)	1536 (3)	1554 (4)	34 (1)
C(2)	5611 (5)	1625 (3)	550 (4)	38 (1)
C(3)	4524 (5)	2276 (3)	417 (4)	41 (1)
C(4)	4578 (5)	2816 (3)	1326 (4)	36 (1)
C(5)	5706 (5)	2729 (3)	2405 (4)	30 (1)
C(6)	7981 (6)	1339 (4)	4965 (4)	60 (2)
C(7)	9230 (6)	2971 (3)	4659 (4)	55 (2)
C(8)	10048 (5)	1400 (4)	3782 (5)	53 (1)
C(9)	3158 (5)	356 (3)	1236 (4)	39 (1)
C(10)	4425 (5)	38 (3)	2068 (4)	33 (1)
C(11)	2886 (5)	1349 (3)	2538 (4)	37 (1)
C(12)	4154 (5)	1030 (3)	3370 (4)	33 (1)
C(13)	2089 (5)	558 (3)	1859 (4)	42 (1)
C(14)	4127 (5)	45 (3)	3190 (4)	34 (1)
C(15)	2477 (5)	-146 (3)	2779 (4)	42 (1)
B(1)	6964 (6)	2100 (3)	2550 (4)	29 (1)
B(2)	1618 (6)	3951 (4)	2596 (5)	40 (1)

Table 9. Bond lengths [Å] and angles [°] for 1.

Rh-C(11)	2.114(4)	Rh-C(12)	2.120(4)
Rh-C(10)	2.139(4)	Rh-C(9)	2.146(5)
Rh-C(2)	2.247(4)	Rh-C(5)	2.269(4)
Rh-C(3)	2.280(4)	Rh-C(4)	2.286(4)
Rh-C(1)	2.339(4)	Rh-B(1)	2.369(5)
P-C(8)	1.790(5)	P-C(6)	1.790(5)
P-C(7)	1.797(5)	P-B(1)	1.928(5)
F(1)-B(2)	1.366(7)	F(2)-B(2)	1.359(7)
F(3)-B(2)	1.364(6)	F(4)-B(2)	1.380(6)
C(1)-C(2)	1.414(6)	C(1)-B(1)	1.494(7)
C(2)-C(3)	1.425(7)	C(3)-C(4)	1.399(7)
C(4)-C(5)	1.425(6)	C(5)-B(1)	1.522(7)
C(9)-C(10)	1.400(6)	C(9)-C(13)	1.533(7)
C(10)-C(14)	1.533(6)	C(11)-C(12)	1.402(6)
C(11)-C(13)	1.536(7)	C(12)-C(14)	1.535(6)
C(13)-C(15)	1.534(6)	C(14)-C(15)	1.535(6)
C(11)-Rh-C(12)	38.7(2)	C(11)-Rh-C(10)	78.8(2)
C(12)-Rh-C(10)	65.9(2)	C(11)-Rh-C(9)	66.0(2)
C(12)-Rh-C(9)	79.2(2)	C(10)-Rh-C(9)	38.1(2)
C(11)-Rh-C(2)	153.2(2)	C(12)-Rh-C(2)	167.3(2)
C(10)-Rh-C(2)	107.2(2)	C(9)-Rh-C(2)	102.1(2)
C(11)-Rh-C(5)	106.9(2)	C(12)-Rh-C(5)	103.4(2)
C(10)-Rh-C(5)	155.9(2)	C(9)-Rh-C(5)	165.3(2)
C(2)-Rh-C(5)	78.6(2)	C(11)-Rh-C(3)	120.8(2)
C(12)-Rh-C(3)	155.4(2)	C(10)-Rh-C(3)	132.4(2)
C(9)-Rh-C(3)	106.2(2)	C(2)-Rh-C(3)	36.7(2)
C(5)-Rh-C(3)	65.5(2)	C(11)-Rh-C(4)	102.9(2)
C(12)-Rh-C(4)	123.4(2)	C(10)-Rh-C(4)	166.8(2)
C(9)-Rh-C(4)	130.4(2)	C(2)-Rh-C(4)	65.4(2)
C(5)-Rh-C(4)	36.5(2)	C(3)-Rh-C(4)	35.7(2)
C(11)-Rh-C(1)	170.1(2)	C(12)-Rh-C(1)	133.0(2)
C(10)-Rh-C(1)	103.1(2)	C(9)-Rh-C(1)	121.4(2)
C(2)-Rh-C(1)	35.8(2)	C(5)-Rh-C(1)	67.5(2)
C(3)-Rh-C(1)	65.2(2)	C(4)-Rh-C(1)	77.5(2)
C(11)-Rh-B(1)	134.0(2)	C(12)-Rh-B(1)	107.9(2)
C(10)-Rh-B(1)	121.9(2)	C(9)-Rh-B(1)	155.1(2)
C(2)-Rh-B(1)	65.8(2)	C(5)-Rh-B(1)	38.2(2)
C(3)-Rh-B(1)	77.6(2)	C(4)-Rh-B(1)	66.4(2)
C(1)-Rh-B(1)	37.0(2)	C(8)-P-C(6)	107.4(3)
C(8)-P-C(7)	107.1(3)	C(6)-P-C(7)	106.7(3)
C(8)-P-B(1)	110.7(2)	C(6)-P-B(1)	111.8(2)
C(7)-P-B(1)	112.9(2)	C(2)-C(1)-B(1)	119.2(4)
C(2)-C(1)-Rh	68.5(2)	B(1)-C(1)-Rh	72.6(3)
C(1)-C(2)-C(3)	122.6(4)	C(1)-C(2)-Rh	75.6(2)
C(3)-C(2)-Rh	72.9(3)	C(4)-C(3)-C(2)	120.4(4)
C(4)-C(3)-Rh	72.4(3)	C(2)-C(3)-Rh	70.4(2)
C(3)-C(4)-C(5)	121.3(4)	C(3)-C(4)-Rh	71.9(3)
C(5)-C(4)-Rh	71.1(2)	C(4)-C(5)-B(1)	119.8(4)
C(4)-C(5)-Rh	72.4(2)	B(1)-C(5)-Rh	74.5(2)
C(10)-C(9)-C(13)	105.6(4)	C(10)-C(9)-Rh	70.7(3)
C(13)-C(9)-Rh	97.3(3)	C(9)-C(10)-C(14)	106.6(4)
C(9)-C(10)-Rh	71.2(3)	C(14)-C(10)-Rh	97.6(3)
C(12)-C(11)-C(13)	106.3(4)	C(12)-C(11)-Rh	70.9(3)
C(13)-C(11)-Rh	98.5(3)	C(11)-C(12)-C(14)	105.8(4)

C(11)-C(12)-Rh	70.4(2)	C(14)-C(12)-Rh	98.3(3)
C(9)-C(13)-C(15)	101.9(4)	C(9)-C(13)-C(11)	98.2(4)
C(15)-C(13)-C(11)	101.5(4)	C(10)-C(14)-C(15)	101.4(4)
C(10)-C(14)-C(12)	98.1(3)	C(15)-C(14)-C(12)	101.7(4)
C(13)-C(15)-C(14)	94.3(4)	C(1)-B(1)-C(5)	116.2(4)
C(1)-B(1)-P	121.4(4)	C(5)-B(1)-P	122.2(3)
C(1)-B(1)-Rh	70.4(3)	C(5)-B(1)-Rh	67.3(2)
P-B(1)-Rh	128.3(2)	F(2)-B(2)-F(3)	110.0(5)
F(2)-B(2)-F(1)	109.1(5)	F(3)-B(2)-F(1)	108.9(5)
F(2)-B(2)-F(4)	109.2(5)	F(3)-B(2)-F(4)	109.1(5)
F(1)-B(2)-F(4)	110.5(5)		

Symmetry transformations used to generate equivalent atoms:

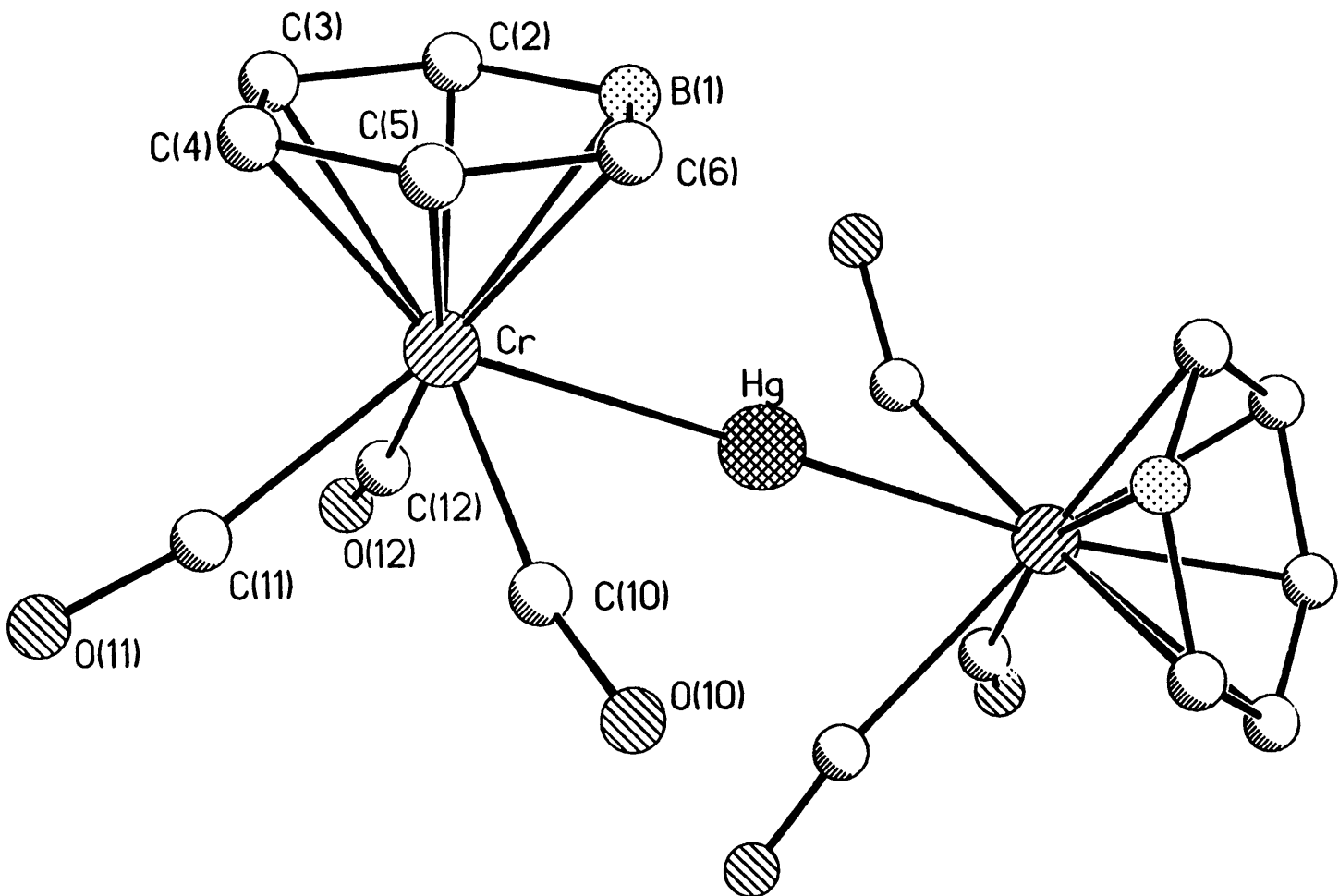


Table 1. Crystal data and structure refinement for 1.

A. Crystal Data

Identification code	93004
Empirical formula	$C_{16}H_{12}B_2Cr_2HgO_3$
Formula weight	578.47
Temperature	293(2) K
Wavelength	0.71073 Å
Crystal morphology	block
Crystal size	0.03 x 0.03 x 0.03 mm
Crystal system	Monoclinic
Space group	C2
Unit cell dimensions	$a = 12.57(10) \text{ Å}$ $\alpha = 90^\circ$ $b = 7.73(7) \text{ Å}$ $\beta = 117.9(2)^\circ$ $c = 10.70(5) \text{ Å}$ $\gamma = 90^\circ$
Volume, Z	$918(12) \text{ Å}^3$, 2
Density (calculated)	2.092 Mg/m^3
Absorption coefficient	9.511 mm^{-1}
F(000)	540

B. Data Collection and Reduction

Diffractionmeter	Siemens SMART/CCD
Scan Type	ω Scans
Scan angle	0.30°
θ range for data collection	2.15 to 23.24°
Limiting indices	$-11 \leq h \leq 7$, $-4 \leq k \leq 8$, $-10 \leq l \leq 11$

Reflections collected	877
Independent reflections	671 ($R_{int} = 0.0562$)
Absorption correction	Semi-empirical from psi-scans
Max. and min. transmission	0.9804 and 0.5292

C. Solution and Refinement

Refinement method	Full-matrix least-squares on F^2
Data / restraints / parameters	671 / 1 / 59
Goodness-of-fit on F^2	1.109
Final R indices [$I > 2\sigma(I)$]	$R_1 = 0.0481$, $wR_2 = 0.1254$
R indices (all data)	$R_1 = 0.0484$, $wR_2 = 0.1261$
Absolute structure parameter	0.00
Largest diff. peak and hole	0.986 and $-1.180 \text{ e}\text{\AA}^{-3}$

Table 2. Atomic coordinates [$\times 10^4$] and equivalent isotropic displacement parameters [$\text{\AA}^2 \times 10^3$] for 1. $U(\text{eq})$ is defined as one third of the trace of the orthogonalized U_{ij} tensor.

	x	y	z	$U(\text{eq})$
Hg	0	140	0	45 (1)
Cr	-2083 (3)	115 (28)	-2376 (3)	67 (2)
O(10)	-2714 (20)	58 (152)	11 (20)	127 (14)
O(11)	-3975 (20)	-3002 (30)	-3466 (22)	64 (6)
O(12)	-618 (18)	-3404 (22)	-2108 (17)	49 (5)
B(1)	-1038	2231	-2374	112
C(2)	-1192	1167	-3494	52
C(3)	-2337	598	-4450	42
C(4)	-3328	1092	-4286	73
C(5)	-3174	2156	-3166	26
C(6)	-2028	2725	-2210	30
C(10)	-2361 (23)	-320 (24)	-875 (22)	35 (7)
C(11)	-3103 (43)	-2103 (61)	-2928 (43)	91 (12)
C(12)	-1093 (23)	-2249 (31)	-2101 (22)	33 (5)

Table 3. Bond lengths [Å] and angles [°] for 1.

Hg-Cr	2.66 (2)	Hg-Cr#1	2.66 (2)
Hg-C(12)	2.73 (3)	Hg-C(12) #1	2.73 (3)
Hg-C(10) #1	2.68 (3)	Hg-C(10)	2.68 (3)
Hg-B(1) #1	2.767 (13)	Cr-C(10)	1.83 (2)
Cr-C(11)	2.05 (5)	Cr-C(5)	2.00 (2)
Cr-C(6)	2.02 (3)	Cr-C(4)	2.049 (13)
Cr-B(1)	2.10 (2)	Cr-C(3)	2.122 (12)
Cr-C(12)	2.15 (3)	Cr-C(2)	2.145 (13)
O(10)-C(10)	1.26 (4)	O(11)-C(11)	1.19 (5)
O(12)-C(12)	1.08 (3)	B(1)-C(6)	1.39
B(1)-C(2)	1.39	C(2)-C(3)	1.39
C(3)-C(4)	1.39	C(4)-C(5)	1.39
C(5)-C(6)	1.39		
Cr-Hg-Cr#1	179.2 (9)	Cr-Hg-C(12)	47.0 (7)
Cr#1-Hg-C(12)	132.2 (8)	Cr-Hg-C(12) #1	132.2 (8)
Cr#1-Hg-C(12) #1	47.0 (7)	C(12)-Hg-C(12) #1	94.9 (11)
Cr-Hg-C(10) #1	139.8 (5)	Cr#1-Hg-C(10) #1	40.0 (5)
C(12)-Hg-C(10) #1	104.2 (7)	C(12) #1-Hg-C(10) #1	64.9 (7)
Cr-Hg-C(10)	40.0 (5)	Cr#1-Hg-C(10)	139.8 (5)
C(12)-Hg-C(10)	64.9 (7)	C(12) #1-Hg-C(10)	104.2 (7)
C(10) #1-Hg-C(10)	164.8 (8)	Cr-Hg-B(1) #1	135.3 (5)
Cr#1-Hg-B(1) #1	45.4 (5)	C(12)-Hg-B(1) #1	171.6 (4)
C(12) #1-Hg-B(1) #1	78.5 (7)	C(10) #1-Hg-B(1) #1	77.8 (5)
C(10)-Hg-B(1) #1	111.5 (5)	C(10)-Cr-C(11)	75.4 (14)
C(10)-Cr-C(5)	98.1 (9)	C(11)-Cr-C(5)	108.9 (14)
C(10)-Cr-C(6)	96.8 (9)	C(11)-Cr-C(6)	148.0 (14)
C(5)-Cr-C(6)	40.4 (5)	C(10)-Cr-C(4)	125.0 (9)
C(11)-Cr-C(4)	86.5 (13)	C(5)-Cr-C(4)	40.1 (3)
C(6)-Cr-C(4)	72.5 (7)	C(10)-Cr-B(1)	121.3 (10)
C(11)-Cr-B(1)	163.2 (11)	C(5)-Cr-B(1)	72.0 (9)
C(6)-Cr-B(1)	39.4 (5)	C(4)-Cr-B(1)	84.2 (8)
C(10)-Cr-C(3)	162.6 (8)	C(11)-Cr-C(3)	94.5 (12)
C(5)-Cr-C(3)	71.4 (4)	C(6)-Cr-C(3)	84.2 (6)
C(4)-Cr-C(3)	38.9 (3)	B(1)-Cr-C(3)	69.6 (4)
C(10)-Cr-C(12)	93.4 (12)	C(11)-Cr-C(12)	65 (2)
C(5)-Cr-C(12)	165.0 (7)	C(6)-Cr-C(12)	147.2 (9)
C(4)-Cr-C(12)	124.9 (8)	B(1)-Cr-C(12)	109.9 (9)
C(3)-Cr-C(12)	95.0 (7)	C(10)-Cr-C(2)	157.6 (10)
C(11)-Cr-C(2)	125.1 (13)	C(5)-Cr-C(2)	84.2 (8)
C(6)-Cr-C(2)	70.5 (6)	C(4)-Cr-C(2)	70.0 (6)
B(1)-Cr-C(2)	38.2 (3)	C(3)-Cr-C(2)	38.0 (3)
C(12)-Cr-C(2)	88.8 (7)	C(10)-Cr-Hg	70.7 (9)
C(11)-Cr-Hg	119 (2)	C(5)-Cr-Hg	124.8 (9)
C(6)-Cr-Hg	86.1 (5)	C(4)-Cr-Hg	154.2 (9)
B(1)-Cr-Hg	70.0 (4)	C(3)-Cr-Hg	126.6 (5)
C(12)-Cr-Hg	68.2 (7)	C(2)-Cr-Hg	89.6 (6)
C(6)-B(1)-C(2)	120.0	C(6)-B(1)-Cr	67.4 (6)
C(2)-B(1)-Cr	72.8 (4)	C(3)-C(2)-B(1)	120.0
C(3)-C(2)-Cr	70.1 (5)	B(1)-C(2)-Cr	69.0 (6)
C(2)-C(3)-C(4)	120.0	C(2)-C(3)-Cr	71.9 (4)
C(4)-C(3)-Cr	67.7 (3)	C(5)-C(4)-C(3)	120.0
C(5)-C(4)-Cr	68.0 (7)	C(3)-C(4)-Cr	73.4 (5)
C(4)-C(5)-C(6)	120.0	C(4)-C(5)-Cr	71.9 (5)
C(6)-C(5)-Cr	70.7 (6)	B(1)-C(6)-C(5)	120.0

B(1)-C(6)-Cr	73.2(2)	C(5)-C(6)-Cr	68.8(2)
O(10)-C(10)-Cr	154(5)	O(10)-C(10)-Hg	115(2)
Cr-C(10)-Hg	69.3(8)	O(11)-C(11)-Cr	159(4)
O(12)-C(12)-Cr	172(2)	O(12)-C(12)-Hg	120(2)
Cr-C(12)-Hg	64.8(8)		

Symmetry transformations used to generate equivalent atoms:

#1 -x, y, -z

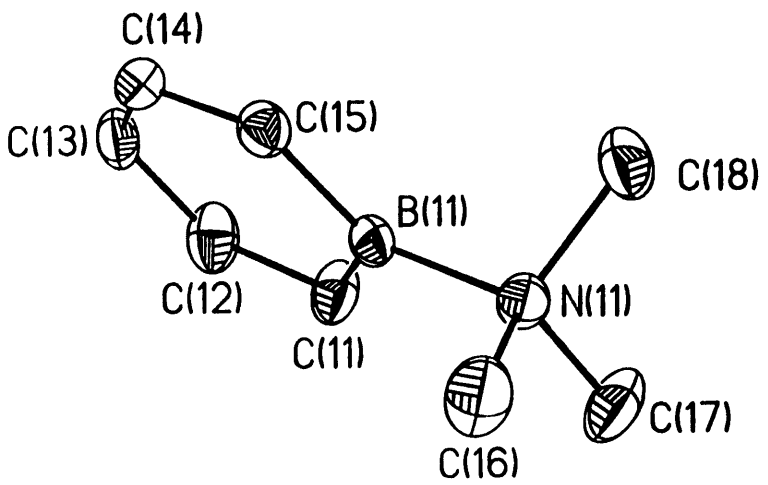
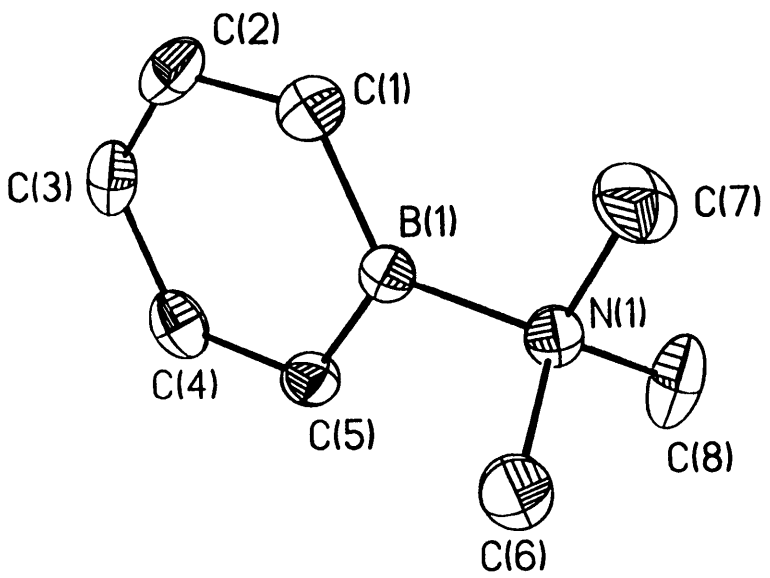


Table 7. Crystal data and structure refinement for 1.

A. Crystal Data

Identification code	98005
Empirical formula	$C_8H_{14}BN$
Formula weight	135.01
Temperature	293(2) K
Wavelength	0.71073 Å
Crystal morphology	irregular block
Crystal size	.17 x .17 x .08 mm
Crystal system	Monoclinic
Space group	$P2_1/c$
Unit cell dimensions	$a = 12.655(6)$ Å $\alpha = 90^\circ$ $b = 10.954(4)$ Å $\beta = 115.13(3)^\circ$ $c = 13.640(8)$ Å $\gamma = 90^\circ$
Volume, Z	$1712(2)$ Å ³ , 8
Density (calculated)	1.048 Mg/m ³
Absorption coefficient	0.059 mm ⁻¹
F(000)	592

B. Data Collection and Reduction

Diffractometer	Siemens SMART/CCD
Scan Type	ω Scans
Scan angle	0.30°
θ range for data collection	1.78 to 22.49°
Limiting indices	$-8 \leq h \leq 14$, $-12 \leq k \leq 11$, $-15 \leq l \leq 15$

Reflections collected	6243
Independent reflections	2230 ($R_{int} = 0.0791$)
Absorption correction	None

C. Solution and Refinement

Refinement method	Full-matrix least-squares on F^2
Data / restraints / parameters	2013 / 0 / 181
Goodness-of-fit on F^2	1.095
Final R indices [$I > 2\sigma(I)$]	$R_1 = 0.0682$, $wR_2 = 0.1258$
R indices (all data)	$R_1 = 0.1183$, $wR_2 = 0.1552$
Largest diff. peak and hole	0.162 and $-0.185 \text{ e}\text{\AA}^{-3}$

Table 8. Atomic coordinates [$\times 10^4$] and equivalent isotropic displacement parameters [$\text{\AA}^2 \times 10^3$] for 1. $U(\text{eq})$ is defined as one third of the trace of the orthogonalized U_{ij} tensor.

	x	y	z	$U(\text{eq})$
N(11)	9075 (2)	5198 (2)	2138 (2)	33 (1)
N(1)	4248 (2)	4709 (2)	1897 (2)	34 (1)
C(5)	4426 (3)	2903 (3)	675 (3)	36 (1)
C(15)	7795 (3)	3179 (3)	1427 (3)	35 (1)
C(4)	3961 (3)	1870 (3)	45 (3)	42 (1)
C(12)	8801 (3)	2697 (3)	-29 (3)	46 (1)
C(1)	2600 (3)	2979 (3)	1009 (3)	39 (1)
C(2)	2235 (3)	1933 (3)	369 (3)	43 (1)
C(3)	2887 (3)	1399 (3)	-110 (3)	42 (1)
C(18)	8052 (3)	5987 (3)	1962 (3)	49 (1)
C(14)	7478 (3)	2172 (3)	750 (3)	38 (1)
C(13)	7963 (3)	1930 (3)	34 (3)	40 (1)
B(11)	8684 (3)	4024 (3)	1375 (3)	31 (1)
C(17)	9934 (3)	5965 (3)	1940 (3)	58 (1)
C(11)	9191 (3)	3730 (3)	609 (3)	40 (1)
B(1)	3735 (3)	3512 (3)	1186 (3)	29 (1)
C(8)	4520 (4)	5654 (3)	1249 (3)	61 (1)
C(7)	3422 (3)	5256 (4)	2290 (3)	63 (1)
C(16)	9612 (4)	4799 (3)	3293 (3)	59 (1)
C(6)	5349 (3)	4394 (3)	2857 (3)	51 (1)

Table 9. Bond lengths [Å] and angles [°] for 1.

N(11)-C(17)	1.487(4)	N(11)-C(18)	1.489(4)
N(11)-C(16)	1.491(4)	N(11)-B(11)	1.595(4)
N(1)-C(7)	1.488(4)	N(1)-C(6)	1.492(4)
N(1)-C(8)	1.493(4)	N(1)-B(1)	1.596(4)
C(5)-C(4)	1.392(5)	C(5)-B(1)	1.488(5)
C(15)-C(14)	1.384(4)	C(15)-B(11)	1.481(5)
C(4)-C(3)	1.383(5)	C(12)-C(13)	1.383(5)
C(12)-C(11)	1.384(5)	C(1)-C(2)	1.395(5)
C(1)-B(1)	1.473(5)	C(2)-C(3)	1.381(5)
C(14)-C(13)	1.383(5)	B(11)-C(11)	1.476(5)
C(17)-N(11)-C(18)	107.2(3)	C(17)-N(11)-C(16)	108.5(3)
C(18)-N(11)-C(16)	108.4(3)	C(17)-N(11)-B(11)	112.7(3)
C(18)-N(11)-B(11)	110.8(3)	C(16)-N(11)-B(11)	109.2(3)
C(7)-N(1)-C(6)	108.3(3)	C(7)-N(1)-C(8)	107.9(3)
C(6)-N(1)-C(8)	108.4(3)	C(7)-N(1)-B(1)	112.6(3)
C(6)-N(1)-B(1)	109.3(3)	C(8)-N(1)-B(1)	110.2(2)
C(4)-C(5)-B(1)	118.4(3)	C(14)-C(15)-B(11)	118.5(3)
C(3)-C(4)-C(5)	121.9(3)	C(13)-C(12)-C(11)	122.4(3)
C(2)-C(1)-B(1)	118.0(3)	C(3)-C(2)-C(1)	122.6(3)
C(2)-C(3)-C(4)	121.0(3)	C(13)-C(14)-C(15)	122.3(3)
C(12)-C(13)-C(14)	120.6(3)	C(11)-B(11)-C(15)	117.7(3)
C(11)-B(11)-N(11)	122.0(3)	C(15)-B(11)-N(11)	120.3(3)
C(12)-C(11)-B(11)	118.5(3)	C(1)-B(1)-C(5)	118.1(3)
C(1)-B(1)-N(1)	122.8(3)	C(5)-B(1)-N(1)	119.0(3)

Symmetry transformations used to generate equivalent atoms:

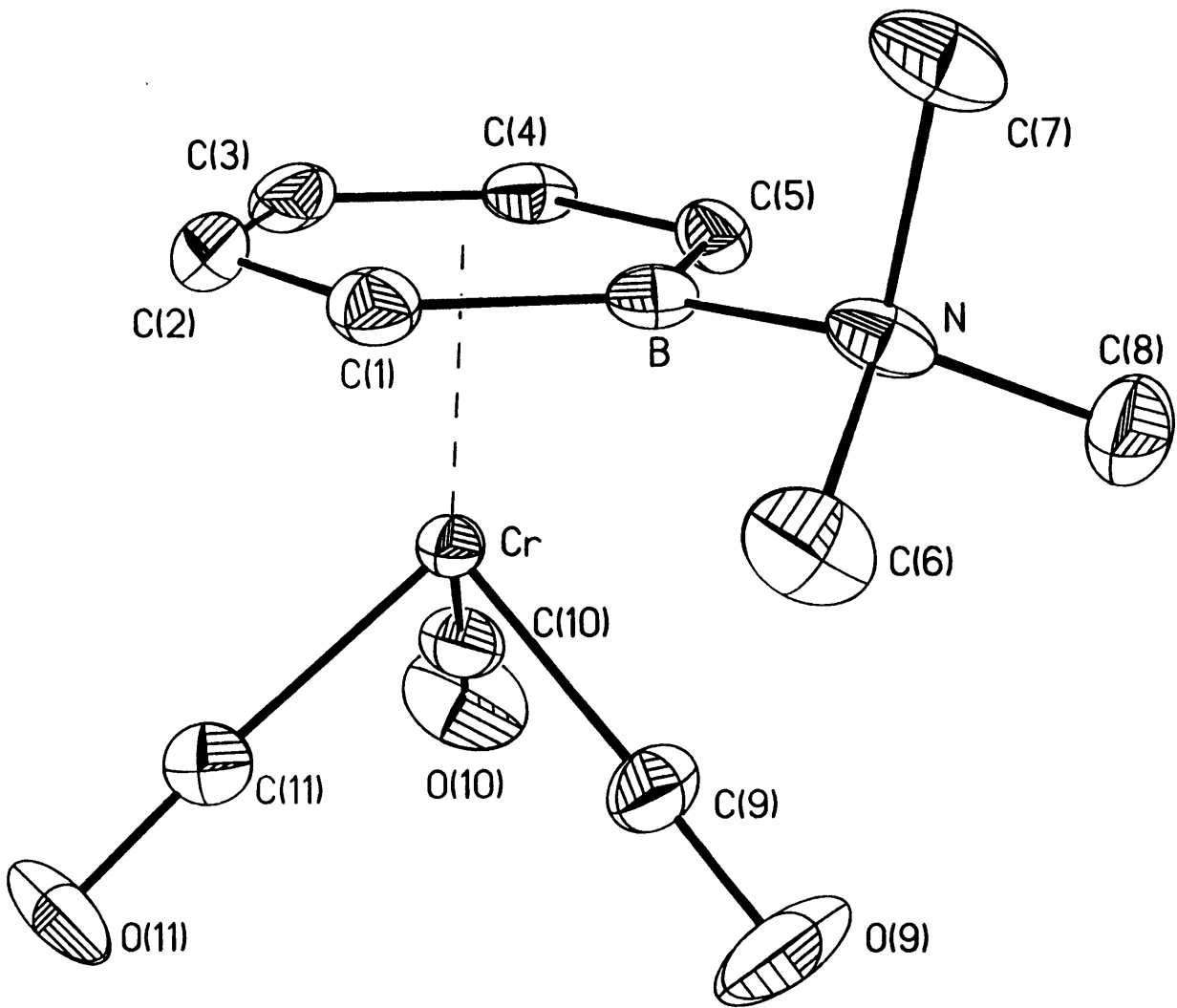


Table 1. Crystal data and structure refinement for 1.

A. Crystal Data

Identification code	98007
Empirical formula	$C_{11}H_{14}BCrNO_3$
Formula weight	271.04
Temperature	293(2) K
Wavelength	0.71073 Å
Crystal morphology	yellow needle
Crystal size	.33 x 0.08 x 0.08 mm
Crystal system	Monoclinic
Space group	$P2_1$
Unit cell dimensions	$a = 6.3919(2)$ Å $\alpha = 90^\circ$ $b = 11.1797(4)$ Å $\beta = 101.126(2)^\circ$ $c = 8.9471(2)$ Å $\gamma = 90^\circ$
Volume, Z	$627.34(3)$ Å ³ , 2
Density (calculated)	1.435 Mg/m ³
Absorption coefficient	0.905 mm ⁻¹
F(000)	280

B. Data Collection and Reduction

Diffractionmeter	Siemens SMART/CCD
Scan Type	ω Scans
Scan angle	0.30°
θ range for data collection	2.32 to 23.23°
Limiting indices	$-7 \leq h \leq 6$, $-12 \leq k \leq 6$, $-9 \leq l \leq 9$

Reflections collected	2536
Independent reflections	1305 ($R_{int} = 0.0327$)
Absorption correction	Semi-empirical from psi-scans
Max. and min. transmission	0.5959 and 0.4744

C. Solution and Refinement

Refinement method	Full-matrix least-squares on F^2
Data / restraints / parameters	1304 / 1 / 154
Goodness-of-fit on F^2	1.258
Final R indices [$I > 2\sigma(I)$]	$R1 = 0.0359$, $wR2 = 0.0731$
R indices (all data)	$R1 = 0.0397$, $wR2 = 0.0761$
Absolute structure parameter	0.01(4)
Largest diff. peak and hole	0.204 and $-0.244 \text{ e}\text{\AA}^{-3}$

Table 2. Atomic coordinates [$\times 10^4$] and equivalent isotropic displacement parameters [$\text{\AA}^2 \times 10^3$] for 1. $U(\text{eq})$ is defined as one third of the trace of the orthogonalized U_{ij} tensor.

	x	y	z	U(eq)
Cr	3154 (1)	4236 (1)	8039 (1)	22 (1)
O (9)	4789 (10)	6321 (5)	6557 (6)	84 (2)
O (10)	6936 (6)	4418 (6)	10560 (5)	63 (2)
O (11)	1203 (7)	6050 (5)	9806 (5)	57 (1)
N	1715 (7)	3979 (4)	3945 (4)	30 (1)
C (1)	113 (8)	3603 (5)	6459 (6)	31 (1)
C (2)	291 (9)	3059 (6)	7886 (6)	38 (2)
C (3)	2102 (10)	2412 (6)	8583 (7)	40 (2)
C (4)	3831 (9)	2295 (5)	7831 (6)	32 (1)
C (5)	3843 (9)	2789 (6)	6386 (6)	27 (1)
C (6)	403 (11)	5097 (6)	3676 (7)	47 (2)
C (7)	626 (10)	3027 (6)	2889 (6)	44 (2)
C (8)	3827 (7)	4239 (10)	3521 (5)	44 (1)
C (9)	4171 (12)	5495 (7)	7136 (7)	43 (2)
C (10)	5486 (7)	4339 (9)	9579 (5)	36 (1)
C (11)	1916 (9)	5323 (6)	9117 (7)	34 (2)
B	1899 (9)	3478 (6)	5621 (7)	27 (2)

Table 3. Bond lengths [Å] and angles [°] for 1.

Cr-C(9)	1.805 (7)	Cr-C(11)	1.823 (6)
Cr-C(10)	1.828 (5)	Cr-C(4)	2.228 (6)
Cr-C(3)	2.230 (6)	Cr-C(2)	2.236 (6)
Cr-C(1)	2.284 (5)	Cr-C(5)	2.292 (6)
Cr-B	2.318 (6)	O(9)-C(9)	1.164 (8)
O(10)-C(10)	1.150 (6)	O(11)-C(11)	1.165 (7)
N-C(8)	1.499 (6)	N-C(6)	1.499 (7)
N-C(7)	1.502 (7)	N-B	1.583 (7)
C(1)-C(2)	1.398 (8)	C(1)-B	1.489 (8)
C(2)-C(3)	1.405 (8)	C(3)-C(4)	1.406 (8)
C(4)-C(5)	1.407 (8)	C(5)-B	1.509 (8)
C(9)-Cr-C(11)	87.0 (3)	C(9)-Cr-C(10)	88.7 (3)
C(11)-Cr-C(10)	86.2 (3)	C(9)-Cr-C(4)	129.0 (3)
C(11)-Cr-C(4)	143.5 (3)	C(10)-Cr-C(4)	88.9 (3)
C(9)-Cr-C(3)	163.8 (3)	C(11)-Cr-C(3)	108.3 (3)
C(10)-Cr-C(3)	97.4 (3)	C(4)-Cr-C(3)	36.8 (2)
C(9)-Cr-C(2)	142.4 (3)	C(11)-Cr-C(2)	89.5 (2)
C(10)-Cr-C(2)	128.5 (3)	C(4)-Cr-C(2)	65.9 (2)
C(3)-Cr-C(2)	36.7 (2)	C(9)-Cr-C(1)	107.6 (3)
C(11)-Cr-C(1)	97.5 (2)	C(10)-Cr-C(1)	163.5 (3)
C(4)-Cr-C(1)	78.6 (2)	C(3)-Cr-C(1)	66.1 (2)
C(2)-Cr-C(1)	36.0 (2)	C(9)-Cr-C(5)	97.5 (3)
C(11)-Cr-C(5)	165.6 (2)	C(10)-Cr-C(5)	107.5 (3)
C(4)-Cr-C(5)	36.2 (2)	C(3)-Cr-C(5)	66.3 (2)
C(2)-Cr-C(5)	78.6 (2)	C(1)-Cr-C(5)	68.2 (2)
C(9)-Cr-B	87.5 (3)	C(11)-Cr-B	129.0 (2)
C(10)-Cr-B	144.2 (3)	C(4)-Cr-B	66.6 (2)
C(3)-Cr-B	78.7 (2)	C(2)-Cr-B	66.2 (2)
C(1)-Cr-B	37.7 (2)	C(5)-Cr-B	38.2 (2)
C(8)-N-C(6)	107.5 (6)	C(8)-N-C(7)	108.0 (5)
C(6)-N-C(7)	108.2 (4)	C(8)-N-B	113.7 (4)
C(6)-N-B	112.6 (4)	C(7)-N-B	106.6 (4)
C(2)-C(1)-B	119.0 (5)	C(2)-C(1)-Cr	70.1 (3)
B-C(1)-Cr	72.4 (3)	C(1)-C(2)-C(3)	122.9 (5)
C(1)-C(2)-Cr	73.8 (3)	C(3)-C(2)-Cr	71.4 (3)
C(2)-C(3)-C(4)	119.5 (5)	C(2)-C(3)-Cr	71.9 (4)
C(4)-C(3)-Cr	71.5 (3)	C(3)-C(4)-C(5)	123.1 (6)
C(3)-C(4)-Cr	71.7 (4)	C(5)-C(4)-Cr	74.3 (4)
C(4)-C(5)-B	117.9 (5)	C(4)-C(5)-Cr	69.4 (3)
B-C(5)-Cr	71.8 (3)	O(9)-C(9)-Cr	178.5 (7)
O(10)-C(10)-Cr	178.9 (6)	O(11)-C(11)-Cr	177.0 (6)
C(1)-B-C(5)	117.6 (5)	C(1)-B-N	121.3 (5)
C(5)-B-N	121.0 (5)	C(1)-B-Cr	69.9 (3)
C(5)-B-Cr	69.9 (3)	N-B-Cr	134.8 (4)

Symmetry transformations used to generate equivalent atoms:

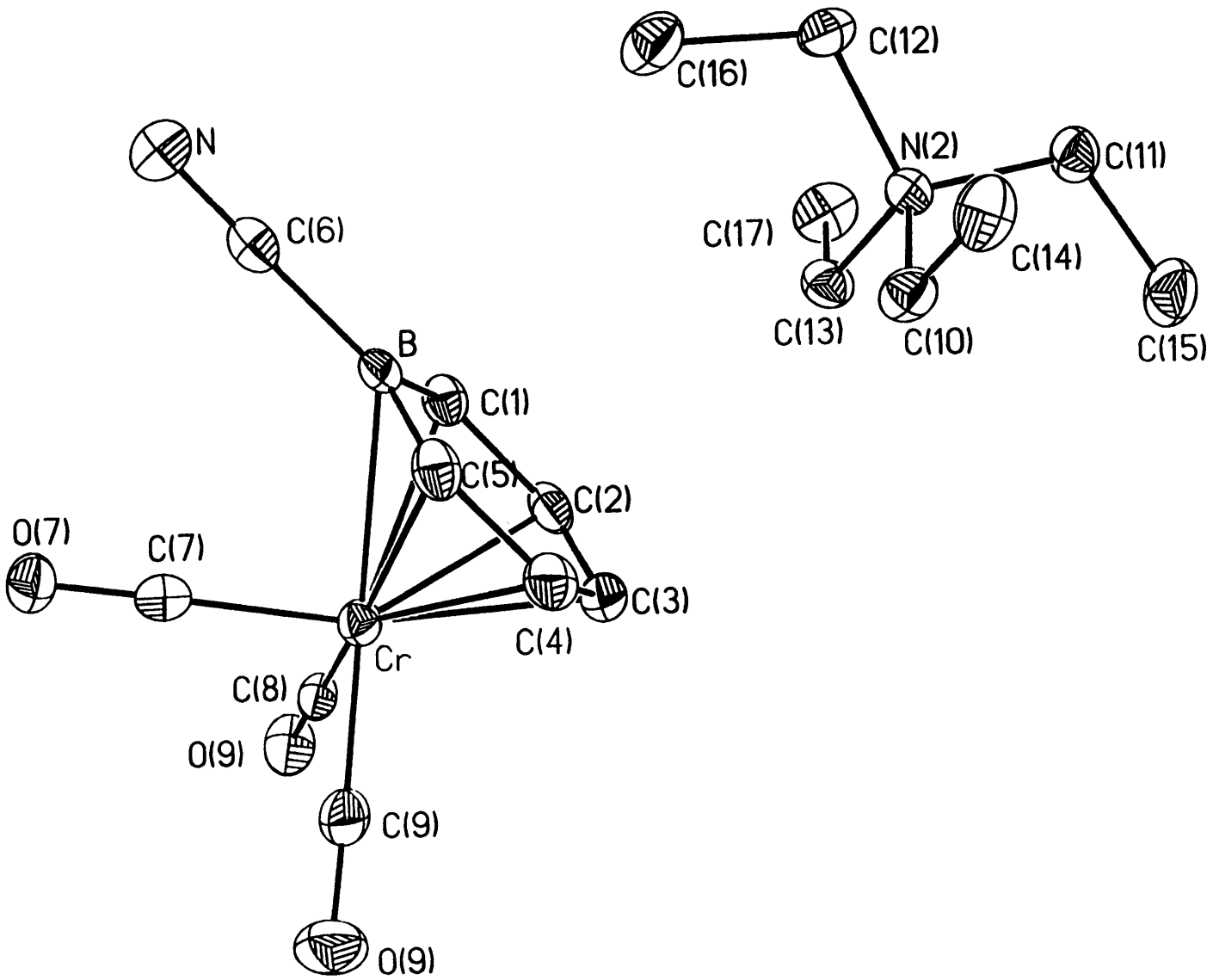


Table 1. Crystal data and structure refinement for 1.

A. Crystal Data

Identification code	98045
Empirical formula	$C_{17}H_{25}BCrN_2O_3$
Formula weight	368.20
Temperature	183(2) K
Wavelength	0.71073 Å
Crystal morphology	block
Crystal size	.12 x .15 x .15 mm
Crystal system	Monoclinic
Space group	$P2_1/n$
Unit cell dimensions	$a = 7.1171(2)$ Å $\alpha = 90^\circ$ $b = 20.9934(7)$ Å $\beta = 103.9090(10)^\circ$ $c = 13.1154(3)$ Å $\gamma = 90^\circ$
Volume, Z	1902.14(9) Å ³ , 4
Density (calculated)	1.286 Mg/m ³
Absorption coefficient	0.617 mm ⁻¹
F(000)	776

B. Data Collection and Reduction

Diffractometer	Siemens SMART/CCD
Scan Type	ω Scans
Scan angle	0.30°
θ range for data collection	1.87 to 23.30°
Limiting indices	$-7 \leq h \leq 7, -23 \leq k \leq 23, -9 \leq l \leq 14$

Reflections collected	7559
Independent reflections	2730 ($R_{int} = 0.0656$)
Absorption correction	Semi-empirical from psi-scans
Max. and min. transmission	0.8105 and 0.7103

C. Solution and Refinement

Refinement method	Full-matrix least-squares on F^2
Data / restraints / parameters	2728 / 0 / 217
Goodness-of-fit on F^2	1.149
Final R indices [$I > 2\sigma(I)$]	$R1 = 0.0567$, $wR2 = 0.1087$
R indices (all data)	$R1 = 0.0964$, $wR2 = 0.1285$
Largest diff. peak and hole	0.302 and $-0.322 \text{ e}\text{\AA}^{-3}$

Table 2. Atomic coordinates [$\times 10^4$] and equivalent isotropic displacement parameters [$\text{\AA}^2 \times 10^3$] for 1. $U(\text{eq})$ is defined as one third of the trace of the orthogonalized U_{ij} tensor.

	x	y	z	$U(\text{eq})$
Cr	1191(1)	727(1)	3255(1)	26(1)
O(9)	460(6)	1531(2)	5007(3)	42(1)
N(2)	-1702(5)	-1982(2)	1519(3)	27(1)
O(7)	1185(5)	1941(2)	2054(3)	39(1)
C(6)	-1942(7)	709(2)	691(4)	30(1)
C(2)	-823(8)	-36(2)	3543(4)	34(1)
C(3)	1019(8)	-301(2)	3635(4)	36(1)
C(4)	1938(8)	-253(2)	2799(4)	37(1)
C(5)	1072(8)	61(2)	1856(4)	32(1)
C(1)	-1827(7)	290(2)	2628(4)	29(1)
C(10)	421(7)	-1966(2)	1480(4)	32(1)
O(9)	5378(6)	935(2)	4291(3)	57(1)
C(12)	-3020(7)	-1809(2)	458(4)	32(1)
C(7)	1187(7)	1460(3)	2515(4)	29(1)
C(13)	-1921(7)	-1502(2)	2345(4)	32(1)
C(17)	-3930(8)	-1463(3)	2556(4)	44(2)
C(8)	700(7)	1207(2)	4322(4)	30(1)
B	-904(9)	348(3)	1724(5)	29(1)
N	-2722(7)	970(2)	-68(4)	42(1)
C(11)	-2293(7)	-2647(2)	1789(4)	32(1)
C(16)	-2647(8)	-1161(3)	35(4)	42(2)
C(15)	-1240(8)	-2896(3)	2861(4)	47(2)
C(9)	3754(8)	841(2)	3875(4)	36(1)
C(14)	942(8)	-2382(3)	644(4)	41(1)

Table 3. Bond lengths [Å] and angles [°] for 1.

Cr-C(7)	1.819(6)	Cr-C(8)	1.825(6)
Cr-C(9)	1.826(6)	Cr-C(3)	2.224(5)
Cr-C(4)	2.241(5)	Cr-C(2)	2.241(5)
Cr-C(5)	2.291(5)	Cr-C(1)	2.298(5)
Cr-B	2.334(6)	O(9)-C(8)	1.172(6)
N(2)-C(13)	1.515(6)	N(2)-C(11)	1.523(6)
N(2)-C(12)	1.524(6)	N(2)-C(10)	1.525(6)
O(7)-C(7)	1.177(6)	C(6)-N	1.154(6)
C(6)-B	1.573(8)	C(2)-C(3)	1.402(7)
C(2)-C(1)	1.417(7)	C(3)-C(4)	1.408(7)
C(4)-C(5)	1.407(7)	C(5)-B	1.501(8)
C(1)-B	1.492(8)	C(10)-C(14)	1.516(7)
O(9)-C(9)	1.170(6)	C(12)-C(16)	1.516(7)
C(13)-C(17)	1.522(7)	C(11)-C(15)	1.518(7)
C(7)-Cr-C(8)	88.0(2)	C(7)-Cr-C(9)	90.0(2)
C(8)-Cr-C(9)	86.6(2)	C(7)-Cr-C(3)	161.3(2)
C(8)-Cr-C(3)	109.4(2)	C(9)-Cr-C(3)	97.5(2)
C(7)-Cr-C(4)	127.2(2)	C(8)-Cr-C(4)	144.3(2)
C(9)-Cr-C(4)	88.0(2)	C(3)-Cr-C(4)	36.8(2)
C(7)-Cr-C(2)	140.8(2)	C(8)-Cr-C(2)	91.0(2)
C(9)-Cr-C(2)	129.1(2)	C(3)-Cr-C(2)	36.6(2)
C(4)-Cr-C(2)	65.9(2)	C(7)-Cr-C(5)	95.4(2)
C(8)-Cr-C(5)	166.8(2)	C(9)-Cr-C(5)	106.1(2)
C(3)-Cr-C(5)	66.1(2)	C(4)-Cr-C(5)	36.1(2)
C(2)-Cr-C(5)	78.3(2)	C(7)-Cr-C(1)	105.4(2)
C(8)-Cr-C(1)	99.2(2)	C(9)-Cr-C(1)	163.7(2)
C(3)-Cr-C(1)	66.2(2)	C(4)-Cr-C(1)	78.4(2)
C(2)-Cr-C(1)	36.3(2)	C(5)-Cr-C(1)	67.6(2)
C(7)-Cr-B	84.9(2)	C(8)-Cr-B	130.3(2)
C(9)-Cr-B	142.3(2)	C(3)-Cr-B	78.7(2)
C(4)-Cr-B	66.5(2)	C(2)-Cr-B	66.4(2)
C(5)-Cr-B	37.9(2)	C(1)-Cr-B	37.6(2)
C(13)-N(2)-C(11)	111.2(4)	C(13)-N(2)-C(12)	110.4(4)
C(11)-N(2)-C(12)	106.7(4)	C(13)-N(2)-C(10)	106.4(4)
C(11)-N(2)-C(10)	111.1(4)	C(12)-N(2)-C(10)	111.2(4)
N-C(6)-B	179.2(5)	C(3)-C(2)-C(1)	122.4(5)
C(3)-C(2)-Cr	71.0(3)	C(1)-C(2)-Cr	74.0(3)
C(2)-C(3)-C(4)	120.3(5)	C(2)-C(3)-Cr	72.4(3)
C(4)-C(3)-Cr	72.3(3)	C(5)-C(4)-C(3)	122.0(5)
C(5)-C(4)-Cr	73.8(3)	C(3)-C(4)-Cr	71.0(3)
C(4)-C(5)-B	119.3(5)	C(4)-C(5)-Cr	70.0(3)
B-C(5)-Cr	72.6(3)	C(2)-C(1)-B	118.9(5)
C(2)-C(1)-Cr	69.6(3)	B-C(1)-Cr	72.5(3)
C(14)-C(10)-N(2)	115.3(4)	C(16)-C(12)-N(2)	115.2(4)
O(7)-C(7)-Cr	178.7(4)	N(2)-C(13)-C(17)	115.4(4)
O(9)-C(8)-Cr	176.9(4)	C(1)-B-C(5)	117.0(5)
C(1)-B-C(6)	121.2(5)	C(5)-B-C(6)	121.7(5)
C(1)-B-Cr	69.9(3)	C(5)-B-Cr	69.5(3)
C(6)-B-Cr	130.4(3)	C(15)-C(11)-N(2)	115.4(4)
O(9)-C(9)-Cr	177.5(4)		

Symmetry transformations used to generate equivalent atoms:

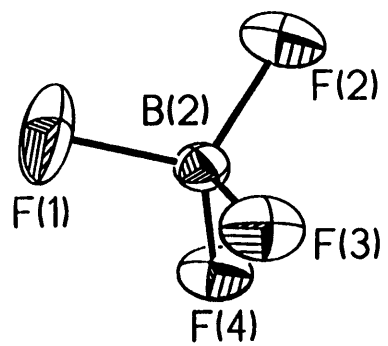
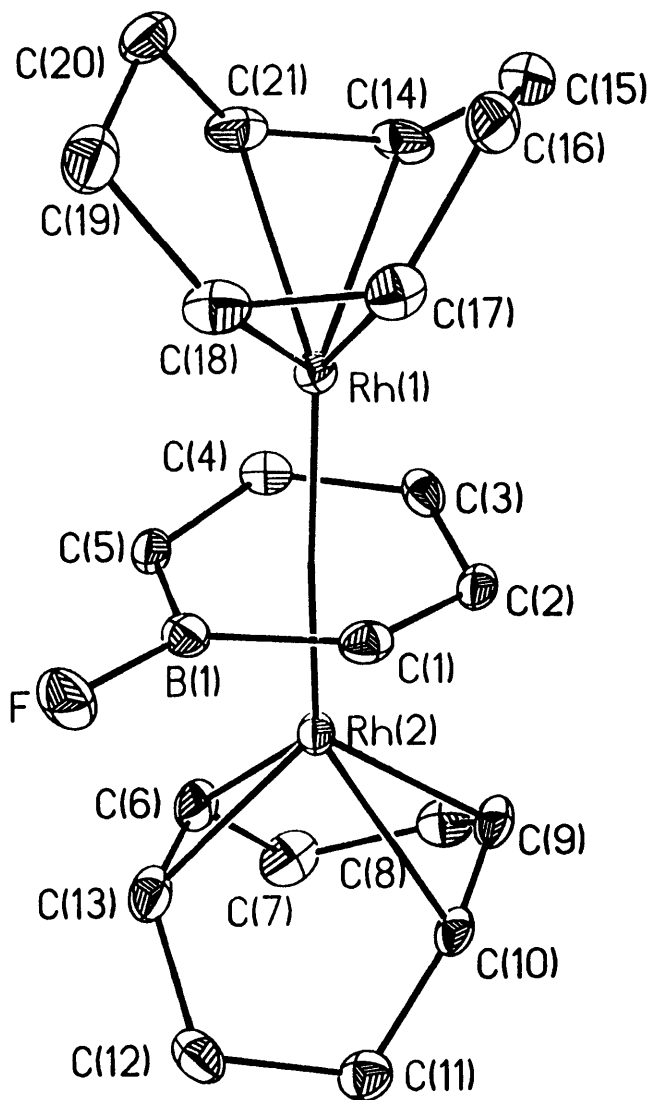


Table 1. Crystal data and structure refinement for 1.

A. Crystal Data

Identification code	98130
Empirical formula	$C_{21}H_{29}B_2F_5Rh_2$
Formula weight	603.88
Temperature	183(2) K
Wavelength	0.71073 Å
Crystal morphology	block
Crystal size	0.08 x 0.08 x 0.15 mm
Crystal system	Monoclinic
Space group	$P2_1/c$
Unit cell dimensions	$a = 7.2488(3) \text{ \AA}$ $\alpha = 90^\circ$ $b = 19.6666(9) \text{ \AA}$ $\beta = 95.9770(10)^\circ$ $c = 14.9330(7) \text{ \AA}$ $\gamma = 90^\circ$
Volume, Z	$2117.3(2) \text{ \AA}^3$, 4
Density (calculated)	1.894 Mg/m^3
Absorption coefficient	1.608 mm^{-1}
F(000)	1200

B. Data Collection and Reduction

Diffractometer	Siemens SMART/CCD
Scan Type	ω Scans
Scan angle	0.30°
θ range for data collection	1.72 to 23.28°
Limiting indices	$-8 \leq h \leq 7$, $-19 \leq k \leq 21$, $-16 \leq l \leq 16$

Reflections collected	8435
Independent reflections	3021 ($R_{int} = 0.0408$)
Absorption correction	Semi-empirical from psi-scans
Max. and min. transmission	0.7891 and 0.6953

C. Solution and Refinement

Refinement method	Full-matrix least-squares on F^2
Data / restraints / parameters	3014 / 0 / 272
Goodness-of-fit on F^2	1.115
Final R indices [$I > 2\sigma(I)$]	$R1 = 0.0303$, $wR2 = 0.0601$
R indices (all data)	$R1 = 0.0428$, $wR2 = 0.1065$
Extinction coefficient	0.00041(9)
Largest diff. peak and hole	0.380 and $-0.365 \text{ e}\text{\AA}^{-3}$

Table 2. Atomic coordinates [$\times 10^4$] and equivalent isotropic displacement parameters [$\text{\AA}^2 \times 10^3$] for 1. $U(\text{eq})$ is defined as one third of the trace of the orthogonalized U_{ij} tensor.

	x	y	z	U(eq)
Rh(1)	2320 (1)	6013 (1)	3613 (1)	19 (1)
Rh(2)	3409 (1)	7750 (1)	4425 (1)	20 (1)
F(1)	-949 (6)	7172 (2)	6257 (3)	76 (1)
F(2)	-3771 (5)	6934 (2)	6706 (2)	63 (1)
F(3)	-1187 (5)	6773 (2)	7645 (2)	54 (1)
F(4)	-2130 (4)	7836 (2)	7272 (2)	46 (1)
F	6818 (4)	6520 (2)	4200 (2)	40 (1)
C(1)	3735 (7)	6547 (2)	4854 (3)	25 (1)
C(2)	1855 (7)	6792 (2)	4766 (3)	24 (1)
C(3)	996 (7)	7028 (2)	3912 (3)	25 (1)
C(4)	2071 (7)	7137 (2)	3181 (3)	25 (1)
C(5)	4028 (7)	7060 (2)	3289 (3)	25 (1)
C(6)	4088 (8)	8678 (3)	3829 (4)	34 (1)
C(7)	2993 (8)	9282 (3)	4136 (4)	39 (1)
C(8)	1362 (7)	9061 (3)	4648 (4)	35 (1)
C(9)	1779 (7)	8405 (2)	5176 (3)	27 (1)
C(10)	3439 (6)	8263 (2)	5700 (3)	23 (1)
C(11)	5027 (7)	8767 (3)	5885 (4)	32 (1)
C(12)	6486 (7)	8660 (3)	5231 (4)	36 (1)
C(13)	5689 (8)	8416 (2)	4319 (3)	33 (1)
C(14)	-172 (6)	5599 (3)	2904 (3)	31 (1)
C(15)	-789 (8)	5008 (3)	3433 (4)	40 (1)
C(16)	779 (8)	4595 (3)	3919 (4)	35 (1)
C(17)	2475 (7)	5027 (2)	4181 (3)	28 (1)
C(18)	3941 (7)	5116 (2)	3656 (3)	31 (1)
C(19)	4035 (8)	4825 (3)	2730 (4)	38 (1)
C(20)	2232 (8)	4913 (2)	2130 (3)	33 (1)
C(21)	1247 (7)	5564 (3)	2335 (3)	32 (1)
B(1)	5004 (8)	6703 (3)	4122 (4)	26 (1)
B(2)	-2011 (9)	7173 (3)	6965 (4)	34 (2)

Table 3. Bond lengths [Å] and angles [°] for 1.

Rh(1)-C(17)	2.115(5)	Rh(1)-C(18)	2.117(5)
Rh(1)-C(14)	2.156(5)	Rh(1)-C(21)	2.172(5)
Rh(1)-C(1)	2.279(5)	Rh(1)-C(3)	2.279(4)
Rh(1)-C(4)	2.304(5)	Rh(1)-C(2)	2.356(4)
Rh(1)-B(1)	2.429(6)	Rh(1)-C(5)	2.476(5)
Rh(2)-C(6)	2.111(5)	Rh(2)-C(13)	2.127(5)
Rh(2)-C(9)	2.142(4)	Rh(2)-C(10)	2.153(4)
Rh(2)-C(5)	2.254(4)	Rh(2)-C(2)	2.280(4)
Rh(2)-C(3)	2.322(5)	Rh(2)-C(4)	2.339(5)
Rh(2)-B(1)	2.428(5)	Rh(2)-C(1)	2.457(5)
F(1)-B(2)	1.371(7)	F(2)-B(2)	1.377(7)
F(3)-B(2)	1.372(7)	F(4)-B(2)	1.388(7)
F-B(1)	1.357(6)	C(1)-C(2)	1.439(7)
C(1)-B(1)	1.532(7)	C(2)-C(3)	1.437(7)
C(3)-C(4)	1.422(7)	C(4)-C(5)	1.419(7)
C(5)-B(1)	1.535(8)	C(6)-C(13)	1.404(7)
C(6)-C(7)	1.525(7)	C(7)-C(8)	1.536(7)
C(8)-C(9)	1.528(7)	C(9)-C(10)	1.394(7)
C(10)-C(11)	1.522(7)	C(11)-C(12)	1.526(7)
C(12)-C(13)	1.503(7)	C(14)-C(21)	1.402(7)
C(14)-C(15)	1.499(7)	C(15)-C(16)	1.518(8)
C(16)-C(17)	1.512(7)	C(17)-C(18)	1.395(7)
C(18)-C(19)	1.505(7)	C(19)-C(20)	1.515(7)
C(20)-C(21)	1.514(7)		
C(17)-Rh(1)-C(18)	38.5(2)	C(17)-Rh(1)-C(14)	81.8(2)
C(18)-Rh(1)-C(14)	97.7(2)	C(17)-Rh(1)-C(21)	88.8(2)
C(18)-Rh(1)-C(21)	80.5(2)	C(14)-Rh(1)-C(21)	37.8(2)
C(17)-Rh(1)-C(1)	95.5(2)	C(18)-Rh(1)-C(1)	99.1(2)
C(14)-Rh(1)-C(1)	148.9(2)	C(21)-Rh(1)-C(1)	172.6(2)
C(17)-Rh(1)-C(3)	136.9(2)	C(18)-Rh(1)-C(3)	165.4(2)
C(14)-Rh(1)-C(3)	94.5(2)	C(21)-Rh(1)-C(3)	114.1(2)
C(1)-Rh(1)-C(3)	66.4(2)	C(17)-Rh(1)-C(4)	172.4(2)
C(18)-Rh(1)-C(4)	146.6(2)	C(14)-Rh(1)-C(4)	100.9(2)
C(21)-Rh(1)-C(4)	97.7(2)	C(1)-Rh(1)-C(4)	78.5(2)
C(3)-Rh(1)-C(4)	36.2(2)	C(17)-Rh(1)-C(2)	108.0(2)
C(18)-Rh(1)-C(2)	129.9(2)	C(14)-Rh(1)-C(2)	115.4(2)
C(21)-Rh(1)-C(2)	147.3(2)	C(1)-Rh(1)-C(2)	36.1(2)
C(3)-Rh(1)-C(2)	36.1(2)	C(4)-Rh(1)-C(2)	64.4(2)
C(17)-Rh(1)-B(1)	112.3(2)	C(18)-Rh(1)-B(1)	91.8(2)
C(14)-Rh(1)-B(1)	165.4(2)	C(21)-Rh(1)-B(1)	134.8(2)
C(1)-Rh(1)-B(1)	37.8(2)	C(3)-Rh(1)-B(1)	77.8(2)
C(4)-Rh(1)-B(1)	65.7(2)	C(2)-Rh(1)-B(1)	65.1(2)
C(17)-Rh(1)-C(5)	146.5(2)	C(18)-Rh(1)-C(5)	114.3(2)
C(14)-Rh(1)-C(5)	129.0(2)	C(21)-Rh(1)-C(5)	107.9(2)
C(1)-Rh(1)-C(5)	65.4(2)	C(3)-Rh(1)-C(5)	62.6(2)
C(4)-Rh(1)-C(5)	34.3(2)	C(2)-Rh(1)-C(5)	73.4(2)
B(1)-Rh(1)-C(5)	36.5(2)	C(6)-Rh(2)-C(13)	38.7(2)
C(6)-Rh(2)-C(9)	82.4(2)	C(13)-Rh(2)-C(9)	98.3(2)
C(6)-Rh(2)-C(10)	89.3(2)	C(13)-Rh(2)-C(10)	80.9(2)
C(9)-Rh(2)-C(10)	37.9(2)	C(6)-Rh(2)-C(5)	97.4(2)
C(13)-Rh(2)-C(5)	95.6(2)	C(9)-Rh(2)-C(5)	156.9(2)
C(10)-Rh(2)-C(5)	164.5(2)	C(6)-Rh(2)-C(2)	162.0(2)
C(13)-Rh(2)-C(2)	158.6(2)	C(9)-Rh(2)-C(2)	93.8(2)
C(10)-Rh(2)-C(2)	98.6(2)	C(5)-Rh(2)-C(2)	79.2(2)

C(6)-Rh(2)-C(3)	126.2(2)	C(13)-Rh(2)-C(3)	156.4(2)
C(9)-Rh(2)-C(3)	95.9(2)	C(10)-Rh(2)-C(3)	121.1(2)
C(5)-Rh(2)-C(3)	65.5(2)	C(2)-Rh(2)-C(3)	36.4(2)
C(6)-Rh(2)-C(4)	101.9(2)	C(13)-Rh(2)-C(4)	121.3(2)
C(9)-Rh(2)-C(4)	121.3(2)	C(10)-Rh(2)-C(4)	155.4(2)
C(5)-Rh(2)-C(4)	35.9(2)	C(2)-Rh(2)-C(4)	65.0(2)
C(3)-Rh(2)-C(4)	35.5(2)	C(6)-Rh(2)-B(1)	121.2(2)
C(13)-Rh(2)-B(1)	96.8(2)	C(9)-Rh(2)-B(1)	155.1(2)
C(10)-Rh(2)-B(1)	127.0(2)	C(5)-Rh(2)-B(1)	38.1(2)
C(2)-Rh(2)-B(1)	66.2(2)	C(3)-Rh(2)-B(1)	77.1(2)
C(4)-Rh(2)-B(1)	65.2(2)	C(6)-Rh(2)-C(1)	157.3(2)
C(13)-Rh(2)-C(1)	123.9(2)	C(9)-Rh(2)-C(1)	119.1(2)
C(10)-Rh(2)-C(1)	103.2(2)	C(5)-Rh(2)-C(1)	66.1(2)
C(2)-Rh(2)-C(1)	35.1(2)	C(3)-Rh(2)-C(1)	62.9(2)
C(4)-Rh(2)-C(1)	74.4(2)	B(1)-Rh(2)-C(1)	36.5(2)
C(2)-C(1)-B(1)	120.1(4)	C(2)-C(1)-Rh(1)	74.9(3)
B(1)-C(1)-Rh(1)	76.4(3)	C(2)-C(1)-Rh(2)	65.7(3)
B(1)-C(1)-Rh(2)	70.7(3)	Rh(1)-C(1)-Rh(2)	102.1(2)
C(3)-C(2)-C(1)	120.5(4)	C(3)-C(2)-Rh(2)	73.4(3)
C(1)-C(2)-Rh(2)	79.2(3)	C(3)-C(2)-Rh(1)	69.0(2)
C(1)-C(2)-Rh(1)	69.0(3)	Rh(2)-C(2)-Rh(1)	105.2(2)
C(4)-C(3)-C(2)	120.6(4)	C(4)-C(3)-Rh(1)	72.9(3)
C(2)-C(3)-Rh(1)	74.9(3)	C(4)-C(3)-Rh(2)	72.9(3)
C(2)-C(3)-Rh(2)	70.2(3)	Rh(1)-C(3)-Rh(2)	106.4(2)
C(5)-C(4)-C(3)	121.2(4)	C(5)-C(4)-Rh(1)	79.5(3)
C(3)-C(4)-Rh(1)	70.9(3)	C(5)-C(4)-Rh(2)	68.8(3)
C(3)-C(4)-Rh(2)	71.6(3)	Rh(1)-C(4)-Rh(2)	105.0(2)
C(4)-C(5)-B(1)	120.8(4)	C(4)-C(5)-Rh(2)	75.3(3)
B(1)-C(5)-Rh(2)	77.1(3)	C(4)-C(5)-Rh(1)	66.2(3)
B(1)-C(5)-Rh(1)	70.1(3)	Rh(2)-C(5)-Rh(1)	102.2(2)
C(13)-C(6)-C(7)	123.9(5)	C(13)-C(6)-Rh(2)	71.3(3)
C(7)-C(6)-Rh(2)	113.3(3)	C(6)-C(7)-C(8)	112.4(4)
C(9)-C(8)-C(7)	112.0(4)	C(10)-C(9)-C(8)	124.9(4)
C(10)-C(9)-Rh(2)	71.5(3)	C(8)-C(9)-Rh(2)	109.1(3)
C(9)-C(10)-C(11)	124.4(4)	C(9)-C(10)-Rh(2)	70.6(3)
C(11)-C(10)-Rh(2)	113.7(3)	C(10)-C(11)-C(12)	110.9(4)
C(13)-C(12)-C(11)	113.4(4)	C(6)-C(13)-C(12)	125.0(5)
C(6)-C(13)-Rh(2)	70.0(3)	C(12)-C(13)-Rh(2)	110.9(3)
C(21)-C(14)-C(15)	124.0(5)	C(21)-C(14)-Rh(1)	71.7(3)
C(15)-C(14)-Rh(1)	108.4(3)	C(14)-C(15)-C(16)	114.6(4)
C(17)-C(16)-C(15)	111.8(4)	C(18)-C(17)-C(16)	124.9(5)
C(18)-C(17)-Rh(1)	70.8(3)	C(16)-C(17)-Rh(1)	113.8(3)
C(17)-C(18)-C(19)	125.3(5)	C(17)-C(18)-Rh(1)	70.7(3)
C(19)-C(18)-Rh(1)	111.5(3)	C(18)-C(19)-C(20)	112.4(4)
C(21)-C(20)-C(19)	111.9(4)	C(14)-C(21)-C(20)	123.7(5)
C(14)-C(21)-Rh(1)	70.5(3)	C(20)-C(21)-Rh(1)	112.8(3)
F-B(1)-C(1)	122.2(5)	F-B(1)-C(5)	123.6(5)
C(1)-B(1)-C(5)	114.2(4)	F-B(1)-Rh(2)	133.3(4)
C(1)-B(1)-Rh(2)	72.8(3)	C(5)-B(1)-Rh(2)	64.8(3)
F-B(1)-Rh(1)	128.0(3)	C(1)-B(1)-Rh(1)	65.8(3)
C(5)-B(1)-Rh(1)	73.5(3)	Rh(2)-B(1)-Rh(1)	98.7(2)
F(1)-B(2)-F(3)	109.5(5)	F(1)-B(2)-F(2)	111.2(5)
F(3)-B(2)-F(2)	109.4(5)	F(1)-B(2)-F(4)	108.4(5)
F(3)-B(2)-F(4)	109.4(5)	F(2)-B(2)-F(4)	109.0(5)

Symmetry transformations used to generate equivalent atoms:

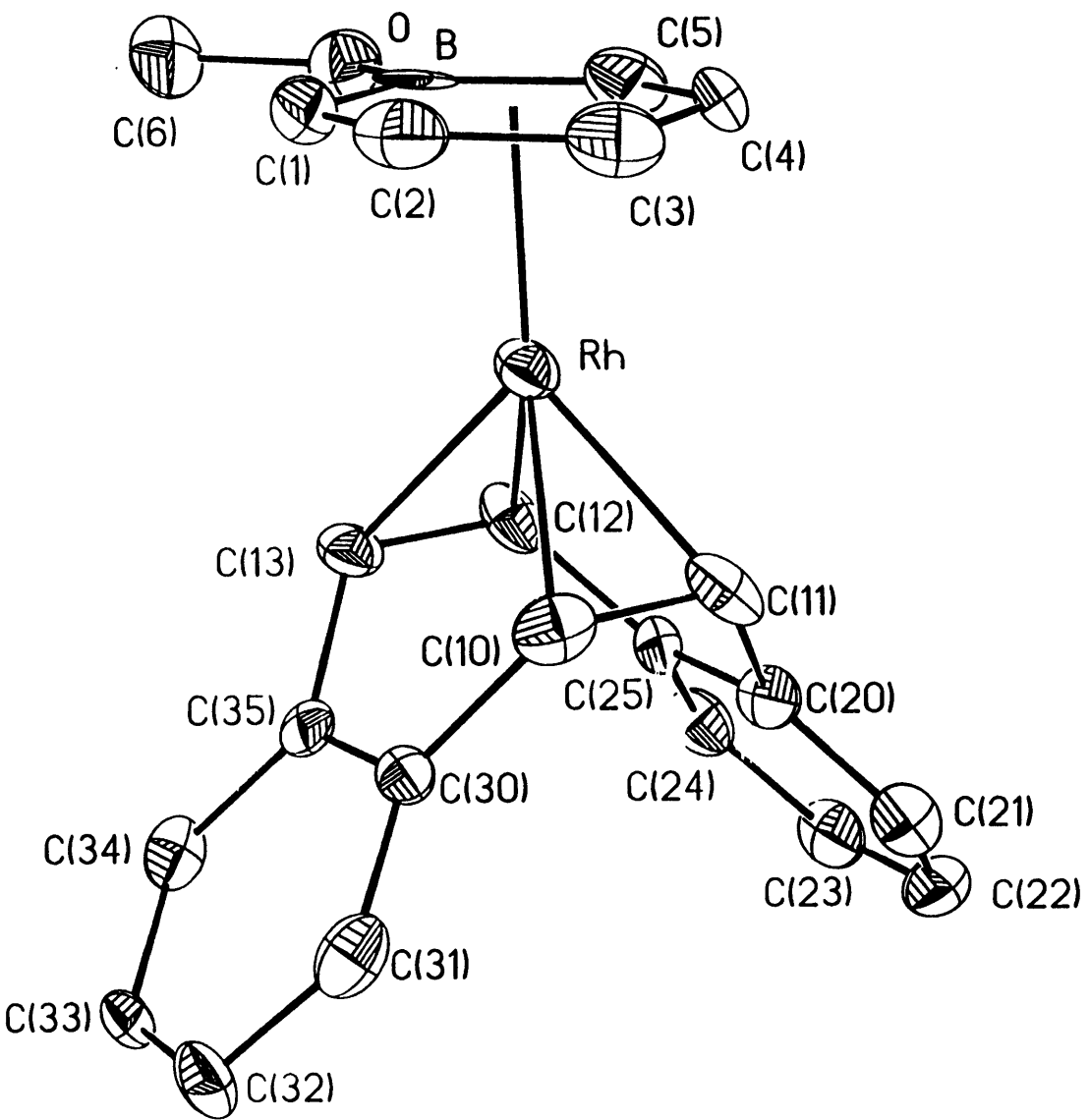


Table 1. Crystal data and structure refinement for 1.

A. Crystal Data

Identification code	98147
Empirical formula	$C_{22}H_{20}BORh$
Formula weight	414.10
Temperature	293(2) K
Wavelength	0.71073 Å
Crystal morphology	yellow
Crystal size	0.30 x 0.30 x 0.08 mm
Crystal system	Monoclinic
Space group	$P2_1/n$
Unit cell dimensions	$a = 11.1151(4)$ Å $\alpha = 90^\circ$ $b = 11.4384(4)$ Å $\beta = 93.481(2)^\circ$ $c = 13.8172(3)$ Å $\gamma = 90^\circ$
Volume, Z	1753.46(10) Å ³ , 4
Density (calculated)	1.569 Mg/m ³
Absorption coefficient	0.980 mm ⁻¹
F(000)	840

B. Data Collection and Reduction

Diffractometer	Siemens SMART/CCD
Scan Type	ω Scans
Scan angle	0.30°
θ range for data collection	2.29 to 22.50°
Limiting indices	$-8 \leq h \leq 12$, $-12 \leq k \leq 12$, $-13 \leq l \leq 15$

Reflections collected	6528
Independent reflections	2288 ($R_{int} = 0.1371$)
Absorption correction	Semi-empirical from psi-scans
Max. and min. transmission	0.3039 and 0.1873

C. Solution and Refinement

Refinement method	Full-matrix least-squares on F^2
Data / restraints / parameters	2071 / 0 / 227
Goodness-of-fit on F^2	1.203
Final R indices [$I > 2\sigma(I)$]	$R1 = 0.0814$, $wR2 = 0.1832$
R indices (all data)	$R1 = 0.1240$, $wR2 = 0.2377$
Extinction coefficient	0.0000(6)
Largest diff. peak and hole	1.646 and -1.073 $e\text{\AA}^{-3}$

Table 2. Atomic coordinates [$\times 10^4$] and equivalent isotropic displacement parameters [$\text{\AA}^2 \times 10^3$] for 1. $U(\text{eq})$ is defined as one third of the trace of the orthogonalized U_{ij} tensor.

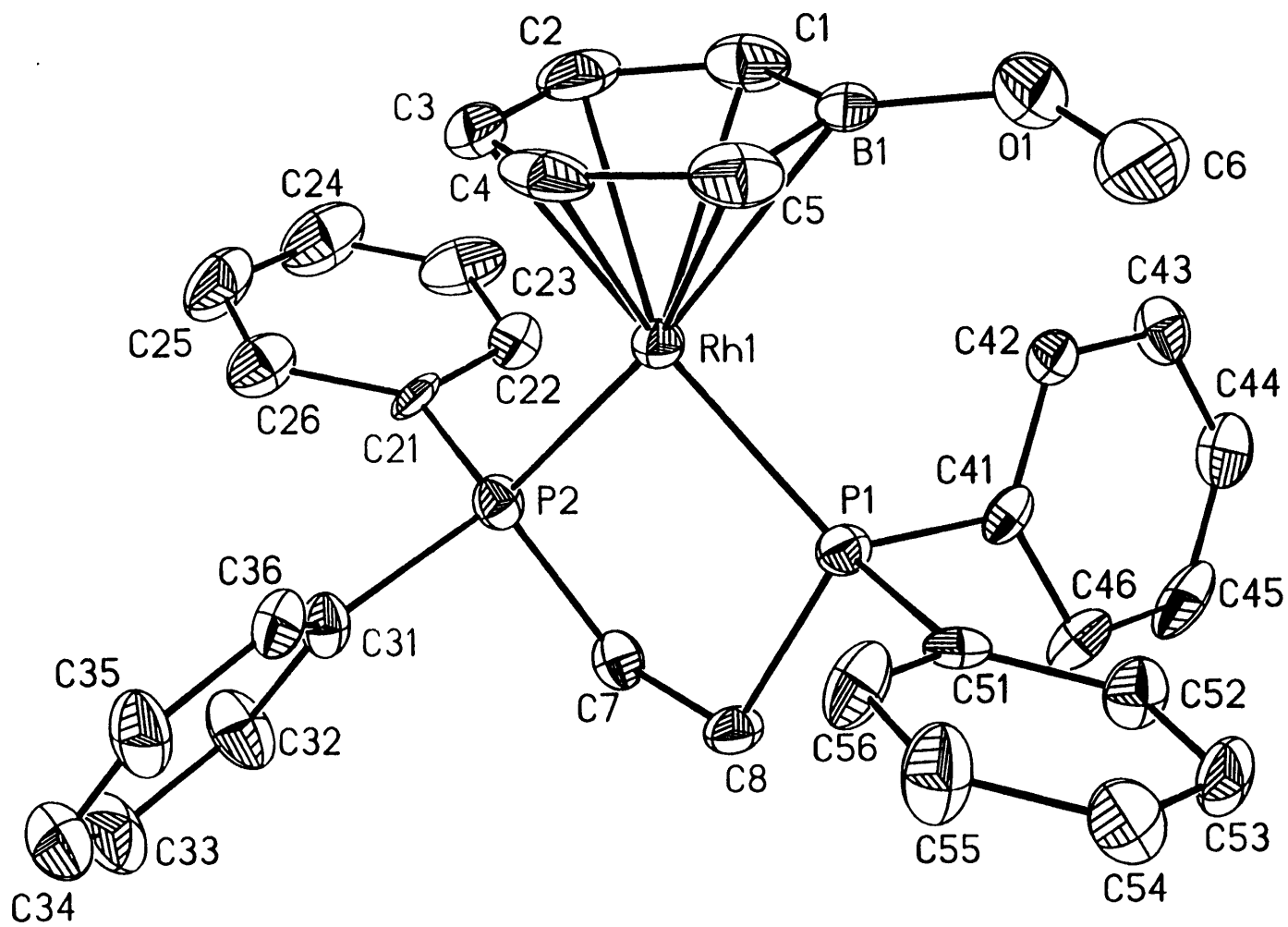
	x	y	z	$U(\text{eq})$
Rh	4963 (1)	5251 (1)	2796 (1)	31 (1)
O	1917 (9)	5231 (9)	3244 (7)	44 (2)
B	2934 (14)	4579 (13)	3059 (13)	35 (4)
C (1)	3313 (13)	4211 (13)	2084 (10)	36 (3)
C (2)	4379 (15)	3594 (13)	2008 (12)	47 (4)
C (3)	5150 (15)	3367 (13)	2823 (12)	51 (4)
C (4)	4816 (13)	3647 (12)	3769 (10)	36 (4)
C (5)	3795 (13)	4276 (13)	3914 (11)	43 (4)
C (6)	1046 (15)	5531 (12)	2516 (12)	53 (4)
C (10)	6593 (12)	5659 (12)	2128 (10)	35 (3)
C (11)	6768 (12)	5694 (12)	3125 (10)	36 (4)
C (12)	4662 (14)	6992 (11)	3239 (10)	36 (4)
C (13)	4478 (13)	6941 (11)	2235 (10)	32 (3)
C (20)	6851 (14)	6875 (13)	3702 (9)	39 (4)
C (21)	7872 (14)	7286 (14)	4148 (11)	46 (4)
C (22)	7870 (15)	8301 (15)	4709 (11)	52 (5)
C (23)	6813 (16)	8893 (14)	4784 (10)	49 (4)
C (24)	5773 (14)	8494 (12)	4310 (9)	38 (4)
C (25)	5731 (12)	7483 (12)	3760 (9)	31 (3)
C (30)	6435 (11)	6701 (11)	1512 (9)	24 (3)
C (31)	7254 (13)	7026 (13)	826 (10)	38 (4)
C (32)	7038 (14)	7983 (13)	230 (9)	39 (4)
C (33)	6021 (12)	8619 (12)	327 (9)	30 (3)
C (34)	5195 (12)	8329 (12)	969 (10)	33 (3)
C (35)	5375 (11)	7347 (11)	1565 (9)	27 (3)

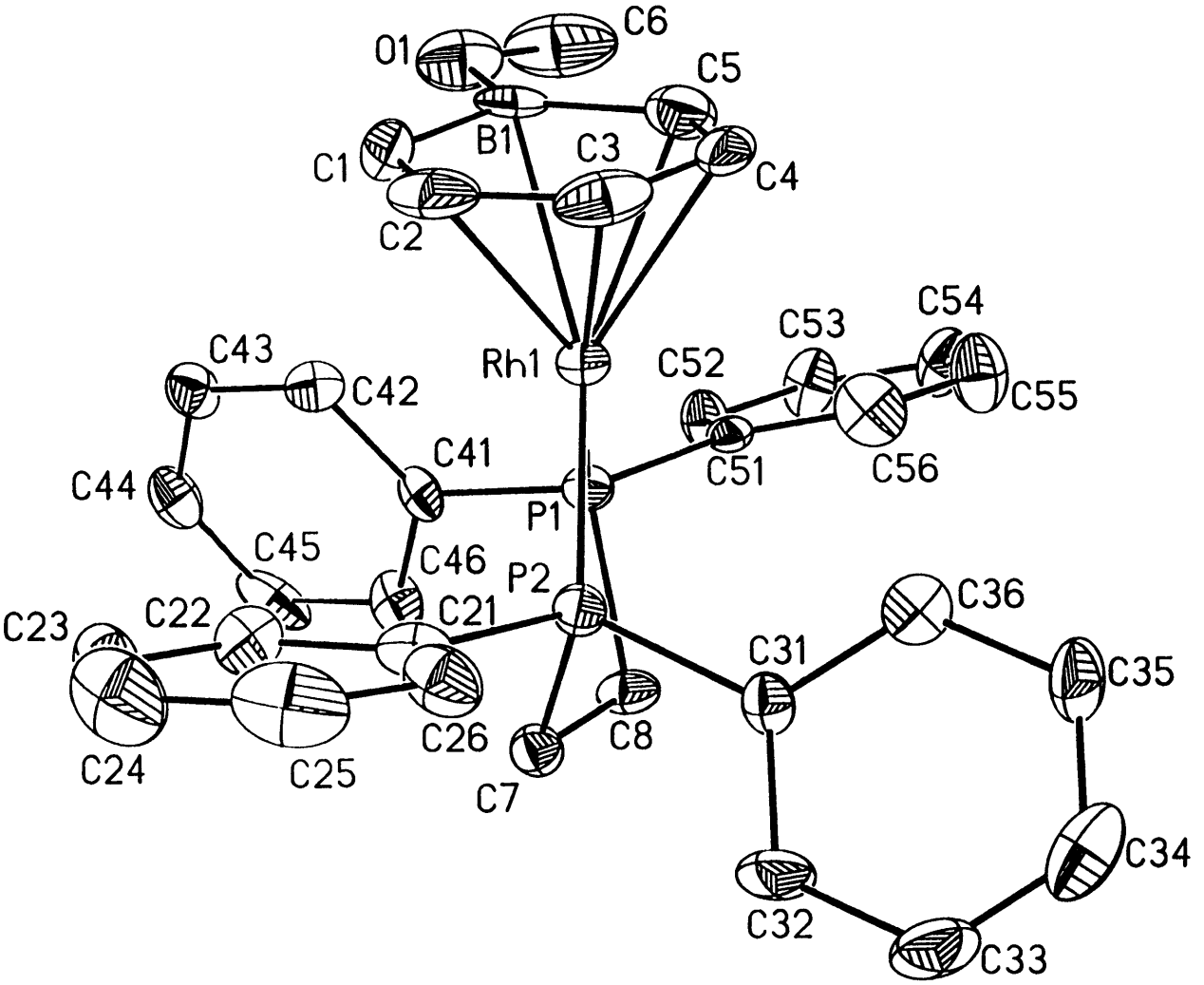
Table 3. Bond lengths [Å] and angles [°] for 1.

Rh-C(11)	2.093 (14)	Rh-C(12)	2.116 (13)
Rh-C(10)	2.135 (13)	Rh-C(13)	2.140 (13)
Rh-C(3)	2.16 (2)	Rh-C(2)	2.26 (2)
Rh-C(4)	2.286 (13)	Rh-C(1)	2.351 (14)
Rh-C(5)	2.358 (13)	Rh-B	2.430 (14)
O-B	1.39 (2)	O-C(6)	1.40 (2)
B-C(1)	1.50 (2)	B-C(5)	1.52 (2)
C(1)-C(2)	1.39 (2)	C(2)-C(3)	1.40 (2)
C(3)-C(4)	1.42 (2)	C(4)-C(5)	1.37 (2)
C(10)-C(11)	1.38 (2)	C(10)-C(30)	1.47 (2)
C(11)-C(20)	1.57 (2)	C(12)-C(13)	1.39 (2)
C(12)-C(25)	1.46 (2)	C(13)-C(35)	1.48 (2)
C(20)-C(21)	1.34 (2)	C(20)-C(25)	1.43 (2)
C(21)-C(22)	1.40 (2)	C(22)-C(23)	1.37 (2)
C(23)-C(24)	1.37 (2)	C(24)-C(25)	1.38 (2)
C(30)-C(35)	1.40 (2)	C(30)-C(31)	1.40 (2)
C(31)-C(32)	1.38 (2)	C(32)-C(33)	1.36 (2)
C(33)-C(34)	1.36 (2)	C(34)-C(35)	1.40 (2)
C(11)-Rh-C(12)	82.9 (6)	C(11)-Rh-C(10)	38.1 (5)
C(12)-Rh-C(10)	94.1 (6)	C(11)-Rh-C(13)	94.4 (5)
C(12)-Rh-C(13)	38.2 (5)	C(10)-Rh-C(13)	81.2 (5)
C(11)-Rh-C(3)	98.5 (6)	C(12)-Rh-C(3)	161.6 (6)
C(10)-Rh-C(3)	98.1 (6)	C(13)-Rh-C(3)	158.0 (6)
C(11)-Rh-C(2)	123.4 (6)	C(12)-Rh-C(2)	151.9 (6)
C(10)-Rh-C(2)	101.6 (6)	C(13)-Rh-C(2)	121.6 (6)
C(3)-Rh-C(2)	36.7 (6)	C(11)-Rh-C(4)	99.7 (5)
C(12)-Rh-C(4)	124.6 (5)	C(10)-Rh-C(4)	121.5 (5)
C(13)-Rh-C(4)	155.9 (5)	C(3)-Rh-C(4)	37.0 (5)
C(2)-Rh-C(4)	65.3 (6)	C(11)-Rh-C(1)	157.9 (5)
C(12)-Rh-C(1)	117.7 (5)	C(10)-Rh-C(1)	126.2 (5)
C(13)-Rh-C(1)	97.6 (5)	C(3)-Rh-C(1)	64.9 (6)
C(2)-Rh-C(1)	35.0 (5)	C(4)-Rh-C(1)	76.0 (5)
C(11)-Rh-C(5)	122.1 (5)	C(12)-Rh-C(5)	98.8 (5)
C(10)-Rh-C(5)	154.5 (5)	C(13)-Rh-C(5)	121.9 (5)
C(3)-Rh-C(5)	64.8 (6)	C(2)-Rh-C(5)	76.5 (5)
C(4)-Rh-C(5)	34.2 (5)	C(1)-Rh-C(5)	65.7 (5)
C(11)-Rh-B	158.5 (5)	C(12)-Rh-B	95.2 (6)
C(10)-Rh-B	162.4 (6)	C(13)-Rh-B	97.1 (5)
C(3)-Rh-B	76.8 (6)	C(2)-Rh-B	64.2 (6)
C(4)-Rh-B	63.8 (5)	C(1)-Rh-B	36.4 (5)
C(5)-Rh-B	36.9 (5)	B-O-C(6)	122.3 (12)
O-B-C(1)	126.4 (14)	O-B-C(5)	117.5 (13)
C(1)-B-C(5)	116.0 (13)	O-B-Rh	129.0 (10)
C(1)-B-Rh	68.9 (8)	C(5)-B-Rh	69.0 (7)
C(2)-C(1)-B	120.0 (14)	C(2)-C(1)-Rh	69.0 (9)
B-C(1)-Rh	74.7 (8)	C(1)-C(2)-C(3)	121 (2)
C(1)-C(2)-Rh	76.0 (9)	C(3)-C(2)-Rh	67.9 (9)
C(2)-C(3)-C(4)	121 (2)	C(2)-C(3)-Rh	75.4 (9)
C(4)-C(3)-Rh	76.2 (9)	C(5)-C(4)-C(3)	121.3 (14)
C(5)-C(4)-Rh	75.8 (8)	C(3)-C(4)-Rh	66.8 (8)
C(4)-C(5)-B	119.7 (13)	C(4)-C(5)-Rh	70.0 (7)
B-C(5)-Rh	74.2 (7)	C(11)-C(10)-C(30)	124.1 (13)
C(11)-C(10)-Rh	69.3 (8)	C(30)-C(10)-Rh	110.7 (8)
C(10)-C(11)-C(20)	122.2 (12)	C(10)-C(11)-Rh	72.6 (8)

C(20)-C(11)-Rh	110.2(9)	C(13)-C(12)-C(25)	124.9(13)
C(13)-C(12)-Rh	71.9(8)	C(25)-C(12)-Rh	111.4(9)
C(12)-C(13)-C(35)	123.2(13)	C(12)-C(13)-Rh	70.0(8)
C(35)-C(13)-Rh	110.3(9)	C(21)-C(20)-C(25)	121.2(14)
C(21)-C(20)-C(11)	124(2)	C(25)-C(20)-C(11)	115.0(11)
C(20)-C(21)-C(22)	121(2)	C(23)-C(22)-C(21)	119(2)
C(22)-C(23)-C(24)	120(2)	C(23)-C(24)-C(25)	122.7(14)
C(24)-C(25)-C(20)	115.9(12)	C(24)-C(25)-C(12)	126.2(13)
C(20)-C(25)-C(12)	117.9(12)	C(35)-C(30)-C(31)	118.6(12)
C(35)-C(30)-C(10)	118.1(11)	C(31)-C(30)-C(10)	123.2(12)
C(32)-C(31)-C(30)	121.1(13)	C(33)-C(32)-C(31)	118.7(12)
C(34)-C(33)-C(32)	122.3(12)	C(33)-C(34)-C(35)	120.2(12)
C(30)-C(35)-C(34)	119.0(12)	C(30)-C(35)-C(13)	118.0(11)
C(34)-C(35)-C(13)	122.9(12)		

Symmetry transformations used to generate equivalent atoms:





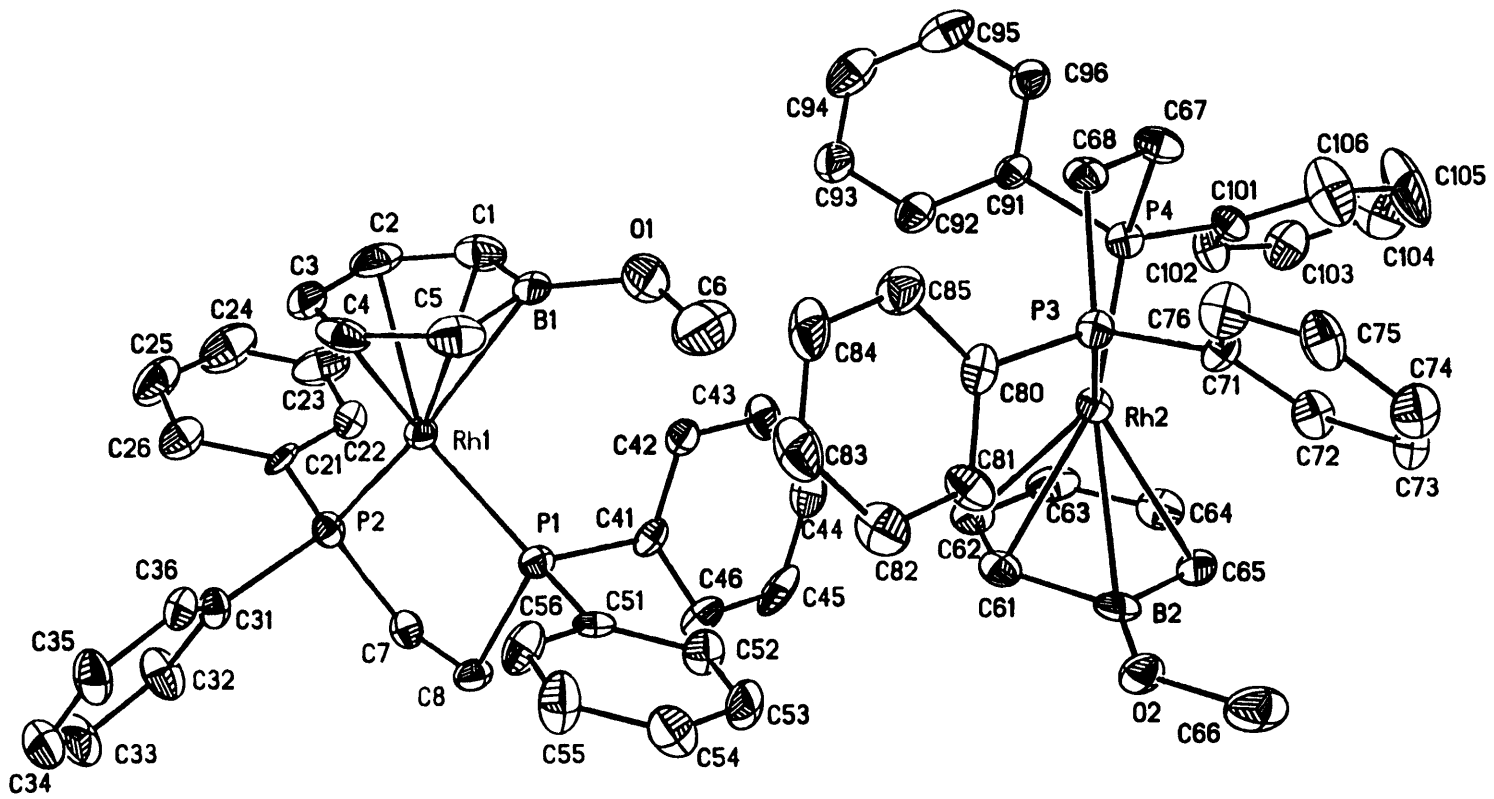


Table 1. Crystal data and structure refinement for 1.

A. Crystal Data

Identification code	98148
Empirical formula	$C_{32}H_{32}BOP_2Rh$
Formula weight	608.24
Temperature	293(2) K
Wavelength	0.71073 Å
Crystal morphology	orange block
Crystal size	.20 x .12 x .04 mm
Crystal system	Monoclinic
Space group	$P2_1/c$
Unit cell dimensions	$a = 8.81(2) \text{ \AA}$ $\alpha = 90^\circ$ $b = 25.99(5) \text{ \AA}$ $\beta = 94.35(8)^\circ$ $c = 24.06(3) \text{ \AA}$ $\gamma = 90^\circ$
Volume, Z	5496(16) Å ³ , 8
Density (calculated)	1.470 Mg/m ³
Absorption coefficient	0.762 mm ⁻¹
F(000)	2496

B. Data Collection and Reduction

Diffractometer	Siemens SMART/CCD
Scan Type	ω Scans
Scan angle	0.30°
θ range for data collection	1.16 to 23.27°
Limiting indices	$-9 \leq h \leq 9, -18 \leq k \leq 28, -21 \leq l \leq 26$

Reflections collected	21334
Independent reflections	7889 ($R_{int} = 0.1194$)
Absorption correction	Semi-empirical from psi-scans
Max. and min. transmission	0.7740 and 0.7069

C. Solution and Refinement

Refinement method	Full-matrix least-squares on F^2
Data / restraints / parameters	7871 / 0 / 668
Goodness-of-fit on F^2	1.125
Final R indices [$I > 2\sigma(I)$]	$R1 = 0.0671$, $wR2 = 0.0885$
R indices (all data)	$R1 = 0.1461$, $wR2 = 0.1328$
Extinction coefficient	0.00033(5)
Largest diff. peak and hole	0.615 and $-0.528 \text{ e}\text{\AA}^{-3}$

Table 2. Atomic coordinates [$\times 10^4$] and equivalent isotropic displacement parameters [$\text{\AA}^2 \times 10^3$] for 1. $U(\text{eq})$ is defined as one third of the trace of the orthogonalized U_{ij} tensor.

	x	y	z	U(eq)
Rh(1)	2264(1)	4630(1)	8055(1)	26(1)
Rh(2)	4348(1)	1910(1)	9869(1)	26(1)
P(1)	800(3)	4198(1)	8592(1)	27(1)
P(2)	110(3)	4952(1)	7677(1)	28(1)
P(3)	6462(3)	2247(1)	10257(1)	28(1)
P(4)	5864(3)	1508(1)	9326(1)	28(1)
O(1)	4998(7)	3677(3)	8478(3)	62(2)
O(2)	2638(7)	2271(2)	11122(2)	41(2)
B(1)	4670(11)	4153(5)	8220(5)	35(3)
B(2)	2502(11)	2085(5)	10583(4)	32(3)
C(1)	4185(10)	4159(4)	7601(4)	46(3)
C(2)	3876(10)	4612(5)	7339(4)	54(3)
C(3)	3954(11)	5084(5)	7619(5)	54(3)
C(4)	4412(10)	5114(4)	8190(5)	54(3)
C(5)	4685(10)	4664(5)	8506(4)	50(3)
C(6)	5185(12)	3648(5)	9060(5)	90(5)
C(7)	-1490(9)	4581(3)	7900(3)	31(2)
C(8)	-1135(9)	4467(4)	8512(3)	33(2)
C(21)	-99(10)	4926(4)	6922(4)	31(2)
C(22)	-189(10)	4444(4)	6667(4)	40(3)
C(23)	-290(11)	4397(5)	6094(4)	59(3)
C(24)	-280(13)	4815(6)	5771(5)	73(4)
C(25)	-152(12)	5300(5)	6010(5)	65(4)
C(26)	-71(10)	5358(4)	6587(4)	45(3)
C(31)	-472(10)	5607(3)	7839(3)	30(2)
C(32)	-1870(11)	5808(4)	7646(4)	50(3)
C(33)	-2291(12)	6295(4)	7815(5)	59(3)
C(34)	-1363(15)	6583(4)	8171(5)	64(3)
C(35)	26(13)	6399(4)	8359(4)	49(3)
C(36)	459(11)	5909(4)	8193(4)	38(3)
C(41)	477(10)	3509(3)	8459(3)	27(2)
C(42)	1531(10)	3237(3)	8183(3)	33(2)
C(43)	1316(11)	2716(4)	8058(4)	39(3)
C(44)	47(12)	2470(4)	8197(4)	43(3)
C(45)	-1005(11)	2737(4)	8469(4)	48(3)
C(46)	-821(11)	3246(4)	8609(3)	39(3)
C(51)	1267(9)	4229(4)	9346(3)	26(2)
C(52)	1229(10)	3818(4)	9709(4)	37(3)
C(53)	1595(11)	3883(4)	10275(4)	44(3)
C(54)	1979(12)	4357(4)	10482(4)	50(3)
C(55)	2032(12)	4765(4)	10132(4)	55(3)
C(56)	1672(11)	4696(4)	9563(4)	50(3)
C(61)	2441(9)	2458(4)	10102(4)	33(2)
C(62)	2127(9)	2300(4)	9548(4)	38(3)
C(63)	2098(10)	1769(4)	9426(4)	43(3)
C(64)	2218(9)	1394(4)	9847(4)	39(3)
C(65)	2403(9)	1524(4)	10408(4)	35(2)
C(66)	2753(11)	1923(5)	11582(4)	68(4)

C (67)	7871 (9)	1591 (4)	9595 (4)	36 (3)
C (68)	8036 (9)	2131 (3)	9820 (4)	32 (2)
C (71)	7205 (10)	2024 (3)	10946 (3)	25 (2)
C (72)	6491 (10)	1640 (4)	11209 (4)	35 (2)
C (73)	6945 (11)	1502 (4)	11755 (4)	46 (3)
C (74)	8130 (12)	1756 (4)	12030 (4)	43 (3)
C (75)	8896 (11)	2118 (4)	11769 (4)	44 (3)
C (76)	8452 (10)	2255 (4)	11224 (4)	42 (3)
C (80)	6511 (10)	2936 (3)	10401 (3)	28 (2)
C (81)	5481 (10)	3126 (4)	10756 (4)	39 (3)
C (82)	5441 (11)	3636 (4)	10887 (4)	49 (3)
C (83)	6435 (12)	3981 (4)	10657 (5)	55 (3)
C (84)	7488 (12)	3802 (4)	10323 (4)	52 (3)
C (85)	7535 (11)	3276 (4)	10191 (4)	46 (3)
C (91)	5895 (10)	1730 (3)	8596 (3)	29 (2)
C (92)	5195 (10)	2178 (4)	8443 (4)	38 (3)
C (93)	5276 (10)	2376 (4)	7914 (4)	48 (3)
C (94)	6047 (12)	2112 (5)	7534 (4)	58 (3)
C (95)	6737 (12)	1656 (5)	7673 (4)	55 (3)
C (96)	6680 (10)	1462 (4)	8214 (4)	39 (3)
C (101)	5608 (10)	817 (4)	9231 (4)	31 (2)
C (102)	4465 (11)	633 (4)	8862 (4)	40 (3)
C (103)	4152 (13)	113 (5)	8810 (4)	54 (3)
C (104)	4996 (13)	-227 (4)	9101 (5)	63 (3)
C (105)	6149 (16)	-57 (5)	9471 (6)	103 (5)
C (106)	6451 (13)	468 (4)	9536 (5)	71 (4)

Table 3. Bond lengths [Å] and angles [°] for 1.

Rh(1)-P(1)	2.203(3)	Rh(1)-P(2)	2.207(4)
Rh(1)-C(3)	2.223(10)	Rh(1)-C(4)	2.276(10)
Rh(1)-C(2)	2.314(10)	Rh(1)-C(5)	2.321(10)
Rh(1)-C(1)	2.417(10)	Rh(1)-B(1)	2.463(11)
Rh(2)-P(3)	2.201(4)	Rh(2)-P(4)	2.204(3)
Rh(2)-C(63)	2.211(9)	Rh(2)-C(62)	2.287(9)
Rh(2)-C(61)	2.304(9)	Rh(2)-C(64)	2.305(9)
Rh(2)-C(65)	2.443(9)	Rh(2)-B(2)	2.496(11)
P(1)-C(51)	1.831(9)	P(1)-C(41)	1.835(10)
P(1)-C(8)	1.840(8)	P(2)-C(21)	1.815(9)
P(2)-C(7)	1.823(9)	P(2)-C(31)	1.827(9)
P(3)-C(80)	1.823(9)	P(3)-C(71)	1.829(8)
P(3)-C(68)	1.828(8)	P(4)-C(101)	1.820(10)
P(4)-C(67)	1.850(9)	P(4)-C(91)	1.849(9)
O(1)-C(6)	1.399(11)	O(1)-B(1)	1.405(13)
O(2)-B(2)	1.381(11)	O(2)-C(66)	1.426(11)
B(1)-C(5)	1.50(2)	B(1)-C(1)	1.519(14)
B(2)-C(61)	1.508(13)	B(2)-C(65)	1.518(14)
C(1)-C(2)	1.355(13)	C(2)-C(3)	1.396(14)
C(3)-C(4)	1.406(14)	C(4)-C(5)	1.404(14)
C(7)-C(8)	1.511(10)	C(21)-C(26)	1.383(12)
C(21)-C(22)	1.392(12)	C(22)-C(23)	1.380(12)
C(23)-C(24)	1.334(14)	C(24)-C(25)	1.39(2)
C(25)-C(26)	1.393(12)	C(31)-C(36)	1.381(11)
C(31)-C(32)	1.385(11)	C(32)-C(33)	1.388(13)
C(33)-C(34)	1.362(14)	C(34)-C(35)	1.359(13)
C(35)-C(36)	1.398(12)	C(41)-C(42)	1.378(11)
C(41)-C(46)	1.404(11)	C(42)-C(43)	1.394(12)
C(43)-C(44)	1.353(12)	C(44)-C(45)	1.365(13)
C(45)-C(46)	1.373(13)	C(51)-C(56)	1.360(13)
C(51)-C(52)	1.383(11)	C(52)-C(53)	1.385(11)
C(53)-C(54)	1.361(12)	C(54)-C(55)	1.357(12)
C(55)-C(56)	1.395(12)	C(61)-C(62)	1.401(12)
C(62)-C(63)	1.410(13)	C(63)-C(64)	1.405(12)
C(64)-C(65)	1.389(12)	C(67)-C(68)	1.508(11)
C(71)-C(72)	1.361(11)	C(71)-C(76)	1.381(11)
C(72)-C(73)	1.391(11)	C(73)-C(74)	1.362(12)
C(74)-C(75)	1.342(12)	C(75)-C(76)	1.387(12)
C(80)-C(85)	1.385(11)	C(80)-C(81)	1.384(11)
C(81)-C(82)	1.363(12)	C(82)-C(83)	1.396(13)
C(83)-C(84)	1.356(13)	C(84)-C(85)	1.404(13)
C(91)-C(92)	1.356(12)	C(91)-C(96)	1.381(11)
C(92)-C(93)	1.379(12)	C(93)-C(94)	1.365(13)
C(94)-C(95)	1.361(14)	C(95)-C(96)	1.401(12)
C(101)-C(106)	1.354(12)	C(101)-C(102)	1.377(12)
C(102)-C(103)	1.382(13)	C(103)-C(104)	1.322(14)
C(104)-C(105)	1.37(2)	C(105)-C(106)	1.396(14)
P(1)-Rh(1)-P(2)	84.9(2)	P(1)-Rh(1)-C(3)	172.0(4)
P(2)-Rh(1)-C(3)	101.0(3)	P(1)-Rh(1)-C(4)	135.7(4)
P(2)-Rh(1)-C(4)	122.0(3)	C(3)-Rh(1)-C(4)	36.4(4)
P(1)-Rh(1)-C(2)	147.8(4)	P(2)-Rh(1)-C(2)	105.0(3)
C(3)-Rh(1)-C(2)	35.8(4)	C(4)-Rh(1)-C(2)	64.3(4)
P(1)-Rh(1)-C(5)	107.7(3)	P(2)-Rh(1)-C(5)	155.5(3)
C(3)-Rh(1)-C(5)	64.9(4)	C(4)-Rh(1)-C(5)	35.5(4)

C(2)-Rh(1)-C(5)	75.8(4)	P(1)-Rh(1)-C(1)	117.9(3)
P(2)-Rh(1)-C(1)	128.1(3)	C(3)-Rh(1)-C(1)	62.5(4)
C(4)-Rh(1)-C(1)	75.0(4)	C(2)-Rh(1)-C(1)	33.2(3)
C(5)-Rh(1)-C(1)	65.2(4)	P(1)-Rh(1)-B(1)	100.6(3)
P(2)-Rh(1)-B(1)	164.0(3)	C(3)-Rh(1)-B(1)	75.2(4)
C(4)-Rh(1)-B(1)	63.8(4)	C(2)-Rh(1)-B(1)	62.7(4)
C(5)-Rh(1)-B(1)	36.3(4)	C(1)-Rh(1)-B(1)	36.3(3)
P(3)-Rh(2)-P(4)	84.8(2)	P(3)-Rh(2)-C(63)	166.0(3)
P(4)-Rh(2)-C(63)	101.4(3)	P(3)-Rh(2)-C(62)	130.0(3)
P(4)-Rh(2)-C(62)	123.5(3)	C(63)-Rh(2)-C(62)	36.5(3)
P(3)-Rh(2)-C(61)	105.2(3)	P(4)-Rh(2)-C(61)	157.5(2)
C(63)-Rh(2)-C(61)	64.8(4)	C(62)-Rh(2)-C(61)	35.5(3)
P(3)-Rh(2)-C(64)	154.6(3)	P(4)-Rh(2)-C(64)	103.8(3)
C(63)-Rh(2)-C(64)	36.2(3)	C(62)-Rh(2)-C(64)	64.9(4)
C(61)-Rh(2)-C(64)	75.9(4)	P(3)-Rh(2)-C(65)	123.0(2)
P(4)-Rh(2)-C(65)	127.0(3)	C(63)-Rh(2)-C(65)	63.1(3)
C(62)-Rh(2)-C(65)	75.2(3)	C(61)-Rh(2)-C(65)	64.6(3)
C(64)-Rh(2)-C(65)	33.9(3)	P(3)-Rh(2)-B(2)	102.2(3)
P(4)-Rh(2)-B(2)	162.0(3)	C(63)-Rh(2)-B(2)	75.8(4)
C(62)-Rh(2)-B(2)	64.3(3)	C(61)-Rh(2)-B(2)	36.4(3)
C(64)-Rh(2)-B(2)	63.2(4)	C(65)-Rh(2)-B(2)	35.8(3)
C(51)-P(1)-C(41)	103.7(4)	C(51)-P(1)-C(8)	102.9(4)
C(41)-P(1)-C(8)	102.9(4)	C(51)-P(1)-Rh(1)	117.5(3)
C(41)-P(1)-Rh(1)	119.0(3)	C(8)-P(1)-Rh(1)	108.9(3)
C(21)-P(2)-C(7)	104.7(4)	C(21)-P(2)-C(31)	103.9(4)
C(7)-P(2)-C(31)	101.2(4)	C(21)-P(2)-Rh(1)	114.6(3)
C(7)-P(2)-Rh(1)	109.8(3)	C(31)-P(2)-Rh(1)	120.8(3)
C(80)-P(3)-C(71)	97.9(4)	C(80)-P(3)-C(68)	105.2(4)
C(71)-P(3)-C(68)	103.5(4)	C(80)-P(3)-Rh(2)	118.6(3)
C(71)-P(3)-Rh(2)	119.4(3)	C(68)-P(3)-Rh(2)	110.2(3)
C(101)-P(4)-C(67)	105.4(4)	C(101)-P(4)-C(91)	101.6(4)
C(67)-P(4)-C(91)	102.3(4)	C(101)-P(4)-Rh(2)	117.8(3)
C(67)-P(4)-Rh(2)	110.0(3)	C(91)-P(4)-Rh(2)	117.9(3)
C(6)-O(1)-B(1)	119.6(10)	B(2)-O(2)-C(66)	120.2(8)
O(1)-B(1)-C(5)	125.8(10)	O(1)-B(1)-C(1)	118.4(11)
C(5)-B(1)-C(1)	115.7(10)	O(1)-B(1)-Rh(1)	131.4(7)
C(5)-B(1)-Rh(1)	66.7(6)	C(1)-B(1)-Rh(1)	70.2(5)
O(2)-B(2)-C(61)	119.5(9)	O(2)-B(2)-C(65)	126.6(9)
C(61)-B(2)-C(65)	113.9(9)	O(2)-B(2)-Rh(2)	134.1(7)
C(61)-B(2)-Rh(2)	64.9(5)	C(65)-B(2)-Rh(2)	70.2(5)
C(2)-C(1)-B(1)	119.8(10)	C(2)-C(1)-Rh(1)	69.2(6)
B(1)-C(1)-Rh(1)	73.5(6)	C(1)-C(2)-C(3)	122.6(10)
C(1)-C(2)-Rh(1)	77.6(6)	C(3)-C(2)-Rh(1)	68.6(6)
C(2)-C(3)-C(4)	121.4(11)	C(2)-C(3)-Rh(1)	75.7(6)
C(4)-C(3)-Rh(1)	73.8(6)	C(3)-C(4)-C(5)	120.5(10)
C(3)-C(4)-Rh(1)	69.8(6)	C(5)-C(4)-Rh(1)	74.0(6)
C(4)-C(5)-B(1)	119.8(9)	C(4)-C(5)-Rh(1)	70.5(6)
B(1)-C(5)-Rh(1)	77.0(6)	C(8)-C(7)-P(2)	106.4(6)
C(7)-C(8)-P(1)	107.4(6)	C(26)-C(21)-C(22)	118.4(9)
C(26)-C(21)-P(2)	123.2(8)	C(22)-C(21)-P(2)	118.3(7)
C(23)-C(22)-C(21)	121.1(10)	C(24)-C(23)-C(22)	120.5(11)
C(23)-C(24)-C(25)	120.1(11)	C(24)-C(25)-C(26)	120.4(11)
C(21)-C(26)-C(25)	119.4(11)	C(36)-C(31)-C(32)	117.7(9)
C(36)-C(31)-P(2)	119.8(7)	C(32)-C(31)-P(2)	122.4(7)
C(31)-C(32)-C(33)	119.8(10)	C(34)-C(33)-C(32)	121.6(10)
C(35)-C(34)-C(33)	120.0(11)	C(34)-C(35)-C(36)	118.9(10)
C(31)-C(36)-C(35)	122.1(9)	C(42)-C(41)-C(46)	117.8(9)
C(42)-C(41)-P(1)	119.0(7)	C(46)-C(41)-P(1)	123.2(7)
C(41)-C(42)-C(43)	121.1(9)	C(44)-C(43)-C(42)	120.5(10)

C(43)-C(44)-C(45)	118.8(10)	C(44)-C(45)-C(46)	122.4(9)
C(45)-C(46)-C(41)	119.4(9)	C(56)-C(51)-C(52)	117.7(8)
C(56)-C(51)-P(1)	116.9(7)	C(52)-C(51)-P(1)	125.4(7)
C(51)-C(52)-C(53)	120.8(9)	C(54)-C(53)-C(52)	120.3(9)
C(55)-C(54)-C(53)	120.0(9)	C(54)-C(55)-C(56)	119.5(10)
C(51)-C(56)-C(55)	121.7(9)	C(62)-C(61)-B(2)	122.4(9)
C(62)-C(61)-Rh(2)	71.6(5)	B(2)-C(61)-Rh(2)	78.8(5)
C(61)-C(62)-C(63)	118.9(9)	C(61)-C(62)-Rh(2)	72.9(5)
C(63)-C(62)-Rh(2)	68.8(5)	C(64)-C(63)-C(62)	122.0(9)

C(64)-C(63)-Rh(2)	75.6(5)	C(62)-C(63)-Rh(2)	74.7(5)
C(65)-C(64)-C(63)	121.9(9)	C(65)-C(64)-Rh(2)	78.5(5)
C(63)-C(64)-Rh(2)	68.3(5)	C(64)-C(65)-B(2)	120.2(9)
C(64)-C(65)-Rh(2)	67.6(5)	B(2)-C(65)-Rh(2)	74.0(5)
C(68)-C(67)-P(4)	107.3(6)	C(67)-C(68)-P(3)	107.6(6)
C(72)-C(71)-C(76)	118.1(8)	C(72)-C(71)-P(3)	120.5(7)
C(76)-C(71)-P(3)	121.2(7)	C(71)-C(72)-C(73)	121.3(9)
C(74)-C(73)-C(72)	119.3(9)	C(75)-C(74)-C(73)	120.5(10)
C(74)-C(75)-C(76)	120.4(10)	C(71)-C(76)-C(75)	120.3(9)
C(85)-C(80)-C(81)	118.2(9)	C(85)-C(80)-P(3)	124.3(8)
C(81)-C(80)-P(3)	117.4(7)	C(82)-C(81)-C(80)	121.3(10)
C(81)-C(82)-C(83)	120.3(10)	C(84)-C(83)-C(82)	119.5(10)
C(83)-C(84)-C(85)	120.1(10)	C(80)-C(85)-C(84)	120.5(10)
C(92)-C(91)-C(96)	119.5(9)	C(92)-C(91)-P(4)	119.2(7)
C(96)-C(91)-P(4)	121.3(7)	C(91)-C(92)-C(93)	121.2(9)
C(94)-C(93)-C(92)	119.6(10)	C(95)-C(94)-C(93)	120.7(11)
C(94)-C(95)-C(96)	119.6(10)	C(91)-C(96)-C(95)	119.5(9)
C(106)-C(101)-C(102)	117.5(9)	C(106)-C(101)-P(4)	122.4(7)
C(102)-C(101)-P(4)	120.0(7)	C(101)-C(102)-C(103)	122.0(10)
C(104)-C(103)-C(102)	120.4(11)	C(103)-C(104)-C(105)	119.2(11)
C(104)-C(105)-C(106)	120.8(12)	C(101)-C(106)-C(105)	120.2(11)

Symmetry transformations used to generate equivalent atoms:

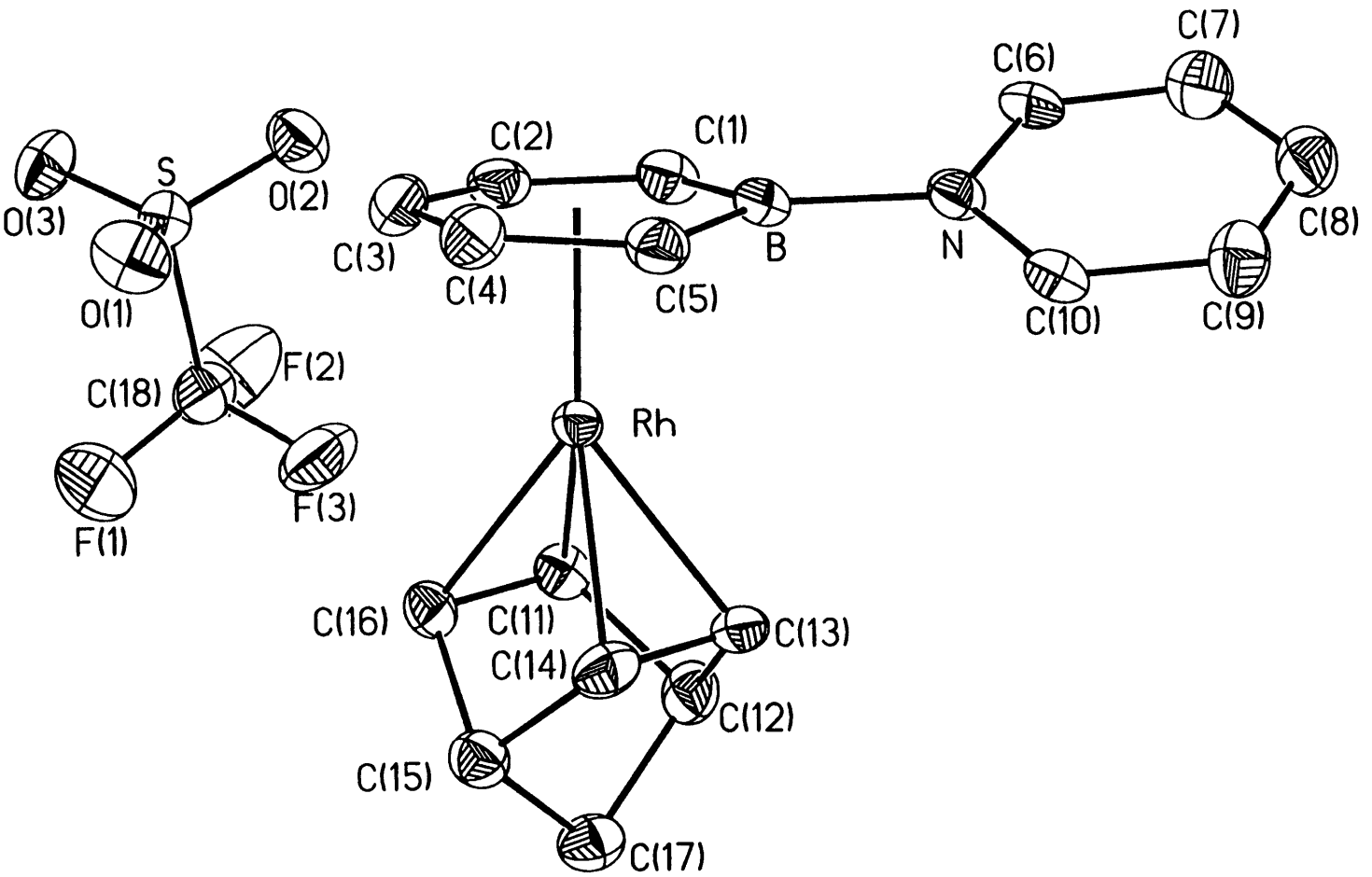


Table 1. Crystal data and structure refinement for 1.

A. Crystal Data

Identification code	98157
Empirical formula	$C_{18}H_{18}BF_3NO_3RhS$
Formula weight	499.11
Temperature	206(2) K
Wavelength	0.71073 Å
Crystal morphology	block
Crystal size	0.08 x 0.20 x 0.20 mm
Crystal system	Triclinic
Space group	$P\bar{1}$
Unit cell dimensions	$a = 9.3769(3)$ Å $\alpha = 116.7200(10)^\circ$ $b = 10.3573(3)$ Å $\beta = 90.2090(10)^\circ$ $c = 10.9920(4)$ Å $\gamma = 101.1900(10)^\circ$
Volume, Z	930.36(5) Å ³ , 2
Density (calculated)	1.782 Mg/m ³
Absorption coefficient	1.079 mm ⁻¹
F(000)	500

B. Data Collection and Reduction

Diffractionmeter	Siemens SMART/CCD
Scan Type	ω Scans
Scan angle	0.30 ^o
θ range for data collection	2.09 to 23.26 ^o
Limiting indices	$-5 \leq h \leq 10, -10 \leq k \leq 11, -12 \leq l \leq 12$

Reflections collected	3010
Independent reflections	2383 ($R_{int} = 0.0963$)
Absorption correction	None

C. Solution and Refinement

Refinement method	Full-matrix least-squares on F^2
Data / restraints / parameters	2363 / 0 / 254
Goodness-of-fit on F^2	1.101
Final R indices [$I > 2\sigma(I)$]	$R_1 = 0.0307$, $wR_2 = 0.0834$
R indices (all data)	$R_1 = 0.0538$, $wR_2 = 0.1766$
Extinction coefficient	0.037(3)
Largest diff. peak and hole	0.583 and $-0.719 \text{ e}\text{\AA}^{-3}$

Table 2. Atomic coordinates [$\times 10^4$] and equivalent isotropic displacement parameters [$\text{\AA}^2 \times 10^3$] for 1. $U(\text{eq})$ is defined as one third of the trace of the orthogonalized U_{ij} tensor.

	x	y	z	U(eq)
Rh	2359(1)	2314(1)	2271(1)	25(1)
S	2883(1)	2784(1)	-2401(1)	34(1)
F(1)	585(5)	3916(6)	-2126(7)	122(2)
F(2)	260(4)	1692(7)	-3677(5)	113(2)
F(3)	333(4)	2156(5)	-1601(4)	81(1)
O(1)	3413(4)	3868(4)	-1031(4)	57(1)
O(2)	3017(4)	1316(4)	-2718(4)	52(1)
O(3)	3277(4)	3213(4)	-3452(4)	54(1)
N	3503(4)	-599(4)	2648(3)	29(1)
B	3803(5)	675(5)	2255(5)	30(1)
C(1)	3451(5)	411(5)	819(5)	35(1)
C(2)	3770(5)	1620(5)	521(5)	37(1)
C(3)	4484(5)	3075(6)	1518(5)	42(1)
C(4)	4794(5)	3381(5)	2879(5)	39(1)
C(5)	4412(5)	2266(5)	3307(5)	34(1)
C(6)	3461(5)	-2010(5)	1686(5)	34(1)
C(7)	3293(5)	-3166(5)	1996(5)	43(1)
C(8)	3136(5)	-2892(5)	3338(5)	43(1)
C(9)	3157(5)	-1476(5)	4319(5)	41(1)
C(10)	3327(4)	-337(5)	3953(4)	32(1)
C(11)	237(5)	1880(5)	1250(4)	33(1)
C(12)	-662(5)	1573(5)	2292(5)	38(1)
C(13)	601(5)	1842(5)	3321(5)	35(1)
C(14)	1189(5)	3381(5)	3959(5)	36(1)
C(15)	273(5)	4036(5)	3309(5)	36(1)
C(16)	805(5)	3421(5)	1883(4)	31(1)
C(17)	-1238(5)	3005(5)	3018(5)	42(1)
C(18)	915(6)	2642(7)	-2438(6)	53(1)

Table 3. Bond lengths [Å] and angles [°] for 1.

Rh-C(13)	2.120(4)	Rh-C(14)	2.123(5)
Rh-C(11)	2.145(4)	Rh-C(16)	2.169(4)
Rh-C(5)	2.254(4)	Rh-C(2)	2.261(5)
Rh-C(4)	2.286(4)	Rh-C(3)	2.295(5)
Rh-C(1)	2.334(5)	Rh-B	2.363(5)
S-O(1)	1.426(4)	S-O(2)	1.431(4)
S-O(3)	1.438(3)	S-C(18)	1.822(5)
F(1)-C(18)	1.307(7)	F(2)-C(18)	1.324(7)
F(3)-C(18)	1.307(6)	N-C(10)	1.351(6)
N-C(6)	1.358(5)	N-B	1.541(6)
B-C(1)	1.500(7)	B-C(5)	1.515(7)
C(1)-C(2)	1.410(6)	C(2)-C(3)	1.428(7)
C(3)-C(4)	1.399(7)	C(4)-C(5)	1.418(6)
C(6)-C(7)	1.368(6)	C(7)-C(8)	1.385(7)
C(8)-C(9)	1.371(7)	C(9)-C(10)	1.391(6)
C(11)-C(16)	1.409(6)	C(11)-C(12)	1.534(6)
C(12)-C(13)	1.529(7)	C(12)-C(17)	1.543(7)
C(13)-C(14)	1.409(7)	C(14)-C(15)	1.539(6)
C(15)-C(16)	1.531(6)	C(15)-C(17)	1.534(6)
C(13)-Rh-C(14)	38.8(2)	C(13)-Rh-C(11)	65.9(2)
C(14)-Rh-C(11)	78.9(2)	C(13)-Rh-C(16)	78.8(2)
C(14)-Rh-C(16)	65.7(2)	C(11)-Rh-C(16)	38.1(2)
C(13)-Rh-C(5)	107.0(2)	C(14)-Rh-C(5)	102.2(2)
C(11)-Rh-C(5)	167.3(2)	C(16)-Rh-C(5)	153.6(2)
C(13)-Rh-C(2)	151.7(2)	C(14)-Rh-C(2)	169.1(2)
C(11)-Rh-C(2)	102.8(2)	C(16)-Rh-C(2)	108.9(2)
C(5)-Rh-C(2)	78.6(2)	C(13)-Rh-C(4)	134.4(2)
C(14)-Rh-C(4)	108.8(2)	C(11)-Rh-C(4)	155.3(2)
C(16)-Rh-C(4)	122.5(2)	C(5)-Rh-C(4)	36.4(2)
C(2)-Rh-C(4)	65.3(2)	C(13)-Rh-C(3)	169.7(2)
C(14)-Rh-C(3)	133.8(2)	C(11)-Rh-C(3)	123.0(2)
C(16)-Rh-C(3)	105.0(2)	C(5)-Rh-C(3)	65.4(2)
C(2)-Rh-C(3)	36.5(2)	C(4)-Rh-C(3)	35.6(2)
C(13)-Rh-C(1)	119.6(2)	C(14)-Rh-C(1)	154.6(2)
C(11)-Rh-C(1)	105.7(2)	C(16)-Rh-C(1)	132.5(2)
C(5)-Rh-C(1)	67.9(2)	C(2)-Rh-C(1)	35.7(2)
C(4)-Rh-C(1)	77.6(2)	C(3)-Rh-C(1)	65.0(2)
C(13)-Rh-B	101.1(2)	C(14)-Rh-B	121.6(2)
C(11)-Rh-B	130.7(2)	C(16)-Rh-B	167.8(2)
C(5)-Rh-B	38.2(2)	C(2)-Rh-B	65.6(2)
C(4)-Rh-B	66.2(2)	C(3)-Rh-B	77.2(2)
C(1)-Rh-B	37.2(2)	O(1)-S-O(2)	114.5(2)
O(1)-S-O(3)	116.0(2)	O(2)-S-O(3)	114.3(2)
O(1)-S-C(18)	103.3(3)	O(2)-S-C(18)	103.0(2)
O(3)-S-C(18)	103.4(2)	C(10)-N-C(6)	118.7(3)
C(10)-N-B	121.2(4)	C(6)-N-B	120.0(4)
C(1)-B-C(5)	116.4(4)	C(1)-B-N	121.6(4)
C(5)-B-N	121.9(4)	C(1)-B-Rh	70.3(2)
C(5)-B-Rh	67.0(2)	N-B-Rh	131.7(3)
C(2)-C(1)-B	118.9(4)	C(2)-C(1)-Rh	69.3(3)
B-C(1)-Rh	72.4(3)	C(1)-C(2)-C(3)	122.5(4)
C(1)-C(2)-Rh	75.0(3)	C(3)-C(2)-Rh	73.0(3)
C(4)-C(3)-C(2)	120.4(4)	C(4)-C(3)-Rh	71.9(3)
C(2)-C(3)-Rh	70.5(3)	C(3)-C(4)-C(5)	121.3(4)

C(3)-C(4)-Rh	72.5(3)	C(5)-C(4)-Rh	70.5(2)
C(4)-C(5)-B	119.8(4)	C(4)-C(5)-Rh	73.1(3)
B-C(5)-Rh	74.8(3)	N-C(6)-C(7)	122.4(4)
C(6)-C(7)-C(8)	118.8(4)	C(9)-C(8)-C(7)	119.5(4)
C(8)-C(9)-C(10)	119.6(5)	N-C(10)-C(9)	121.0(4)
C(16)-C(11)-C(12)	105.8(4)	C(16)-C(11)-Rh	71.8(2)
C(12)-C(11)-Rh	97.2(3)	C(13)-C(12)-C(11)	98.4(3)
C(13)-C(12)-C(17)	102.0(4)	C(11)-C(12)-C(17)	101.2(4)
C(14)-C(13)-C(12)	106.0(4)	C(14)-C(13)-Rh	70.7(3)
C(12)-C(13)-Rh	98.4(3)	C(13)-C(14)-C(15)	106.1(4)
C(13)-C(14)-Rh	70.5(3)	C(15)-C(14)-Rh	98.5(3)
C(16)-C(15)-C(17)	101.0(3)	C(16)-C(15)-C(14)	98.7(4)
C(17)-C(15)-C(14)	101.7(3)	C(11)-C(16)-C(15)	106.3(4)
C(11)-C(16)-Rh	70.1(2)	C(15)-C(16)-Rh	96.9(3)
C(15)-C(17)-C(12)	94.3(4)	F(1)-C(18)-F(3)	108.3(5)
F(1)-C(18)-F(2)	107.5(5)	F(3)-C(18)-F(2)	106.4(5)
F(1)-C(18)-S	111.6(4)	F(3)-C(18)-S	112.4(3)
F(2)-C(18)-S	110.5(4)		

Symmetry transformations used to generate equivalent atoms:

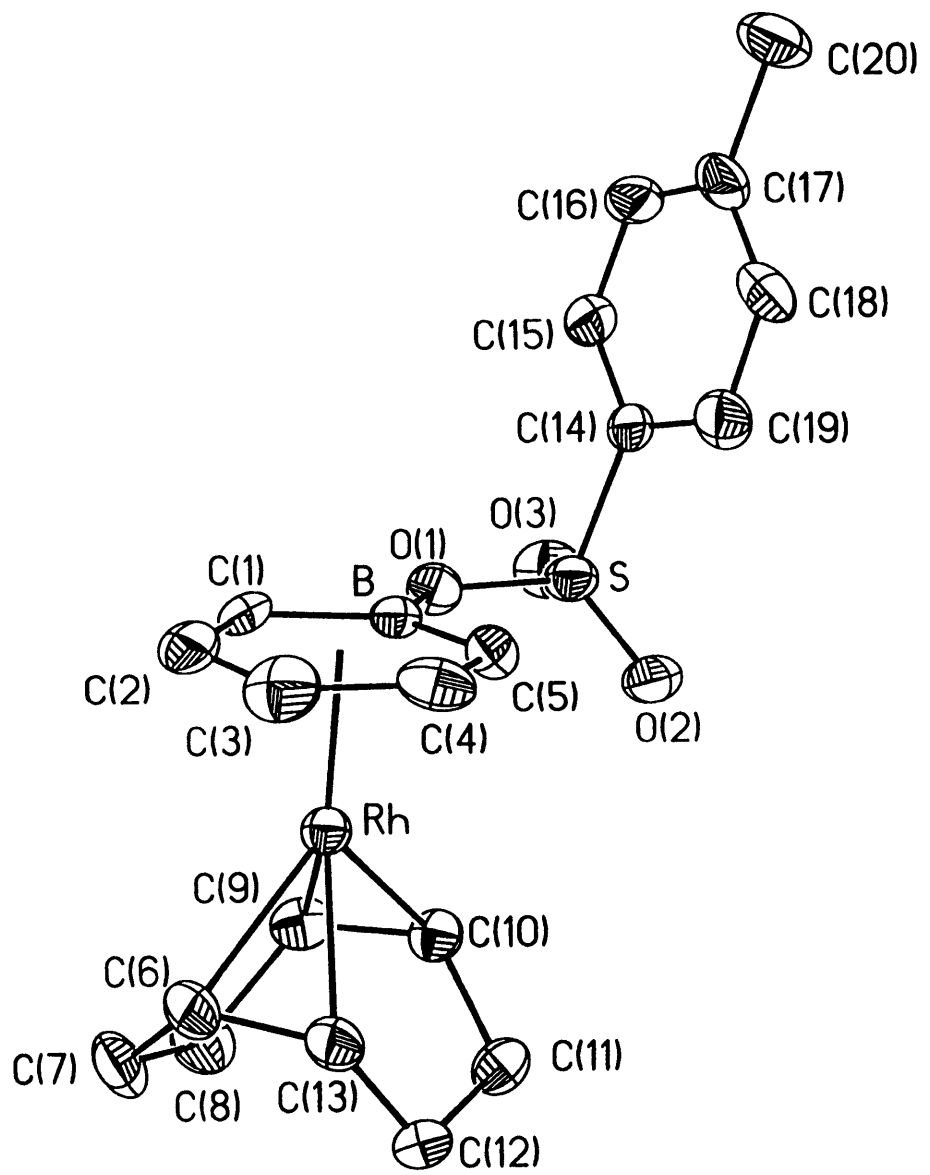


Table 1. Crystal data and structure refinement for 1.

A. Crystal Data

Identification code	98158
Empirical formula	$C_{20}H_{24}BO_3RhS$
Formula weight	458.17
Temperature	205(2) K
Wavelength	0.71073 Å
Crystal morphology	thin plate
Crystal size	0.04 x 0.30 x 0.70 mm
Crystal system	Monoclinic
Space group	Cc
Unit cell dimensions	$a = 6.5653(5) \text{ \AA}$ $\alpha = 90^\circ$ $b = 18.529(2) \text{ \AA}$ $\beta = 93.3020(10)^\circ$ $c = 15.8120(12) \text{ \AA}$ $\gamma = 90^\circ$
Volume, Z	$1920.3(3) \text{ \AA}^3$, 4
Density (calculated)	1.585 Mg/m^3
Absorption coefficient	1.015 mm^{-1}
F(000)	936

B. Data Collection and Reduction

Diffractometer	Siemens SMART/CCD
Scan Type	ω Scans
Scan angle	0.30°
θ range for data collection	2.20 to 23.24°
Limiting indices	$-7 \leq h \leq 3$, $-20 \leq k \leq 20$, $-17 \leq l \leq 17$

Reflections collected	3803
Independent reflections	1812 ($R_{int} = 0.0812$)
Absorption correction	None

C. Solution and Refinement

Refinement method	Full-matrix least-squares on F^2
Data / restraints / parameters	1789 / 2 / 236
Goodness-of-fit on F^2	1.102
Final R indices [$I > 2\sigma(I)$]	$R1 = 0.0333$, $wR2 = 0.0731$
R indices (all data)	$R1 = 0.0557$, $wR2 = 0.1923$
Absolute structure parameter	-0.02(4)
Extinction coefficient	0.0029(4)
Largest diff. peak and hole	0.584 and -0.634 $e\text{\AA}^{-3}$

Table 2. Atomic coordinates [$\times 10^4$] and equivalent isotropic displacement parameters [$\text{\AA}^2 \times 10^3$] for 1. $U(\text{eq})$ is defined as one third of the trace of the orthogonalized U_{ij} tensor.

	x	y	z	U(eq)
Rh	8707 (1)	-7753 (1)	2892 (1)	34 (1)
S	8031 (3)	-5355 (1)	2314 (1)	45 (1)
O(1)	9096 (7)	-6052 (2)	2007 (3)	45 (1)
O(2)	6907 (9)	-5517 (2)	3034 (3)	60 (1)
O(3)	9591 (10)	-4822 (3)	2381 (3)	66 (1)
B	8270 (14)	-6777 (4)	1926 (4)	39 (2)
C(1)	9645 (14)	-7336 (3)	1562 (4)	46 (2)
C(2)	8996 (15)	-8060 (4)	1493 (4)	61 (2)
C(3)	7052 (15)	-8269 (4)	1778 (5)	62 (2)
C(4)	5633 (16)	-7751 (4)	2073 (6)	53 (2)
C(5)	6199 (13)	-7021 (5)	2174 (5)	43 (2)
C(6)	9860 (11)	-8728 (3)	3488 (4)	47 (2)
C(7)	12029 (11)	-8631 (4)	3845 (5)	58 (2)
C(8)	12501 (13)	-7869 (4)	4132 (6)	59 (2)
C(9)	11156 (17)	-7299 (4)	3672 (5)	45 (2)
C(10)	9273 (12)	-7055 (4)	3957 (4)	41 (2)
C(11)	8312 (15)	-7331 (3)	4727 (5)	51 (2)
C(12)	8183 (12)	-8151 (4)	4758 (4)	52 (2)
C(13)	8108 (11)	-8495 (3)	3892 (4)	44 (2)
C(14)	6317 (11)	-5130 (3)	1451 (4)	41 (2)
C(15)	7015 (12)	-4777 (3)	768 (4)	51 (2)
C(16)	5683 (16)	-4618 (4)	78 (4)	60 (2)
C(17)	3640 (15)	-4807 (4)	78 (5)	60 (2)
C(18)	2964 (13)	-5152 (4)	778 (5)	56 (2)
C(19)	4245 (12)	-5304 (4)	1480 (5)	54 (2)
C(20)	2196 (19)	-4635 (5)	-665 (6)	83 (3)

Table 3. Bond lengths [Å] and angles [°] for 1.

Rh-C(10)	2.139(6)	Rh-C(9)	2.141(9)
Rh-C(13)	2.150(6)	Rh-C(6)	2.155(5)
Rh-C(3)	2.231(7)	Rh-C(2)	2.302(7)
Rh-C(4)	2.334(10)	Rh-C(1)	2.354(7)
Rh-C(5)	2.371(8)	Rh-B	2.374(7)
S-O(3)	1.423(6)	S-O(2)	1.424(5)
S-O(1)	1.560(4)	S-C(14)	1.768(6)
O(1)-B	1.450(9)	B-C(5)	1.507(12)
B-C(1)	1.511(10)	C(1)-C(2)	1.408(11)
C(2)-C(3)	1.431(13)	C(3)-C(4)	1.434(12)
C(4)-C(5)	1.409(11)	C(6)-C(13)	1.416(10)
C(6)-C(7)	1.512(10)	C(7)-C(8)	1.511(10)
C(8)-C(9)	1.532(12)	C(9)-C(10)	1.414(14)
C(10)-C(11)	1.494(11)	C(11)-C(12)	1.522(11)
C(12)-C(13)	1.509(10)	C(14)-C(15)	1.364(9)
C(14)-C(19)	1.401(10)	C(15)-C(16)	1.391(11)
C(16)-C(17)	1.387(13)	C(17)-C(18)	1.373(11)
C(17)-C(20)	1.501(12)	C(18)-C(19)	1.383(11)
C(10)-Rh-C(9)	38.6(4)	C(10)-Rh-C(13)	80.7(3)
C(9)-Rh-C(13)	89.5(3)	C(10)-Rh-C(6)	97.0(3)
C(9)-Rh-C(6)	81.0(3)	C(13)-Rh-C(6)	38.4(3)
C(10)-Rh-C(3)	159.3(3)	C(9)-Rh-C(3)	159.8(4)
C(13)-Rh-C(3)	101.8(3)	C(6)-Rh-C(3)	97.4(3)
C(10)-Rh-C(2)	152.3(3)	C(9)-Rh-C(2)	123.4(4)
C(13)-Rh-C(2)	125.3(3)	C(6)-Rh-C(2)	99.6(3)
C(3)-Rh-C(2)	36.8(3)	C(10)-Rh-C(4)	122.7(3)
C(9)-Rh-C(4)	156.3(3)	C(13)-Rh-C(4)	102.7(3)
C(6)-Rh-C(4)	121.0(3)	C(3)-Rh-C(4)	36.5(3)
C(2)-Rh-C(4)	65.4(3)	C(10)-Rh-C(1)	117.5(3)
C(9)-Rh-C(1)	99.2(3)	C(13)-Rh-C(1)	159.3(2)
C(6)-Rh-C(1)	124.2(3)	C(3)-Rh-C(1)	64.9(3)
C(2)-Rh-C(1)	35.2(3)	C(4)-Rh-C(1)	76.5(3)
C(10)-Rh-C(5)	96.6(3)	C(9)-Rh-C(5)	121.9(3)
C(13)-Rh-C(5)	124.5(3)	C(6)-Rh-C(5)	154.9(3)
C(3)-Rh-C(5)	64.8(3)	C(2)-Rh-C(5)	77.0(3)
C(4)-Rh-C(5)	34.8(3)	C(1)-Rh-C(5)	66.1(3)
C(10)-Rh-B	93.1(3)	C(9)-Rh-B	97.5(3)
C(13)-Rh-B	160.1(3)	C(6)-Rh-B	161.2(3)
C(3)-Rh-B	77.5(3)	C(2)-Rh-B	65.4(2)
C(4)-Rh-B	64.7(3)	C(1)-Rh-B	37.3(2)
C(5)-Rh-B	37.0(3)	O(3)-S-O(2)	119.3(3)
O(3)-S-O(1)	105.4(3)	O(2)-S-O(1)	109.7(3)
O(3)-S-C(14)	108.5(3)	O(2)-S-C(14)	109.3(3)
O(1)-S-C(14)	103.4(2)	B-O(1)-S	128.4(5)
O(1)-B-C(5)	126.4(7)	O(1)-B-C(1)	116.1(7)
C(5)-B-C(1)	117.4(7)	O(1)-B-Rh	128.2(5)
C(5)-B-Rh	71.4(4)	C(1)-B-Rh	70.7(4)
C(2)-C(1)-B	119.9(8)	C(2)-C(1)-Rh	70.4(4)
B-C(1)-Rh	72.1(4)	C(1)-C(2)-C(3)	120.3(7)
C(1)-C(2)-Rh	74.5(3)	C(3)-C(2)-Rh	68.9(4)
C(2)-C(3)-C(4)	121.9(7)	C(2)-C(3)-Rh	74.3(4)
C(4)-C(3)-Rh	75.7(5)	C(5)-C(4)-C(3)	120.5(9)
C(5)-C(4)-Rh	74.0(6)	C(3)-C(4)-Rh	67.8(5)
C(4)-C(5)-B	119.7(8)	C(4)-C(5)-Rh	71.1(5)

B-C(5)-Rh	71.6(4)	C(13)-C(6)-C(7)	124.5(6)
C(13)-C(6)-Rh	70.6(3)	C(7)-C(6)-Rh	111.3(4)
C(8)-C(7)-C(6)	113.3(6)	C(7)-C(8)-C(9)	113.5(7)
C(10)-C(9)-C(8)	124.1(8)	C(10)-C(9)-Rh	70.6(5)
C(8)-C(9)-Rh	113.3(4)	C(9)-C(10)-C(11)	124.6(7)
C(9)-C(10)-Rh	70.8(4)	C(11)-C(10)-Rh	111.8(5)
C(10)-C(11)-C(12)	113.3(5)	C(13)-C(12)-C(11)	113.1(5)
C(6)-C(13)-C(12)	123.7(7)	C(6)-C(13)-Rh	71.0(3)
C(12)-C(13)-Rh	113.5(4)	C(15)-C(14)-C(19)	120.5(6)
C(15)-C(14)-S	119.7(5)	C(19)-C(14)-S	119.7(5)
C(14)-C(15)-C(16)	119.9(7)	C(17)-C(16)-C(15)	120.7(7)
C(18)-C(17)-C(16)	118.4(7)	C(18)-C(17)-C(20)	120.7(9)
C(16)-C(17)-C(20)	120.9(9)	C(17)-C(18)-C(19)	122.2(8)
C(18)-C(19)-C(14)	118.2(7)		

Symmetry transformations used to generate equivalent atoms:

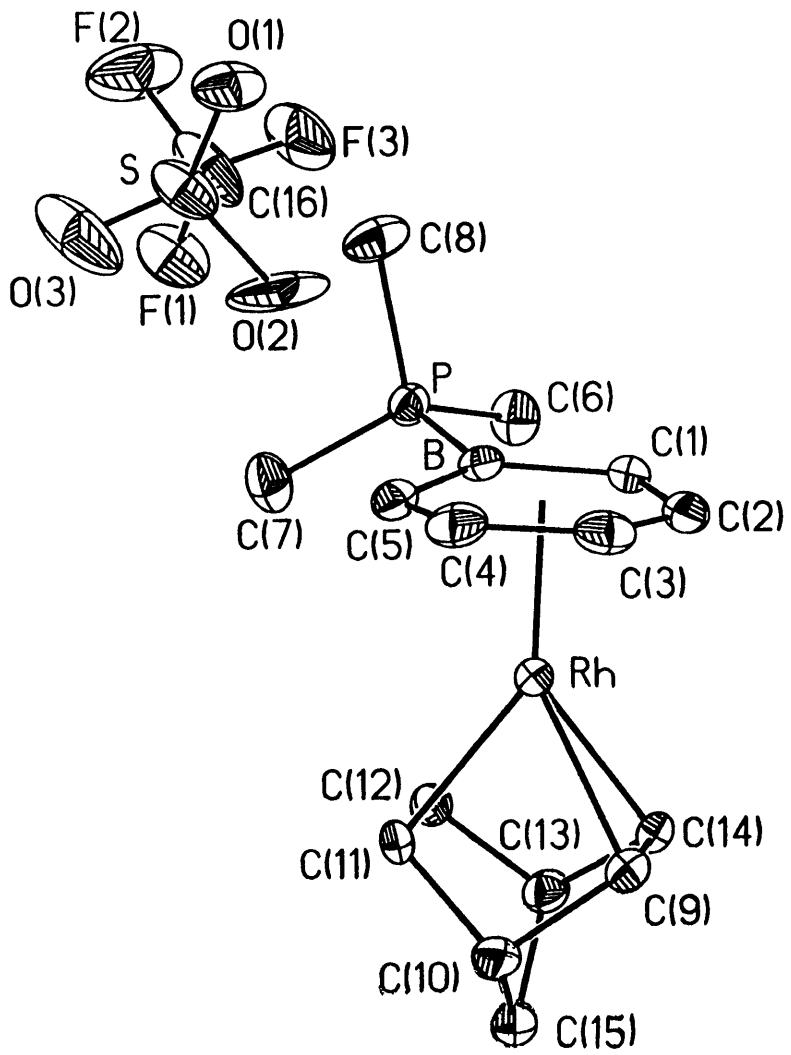


Table 1. Crystal data and structure refinement for 1.

A. Crystal Data

Identification code	98161
Empirical formula	$C_{16}H_{22}BF_3O_3PRhS$
Formula weight	496.09
Temperature	196(2) K
Wavelength	0.71073 Å
Crystal morphology	yellow block
Crystal size	0.05 x 0.20 x 0.20 mm
Crystal system	Monoclinic
Space group	$P2_1/n$
Unit cell dimensions	$a = 9.7678(2) \text{ \AA}$ $\alpha = 90^\circ$ $b = 14.29760(10) \text{ \AA}$ $\beta = 91.0320(10)^\circ$ $c = 14.0012(2) \text{ \AA}$ $\gamma = 90^\circ$
Volume, Z	$1955.04(5) \text{ \AA}^3$, 4
Density (calculated)	1.685 Mg/m^3
Absorption coefficient	1.102 mm^{-1}
F(000)	1000

B. Data Collection and Reduction

Diffractometer	Siemens SMART/CCD
Scan Type	ω Scans
Scan angle	0.30°
θ range for data collection	2.04 to 23.30°
Limiting indices	$-9 \leq h \leq 10$, $-11 \leq k \leq 15$, $-15 \leq l \leq 15$

Reflections collected	7732
Independent reflections	2804 ($R_{int} = 0.0330$)
Absorption correction	Semi-empirical from psi-scans
Max. and min. transmission	0.4790 and 0.3641

C. Solution and Refinement

Refinement method	Full-matrix least-squares on F^2
Data / restraints / parameters	2801 / 0 / 236
Goodness-of-fit on F^2	1.044
Final R indices [$I > 2\sigma(I)$]	$R1 = 0.0429$, $wR2 = 0.1049$
R indices (all data)	$R1 = 0.0517$, $wR2 = 0.1226$
Extinction coefficient	0.0021(6)
Largest diff. peak and hole	1.513 and $-0.986 \text{ e}\text{\AA}^{-3}$

Table 2. Atomic coordinates [$\times 10^4$] and equivalent isotropic displacement parameters [$\text{\AA}^2 \times 10^3$] for 1. U(eq) is defined as one third of the trace of the orthogonalized U_{ij} tensor.

	x	y	z	U(eq)
Rh	1979 (1)	653 (1)	3463 (1)	24 (1)
S	3071 (2)	5932 (2)	6337 (1)	65 (1)
P	1882 (2)	3162 (1)	4685 (1)	30 (1)
F(1)	3188 (5)	6073 (4)	8175 (3)	86 (2)
F(2)	2993 (9)	7394 (4)	7297 (6)	152 (4)
F(3)	1292 (5)	6507 (4)	7564 (4)	102 (2)
O(1)	2304 (6)	6352 (4)	5592 (3)	69 (2)
O(2)	2421 (12)	4959 (4)	6606 (7)	170 (5)
O(3)	4423 (7)	5846 (7)	6339 (5)	135 (4)
B	1627 (7)	2282 (4)	3664 (5)	29 (1)
C(1)	266 (6)	1813 (4)	3483 (4)	29 (1)
C(2)	113 (6)	1227 (4)	2681 (4)	34 (1)
C(3)	1153 (7)	1118 (4)	1996 (4)	38 (1)
C(4)	2448 (7)	1527 (4)	2135 (4)	37 (1)
C(5)	2760 (6)	2051 (4)	2972 (4)	31 (1)
C(6)	611 (6)	3047 (5)	5579 (5)	45 (2)
C(7)	3533 (7)	3095 (5)	5264 (5)	51 (2)
C(8)	1669 (9)	4313 (4)	4181 (5)	53 (2)
C(9)	1824 (6)	-846 (4)	3393 (4)	33 (1)
C(10)	3321 (6)	-1070 (4)	3665 (5)	36 (1)
C(11)	3828 (5)	-56 (4)	3820 (4)	33 (1)
C(12)	3214 (6)	263 (4)	4669 (4)	32 (1)
C(13)	2339 (6)	-558 (4)	5018 (4)	34 (1)
C(14)	1209 (6)	-535 (4)	4230 (4)	29 (1)
C(15)	3182 (6)	-1410 (4)	4705 (5)	38 (2)
C(16)	2540 (10)	6423 (9)	7393 (6)	93 (4)

Table 3. Bond lengths [Å] and angles [°] for 1.

Rh-C(11)	2.122(5)	Rh-C(12)	2.132(5)
Rh-C(9)	2.150(6)	Rh-C(14)	2.152(5)
Rh-C(5)	2.251(5)	Rh-C(2)	2.264(6)
Rh-C(3)	2.292(6)	Rh-C(4)	2.294(6)
Rh-C(1)	2.357(5)	Rh-B	2.372(6)
S-O(3)	1.326(7)	S-O(1)	1.408(5)
S-O(2)	1.578(8)	S-C(16)	1.725(9)
P-C(6)	1.786(6)	P-C(7)	1.794(6)
P-C(8)	1.801(6)	P-B	1.918(7)
F(1)-C(16)	1.351(9)	F(2)-C(16)	1.464(14)
F(3)-C(16)	1.252(10)	B-C(1)	1.506(9)
B-C(5)	1.521(9)	C(1)-C(2)	1.408(8)
C(2)-C(3)	1.418(9)	C(3)-C(4)	1.404(9)
C(4)-C(5)	1.419(9)	C(9)-C(14)	1.398(8)
C(9)-C(10)	1.538(8)	C(10)-C(11)	1.546(8)
C(10)-C(15)	1.543(9)	C(11)-C(12)	1.416(8)
C(12)-C(13)	1.537(8)	C(13)-C(15)	1.538(8)
C(13)-C(14)	1.547(8)		
C(11)-Rh-C(12)	38.9(2)	C(11)-Rh-C(9)	66.0(2)
C(12)-Rh-C(9)	79.3(2)	C(11)-Rh-C(14)	79.0(2)
C(12)-Rh-C(14)	66.2(2)	C(9)-Rh-C(14)	37.9(2)
C(11)-Rh-C(5)	101.8(2)	C(12)-Rh-C(5)	106.5(2)
C(9)-Rh-C(5)	153.5(2)	C(14)-Rh-C(5)	167.5(2)
C(11)-Rh-C(2)	164.0(2)	C(12)-Rh-C(2)	156.5(2)
C(9)-Rh-C(2)	106.5(2)	C(14)-Rh-C(2)	104.0(2)
C(5)-Rh-C(2)	78.7(2)	C(11)-Rh-C(3)	129.3(2)
C(12)-Rh-C(3)	166.2(2)	C(9)-Rh-C(3)	103.0(2)
C(14)-Rh-C(3)	123.7(2)	C(5)-Rh-C(3)	65.4(2)
C(2)-Rh-C(3)	36.3(2)	C(11)-Rh-C(4)	105.7(2)
C(12)-Rh-C(4)	131.8(2)	C(9)-Rh-C(4)	121.4(2)
C(14)-Rh-C(4)	155.7(2)	C(5)-Rh-C(4)	36.4(2)
C(2)-Rh-C(4)	65.2(2)	C(3)-Rh-C(4)	35.7(2)
C(11)-Rh-C(1)	159.1(2)	C(12)-Rh-C(1)	124.5(2)
C(9)-Rh-C(1)	130.7(2)	C(14)-Rh-C(1)	107.2(2)
C(5)-Rh-C(1)	67.8(2)	C(2)-Rh-C(1)	35.4(2)
C(3)-Rh-C(1)	64.4(2)	C(4)-Rh-C(1)	77.2(2)
C(11)-Rh-B	124.5(2)	C(12)-Rh-B	104.1(2)
C(9)-Rh-B	166.8(2)	C(14)-Rh-B	131.5(2)
C(5)-Rh-B	38.3(2)	C(2)-Rh-B	65.4(2)
C(3)-Rh-B	76.8(2)	C(4)-Rh-B	66.0(2)
C(1)-Rh-B	37.1(2)	O(3)-S-O(1)	123.9(4)
O(3)-S-O(2)	108.8(6)	O(1)-S-O(2)	110.0(4)
O(3)-S-C(16)	110.5(5)	O(1)-S-C(16)	107.3(4)
O(2)-S-C(16)	91.5(6)	C(6)-P-C(7)	108.0(3)
C(6)-P-C(8)	106.4(4)	C(7)-P-C(8)	108.8(4)
C(6)-P-B	112.3(3)	C(7)-P-B	113.9(3)
C(8)-P-B	107.1(3)	C(1)-B-C(5)	116.5(5)
C(1)-B-P	121.3(5)	C(5)-B-P	122.1(5)
C(1)-B-Rh	70.9(3)	C(5)-B-Rh	66.5(3)
P-B-Rh	135.7(3)	C(2)-C(1)-B	118.7(5)
C(2)-C(1)-Rh	68.7(3)	B-C(1)-Rh	72.0(3)
C(1)-C(2)-C(3)	122.5(5)	C(1)-C(2)-Rh	75.9(3)
C(3)-C(2)-Rh	72.9(3)	C(4)-C(3)-C(2)	121.0(5)
C(4)-C(3)-Rh	72.2(3)	C(2)-C(3)-Rh	70.8(3)

C(3)-C(4)-C(5)	120.9(5)	C(3)-C(4)-Rh	72.1(3)
C(5)-C(4)-Rh	70.2(3)	C(4)-C(5)-B	119.6(5)
C(4)-C(5)-Rh	73.5(3)	B-C(5)-Rh	75.2(3)
C(14)-C(9)-C(10)	106.2(5)	C(14)-C(9)-Rh	71.1(3)
C(10)-C(9)-Rh	97.5(4)	C(9)-C(10)-C(11)	98.0(4)
C(9)-C(10)-C(15)	101.6(5)	C(11)-C(10)-C(15)	101.3(5)
C(12)-C(11)-C(10)	106.3(5)	C(12)-C(11)-Rh	70.9(3)
C(10)-C(11)-Rh	98.4(3)	C(11)-C(12)-C(13)	105.5(5)
C(11)-C(12)-Rh	70.2(3)	C(13)-C(12)-Rh	98.2(3)
C(12)-C(13)-C(15)	102.1(5)	C(12)-C(13)-C(14)	98.6(4)
C(15)-C(13)-C(14)	101.1(5)	C(9)-C(14)-C(13)	106.3(5)
C(9)-C(14)-Rh	71.0(3)	C(13)-C(14)-Rh	97.0(3)
C(13)-C(15)-C(10)	94.4(4)	F(3)-C(16)-F(1)	108.9(8)
F(3)-C(16)-F(2)	102.9(9)	F(1)-C(16)-F(2)	106.7(8)
F(3)-C(16)-S	120.8(8)	F(1)-C(16)-S	113.6(7)
F(2)-C(16)-S	102.2(7)		

Symmetry transformations used to generate equivalent atoms:

Diego Andrés Hoic

Biographical Note.

The author was born to Carlos Hoic and Viviana Vera Salomon de Hoic in Buenos Aires, Argentina, on July 19, 1970. He has a sister named Magui. He attended Primary School at the Escuela N° 2, Olivos, Argentina from March 1977 to December 1983. He then attended High School at the Colegio Nacional de Buenos Aires, from March 1984 until December 1988. It was at this school that, for better or worse, his character was formed. Simultaneously, he attended the Conservatorio Provincial de Música Juan José Castro, in La Lucila, Argentina, where he studied piano and clarinet, as well as singing in the choir.

In August, 1989, the author left his beloved neighborhood Olivos, moving to the island of Manhattan to attend college at Columbia University. It was at Columbia that, under Professor Tom Katz's guidance, the author's interest in chemistry crystallized. The author worked on two different approaches to the synthesis of optically pure helicenes. However, he developed an interest in organometallic chemistry because of research on Fischer carbenes that was simultaneously taking place in the Katz group.

Upon graduation, the author left the grand metropolis for a beautiful small town named Boston. There he embarked in graduate studies at the MIT Department of Chemistry, choosing Greg Fu as his research advisor. During the following fifty-seven months he strived to become an expert in the area of borabenzene chemistry. The present thesis is a summary of the experiments performed, as well as of the literature read, to achieve that goal.

The author has accepted an offer of employment from the Colgate-Palmolive Company. A résumé is included in the next page.

Diego Andrés Hoic
18-444
Massachusetts Institute of Technology
Cambridge, MA 02139
Telephone: (617) 666-1639
Internet: hoic@mit.edu

Education:

- 1998 Ph.D. in Organic Chemistry. Massachusetts Institute of Technology. Thesis title: The Chemistry of Borabenzene. Research advisor: Gregory Fu.
1993 B. A. in Chemistry, Columbia University. Research advisor: Thomas Katz.

Experience:

Research Assistant: Synthesized organic and organometallic compounds.
Boron heterocycles and their transition metal complexes (graduate): Developed new, highly-efficient syntheses to two families of heterocycles and to their early, middle and late transition metal complexes. Compared the unique properties of these compounds to those of benzene and the Cp anion.
Phenanthrenequinones (undergraduate): Prepared them by Diels-Alder reaction of various styrenes with *p*-benzoquinone, as a model for helicene synthesis. Carefully placed substituents doubled the yield of a 30-year-old transformation.
Operated NMR, IR, GC-MS, HPLC, single-crystal X-ray diffraction instruments.
Teaching Assistant: Five semesters in graduate school and two in college.

Languages:

Fluent in Spanish, English, French and Croatian; basic German.

Computer Literacy:

Macintosh, PC and UNIX-based systems; Word, Excel, ChemDraw, HTML.

Extracurricular Activities:

- 1995-7 President, MIT Argentine Club.
1997 Logistics Manager, MIT Latin American Conference.

References:

Prof. Gregory C. Fu (617) 253-2664 18-411 MIT Cambridge, MA 02139	Prof. Thomas J. Katz (212) 854-2173 Box 259 Havemeyer Columbia University New York, NY 10027	Prof. Christopher C. Cummins (617) 253-5332 2-227 MIT Cambridge, MA 02139
---	--	---

Diego Andrés Hoic

Publications:

"First Synthesis and Structural Characterization of an Enantiomerically Pure Planar-Chiral Lewis Acid Complex" Tweddell, J.; Hoic, D. A.; Fu, G. C. *J. Org. Chem.* **1997**, *62*, 8286-8287.

"Synthesis, Resolution, and Crystallographic Characterization of a C₂-Symmetric Diphosphaferrocene." Qiao, S.; Hoic, D. A.; Fu, G. C. *Organometallics* **1997**, *17*, 773-774.

"Direct Crystallographic Comparison of P-B and N-B π -Bonding: Structural Studies of Diphenylphosphido- and Diphenylamidoboratabenzene" Hoic, D. A.; DiMare, M.; Fu, G. C. *J. Am. Chem. Soc.* **1997**, *119*, 7155-7156.

"Synthesis and Structure of Borabenzene-(4-phenylpyridine), a Heterocyclic Analogue of *p*-Terphenyl" Qiao, S.; Hoic, D. A.; Fu, G. C. *Organometallics* **1997**, *16*, 1501-1502.

"Defining the Conformation of Lewis Acid-Lewis Base Complexes: Crystallographic Evidence for Simultaneous σ and π Donation by a Carbonyl Group to a Divalent Boron Lewis Acid" Amendola, M. C.; Stockman, K. E.; Hoic, D. A.; Davis, W. M.; Fu, G. C. *Angew. Chem., Int. Ed. Engl.* **1997**, *36*, 267-269.

"Diphenylphosphidoboratabenzene: An Anionic Analogue of Triphenylphosphine" Hoic, D. A.; Davis, W. M.; Fu, G. C. *J. Am. Chem. Soc.* **1996**, *118*, 8176-8177.

"Nucleophilic Aromatic Substitution Reactions of Borabenzene: A Versatile Route to 1-Substituted Boratabenzenes" Qiao, S.; Hoic, D. A.; Fu, G. C. *J. Am. Chem. Soc.* **1996**, *118*, 6329-6330.

"Chemistry of Borabenzene: Efficient and General Synthesis of New Neutral Borabenzene-Ligand Complexes" Hoic, D. A.; Wolf, J. R.; Davis, W. M.; Fu, G. C. *Organometallics* **1996**, *15*, 1315-1318.

"A Boron Analogue of Benzene: Synthesis, Structure, and Reactivity of 1-*H*-Boratabenzene" Hoic, D. A.; Davis, W. M.; Fu, G. C. *J. Am. Chem. Soc.* **1995**, *117*, 8480-8481.

"Diels-Alder Reactions of α -Substituted Styrenes with *p*-Benzoquinone" Willmore, N. D.; Hoic, D. A.; Katz, T. J. *J. Org. Chem.* **1994**, *59*, 1889-1891.